



11<sup>th</sup> International Conference  
**Tunnel Safety and Ventilation**

**ITnA-Reports**

Volume 105 | May 09-10, 2022

Series Editor: Helmut Eichlseder

Editor: Peter J. Sturm



**11<sup>th</sup> International Conference**  
**TUNNEL SAFETY AND VENTILATION**

**May 09 – 10, 2022**

Graz, Austria

## **ITnA-Reports, Vol. 105**

Reports of the Institute of Thermodynamics  
and Sustainable Propulsion Systems

Series Editor            Univ.-Prof. Dr. Helmut Eichlseder

Editor                    Ao.Univ.-Prof. Dr. Peter J. Sturm

Cover                    Stefan Schleich

Cover pictures        1. Chalabala / Adobe Stock

(left to right)        2. Helmut Lunghammer

3. ITnA / TU Graz

4. Helmut Lunghammer

5. ÖBB / isochrom

6. (center) Sakarin Sawasdinaka / Shutterstock.com

Print                    Haltmeyer.at

**2022 Verlag der Technischen Universität Graz**

[www.tugraz-verlag.at](http://www.tugraz-verlag.at)

### **Print:**

ISBN 978-3-85125-883-7

### **E-Book:**

ISBN 978-3-85125-884-4

DOI 10.3217/978-3-85125-883-7



This work – excluding the cover and parts noted otherwise – is licensed under  
a Creative Commons License: *Attribution-NoDerivatives 4.0 International*  
<https://creativecommons.org/licenses/by-nc/4.0/>

## PREFACE

Ladies and Gentlemen, dear Participants,

This conference series started in 2002 in order to provide a forum for information exchange among operators, users, technicians, scientists and companies involved in the design, construction and equipping of road and rail tunnels. The success of the 2002 conference led to the organization of biennial follow up meetings.

While the first conferences were strongly influenced by the tunnel incidents of the late 1990's and related safety issues, nowadays road tunnel operation, the conflict between the needs for upgrading existing road tunnels and requirements given in a legal framework dominate. With the introduction of vehicles propelled by new energy carriers (NEC) new challenges for tunnel safety popped up. Especially the management and handling of fires with battery electric vehicles and hydrogen vehicles require attention and research into these issues is still going on.

Road traffic is increasing, at both a national as well as an international level. Thus, while in densely populated areas there is much greater demand for sub-surface transportation, in rural areas there is an increasing need to upgrade the road infrastructure. The upgrading process constitutes a big challenge in practice, as – in contrast to new tunnel construction – several prevailing structures and systems act as constraints and have to be taken into consideration in planning. There is also the additional need to ensure that traffic flow can be maintained throughout the construction period.

Investments in rail traffic in Austria resulted in the construction of three major rail tunnel. While the construction of the tracks and electrical installations is already underway in the 38 km long Koralm Tunnel, the breakthrough of the first tube in the Semmering Base Tunnel (28 km) is expected in mid-May 2022 and the second tube in autumn 2022. The Brenner Base tunnel with 55 km connects Austria and Italy, construction is in progress. These projects exhibit, based on their history and complexity, very high requirements and challenges for all parties involved in construction and operation.

The question of tunnel safety is a highly controversial field. It is often claimed that several new techniques are now on the market and that these can help improve safety due to quicker and more reliable detection, more efficient installations and/or additional equipment. However, such 'improvements' often result in significant increases in complexity, as well as in the cost of operation and maintenance of the new safety equipment.

This conference wouldn't be the "Graz" conference without the related exhibition. Many companies have put a lot of effort into presenting their latest developments and technologies. Conference participants now have the chance to get into contact with leading companies in the electro-mechanical tunnel business, to establish new contacts, and also to strengthen existing ones.

Another exciting and distinguishing aspect of the "Graz" conference is the accompanying technical visit. After many years of negotiations concerning financing, legal aspects, and finally it's erection, the research center "ZaB - Zentrum am Berg" is now under operation in a dedicated part of the Styrian Erzberg (an open-pit iron mine in operation since the 11th century). Trainings of first responders to tunnel incidents are also part of the daily business, as well as research in

mining and construction of tunnels. A special focus is on full scale fire tests for system development and tunnel safety related issues. The visit of the ZaB in the framework of the conference contains a tour to the new tunnel tubes currently under construction followed by fire tests.

We wish to extend a special thank you to our scientific committee for its valuable work in defining the objectives of this conference, and in selecting the presentations.

We also extend our professional thanks to the authors for their hard work in preparing abstracts, papers, posters, and of course their presentations.

And finally, we wish to offer our sincere thanks to all the people in the background who have been working to ensure that this will be a smooth, enjoyable and effective conference for us all.

After holding the last conference as a virtual event and missing all positive effects of face to face meetings, I hope that this years' conference will build on the very successful events of the pre-Corona years. It is my pleasure to welcome you all on behalf of the conference scientific committee and to wish you all a successful meeting and a sound basis for fertile networking in the future.

Peter J. Sturm

Graz, May 2022

**CONTENS**  
“TUNNEL SAFETY AND VENTILATION”  
Graz, 09. – 11. May 2022

**Preface**

<b>TUNNEL VENTILATION AND SAFETY, 10 CONFERENCES – THE STORY SO FAR</b>	<b>1</b>
Peter Sturm Graz University of Technology	
<b>ROAD INFRASTRUCTURE AND SUSTAINABILITY – HOW DOES IT FIT TOGETHER?</b>	<b>11</b>
Andreas Fromm ASFINAG Bau Management GmbH, AT	
<b>TUNNEL VENTILATION AND UN 2030 SUSTAINABILITY GOALS – WE HAVE A STORY TO TELL</b>	<b>13</b>
Arnold Dix Legal Counsel White & Case Professor of Engineering Tokyo City University, JP President Elect ITA	
<b>CURRENT STATUS OF THE WORK IN PIARC'S TECHNICAL COMMITTEE 4.4 TUNNELS</b>	<b>18</b>
Ingo Kaundinya Federal Highway Research Institute (BASt), Chairman of PIARC TC 4.4 Tunnels, DE	
<b>TUNNEL PERFORMANCE TEST</b>	<b>25</b>
<sup>1</sup> Günter Rattei, <sup>2</sup> Ulrike Stiefvater <sup>1</sup> ASFINAG Service GmbH, AT, <sup>2</sup> KFV, Kuratorium für Verkehrssicherheit, AT	
<b>NFPA 502: A REPORT ON STANDARD UPDATES AND ACTIVITY</b>	<b>31</b>
<sup>1</sup> Norris Harvey, <sup>2</sup> Iain Bowman, <sup>2</sup> Yinan Scott Shi <sup>1</sup> Mott MacDonald, US <sup>2</sup> Mott MacDonald, CA	
<b>ON SMOKE STRATIFICATION IN A 1-D TUNNEL VENTILATION MODEL</b>	<b>39</b>
Ingo Riess, Riess Ingenieur-GmbH, CH	
<b>NUMERICAL INVESTIGATION OF THE KORALM TUNNEL FIRE TESTS USING AN AUTONOMOUS MESHING APPROACH WITH ADAPTIVE MESH REFINEMENT</b>	<b>47</b>
<sup>1</sup> Mathias Vångö, <sup>1</sup> Pietro Scienza, <sup>2</sup> Patrik Föbtleitner, <sup>3</sup> Daniel Fruhwirt <sup>1</sup> Convergent Science GmbH, AT <sup>2</sup> FVT mbH, AT <sup>3</sup> Graz University of Technology, AT	
<b>CFD VALIDATION FOR TUNNEL SMOKE CONTROL DESIGN</b>	<b>55</b>
<sup>1</sup> Michael Beyer, <sup>1,2</sup> Conrad Stacey <sup>1</sup> Stacey Agnew Pty Ltd, AU <sup>2</sup> SAMJ LLC, US	

<b>SELECTION OF A ROAD TUNNEL VENTILATION SYSTEM USING VENTSIM SOFTWARE</b>	<b>75</b>
<u><sup>1</sup>Marek Borowski</u> , <sup>1</sup> Szmuk Andrzej, <sup>1</sup> Zwolińska Klaudia <sup>1</sup> AGH University of Science and Technology, PL	
<b>ON HEAT TRANSFER COEFFICIENTS AND TEMPERATURE DISTRIBUTION IN LONGITUDINALLY VENTILATED TUNNEL FIRES</b>	<b>83</b>
Milan Šekularac University of Montenegro, ME	
<b>METHODOLOGY FOR INVESTIGATIONS ON THE TUNNEL CLIMATE IN LONG RAILWAY TUNNELS - OPTIMIZATION OF THE DESIGN PROCESS FOR CROSS-PASSAGE COOLING SYSTEMS</b>	<b>93</b>
<u><sup>1</sup>Daniel Fruhwirt</u> , <sup>1</sup> Peter Sturm, <sup>2</sup> Helmut Steiner <sup>1</sup> Graz University of Technology, ITnA, AT <sup>2</sup> ÖBB Infrastruktur AG, AT	
<b>EMPIRICAL VALIDATION OF SEASONAL 1D TEMPERATURE PREDICTIONS IN A 9 KM NORDIC TRAIN TUNNEL</b>	<b>113</b>
<u><sup>1</sup>Erik Östblom</u> , <sup>2</sup> Per Sahlin <sup>1</sup> EQUA Solutions AB, SE <sup>2</sup> EQUA Simulation AB, SE	
<b>THE PISTON EFFECT TEST BENCH FOR THE GRAND PARIS EXPRESS</b>	<b>121</b>
<u><sup>1</sup>Elisa BERAUD</u> , <sup>1</sup> Fabien JOUVE, <sup>1</sup> Benoît HOUSEAUX <sup>1</sup> Eiffage Énergie Systèmes, Ventilation of tunnel & underground spaces, FR	
<b>RAPID FIRE DETECTION AND NOTIFICATION USING A DUAL THERMAL+OPTICAL CAMERA</b>	<b>129</b>
<u><sup>1</sup>Takuya Matsumoto</u> , <sup>1</sup> Tatsuya Oshiro, <sup>1</sup> Kazuki Furuhashi, <sup>2</sup> Hideyuki Uemura, <sup>3</sup> Alan Vardy <sup>1</sup> Sohatsu Systems Laboratory Inc., Kobe, JP <sup>2</sup> Teledyne FLIR, Osaka, JP <sup>3</sup> University of Dundee, Dundee, Scotland, UK	
<b>EXPERIMENTAL STUDY ON GENDER DIFFERENCE IN MENTAL STRESS AND WALKING SPEED DURING TUNNEL FIRES</b>	<b>136</b>
<u><sup>1</sup>Wenhao Li</u> , <sup>1</sup> Miho Seike, <sup>1</sup> Akimasa Fujiwara, <sup>1</sup> Makoto Chikaraishi <sup>1</sup> Hiroshima University, JP	
<b>ON THE ACCURACY OF FDS SMOKE PROPAGATION MODELS IN THE CONTEXT OF TUNNEL RISK ANALYSIS</b>	<b>144</b>
<u><sup>1</sup>Oliver Heger</u> , <sup>2</sup> Peter Sturm <sup>1</sup> ILF Consulting engineers Austria GmbH, AT <sup>2</sup> Institute of Thermodynamics and Sustainable Propulsion Systems, Graz University of Technology, AT	
<b>UPGRADE OF THE GERMAN METHODOLOGY FOR TUNNEL RISK ASSESSMENT</b>	<b>155</b>
<u><sup>1</sup>Georg Mayer</u> , <sup>2</sup> Harald Kammerer, <sup>3</sup> Christoph Zulauf, <sup>4</sup> Christof Sistenich <sup>1</sup> BUNG Ingenieure AG, DE <sup>2</sup> ILF Consulting Engineers Austria GmbH, AT, <sup>3</sup> EBP Schweiz AG, CH, <sup>4</sup> Bundesanstalt für Straßenwesen (BASt), DE	



<b>INFLUENCE OF ALTERNATIVE ENERGY CARRIERS ON TUNNEL SAFETY – A QUANTITATIVE CONSEQUENCE ANALYSIS</b>	<b>161</b>
<sup>1</sup> Anne Lehan, <sup>2</sup> Regina Schmidt, <sup>3</sup> Patrik Föbtleitner, <sup>1</sup> Harald Kammerer <sup>1</sup> BAST, DE <sup>2</sup> ILF Consulting Engineers, AT <sup>3</sup> FVTmbH, AT	
<b>THE APPLICATION OF ZONE MODELLING IN THE RISK ANALYSIS OF TUNNELS WITH ARTU SOFTWARE</b>	<b>169</b>
<sup>1</sup> Michele Fronterre, <sup>1</sup> Rugiada Scozzari <sup>1</sup> Cantene s.r.l., IT	
<b>FIERCE: A COST BENEFIT ANALYSIS FOR TUNNEL FIRE SAFETY</b>	<b>178</b>
<sup>1</sup> Melchior Schepers, <sup>1</sup> Xavier Deckers, <sup>2</sup> Jovanović Balša, <sup>2</sup> Chaudhary Ranjit Kumar, <sup>2</sup> Van Coile Ruben <sup>1</sup> Jensen Hughes, Ghent, BE <sup>2</sup> Department of Structural Engineering and Building Materials, Ghent University, Ghent, BE	
<b>INFLUENCE OF THE REDUNDANCY OF TUNNEL VENTILATION SYSTEMS ON THE AVAILABILITY OF ROAD TUNNELS</b>	<b>185</b>
<sup>1</sup> Leonhard Pölzer, <sup>1</sup> Maximilian Weithaler, <sup>1</sup> Reinhard Gertl, <sup>2</sup> Markus Gröblacher ; <sup>1</sup> ILF Consulting Engineers Austria GmbH, AT <sup>2</sup> ASFINAG Bau Management GmbH, AT	
<b>VALIDATION OF A MODEL ROAD TUNNEL USING FIRE EXPERIMENTS DATA</b>	<b>193</b>
<sup>1</sup> Andreas Klein, <sup>2</sup> Wilhelm Jessen, <sup>3</sup> Christof Sistenich <sup>1</sup> ISAC GmbH, Aachen, DE <sup>2</sup> Institute of Aerodynamics, RWTH Aachen University, DE <sup>3</sup> Federal Highway Research Institute (BAST), Bergisch Gladbach, DE	
<b>EGRESS-DOORS IN ÖBB RAILWAY TUNNELS - BASICS, DECISIONS, RECOMMENDATIONS</b>	<b>201</b>
<sup>1</sup> Helmut Steiner, <sup>2</sup> Michael Bacher <sup>1</sup> ÖBB Infra, AT <sup>2</sup> Graz University of Technology, AT	
<b>RECOMMENDATIONS TOWARDS THE STANDARDIZATION OF THE VENTILATION EQUIPMENT IN ROAD TUNNELS</b>	<b>210</b>
Justo Suárez INGENIERIC, ES	
<b>ON THE RISK OF A PRESSURE VESSEL EXPLOSION INSIDE ROAD TUNNELS</b>	<b>217</b>
<sup>1</sup> Jonatan Gehandler, <sup>1</sup> Chen Huang, <sup>1</sup> Ying Zhen Li, <sup>1</sup> Anders Lönnermark <sup>1</sup> RISE Research Institutes of Sweden, SE	
<b>DETERMINATION OF AERODYNAMIC LOADS IN RAIL TUNNELS USING MEASUREMENTS</b>	<b>223</b>
Johannes Rodler FVTmbH, AT	

<b>INCREASING SAFETY AND SECURITY BY USING MODERN INTERDISCIPLINARY APPROACHES FOR UNDERGROUND FACILITIES</b>	<b>232</b>
<u><sup>1</sup>Nina Gegenhuber</u> , <sup>1</sup> Robert Galler <sup>1</sup> Montanuniversität Leoben/Chair of Subsurface Engineering, AT	
<b>FEASIBILITY STUDY INTO THE IMPLEMENTATION OF ZERO FLOW TUNNEL VENTILATION IN THE SCHIPHOL KAAGBAAN TUNNEL</b>	<b>240</b>
Hans Beljaars Royal HaskoningDHV, NL	
<b>VENTILATION STRATEGY AND DESIGN OF INTERTWINING TUNNELRAMPS, OOSTERWEEL LINK ANTWERP</b>	<b>249</b>
<u><sup>1</sup>Thijs Bouwhuis</u> , <sup>1</sup> Tamara Dolle, <sup>2</sup> Aryan Snel <sup>1</sup> RoTS / Witteveen+Bos, Amsterdam, NL <sup>2</sup> Lantis / RoTS, Antwerpen, BE	
<b>RISK-BASED VENTILATION DESIGN STUDY FOR THE LA LINEA TUNNEL</b>	<b>257</b>
<sup>1</sup> Jorge Luis Rios Portilla, <u><sup>2</sup>Juan-Carlos Rueda</u> , <sup>2</sup> Harald Kammerer, <sup>2</sup> Reinhard Gertl, <sup>3</sup> Bernhard Kohl <sup>1</sup> DISICO S.A Ingeniería Eléctrica, Civil y Telecomunicaciones, CO <sup>2</sup> ILF Consulting Engineers Austria GmbH, AT <sup>3</sup> ILF Group Holding GmbH, AT	
<b>TESTING THE THRUST OF JET FANS IN A WIND TUNNEL</b>	<b>265</b>
<sup>1</sup> Tomasz Burdzy, <u><sup>1</sup>Wojciech Węgrzyński</u> , <sup>2</sup> Marek Borowski <sup>1</sup> Fire Research Department, Building Research Institute (ITB), PL <sup>2</sup> AGH University of Science and Technology, Krakow, PL	
<b>MEASUREMENTS AND CFD CALCULATIONS WITH A MOJET AND A CONVENTIONAL JET FAN</b>	<b>275</b>
<u><sup>1</sup>Fathi Tarada</u> , <sup>2</sup> Lars Lehmann, <sup>1</sup> Pier Bertacche <sup>1</sup> Mosen Ltd, Forest Row, UK <sup>2</sup> TLT-Turbo GmbH, Zweibrücken, DE	
<b>BEST PRACTICE FOR SELECTION OF FAN- AND DRIVE TECHNOLOGY IN TUNNEL VENTILATION APPLICATIONS</b>	<b>283</b>
<u><sup>1</sup>Simon Frey</u> , <sup>1</sup> Matthias Lempp, <sup>1</sup> Christina Zimmermann, <sup>2</sup> Stefan Herger, <sup>3</sup> Jürg Pargätzi, <sup>4</sup> Diego Tschuppert <sup>1</sup> HBI Haerter AG, CH <sup>2</sup> Brüniger + Co. AG, CH, <sup>3</sup> Parmeltec GmbH, CH, <sup>4</sup> FEDRO, CH	
<b>EVERY SECOND COUNTS - THE SAFETY OF PEOPLE AND GOODS IN TUNNELS. BEST PRACTICE: INNOVATIVE FIRE AND SECURITY SOLUTION USING THE EXAMPLE OF "ZENTRUM AM BERG".</b>	<b>291</b>
Wolfgang Lahner Honeywell/Honeywell Life Safety Austria GmbH, AT	
<b>AN AFFORDABLE &amp; SUITABLE ALTERNATIVE: LED RETROFIT TUNNEL LIGHTING</b>	<b>295</b>
<sup>1</sup> Thomas Nessel, <u><sup>2</sup>Markus Keller</u> , <sup>1</sup> ASFiNAG Service GmbH, AT <sup>2</sup> ASFiNAG BMG, At	

**VENTILATION IN SHORT TUNNELS AS A RISK MITIGATION MEASURE:  
"A SHORT TUNNEL CAN BE AS DANGEROUS AS A LONG ONE"**

**300**

D. Benitez Forero

Electromechanics Department, Integral S.A., CO



# **TUNNEL VENTILATION AND SAFETY, 10 CONFERENCES – THE STORY SO FAR**

Peter Sturm  
Graz University of Technology, A

## **1. BACKGROUND**

Austria's topography presents a major challenge when attempting to establish an efficient transport network. For most of the past, routes traversing mountain ranges were time consuming and dangerous. Traffic and civil engineers thus started early on to focus on the possibility of tunnels. In the east of the country, in 1854, the first mountain railway with a standard gauge track, and gradients of up to 2.5%, was built to cross the Semmering Mountain range and to provide a rail link from Vienna to the Mediterranean region. A total of 14 tunnels and 16 viaducts had to be constructed in very difficult terrain. Looking to the west of Austria, the Arlberg massif is the main obstacle between the regions of Tirol and Vorarlberg. Here, an 11 km long rail tunnel was constructed as early as 1884. Between these two ends of Austria, a number of long railway tunnels pass through the Alps in a north-south direction. In the 1970s, the strong increase in road traffic and goods transport required the construction of various long road tunnels. The Tauern tunnel (length 6.5 km) and the Katschberg tunnel (5.9 km) were both opened in 1975, the 14 km long Arlberg road tunnel – running almost in parallel to the rail tunnel – was opened in 1978. These are only a few of the many long tunnels now in existence. Almost all of them originally operated using a counter-flow system. This poses a major challenge in terms of fresh air supply and the maintenance of in-tunnel air quality needed to allow for safe tunnel passage. Owing to the relatively high vehicle-specific CO emissions at the time, many of the tunnels were equipped with a transverse ventilation system. The first tunnel with a full transverse ventilation system in Austria was opened in 1958 (Dürnstein tunnel). In all of these tunnels the design chosen had to ensure a tenable environment for users.

Today, as a result of such a long history, Austrian engineers are well-known experts, not only in tunnel construction, but also in the design of the electro-mechanical systems needed in tunnel operation. Currently, more than 165 tunnels are in operation within the Austrian highway network and roughly the same number in the secondary road network. The technological standard is very high and often taken as a benchmark for projects in other countries. Safety standards are also second to none. Even though in the last 15 years the number of tunnel km driven has increased almost by a factor of 5, the number of fatalities due to tunnel incidents has fallen from 18 to 5 per year.

## **2. THE ROLE OF THE HOST INSTITUTE AT GRAZ UNIVERSITY OF TECHNOLOGY IN TUNNEL VENTILATION AND SAFETY**

The design of tunnel ventilation systems requires extensive knowledge in aerodynamics, thermodynamics, and in the emission behaviour of vehicles propelled by internal combustion engines. As the Institute for Internal Combustion Engines and Thermodynamics (IVT)<sup>1</sup> at Graz University of Technology (TUG) has provided just such a combination of knowledge for several decades, it should come as no surprise that the institute has been at the centre of such

---

<sup>1</sup> Since January 1<sup>st</sup> 2022 Institute of Thermodynamics and Sustainable Propulsion Systems (ITnA)

research questions for already a considerable time. The tunnel-related research topics dealt with at ITnA can be split into the following areas of research:

- Investigation of fresh air requirement due to vehicle emissions
- Thermo- and aerodynamics
- Ventilation control strategy
- Environmental topics related to road and rail tunnels

### **2.1. Fresh air requirement due to vehicle emissions**

Airborne pollutants from internal combustion engines have always been a major topic in engine development. For decades, emission measurements were only performed on a stationary test bed. However, it was well-known that this did not represent the emission behaviour of vehicles in road tunnels. Thus, from the late 1960s onwards, a major effort was made to measure carbon monoxide concentration and visibility in road tunnels, and to relate this to vehicle emissions [1][2]. The growing share of heavy goods vehicles in road tunnels over the years meant that the issue of particle/soot emissions, and of visibility, gained more and more in priority. Intense work was thus undertaken in order to investigate the correlation between particle concentration in tunnel air and light extinction [3][4]. Subsequent co-operation with Switzerland and Germany meant that the work could be extended in order to get a broader view of the impact of variations in vehicle fleet, and to gain a better understanding of the influence of altitude on vehicle emissions [6].

Such work, for the most part driven by our institute, was subject to a continual process of updating concerning new developments in vehicle technology and measurements of real-world emissions. This work resulted in the well-known emission factor database for calculation for road tunnel air demand, published by PIARC [9][10][12][13][14].

### **2.2. Thermo- and aerodynamics**

Ventilation design is based on the application of aerodynamics, combined with empirically-gained knowledge. The possibility of a tunnel fire obviously requires the inclusion of various matters related to thermodynamics. From very early on, a tunnel fire was perceived as presenting a major source of risk for tunnel users, and appropriate tests were performed as early as the 1960s [15]. In Austria, a relatively large fire experiment was performed in 1974/75 in the Zwenbergtunnel, an abandoned railway tunnel which was upgraded to a road tunnel test facility with a full transverse ventilation system. For a long time, such tests served as a benchmark in investigations of tunnel smoke propagation and the impact of the different ventilation strategies [7][8]. In 1978, the report ‘Conception of Ventilation Systems for Road Tunnels’, was published. This report was the starting point for the development of Austrian guidelines for tunnel ventilation. With respect to research on full-scale fires, the EUREKA 499 FIRETUN project, from 1990 to 1995, represented a further milestone. Multiple fire experiments were performed in the Repafjord in Norway [16][17]. Here, ITnA provided measurement technique. While fire tests in tunnels continued to remain a core area of research, the focus slowly shifted more towards smoke propagation and smoke management. In 2017 full-scale fire tests with heat release rates up to 21 MW were performed in the Koralm rail tunnel. This was done in order to investigate smoke propagation in the region of cross passages, and to assess the most efficient measures needed to keep egress ways smoke-free [18]. Current research now focuses on the combustion behaviour of battery electric vehicles in tunnels.

### **2.3. Ventilation design and ventilation control strategy**

Ventilation design and operation is strongly related to the associated control strategy. While the ventilation strategy is clear under conditions of normal operation, i.e. the need to maintain in-tunnel air quality through sufficient ventilation – a different strategy is required in cases of fire. For example, achieving critical velocity in order to avoid backlayering represents one possible

strategy, and maintaining a controlled velocity (at lower speeds) to support self-rescue, represents another. These strategies are mainly relevant for longitudinally ventilated tunnels. In transverse ventilation systems smoke is extracted via the return air duct. However, the big fires in the Mt. Blanc and the Tauertunnel in the late 1990s totally changed the prevailing ventilation philosophy for transverse ventilated tunnels. Instead of extracting smoke over a series of small openings in the false ceiling between traffic room and return air duct, massive point extraction systems with remotely controlled dampers and large cross sections were introduced [19]. This also made it necessary to introduce closed loop control systems into ventilation control. One of the first fully automatic closed loop ventilation systems was developed in 2003 by IVT for the 10 km long, fully transverse ventilated Plabutsch tunnel in Graz, Austria [20]. These systems subsequently became state of the art in tunnel ventilation control. Despite such advances, the associated increase in complexity with respect to sensor technique and control mechanisms requires intense research in optimizing methods for system tests, especially in the case of complex road tunnels. As a result of such new developments, IVT now focuses strongly on ventilation control and system tests [21] [22] [27].

The institute is a sought-after partner when it comes to solving complex tasks in the area of tunnel ventilation design. This is especially true when aging tunnel systems are to be upgraded to the latest safety standards. Requirements that were once state of the art, are no longer acceptable today. In particular, today's higher traffic volume now means that much higher fire loads have to be taken into account. The extraction of any fire gases that may occur requires a completely different approach. However, this also requires a change in the mechanical equipment that is now required to control the tunnel airflows. As part of the renovation of transverse-ventilated tunnel systems, a system was developed with targeted fresh air injection using air momentum. This was first used in the Katschberg tunnel in 2010 and is now often used in all long tunnels with full transverse ventilation systems [23]. Refurbishment of the ventilation system in the Arlberg tunnel was particularly challenging. In addition to the necessary ventilation requirements, the supply air duct also had to be used as an escape route. This project required the combined use of fresh air impulse dampers and jet fans in order to meet the most advanced requirements with regard to ventilation and smoke evacuation [24]. In order to better understand the efficiency losses of jet fans, and to improve related installation factors [25], intense work was performed based on full-scale experiments, and supplemented with detailed CFD simulations. This work showed that the widely used installation factors based on the work of Kempf [26] clearly underestimated jet fan efficiency loss.

#### **2.4. Environmental topics related to road and rail tunnels**

The interface between emissions from transport and their effects on the environment has always been a key focus of research at IVT. What applies to the environment, naturally applies also to tunnels. Two aspects require particular consideration. One is the tunnel air itself, and the other, the effects resulting from polluted tunnel air.

When considering in-tunnel air quality, the main pollutants are carbon monoxide, nitrogen oxides and soot. Treatment of tunnel air may be one means of improving in-tunnel air quality and/or minimizing the negative effects of tunnel air upon the environment. In 1990 the IVT started field tests in various tunnels in Austria in order to investigate filtration of dust/aerosols and airborne pollutants. These tests lasted over a decade and are still ongoing, albeit on a smaller scale. Electrostatic dust filters as well as catalytic and biogenic treatment of airborne gases were investigated. Although some positive results were found, in general tunnel air treatment proved not feasible except for special applications (mainly PM filters) [28][29][30][31].

The dispersion of tunnel-generated pollution is a further area of research. This has mainly to be considered for city tunnels or for portal or stack locations in close proximity to built-up areas. In the 1980s, IVT started to investigate this topic in detail. As simple dispersion models failed

to correctly model the dispersion of the tunnel jet wind, model tests were performed to simulate the interaction between portal air and built-up areas [32]. Such wind tunnel tests supplemented by full-scale experiments at tunnel portals were then used to validate first generation CFD models for applications in ambient air [33][34][35]. Based on all these experimental data, and supported by other international research, a numerical code, called GRAL, was eventually developed. This was designed to model pollution dispersion from low level sources like road traffic, tunnel portals and stacks [36][37]. This software code has since become state of the art in dispersion modelling of airborne pollution in complex terrain [38].

### **3. THE CONFERENCES**

Graz University of Technology, together with the Mining University in Leoben, has always been a focal point for knowledge exchange in tunnel construction. That it has also become a focal point with respect to research on tunnel equipment, operation and safety, is thus no surprise. Based on IVT's long history of experience in tunnel ventilation and tunnel safety, a decision was made in 2002 - following upon the almost revolutionary changes in tunnel safety arising from the fires of the late 1990s - to organize a small venue for information exchange within the Alpine countries. The resulting conference was hosted on the campus of the university and attracted almost 150 persons, mainly from Europe, but also with a noticeable overseas contingent. As a result of the positive feedback from this initial event, a second meeting was organized two years later. This latter event even included a small trade fair. By 2004, the event already had so many participants that it had outgrown campus facilities. A decision was therefore made to organise the conference biannually and to move to a more suitable off-campus venue. The next event was held in the Graz Congress Centre but once again, due to the growing demand for space, had to be moved to the Messecongress Graz. While the initial conferences were strongly related to road tunnels, the later ones had already begun to shift their focus more towards the requirements and safety issues concerning long trans-Alpine and sub-sea rail tunnels.

The following section is intended to point out several highlights from past conferences, covering, amongst other things, both the successful and the less successful innovations in tunnel safety. All conference papers can be downloaded from [www.tunnel-graz.at/archive](http://www.tunnel-graz.at/archive).

#### **3.1. Conference 2002**

The fires in the Mt. Blanc and Tauern tunnel, together with their consequences, had a major impact on the conference in 2002. The subsequent rise in public awareness concerning tunnel fires has also had a significant impact on activities in the field of tunnel safety. It is worth mentioning, however, that this problem was not at all new to safety experts. Various contributions in the 2002 conference proceedings refer to the 1999 PIARC report, Fire and Smoke Control in Road Tunnels [11], which was, and still is, a crucial reference point for many activities in this area. At the time, there was a definite change of opinion among several decision-makers regarding potential problems and solutions.

There were also far-reaching consequences with respect to tunnel safety equipment. This is illustrated in the presentations concerning the new directives in Austria and Switzerland. In particular, the new design of the ventilation systems helped to achieve a breakthrough in terms of the acceptability of massive smoke extraction in long tunnels, and as a result, remote-controlled smoke extraction dampers have since become state of the art in tunnels with a transverse ventilation system.

Various presentations on theoretical and numerical work (smoke behaviour, escape behaviour) as well as practical work (tests, component development) provided a new basis for the design



of the requisite installations. For example, the article by Rudolf Hörhan, emphasized the need to allow for interaction between the different safety systems. Several articles underlined the necessity of tests, pointing to existing uncertainties in the theoretical considerations, as well as the need for maintenance and servicing of the more complex systems.

One presentation even dealt with qualitative risk assessments, using the new ventilation design for the Tauern Tunnel as an example. Arnold Dix emphasized legal aspects, and the importance of clear documentation in the implementation of new systems. He foresaw the impact of increasingly complex systems and pointed to the acute problems that can arise at the interface between design and operations, when, for example, an innovative engineer and a high-performing maintenance worker must work together. The problem of quantifying the effectiveness of safety measures was pinpointed and a warning was voiced concerning the possibility of confusing low probability/high consequence events with successful risk reduction.

### **3.2. Conference 2004**

The catastrophic tunnel fires that had occurred in the late 1990s continued to exert an influence on the second conference in 2004. Hence, a majority of the papers presented dealt with issues concerning optimized ventilation and smoke control strategies, new generations of incident detection systems, and methods for assessing tunnel safety.

A highlight of the conference was the presentation of the first closed loop ventilation control system. This system was installed in the 10 km long twin-tube Plabutsch tunnel (Almbauer, Waltl). The tunnel was equipped with a full transverse ventilation system and the ventilation control system was designed to manage up to 12 axial fans per tube in parallel. Fire tests confirmed that the system worked but also revealed that problems may arise when important sensors react too slowly or malfunction.

In one presentation, John Day addressed the discrepancy that often exists concerning the effort made to reduce the effects of tunnel fires and the unpredictable behaviour of tunnel users. He highlighted the growing gap between the costs of training tunnel users and the costs of improving safety installations. He concluded that the most cost-efficient option would be improving the behaviour of tunnel users and the weakest one is to invest in additional safety systems.

### **3.3. Conference 2006**

The 3<sup>rd</sup> conference in 2006 was strongly influenced by topics such as video detection and incident management, with particular focus on the early detection of incidents and on establishing a well designed management system. A further focus was on the usage of fixed fire fighting systems (FFFS). While papers from Australia (A. Irvin) dealt with deluge systems, high water mist systems were also presented for use in road tunnel applications (S. Kratzmeir, G. Reichsthaler), and implementations of fixed water shield systems in Japan (R. Amano) were also discussed. The PIARC position with respect to FFFS was presented by A. Haack. The safety issues in operation were complemented by presentations concerning a broad range of topics dealing with issues such as sudden wind shield fogging, safe cabling systems, and as a novelty, data security in the ethernet network.

### **3.4. Conference 2008**

In 2008 the focus was placed on differentiating between theoretical simplifications and the reality of tunnel operating requirements. Of particular interest were papers exploring the difference between actual human behaviour and model simplification, as well as those covering the challenges pertaining to refurbishments and emerging technologies in incident detection.

Of particular note was the paper by Porizek, Zaparka and Ferkl. Their paper “Ventilation Control of the Blanka Tunnel: A mathematical programming approach” described the use of model-based predictive controllers that adapt to changes in operational conditions in real time, and thereby optimise system performance in terms of both safety and energy consumption. The level of complexity revealed in their case study on the Blanka Tunnel was sufficient to demonstrate that their proposed methodology was well-suited to real world application. The pragmatic evidence they presented clearly demonstrated that such emerging techniques can be quite useful in practice, and need not be confined to the realm of theory.

Their proposed technique now forms part of the intellectual framework that is being developed for the optimisation of tunnel systems using artificial intelligence. Their 2008 contribution may thus quite legitimately be regarded as an especially significant paper.

### **3.5. Conference 2010**

The 5<sup>th</sup> Conference took place in 2010. The conference topics continued to be heavily influenced by ventilation and detection problems. Ventilation as a safety feature has been featured in several papers reflecting the changes brought about by the major fire events of the past decade. Franz Zumsteg pointed out that many of the most drastic changes in tunnel ventilation that have been proposed in recent years have already become more or less a matter of course. However, since many new ideas are based on predictions, and since predictions are fraught with uncertainty, it is important to remain critical lest we fall under the illusion that most incidents are relatively easy to deal with.

Many of the systems presented at this conference have now become state of the art, e.g. sensor technology in relation to incident detection, recognition of hazmat in tunnels, and detection of thermal problems in heavy goods vehicles before entering a tunnel. A very interesting paper about the usage of incident information and safety systems by tunnel users was presented by Günter Rattei from the Austrian highway operator ASFINAG. He showed quite clearly that automatic detection systems, e.g. linear heat detectors, video systems etc. are really quite efficient, while, in contrast, all the possibilities available to tunnel users, such as emergency phones, emergency call buttons etc. failed to have the desired effect.

A further cornerstone of the conference was the topic of fixed fire fighting systems, such as deluge, or high-pressure water mist systems. While some papers covered different installations and system acceptance tests, the paper of Arnold Dix concerning, from a legal point of view, the review of the Burnley fire accident (AUS), also demonstrated the positive effect of such a system.

The closing paper by John Day brought the participants of the conference back to reality. He clearly pointed out that ‘equipping a tunnel with each and every safety measure does not mean that the tunnel is safe’. He further demanded that ‘a minimum level of operating safety measures should be determined for each tunnel and the tunnel should be closed when that level is not achieved’. This requirement is now generally accepted, even though it causes severe problems for tunnel operators as they need to keep the tunnel under operation as long as possible.

### **3.6. Conference 2012**

In 2012 risk assessment was a hot topic. Papers looked at the topic from a number of different perspectives, and the application of risk assessment tools was subjected to considerable critical analysis. The paper by Bernhard Kohl demonstrated that a risk analysis can provide a solid basis for safety-relevant decisions in tunnel design and operation. However, risk analysis is only one of a variety of aspects which have to be included in a decision-making process. Discussion in this area was completed by looking at applications of QAR for complex tunnel systems (R. Brandt) and galleries (G. Mayer).

A further key aspect in this conference concerned rail tunnels. Here, several complementary contributions were made, concerning, for example, the ventilation system of the new Semmering Base Tunnel in Austria (G. Gobiet), selected topics from Russia (S. Gendler), and the safety concept for the Crossrail in London (Y. Ting). Finally, Franz Zumsteg pointed out that, particularly where short, steep road tunnels are concerned, improvements in escape possibilities are much more important than any additional technical safety installation.

### **3.7. Conference 2014**

The 2014 symposium covered a broad range of high-quality papers. Ever stricter regulatory requirements for ventilation control in normal and incident tunnel operating mode, call for complex control mechanisms. As soon as these requirements have to be applied in complex tunnel systems with multiple on/off ramps and connections to other tunnels, control system complexity increases non-linearly. This then requires significant and time-consuming on-site testing in order to adjust the control systems. L. Elertson demonstrated how such systems can be successfully applied and tested, taking the Norra Länken in Stockholm as an example. T. Aralt gave an overview of the future needs of automated response systems, based on the requirements for the Bergen Control Center in Norway, which is responsible for monitoring more than 250 tunnels.

Another focus was on the refurbishment of tunnels and tunnel infrastructure. Upgrading of relatively old tunnels means that, in most cases, project-specific solutions are needed in order to meet modern tunnel requirements. M. Bacher demonstrated the cornerstones entailed in the upgrading of the 14 km long Arlberg Tunnel (A), where the fresh air duct of the transverse ventilation system has to be used as an egress way, and a combination of Saccardo nozzles and jet fans are employed to overcome the large pressure differences acting between the portals. Discussion of refurbishment work in Spain (F. Portugues) as well as of the usage of water-based FFFS as passive protection systems (R. Rothe, M. Lakkonen, A. Wierer) complemented the topic.

A very critical paper by C. Stacey, concerning the controversial topics of fire, risk and project governance, as well as a presentation by R. Brandt on ‘the four elements of tunnel safety’ served to round off the conference.

### **3.8. Conference 2016**

The 2016 meeting provided the usual collection of content-rich papers. This conference saw studies on the consequences of false alarms, intended as an incentive for stimulating advancements in sensors (Sakaguchi et al), and leading to an LHD signal processing paper in 2018. Traxler et al explained how AI might be applied in order to reduce the occurrence of false alarms.

For anyone involved in even slightly complicated tunnel projects, there were six interesting papers on control design, testing, and simulation of tunnel ventilation, which together, still form quite a valuable resource.

In addition, there was some great information on motorist responses to emergencies, from Japan, Germany and Austria.

And there was also good design information on jet fan performance, lighting efficiency, and the use of the PIARC emission data.

### **3.9. Conference 2018**

The 9<sup>th</sup> conference focused on the big rail tunnel projects currently under construction in Austria. The Koralm Tunnel (KAT, 33 km), and the Semmering Base Tunnel (SBT, 28 km), are the core parts of the new Baltic – Adriatic Rail Corridor. The tunnels are to go into operation

in 2026 and 2027, respectively. In the KAT, large-scale fire tests were carried out up to a maximum heat release rate of 21 MW in order to examine the spread of smoke in the tunnel. With cross-passage equipment reduced to a minimum, it was possible to prove that the over-pressure ventilation of the safe tunnel tube is sufficient to prevent smoke from entering the cross passage. Further investigations looked at the thermal management necessary for maintaining acceptable temperatures inside the utility rooms, so as to support operation and communication purposes. Such utility rooms are located at every 500 m inside the tunnel. They require a lot of electrical energy and produce remarkable amounts of waste heat. As the rock temperature can go up to 36°C, a cost-efficient cooling system is essential. Furthermore, it was demonstrated that the effects of climate change also need to be considered as increasing ambient temperatures strongly reduce the scope of using ventilation for cooling.

One further challenging presentation concerned the usage of a sound-based incident detection system in road tunnels. The so-called AKUT system was introduced some 8 years ago into Austrian tunnels (after 8 years of research and development) and has now become almost standard in road tunnels. The period of its permanent operation has revealed that the system provides the fastest identification of a tunnel incident, and that it exhibits a very low failure rate.

### **3.10. Conference 2020**

A celebration was planned for the 10th Tunnel Safety and Ventilation Conference in April of 2020. Then COVID-19 happened and all of the event preparation was lost. The conference venue and social events had been booked but had to be cancelled and ultimately the 2020 conference became a virtual event.

In spite of the challenges faced in 2020, the conference was a strong technical success. Published papers and presentations included advances in the state-of-the art in alternative fueled vehicles, critical velocity and safety of rail transport of dangerous goods through tunnels. Specifically, battery and fuel cell vehicles were demonstrated to be as safe as gasoline and diesel driven vehicles and an intense discussion on critical velocity has led to a detailed re-examination of the topic.

While we all missed the networking opportunities and the trade exhibition in 2020, the conference was a great success, both interesting and informative.

## **4. ACKNOWLEDGEMENTS**

Section 3, concerning the highlights of the individual conferences, was co-authored by Franz Zumsteg (2002), Arnold Dix (2008), Norris Harvey (2010, 2020), Conrad Stacey (2016). Their contributions are very much appreciated.

## **5. REFERENCES**

- [1] Pischinger R.: Rußemissionen von Lastkraftwagen, Bundeministerium für Bauten und Technik, Schriftenreihe Straßenforschung, Heft 28, 1974
- [2] Haerter A.: Fresh air requirement of road tunnels. International Symposium on the Aerodynamics of Road Tunnels, (BHRA), Canterbury 1973
- [3] Pischinger R., Puchwein H.: Sichtweitenbestimmung in Straßentunnel, Bundeministerium für Bauten und Technik, Schriftenreihe Straßenforschung, Heft 75, 1977
- [4] Pischinger R., Puchwein H.: The Influence of Air Pollution on the Visual Range in Road Tunnels. 2<sup>nd</sup> International Symposium on the Aerodynamics of Road Tunnels, (BHRA), Cambridge 1976

- [5] Pischinger R., Pucher K., Schweiger H., Haghofer J.: Messung der Trübungsemission in Straßentunnel, Bundeministerium für Bauten und Technik, Schriftenreihe Straßenforschung, Heft 183, 1982
- [6] Pischinger R., Pucher K., Schweiger H., Haerter A.: Internationale Emissionsmessungen in Straßentunnel, Bundeministerium für Bauten und Technik, Schriftenreihe Straßenforschung, Heft 245, 1984
- [7] Feizlmayr A., Winter H., Pischinger R., Erhäusl A.: Brandversuche in einem Tunnel, Bundeministerium für Bauten und Technik, Schriftenreihe Straßenforschung, Heft 50, Teil 1 und 2, 1976
- [8] Schweiger H.: Thermodynamische Untersuchungen von Tunnelbränden, Bundeministerium für Bauten und Technik, Schriftenreihe Straßenforschung, Heft 78, 1977
- [9] PIARC 1987: 28<sup>th</sup> World Road Congress, Technical Committee Report No 5, Road tunnels, Brussels 13-19. September 1987
- [10] PIARC 1995: Vehicle Emissions, Air Demand, Environment, Longitudinal Ventilation, Report 05.02.B-1995
- [11] PIARC 1999: Fire and Smoke Control in Road Tunnels, Report 05.05.B-1999
- [12] PIARC 2004: Vehicle Emissions and Air Demand for Ventilation, Report 05.14.B-2004
- [13] PIARC 2012: Vehicle Emissions and Air Demand for Ventilation, Report 2012R05EN\_revised version December 2012
- [14] PIARC 2019: Vehicle Emissions and Air Demand for Ventilation, Report 2019R02EN
- [15] Kommission für Sicherheitsmaßnahmen in Straßentunneln in der Schweiz. Schlussbericht über die Brandversuche im Tunnel Ofenegg vom 17.5. bis 31.5 1965
- [16] EUREKA 499: <https://www.eurekanetwork.org/project/id/499>
- [17] Haack A.: Fire protection in road tunnels: general aspects and results of the EUREKA project, Tunnelling and Underground Space technology, Vol. 13 Issue 4, pp 377-381, 1998
- [18] Sturm P., Rodler J., Thaller T., Fruhwirt D., Föbtleitner P.: Hot smoke tests for smoke propagation investigations in long rail tunnels, Fire Safety Journal 105 (2019) 196–203
- [19] Speiser M., Pucher K.: Adjustable tunnel dampers – an essential component for smoke extraction during fires, International Conference Tunnel Safety and Ventilation, 8-10. April 2002, pp 37-44, ISBN 3-901351-57-4
- [20] Almbauer R., Sturm P., Bacher M., Pretterhofer G. Simulation of ventilation and smoke management, 2<sup>nd</sup> International Conference Tunnel Safety and Ventilation, 19. – 21. April 2004, pp 32-38, ISBN 3-901351-95-7
- [21] Sturm P., Bacher M., Pretterhofer G., Kalz U., Maier J.: Problems on ventilation in complex city tunnels, 3<sup>rd</sup> International Conference Tunnel Safety and Ventilation, 15 – 17. May 2006, pp 15-24, ISBN 3-902465-33-6
- [22] Schmölzer G., Sturm P., Zettl D., Koppensteiner W., Wierer A.: Ventilation control in case of a fire: a practical approach to the implementation of PI controllers, 8<sup>th</sup> International Conference Tunnel Safety and Ventilation, 25.-26. April 2016, pp 220-229, ISBN 978-3-85125-464-8
- [23] Sturm P., Bacher M. Brandt R.: Evolving needs of tunnel ventilation in a changing world, 4<sup>th</sup> International Conference Tunnel Safety and Ventilation, 21.-23. April 2008, pp 8-21, ISBN 978-3-85125-008-4
- [24] Sturm P., Bacher M.: Upgrading the Arlberg tunnel to current safety standards, Tunnelling and Underground Space Technology 48 (2015) 140–146
- [25] Beyer M., Sturm P., Sauerwein M., Bacher M.: Evaluation of Jet Fan Performance in Tunnels, 8<sup>th</sup> International Conference Tunnel Safety and Ventilation, 25.-26. April 2016, pp 298-314, ISBN 978-3-85125-464-8

- [26] Kempf J.: Einfluss der Wandeffekte auf die Treibstrahlwirkung eines Strahlgebläses, Schweizerische Bauzeitung Vol 4, 1965 pp 47-52
- [27] Rodler J., Sturm P., Schmölzer G., Föbtleitner P., Bacher M., Fruhwirt D.: Ventilation control in complex tunnels – results from system tests, 9<sup>th</sup> International Symposium on Tunnel Safety and Security – ISTSS 2020, 11.13 March 2020
- [28] Pischinger R., Pucher K., Söllmann G.: Abgasreinigung bei Tunnelanlagen, Bundesministerium für Wirtschaftliche Angelegenheiten, Schriftenreihe Straßenforschung, Heft 384, 1990
- [29] Pischinger R., Pucher K., Herzog G., Söllmann G.: Abluftreinigung mit Katalysatoren in Straßentunneln, Bundesministerium für Wirtschaftliche Angelegenheiten, Schriftenreihe Straßenforschung, Heft 423, 1994
- [30] Pischinger R., Pucher K., Herzog G., Rodler J.: Regenerationsverfahren für einen Tunnelkatalysator, Bundesministerium für Wirtschaftliche Angelegenheiten, Schriftenreihe Straßenforschung, Heft 458, 1996
- [31] Pucher K., Leistentritt R., Rodler J., Robra K.-H., Wellacher M.: Exhaust Air Purification for Road Tunnels, International Conference Transport and Air pollution, Graz, April 1996
- [32] Pucher K., Sturm P.: Measurement of CO concentrations in the vicinity of tunnel portals and exhaust air chimneys by model tests, 5<sup>th</sup> International Symposium on the Aerodynamics and ventilation of Vehicle Tunnels, Lille 20-22 may 1985, paper H3
- [33] Pischinger R., Pucher K., Landfahrer K., Schweiger H.: Schadstoffausbreitung bei Tunnelportalen, Bundesministerium für Bauten und Technik, Schriftenreihe Straßenforschung, Heft 228, 1983
- [34] Pischinger R., Pucher K., Sturm P.: Räumliche Schadstoffausbreitung bei Straßen, Bundesministerium für Wirtschaftliche Angelegenheiten, Schriftenreihe Straßenforschung, Heft 351, 1988
- [35] Puxbaum H., Ellinger R., Gresslehner K.-H., Mursch-Radlgruber E., Öttl D., Staudinger M., Sturm P.: Messung und Modellierung der Schadstoffausbreitung im Nahbereich von Tunnelportalen, Bundesministerium für Verkehr, Innovation und Technologie, Schriftenreihe Straßenforschung, Heft 532, 2003
- [36] Öttl D., Sturm P., Almbauer R.: Evaluation of GRAL for the pollutant dispersion from a city street tunnel portal at depressed level, Environmental modelling & software, Vol 20, Issue 5, DOI: 10.1016/j.envsoft.2004.06.001, 2005
- [37] Öttl D., Sturm P., Bacher M., Pretterhofer G., Almbauer R.: A simple model for the dispersion of pollutants from a road tunnel portal, Atmospheric Environment, Vol 36, Issue 18, DOI: 10.1016/S1352-2310(02)00254-6, 2002
- [38] Uhrner U., Reifeltshammer R., Sturm P.: Assessment of NO<sub>2</sub> concentration levels within a street canyon and a tunnel portal micro environment, 18th International Conference on Harmonisation within Atmospheric Dispersion Modelling for Regulatory Purposes, Bologna, 9-12. October 2017
- [39] Sturm P., Minarik S.: Proceedings of the International Conference Tunnel Safety and Ventilation, 8.-10. April 2002, Graz Austria, ISBN 3-901351-57-4 ([https://www.tunnel-graz.at/assets/files/tagungsbaende/Tunnel-Safety-and-Ventilation-GRAZ-01\\_2002.pdf](https://www.tunnel-graz.at/assets/files/tagungsbaende/Tunnel-Safety-and-Ventilation-GRAZ-01_2002.pdf))

## **ROAD INFRASTRUCTURE AND SUSTAINABILITY – HOW DOES IT FIT TOGETHER?**

<sup>1</sup>Andreas Fromm

<sup>1</sup>ASFINAG Bau Management GmbH, AUT

*Keywords: highway, motorway, sustainability, safety*

### **1. ROAD INFRASTRUCTURE AND SUSTAINABILITY – HOW DOES IT FIT TOGETHER?**

The Austrian high-level road network, consisting of 2249 km of motorways and speedways, is part of the “veins” of Austria and connects the biggest cities and centers of Austria with efficient and fast mobility paths. The responsibility for planning, constructing and maintaining the high-level road network lies within the ASFINAG Construction Management Company. It had to continuously adapt to the ever-changing environmental protection and safety requirements. The overall system can only endure by balancing all three pillars of sustainability – ecology, society and economy. Continuous development and improvement are a prerequisite for keeping the balance.

#### **Ecology**

In the 60ies, it was state of the art to build high-level roads without noise barriers, water protection systems or retention systems – nowadays all of the aforementioned protective measures are included in the high-level road network, supplemented by further measures such as traffic guidance systems, roadside greenery and compensation areas.

ASFINAGs compensation areas are made up of high-quality nature conservation compensation areas, wooded areas along embankments as well as mowing and meadow areas.

In the future, the high-level network will also include e-charging infrastructure and different installation for own energy production. Until 2030 ASFINAG aims to cover its own electricity requirements with its own energy production. To reach this goal, the company’s overall power consumption additionally needs to fall by 20%.

#### **Society**

The ASFINAG road network is being equipped with an increasing number of intermodal transfer points – e.g. Park & Drive facilities. Intermodality stands for the interweaving and interlocking of modes of transport, not only considering the car as the sole means of transportation. To make the best use of intermodal transfer points, ASFINAG’s customers need to have a precise overview of all transport carriers, in order to make an informed decisions when it comes to choosing the mode of transportation. All relevant data is already being bundled via the VAO (Verkehrsauskunft Österreich), the Austrian Traffic Information Platform.

#### **Economy**

Investments in the Austrian high-level road network have positive effects on the job market. An optimized infrastructure system also reduces the price of transportation and provides better connections for neighboring markets and regions. In the following 6 years, the ASFINAG Construction Management Company will invest approximately 7 billion EUR in maintaining and optimizing the existing network and facilities – with a focus on responsible construction.

In many areas, innovative construction methods are being carried out in order to improve the existing network. This includes CO<sub>2</sub>-reduced concrete, high recycling rates and sustainable logistics concepts. Additionally, ASFINAG is working with alternative contract models, eco-social procurement criteria and digital construction methods and tools.

With proactive and innovative solutions, ASFINAG plays an active part of the transition to sustainable mobility in Austria and, together with its partners, enables mobility for generations.

### **Aspects and Challenges of Tunnel Safety**

The Road Tunnel Safety Act applies to all 166 tunnel structures in Austria. It aims to achieve a constant and high level of safety for all road tunnels in Austria. Implementing and upholding this law is a top priority for ASFINAG.

Tunnel safety can be categorized in the following three areas:

- Safety of people
- Operational stability
- Data protection and information security

The safety of people is the top priority and is continuously being optimized by ASFINAG by upgrading the technical standard in tunnel systems, installing kerb reflectors, using variable traffic signs, traffic lights, information boards and LED escape route markings. The success of these measures can be seen in the development of accidents since the year 2000: while tunnel structures have continuously increased, the number of accidents with personal injuries has declined significantly.

The maintenance of operational stability is essential for smooth traffic handling. This is ensured by comprehensive maintenance work. Regarding the challenge of securing tunnel facilities in terms of energy technology, ASFINAG is currently testing the energy self-sufficiency of individual tunnel objects by using solar energy. In the event of a blackout, this will continue to guarantee the functionality of the tunnel facilities. A project in this context is the S 1 Vienna Bypass. Starting autumn 2022, the photovoltaic systems installed on this road will be a first step towards energy self-sufficiency.

Tunnel safety is completed by the area of data protection and information security. A legal basis for this area is the Federal Act to Ensure a High Level of Security of Network and Information Systems, the so-called NIS-act. It requires to evaluate existing safety concept as well as implement further measures. ASFINAG is, among other aspects, focused in optimizing user entrances, adapting privileged access rights and installing electric safety doors in areas of highly sensible tunnel facilities. The implementation of the measures needs to be validated by the Austrian Federal Ministry of Internal Affairs in November 2022.

Since planning, constructing and maintaining high-level road network and especially tunnels are highly complex tasks that also bear financial risks and require highly specialized personnel, ASFINAG tries to identify risks as soon as possible, take targeted countermeasures or aims to prevent risks from arising in the first place.



# **Tunnel Ventilation and UN 2030 Sustainability Development Goals – we have a story to tell**

By Arnold Dix

Legal Counsel White & Case, Professor of Engineering Tokyo City University,  
President Elect ITA

## **ABSTRACT**

The 2030 Agenda for Sustainable Development, adopted by all United Nations Member States, provides a shared blueprint for peace and prosperity for people and the planet, now and into the future. Politically tunnel projects must be seen and actually be responsive to the United Nations climate change agenda. This means we, as tunnel ventilation experts, must articulate the benefits and efficiencies of the ventilation systems we design, operate, and refurbish using this modern narrative. From energy consumption minimisation to control systems that will respond to decreased emissions – our emphasis must be on explaining our approaches focused on the principles of sustainability. If we do not focus on these messages, we risk catastrophic rejection of our projects on sustainability grounds. The biggest threat to tunnelling and tunnelling projects is our industries lack of focus on adequately promoting underground infrastructure contribution to achieving the UNs sustainability objectives of 2030 and transformational opportunities, in the face of climate change. This paper proposes a framework for articulating tunnel ventilation opportunities that embraces the United Nations 2030 agenda for sustainable development.

*Keywords: Sustainability, ventilation, underground, infrastructure, climate change*

## **1. INTRODUCTION**

On 28 February 2022 the Intergovernmental Panel on Climate Change (IPCC) [1] being the United Nations (UN) body for assessing the science of climate change established by the United Nations Environment Programme (UNEP) and the World Meteorological Organization (WMO), published a, ‘... *dire warning about the consequences of inaction ...*’ advising that, ‘... *climate change is a grave and mounting threat to our wellbeing and a healthy planet. Our actions today will shape how people adapt and nature responds to the increasing climate risks.*’

The 195 member governments of the UN IPCC have collectively warned of acute food and water insecurity, loss of life, and loss of infrastructure. The report urges immediate adaptive action be taken including more resilient life critical services such as clean water, critical infrastructure such as energy and transportation systems, storm drought and flooding controls, and sustainable transport systems.

The United Nations (UN) Department of Economic and Social Affairs revised its 2030 Sustainability Development Goals (SDGs) [2] in recognition of the declaration on 12 December 2020 by the United Nations Secretary General of a climate emergency [3] and consistent with the findings of COP26 [4].

Underground infrastructure, tunnels, are a proven method for robustly addressing adaptive and transitional climate change issues. Tunnels are a proven method for improving the human condition and are well suited to responding to the world’s most pressing climate change and sustainability issues.

However, tunnels are carbon heavy during construction and consume energy over very long periods of time.

Tunnel ventilation is one of the big consumers of energy during the lifetime of a tunnel and we as tunnel ventilation practitioners must be mindful of that energy burden and adjust our approach to tunnel ventilation and how we describe the systems we design, operate and refurbish, with the declared climate emergency and sustainability development goals in mind.

There is a common and populist view that all governments must exercise their decision making powers on behalf of their people to mitigate climate change by the most appropriate spending of limited public funds.

This means that most decisions relating to underground infrastructure in all countries include a requirement to demonstrate how the project will benefit the environment more than other projects competing for the same limited resources. Even during competitive bidding for tunnel projects – sustainability issues are often weighted and can be decisive for successful bidding.

Modern history demonstrates that there is a close relationship between underground infrastructure and underground development and positive environmental and social outcomes. From the provision of clean water and sewerage to highly efficient underground transportation systems, to the efficient and effective delivery of energy and other resource, the association between underground infrastructure and social and environmental benefits is clear. However, collectively as a global industry, we have failed to keep pace with the narrative, language, and metrics used to measure and communicate the collective benefits (and disbenefits) of the use and development of underground space.

This failure was recently highlighted in Germany by a legal challenge to a metro project on the basis of its adverse environmental impact due to its high construction carbon footprint.

There will be more such challenges as communities and their governments critically review their investment strategies through the new lenses of a perceived climate emergency and the urgency of taking action. Internationally this is now being evidenced in project procurement documentation which assesses the merits of projects using criteria designed to measure likely adverse impact on climate and the environment generally. As a professional industry we must rise to this challenge and better and more transparently articulate the implications of underground works projects and their long term operational implications for humanity and the planet.

## **2. Tunnel Ventilation**

There are a range of metrics associated with tunnel ventilation which can inform and assist decision makers assess the merits of underground projects generally and competing design and operational regimes specifically. For transportation tunnels it is possible to calculate the impact on carbon emissions due to increased vehicle efficiency and reduced journey times [5]. For utility tunnels such as water, sewerage and power, calculations can be undertaken to demonstrate the overall reduced carbon footprint of the underground option and offset that from the ventilation energy carbon footprint.

### **2.1. Ventilation - Energy Consumption**

The practice has been to describe energy consumption of competing ventilation design options primarily based on cost. By adopting a sustainability development goal (SDG) criteria various design options can be assessed in an SDG framework that better informs the decision making process.

The source of energy for tunnel ventilation should be a factor in assessing the impact of energy consumption on achieving sustainability performance. A naturally ventilated tunnel will likely have minimal mechanical ventilation, a tunnel powered by renewable energy sources has a smaller footprint than the equivalent tunnel powered by fossil fuel electricity generators. An example of the difference of the source of electricity can have on the environmental footprint of a tunnel was examined in the context of tunnel air cleaning technologies comparing a nuclear powered option with a coal powered option [6]. The analysis found that it was better not to clean tunnel air if the power source was from a coal powered electricity generator.

### **2.2. Using United Nations Sustainability Goals**

The United Nations Department of Social and Economic Affairs has created a set of 17 goals which can be used as a method to link ventilation engineering to positive sustainability outcomes. In doing so ventilation practitioners can assist decision makers positively assess ventilation proposals.

Sustainable Development Goal 7 is to ensure access to affordable, reliable, sustainable and modern energy for all. The UN is promoting accelerated action on modern renewable energy especially in the heating and transport sectors. When designing a tunnel passive ventilation (such as regular openings and innovative use of the piston effect) could be explored (if appropriate) and their benefits weighted to reflect the emerging importance of lower energy consumption in underground transportation assets. This is often difficult because until very recently the environmental effects of emissions from many road tunnels were driven by the prudent management of emissions from fossil fuel engines. That situation is changing rapidly, and tunnel ventilation designers can now embrace improved fossil fuel vehicle emissions and thereby engage in an SDG discussion from a tunnel ventilation perspective. In doing so tunnel ventilation engineers assist projects navigate increasingly rigorous sustainability based assessments of projects.

### **2.3. Efficiency of Tunnel Ventilation**

There are many opportunities to improve the efficiency of tunnel ventilation systems.

The configuration and exact location of fans (of whatever type) impact the efficiency of the ventilation system. Detailed consideration of fan location and orientation, overall cross section, niche design, duct size and detailed geometry to energy consumption and therefore the SDGs is a powerful tool for project advocacy. For example providing a greater distance between a tunnel lining and jet fan can greatly increase the efficiency of the jet fan because the plume of the jet fan is not impinged by the tunnel wall and the energy of the jet fan can be transferred more efficiently into momentum.

By describing the advantages of alternative tunnel geometries in terms of impact on energy efficiency of the ventilation system in an SDG context decision making can better balance construction costs with the overall SDG outcomes or the design life of the infrastructure. It is best to translate the energy consumption and efficiency performance into a SDG context to help inform the decision makers.

### **2.4. Duct Work – Detailed Design**

The aerodynamic efficiency of tunnel ventilation has been a consistent theme was the hallmark of renowned scientists at the Technical University of Graz such as the generation of Karl Pucher, Alex Härter and Ferro whom carefully explored energy efficient designs, proposing guiding vanes and curved ducts wherever possible. In recent years a focus on construction costs has driven cheaper and less efficient designs – the SDGs provide a narrative that values efficiency – for the collective good of our people and shared planet.

In 2022 there are opportunities to deliver energy savings in project ventilation through detailed design of ducts. Such detailed design work can rightly inform SDGs and become part of the advocacy for tunnel projects. Describing these efficiencies in the context of modern SDGs allows decision makers to better consider the merits of tunnel projects and alternative tunnel ventilation solutions.

### **2.5. Fan Efficiencies**

There are a range of techniques and technologies that improve the efficiency of fans either through refinement of their physical design or the control systems that regulate their use.

#### **2.5.1. Design**

Various fan manufacturers claim efficiencies in their fan design. As part of the narrative to assist the decision making process these efficiencies should be described in terms of achieving the UN SDGs. It is not enough to merely talk about the improved efficiency because decision makers need information

in a form and usable language that helps them meet requirements in policy and contractual documents of evidence of improved energy efficiency in major infrastructure.

### 2.5.2. Control

The ability to better control ventilation systems is also an opportunity to reduce energy consumption and usually reduce peak energy consumption by a range of techniques and technologies that reduce start up peak energy demand and optimise energy usage for a given ventilation outcome.

By framing the narrative that describes these energy consumption changes in terms of reduced peak energy demand and decreased overall energy usage provides a basis for making evidence based claims about how a control system contributes to achieving United Nations Sustainability Development Goals. This in turn helps decision makers make informed decisions about how best to spend their limited resources.

## 3. Lateral Thinking

It is not common for technical practitioners to embrace translating their technical engineering data and evidence into a narrative that informs broader public policy and decision making. However, the UN has declared a climate emergency and popular opinion is demanding that limited financial and technical resources be mobilised to address the emergency.

A reduction in peak energy consumption of underground infrastructure makes more energy available to the community because the reduction in peak demand allows more users of the same overall amount of energy with no reduction in the level of service. In making more energy available, such a strategy meets the requirements of SDGs 7, 8, 9, 11, 12, and 13.

The energy reduction meets SDG 7 as it increases access for others to the existing available energy, SDG 8 as it promotes more sustained use of underground infrastructure, SDG 9 as it promotes resilient infrastructure, makes the infrastructure more sustainable and is an innovation, SDG 11 as it makes the network it forms part of more resilient and sustainable, SDG 12 by making energy consumption more sustainable, and SDG 13 as it is an example of urgent action to reduce energy consumption and thereby combat climate change.



Figure 1: SDG Icons 7 to 9 and 11 to 13

By embracing more energy efficient underground designs and including either in new build or refurbishment higher efficiency and better control of tunnel ventilation a project is directly contributing to the stated United Nations objectives. In linking our tunnel ventilation outcome to these United Nations goals our outputs become more persuasive to decisions makers and the general public demonstrating we are taking urgent action to combat climate change by reducing energy consumption and better articulating the benefits of tunnels and underground space.

More action is required to better quantify and capture the benefits of improved approaches to tunnel ventilation specifically and underground infrastructure generally. The ITA is embarking on a program to help formalise a process of capturing the tremendous benefits and innovations in the use and development of underground space for the benefit of humanity and the planet.

## 4. CONCLUSION

We, as tunnel ventilation practitioners, can do our part in ensuring that the positive contribution we make to humanity and the planet is captured and recognised by decision makers and the public. The most fundamental step in achieving that outcome is embracing the language and concepts of sustainability and climate change in the narratives we generate. Furthermore, by describing the innovations in tunnel ventilation using the SDGs it makes it easier for allied professionals to perform carbon footprint offset calculations to address the considerable carbon cost of building underground infrastructure and places.

Describing our advances in tunnel ventilation, the great innovations and improvements we are making in reducing energy consumption, and describing the energy tunnels consume in terms of the offset of emissions generated by above ground activity without the tunnels is increasingly critical to ensuring the true environmental value of underground solutions is not overlooked by decision makers focused on addressing the climate emergency and the competing projects seeking to transition and adjust our human activities.

## REFERENCES

- [1] <https://IPCC.CH>
- [2] <https://SDGS.UN.org/goals>
- [3] <https://un.org/en/climatechange>
- [4] <https://UKCOP26.org>
- [5] Ridley, P., & Stacey, C., 2009: *Greenhouse Cost-Benefit Analysis for Urban Road Tunnels*, SSEE International Conference, Solutions for a Sustainable Planet, Melbourne, Australia 23 & 24 November 2009
- [6] Dix, A., & Katatani, A., 2010: Differing Environmental Footprints of Tunnel Air Cleaning Technology in Nuclear and Coal based electricity economies. *Scribd*:  
<https://www.scribd.com/document/242260307/Differing-Environmental-Footprints-of-Tunnel-Air-Cleaning-Technology-in-Nuclear-and-Coal-based-electricity-economies>

## CURRENT STATUS OF THE WORK IN PIARC'S TECHNICAL COMMITTEE 4.4 TUNNELS

<sup>1</sup>Ingo Kaundinya

<sup>1</sup>Federal Highway Research Institute (BASt),  
Chairman of PIARC TC 4.4 Tunnels, Germany

### ABSTRACT

This paper presents the outputs of PIARC's road tunnel committee of the current work cycle 2020-2023. Due to the new PIARC approach in this cycle to have more and earlier outputs, TC4.4 will deliver in total 13 outputs until the end of 2023. Current topics include: Increasing resilience of tunnels, management of urban and heavily trafficked tunnels, impact of new propulsion technologies on tunnel operation and safety, ITS in tunnels, update of the online Road Tunnel Manual, updating and improving of the DG-QRAM Software, organization of the 2<sup>nd</sup> International Conference on Road Tunnels Operation and Safety and organization of two International Seminars in Low- and Medium-Income Countries (LMIC).

*Keywords: Tunnel operation, tunnel safety & resilience, tunnel maintenance, Online Tunnel Manual, transport of dangerous goods, Intelligent Transport Systems (ITS) in tunnels, New Energy Carriers (NEC).*

### 1. INTRODUCTION

The World Road Association PIARC is an international, non-political, non-profit organization, established in 1909. The mission of PIARC is to promote international cooperation on issues related to roads and road transport. Since more than 100 years PIARC continues to foster and facilitate global discussion and knowledge sharing on roads and road transport. The Association now boasts 122 government members worldwide and retains consultative status to the Economic and Social Council of the United Nations. The main objective of PIARC is to facilitate exchange of knowledge on roads and road transport policy and practices within the context of integrated, sustainable transport. PIARC is worldwide acknowledged for the quality of its outputs. The work within PIARC is organized in Technical Committees (TC) which are regularly nominated for a working period of 4 years (so-called work cycles). PIARC's tunnel committee is one of the oldest and one of the largest committees in PIARC. During the past decades the TC Tunnels has produced

- a total of approximately 48 technical reports, covering all matters relating to the operation of road tunnels: geometry, equipment and maintenance, operating, safety and environment,
- numerous articles in PIARC's quarterly magazine Routes/Roads,
- a comprehensive Online Tunnel Manual and
- many more contributions to international events.

Work topics for the TC's are defined in the 4-years Strategic Plan (SP) [1]. The SP for the cycle 2020-2023 includes a new structure of PIARC Technical Committees and task Forces (Figure 1). TC 4.4 Tunnels is part of the Strategic Theme 4 "Resilient Infrastructure".

Strategic Theme 1 Road Administration	Strategic Theme 2 Mobility	Strategic Theme 3 Safety and Sustainability	Strategic Theme 4 Resilient Infrastructure
<b>TECHNICAL COMMITTEES</b>			
TC 1.1 Performance of Transport Administrations	TC 2.1 Mobility in Urban Areas	TC 3.1 Road Safety	TC 4.1 Pavements
TC 1.2 Planning Road Infrastructure and Transport to Economic and Social Development	TC 2.2 Accessibility and Mobility in Rural Areas	TC 3.2 Winter Service	TC 4.2 Bridges
TC 1.3 Finance and Procurement	TC 2.3 Freight	TC 3.3 Asset Management	TC 4.3 Earthworks
TC 1.4 Climate change and resilience of Road Network	TC 2.4 Road Network Operation/ITS	TC 3.4 Environmental Sustainability in Road Infrastructure and Transport	TC 4.4 Tunnels
TC 1.5 Disaster management			
<b>CROSS-CUTTING COMMITTEES</b>			
Terminology Committee			
Road Statistics Committee			
<b>RESPONSE TEAM</b>			
PIARC Covid-19 Response Team			
<b>TASK FORCES</b>			
TF 1.1 Well-Prepared Projects	TF 2.1 New mobility and its impact on road infrastructure and Transport	TF 3.1 Road Infrastructure and Transport Security	TF 4.1 Road Design Standards
TF 1.2 HDM-4	TF 2.2 Electric Road Systems		

Figure 1: New PIARC Structure according to 2020-2023 Strategic Plan (SP) [1]

The TC 4.4 Tunnels has currently 150 members (including working group members) representing 37 countries around the world. The work is organized in biannual TC meetings, 4 thematic working groups (WG) and 3 smaller Task Forces (TF) (Figure 2).

<b>Working Groups (WG) cycle 2020-2023</b>	<b>Responsible for Topic (according to the SP)</b>
WG 1 “Sustainable Operations and Maintenance”	4.4.2
WG 2 “Safety and Resilience”	4.4.1
WG 3 “ITS in Tunnels”	4.4.4
WG 4 “New Propulsion Technologies & Ventilation”	4.4.3
Task Force “Knowledge Management / Tunnel Manual”	4.4.5
Task Force “2 <sup>nd</sup> International Conference”	4.4.6
Task Force DG-QRAM	4.4.7

Figure 2: Working Groups and Task Forces in TC4.4 Tunnels

## 2. CURRENT ACTIVITIES IN THE 2020-2023 PIARC WORK CYCLE

In the following subchapters the planned activities and first results already achieved in the 2020-2023 work cycle are discussed. For detailed information and the free download of already published outputs please refer to the PIARC website ([www.piarc.org](http://www.piarc.org)).

### 2.1. Measures for increasing resilience of tunnels (topic 4.4.1)

The activities and outputs in relation to the topic “Measures for increasing the resilience of tunnels (4.4.1)” focus on increasing the resilience of a tunnel system, i.e. measures to increase the availability of the tunnel for users and measures to increase the robustness of the tunnel system. A “tunnel system” is defined as the system that consists of e.g. the road (in and nearby

the tunnel), the tunnel construction, the tunnel technical installations, including the control systems / control center from which the tunnel is operated, etc. All these elements work together as a system to assure the safety and availability for the tunnel users, at a certain designated service level (based on requirements set by the tunnel manager). Hence, the integrated performance of all these elements defines the resilience of the tunnel system.

As a first output a comprehensive Literature Review Report “Improving Road Tunnel Resilience, considering Safety and Availability (2021LR01EN)” [2] was produced by WG2. In the report more than 100 literature sources on road tunnel resilience, including more general literature on resilience principles or aspects that could be applied to tunnels, were reviewed and the results were synthesized. Many definitions for “resilience” were found, but the Working Group decided on the following definition in the context of tunnels:

“The ability to prepare and plan for, absorb, recover from, or more successfully adapt to actual or potential negative effects of events or developments affecting the availability of a road tunnel. In this context, an acceptable safety level is a mandatory constraint for the availability of the road tunnel”.

The literature review focusses on the following topics:

- General concepts and approaches for resilience management;
- Legislation, standards, strategies and policies;
- Criteria and requirements for resilience, availability and safety as a mandatory constraint;
- Various events and future developments to be resilient for, like weather conditions, climate change and other natural hazards like earthquakes and flooding, traffic incidents and traffic developments, calamities like fire, physical and cyber-security incidents, failure of technical or operational safety measures, including pandemics threatening the availability of the tunnel staff, maintenance and refurbishment works and technical and social developments like SMART mobility and the growing use of new energy carriers for vehicles;
- Possible measures to improve road tunnel resilience for these events;
- Organizational and managerial aspects of resilience improvement.

The report is completed with conclusions and recommendations (for decision makers and for PIARC), an extensive reference list, a glossary and appendices.

The literature review is the first step in the development of a full technical report on road tunnel resilience. The second step is a briefing note including 18 case studies on tunnel resilience collected from 12 countries world-wide. The collection of case studies in the briefing note covers the wide range of resilience topics and aspects mentioned above, thus providing valuable insight in current practices worldwide. Included are cases from Australia, Austria, Belgium, France, Germany, Italy, Japan, The Netherlands, South Africa, South Korea, Spain, Switzerland and The United Kingdom. The briefing note including collection of case studies “Improving Road Tunnel Resilience, considering Safety and Availability (2022R04EN)” [3] has been published in March 2022. The last and final output on the topic of tunnel resilience will be a full technical report which will include a practical road map to manage and improve resilience, “measure sheets” with assessment of effectiveness and cost-effectiveness of various resilience measures with main focus on recovery and recommendations for the target group. The publication of this final output on the resilience topic is foreseen for end of 2023.



## **2.2. Best practices in management particularly in of urban and heavily trafficked tunnels (topic 4.4.2)**

In the past years numerous technical equipment has been installed in road tunnels. The maintenance of this equipment is increasingly complex and has become an important issue. This is notably the case in urban tunnels or tunnels with high traffic volume where accessing equipment and conducting road works while the tunnel is open to traffic can be particularly challenging.

The aim of the case study collection report (2022R06EN) [4] was to gather, evaluate and comment on international expertise related to maintenance and traffic management in highly trafficked urban road tunnels. A large number of cases were collected, which were particularly suitable for providing an insight into the implementation of these special requirements for urban road tunnels. It became apparent that it was useful to divide the cases into 3 categories, which pursued similar goals:

- Implementation of the "quick responders" concept with different approaches,
- Measures to organize work and to reduce nuisance to users during the renovation of tunnels,
- New tools for maintenance and operation.

The quick responder's approach is generally considered to be an appropriate measure. However, local requirements must be carefully considered. Specially equipped motorcycles are recommended as suitable responding vehicles. In the second category, various approaches are possible, and these should be tailored as closely as possible to the renovation project in question. Public information campaigns can be just as important as technically sophisticated traffic guidance installations and design adaptations. Probabilistic approaches, e.g. on the basis of the RAMS ISO-standard (reliability, availability, maintainability, safety), can be used to take failure probabilities into account. Such methods are already in use in some cases, but are particularly effective if the methodology can already be deployed during the initial design and construction phase. The final output in this work topic will be a full technical report including recommendations in the fields of traffic, operation maintenance, equipment and refurbishment strategies. The publication is foreseen by end of this year.

## **2.3. Impact of new propulsion technologies on road tunnel operations and safety (topic 4.4.3)**

Alternative propulsion technologies, including battery-electric vehicles, are becoming more prevalent. Whilst such vehicles remain a small overall proportion of the vehicle fleet, the combination of impacts of government policy and technological advances in alternative fuels is expected to accelerate their increase in numbers on the road and in tunnels in coming years. There may also be particular initiatives in certain geographical areas, such as on airport land for example, where higher proportions of alternatively fuelled vehicles are seen sooner than on the open road.

As a result of these changes, the nature of tunnel safety risk (including from fire) is expected to change with time, and detailed consideration of the risk of significant incidents involving such vehicles is required. This should include the evaluation of incident consequences with particular attention paid to fire characteristics and toxic emissions and their impact on tunnel users and on emergency intervention strategies.

The first output of WG4 prepared during this cycle is a case study report "Impact of new propulsion technologies on road tunnel operation and safety (2022R05EN)" [5]. The topic has too few incidents to be able to make statistically relevant statements about the effects of

accidents with vehicles propelled by new propulsion technologies, commonly called new energy carriers (NEC) on the tunnel design and infrastructure. It is also currently not possible to derive specific instructions from experience gained from incidents of such vehicles. Hence, this report collates currently available information on existing or just finished research programs and highlights the most important findings from these projects. The report also presents findings of a “Webinar on New Energy Carriers in Road Tunnels” organized in cooperation with ITA-Cosuf and KPT (Dutch knowledge platform for tunnel safety).

The final output on this topic will be a full technical report to be published at the end of the work cycle (2023).

#### **2.4. Intelligent Transportation Systems in Tunnels (topic 4.4.4)**

Regarding Intelligent Transport Systems (ITS), the last few years have seen considerable technological advances in this field. In a road tunnel environment, these systems can have a significant impact on operation and user safety. The objective of this topic is to focus on the impacts of such systems on road tunnel operations and safety. Regarding ITS in tunnels there are a few main issues that need to be assessed and discussed from a tunnel community perspective:

- Given the very quick development of ITS on open roads, how can service continuity of such systems be guaranteed in the specific context of road tunnels?
- Are there any obstructions for the development of ITS in current tunnels that should be dealt with?
- What changes do we expect in terms of required safety and traffic management systems in a tunnel: what systems could possibly be deleted (under which conditions) and what new systems do we need (under what conditions)?
- What are the tunnel community’s expectations with regard to these ITS: safety distance control, lane departure warning systems (LDWS), heavy vehicle guidance systems, vehicle localization and counting systems, identification of hazardous goods vehicles, etc.?
- More generally speaking, how can these ground-breaking systems improve user safety in road tunnels?

The objective of WG3 is to prepare a full technical report answering these questions.

#### **2.5. Update of the Online Road Tunnels Manual (topic 4.4.5)**

During the last cycles the TC on Road Tunnel Operations has produced a total of approximately 45 technical reports plus many Routes/Roads-Magazine articles and special issues. In the current work cycle some reports are also already published [2, 3, 4, 5]. The main added value of the Online Tunnel Manual is to incorporate and disseminate this information through an electronic document currently published in a new (2019) version, so as to reach the widest possible audience. The current version of the online Tunnel Manual is available in English and Spanish. The French translation is also finished and the updated pages will be uploaded soon.

The update of the Tunnel Manual will be managed by a Task Force with the support of all Working Groups of TC 4.4. The Tunnel Manual is accessible at <https://tunnels.piarc.org/>.

#### **2.6. Preparation of the 2nd International Conference on Tunnels (topic 4.4.6)**

The previous 1<sup>st</sup> International conference in Lyon (October 2018) was a very successful event. The 2<sup>nd</sup> PIARC International Conference on Tunnels will be held from 25 to 28 October 2022 in Granada/ Spain. A Task Force with participation of members of TC4.4 is responsible for the preparation of the technical program in closed collaboration with the Spanish National

11<sup>th</sup> International Conference ‘Tunnel Safety and Ventilation’ 2022, Graz

Committee of Road Tunnels and other relevant international organizations in the field of Road Tunnels. Important topics which will be addressed are: New challenges of the tunnels with the 2030 objective, Resilience in road tunnels, Management of urban and high traffic road tunnels, ITS systems and their contribution to improved operations, New vehicle propulsion energies and their impact on tunnels, Risk Analysis, Ventilation and Lighting, Emergency Management and Current state of tunnels and adaptation to the regulations. More information about the event, the draft program and registration is available at <https://www.piarc-tunnels-spain2022.org/>.

## 2.7. Support for updating and improving of DG-QRAM (topic 4.4.7)

The Dangerous Goods Quantitative Risk Assessment Model, known as “DG-QRAM” is a software tool, which enables its users to perform a specific risk analysis for dangerous goods transport.

Since the release of this software, the DG-QRAM software has been widely used by many European countries to perform risk analysis for dangerous goods transport as required by the European Directive 2004/54/EC on minimum safety requirements for tunnels in the trans-European road network, and to support the choice of a tunnel category according to ADR (dangerous goods regulations).

In the 2016-2019 work cycle the tool was updated to make it compatible with more recent versions of the software that it is based on. Thanks to initial financial contributions provided by 8 funding countries, the updated version of the software tool is available for sale on PIARC website. User training sessions were organized for both expert users and new users. In the current work cycle a further upgrade of the tool, based on feedback of users, is in progress. Preliminary results and more information on the tool were communicated in an International Webinar which was organized by the responsible Task Force in June last year. The presentations and a video are available on PIARC website. It is expected that the upgraded DG-QRAM software will be finalized at the end of the work cycle (2023).

## 2.8. PIARC Tunnel events

In the current work cycle several events have already been organized by TC4.4:

- International Webinar on „Road Tunnel: Recent Trends, Innovations and Way Forward“ streamed from Delhi / India (5 – 6 May 2021),
- Worldwide webinar on the DGQRAM software “A dangerous goods transport risk assessment tool that is being upgraded!”, streamed from Lyon / France (23 June 2021),
- Webinar on “New Energy Carriers in Road Tunnels” streamed from Utrecht / The Netherlands (20 – 21 Oct. 2021),
- Technical workshop on road tunnels at 34<sup>th</sup> Japan Road Conference (4 Nov 2021),
- Technical Session R14 „Increasing Resilience of Tunnels“ at the virtual 16<sup>th</sup> World Winter Service and Road Resilience Congress (9<sup>th</sup> Feb. 2022),
- World Road Tunnels Seminar, Medellín / Colombia (29<sup>th</sup> March – 1<sup>st</sup> April, 2022),
- Several contributions to conferences where PIARC is co-organizer like 10<sup>th</sup> International (virtual) Conference ‘Tunnel Safety and Ventilation’ (1 – 3 Dec. 2020), 3<sup>rd</sup> International Polish Tunnel Forum (3 – 4 Feb. 2021).

The most important upcoming events are:

- GTFE/PIARC France Conference on Tunnel Asset Management, 2 June 2022, Lyon / France (<https://www.gtf.fr/evenements/la-conference-du-gtfe-piarc-france/>),
- 2<sup>nd</sup> PIARC International Conference on Road Tunnel Operations and Safety, 25 – 28 October 2022 – Granada / Spain (<https://www.piarc-tunnels-spain2022.org/>),

- PIARC International Seminar "Advances in Design, Construction and Maintenance of Tunnels", April 2023 – Delhi & Dehradun / India,
- 27<sup>th</sup> World Road Congress, 2 – 6 October 2023, Prague / Czech Republic (<https://www.wrc2023prague.org/>).

### 3. SUMMARY AND CONCLUSION

Since 1957, date of creation by PIARC of the "Committee on Road Tunnels", the Association has conducted an ongoing activity on all matters relating to the operation of road tunnels: geometry, equipment and maintenance, operating, safety and environment. All outputs are available online (free download) on the PIARC website. In the current work cycle several outputs have already been completed and published on the PIARC website [2 – 5]. A large number of successful events have been organized in the first 2 years of the current work cycle. A number of important tunnel conferences and seminars will follow until the end of the work cycle in 2023.

There will be continuous publications on the PIARC website during the next years because not only full technical reports are published but also intermediate deliverables like a literature review, a collection of case studies or a briefing note. Please visit the PIARC website regularly to stay updated. Anyone interested in contributing to the topics mentioned above is cordially invited to participate in TC 4.4.

### 4. REFERENCES

- [1] PIARC (2020). *Strategic Plan 2020-2023*. <https://www.piarc.org/en/PIARC-Association-Roads-and-Road-Transportation/strategic-plan>.
- [2] PIARC Technical Committee 4.4 (2021). *Literature Review Report: Improving Road Tunnel Resilience, considering Safety and Availability*. PIARC Ref.: 2021LR01EN, <https://www.piarc.org/en/>.
- [3] PIARC Technical Committee 4.4 (2022). *Briefing Note including Collection of Case Studies: Improving Road Tunnel Resilience – Considering Safety and Availability*. PIARC Ref.: 2022R04EN, <https://www.piarc.org/en/>.
- [4] PIARC Technical Committee 4.4 (2022). *Case Study Report: Maintenance and Traffic Operation of Heavily Trafficked (Urban) Road Tunnels*. PIARC Ref.: 2022R06EN, <https://www.piarc.org/en/>.
- [5] PIARC Technical Committee 4.4 (2022). *Case Study Report : Impact of New Propulsion Technologies on Road Tunnel Operations and Safety*. PIARC Ref.: 2022R05EN, <https://www.piarc.org/en/>.

## TUNNEL PERFORMANCE TEST

<sup>1</sup>Günter Rattei, <sup>2</sup>Ulrike Stiefvater

<sup>1</sup>ASFINAG Service GmbH, <sup>2</sup>KFV, Kuratorium für Verkehrssicherheit, AT

### ABSTRACT

The life cycle of a tunnel structure over 500 m officially begins for operation with the first opening in accordance with the Road Tunnel Safety Act (STSG) and thus after acceptance by the tunnel management authority. In the course of such an acceptance with an officially appointed and sworn expert, the tunnel is structurally and technically inspected for functionality and conformity with regulations.

After the first opening, the tunnel is not tested any more across all trades until the next refurbishment according to STSG §§ 7 and 8 STSG. ASFINAG Performance Tests have been working against this since 2018. With the voluntary internal ASFINAG tests of the entire system, conclusions can be drawn about the life cycle of a tunnel system and traffic and tunnel safety can be increased. The aim of these tests is to check systems between partial and general refurbishment and to initiate any necessary measures to restore the approved system condition.

*Keywords: Tunneltest, Life Cycle, Commissioning, Recommissioning, Performance Test, system-wide*

### 1. FIGURES, DATA AND FACTS LIFE CYCLE

At present, 166 tunnel systems are in operation on Austrian motorways and expressways, 87 of which are over 500 m long and therefore subject to the Road Tunnel Safety Act. (STSG)

With the entry into force of the Road Tunnel Safety Act 2006, all tunnel installations more than 500 m before being opened for the first time (new construction) or reopened (refurbishment) must undergo an acceptance or test procedure by the tunnel management authority and an external expert. The official acceptance procedure takes place after a cross-system test and trial run by the contractor, which can last up to 12 weeks, depending on the size of the facility. On the basis of the official acceptance procedure, a notice of initial opening or reopening of the tunnel is issued.

Before opening or reopening tunnels run through several test procedures until they are open to traffic in accordance with §§ 7, 8. After that, partial or general refurbishments with closure of the tunnels are planned every 15 to 20 years. Between opening or reopening and the refurbishments, only maintenance and repair work at the maintenance intervals in accordance with the guidelines can be carried out by external contractors and/or the operating technology department of ASFINAG.

For tunnels under 500 m length, no official acceptance procedure with cross-trade inspections is provided.

## **2. TUNNEL PERFORMANCE TEST**

Due to the lack of cross-system tests between the refurbishment phases, ASFINAG started with the first performance tests in 2018.

A performance test aims to check the tunnel for approved functionality and guideline conformity (status of the guidelines at the time of the first opening or last refurbishment). A target-actual comparison is carried out in order to derive measures for operation from it if necessary.

### **2.1 GENERAL CONDITIONS**

In order to ensure a reasonable and efficient planning of the systems to be tested, 5 parameters were identified which can trigger a performance test in tunnel systems:

- Age of the system (year of first opening or last reopening)
- Safety assessment (year of the last external safety assessment carried out)
- Exchange of the tunnel head computer
- Implementation of a notification procedure according to § 10 STSG
- Partial or general refurbishment (year of the next planned refurbishment)

The above mentioned parameters flow into the planning matrix and thus support the selection of the systems to be tested and the preparation of the annual planning.

Currently, a test interval of max. 5 years is planned.

### **2.2 SCOPE AND PROCEDURE OF THE TEST**

A performance test looks at the tunnel holistically and across all the different trades. The technical function of the individual field devices on site, visual inspections of the system status and the integral automated processes according to the event and incident matrix and traffic matrix are documented in the tunnel and in the traffic management centre. In addition, the equipment of the tunnel is checked for compliance with planning and guidelines.

- Video detection incl. correct video image switching and text insertion (ghost drivers, slow drivers, standstill/congestion)
- Occupied, counting and double counting loops (triggering parameters, reflexes)
- Traffic programs according to traffic matrix
- Emergency call (voice quality, door contacts and reflexes)
- Fire alarm system incl. ventilation control (reflexes, plausibility check ventilation control, fire extinguishing niches, extinguishing equipment)
- Sound reinforcement (FM or loudspeakers, free text or canned music)
- Lighting (step switching and control in case of an event)
- Automated processes according to event and incident matrix (if available)
- Visual inspection of all system components (incl. pictograms) for damage
- Doors and gates (contacts, door opening forces)
- Inspection of signage and inscriptions conforming to guidelines and planning

A minimum of 3 persons (excluding operating personnel for setting up the barrier) must be scheduled for the tests. When setting up the barrier, care must be taken to ensure that it is kept as short as possible and that it takes place during periods of low traffic. Especially in urban areas, these factors are an enormous challenge in planning the test procedures.

Visual inspections and functional tests of the emergency call system can in principle be carried out during lane closures. Testing of counting and double counting loops, and here especially the detection of wrong-way drivers, is only permitted with a blocking of the affected tube. Integral and thus cross-tube tests are only possible in the course of stops on both sides or during the blocking of both tunnel tubes. Experience has shown that cross-system tests during or after exercises and/or tunnel washing are not useful due to the time factor and the simultaneous work to be carried out in the tunnel. As a rule, the tests take place during exclusive night closures.

The tests carried out are documented in pre-prepared sheets with the date, time, tunnel tube and the name of the tested component and the reflex triggered by it. In order to ensure traceability and, if necessary, to reconstruct defects, test sheets per trade must be filled in for each trade for the documentation of the test activities/triggers in the tunnel and for the documentation of the resulting visualisation of the reflexes in the traffic management centre. In addition, photos are taken in case of deviations from the target state as well as videos of the ventilation tests.

After the tests, all test activities carried out must be listed in a protocol, if necessary with a list of the deviations from the target state and the measures to be derived from them.

### **3. EXAMPLE OF A TUNNEL PERFORMANCE TEST IN THE GANZSTEIN TUNNEL**

The almost 2 km long, longitudinally ventilated Ganzstein Tunnel on the S 6 Semmering Expressway was tested in 2019 as part of a performance test. The first tube of the Ganzstein tunnel was completed in 1980 and the second in 2009. Since the opening of the second tube, no refurbishment procedure and therefore no official acceptance has been carried out. The start of the next refurbishment is planned for 2025 at the earliest.

The inspections/tests were carried out or accompanied by 8 persons (excluding operational staff for the closure). Two employees documented the procedures from the traffic management centre in Bruck; 5 employees carried out the visual inspections and releases on site in the tunnel. Furthermore, the operators on duty supported the operation of the system.

The tests took place during a 7-hour night closure from 20:00 to 03:00 in the morning. A total of 36 SOS manual hazard alarms were pressed, 74 niche doors and 10 escape route doors were tested, the fire alarm centre and the fire programme were activated 12 times, 36 emergency calls were made via the emergency call receivers, 39 cameras and 16 double counting and occupancy loops were tested. Table 1 shows an overview of the size of the system, the time required and the documented deviations.

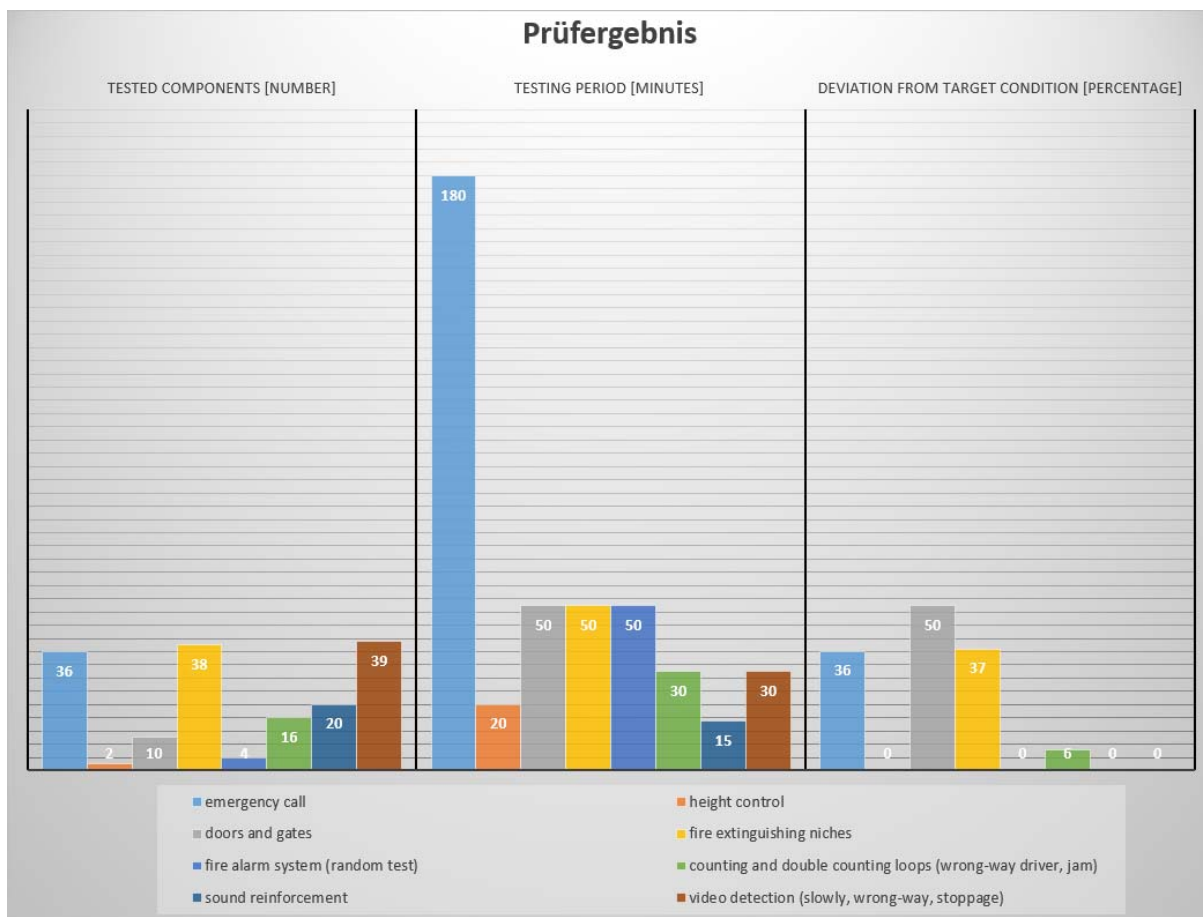


Table 1: Total expenditure for Tunnel Ganzstein test procedure

Finally, a very good plant condition was documented. Nevertheless, over 30 deviations from the target condition were detected. Safety-critical deviations were not determined. Corrective action could be taken promptly by taking appropriate measures.

#### 4. EXPERIENCES AND FINDINGS

Since 2018, about 50 tunnels were tested. Experience shows that the time required for tunnels under 3 km can be calculated as 7 hours (one night). For the remaining tunnels, night closures, lane closures or stops lasting several days had to be planned.

The deviations are divided into three categories, firstly deviations of the technical function, then deviations of the system condition and deviations from the approved technical regulations (RVS, planning manuals, etc.). Deviations from the state of the system include all visual inspections (pictograms, escape route orientation boards, etc.).

A large part of the deviations concern the general condition of the system. This is followed by technical deviations in the area of control technology, video detection and loop detection. Insignificant faults can usually be rectified by the plant engineering department during the tests.

The measures are recorded in a results or measures list and assigned to the responsible departments. A priority ranking according to short, medium and long-term measures as well as clear responsibilities can be read from this list. The monitoring of the fulfilment of these measures is ensured by the tunnel management.





Fig. 1: Example of a faulty display WVZ



Fig. 2: Example: LG measuring device malfunction during fire simulation



Fig. 3: Example of a faulty escape route indication sign

The system tests between the planned refurbishments ensure that the tunnel systems function perfectly and comply with the planning and guidelines, thus actively contributing to tunnel safety.

## **5. SUMMARY**

The performance tests that have been carried out voluntarily by ASFINAG since 2018 ensure a high level of safety in Austrian tunnels. They provide support in fault rectification and are in the meantime a fixed component of a tunnel life cycle. The aim is to test up about 20 tunnels (STSG and short tunnels) per year.

Similar to the performance tests, the Road Tunnel Safety Act provides for inspections by the tunnel administration authority according to § 3 (5). In order to minimize traffic disruptions for road users the tunnel administration authority and ASFINAG decided to carry out joint inspections and tunnel performance tests. In 2022, 14 tunnel performance tests and additional 14 joint inspections and tunnel performance tests are planned.

Such tests are preventive measures to maintain and increase safety standards in tunnels. Furthermore, conclusions can be drawn about the life cycle of the operation and safety facilities and refurbishment measures can be adapted accordingly.

## NFPA 502: A REPORT ON STANDARD UPDATES AND ACTIVITY

<sup>1</sup>Norris Harvey, <sup>2</sup>Iain Bowman, <sup>2</sup>Yinan Scott Shi

<sup>1</sup>Mott MacDonald, USA

<sup>2</sup> Mott MacDonald, Canada

### ABSTRACT

The NFPA 502 Standard provides fire protection and fire life safety requirements for limited access highways, road tunnels, bridges, elevated highways, depressed highways, and roadways that are located beneath air-right structures. The NFPA 502 three year cycle is closing and the next edition of the standard will be published in September, 2022.

The revisions to the Standard are nearly finalized, so this paper will impart an understanding of what the key changes are. The subjects addressed in the revision cycle include these:

1. Updates to the Critical Velocity Calculations Annex;
2. Changes to criteria from prevention of backlayer to control of backlayer;
3. Updates to the Autonomous Vehicles Annex;
4. Updates to the Alternative Fuels Annex;
5. Application of NFPA 72 (Fire Alarms);
6. Updates to the Tunnel Categories;
7. Structural fire protection.

Keywords: NFPA 502; Critical Velocity; Autonomous Vehicles; Alternative Fuels; Fire Protection.

### 1. INTRODUCTION

The 2023 Edition of NFPA 502 will be issued around September 2022. This issuance is the culmination of a lengthy process that all NFPA documents must traverse, see Figure 1. The NFPA 502 Standard received 57 Public Inputs for review and revision.

The process broadly follows four steps:

1. **Input stage:** There is a 9-month public input period for proposed revisions to a standard. This period begins almost immediately after the new NFPA Edition is published. Typically, this is from October to June. Comments must be entered via the NFPA website and anyone can participate. After closing, the First Draft meeting takes place where each comment is discussed in detail. After an official on-line balloting process, the results of the First Draft Process are posted on the NFPA website and are available for additional comments.
2. **Step 2:** This step begins with a time period to submit comments to the First Draft responses. Once comments are received, each comment is discussed in detail at the Second Draft meeting. After an official on-line balloting process, the results of the Second Draft Process are posted on the NFPA website. At this point, if a comment proponent still disagrees with the outcome of the process, a NITMAM (Notice of Intent to Make a Motion) may be submitted. Once certified, NITMAMs are dealt with in Step 3. If no public comments are received, there is not a second revision by the committee and the NITMAM process does not occur.
3. **Step 3:** NITMAM's are resolved at the annual NFPA Technical Meeting. This represents the last opportunity for changes to the Standard.

4. **Step 4:** The NFPA Council meets and the Standard is issued.

The four steps are a 3-year process that allows public input and comment with an appropriate review provided by the Standard Committee. The process is a consensus approach where changes are enacted upon a majority vote, in this case, on the NFPA 502 Committee.

For this cycle, the meetings occurred via conference call, due to the COVID-19 isolation measures taken by most countries. The meetings were held in October 2020 and October 2021. Preparation for these meetings was done by sub-committees which did a preliminary review of comments and recommended a path forward. These recommendations were then discussed at the technical meetings.

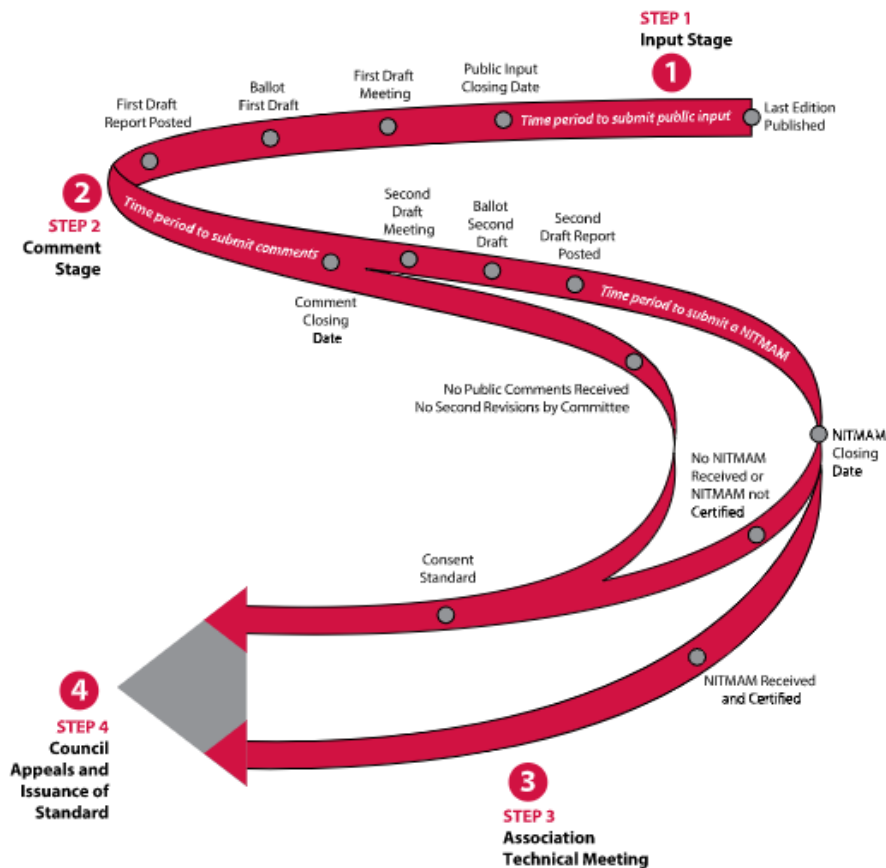


Figure 1: The NFPA standards development process [1]

The process is now coming to a close and the changes to NFPA 502 will be finalized in June at the Annual meeting. The key changes follow:

## 2. CHANGES TO NFPA 502

### 2.1. Annex D: Critical Velocity Calculations

The Critical Velocity Calculations Annex received a complete revision as the result of public comments and inputs. A Tentative Interim Amendment (TIA) was processed by the Technical Committee on Road Tunnel and Highway Fire Protection, and was issued by the Standards Council on August 26, 2021, with an effective date of September 15, 2021[2]. The TIA effectively removed the 2020 critical velocity equations from the Standard. To fill the void, new annex material was established by the committee via the extensive efforts of a sub-committee.

The new Annex D provided critical velocity calculation methods from the NFPA 502 2014 edition and the 2017 edition. The only difference between the two equations is the introduction of the variable critical Froude number factors in the 2017 edition which is dependent on the convective Fire Heat Release Rate (FHRR). The annex recognizes that both equations have their advantages and limitations. Both equations are compared with the Memorial Tunnel Fire Ventilation Test Program (MTFVTP) [3] data as shown in Figure 2. The intent is to allow the reader to make an informed decision about which equation to use.

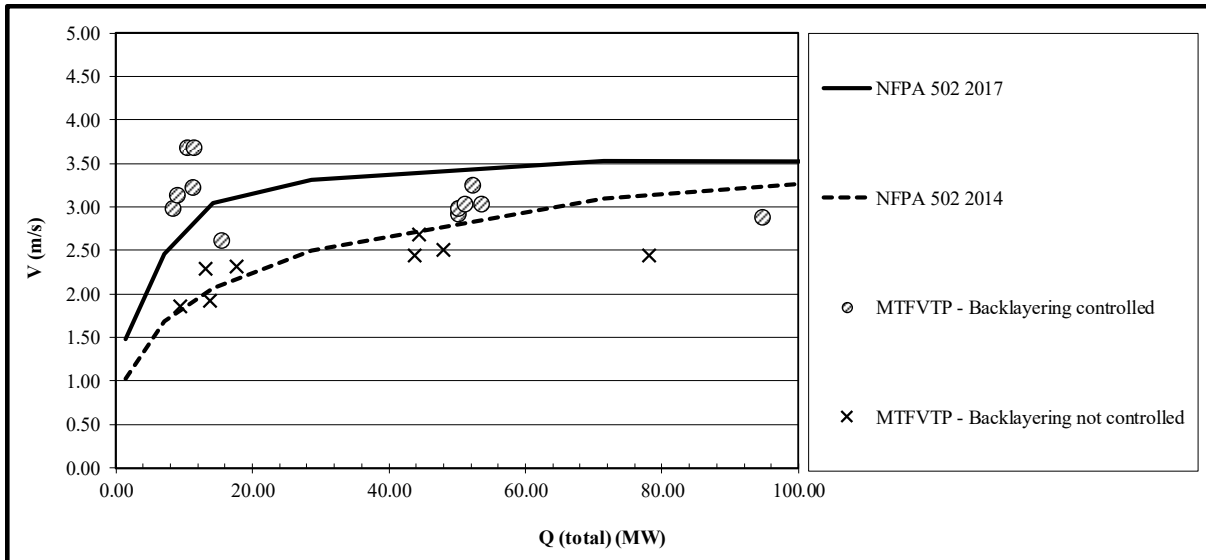


Figure 2: Critical velocity equation from NFPA 502 2014 and 2017 versus MTFVTP

Furthermore, the limitations of each equation are documented:

1. Both the 2014 and the 2017 equations are limited to the tunnel aspect ratio being similar to a two-lane tunnel (width to height on the order of 1 to 2 with a typical lane being 3.5 meters wide). For very wide road tunnels, the equations should be solved for velocity (not flow rate) as though the tunnel were two lanes wide [4].
2. The 2014 equations assume that the fire must be sufficiently wide and high such that no air can move past the fire without cooling it. (The fire plume and incoming airflow are well mixed, known as the complete mixing assumption). The equations use a constant critical Froude number factor equal to 0.606.
3. With the variable critical Froude number factors in the 2017 equations, different mixing conditions between the incoming airflow and the fire plume are better captured. However, the critical Froude number factors are based on small-scale tests and are still subject to uncertainty, and can only provide an indicative prediction of the critical velocity.

Recognizing that both equations are imperfect and that various parameters affect the critical velocity — including but not limited to tunnel geometry, design fire, tunnel blockage ratio, and tunnel wall and ceiling heat transfer — the annex acknowledges several other forms of smoke control equations exist that this is an area of active research and discussion in the industry.

The annex also introduced the term “confinement velocity” to recognize the possibility of achieving a tenable environment by controlling smoke backlayering especially during a fire incident with a relatively high FHRR. The confinement velocity is defined as the minimum steady-state velocity of the ventilation airflow moving toward the fire, within a tunnel or passageway, that is required to achieve steady-state smoke backlayer control. This is a significant change as critical velocity does not allow any backlayer by definition. To achieve

the confinement velocity, it is recommended to follow Section B.3(2) on the zone of tenability. An equation to calculate the confinement velocity is not provided, instead the annex recognizes the performance-based tunnel fire safety design methods involving computational fluid dynamics (CFD). It also urges engineers to use industry best practices for CFD.

## 2.2. Confinement Velocity

The update to Annex D has shifted the previous view on smoke management from strictly preventing smoke backlayering to controlling smoke backlayering while concentrating on providing tenable environment. To execute the implementation, multiple updates are made within the Standard:

- The term confinement velocity is introduced in Section 3.3.14, meaning the steady-state velocity of the longitudinal ventilation airflow moving towards the fire, within a tunnel or passageway that controls the backlayering distance. It co-exists alongside the definition of critical velocity.
- Sections 11.2.1, 11.2.3, 11.2.4 and 11.3 add an emphasis on providing or maintaining a tenable environment as the key objective.
- Annex A.11.2.4, A.11.4.2 and C.3.3 update the word “prevent” to “control” when applied to smoke backlayering.
- The illustrations in annex A.3.3.5 are updated to reflect the inclusion of confinement velocity and to provide a visual comparison with the critical velocity as shown in Figure 3:

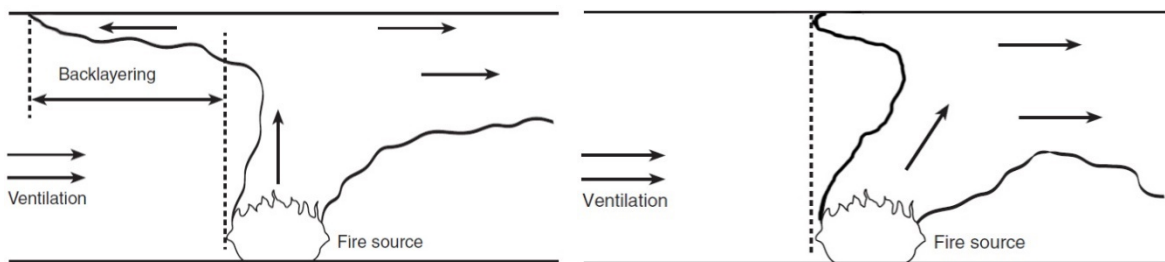


Figure 3 confinement velocity (left) vs. critical velocity (right)

## 2.3. Annex G: Alternative Fuels

Alternative fuels are advancing in the global automotive community. As a result, extensive editing was incorporated into the Alternative Fuels annex as the result of 9 of the 57 public inputs on this subject. The result was a significantly edited annex.

In summary the edits to the document are as follows (not inclusive):

In section G.2.1, additional information regarding compressed natural gas (CNG) storage was added. This information informs the reader about Standard FMVSS 304 “Compressed Natural Gas Fuel Container Integrity” and ANSI NGV2 “American National Standard for Natural Gas Vehicle Containers”. A brief summary about full-scale testing of storage containers, pressure relief devices (PRDs), and other testing required by the Standard was provided.

In the section on hydrogen fuel, G.2.4, additional information was provided on the storage tanks and the hydrogen process in vehicles. It was noted that medium- and heavy-duty gaseous hydrogen vehicles are in their demonstration phase.

In section G.2.5, information was provided on battery electric vehicles (BEV). Many of the hazards were described which include thermal runaway and hazards deriving from lithium-ion smoke such as hazards from heavy metals and hydrogen flourides. The corrosive nature is also

noted as the smoke can attack concrete and steel structures. Currently there is limited data on BEV fires.

Section G.2.5 on hybrid electric vehicles (HEV) was included to suggest that the risks from these vehicles is less than that of vehicles solely powered by batteries, as the battery bank is much smaller.

#### 2.4. Application of NFPA 72 (Fire Alarms)

Typically, US codes and standards push for fire alarms and fire protection systems to be completely independent of the normal operation of supervisory control and data acquisition (SCADA) and building management systems. Underwriter Laboratories (UL) listing of these systems is based on an independent fire management system operating the tunnel fire protection systems. However, almost all tunnel systems are used for both normal and emergency operations which in many cases invalidates the UL listing for components. The changes in NFPA 502 are intended to address this issue which is US code related.

The Standard now allows the fire alarm control panel (FACP) to interface with the SCADA for the purpose of reporting alarms, but also requires a minimum safety integrity level (SIL) of SIL-2 for the SCADA system in accordance with IEC 61508 “Standard for Functional Safety of Electrical/Electronic/Programmable Electronic Safety-Related Systems.”

#### 2.5. Passive Fire Protection

Passive fire protection in road tunnels has for many years referenced the time-temperature curve developed by the Dutch Ministry of Transport (Rijkwaterstaat, RWS) and the Netherlands Organisation for Applied Scientific Research (TNO) from a series of tests done in the 1970s and later verified by the Runehamar tunnel tests done by the UPTUN project in Norway in 2003.

The RWS curve has been included for a number of editions in the Standard as a performance requirement in Clause 7.3.2, which also allows use of another time-temperature curve “acceptable to the AHJ.” Related informational material has also been included in Annex A.7.3.2.

Since publication of the current edition of the Standard, a new edition of a test standard has been published, ASTM E3134, Standard Specification for Transportation Tunnel Structural Components and Passive Fire Protection Systems **Fehler! Verweisquelle konnte nicht gefunden werden.** This standard now incorporates a time-temperature curve similar to the RWS curve. It also contains an option of conducting a surface burning test on fire-resistive materials potentially used on tunnel surfaces and a fire-resistance rating test on any joint materials being considered.

Consequently, it was decided to add a reference to this newly revised standard in Annex A.7.3.2.

Section 9.4.4.2 now also permits a fixed water-based firefighting system to be an alternative to, or an augmentation of, passive fire protection.

#### 2.6. Tunnel Categories

The classification of tunnel by length was revised. In the previous edition of the Standard, tunnels were classified by length into five Categories (X, A, B, C, D) in Clause 7.2, with Annex material in A.7.2, Table A.7.2, Figure A.7.2

The Category B tunnel was defined by length (240m / 800ft) qualified by distance to a “point of safety” (120m / 400ft). The stated maximum distance to a “point of safety” is not a prescribed

requirement of the Standard, nor is it consistent with the requirement for maximum spacing between exits (300m / 1000ft) prescribed within the Standard.

Consequently, it was decided to revise the categorisation by deletion of the previous Category B, and to thus rename the two subsequent Categories i.e. C becomes B and D becomes C. There will now be four Categories (X, A, B, C). The differences are summarised in a comparison of the current Figure A.7.2 in the 2020 Edition (Figure 4) and a draft of Figure A.7.2 as it will appear in the 2023 Edition (Figure 5).

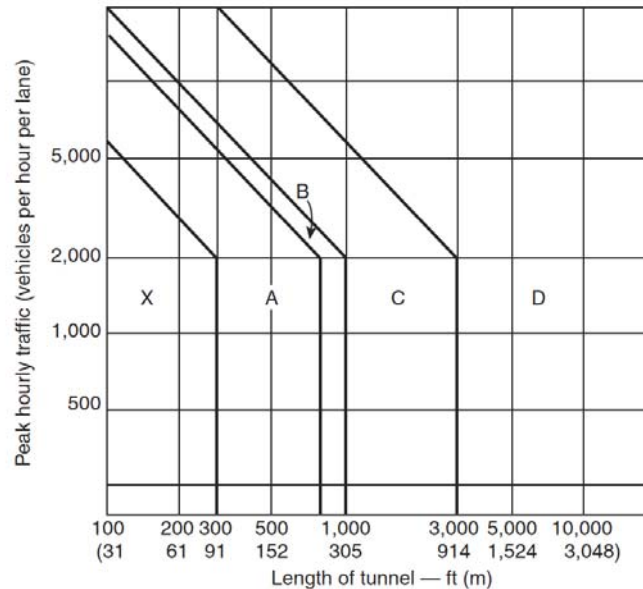


Figure 4. Figure A.7.2 NFPA 502, 2020 Edition

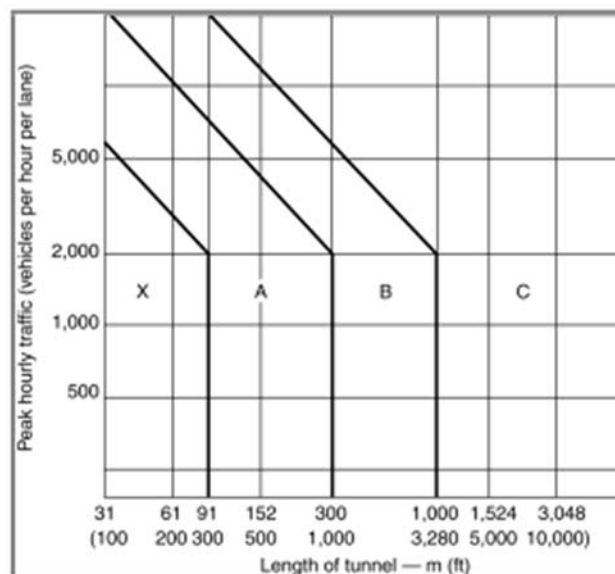


Figure 5. Draft Figure A.7.2 NFPA 502, 2023 Edition

The Reference Guide table (Table A.7.2) and Figure A.7.2 in the Annex were also reviewed and edited for consistency with the revised definitions, considering the increase of 60m (200ft) for tunnels that previously were classified as Category B.

With reference to Table A.7.2 of the Standard, noting that as Annex material this table is provided for information only, for items that were decreased in stringency from Mandatory Requirement (MR) to Conditionally Mandatory Requirement (CMR), it was decided that the



minor length increase does not warrant maintaining these items as MR. One example is the increase in fires reported by cell phone, which could negate the need for mandatory installation of automatic fire detection.

For items that were retained in stringency at CMR, the length increase was not expected to have a material impact on risk for these items, however that could be confirmed via engineering analysis as required by Clause 4.3.1.

For items that were increased in stringency from “-” (“dash” i.e. no requirement) to CMR, it was decided that the length increase could have an impact on risks for these items, to be confirmed through the engineering analysis required by Clause 4.3.1.

## 2.7. Annex N: Autonomous Vehicles

In light of the increasing use of semi-autonomous vehicles on road networks globally and the presumption that autonomous vehicles may soon also become a reality, the current edition of the Standard introduced an Annex N providing background information on autonomous vehicles.

For the next edition, this Annex was revised to account for recent developments in the area.

Table N.2 was revised to update the SAE autonomous vehicles (AV) definitions to the latest used in SAE J3016, “Taxonomy and Definitions for Terms Related to Automated Driving Systems for On-Road Motor Vehicles” **Fehler! Verweisquelle konnte nicht gefunden werden..**

Terminology used in describing AV systems was updated. For example, since publication of the current edition of the Standard, the term V2X (vehicle-to-everything) has entered usage as a generic term to describe wireless communications between connected vehicles and other similar vehicles and infrastructure. V2X encompasses V2V (vehicle-to-vehicle), V2I (vehicle-to-infrastructure), and V2N (vehicle-to-network).

Other tests were revised to account for the current regulatory environment for AVs. For example, within the United States some local, state and federal agencies have authorized designated trial testing grounds for demonstration and development of AV technology for automobiles, buses and heavy goods vehicles (HGV).

The description of platooning in Section N.5 was updated to highlight new developments. Platooning is the synchronized movement of multiple AVs with minimal separation distances, such that the vehicles are separated by much smaller distances than is usual with driver-operated vehicles. Platooning of HGVs is attractive to the trucking and freight industry. However, its application within facilities addressed by NFPA 502 has potential implications for, among other things, the range of fire emergencies, design fire size, emergency response time and fire protection features. This places additional emphasis on the engineering analysis requirements in Section 4.3. Particular emphasis should be given to the type of facility, since platooning could have significant impacts previously not considered for bridges and limited-access highways.

## 3. SUMMARY AND CONCLUSION

The updates to the NFPA 502 Standard were extensive and many hours of time were spent considering and debating the resulting changes. The Standard is improved as a result.

There is always room for improvement. This is one of the reasons that the NFPA process updates the Standard every three years. End users are encouraged to submit recommended

changes to the NFPA website during the open comment period. These comments should be concise, measurable, and enforceable.

At the time of publication, the information contained herein represents the views and opinions of the authors and is not the official opinion of NFPA. The official stance of NFPA will be published in the third quarter of this year.

#### 4. REFERENCES

- [1] “NFPA Standards Development Process”, NFPA, 2021
- [2] Tentative Interim Amendment (TIA 20-1 SC 21-8-36 / TIA Log #1561) Annex D NFPA 502 2020 Edition. NFPA, 2021.
- [3] Bechtel - Parsons Brinckerhoff, “Memorial Tunnel Fire Ventilation Comprehensive Test Report Volume 1.” Massachusetts Highway Department, 1995.
- [4] W. D. Kennedy, “Critical Velocity Past, Present and Future,” in Independent Technical Conferences - Smoke and Critical Velocity in Tunnels, 1997, pp. 58–67.
- [5] “Standard Specification for Transportation Tunnel Structural Components and Passive Fire Protection Systems,” ASTM E3134-2020, ASTM, January, 2020
- [6] “Taxonomy and Definitions for Terms Related to Driving Automation Systems for On-Road Motor Vehicles,” SAE J3016, 2021
- [7] NFPA 502, “Standard for Road Tunnels, Bridges, and Other Limited Access Highways, 2020“, 1 Batterymarch Park, Quincy, MA USA.



# ON SMOKE STRATIFICATION IN A 1-D TUNNEL VENTILATION MODEL

Ingo Riess,  
Riess Ingenieur-GmbH, CH

## ABSTRACT

Tunnel ventilation design and risk analysis rely on modelling smoke propagation. I often read that 3-D numerical models are required, commonly Fire Dynamic Simulator in combination with the egress model EVAC. But these simulations are costly. Design decisions are made following one simulation scenario with the design fire in a single location and with steady-state boundary conditions.

1-D models cannot represent the nature of the flow? This is where I disagree. The paper includes references to analytical and empirical models, as the underlying equations have been published elsewhere. Here, we concentrate on a simple model to represent smoke stratification as a function of the local flow velocity and smoke temperature. As a result, we have a 1-D numerical model that gives a plausible representation of tunnel aerodynamics, thermodynamics of the fire, moving and stopping vehicles, smoke propagation, stratification, and egress.

Such a model must be validated against data from tunnel fires, fire tests and/or 3-D CFD simulations. Once validated, the computation of a fire scenario only takes a few seconds. This allows us to run multiple scenarios with a variation of boundary conditions for better system understanding and consequently for better design decisions.

*Keywords: tunnel ventilation, simulation, fire, smoke, back-layering, stratification.*

## 1. INTRODUCTION

About 20 years ago, there was a significant change in tunnel ventilation design. The focus shifted from normal operation to smoke control. And a new ventilation concept was born: smoke control by means of local smoke extraction with remote controlled dampers and feedback controlled longitudinal airflow in the tunnel. Tunnel ventilation concepts became more complex and more dynamic.

Two further developments had an impact on tunnel ventilation design as we know it today: the advance of CFD models with increasing computational power available to the designer and the development of risk analysis tools that provide black-box answers to any design variation. It appears that any design decision can be made based on CFD simulation and risk analysis.

However, this neglects the dynamic processes in a real fire scenario. CFD simulations usually start with the initial condition of standing traffic. Ventilation operation is pre-defined, thereby neglecting the dynamics of the ventilation control system. To understand the dynamics of a fire scenario, 1-D models still have their place.

There are two weaknesses in 1-D tunnel ventilation models: Effects that are caused by 3-D flow phenomena must be included by sub-models – including smoke stratification and smoke back-layering. And every physical effect that is relevant for the flow regime must be included explicitly, for example the throttling effect or the inertia of ventilation control.

## 2. PREVIOUS WORK

The complete description of the flow model goes beyond the scope of this paper. The underlying equations have been published before. The equations for the longitudinal airflow in the tunnel

are the core of the model: Friction, pressure force of moving and standing vehicles against the longitudinal airflow, local losses at the portals, stack effect due to longitudinal gradient and the temperature distribution. These equations are given in [1] for longitudinal ventilation and in [2] for combined ventilation systems. Later, the model has been extended to include a transport equation for smoke concentration and a deterministic egress model [3].

A few years ago, the model SPITFIRE was re-written, simplified and extended. Heat radiation is no longer modelled explicitly but included in the heat transfer coefficient. The model for the in-tunnel temperature now follows the model described in Austrian design guideline RVS 09.02.32. The heat capacity of the tunnel wall was removed, as this caused problems with long simulation times. Long simulation times (>20 min) may be required for egress simulations in tunnels with a long distance between egress doors. For short simulation times, there are no significant differences between the previous temperature model and the simplified one.

The most notable inclusion in this model is the propagation of hot smoke under the tunnel ceiling. The model can predict back-layering of smoke with the density driven smoke propagation superimposed to the 1-D analysis [1]. Smoke propagation is driven by density differences between the hot smoke and the cooler tunnel air.

The relation between the smoke temperature and the smoke front velocity has been derived from buoyancy driven flow problems, such as the lock-exchange experiment, see Figure 1 [4]. The light fluid intrusion front into the heavy fluid represents a model for the smoke front in a tunnel fire.

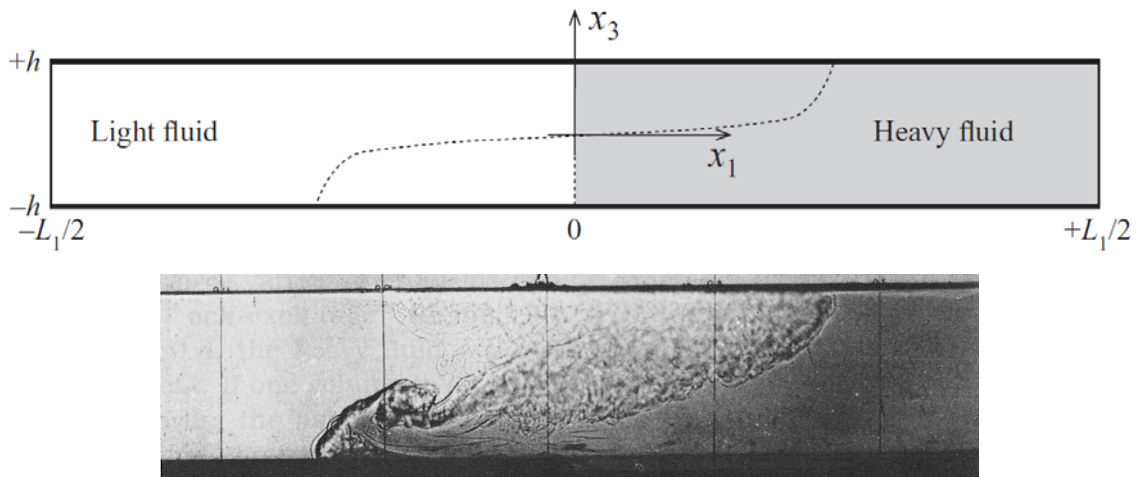


Figure 1: Definition and shadowgraph image of the lock-exchange experiment [4]

The velocity of the hot smoke front intruding into the colder tunnel air can be expressed as

$$u_{smoke} = k \cdot \sqrt{g H \frac{T_{smoke} - T_0}{2 T_{smoke}}}$$

with the velocity of the smoke front  $u_{smoke}$ , the gravitational acceleration  $g$ , the height of the tunnel profile  $H$ , the tunnel air temperature  $T_0$  and the smoke temperature  $T_{smoke}$  (the average smoke temperature between the fire and the smoke front). This is a simple model for the gravity driven flow. It does not include the height of the smoke layer. An empirical parameter  $k = 0.62$  is defined to match the smoke front velocity to experimental data for the back-layering length and to predict critical velocity.  $k$  is expected to depend on the shape of the cross-section [4]. It applies to the geometry corresponding to the experiments. The calculation of the smoke front velocity must be combined with a transport equation for heat propagating with the smoke (and

heat conduction to the tunnel wall as described above). The model assumes stable temperature stratification. Any drastic disturbance, such as jet fan operation in the smoke, will limit the extent of gravity driven smoke propagation. Temperature stratification may still be present in scenarios where smoke stratification is no longer visible [5].

SPITFIRE includes a variation of air density as a function of temperature. This feature captures the increased flow velocity downstream of a large fire and the reduced thrust of jet fans operating in hot smoke. The model is still incompressible, as pressure variations do not affect air density. Jet fan operation in a fire scenario may be pre-defined or automatically controlled using a PI-controller. The parameters of the PI-controller are defined automatically using the procedure described in the ASFINAG design guideline [6]. The parameters can then be optimized by the user.

The airflow resistance of the tunnel fire in longitudinal ventilation is captured using the equation proposed in [7]. The more conservative approach described in [8] and [9] has not yet been adopted, as the validation of these findings is still work in progress.

### 3. STRATIFICATION MODEL

The application of the combined model for 1-D smoke propagation and egress may lead to non-plausible results when stratification is not included. People that are in the smoke affected part of the tunnel would be exposed to the average concentration in the cross-section. Applying such a model to a longitudinal ventilation system leads to the conclusion that the best ventilation strategy is to run the system at maximum capacity to reduce exposure by dilution of smoke. As we know, the recommended approach is to maintain flow direction and to limit the airflow velocity between 1 to 1.5 m/s to maintain smoke stratification. For a more plausible egress evaluation, stratification is included in SPITFIRE.

A simple model for the stability of smoke stratification is given by Newman [10]. A measure for smoke layer stability can be defined by the local Froude number. The Froude number is a dimensionless parameter defined by the ratio of flow inertia to buoyancy forces. Increased flow inertia causes flow disturbances and de-stratification. Increased buoyancy leads to more stable temperature stratification. Here, the Froude number is defined by

$$Fr(x) = \frac{u_x}{\sqrt{g H \Delta T / T_{ave}}}$$

with the local Froude number  $Fr(x)$ , the flow velocity  $u_x$  (average in the cross-section), the gravitational acceleration  $g$ , the tunnel height  $H$ , the temperature difference between smoke and cold air  $\Delta T$  and the average temperature in the cross-section  $T_{ave}$ . In [10], three regions are defined:  $Fr \leq 0.9$  as a region for stable temperature stratification,  $0.9 < Fr \leq 10$  described as region of increased mixing and  $Fr > 10$ , a region without significant temperature stratification. For an assessment of smoke stratification, it is sufficient to include the limit of  $Fr = 0.9$ . The smoke layer may be disturbed even when temperature stratification is still present.

The 1-D stratification model is based on the following assumptions:

- The propagation of a smoke layer against the mean airflow (back-layering) is only possible if stratification is present.
- The stability of stratification downstream of the fire can be estimated by evaluation of the local Froude number. Stratification is destroyed for  $Fr > 0.9$ .
- When smoke is de-stratified close to the fire, stratification in further distance of the fire is very unlikely due to smaller temperature differences.

Figure 2 (right) shows smoke propagation, airflow, and egress for a fire scenario with a fast-developing 30MW fire. The x-axis shows the location in the tunnel, the y-axis shows the time. The fire is at  $x=1050\text{m}$ . The scenario assumes uni-directional traffic from left to right. Egress doors are marked in green, people movement in red lines. Smoke is shown in grey with the stratified smoke being indicated by a lighter shade. The ventilation schematic is shown above. In Figure 2 (left), the longitudinal airflow is shown left (red) and right (green) of the extraction section over the vertical time axis.

Initially, the smoke is de-stratified due to high mean flow velocity in the tunnel. The ventilation response is defined by smoke extraction beginning at  $t=3\text{min}$ . Full capacity is reached one minute later. At the same time, jet fans close to the entry portal are used to control the longitudinal airflow to  $2\text{m/s}$  resp.  $-2\text{m/s}$ .

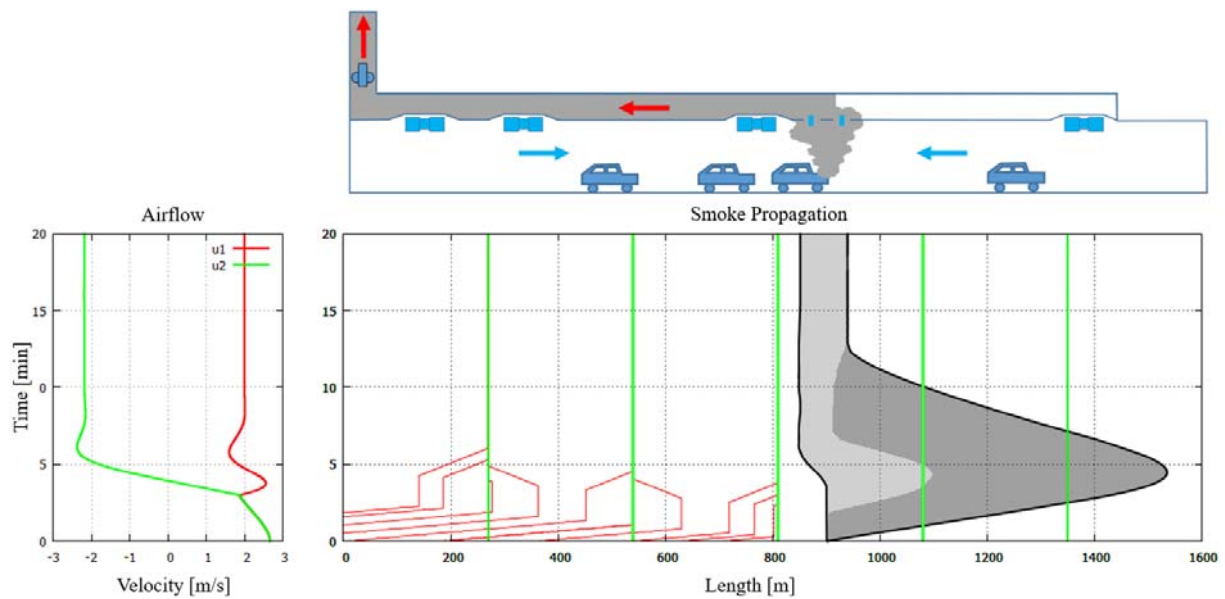


Figure 2: Smoke control – PI-control of longitudinal airflow

The graph shows that due to the initial flow velocity, smoke stratification downstream of the fire is unlikely. When the fire develops more heat and when the airflow is controlled, a section of stratified smoke is developed close to the fire. In this scenario, stratification does not influence egress, as smoke back-layering to the left is mostly avoided and tunnel users can evacuate to the nearest egress door.

## 4. VALIDATION

Model validation has been performed over the years with every available dataset from fire tests or CFD simulations. Most test cases have been derived from site acceptance fire tests. These are tests required for project approval of Austrian highway tunnels. Usually, validation is limited to parts of the model, depending on the dataset. Test heat release rates are small; and there is no moving traffic present.

### 4.1. Smoke stratification

The model for smoke stratification has not yet been validated due to lack of reliable data. The model has been adopted from literature without further empirical coefficients. And the results are plausible.

#### 4.2. Control dynamics

Control dynamics are unrelated to smoke propagation and stratification. But these models must include system properties explicitly. In this case the inertia of system reaction. Figure 3 shows a comparison of test data and a SPITFIRE simulation. The graph depicts the system response (flow velocity) to a fire alarm and start of the emergency ventilation.

The fuel pan fire was started at about 22:30:00. Only a few seconds after ignition the fire alarm was set manually to avoid damage to the tunnel structure. The controlled airflow conditions limit the maximum temperature. The test was then run continuously until the fuel was burnt completely, see Figure 4.

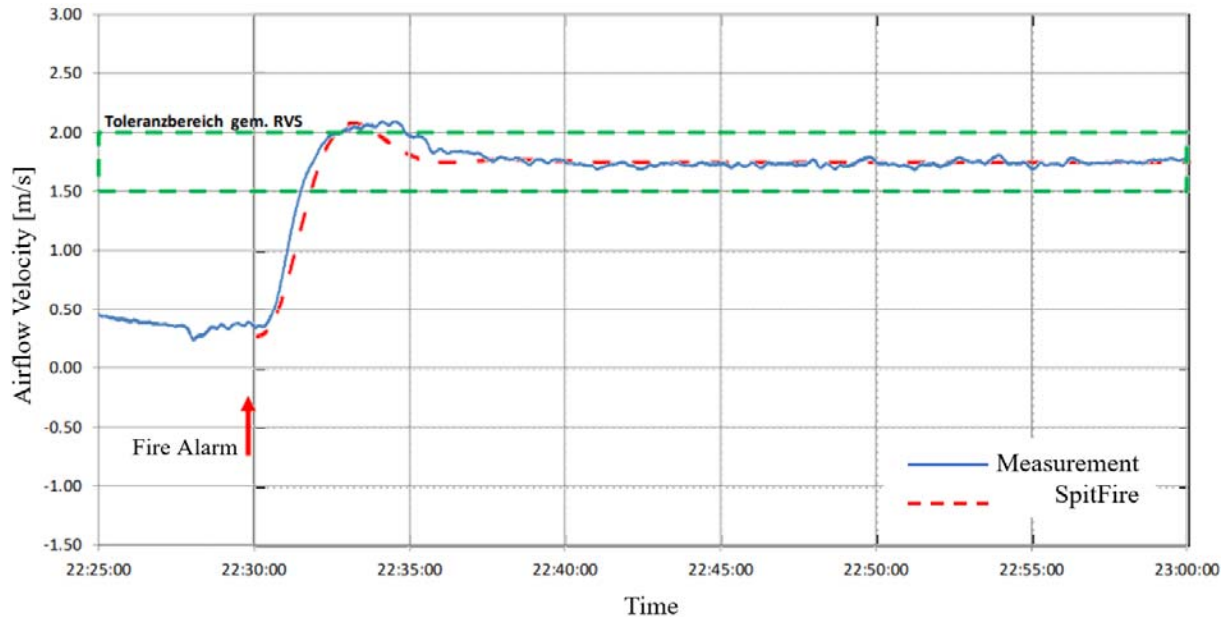


Figure 3: Flow velocity – fire test and SPITFIRE model



Figure 4: Smoke back-layering and downstream stratification in the first minutes of the test

The simulation uses the tunnel geometry data. The heat release rate is estimated from the area of the fuel pan. Deviations between measurement and numerical model may be attributed to the detailed control parameter settings. The ventilation control system was optimized in preparation of the site acceptance test. The simulation includes the calculated default parameter settings. Other potential sources of deviations may be the ramp settings in the jet fans' variable speed drives. The detailed settings were not documented in the test report.

In the fire test, back-layering is mostly controlled due to the small heat release rate. This is confirmed in the test report, stating that back-layering extended to a maximum of 15m. It was quickly driven back to the fire. The simulation shows a maximum back-layering of 2m.

#### 4.3. Critical velocity

The critical velocity is defined as the upstream airflow towards a fire that prevents the propagation of smoke back-layering beyond the source of the fire. In the past couple of years, several methods to calculate critical velocity have been published. The current consensus for practical applications appears to be the relation published in NFPA502:2017 [11].

SPITFIRE has been tested against this standard. The geometry has been assumed for the tunnel shown in Figure 4 without longitudinal gradient. Ventilation control is set up to achieve the critical velocity as calculated from NFPA. The back-layering for the quasi-steady state case is evaluated. For heat release rates increasing from 20MW to 90MW, the model shows back-layering increasing from 1.3m up to 8.6m. This is only slightly more than the hydraulic tunnel diameter or the length of a single grid cell, which is deemed acceptable. The model has been developed for the assessment of dynamic fire scenarios and not for steady-state design.

#### 4.4. Smoke back-layering

Most of the published research on smoke propagation in tunnels appears to concentrate on the critical velocity. At the 2020 conference in Graz, a paper [12] has been presented, comparing smoke back-layering in seven full size fire tests with corresponding FDS simulations and two analytical models. This paper provides an ideal collection of experimental, numerical, and analytical data to allow a validation/verification of the smoke propagation in SPITFIRE.

While the paper does not list the detailed tunnel geometry of the fire tests, the missing information can be derived from the back-layering lengths calculated using the models by Li/Ingason and Thomas. The data used in the SPITFIRE simulation is shown in Table 1. The analytical models show good agreement for all cases except Test 7, where my calculation using the model by Thomas gives a back-layering length of 338m instead of 256m as shown in Table 2 [12]. For this case, the model by Li/Ingason gives a back-layering length of 112m instead of 103m.

Table 1: Tunnel geometry

Parameter	Symbol	Value
Tunnel cross-section	A	36.0 m <sup>2</sup>
Tunnel height	H	6.15 m
Air density	$\rho_0$	1.251 kg/m <sup>3</sup>
Initial Temperature	T <sub>0</sub>	283.15 K

Table 2 describes qualitatively the deviations of the back-layering length, taking observations from fire tests as reference. A graphical representation of Table 2 is shown in Figure 5. Please note that the column for Test 7 and the model by Thomas is cut at 200m to allow an easier comparison for the cases with shorter back-layering.

Although SPITFIRE includes a very simple model for the smoke front velocity, it provides a surprisingly good agreement with backlayering observed in fire tests and in FDS simulations. The most notable deviation is visible in Test 6, where SPITFIRE underpredicts back-layering similar to the analytical models by Li/Ingason and Thomas. In the other test cases, SPITFIRE appears to underpredict smoke back-layering by 10 to 20%.



Table 2: Back-layering lengths – comparison experiment/FDS/literature [12] and SpitFire

# Test	Experiment			FDS simulation		Thomas		Li/Ingason		SPITFIRE	
	Peak HRR Q	airflow $v_0$	back-layering length	back-layering length	% from experiment	back-layering length	% from experiment	back-layering length	% from experiment	back-layering length	% from experiment
	[MW]	[m/s]	[m]	[m]	[%]	[m]	[%]	[m]	[%]	[m]	[%]
3	4.0	1.10	90	130	145	85	71	77	86	78	86
4	7.7	1.30	90	140	156	103	114	83	92	99	109
5	11.5	1.61	120	100	84	79	66	74	94	85	71
6	14.3	2.00	110	100	90	43	39	57	52	50	45
7	19.5	1.25	160	150	94	256	160	103	64	142	89
8	6.7	1.32	100	140	140	82	82	76	76	78	78
13	21.0	1.72	140	135	97	124	89	75	54	127	91

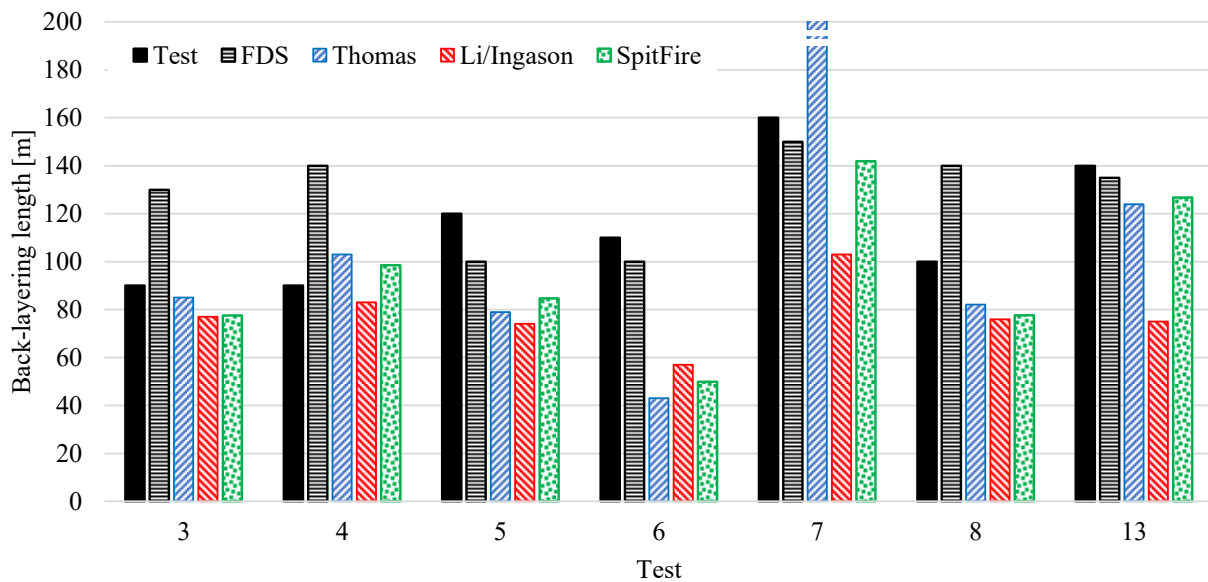


Figure 5: Back-layering lengths – comparison experiment/FDS/literature [12] and SPITFIRE

## 5. SUMMARY AND CONCLUSION

1-D models can represent airflow, smoke propagation and ventilation operation in road tunnels. In this paper – together with previously published work – a simple 1-D numerical model is described that gives a plausible representation of tunnel aerodynamics, thermodynamics of the fire, moving and stopping vehicles, automated ventilation control, smoke propagation, stratification, and egress.

The model has been validated against test cases showing specific aspects of the model, namely the dynamic system reaction in a fire scenario, smoke control towards critical velocity and smoke back-layering in scenarios with reduced longitudinal flow. The model performed reasonably well in all test cases.

The main advantage of a 1-D model against 3-D CFD lies in the short computation time. For a typical tunnel, SPITFIRE computes a fire scenario in 5 to 10 seconds. This allows a wide

variation of boundary conditions in short time and a better understanding of the dynamic behaviour of the tunnel ventilation system in a fire scenario. This may lead to better design decisions.

The main disadvantage of a 1-D model lies in the simplifications. If the model does not include a sub-model for smoke stratification, there is no stratification. If the model does not include a sub-model for the pressure loss of a fire in longitudinal flow, there is no pressure loss. We are required to observe the limitations of the model – always. And we must test the model against available data – always.

Only by regular and frequent validation, the special cases are identified where the model is not applicable in its current form. And when these cases are identified, the model can be developed for a wider range of applications – but only after further validation.

## 6. REFERENCES

- [1] Riess, I., Bettelini, M. (1999). The prediction of smoke propagation due to tunnel fires. ITC Conference Tunnel Fires and Escape from Tunnels. Lyon.
- [2] Riess, I., Bettelini, M., & Brandt, R. (2000). Sprint - a design tool for fire ventilation. 10<sup>th</sup> International Symposium on Aerodynamics and Ventilation of Vehicle Tunnels. Boston.
- [3] Riess, I., Brandt, R. (2010). ODEM - a one-dimensional egress model for risk assessment. 5<sup>th</sup> International Conference "Tunnel Safety and Ventilation". Graz.
- [4] Fanneløp, T.K. (1994). *Fluid Mechanics for Industrial Safety and Environmental Protection*. Industrial Safety Series. Elsevier.
- [5] Federal Highway Administration. (1995). *Memorial Tunnel Fire Ventilation Test Program*. Denver: Massachusetts Highway Department Central Artery/Tunnel Project.
- [6] ASFINAG. (2018). *PI-Regler in der Lüftungssteuerung*. PLaPB 800.542.1604.
- [7] Dutrieue, R., Jacques, E. (2006). Pressure loss caused by fire in a tunnel. 12<sup>th</sup> International Symposium Aerodynamics and Ventilation of Vehicle Tunnels. Portoroz.
- [8] Riess, I. (2020). *Aerodynamic Resistance of Fires in Tunnels*. Riess Ingenieur-GmbH, Zürich.
- [9] Riess, I., Weber, D., Steck, M. (2020). On the air-flow resistance of tunnel fires in longitudinal ventilation – the “Throttling Effect”. 10<sup>th</sup> International Conference Tunnel Safety and Ventilation. Graz.
- [10] Newman, J.S. (1984). Experimental evaluation of fire-induced stratification. *Combustion and Flame* 57:33–39.
- [11] NFPA (2017). *Standard for Road Tunnels, Bridges and Other Limited Access Highways*. NFPA 502. 2017 Edition.
- [12] Fruhwirt, D., Sturm, P. Bacher, M. Schwingenschlögl, H. (2020). Smoke propagation in tunnels – comparison of in-situ measurements, simulations and literature, 10<sup>th</sup> International Conference Tunnel Safety and Ventilation. Graz.

# NUMERICAL INVESTIGATION OF THE KORALM TUNNEL FIRE TESTS USING AN AUTONOMOUS MESHING APPROACH WITH ADAPTIVE MESH REFINEMENT

<sup>1</sup>Mathias Vångö, <sup>1</sup>Pietro Scienza, <sup>2</sup>Patrik Föbbleitner, <sup>3</sup>Daniel Fruhwirt

<sup>1</sup>Convergent Science GmbH, AT,  
<sup>2</sup>FVT mbH, AT, <sup>3</sup>Graz University of Technology, AT

## ABSTRACT

Understanding smoke propagation and temperature stratification in tunnels during fire incidents is crucial in order to ensure the road user's safety. To accurately predict these phenomena, numerical tools such as Computational Fluid Dynamics (CFD) are invaluable.

We present in this work a CFD model, which features an improved workflow and turnaround time by utilizing an autonomous mesh generation technology. A high-quality mesh is generated on the fly and enables the use of adaptive mesh refinement (AMR) based on local flow gradients.

To assess the proposed method, simulation results are compared with measurements from full-scale fire tests performed by the Institute of Thermodynamics and Sustainable Propulsion Systems (ITnA) at Graz University of Technology in the Koralm tunnel (Austria). Namely, temperature readings from several sensors were used as validation data, along with the observed maximum backlayering length.

*Keywords: CFD, autonomous mesh, adaptive mesh refinement, tunnel smoke propagation*

## 1. INTRODUCTION

Safety and risk-scenario assessments are key part of the design and certification for infrastructures such as road and railway tunnels. Computational Fluid Dynamics (CFD) could provide a suitable solution, avoiding the necessity to build physical models and allowing to test several different scenarios, even considering full scale conditions. Additionally, it allows to take a closer look to complex physical phenomena which are difficult to study otherwise.

To that end, Fruhwirt et al. [1] used numerical CFD simulations to assess fire and smoke propagation in the Austrian Koralm tunnel, validating the model against experimental data. Furthermore, Truchot et al. [2] simulated the venting of toxic gases from a truck loaded with batteries, and consequently the implications of the dangerous gas release and combustion inside a tunnel. Temperature profiles and smoke distribution were among the analyzed quantities.

Not only fire occurrences, smoke propagation and other hazardous conditions, but also mitigation scenarios are often addressed and modeled through CFD. On this line, Riess et al. [3] simulated the water mist spray from a fire extinguishing system on a burning area in different flow regimes.

Forced ventilation in tunnels is also a key topic of interest and CFD has been proven as a valuable tool to address such scenarios, being able to model turbulence, heat transfer and buoyancy [4]. This also applies in scenarios where the ventilation system has to handle smoke and fire occurrences. Sturm et al. [5] provide a precise and general insight of the ventilation control in case of a fire in a tunnel, while Khattri et al. [6] looked at the longitudinal ventilation, focusing on the oxygen content and its impact on the fire dynamics.

In this work, we introduce a numerical model intended to address these challenges, while keeping simplifications to the geometry to a minimum and overall improving the workflow. More specifically, we present a comparison between in-situ measurements from the Koralm tunnel presented by Fruhwirt et al. [1] and numerical results obtained by our model. This comparison serves as validation of the model for the complex near-fire region, in the case of a longitudinally well-ventilated fire situation.

## 2. COMPUTATIONAL MODEL

In this work, we used CONVERGE [7] version 3.0.19 for all the simulations. A fully compressible URANS (Unsteady Reynolds-Averaged Navier-Stokes) methodology was employed using the well-known two-equation standard k- $\epsilon$  model, along with the real gas Redlich-Kwong equation of state. A second-order central difference spatial discretization scheme was employed, and a modified SIMPLE (Semi-Implicit Method for Pressure-Linked Equations) algorithm was used to solve the pressure velocity coupling. Although CONVERGE have not previously been used for large scale fire simulations, it has been extensively used and validated in other application areas, such as internal combustion engines, gas turbines as well as pumps and compressors [8, 9, 10]. Detailed descriptions of the governing equations and numerics are given in Richards et al. [11].

### 2.1. Physical models

Although CONVERGE possesses capabilities to model combustion by directly solving detailed chemical reaction mechanisms, we employed in this work the Eddy Dissipation combustion model (EDM) [12], which has been found reasonable considering computational cost and accuracy tradeoff.

Radiation was accounted for by solving the radiative transfer equation (RTE) using the Discrete Ordinates Method (DOM). Typically for large-scale fire simulations the flame temperatures are not properly resolved due to prohibitive computational expense, hence we applied the Optically-Thick, Specified Radiative Fraction model [13] to scale the radiative emission at the flame based on a pre-determined, user-specified radiative fraction.

In order to accurately model the wall heat transfer, we incorporated the solids into our model through the Conjugate Heat Transfer (CHT) method. Two CHT models were used, 3D-CHT and 1D-CHT, where the former includes the solid walls in the computational domain, and the latter uses virtual one-dimensional layers normal to the wall boundary.

### 2.2. Mesh

CONVERGE uses a modified Cartesian cut-cell meshing method which allows to retain the real geometry details without introducing any modification to the boundary shape. In this framework, the mesh generation process is fully automated and the grid is regenerated every time step, thus allowing moving and deforming boundaries. Furthermore, in traditional CFD, *a priori* knowledge of local flow features is often required to achieve satisfactory results, which is especially challenging in complex scenarios. As the mesh is continuously updated in CONVERGE, the mesh is allowed to be locally refined during runtime using the Adaptive Mesh Refinement (AMR) approach. More precisely, AMR evaluates the magnitude of the sub-grid field  $\phi'$  of user-specified variables (e.g., temperature and velocity) to assess if mesh refinement should be applied, satisfying user defined criteria.  $\phi'$  is defined as  $\phi' = \phi - \bar{\phi}$ , where  $\phi$  and  $\bar{\phi}$  are the actual and resolved field respectively.

The sub-grid field is approximated as the second order derivative

$$\phi' = -\alpha_{[k]} \frac{\partial^2 \bar{\phi}}{\partial x_k \partial x_k}, \quad (1)$$

arising from an infinite series expression of  $\phi'$ , where,  $\alpha_k$  is  $(\Delta x_k)^2/24$  for rectangular shaped cell. This methodology allows the mesh to be refined only when and where necessary, making optimal use of the cell count.

### 3. FIRE TEST DESCRIPTION

As means for validation of our approach we use the full-scale fire tests performed by ITnA in the Koralm tunnel, Austria. The aim of these tests was primarily to study smoke propagation to obtain information on keeping escape routes free of smoke. Hence, temperature measurements were taken at several locations downstream of the fire location, as well as the upstream smoke propagation (backlayering) length was measured.

In these tests, fire pools were used as fire source, placed in a protective fire box within the tunnel as shown in Fig. 1. Fourteen fire tests were performed with varying test duration and fire intensities. In this work, we focused on one particular test with eight pool fires giving approximately 18 MW sustained intensity, with a burn duration of eight minutes. For a detailed description of the fire tests see Sturm et al. [14].

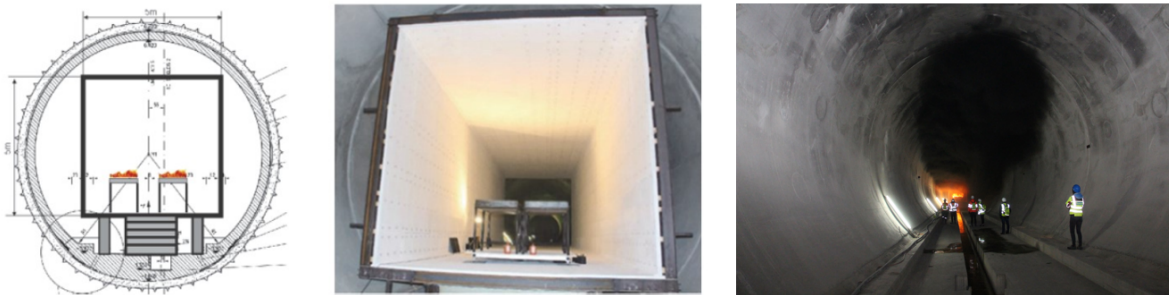


Figure 1: Visualization of the test pool fire setup and the protective box.

During the tests, many temperature measurements were taken. In this work, we used the temperature measurements obtained from the sensor arrays MP5 and MP6, as illustrated in Fig. 2, to evaluate the simulated temperature stratification. Furthermore, a comparison of the concrete temperature was carried out with sensor S7.1 and S7.2, as well as with the maximum observed backlayering length from the test.

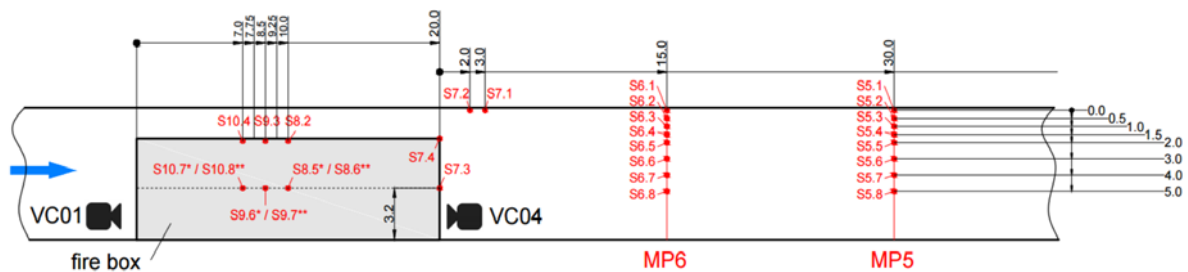


Figure 2: Temperature sensors locations within the test configuration.

## 4. SIMULATION SETUP

In order to evaluate our approach, we aimed to replicate the test case scenario described above within the numerical framework.

### 4.1. Simulation domain and mesh settings

The domain used for the simulations is shown in Fig. 3. It can be noted that little to no simplifications has been made to the geometry, as it includes the correct cross-section profile of the tunnel, the detailed fire box, as well as the solid concrete tunnel wall.

Determining the correct mesh size is not trivial in CFD, but the characteristic fire diameter

$$D^* = \left( \frac{\dot{Q}}{\rho c_p T \sqrt{g}} \right)^{\frac{2}{5}}, \quad (2)$$

is often used in this context as a comparative length scale to define how well the flow is resolved [10]. Here,  $\dot{Q}$ ,  $\rho$ ,  $c_p$ ,  $T$  and  $g$  refer to fire heat release rate, density, specific heat, temperature and gravity respectively. In this work, we used a relatively coarse mesh size of  $\Delta x = D^*/5$  towards the ends of the tunnel, whereas the centre part of the tunnel, close to the fire, was refined to  $\Delta x = D^*/10$ . The grid was further refined in the direct vicinity of the fire source with the size  $\Delta x = D^*/40$  using AMR based on temperature.

Consequently, the coarsest element size was 0.6 m, while the fire zone was refined with AMR using 0.075 m cells. Furthermore, in order to capture the strong temperature gradient close to the wall, additional fixed local refinement at the tunnel wall was applied via a boundary fitted grid, extruded from the surface with the first layer height being 0.01 m, an expansion ratio of 1.5 and a total of seven layers. The total cell count ranged from approximately 800 000 to 950 000 during the simulation due to AMR. The mesh used in the center part of the tunnel is visualized in Fig. 4.

The chosen mesh element size was rather small according to similar studies, as achieving mesh independence is in general challenging for large scale fire simulations, with temperature over-prediction being common for too coarse meshes [15]. We did however compare with a near-fire mesh of  $\Delta x = D^*/30$  and  $\Delta x = D^*/60$ , but concluded that the chosen mesh resolution was sufficient for this study.

### 4.2. Boundary conditions

As boundary condition for the tunnel supply air velocity, we used the temporally varying profile measured in the fire test, ranging between 1.2 and 2.5 m/s. The fire size was imposed based on the measured fuel consumption rate of approximately 0.4 kg/s during the sustained burn phase. More specifically, the temporally noisy measured fuel consumption rate was approximated as a fitted polynomial, as shown in Fig. 5, and imposed as a fuel inflow rate at the fire pool patches.

In the experiment, a mixture of diesel and gasoline was used as fuel, whereas in our simulation we used pure isooctane with a specified lower heating value (LHV) of 42.2 MJ/kg based on the fuel mixture. Furthermore, a specified radiative fraction of 0.4 was used together with yield factors 0.1 and 0.001 kg/kg<sub>fuel</sub> for CO and soot respectively.

Due to the relatively thin layer of protective material in the fire box, the fire box walls were modelled using 1D-CHT. Material properties of Promatect-T were used and the wall thickness was divided into 20 evenly-spaced layers.

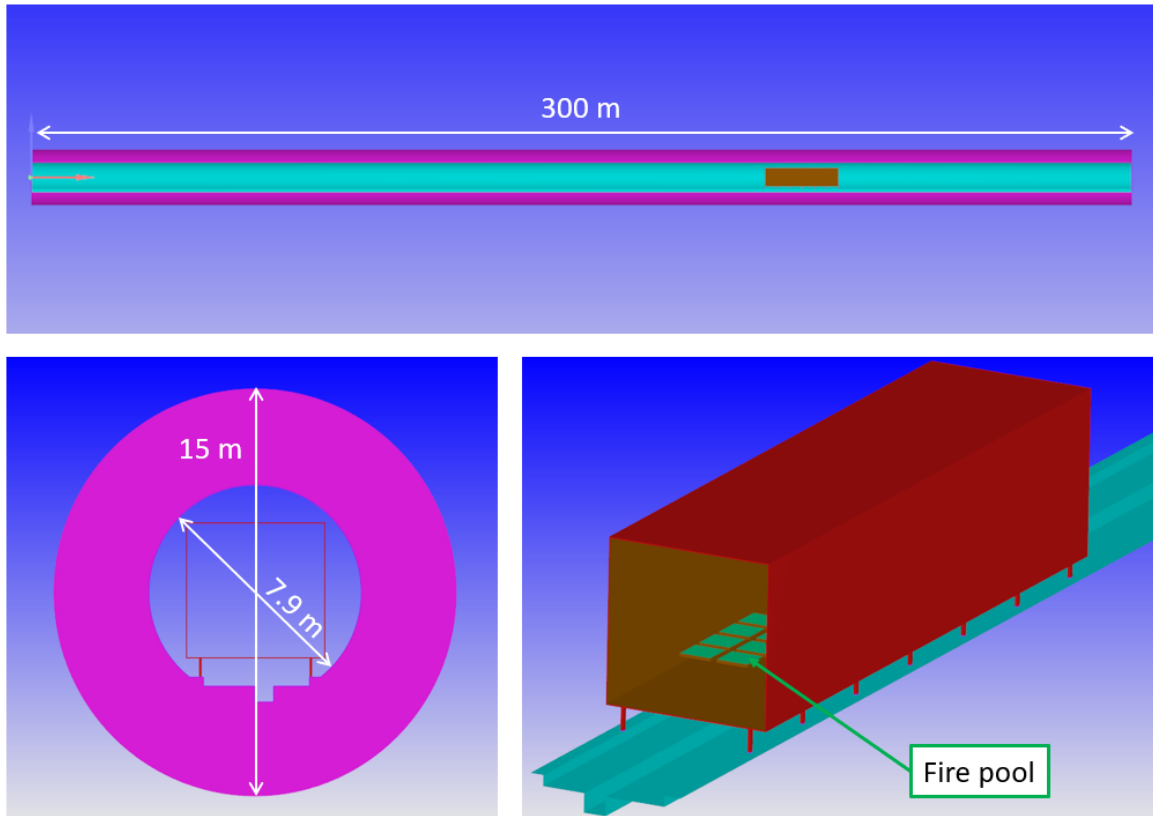


Figure 3: Simulation domain visualization. The top image is showing a clipped view at the centerline along the x-axis, the bottom left the tunnel cross section and the bottom right a zoom of the fire box.

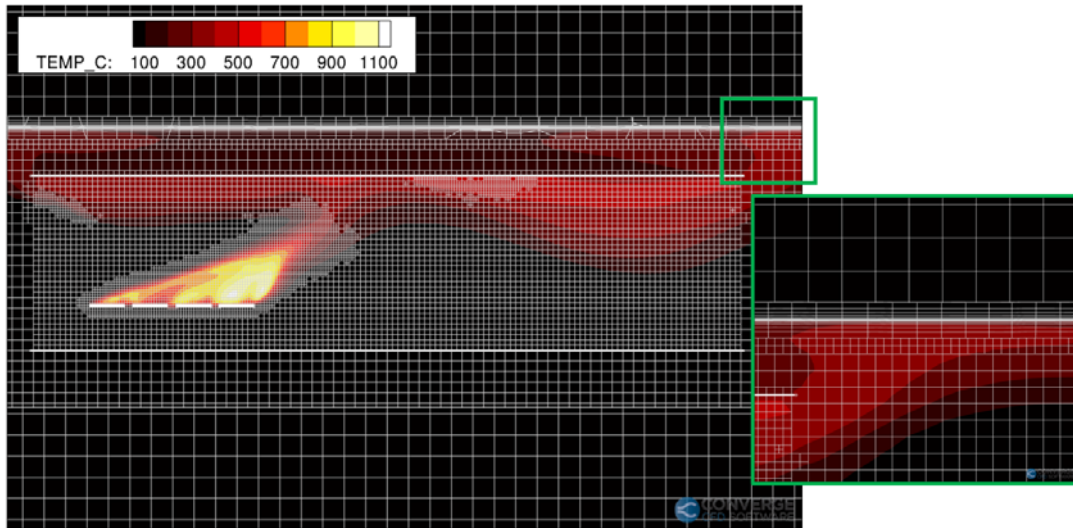


Figure 4: Visualization of the computational mesh in the center part of the tunnel.

## 5. RESULTS

In this section we present our findings from the previously described simulations. Figures 6 and 7 show the temperature stratification at various times at temperature sensor arrays S5 and

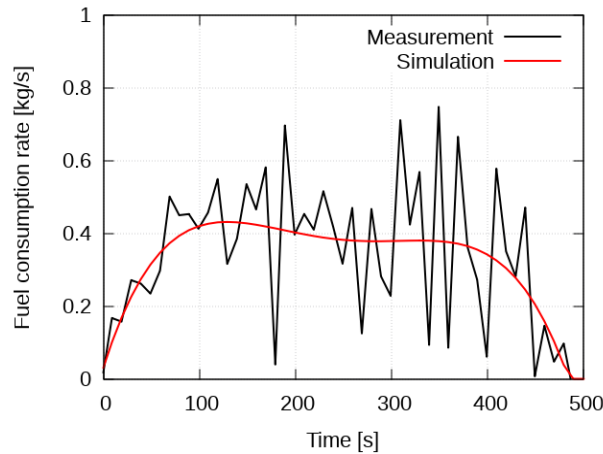


Figure 5: Comparison of the fuel consumption rate used in the simulation and the measured one from the fire test.

S6 respectively, for the measured values from the fire test (left) and simulation (right). In general, the trends and temperature magnitudes are well captured, especially in the upper part of the tunnel where hot smoke is present. This suggests that the downstream smoke propagation was adequately predicted and that the chosen methodology for the fire dynamics and radiative behaviour are well represented. The temperature gradient close to the upper wall is also adequately captured by the simulation when compared to the measurement. This indicates that the near-wall mesh strategy allows to satisfactorily capture the wall heat transfer. It should be noted that the temperature gradient at the upper wall is large and the temperature obtained in that region is highly sensitive to the exact sensor location, which is difficult to perfectly replicate in the simulation.

Figure 8 visualizes the concrete surface temperature at sensor location S7.1 and S7.2, which further indicate that the wall heat transfer trend is reasonably captured, although some underprediction of the temperature can be observed. Similarly here, the results experience high sensitivity to the sensor location, so it's difficult to precisely determine the cause of the observed surface temperature differences. To fully understand that behavior, more specific tests would need to be conducted which was outside the scope of this work, as the primary focus was the smoke propagation.

Furthermore, the simulated backlayering length was compared with the carried out measurements. As no time history of the backlayering length was available from the fire tests, the maximum observed backlayering are compared and presented in Table 1. Also here a satisfactory agreement can be observed.

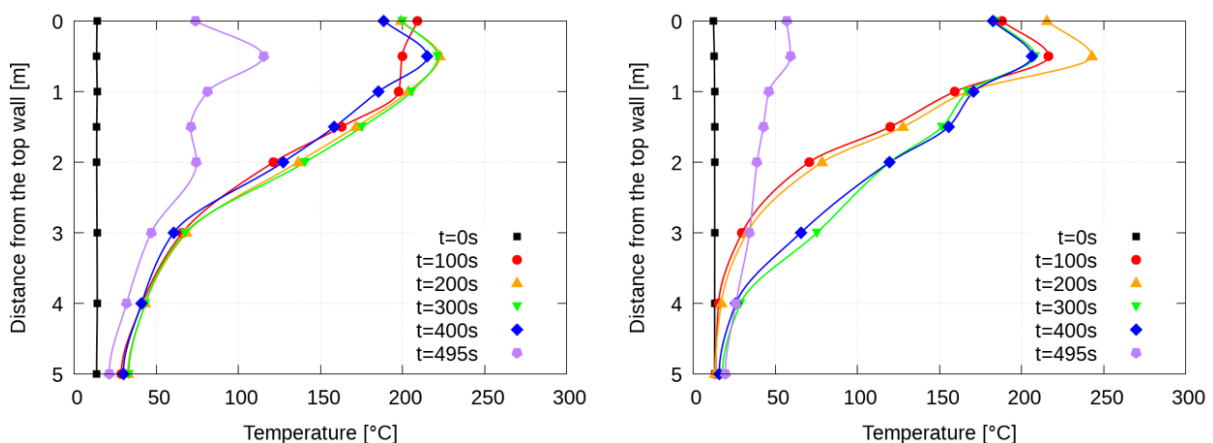


Figure 6: Vertical temperature profiles at sensor location S5 from measurement (left) and simulation (right) at various times.



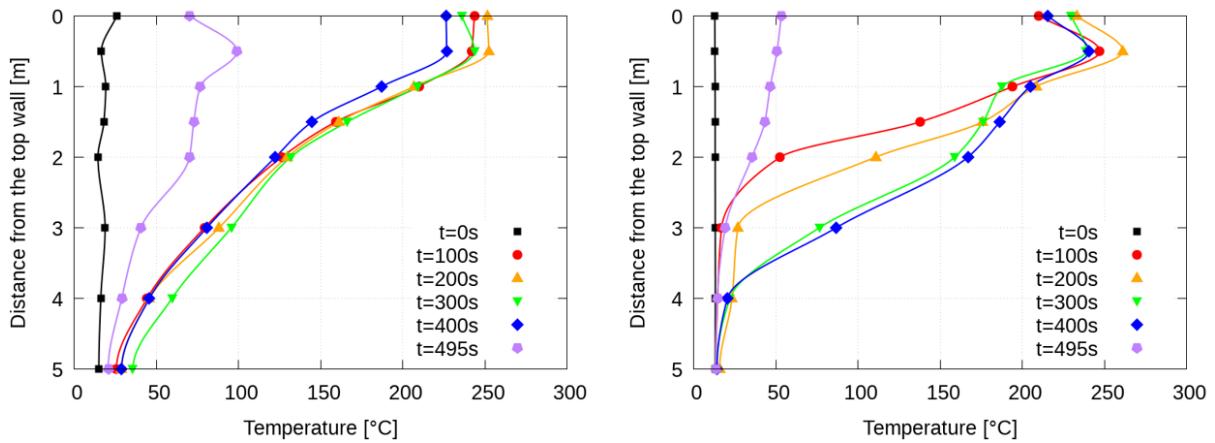


Figure 7: Vertical temperature profiles at sensor location S6 from measurement (left) and simulation (right) at various times.

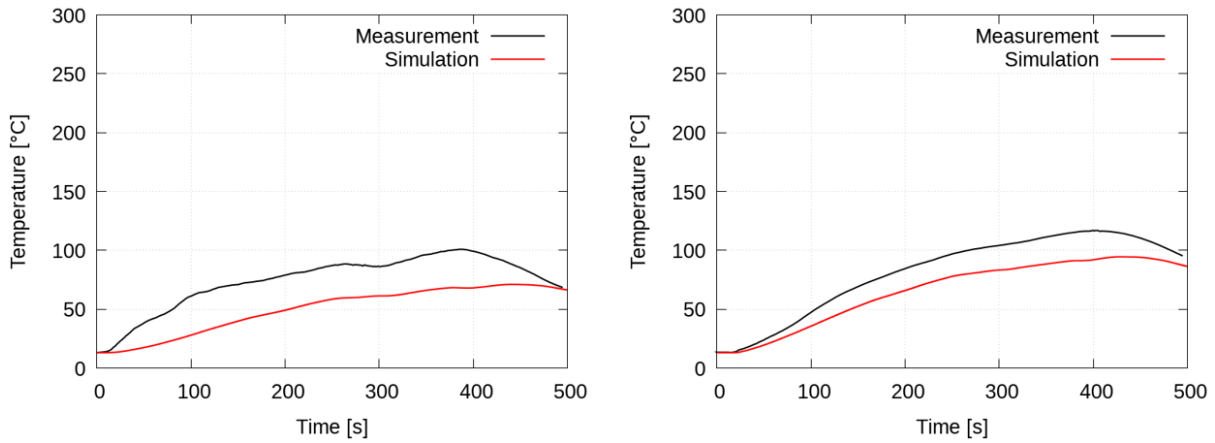


Figure 8: Comparison of the concrete temperature at sensor S7.1 (left) and S7.2 (right) between measurement and simulation.

Table 1: Comparison of the maximum observed backlayering length between the simulation and measurement.

	Measurement	Simulation
<b>Backlayering length</b>	160 m	155 m

## 6. CONCLUSION

In this work, we have presented a numerical model using a truly autonomous mesh approach to simulate large scale fire scenarios, intended to accurately predict smoke propagation during fire incidents to ensure smoke free evacuation paths. The chosen numerical strategy for important physical phenomena was presented, along with a discussion of necessary simplifications and special modelling requirements for this particular application.

The model was validated against real fire tests carried out by ITnA in the Austrian Koralm tunnel, where several measurements for both downstream and upstream smoke propagation were taken. Namely, downstream temperature stratification and concrete surface temperatures were directly compared with measurements from temperature sensors, as well as the maximum backlayering length was compared with observations from the fire test.

Generally, the simulation showed good agreement with the measured data. The downstream temperature stratification was well represented, showing very reasonable magnitudes with the exception of a slight underprediction for the lower part of the tunnel. We did also see some

underprediction of the concrete surface temperature, although it should be noted that the exact sensor location was of great importance due to the strong temperature gradient observed in the vicinity of the wall. Additionally, the observed backlayering length was in good agreement, further highlighting the accurate capturing of the smoke propagation, suggesting that the chosen numerical approach could be a relevant tool in fire safety scenarios.

## 7. REFERENCES

1. Fruhwirt, D., Sturm, P., Bacher, M., & Schwingenschlögl, H. (2020). Smoke propagation in tunnels-comparison of in-situ measurements, simulation and literature. In *10th International Conference Tunnel Safety and Ventilation*.
2. Truchot, B., Leroy, G., & Marlair, G. (2016). CFD and engineering method coupling for evaluating the fire relative to battery transportation. In *8. International Conference on Tunnel Safety and Ventilation* (pp. 132-140).
3. Riess, I., & Steck, M. (2018). On the aerodynamics of water mist from a ventilation designer's perspective. In *International Conference Tunnel Safety and Ventilation, Graz*.
4. Fleming, & C., Rhodes, N. (2018). A validation of the fire dynamics simulator for smoke dispersion from metro stations. In *International Conference Tunnel Safety and Ventilation, Graz*.
5. Sturm, P., Beyer, M., & Rafiei, M. (2017). On the problem of ventilation control in case of a tunnel fire event. *Case Studies in Fire Safety*, 7, 36-43.
6. Khattri, S. K., Log, T., & Kraaijeveld, A. (2019). Tunnel fire dynamics as a function of longitudinal ventilation air oxygen content. *Sustainability*, 11(1), 203.
7. Richards, K. J., Senecal, P. K., and Pomraning, E., CONVERGE 3.0, Convergent Science, Madison, WI (2022)
8. Senecal, P. K., Pomraning, E., Richards, K. J., & Som, S. (2012). Grid-convergent spray models for internal combustion engine CFD simulations. In *Internal Combustion Engine Division Fall Technical Conference* (Vol. 55096, pp. 697-710). American Society of Mechanical Engineers.
9. Li, Y., Rowinski, D. H., Bansal, K., & Rudra Reddy, K. (2018). CFD modeling and performance evaluation of a centrifugal fan using a cut-cell method with automatic mesh generation and adaptive mesh refinement.
10. Omote, H., Hirota, K., Hotta, T., Kumar, G., & Drennan, S.A (2015). Combustion and Conjugate Heat Transfer CFD Simulations to Support Combustor Design. In *International Gas Turbines Conference*, Tokyo, Japan.
11. Richards, K. J., Senecal, P. K., and Pomraning, E., CONVERGE 3.0 Manual, Convergent Science, Madison, WI (2022)
12. Magnussen, B. F., & Hjertager, B. H. (1977). On mathematical modeling of turbulent combustion with special emphasis on soot formation and combustion. In *Symposium (international) on Combustion* (Vol. 16, No. 1, pp. 719-729). Elsevier.
13. McGrattan, K., Hostikka, S., McDermott, R., Floyd, J., Weinschenk, C., & Overholt, K. (2013). Fire dynamics simulator user's guide. *NIST special publication*, 1019(6), 1-339.
14. Sturm, P., Rodler, J., Thaller, T., Fruhwirt, D., & Föbleitner, P. (2019). Hot smoke tests for smoke propagation investigations in long rail tunnels. *Fire safety journal*, 105, 196-203.
15. Vigne, G., & Jonsson, J. (2009). Experimental research-large scale tunnel fire tests and the use of CFD modelling to predict thermal behaviour. In *Advanced Research Workshop on Fire Protection and Life Safety in Buildings and Transportation Systems*, Santander, Spain (pp. 255-272).

## CFD VALIDATION FOR TUNNEL SMOKE CONTROL DESIGN

<sup>1</sup>Michael Beyer, <sup>1,2</sup>Conrad Stacey

<sup>1</sup>Stacey Agnew Pty Ltd, Australia

<sup>2</sup>SAMJ LLC, USA

### ABSTRACT

With no reliable formula for determining minimum required upstream velocity to control smoke in tunnels, attention has turned to CFD for answers. However, CFD must be used with caution, as it produces many different answers, depending on the quality of the algorithms and coding, and how parameters and numerical models are selected. It is really only valid when the whole system of analysis (analyst + software + parameter/model choices) has been validated against known and relevant real fire scenarios. If the analyst is new, the software is different, solution parameters change, or there is no real case for comparison, perhaps it can no longer be relied on. A validation of a system of analysis against the best available tunnel fire data (Memorial Tunnel tests) is presented, with discussion on how different modelling options and software can affect the outcome, leading to conclusions as to how to model smoke control in tunnels that are not so different (in the physics and flow regimes present) to the Memorial Tunnel tests. How far the techniques might be stretched to different geometries or fire scenarios is also discussed briefly.

*Keywords: CFD, tunnel fire, CFD validation, smoke propagation*

### 1. INTRODUCTION

Smoke control during a tunnel fire is an ongoing discussion, with different strategies/philosophies established in different countries by their national standards or experiences. A common approach is the ‘critical velocity philosophy’, where upstream propagation of a hot smoke layer is just prevented. Avoiding any onset of backlayering with sufficiently high upstream velocities causes higher smoke/air mixing, and even higher downstream velocities, due to expansion of the air/smoke mixture caused by the heat addition. Besides the smoke mixing effect, a high upstream air velocity is also likely to cause faster fire growth, a higher peak heat release rate, and greater fire spread, as concluded in [1].

In Europe, a low velocity philosophy is usually recommended, to facilitate evacuation. A lower upstream tunnel air velocity might allow some backlayering of smoke (depending on the realised heat release rate) but reduces the risk of destroying any possible smoke stratification and leads to a lower smoke propagation speed downstream of the fire. Lower velocities are more likely to support tenable escape conditions downstream of a fire.

Further discussion on different smoke control philosophies can be found in [2] and [3]. NFPA 502, the national standard in the US, which historically proposed a ‘critical velocity’ approach, will now change its terminology from preventing backlayering to controlling backlayering (with the 2023 edition). That change allows for some backlayering of hot smoke, especially within the zone close to a fire that can already be considered as untenable due to radiation or other risks. It will then be more aligned with the European approach. The backlayering distance which may be judged as acceptable might depend on the available clearance and space/room above tunnel users and responders for hot smoke, and on the length of the zone already made untenable by the fire.

There is currently no sufficiently accurate or reliable formula for critical velocity, see [4], let alone the “confinement” velocity required to “control” smoke in tunnels by targeting a backlayering length for a specific design fire scenario. Lacking such knowledge, attention has turned to computational fluid dynamics (CFD) for answers. However, CFD must be used with

care, as the results can vary widely, depending on the selection of parameters and numerical models. To avoid design errors and to generate reliable answers, it is necessary to validate a CFD model against at least one relevant real fire test. This paper presents a validation, for different fire heat release rates (HRR), of a CFD model using ANSYS Fluent, against the best available tunnel fire data [5], [6]. Fire Dynamics Simulator (FDS) has also been used and compared with the test data, as it is a simulation tool often used for analysing tunnel fires.

## 2. TEST DATA FOR VALIDATION

The Memorial Tunnel test data are the best documented full scale fire test available and were therefore selected as a base for a reliable model validation. Geometrical details and raw data of temperature sensors, velocity sensors, fuel pumping rates, change in fire pan fuel weights etc. were packed in a 9 CD set and are still publicly available [6]. The processed raw data with the comprehensive test reports, graphics, plots, pictures, videos, and test results are also summarised on a two-disc interactive CD-ROM package [5]. The information from those packages that are relevant to the CFD validation are mentioned here.

During the test program from 1993 to 1995, in total 98 fire ventilation tests were conducted, with fire sizes of 10, 20, 50 and 100 MW, and with a series of ventilation configurations including different fully and semi transverse ventilation strategies, point supply and extraction, natural ventilation, and longitudinal ventilation with jet fans. After the completion of the tests with the transverse ventilation configuration (using the central fans in the ventilation building), the false ceiling was removed, and the ventilation system was transformed into longitudinal ventilation with jet fans. The tunnel configuration and test setup after the ceiling was removed was used as the base for the CFD model validation.

Before using the test parameter data as input parameters for the CFD model, the raw data (readings of the individual sensors) have been processed according to the details given in the Memorial Tunnel Test Data Report [6] and compared with the processed and documented test data of the comprehensive test report [5] to see if the data are consistent and reliable. The reported bulk flow rates and temperatures as well as the averaged flow parameters could be reproduced, based on the documented parameters and calibration factors.

The Memorial Tunnel report [5] concluded that the most reliable measurement loop for bulk flow is Loop 214 at the northern end of the tunnel. Review for this work revealed that other loops are clearly affected by jet fan and radiation influences on the temperature correction for pitot measurements. Local upstream average velocities are calculated based on the flow rate measured at Loop 214 and the local tunnel cross sectional area.

As an example, Figure 1 illustrates the mass flow rate at the different measurement loops for test 611 (50 MW pan fire) at three different times (89 s, 59 s and 29 s) before ignition (0 s) when there were no jet fans running and flow was being driven by a natural pressure difference, and at several time stamps after ignition (from 856 s to 976 s) when both jet fans and heat were affecting readings.

That plot shows that the mass flow rate before ignition (at cold flow) is nearly constant, as it must be by continuity. However, after ignition, the reported mass flow is not constant, indicating increased errors in the measurements and data processing. It is believed that the errors relate to the area-weighted averaging of velocities in combination with blockages and stratification, jet fan influences, and radiation effects on the temperatures used to calculate velocity from the pitot probes.

Jet fans were running just upstream of Loops 209 and 207. Figure 1 suggests that Loops 209 and 207 were affected by those jet fans. Mass flow estimation at Loops 304 and 302 appears to be influenced by temperature effects. Beneath the plot of the flow rates, the temperature

contour plot of the corresponding test, extracted from the test report [5], shows that upstream mass flow anomalies were not due to backlayering (826.5 s after ignition).

The difficulties with interpreting these data precisely led to temperature readings from the tests being the comparison basis for CFD validation. While they are still subject to radiation close to the fire, they are not sensitive to stratification, area-weighted averaging, or jet fans.

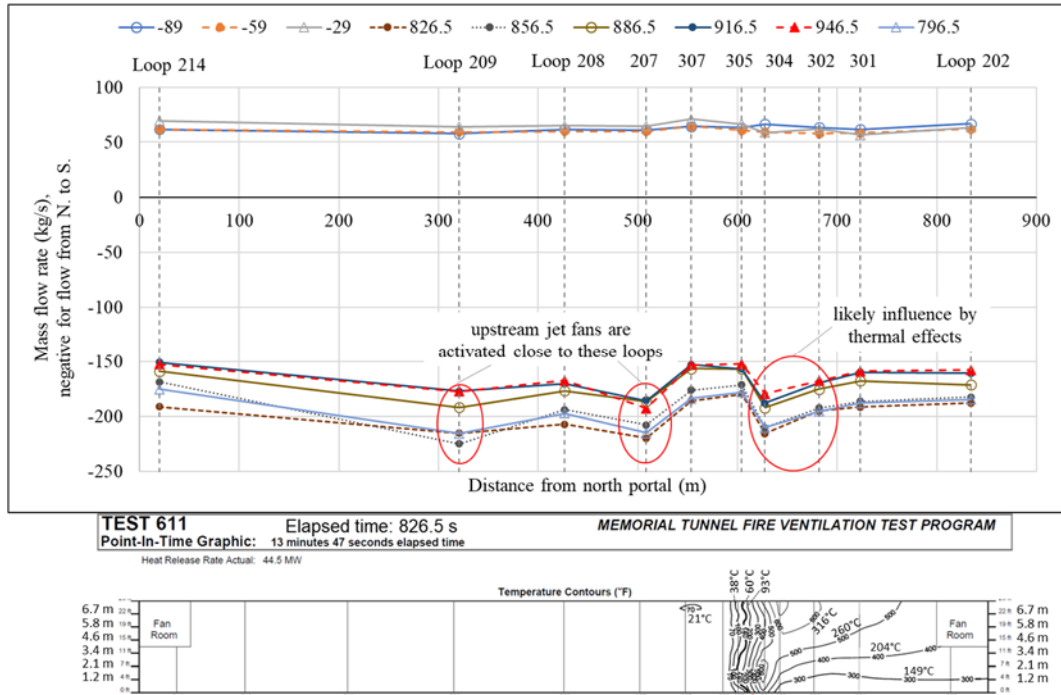


Figure 1: The upper plot shows mass flow rate at different measurement loops prior to ignition (89 s, 59 s and 29 s prior to ignition, all above the axis) and for several time stamps after ignition (826.5 s to 976.5 s after ignition) for test 611 (50 MW pan fire). The lower plot depicts the temperature contours at 826.5 s after ignition, to illustrate the smoke propagation at that time [5], [6].

To validate the CFD model for low as well as high fire heat release rates (HRR), pan fire tests with HRRs of 10 MW, 50 MW and 100 MW were selected. The essential case parameters are listed in Table 1. The flow parameters listed are averages over a period when the flow and smoke layer were fairly constant. This allows the comparison of the measured values with a steady-state simulation in a reasonable way.

Table 1. Input and test parameters extracted from the Memorial Tunnel test data [5], [6], [7] for three validation cases. Bulk temperatures are mass-averaged temperatures.

Parameter	Case 1	Case 2 (base)	Case 3
Test number	606A	610	615B
Elapsed time used for averaging (sec.)	1651 to 1680.5	191.5 to 281	678.5 to 828.5
Measured total HRR <sup>1</sup> (MW)	11.1	54.3	104.6
Activated jet fan/s	JF3	JF2, 5, 8, 11 & 14	JF1, 3, 4, 6, 7 & 9
Fire pan/s used, according to Figure 2	10 MW	50 MW	50, 30 & 20 MW
Flow rate - Loop 214 (m <sup>3</sup> /s)	143.2	148.3	139.8
Average velocity - Loop 305 (m/s)	2.92	3.00	2.85
Blockage area at Loop 305 <sup>3</sup> (m <sup>2</sup> ) [5], [7]	10.2	10.2	10.2
Free tunnel cross sectional area (m <sup>2</sup> )	59.9	59.9	59.9
Average velocity unobstructed tunnel section (m/s)	2.44	2.51	2.38
Upstream temperature - Loop 214 (°C)	3.6	4.0	6.8
Upstream temperature - Loop 207 (°C)	8.5	7.3	12.0
Upstream temperature - Loop 307 (°C)	9.0	7.2	14.8

Measured bulk temperature after fire - Loop 302 (°C)	53	190	451
Measured bulk temperature after fire - Loop 303 (°C)	57	217	475
Upstream density - Loop 214 (kg/m <sup>3</sup> )	1.28	1.27	1.26
Specific heat capacity (kJ/kgK)	1.014	1.044	1.096
Theoretical bulk temperature after the fire based on total HRR(°C)	69	282	554
Radiative fraction <sup>2</sup> (-)	0.21	0.24	0.17

<sup>1</sup> Measured heat release rate corrected by the CO to CO<sub>2</sub> ratio to account for non-ideal combustion [5], [6]

<sup>2</sup> Ratio between measured bulk temperature and the theoretical bulk temperature rise resulting from the total HRR is assumed to be the radiative fraction.

<sup>3</sup> Value as stated in Section 8.8.4 in the comprehensive test report [5], and in the paper from Kile&Gonzalez [7]. The fraction of the tunnel area blocked is about 17%, as also reported in the same references.

### 3. CFD MODEL

The CFD validation was carried out by using the simulation software ANSYS Fluent version 2021 R1 [8], [9], [10]. During the validation process, a fire test with a nominal fire heat release rate of 50 MW was chosen as the base case (Case 2 in Table 1) and analysed with two different common approaches as to how the fire is represented in the numerical model. The two methods for representing the fire are “volumetric heat source” and “simulation of the combustion process” and explained in more detail in Section 3.2.

To validate against a wide range of fire sizes, the fire representation with the most promising results was also applied to simulating 10 MW and 100 MW fire tests.

As a final step and comparison, the base case validation (50 MW) was also analysed with FDS (Fire Dynamic Simulator version 6.7.1) [11], as outlined in Sections 4 and 5.3.

#### 3.1. Geometry and Computational Mesh

Geometric parameters were mainly extracted from the test reports [5], [6] to create a detailed model of the Memorial Tunnel including the jet fans, fire pans, measurement loops and measurement equipment/data acquisition units obstructing part of the tunnel cross section around the loops. Setup sketches and test notes made at the time were also provided by [12], to assist in reproducing the size and position of the data acquisition, measurement units, and instrument loops. Unfortunately, the sketches were made when the false ceiling was still in place. However, it has been confirmed that the position and size of the recorded obstacles were similar after the ceiling was removed [12]. Also, the reconstruction of the geometry based on photos and those sketches confirmed the obstruction area as being 10.2 m<sup>2</sup> at Loop 305. As a figure of 110 ft<sup>2</sup> (10.2 m<sup>2</sup>) is noted for Loop 305 in the test reports [5] and [7]. This is important, since the average air velocity at Loop 305 (11.3 m upstream of the fire site centre-line) was used as the measure for the critical velocity (about 20% higher than the unobstructed upstream average velocity [5], [7]). In the Memorial Tunnel report, slightly different cross sectional areas are stated, ranging from 59.6 m<sup>2</sup> to 60.4 m<sup>2</sup>. The replication of the tunnel geometry based on the plotted tunnel profile with detailed dimensions, as depicted in Figure 2, resulted in a cross-sectional area of 59.91 m<sup>2</sup>, which is in the quoted range, has a basis in the records, and was therefore adopted. At the portal sections, the northern and southern central fan rooms limit the ceiling height so that the cross-sectional area reduces to 37.1 m<sup>2</sup>. The position and size of the fire pans was incorporated as shown in Figure 2. In total, 24 jet fans, each with a flow rate of 42.95 m<sup>3</sup>/s and a discharge velocity of 34.2 m/s were installed in banks of three upstream and downstream of the fire, as depicted in Figure 3. Jet fans influence the velocity profile and turbulence in the tunnel and so the operating jet fans were also implemented in the CFD model. The groups of jet fans downstream of the fire were installed in a later stage of the tests and were not relevant to include in the model for the tests analysed. The total tunnel length from portal to portal is 853.75 m. Location of the measurement loops, as well as of the individual sensors in the tunnel profile, are illustrated in Figure 3.

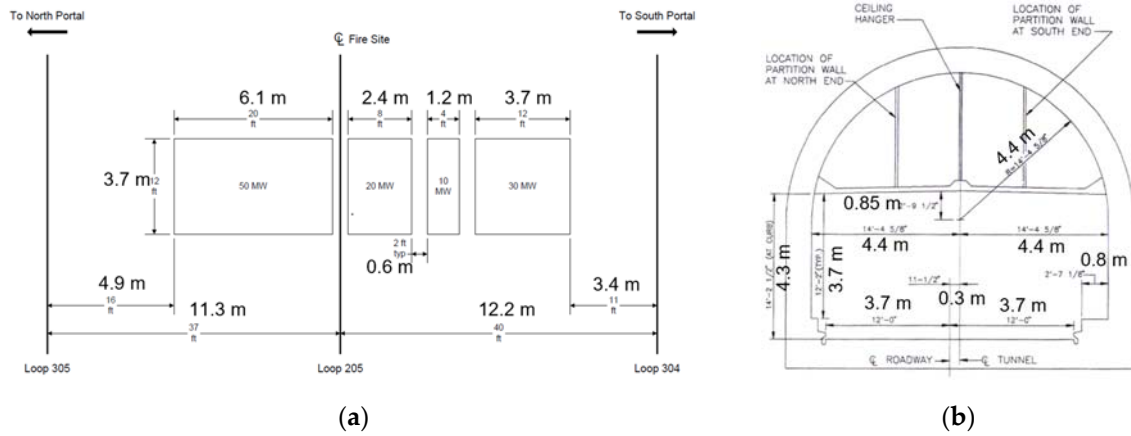


Figure 2. Sketches from the Memorial Tunnel report [5], [6].  
 (a) Configuration and dimensions of the fire pans used, which were set about 0.76 m above the tunnel floor; (b) Memorial Tunnel cross-section with dimensions (looking north).

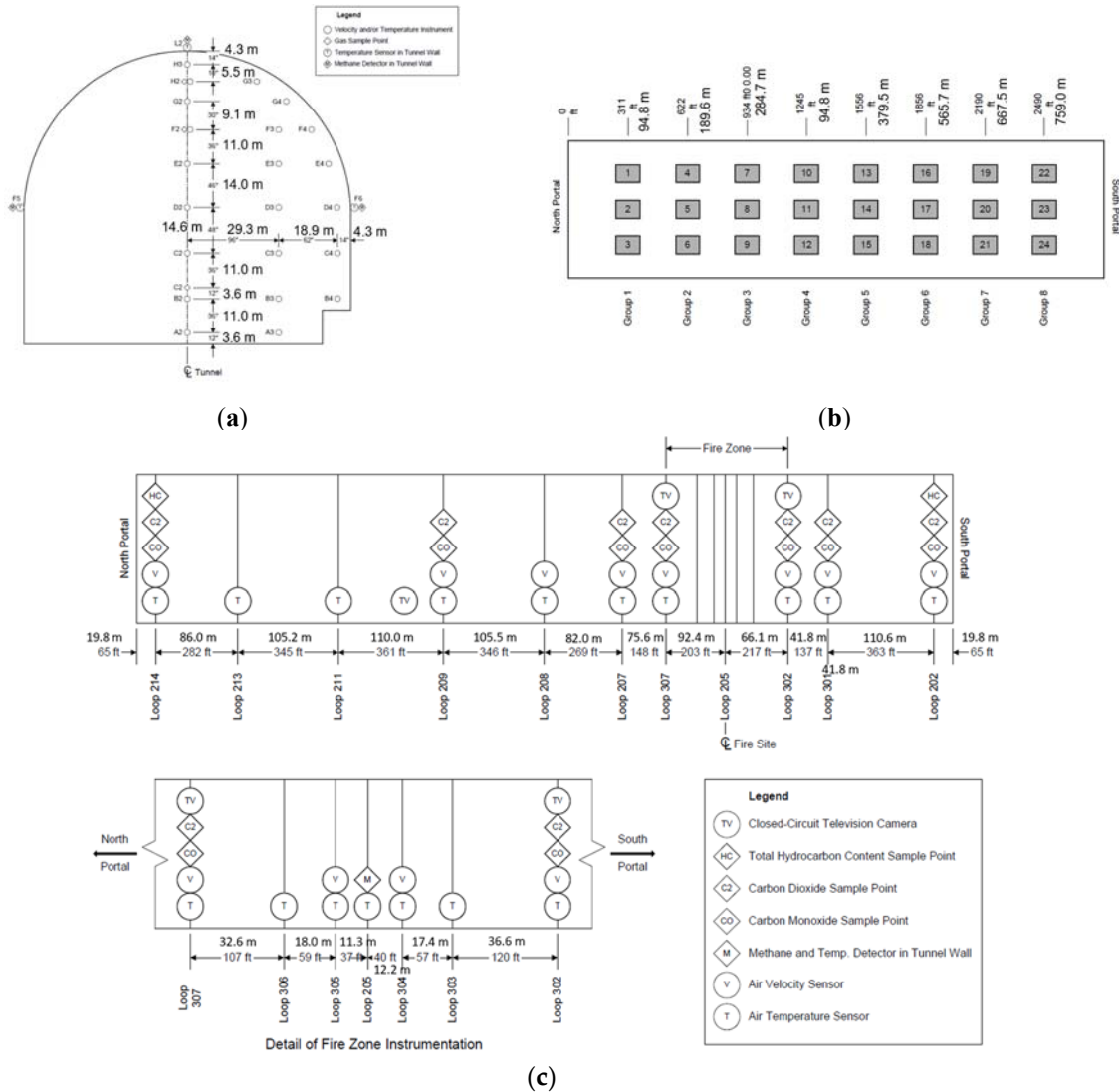


Figure 3. Sketches from the Memorial Tunnel report [5], [6].  
 (a) Location of the different sensors at the measurement loops (looking north);  
 (b) Location and description of the jet fan groups throughout the tunnel. Jet fans 16 to 24 were installed at a later stage of the tests and are not relevant for the cases considered.  
 (c) Instrument loop locations, with instrument types at each loop.

The whole domain was meshed with polyhedral surface elements in combination with hexahedral-core elements. To resolve the boundary layer at the walls, prism elements were created at the solid surfaces (fire pan, instrumentation tree, jet fans etc.). The element size within 40 m of the fire pans ranges from 0.02 to 0.1 m. Beyond the fire location, the elements grow to approximately 0.3 m. For the jets downstream of the jet fans, a finer mesh with a maximum element size of 0.1 m was introduced by means of a conical body of influence. The whole domain was meshed with approximately 35 M numerical elements. Figure 4 depicts the computational mesh around the fire pans (a) and jet fans (b).

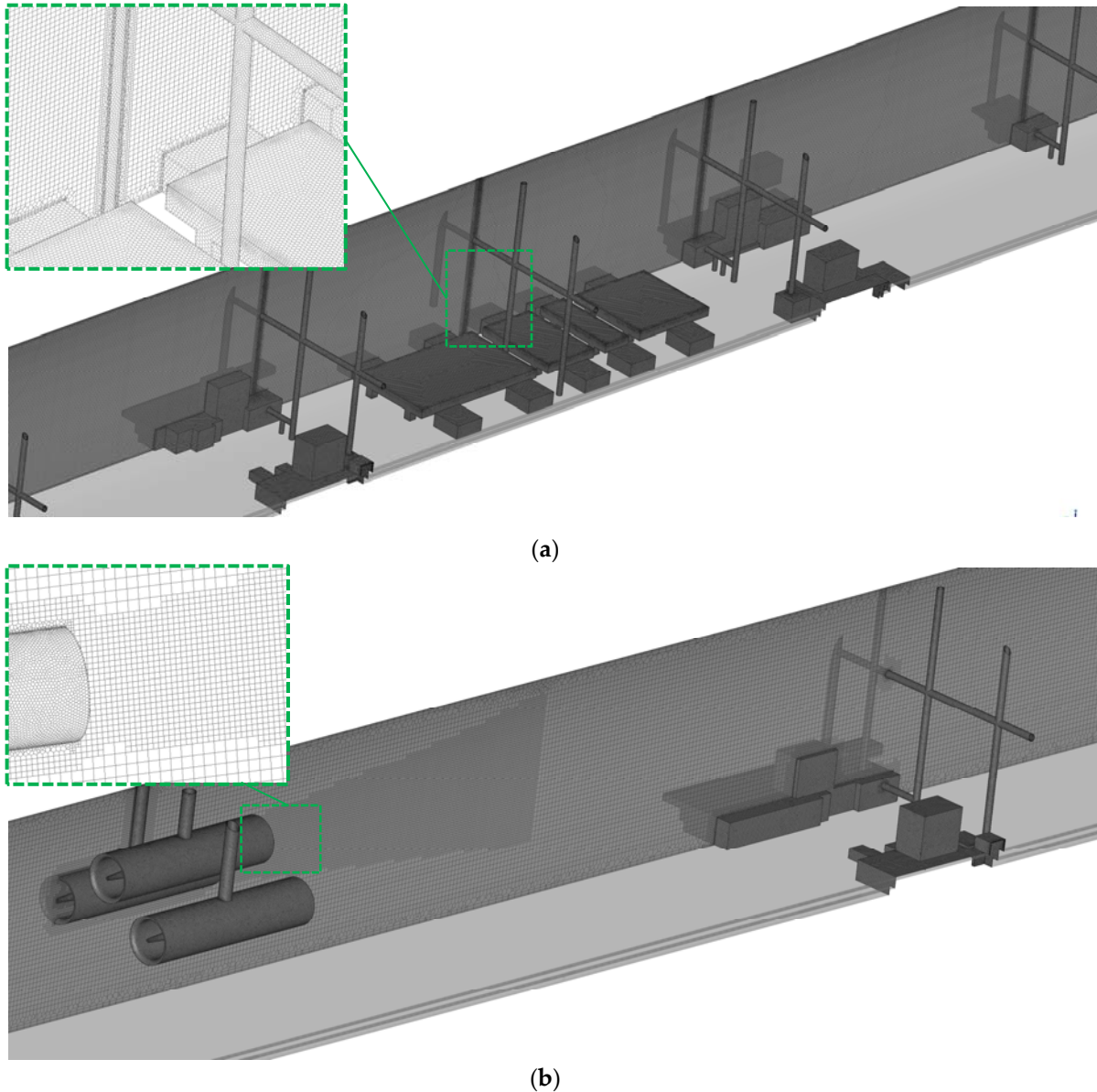


Figure 4. Computational mesh: (a) around the fire pans; (b) around jet fan group 5 and Loop 207.

### 3.2. Simulation Procedure and Methodology

Simulations were carried out in ANSYS Fluent using a pressure based, steady-state, Reynolds-averaged Navier-Stokes (RANS) solver with a spatial discretisation method of 2<sup>nd</sup> order. The realizable  $k$ - $\epsilon$  model with scalable wall function was applied. This turbulence model was developed to more accurately predict the spreading rate of planar and round jets and provides a good performance for flows involving rotation, boundary layers under strong adverse pressure gradients, separation and recirculation [8], [9]. The turbulence model was selected due to the



expected flow behaviour (jet flow at jet fans as well as separation and recirculation around the instrument trees), for its robust and efficient performance, and its accuracy. Buoyancy effects of the smoke are fully considered by using the incompressible ideal gas law. The fire is commonly represented with two different approaches as already noted at the beginning of Section 3, and further described below. Both have been tested and compared for test 610 which is a 50 MW pan fire (Case 2 in Table 1).

**Volumetric heat source:** The fire is represented as a source of heat and mass without simulating the combustion process, as proposed in [13]. In that approach, the heat release rate due to combustion is simplified as a volumetric heat source in an adopted fire region. As the heat is released in that region, the generated temperature depends not only on the heat release rate, but also on the size and definition of the pre-defined volume. This is essentially giving the model information on the flame size and shape, and the distribution of the release of heat. Of course, the size and shape of the flame are not known beforehand, and should be results of the model, not inputs, and so the volumetric heat source approach is adding assumptions that may not represent the real situation. For this validation, different (rectangular prism) heat source dimensions were analysed, and compared with the test results. The fuel mass due to combustion is considered in an additional mass source term in the continuity equations.

**Eddy-dissipation combustion model:** The combustion process is calculated by means of a turbulence-chemistry interaction model based on the work of Magnussen and Hjertager [14]. The chemical reaction rate is controlled by turbulent mixing and shows an acceptable performance for pool fires as suggested in [15]. Owing to the absence of detailed information on the combustion reaction, an ideal stoichiometric combustion was adopted. To reflect the Memorial Tunnel fire tests, a fuel oil with a chemical formula of  $C_{19}H_{30}$  was introduced as fuel vapor coming from the pan surface.

Thermal radiation was not simulated for either the volumetric heat source or the eddy-dissipation combustion model. Instead, a radiative fraction approach as explained in [13] has been adopted, capturing the loss of thermal energy in a gross sense. This approach assumes that the radiative fraction of the total fire heat release rate is lost to the surroundings without affecting the temperature distribution within the tunnel. Particularly in the early stages of any fire, that is a reasonable approximation. The remaining energy heats up the air as it mixes with the plume. The radiative fraction of the individual test cases was estimated by the measured fire heat release rate and the bulk temperature downstream of the fire (see Table 1). The heat release rates during the Memorial Tunnel tests were measured through the fuel flow rate of the fuel supply pipe and the mass change of the fire pan. To account for the combustion efficiency, the HRR was corrected by the CO to CO<sub>2</sub> ratio. The corrected HRR as listed in Table 1 was used for the assessment. For the eddy-dissipation combustion model, a controller was implemented in the simulation, to adjust the fuel mass flow in such a way that the convective heat is achieved and maintained throughout the simulation.

The assumption of ideal combustion, and the radiative fraction approach, both require incorporation of an additional mass source. The simulation allowed for the additional mass source, adjusted to be appropriate to the real/factual fuel mass flow.

As already discussed in Section 2, Loop 214 (see Figure 3) gave the most reliable flow measurement during the tests. Tunnel air mass flow rate as the inlet boundary condition at the northern portal was determined based on the measured flow rate and bulk temperature at Loop 214. The air temperature measured just upstream of the fire was usually a few degrees higher than at the portal. This is caused by the tunnel wall temperature being higher than the ambient air temperature outside the tunnel. In order to have the right temperature and velocity just upstream of the fire, the mass flow at the northern portal was calculated based on the volume flow rate and density (bulk temperature) at Loop 214, but introduced into the tunnel

with the higher temperature that was measured just upstream of the fire (~Loop 208). The wall temperature was taken to be similar to the tunnel air temperature just upstream of the fire. The same approach was used for all simulation cases.

A piecewise-polynomial function for the temperature dependent specific heat capacity for the individual species was considered. The thermal dependency of the thermal conductivity and the dynamic viscosity for the individual species were estimated based on Sutherland's law with three coefficients, in combination with a mass-weighted mixing law.

#### 4. FDS – SIMULATION PARAMETERS

For comparison with the Fluent validation, an FDS (version 6.7.1) simulation has been carried out with a 50 MW fire only (Case 2 as defined in Table 1). The geometry used for the ANSYS Fluent simulations (as described in Section 3.1) was exported as an STL file and imported into FDS via PyroSim (Revision 2020.1.0324). For the mesh, a cell size of 0.1 m x 0.1 m in the tunnel cross section, and 0.2 m longitudinally, was used. In FDS, stepwise representation of curved geometries makes it difficult to match the area precisely, such that either the velocity or the flow rate will be in error. The inlet boundary condition at the northern portal was a velocity inlet as the right tunnel air velocity is essential for reproducing smoke propagation upstream of a tunnel fire. For the southern (downstream) portal, a default open boundary condition was used. The fire in FDS is represented as a Simple Chemistry Reaction with a fuel-oil composed as  $C_{19}H_{30}$  with the fire surface area sitting on the top of the 50 MW fire pan (see Figure 2 and Figure 5). Fire and flow parameters are applied as listed in Table 1 (Case 2). Turbulence in FDS was simulated with VLES (Very Large Eddy Simulation). The assumptions on the thermal radiation and the thermal conditions of the tunnel wall, were the same as discussed in Section 3.2. Jet fans are considered via an HVAC boundary condition with the flow rate as given in Section 3.1. Solver parameters like relaxation factor and velocity tolerance were adjusted to stabilize the numerical simulation and increase the accuracy of the pressure solver.

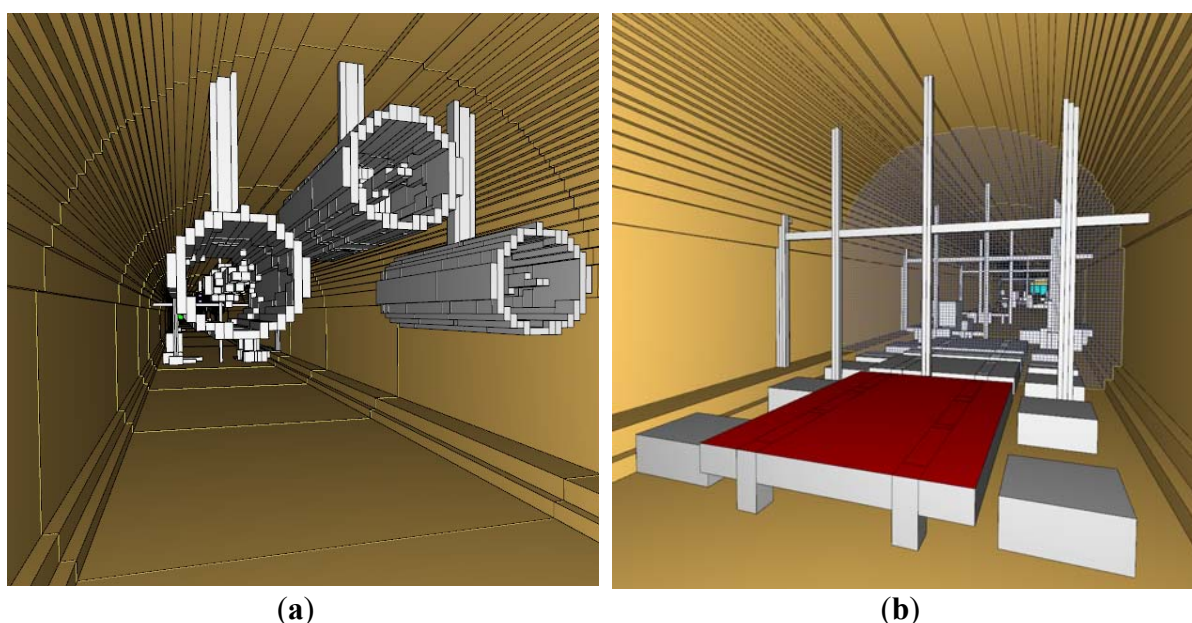


Figure 5. Representation of the tunnel geometry in FDS with a cell size of 0.1 x 0.1 x 0.2 m. (a) Jet fan group 5, looking north. (b) Fire pans at Loop 205, looking south.

The FDS simulation encompasses a mesh of 17 million cells and was run on 128 cores over 3 weeks until it reached nearly steady state conditions. Even if this is considered as an upper limit of a practical usability, the curvatures of the geometry are still not resolved in an accurate way, due to the meshing limitations in FDS. Accurate representation of the geometry is important for resolving boundary and shear layers adjacent to the wall, as well as representing

the correct flow rate vs. velocity through the tunnel or jet fan. All of that is regarded as essential for an accurate prediction of smoke propagation upstream of a fire.

## 5. RESULTS OF THE VALIDATION AND DISCUSSION

For all simulated validation cases, Figure 6 to Figure 11 compare the bulk temperature along the tunnel axis and the temperature profiles over the tunnel height against the corresponding test results [5] and [6]. Thermocouple readings at a given elevation are averaged in the temperature profiles at the different measurement loops. The representative elevation area is a horizontal slice of the tunnel cross-section around the elevation instruments as specified in [5] and [6]. Identical horizontal slices have been used for evaluating the CFD simulations. For a better understanding of the temperature profiles, a contour plot of the temperature through the middle of the tunnel around the vicinity of the fire is also given for each case.

The higher bulk temperature seen in the test data at loops 205, 304, and 303 (close to the fire source) in the plots with the bulk temperature along the tunnel, is believed to be related to the impact of the thermal radiation on the temperature readings, as noted in [5] and [6].

### 5.1. Fluent - Volumetric Heat Source

The volumetric heat source approach was first analysed for a 50 MW fire on a more simplified model with a reduced length of tunnel modelled. Obstacles were only considered in the vicinity of the fire at the Loop 305, 205 and 304 and the influence of jet fans on the velocity profile was also neglected. Fire and input parameters are based on Case 2 as given in Table 1. The simplified model was used to more rapidly analyse and understand the effect of different heat source sizes. The objective of this part of the study was to understand which volumetric heat source definition would replicate the smoke stratification and temperature distribution most accurately. The heat source was placed directly above the 50 MW fire pan (see Figure 2, left), and the volume was varied by changing the height from 2 m to 2.6 m and 3.0 m. That corresponds to volumetric heat sources of  $1.22 \text{ MW/m}^3$ ,  $0.94 \text{ MW/m}^3$  and  $0.81 \text{ MW/m}^3$ , respectively. To quantify the impact of the simplification (neglecting jet fans etc.), the simulation with the 3.0 m heat source was repeated with all relevant details implemented.

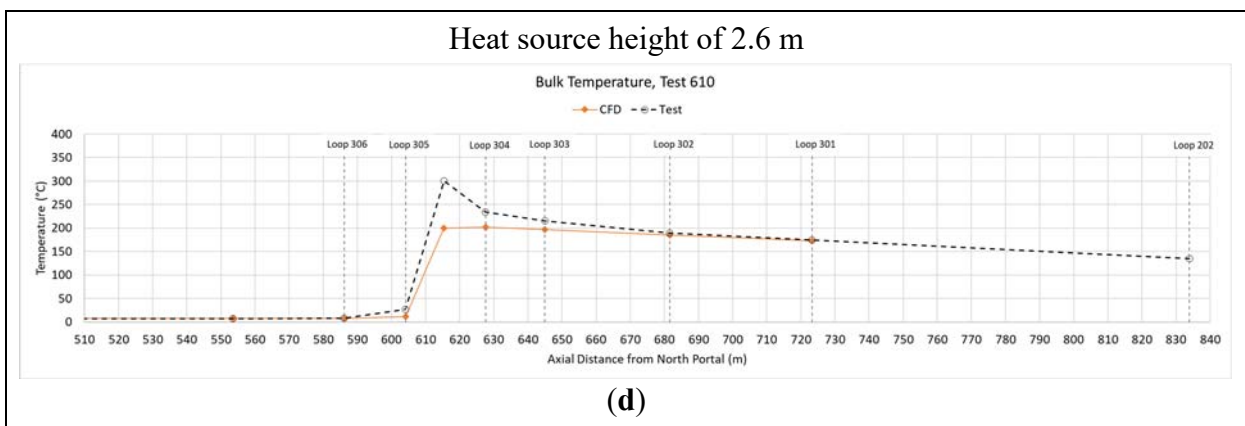
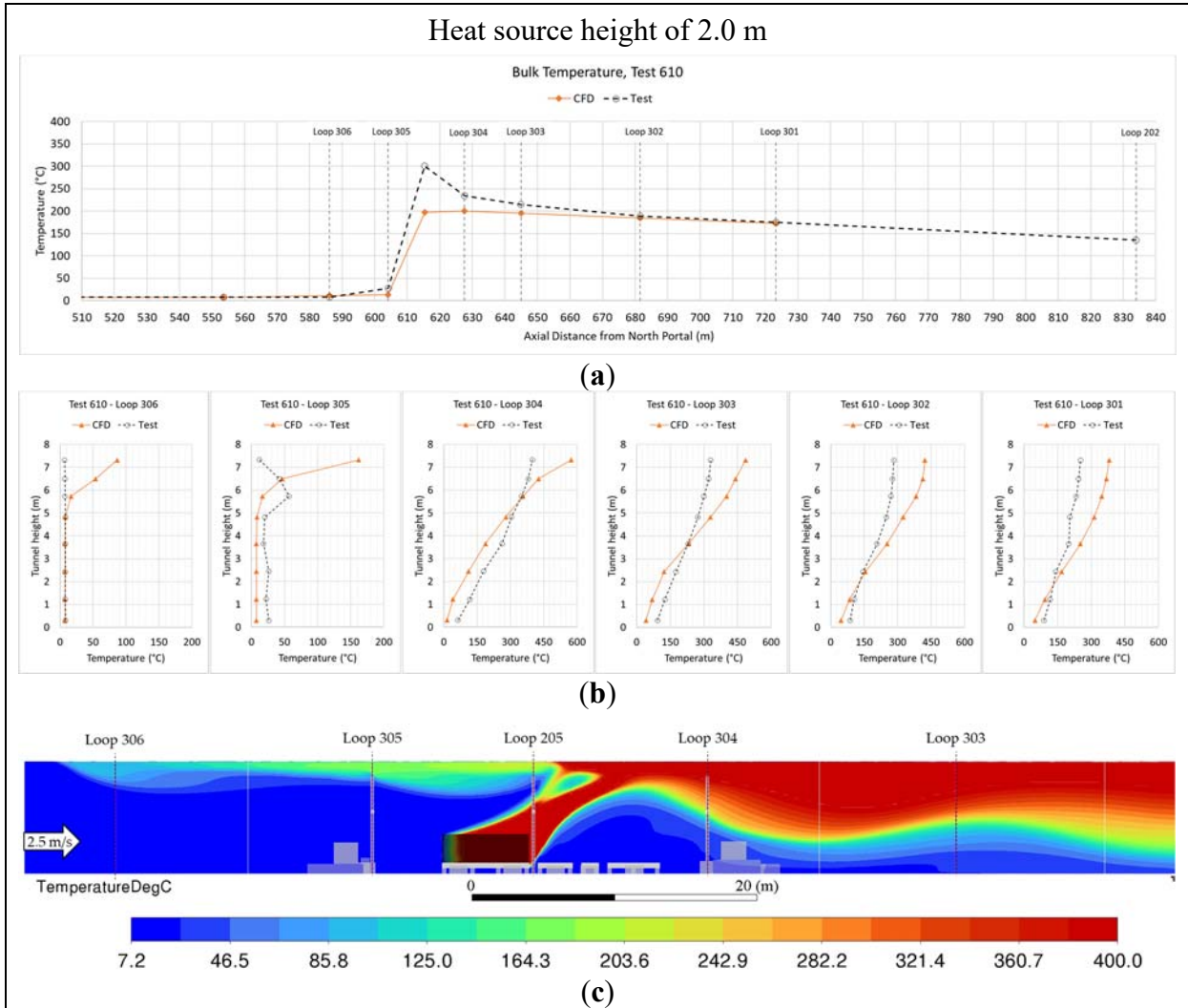
Figure 6 compares the test temperature profiles at the individual instrument loops, against the results of the CFD simulations with the different heat source definitions. The plot below the temperature profiles compares the bulk temperatures along the tunnel axis. A contour plot of the temperature through the middle of the tunnel shows the temperature stratification, and gives an indication of the upstream propagation of the hot smoke.

Looking at the test result, the slight temperature increase at the upper part of Loop 305 indicates that the tip of the backlayering was close to Loop 305 but did not reach Loop 306 further upstream.

In all cases, the extent of the backlayering was not predicted very accurately, with backlayering over-predicted. Backlayering propensity also depends strongly on the definition of the volumetric heat source. The best result in terms of the backlayering prediction were with the 2.6 m high heat source, but the temperature tends to be more stratified than observed in the tests, with higher flow and temperature along the ceiling (less mixing between smoke and air). The latter applies to all cases analysed. Further cases with heat source heights of 1.8 m, 3.5 m and 4.5 m were also analysed, but the predicted backlayering length with the smaller and bigger heat source volumes was higher still (further discussion on the more likely position of the backlayering at that time of the selected test period is provided in Section 5.2).

The detailed simulation with the complete tunnel section, all jet fans and obstacles implemented did improve the prediction of the upstream smoke propagation but did not improve the accuracy of the temperature distribution downstream (see Figure 7).

The volumetric heat source approach is usually very economical, and a robust method to simulate tunnel fires, and is therefore often preferred. However, there is no inherent fire volume definition for any scenario, and as the smoke propagation and temperature distribution strongly depend on the heat source dimensions, this approach is not recommended for analysing confinement or critical velocity in a reliable way.



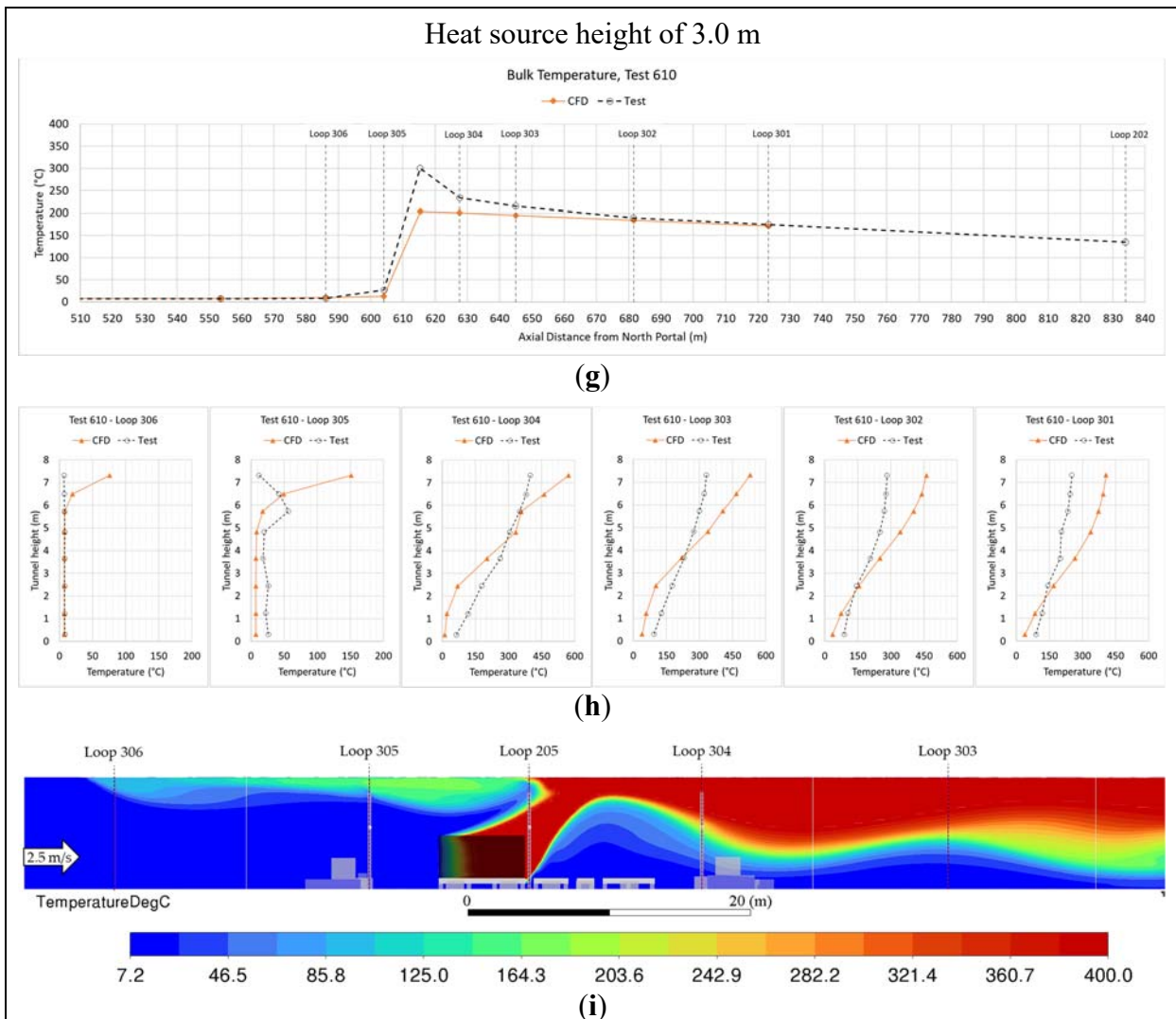
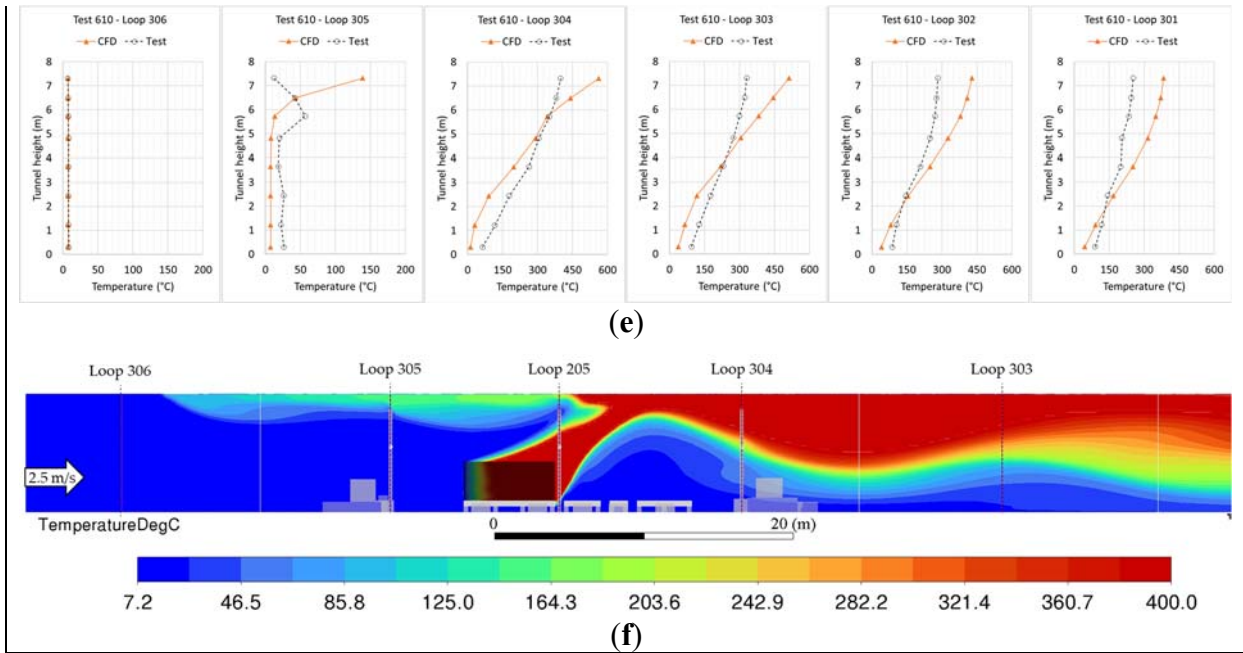


Figure 6. 50 MW validation (Case 2 from Table 1) with volumetric heat source. Comparison of simulation results with test results for test 610: (a), (d) and (g) Bulk temperature along the tunnel axis for different heat source heights, (b), (e) and (h) Temperature profiles over the tunnel height for

different loops in the vicinity of the fire and for different heights of the heat source, (c), (f) and (i) Contour plot of the temperature in °C through the middle of the tunnel and fire pans, for different heat source heights. Temperature is clipped to 400°C for a better visualisation of the temperature layering.

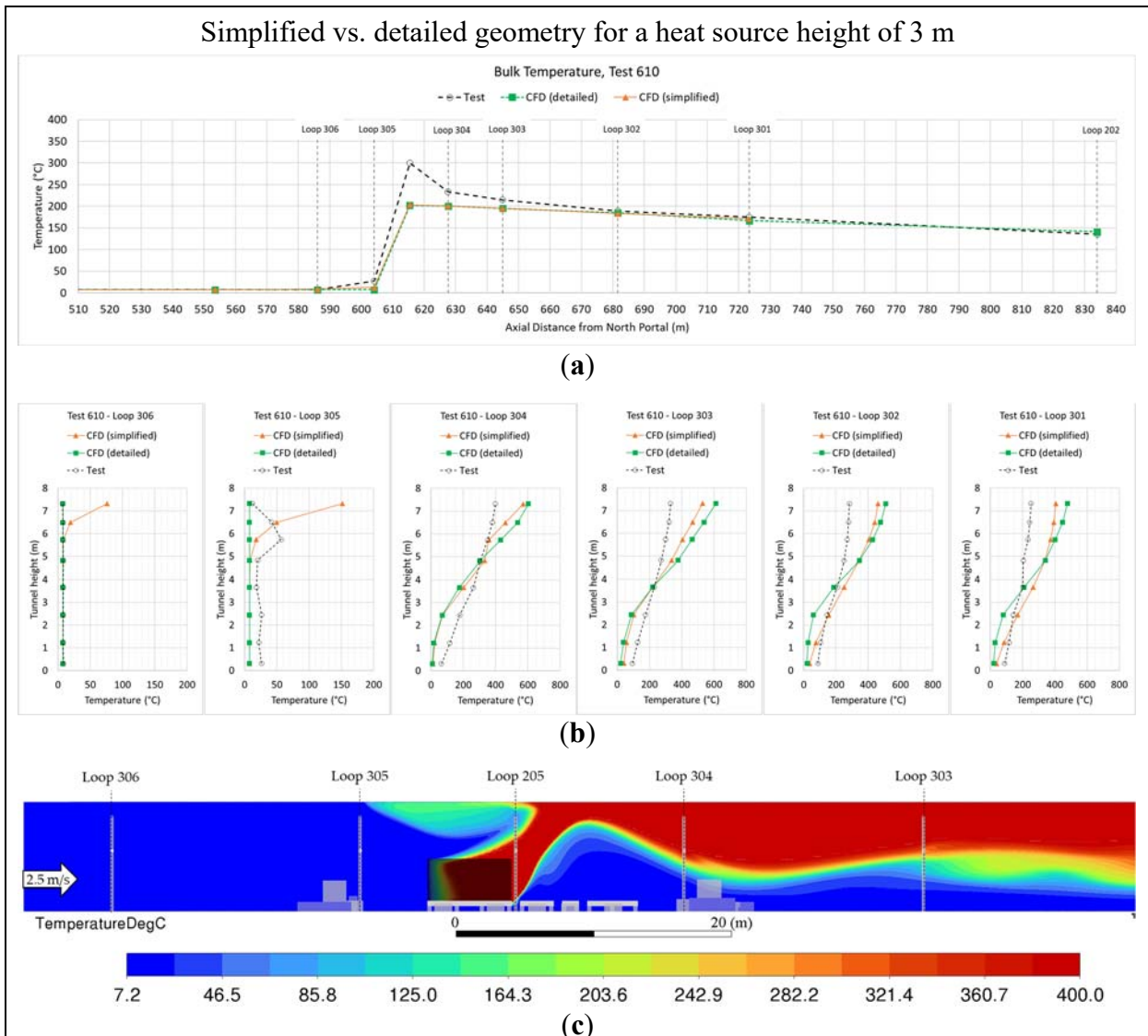


Figure 7. 50 MW validation (Case 2 from Table 1) with volumetric heat source height of 3.0 m. Comparison of: simulation results with simplified geometry; with detailed geometry; and the test results for test 610. (a) Bulk temperature along the tunnel axis, (b) Temperature profiles over the tunnel height for different loops in the vicinity of the fire, (c) Contour plot of the temperature in °C through the middle of the tunnel and fire pans. Temperature is clipped to 400°C for a better visualisation of the temperature layering.

### 5.2. Fluent - Eddy Dissipation Combustion Model

The simulation with the eddy-dissipation combustion model was carried out for all three validation cases listed in Table 1. Results of the temperature distribution along the tunnel and the temperature profiles at the different loops are presented in Figure 8 to Figure 10 for the three different fire cases.

In all cases, the temperature profiles downstream of the fire were predicted with reasonable accuracy. The higher temperature readings of the test data at the upper part of the temperature

profile close to the fire (Loops 304 and 303) might be related to the influence of thermal radiation on the sensors (see Figure 8 and Figure 9).

Besides the deviation of the bulk temperature close to the fire (influence due to thermal radiation on the temperature sensors during the tests), the bulk temperature at Loop 202 also shows a slight deviation, especially at higher downstream temperatures (higher HRR). Loop 202 is located in the smaller cross section near the south portal, with the reduced ceiling height. The step change in the cross-section area is just 1.5 m upstream of Loop 202. This step will have created a separation zone and recirculation close to the ceiling. The difference in bulk temperature seen at Loop 202 may be related to the difficulty in turning point measurements of velocity and temperature into bulk averages, for such a non-uniform flow.

The velocity in the tunnel during the Memorial Tunnel tests was adjusted using the jet fans installed in the tunnel upstream of the fire. These jet fans were not speed controlled. To change the air speed in the tunnel, a jet fan could be switched on or off, making the speed control fairly coarse. The buoyancy force and flow resistance of the 10 MW fire are quite low, certainly much lower than for a 50 MW or 100 MW fire. With the coarse control on jet fan forcing, the low resistance made it difficult to achieve a steady velocity where backlayering was just prevented. For the tests with low heat release rates, two active jet fans were insufficient to stop smoke propagation upstream of the fire, and three jet fans were too strong, so that the approaching air velocity was higher than required for preventing backlayering. The point at which backlayering was just prevented was analysed during the velocity change after turning the third jet fan on or off. This made it difficult to accurately determine the critical velocity for low heat release rates. The scatter in the reported data at low HRR reflects this.

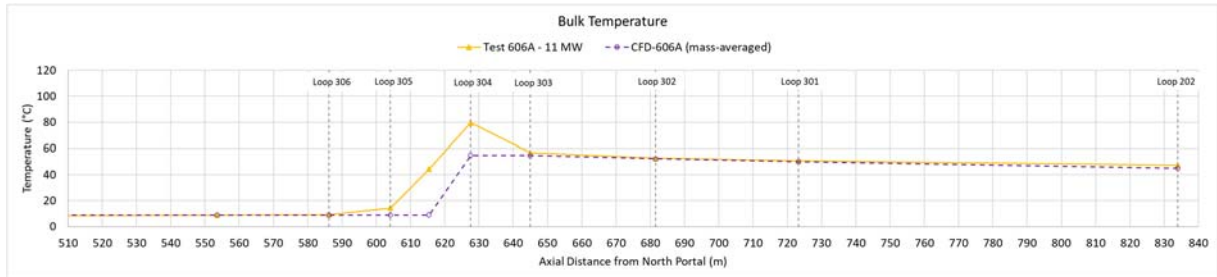
The flow record simulated for test 606A (11.1 MW) was approximately 28 minutes after ignition, when the third jet fan was activated. Before that, smoke was propagating upstream of the fire so that the tops of Loops 304, 305, and partly 306, were covered in smoke for more than 15 minutes. When the smoke went back towards the fire site briefly (for around 2 minutes), the temperature readings show slightly increased values (Figure 8) which may possibly be explained by the thermal inertia of the temperature sensors only recently out of the smoke layer.

Test 610 (54.3 MW) shows backlayering above the deflected flames and plume which stops at the front of the first fire pan, just downstream of Loop 305 (see Figure 9). The sensor temperature at Loop 305 might have been increased by thermal radiation, as the instrument tree is only 5 m upstream of the fire. Also, the backlayering was slowly moving forward and backward with slight fluctuations in the fire dynamics and local velocity during the test.

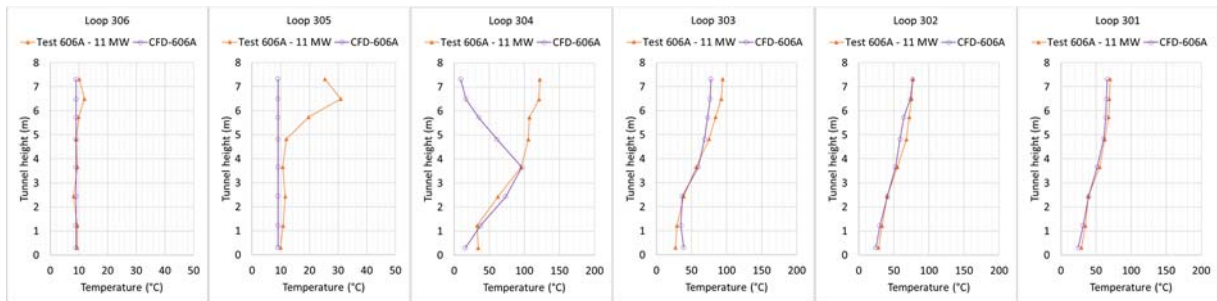
At the beginning of test 615B (104.6 MW), all jet fans were switched off and the smoke was propagating in both directions towards the portals. About 3 minutes after ignition, 6 jet fans (as listed in Table 1) were activated so that the smoke was slowly pushed back towards the fire site. After 10 minutes, the upstream tunnel section was free of smoke. The simulated flow record was at around 12 minutes after ignition, just before one of the six jet fans was turned off and the upstream smoke propagation started again. The simulation shows a backlayering of smoke which stops just upstream of Loop 305 (see Figure 7). Looking at the temporal variation in the original data, the increased temperature around the ceiling at Loop 306 could be related to heated sensors that had been subject to hot smoke for more than 10 minutes and having not yet reached equilibrium with the temperature of the fresh air. It is assumed that the sensor readings at the lower part of Loops 305 and 304 are influenced by thermal radiation. The test results indicate that the smoke downstream of the fire was more mixed than is predicted by the simulation.

Based on the observations above, and acknowledging a few uncertainties in the temperature readings, it can be concluded that the smoke propagation and temperature distribution can be predicted within a reasonable accuracy by the simulation techniques and procedures applied.

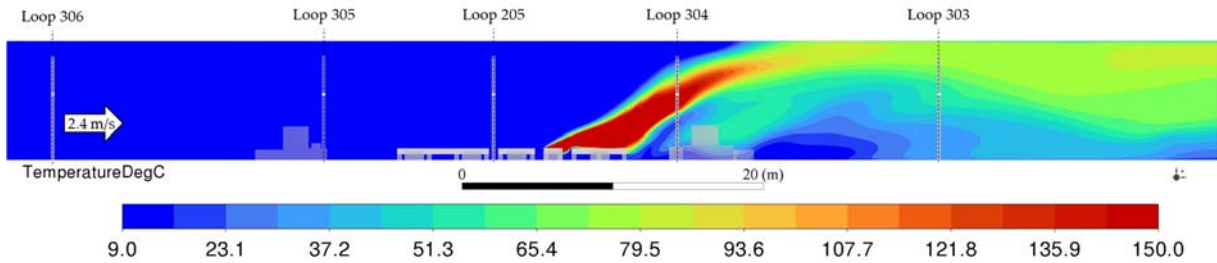
Most importantly for the present purpose, the smoke extent matches the tests very well for the same conditions. However, it is important to also check other parameters, to see that the critical velocity is not correct by an ‘accident’ of compensating errors that may not compensate each other in other scenarios. The temperature profiles away from radiation effects are also predicted quite well, giving confidence that the analysis is a reasonable representation of the plume and smoke layer dynamics. That is; the technique is a reasonable tool for exploring critical velocity, for cases not dissimilar to the validated cases.



(a)



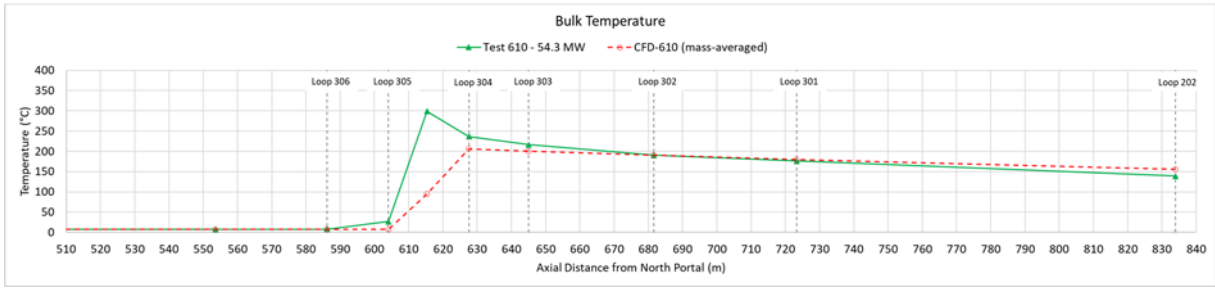
(b)



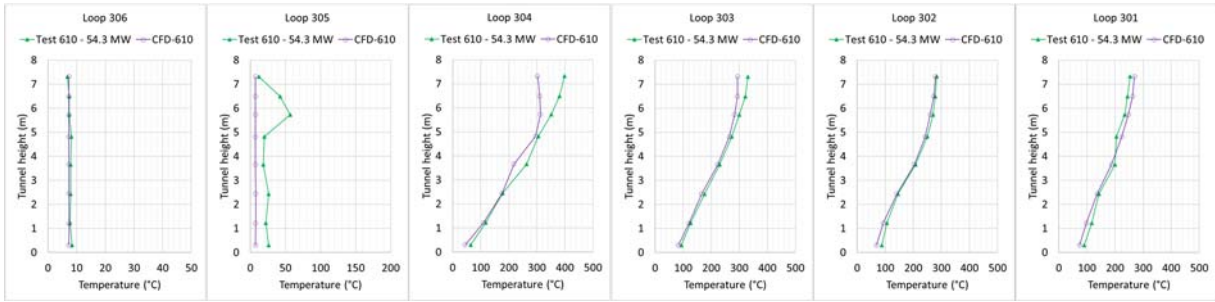
(c)

Figure 8. 11 MW validation (Case 1 from Table 1) with combustion model. Comparison of simulation results with test results for test 606A: (a) Bulk temperature along the tunnel axis, (b) Temperature profiles over the tunnel height for different loops in the vicinity of the fire, (c) Contour plot of the temperature in °C through the middle of the tunnel and fire pans. Temperature is clipped to 150°C for a better visualisation of the temperature layering.

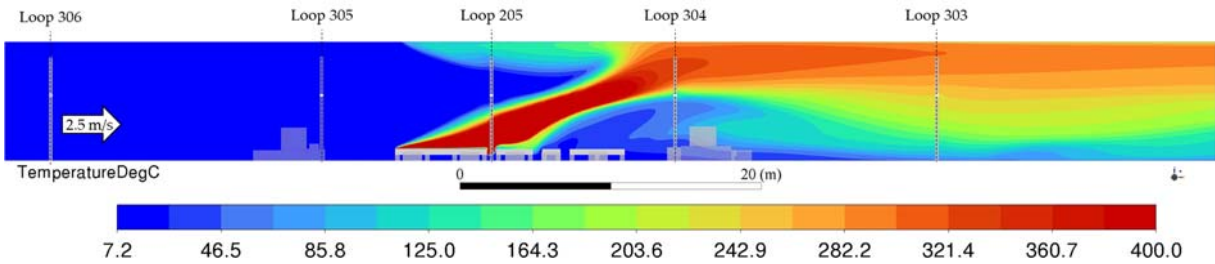




(a)

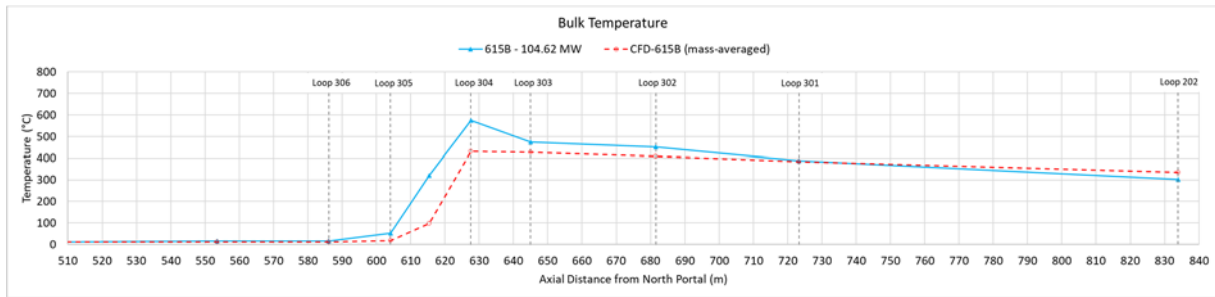


(b)

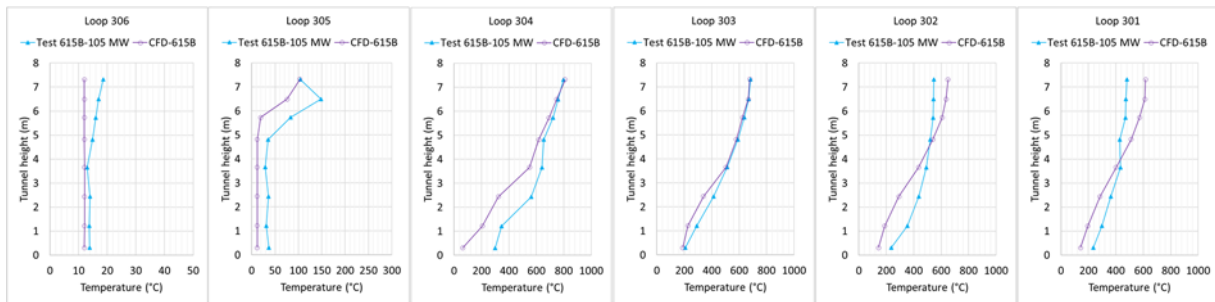


(c)

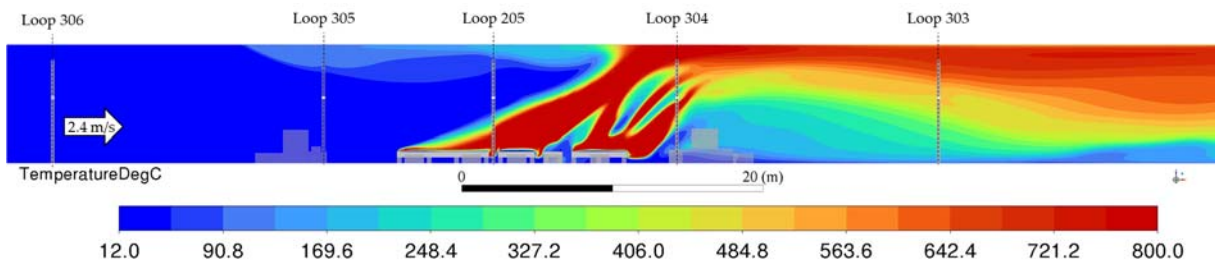
Figure 9. 54.3 MW validation (Case 2 from Table 1). Comparison of simulation results with test results for test 610: (a) Bulk temperature along the tunnel axis, (b) Temperature profiles over the tunnel height for different loops in the vicinity of the fire, (c) Contour plot of the temperature in °C through the middle of the tunnel and fire pans. Temperature is clipped to 400°C for a better visualisation of the temperature layering.



(a)



(b)



(c)

Figure 10. 105 MW validation (Case 3 from Table 1). Comparison of simulation results with test results for test 615B: (a) Bulk temperature along the tunnel axis, (b) Temperature profiles over the tunnel height for different loops in the vicinity of the fire, (c) Contour plot of the temperature in °C through the middle of the tunnel and fire pans. Temperature is clipped to 800°C for a better visualisation of the temperature layer.

### 5.3. FDS

The FDS simulation of Case 2 was run for 600 s. Smoke propagation was established and was almost steady state after 200 s. The values in the temperature profiles as illustrated in Figure 11 are averages over a period of 50 s, close to the end of the simulation. The FDS simulation predicts a smoke propagation upstream of the fire of approximately 360 m, whereas the simulation with the eddy-dissipation combustion model agrees with the test result, with almost no upstream smoke propagation for the 50 MW fire case. The FDS upstream smoke layer stops between Loops 207 and 307, as it is opposed by the running jet fans at JF-Group 5. Without the activated jet fans, the analysis of the simulation results indicates that the backlayering of hot smoke gases would propagate upstream even further. The temperature profile along the tunnel axis shows an increased bulk temperature upstream of the fire due to the upstream smoke layer. The bulk temperature at the southern portal (Loop 202) is missing in the plot as it has not been recorded during the FDS simulation. The comparison of the temperature profiles along the tunnel height shows that the smoke downstream of the fire is less mixed, which results in higher temperatures in the upper part of the tunnel and a more energetic smoke layer.

Based on these observations, it can be concluded that the smoke propagation and temperature distribution are not predicted within a reasonable accuracy by FDS and the applied simulation techniques. Analysing smoke propagation with FDS as described here would lead to overprediction of critical velocity or confinement velocity required for preventing or controlling backlayering.

The poor representation of surface curvatures in FDS compromises efforts to accurately resolve and predict the boundary layer adjacent to the wall, which might be one reason for the unsatisfying results in the smoke propagation. Analysing smoke propagation in straight and rectangular tunnels may potentially improve the results if the boundary layer adjacent to the wall is sufficiently resolved by adequate cell sizes and an appropriate wall function is used. However, caution regarding the accuracy of the flow and pressure field in FDS is required, as several issues with numerical oscillations in the pressure solver have been reported [16], [17] and [18].

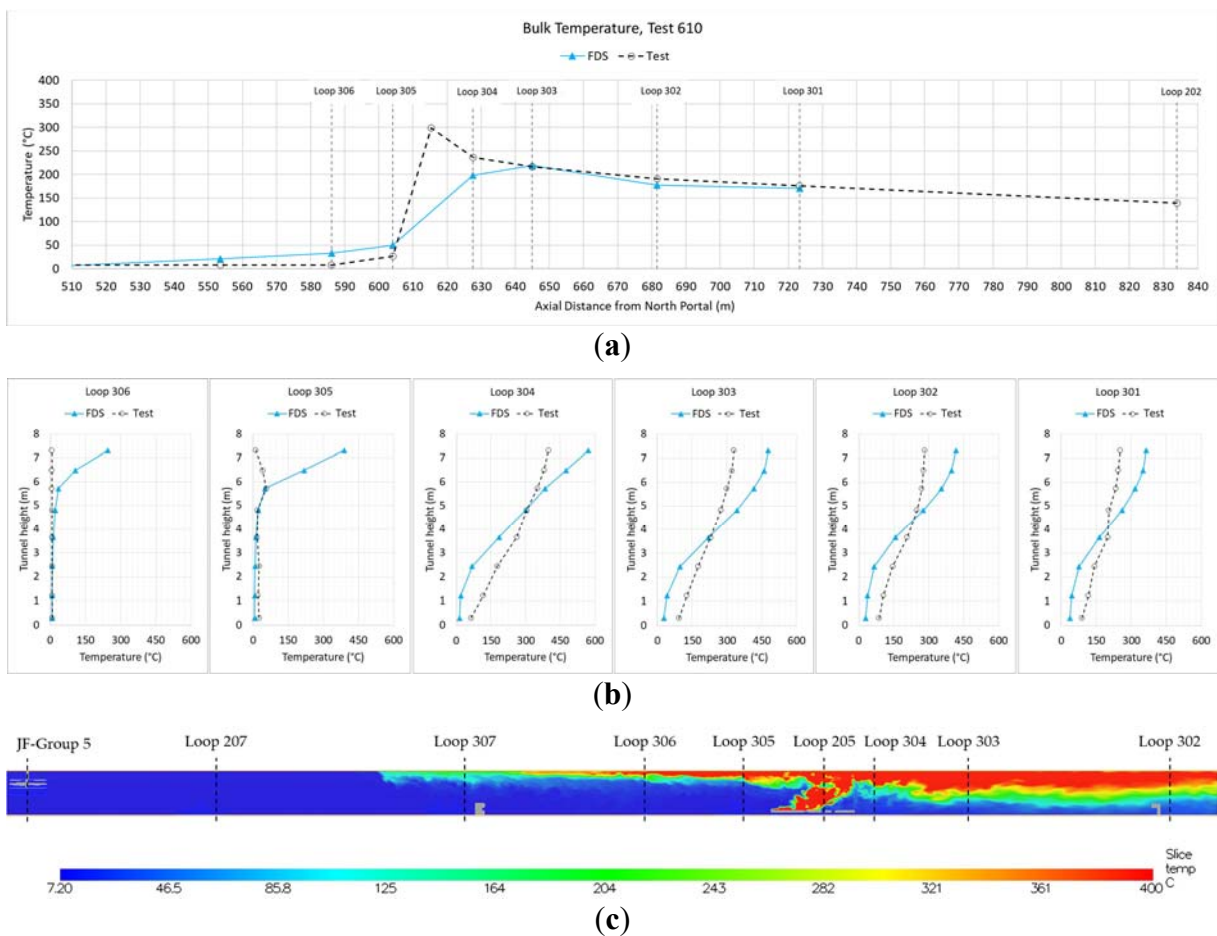


Figure 11. FDS simulation for 50 MW fire (Case 2 from Table 1) after reaching steady state conditions. Comparison of simulation results with test results for test 610: (a) Bulk temperature along the tunnel axis, (b) Temperature profiles over the tunnel height for different loops in the vicinity of the fire, (c) Contour plot of the temperature in °C through the middle of the tunnel and fire pans. Temperature is clipped to 400°C for a better visualisation of the temperature layering.

The current work finds that FDS is not predicting the flow field accurately for tunnel smoke control when applying reasonable parameters. A study for the U.S. Federal Highway Administration [19] explored simulation parameter variations that might bring FDS into some alignment with known data. Best agreement with the Memorial Tunnel test data was only

achieved by using a volumetric heat source, by making the mesh very coarse (0.4 m), and by using unrealistically large wall friction factors (Darcy Weisbach friction factor up to 0.183). Problems with volumetric heat sources are that the plume is artificially constrained, and the temperatures generated may not be real, as discussed earlier. Results from a coarse mesh cannot be relied on when the results vary strongly with mesh size as clearly demonstrated in [19]. When using reasonable parameters for wall friction and mesh size in FDS, the FHWA study [19] shows a considerable overprediction of backlayering. While the conclusions of the FHWA study imply some utility of FDS for tunnel smoke control when using unreasonable inputs, the detail presented supports the current findings. The FHWA work confirms in a more comprehensive way that, using credible simulation parameters, smoke propagation, temperature distribution, and the velocity needed for smoke control, are not predicted within a reasonable accuracy by FDS.

## 6. COMMENTARY AND CONCLUSION

In this CFD validation study, smoke propagation and temperature distributions for tunnel fires were analysed with different fire representations, and compared with the results from the Memorial Tunnel test program.

A volumetric heat source can predict the upstream smoke propagation with reasonable accuracy but provides a poor prediction of the temperature distribution downstream of the fire. However, the results are very sensitive to the heat source size. Without representing the whole flow field reasonably, agreement on backlayering may just result from 'lucky' tuning of an otherwise physically unrealistic approach. The volumetric heat source approach is not recommended as a reliable method.

The eddy-dissipation combustion model in Fluent represents the smoke propagation and temperature distribution with sufficient accuracy for small (10 MW) as well as big (100 MW) tunnel fires.

The results produced with FDS showed a clear overprediction of the upstream smoke propagation and also gave an unconvincing representation of the temperature distribution.

The complexity of the physics and the number of different flow regimes in the critical velocity and backlayering problem make reproduction by CFD very challenging. The answers can be very sensitive to input assumptions about which there is no 'right' answer (e.g. volumetric heat source size), and to modelling approaches, algorithms and coding (FDS, Fluent) as demonstrated here. Without a comparable validation case, the CFD cannot be relied on for design of tunnel smoke control.

The work done establishes a clear method for using CFD to design smoke control in the Memorial Tunnel. That is not directly useful, as the Memorial Tunnel is already designed, built, operated, de-commissioned, and tested for critical velocity. The question is how widely the above method can be applied to the design of new tunnels. The non-committal answer is that the method will be useful where the physics is sufficiently similar to that in the Memorial Tunnel tests. That probably means that is good for fires of 10 MW to 100 MW in all road tunnels designed for truck traffic (reasonably high clearance).

The validation was done for pool fires only. Whether the applied combustion technique can be stretched to other fire types e.g. solid fuel fires, fires with considerable obstructions, battery fires etc. might require further validation. Furthermore, the approach is for fires with a reasonable duration (approximately 20 to 30 minutes). Tunnel wall parameters would need to be re-evaluated when analysing smoke propagation for fires with a longer period than that. The same applies for tunnels with fire board on the walls or any other cover on the wall that limits

the heat transfer. Especially for analysing long-lasting fires, a transient simulation might be required to evaluate the influence of wall heating on the smoke propagation.

It is not clear that the smoke flow regimes in a wide tunnel are physically different to propagation of a smoke layer in a standard tunnel, such that a change in turbulence or combustion models would be called for. It seems likely that the CFD techniques presented here would have some usefulness for a very wide tunnel.

One case where some greater caution might be required is in tunnels where a ceiling velocity deficit is created by a proliferation of fittings (signs, lights, cable trays) above the traffic space. It seems possible that there could be unexpected interactions between smoke and a highly non-uniform velocity profile which requires an accurate representation of the vortices and turbulence induced.

The authors' view is that validation of the CFD system of (analyst + software + model choices) is likely to provide for a far better way of extrapolating from known test results to a particular tunnel, than is offered by any of the formulae past or present for critical velocity. There are no credible formulae for confinement velocity.

Conversely, unvalidated CFD can readily give either incorrect results, or for a more skilled analyst, whatever result the analyst wants. Unvalidated CFD should not be used for designing tunnel smoke control.

## 7. ACKNOWLEDGEMENTS

We thank Joe Gonzalez and Matthew Bilson for providing details and raw data of the Memorial Tunnel Fire Ventilation Test Program. That made it possible to have a better understanding of the test data.

## 8. REFERENCES

- [1] A. Lönnermark, "On the characteristics of fires in tunnels," Dissertation, Department of Fire Safety Engineering, Lund University, Lund, Sweden, 2005.
- [2] P. Sturm, M. Beyer and M. Rafiei, "On the problem of ventilation control in case of a tunnel fire event," *Case Studies in Fire safety, CSFS 22, Elsevier publishing, doi: 10.1016/j.csfs.2015.11.001*, 2015.
- [3] M. Beyer, C. Stacey and A. Dix, "Critical velocity and tunnel smoke control Part 2, Filling the NFPA 502 void," *Australian Tunnelling Society*, p. 6, 2021.
- [4] C. Stacey and M. Beyer, "Critical of critical velocity - An industry practioner's perspective," in *10th International Conference 'Tunnel Safety and Ventilation'*, Graz, 2020a.
- [5] MTFVTP, "Memorial Tunnel Fire Ventilation Test Program - Comprehensive Test Report," Bechtel/Parsons Brinckerhoff, Boston, 1995a.
- [6] MTFVTP, "Memorial Tunnel Fire Ventilation Test Program - Memorial Tunnel Test Data Report incl. 9 discs of raw data," Bechtel/Parsons Brinckerhoff, Boston, 1995b.
- [7] G. W. Kile and J. A. Gonzalez, "The Memorial Tunnel Fire Ventilation Test Program: The Longitudinal and Natural Tests," *ASHRAE Transactions 103, ProQuest Science Journals*, p. 701, 1997.

- [8] Ansys, Inc, "ANSYS Fluent User's Guide, Release January 2021 R1," USA, 2021a.
- [9] Ansys, Inc, "ANSYS Fluent Theory Guide, Release January 2021 R1," USA, 2021b.
- [10] Ansys, Inc, "ANSYS Fluid Dynamics Verification Manual, Release January 2021 R1," USA, 2021c.
- [11] K. McGrattan, S. Hostikka, R. McDermott, J. Floyd and M. Vanella, "Fire Dynamics Simulator User's Guide," National Institute of Standard and Technology, USA, 2013.
- [12] J. Gonzalez and M. Bilson, *Private communication - Sketches of measurement loops and test notes*, 2020.
- [13] K. Karki, S. Patankar, E. Rosenbluth and S. Levy, "CFD Modeler for Jet Fan Ventilation Systems," in *BHR Group 10th ISAVVT*, Boston, USA, 2000.
- [14] B. F. Magnussen and B. H. Hjertager, "On mathematical models of turbulent combustion with special emphasis on soot formation and combustion," in *16th Symp. (Int'l.) on Combustion*, 1976.
- [15] A. A. Attar, M. Pourmahdian and B. Anvaripour, "Experimental Study and CFD Simulation of Pool Fires," *International Journal of Combustion Applications (0975 - 8887)*, vol. Volume 70, no. No. 11, pp. 9-15, May 2013.
- [16] C. Ang, G. Rein and J. Peiro, "Unexpected Oscillations in Fire Modelling Inside a Long Tunnel," *Fire Technology*, no. 56, pp. 1937-1941, 2020.
- [17] K. McGrattan and R. McDermott, "Response to "Unexpected Oscillations in Fire Modelling Inside a Long Tunnel" by Ang et al," National Institute of Standards and Technology, Gaithersburg, Maryland, USA, 2022.
- [18] I. Riess, "Fixed Fire Fighting Szstems and Tunnel Ventilation," Riess Ingeneur-GmbH, Zürich, 2021.
- [19] T. Warren, S. Bartha, M. Bilson, B. Conell and E. Persson, "Fixed Firefighting and Emergency Ventilation Szstems for Highway Tunnels - Computer Modeling Report," U.S. Department of Transport, Federal Highway Administration, New York, 2022.

## SELECTION OF A ROAD TUNNEL VENTILATION SYSTEM USING VENTSIM SOFTWARE

<sup>1</sup>Zwolińska Klaudia, <sup>2</sup>Szmuk Andrzej, <sup>3</sup>Borowski Marek

<sup>1</sup> AGH University of Science and Technology, Krakow, Poland

<sup>2</sup> AGH University of Science and Technology, Krakow, Poland, <sup>3</sup> AGH University of Science and Technology, Krakow, Poland

### ABSTRACT

Designing the ventilation of a road tunnel is a demanding process, as it requires considering many aspects. Usually, the ventilation system, devices, and location of the elements are selected based on legal regulations and appropriate guidelines. Nonetheless, it should not be forgotten that each road tunnel is an individual case. The designer's main goal is to ensure safe and comfortable conditions for users. The analysis includes the operation of the ventilation system in a road tunnel for standard conditions and the case of emergency (occurrence of fire). In the study, VentSim software is used. Using this software allows simulating the flow of air during both normal operation and fire conditions. The paper presents the methodology of designing the ventilation system and the carried-out simulations. Based on the results, the operating parameters of the system and its individual components were determined. The model was prepared based on the construction concept, meteorological data for the surroundings, traffic forecasts, and traffic analysis for nearby areas. As the analysis shows, the use of numerical simulation makes it possible to predict airflow for changing conditions, which highly simplifies the designing process and increases the safety of tunnel users.

*Keywords: ventilation system, road tunnel, fire, safety.*

### 1. INTRODUCTION

In recent years around the world, numerous new road infrastructure investments have been realized or planned. Frequently in such projects, an issue of overcoming terrain obstacles occurs, including mountains, water reservoirs, and highly urbanized areas. Consequently, it is associated with the construction of new engineering facilities, including tunnels. Increasing needs and technical possibilities results in the construction of more and more modern tunnel facilities. There are several thousand road tunnels in operation around the world. They differ in length, width, construction method, and type of traffic.

During the fire, heat, smoke, and toxic products are generated, which may cause material damage and loss of health or even life of tunnel users. Heat is the cause of damage to the structure and technical installations in the tunnel. A primary hazard to people is the loss of visibility caused by smoke (which makes rescue more difficult) and the toxicity of fire gases. Similarly, fires pose a threat to the environment by emitting toxic smoke components into the atmosphere [1]. In terms of safety, the essential and crucial equipment of the tunnel is its ventilation system. The main tasks of the ventilation are to control airflow, remove fire smoke and gases, and enable the safe rescue of tunnel users [2]. The amount of generated smoke and heat depends on the size of the fire. It is assumed that the production of smoke and heat is proportional to the size of the fire, where smoke and gases are the product of incomplete combustion, and the amount of their emission depends on the combustion mechanism of materials. The larger the size of the fire, the more combustion products are generated. Therefore a larger airflow rate is needed to control the flow and remove smoke and hot gases [3].

This article presents ventilation systems for road tunnels when functioning in normal operating mode and during the fire.

## 2. CHARACTERISTICS OF FIRE DEVELOPMENT IN A ROAD TUNNEL

When a fire incident occurs, ventilation in the tunnel is started up in the so-called fire mode. The role of the system is to provide a controlled flow of smoke and fire gases in the tunnel and to discharge them outside the tunnel. The creation of a controlled flow of smoke and fire gases allows the evacuation of users with minimal smoke contamination of escape routes, preventing smoke intrusion to the access routes for rescue teams leading to the place of the incident. Typically, one ventilation system is used in tunnels for normal operation, emergency conditions, as well as in fire conditions. Nevertheless, for each operating mode, different ventilation system parameters are provided.

For tunnel ventilation, both natural and mechanical methods are used. In the light of the regulations in force in Poland, natural ventilation is used in tunnels of not more than 700 m in length for unidirectional traffic. For natural-ventilated tunnels with bidirectional traffic, the length of the tunnel should not exceed 500 m [4]. A limitation in the use of natural ventilation in fire conditions is the risk of an uncontrolled process of fire gas flow. According to NFPA [2], three types of mechanical tunnel ventilation could be distinguished, i.e., longitudinal, transverse, and mixed systems. Whereas, Directive [5] introduces the division of mechanical ventilation systems into longitudinal, semi-transverse and transverse. In longitudinal ventilation systems, the air flows along the tunnel, usually from the inlet portal to the outlet portal. The air movement is forced by the operation of fans located inside the tunnel, e.g., jet fans suspended under the tunnel ceiling or fans installed in the supply and exhaust shafts. Typically, longitudinal ventilation is designed, with axial fans arranged inside the tunnel every 60-120 m. This solution does not require routing of ventilation ducts under the roadway or tunnel ceiling. The fans are to ensure smoke removal over the entire length of the tunnel, and speed of air flow through the tunnel should prevent smoke backflow by providing so-called critical speed. Transverse ventilation is used in long tunnels with heavy traffic, as it allows even distribution of air along the entire length of the tunnel and removal of solid and gaseous pollutants emitted by the vehicles. This solution requires routing supply ducts inside the tunnel, usually under the tunnel roadway, and the gas stream is removed through a ventilation duct located under the tunnel's ceiling. In such a ventilation system, air is supplied at the height of vehicle wheels and discharged under the ceiling of the tunnel. Mixed (semi-transverse) ventilation is a combination of transverse and longitudinal ventilation. Ventilation systems in road tunnels are designed for maximum fire power. Figure 1 shows the principle of operation of the longitudinal and transverse systems during a fire.

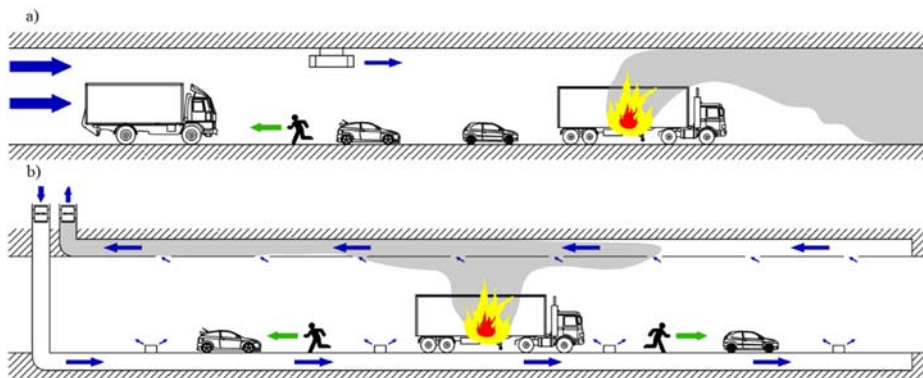


Figure 1: Ventilation of the road tunnels (a) longitudinal system (b) transverse ventilation



### 3. ANALYSIS OF SELECTED ROAD TUNNEL - CASE STUDY

#### 3.1. Assumptions for calculations

The subject of the analysis in the article is the concept of technical equipment in the ventilation system of the TS-33.7 tunnel on the S6 road. The cross-sections of the ventilation ducts were adopted according to the assumptions presented in Figure 2.

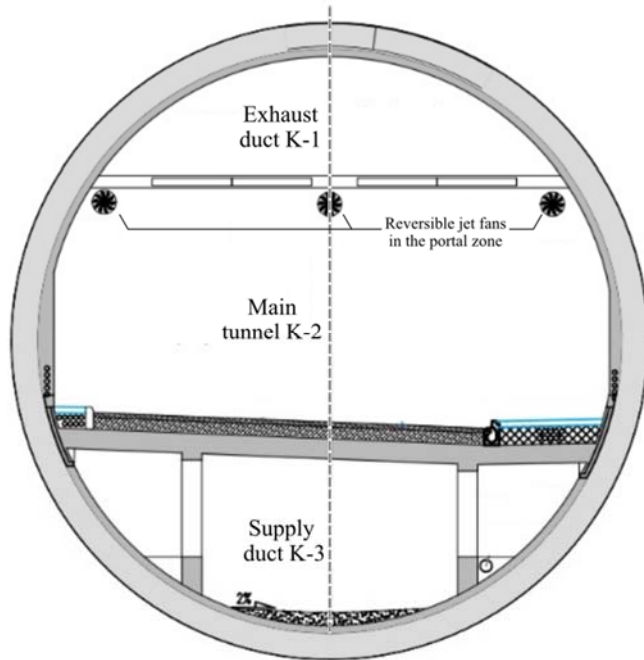


Figure 2: Division of the tunnel cross-section into ventilation ducts

The transverse ventilation system works based on separated functional channels (table 1):

- Smoke exhaust duct **K-1** located under the main ceiling. During normal operation, it is used for exhaust gas extraction along the entire length of the tunnel. During the fire and rescue operation, it allows for the removal of hot air and smoke from the section covered by the fire.
- The main tunnel **K-2**. It is the central space of the tunnel, used to guide vehicle traffic, divided into smoke removal sections with ceiling flaps
- Clean air duct **K-3**. The duct underneath the roadway supplies clean air into the main tunnel K-2 space. The air flows through the duct under the road and is further distributed using transverse ducts with outlets at a height of about 20 cm above the pavement.

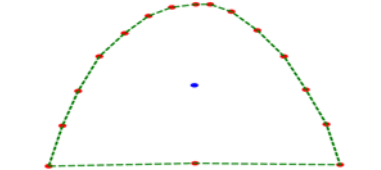
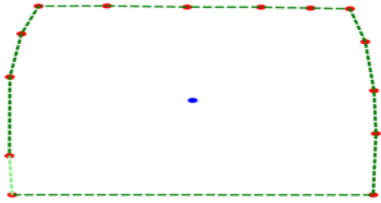
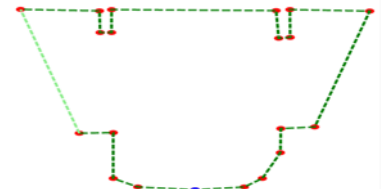
Table 1. Characteristic parameters of the ducts/tunnels:

Duct/ tunnel	Cross-sectional area, m <sup>2</sup>	Length, m	Volume, m <sup>3</sup>
<b>K-1</b>	23,7	5230	123 951
<b>K-2</b>	79,3	5330	422 669
<b>K-3</b>	36,5	5230	190 895

VentSim DESIGN software provided by Howden company was used in this study. Software is a comprehensive package for the design and analysis of mine and tunnel ventilation systems. During the design phase, VentSim enables 3D modeling of the ventilation system, ensuring an

understanding of possible solutions. The system performance could be simulated based on expected operating conditions and evaluated to allow for the selection of an optimized design. The mapping of the cross-sectional area for each part was prepared using the Ventsim DESIGN software. Details are presented below in Table 2. For individual cross-sections, the airflow resistance of the ducts was assumed.

Table 2. Mapping of ducts/tunnels

Duct	Cross-section	Cross-sectional area, m <sup>2</sup>	Details
K1		23,7 m <sup>2</sup>	R= 0,0090 kg/m <sup>7</sup> Concrete duct
K2		79,3 m <sup>2</sup>	R= 0,0419 kg/m <sup>7</sup> Concrete tunnel with "blocked" car traffic
K3		36,5 m <sup>2</sup>	R= 0,0150 kg/m <sup>7</sup> Irregular duct

The view of the duct connection in the ventilation system model in Ventsim Design is shown in Figure 3. Figure 4 shows the entire model of the road tunnel.

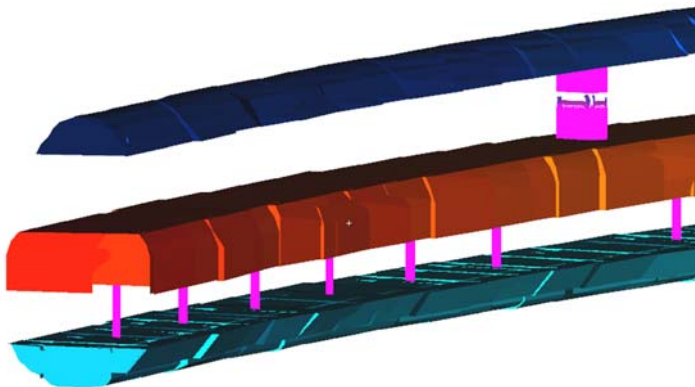


Figure 3: Arrangement of ventilation ducts in the model in the Ventsim Design software

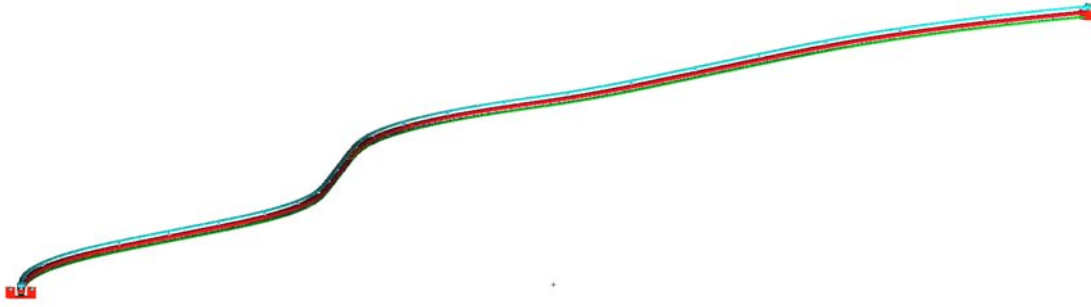


Figure 4: Tunnel model in Ventsim Design software

The view of the ventilation ducts and the mapping of the fan stations are shown in figure 5.

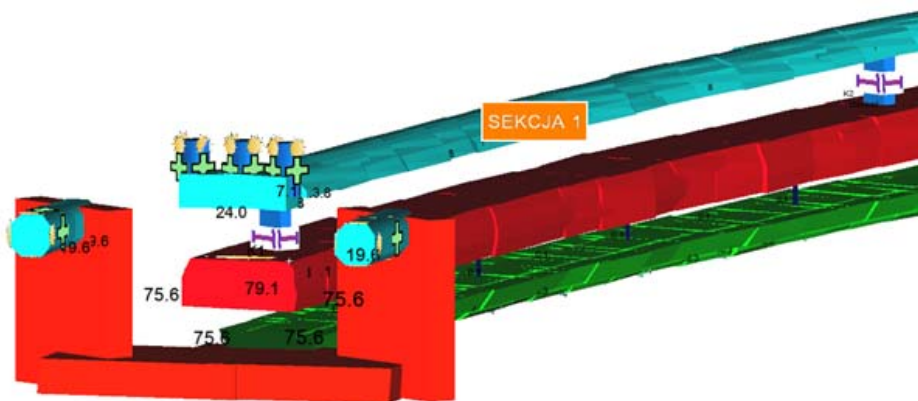
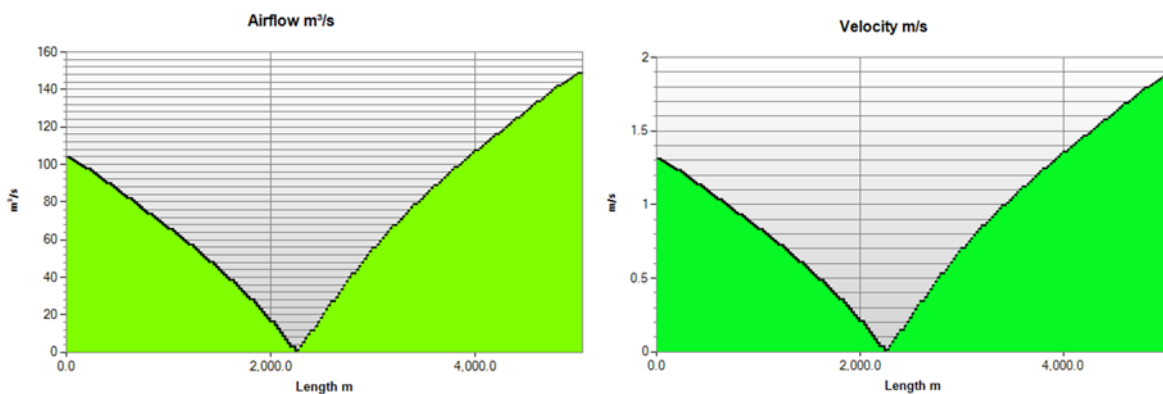


Figure 5: Mapping of ventilation ducts and stations in fans in the Ventsim Design software

The calculations were carried out assuming that the temperature in the summer period is 23 °C and for the winter period it is -3 °C. It results from the location of the tunnel. Additionally, west wind with a maximum value of 10 m / s was assumed, which generates a pressure thrust on the portal of 50 Pa.

### 3.2. Calculations of ventilation parameters

The results of calculations of the airflow and velocity as well as the pressure distribution in the tunnel are shown in Figure 6. The figures show asymmetry in the air distribution and pressure distribution in the tunnel due to the effect of wind. The westerly wind was considered with a barometric pressure difference of 50 Pa between the tunnel inlets.



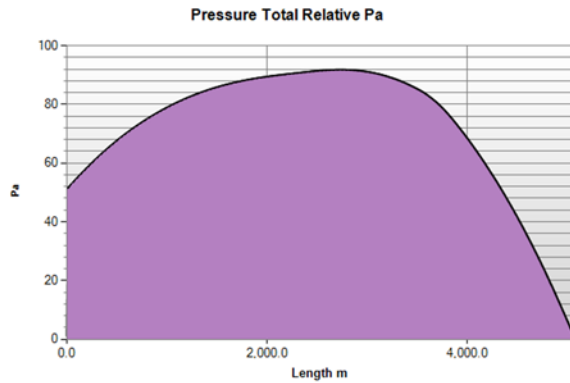


Figure 6: Changes in airflow and velocity, and total pressure distribution in Ventsim Design software

The results of the fan parameters calculation for the airstream of 260 m<sup>3</sup>/s in the K1 and K3 ducts are shown in Table 3.

Table 3: Calculations of the parameters of ventilation ducts

System	Airflow of fans	Flow resistance	Total pressure	Summary
<b>Duct K-3 (Supply ventilation)</b>	4 x 65 m <sup>3</sup> /s (2 fans on each side of the tunnel)	Pressure loss in ducts: 270 Pa Pressure loss on silencers and outlets: 300 Pa (assumed)	Pc = 570 Pa + 30 % = 740 Pa	740 Pa (at 80% of total stagnation pressure) the volume rate is 65 m <sup>3</sup> /s each
<b>Duct K-1 (Exhaust ventilation)</b>	6 x 44,3 m <sup>3</sup> /s (3 fans on each side of the tunnel)	Pressure loss in ducts: 816 Pa Pressure loss on silencers and outlets: 300 Pa (assumed)	Pc = 1116 Pa + 30 % = 1450 Pa	1450 Pa (at 80% of total stagnation pressure) the volume rate is 44,3 m <sup>3</sup> /s each

The calculations show that for the amount of air which is 260 m<sup>3</sup>/s, the maximum pressure loss in the K-3 supply duct is 740 Pa. On the other hand, the maximum pressure loss in the K-1 exhaust duct is 1450 Pa.

### 3.3. Ventilation analysis for a fire located in the middle of the tunnel (13th section)

A scenario was assumed in which a gasoline tanker accident occurs:

- 0 min - 5 min - Start of fire - burning gasoline at a rate of 0 to 8300 kg/h,
- 5 min - 2 hours and 5 min - constant fire - burning gasoline at the rate of 8300 kg/h,
- Peak fire heat release rate: 101 kW,
- The calculations for 2 open fire dampers,
- The calculations for airflow rate: 260 m<sup>3</sup>/s.

Figure 7 shows the location of the fire in the middle of the tunnel for section 13. Figures 8 and 9 show the changes in power and temperature of the fire and changes in the volume rate of air in the ventilation duct exhausting fire fumes, respectively. The performed calculations confirmed the parameters of the designed road tunnel ventilation system.



Figure 7: Location of a fire in a tunnel in Ventsim Design

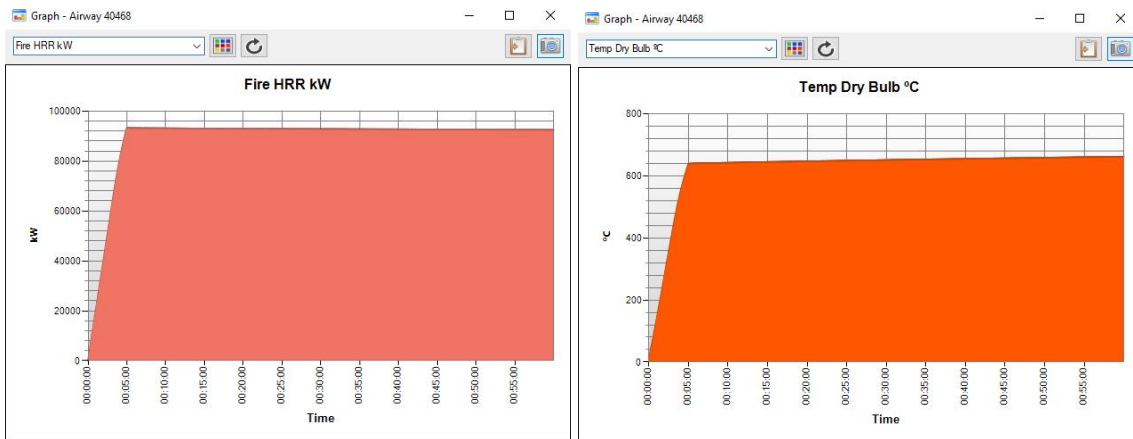


Figure 8: The power of the fire and the temperature changes in the fire location over time

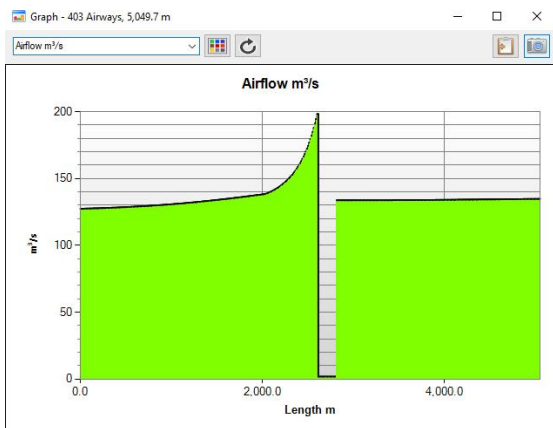


Figure 9: Airflow rate distribution (volume flow) in the exhaust air duct K1.

#### 4. SUMMARY AND CONCLUSION

Regardless of the ventilation system used, the parameters of this system are designed for maximum firepower, taking into account the emission of fire gases produced. The properly designed ventilation system should provide a controlled flow of smoke and fire gases as well as discharge them outside the tunnel. Two primary concepts of fire ventilation solutions are used for these aims. Longitudinal flow is mostly applied for short or unidirectional tunnels,

while exhaust ducts are for long and bidirectional tunnels. In Polish conditions, tunnels are usually built as twin-tube tunnels, which allows for unidirectional traffic. The only exceptions are two tunnels: Emilia (in operation) and under Świnna (under construction), which were designed as bidirectional.

In summarizing, it is observed that designers prefer longitudinal ventilation, which is the most likely applied (if the regulations allow it). In the case of the long tunnels where the lengths do not exceed 3000 m, it is proposed to use semi-transverse ventilation with air supply through the ducts under the roadway and air discharge through the tunnel using jet fans installed under the tunnel ceiling. Such solutions are dictated by economic considerations because the installation of longitudinal or semi-transverse ventilation is less expensive than the installation of fully transverse ventilation.

Of course, the implementation of each of the proposed solutions should be adjusted individually to the designed tunnel. Hence, it is necessary to confirm the correctness of the proposed solution in terms of ensuring safe conditions of operation. As the analysis shows, the use of Ventsim Design software allows for determining the parameters of the road tunnel ventilation system and checking its operation during a fire. The occurrence of a fire is the most important test for the designed system. Therefore, checking the operation in this mode is crucial. Based on the simulation, it is possible to determine whether the proposed airflow rate and selected fans could provide the appropriate conditions and meet the assumed requirements.

## 5. REFERENCES

- [1] Beard A., Carve R., 2012. Handbook of Tunnel Fire Safety, 2nd Edition. ISBN: 0727741535 / 9780727741530.
- [2] NFPA 502. 2014. Standard for Road Tunnels, Bridges, and Other Limited Access Highways, NFPA, Quincy.
- [3] NCHPR. 2011. Report no 425, Design Fires in Road Tunnels, ISBN 978-0-309-14330-1.
- [4] Regulation of the Minister of Transport and Maritime Economy of 30 May 2000 on technical conditions to be met by road engineering structures and their location (Journal of Laws 2007, no 63, item 735).
- [5] Directive 2004/54 / EC of the European Parliament and of the Council of 29 April 2004 on the minimum safety requirements for tunnels in the trans-European road network.

# ON HEAT TRANSFER COEFFICIENTS AND TEMPERATURE DISTRIBUTION IN LONGITUDINALLY VENTILATED TUNNEL FIRES

<sup>1</sup>Milan B. Šekularac

<sup>1</sup>University of Montenegro, Mechanical Engineering faculty(MNE)

## ABSTRACT

Various approximate methods, and guidelines, are followed by tunnel-ventilation designers in the process of sizing the ventilation system. Of particular importance are the heat transfer coefficients used in prediction of the temperature distribution during a fire event. This strongly affects the ventilation exerted trust, and induces a chimney-effect pressure in sloped tunnels. For this purpose, a one-dimensional numerical solution approach is used in this work to evaluate their values. In addition, processing of a selected tunnel-fire-test from the literature data is also used in order assess the heat transfer coefficients values from realistic fire-tests. The results are discussed for final conclusions.

*Keywords: longitudinal tunnel ventilation sizing, fire scenario, transient heat transfer, convection, radiation, conduction, heat transfer coefficients, chimney effect*

## Nomenclature

$a$  – thermal diffusivity ( $m^2/s$ )

$A$  – area of tunnel cross-section ( $m^2$ )

$c_p$  – specific heat of the gas mixture, at a constant pressure ( $J/kgK$ )

$D_h$  – hydraulic diameter,  $4A/P$

$f_D$  – Darcy friction coefficient (-)

$F$  – view factor for radiative heat transfer,

$h$  – coefficient of heat transfer ( $W/m^2 K$ )

$\dot{m}$  – mass flow rate ( $kg/s$ )

$n$  – exponent in the Nusselt number correlation

$Nu$  – Nusselt number,  $hD_h/k$

$Pr$  – Prandtl number,  $\nu/a$

$P$  – perimeter of the tunnel cross-section (m)

$p$  – pressure (Pa)

$\dot{Q}$  – fire heat release rate ( $W$ )

$Re$  – Reynolds number,  $uD_h/\nu$

$s$  – tunnel slope (%)

$St$  – Stanton number,  $Nu/(RePr)$

$T$  – temperature (K)

$u$  – averaged velocity of the gas mixture (m/s)

$y$  – wall-normal coordinate

*Greek symbols*

$\lambda$  – heat conduction coefficient (W/mK)

$\phi$  – heat flux transferred to the tunnel wall (W/m<sup>2</sup>)

$\rho$  – average density of the gas mixture (kg/m<sup>3</sup>),

$\nu$  – kinematic viscosity (m<sup>2</sup>/s),

$\varepsilon$  – coefficient of emission,

$\sigma$  – Stefan–Boltzmann constant (W/m<sup>2</sup>K)

*Subscripts*

$a$  – air

avg – averaged value over the tunnel cross-section

$c$  – convection

$cc$  – convection + conduction

$ch$  – chimney

$cr$  – convection + radiation

$crc$  – convection + radiation + conduction

$m$  – mean value over the tunnel length

$r$  – radiation

$w$  – wall

## 1. INTRODUCTION

The critical regime for longitudinal ventilation system sizing, appears at approx. 15 min after fire onset, when the evacuation of tunnel users is over and fire-suppression and extinction by the fire brigade commences. Of particular importance is the ability to calculate the distribution of the gas-average temperature (at cross section) along the tunnel, at that point in time. The gas-average temperature distribution affects ventilation sizing by: gas acceleration along the tunnel that increases wall friction losses; the chimney-effect is induced in sloped tunnels; the ventilation thrust deteriorates due to a reduced gas density, i.e. mass flow through the fans.

Attention in this paper is given to the heat transfer coefficients, their proper definition, calculation and use in ventilation sizing, which seems overlooked in literature. Thus, a topic where the designer might encounter some difficulty. To this end, a one-dimensional numerical



approach is used, preceded by an assessment on proper use of literature data and heat transfer formulae. In addition, an assessment resulting from processing the literature-available measurement-data obtained during a real-scale-tunnel fire-test, is given.

The energy equation of the gas stream in the tunnel can be written in the form [1], [2]:

$$-\dot{m}c_p \frac{1}{P} \frac{dT_{avg}}{dx} = \dot{q}_c'' + \dot{q}_r'' \quad (1)$$

where  $\dot{q}_c'' = h_c(T_{avg} - T_w)$ , and  $\dot{q}_r'' = F\sigma(\epsilon_g T_{avg}^4 - \alpha_g T_w^4)$ , are local convective and radiative heat transfer rate fluxes from the gas to the tunnel wall, respectively, in  $[W/m^2]$ , [2],[3], whereas conduction heat flux inside the wall, in the wall-normal direction  $y$ , is:  $\dot{q}_{cond}'' = -\lambda(\partial T_w / \partial y)$ . We can define heat transfer coefficients accounting for:  $h_c$  - convection only,  $h_r$  - radiation only, the  $h_{cr}$  - joint convection-radiation (each related to the gas-average to wall-surface temperature difference), and an overall-heat-transfer coefficient (convection-radiation-conduction),  $h_{crc}$  (related to gas-to-rock massive temperature diff.), where the undisturbed wall (rock-mass) temperature  $T_\infty$  is used. Thus, these definitions read:

$$h_c = \frac{\dot{q}_c''}{T_{avg} - T_w}, h_r = \frac{\dot{q}_r''}{T_{avg} - T_w}, h_{cr} = \frac{\dot{q}_c'' + \dot{q}_r''}{T_{avg} - T_w}, h_{crc} = \frac{\dot{q}_c'' + \dot{q}_r''}{T_{avg} - T_\infty}, \quad (2) \text{ (a, b, c, d)}$$

For example, in the literature approaches, the following approximate solutions for the temperature distribution and the chimney-pressure-effect, for use with  $h_{crc,m}$  only, can be found [2], [4],[5],[6], in the form:

$$T_{avg}(x, t) = T_\infty + [T_{max} - T_\infty] e^{-\frac{h_{crc,m} P x}{\dot{m} a c_p}} \quad (3)$$

$$T_{max} = T_a + \eta_r \frac{HRR}{\dot{m} a c_p} \quad (4)$$

$$\Delta p_{ch} = -\frac{\rho_a g s \dot{m} a c_p}{100 h_{crc,m} P} \ln \frac{\eta_r \frac{HRR}{\dot{m} a c_p} e^{-\frac{h_{crc,m} P L}{\dot{m} a c_p}} + T_a}{T_a + \eta_r \frac{HRR}{\dot{m} a c_p}} \quad (5),$$

where:  $HRR$  is the heat-release-rate of the fire,  $L$ -affected length,  $P$ -tunnel perimeter,  $s$ -tunnel slope,  $\eta_r$  (in the range:  $2/3 - 3/4$ ) is the portion of the  $HRR$  available past the local (flame-to-wall) radiative  $HRR$  loss, and the index  $m$  is added in this work to the overall-heat-transfer coefficient  $h_{crc}$  to denote its *mean value over the considered fire-affected length  $L$* . One can assume the cold flow air temperature  $T_a$  and  $T_\infty$  (rock massive undisturbed temperature) to be approx. equal - these were further denoted jointly as  $T_0$ .

## 2. ANALYSIS OF DATA

The following input data, corresponding to a typical horseshoe-shape cross-section 2-lane highway road-tunnel were used as a generic-tunnel numerical example, Table 1.

Table 1: Input data for a generic road-tunnel case computed numerically

Tunnel cross section area $A_t$ [m <sup>2</sup> ]	Considered tunnel length $L_t$ [m]	$D_h$ Tunnel hydraulic diameter[m]	Inflow air velocity: $u_{cr}$ [m/s]	$HRR_{max}$ [MW]	Effective Darcy friction factor $f_D$	Tunnel wall thermal properties
55.1	800	7.7	3	50	0.0275	$\lambda = 1.65$ W/mK $\rho = 2400$ kg/m <sup>3</sup> $c = 920$ J/kgK

The  $HRR(t)$  time-dependence is taken from [2]: a linear increase over 10 min time (0 to  $HRR_{max}$ ), followed by a constant max. value over 10 min time, and a linear decrease back to zero over additional 10 min. A numerical simulation time of 15 min from the fire-onset was selected for the computation presented in sec.2.1., as discussed in the introduction.

### 2.1. One-dimensional numerical solution of the generic example

A transient distribution of tunnel's cross-section flow-averaged variables (density, temperature, pressure, velocity in the tunnel-axis direction) are numerically computed by solving 1D continuity, momentum and energy differential equations of flow using a specialized software package [7], without simplifications required for simplified solutions. Thus, the results can be considered reliable, and its purpose is to serve designers in sizing of the ventilation systems. To this end, it computes the transient temperature distribution of the tunnel wall numerically. The wall temperature is considered as locally dependent on wall normal coordinate and time only, but the solution is carried out independently at numerical locations spread along the tunnel axis  $x$ , spanning the considered tunnel length. The details of the governing numerical model, discretization and the solution procedures can be found in [7]. The heat convection coefficient in this numerical procedure is calculated using Petukhov equation with the user-input of Darcy (Moody-chart) friction factor  $f_D$  value. The heat radiation is accounted for by means of an equivalent heat transfer coefficient  $h_r$ , eq.(2.b). The variables are obtained as cross-section averages, functions of time and the  $x$ -distance. The computed distributions are given in Fig.1.

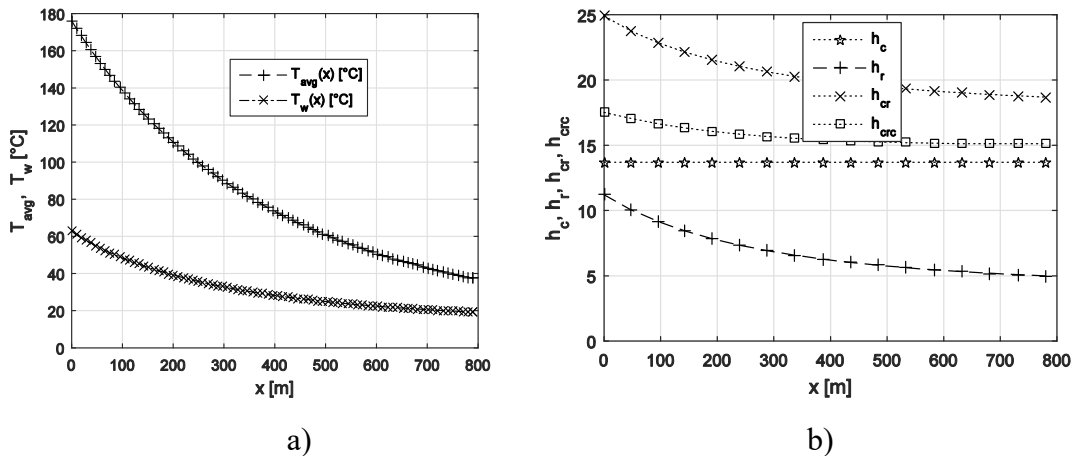


Fig.1. Numerically computed results for the generic-tunnel example in Table1: a) Gas-average and wall-average temperatures,  $T_{avg}(x)$ ,  $T_w(x)$ , b) Heat transfer coefficients:  $h_c$ ,  $h_r$ ,  $h_{cr}$ ,  $h_{crc}$

In Table 2. the mean values for the heat transfer coefficients are given. They are defined as:

$$h_{*,m} = \frac{\int_0^L h_*(T_{avg}(x) - T_w(x)) P dx}{\int_0^L (T_{avg}(x) - T_w(x)) P dx}, \quad h_* \text{ is: } h_c(x), h_r(x), \text{ or } h_{cr}(x) \quad (6)$$

$$h_{crc,m} = \frac{\int_0^L h_{crc}(T_{avg}(x) - T_0) P dx}{\int_0^L (T_{avg}(x) - T_0) P dx} \quad (7)$$

Table 2: Computed mean values of heat-transfer coefficients for the generic road-tunnel numerical case

HRR	$h_{c,m}$	$h_{r,m}$	$h_{cr,m}$	$h_{crc,m}$
50 MW	13.7	7.53	21.33	16.1

## 2.2. Literature predictions for the friction factor $f_D$ and the convective coefficient $h_c$

Comparisons given bellow are for the same generic-tunnel example used in sec.2.1. (fluid properties:  $Pr=0.7$ ,  $T_0=288K$ ,  $T_m=98^\circ C=372K$ :  $\nu=2.2986 \cdot 10^{-5} \text{ m}^2/\text{s}$ ,  $\lambda_{am}=0.0316 \text{ W/mK}$ ). The velocity and the resulting Re numbers, obtained by use of linear-mean or true mean value for gas temperature ( $\sim 98^\circ C$  vs  $\sim 70^\circ C$ , respectively), are:  $u_m = 3.87 \mid 3.57$ , respectively, and Re:  $1.31 \cdot 10^6 \mid 1.33 \cdot 10^6$ . The cold airstream approaching the fire has a Re value:  $1.57 \cdot 10^6$ .

Civil engineering literature provides values for concrete tunnel-wall absolute roughness:  $\sim 3\text{-}9 \text{ mm}$ , thus the Darcy friction factor values, at the Re number given above ( $Re \approx 1.33 \cdot 10^6$ ) by Moody-chart based predictions are:  $f_D = 0.011 \mid 0.016 \mid 0.020$ , for: smooth, minimally rough, maximally rough tubes, respectively. However, the common understanding [8], [9] for cast-concrete-lining traffic-tunnels is that the effective value of the Darcy friction factor  $f_D$  is of the order  $\approx 0.025\text{-}0.030$ , based on real-scale experiments, at Re numbers of interest (critical velocity for smoke control, or higher). A value of  $f_D=0.0275$  is selected and used further as input-data value for all the calculations in this paper, of the generic-tunnel example-case. With rock / sprayed-concrete tunnel linings,  $f_D$  can reach much higher values, which will be discussed later.

### 2.2.1. Smooth-tube tunnel convection coefficient $h_{c,s}$ values

The following values can be obtained by using literature correlations [3], [10]:

$$\text{General formula: } h_{c,s} = 0.0265 \cdot Re_m^{0.8} \cdot Pr^{0.333} \cdot \lambda_{am} / D_h = \dots = 7.58 \text{ W/m}^2\text{K} \quad (8)$$

$$\text{Sieder-Tate formula: } h_{c,s} = 0.027 \cdot Re_m^{0.8} \cdot Pr^{0.3} \cdot \lambda_{am} / D_h \cdot (\nu_m/\nu)^{0.14} \dots = 8.11 \text{ W/m}^2\text{K} \quad (9)$$

$$\text{Newman formula: } h_{c,s} = 0.026 \cdot Re_m^{-0.2} \cdot (1 + (D_h/1500)^{0.7}) \cdot 1.2 \cdot 1010 \cdot u_m = 7.48 \text{ W/m}^2\text{K} \quad (10)$$

$$\text{Petukhov: } h_{c,s} = \frac{\frac{f_D}{8} c_p \rho u}{1.07 + 12.7 \left( Pr^{\frac{2}{3}} - 1 \right) \sqrt{\frac{f_D}{8}}} = \dots = 5.03 \text{ W/m}^2\text{K} \quad (11)$$

### 2.2.2 Rough-wall tunnel heat convection coefficient $h_{c,r}$

The tunnel-ventilation designer can either use the Petukhov formula, with the appropriate friction factor  $f_D$  value, which here the previously adopted value is  $f_D=0.0275$ , and obtain:  $h_c = 13.7 \text{ W/m}^2\text{K}$ . Otherwise, one can use a specific formula by Norris [10], based on forced-convection experiments in rough-wall tubes, eq. (12). This formula gives a prediction for rough-tube forced convection coefficient as a function of its value in the smooth-tube flow at the same Re number, and the ratio of Darcy friction factor values (for rough vs. smooth tube-wall), in the form:

$$h_{c,ro} = h_{c,sm} \left( \frac{f_{D,ro}}{f_{D,sm}} \right)^n, n = 0.68 \cdot Pr^{0.215} \quad (12)$$

with:  $h_{c,sm}$  - the convective heat transfer coefficient for smooth-tube flow,  $f_{D,ro}/f_{D,sm}$  - a ratio of friction factors (both at the same Re number),  $n$  - the exponent depending on the fluid's Prandtl number (here further taken as  $0.7$ , thus  $n = 0.6298$ ). With an important note [10] that there is an upper limit for the formula eq.(12), occurring at the value of roughness which produces the Darcy friction factor 4 times higher than its smooth-tube-flow variant at the same Re number. A further increase of tube roughness above that value does not result in increase of  $h_c$ . This means that for fluid properties approx. equal to air ( $Pr=0.7$ ), a maximum increase factor for  $h_c$  due to friction (*rougher walls*) is of the order:  $\cdot 2.394$  or by 140%, compared to the smooth wall. For the generic-tunnel used here, such limit would be encountered at  $f_{D,ro} = 4 \cdot f_{D,sm} \approx 0.044$ . Depending on the formula one adopts to calculate the smooth tube case (*the Sieder-Tate, the Petukhov, or the Newman formula*), the following  $h_c$  value result for the *rough-wall* case, using the generic-tunnel example input-data:  $h_{c,ro} = 14.45 \mid 8.97 \mid 13.32 \text{ W/m}^2\text{K}$ , respectively, by the use of Norris formula, eq.(12). It is worth noting the effect that the surface roughness, and

the selected formula, plays on  $h_c$ , within the range of  $f_D$  values relevant in tunnel ventilation. Using input data for the generic-tunnel example, the following result is obtained, Fig.2.

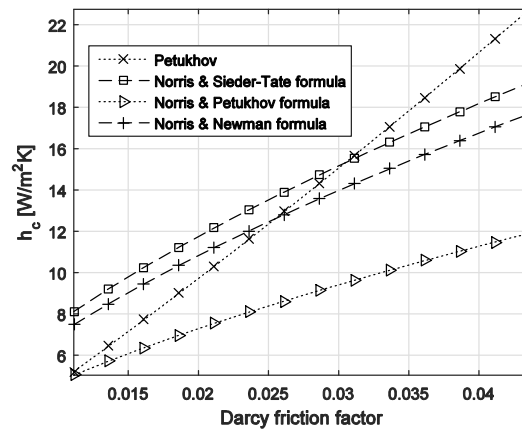


Fig.2. Effect of the Darcy friction factor  $f_D$  on  $h_c$  [W/m²K] value in the relevant  $f_D$  range according to the limit by Norris ( $f_{D,sm} - 4f_{D,sm}$ ) [10], for the generic-tunnel example-data ( $f_{D,sm}=0.0111$ ,  $u=3$  m/s,  $D_h=7.7$ m,  $HRR=50$ MW,  $T_{ref}=0.5(T_{avg,max}+T_0)=372$ K)

A different formula for smoke-to-ceiling convection coefficient  $h_c$  in fire-engineering was used by Zhao et al. [11], to evaluate convection between hot smoke layer and walls but it should be used with a modified *wet perimeter* value of the smoke layer only and will not be discussed here.

### 2.3. Analasys of a real-scale tunnel-fire test data

The data selected correspond to literature-available tunnel-fire test in Norway, (“Runehamar” tunnel) [5]. Conclusions from processing the 70MW and 120MW HRR-value data will be analysed here only. The data correspond to approx. 15-20 min of time from the fire onset. For the 70 MW case, the relevant reported data [5]:  $HRR_{max}=70$ MW,  $P(0-53m)=22$ m,  $P(53-L)=27$ m and  $D_h \approx 7$ m, initial  $u_0 \approx 3.15$  m/s but reduces upon fire development to  $u_0 \sim 2.5$ m/s, fluid properties at  $T_m=436$  K ( $\nu = 30.31 \cdot 10^{-6}$  m²/s,  $\lambda_{am} = 0.0363$  W/mK),  $f_{D,sm} = 0.01145$ ,  $f_{D,ro} = 0.0585$  (thus  $> 4f_{D,sm} = 0.04575$ ), and estimated wall-temperature in fire-near area  $> \sim 100^\circ$ C. The very high relative roughness of the walls (average absolute roughness over 300mm) where these tests were taken, resulted in a reported Darcy friction factor value:  $f_{D,r}=0.0585$ . Data from these tests are available as temperatures measured at two different heights above road surface,  $T_L$  and  $T_C$ , along the tunnel length, which allowed to calculate the estimate for the average-temperature  $T_{avg}(x)$  in this work.

#### 2.3.1. Analysis of the fire-test data and the heat transfer coefficients $h_c$ , $h_r$ , $h_{cr}$ , $h_{crc}$

The following values for  $h_c$ , as the literature-based prediction values, in 70 MW fire-test were obtained: Petukhov (*smooth tube vs rough tube*) case:  $8.11 \mid 36.29$  W/m²K; Norris (with Petukhov for  $h_{c,sm}$ ):  $19.41$  W/m²K, and Norris (with Sieder-Tate for  $h_{c,sm}$ ):  $21.47$  W/m²K. The rough-wall value obtained using Petukhov formula is hardly valid, since the limit  $f_{D,ro}=0.0585 > 4f_{D,sm} = 0.04575$ , given by Norris eq.(10), is met. Thus, the latter two values obtained by use of Norris formula are recommended:  $19.41 \mid 21.47$  W/m²K. For the overall heat transfer coefficient  $h_{crc,m}$ , a best-fit interpolation value of  $\sim 25$  W/m²K was proposed by Ingason in [5], along with use of  $\eta_r$  value 2/3, for use in the approximate-type solutions, eqs.(2)-(3), [2], [5].

Using the above computed  $h_{c,ro}$  value  $21.47$  W/m²K further, the temperature-data processing was carried out to estimate the heat transfer coefficients:  $h_c$ ,  $h_r$ ,  $h_{cr}$ ,  $h_{crc}$ , their

distribution along the tunnel, and their mean values, at the time of the measurements ( $\sim 15-20$  min from fire onset). Ceiling height in this test-tunnel was  $\approx 6\text{m}$ , and temperature measurements were done at:  $1.8\text{m}$  ( $T_L$ ) above road and  $0.3\text{m}$  under ceiling ( $T_C$ ). Assuming local gas velocity to adhere to the relationship  $u = u_0 T/T_0$  [1],[2], using ideal-gas equation of state,  $\rho = \rho_0 T_0/T$ , assuming a roughly linear variation of gas temperature with height, one can obtain an interpolated value estimate for  $T_{avg}(x)$ . The temperature measurement was not available from these tests near the maximum-temperature location (fire-site). But, since  $T_{avg}(x)$  must initiate from a thermodynamically-constrained  $T_{avg,max}$  value, using a recommended radiative loss factor  $\eta_r = 2/3$ ,  $T_{avg,max} = T_0 + \frac{\eta_r \cdot HRR}{\dot{m} c_p}$ , the interpolated  $T_{avg}(x)$  distributions are obtained from the fire-site downstream, and shown in Fig.3.a using  $\eta_r = 1 \mid 3/4 \mid 2/3$  value.

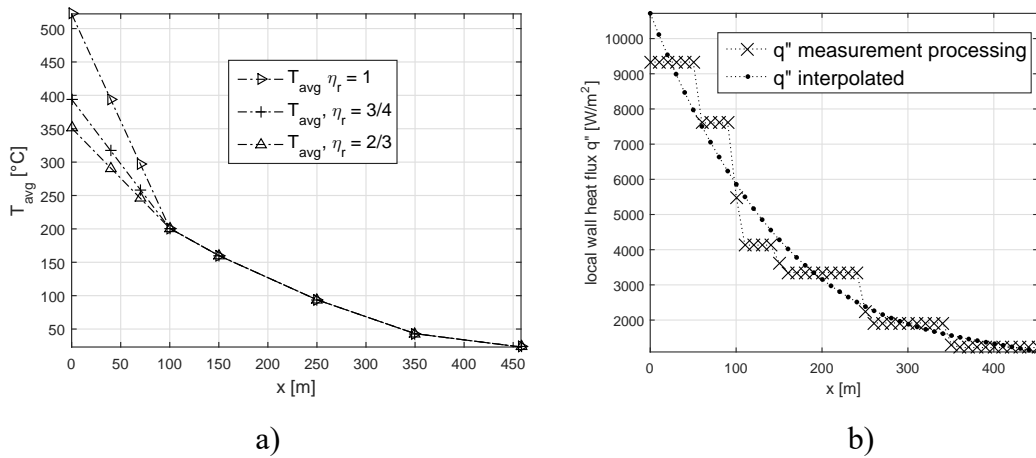


Fig.3. The 70 MW fire-test data processing: a) interpolations for  $T_{avg}(x)$ , step ( $^{\circ}1$ ) of the procedure below, b) local heat flux  $q''$  processing, steps ( $^{\circ}2$ ) and ( $^{\circ}3$ ).

Using further  $\eta_r = 2/3$ , data were further processed according to the following algorithm:

- 1) The rate of change of interpolated  $T_{avg}(x)$  with  $x$  is determined numerically:  $dT_{avg}/dx$ ;
- 2) The local heat flux,  $q''$  [ $\text{W/m}^2$ ] is computed as:  $q''(x) = \rho_0 u_0 A_t \frac{dT_{avg}}{dx}$  [ $\text{W/m}^2$ ];
- 3) An interpolated (smooth) distribution of *measured*  $q''_{meas}$  is obtained by a polynomial interpolation through the  $q''(x)$  result of step ( $^{\circ}2$ ), Fig.3.b, and used further;
- 4) A corrected (smooth) distribution of  $T_{avg}(x)$  is obtained by integrating back the  $q''_{meas}$  with respect to  $x$ , and used further, Fig.4.a;
- 5) The average wall temperature  $T_w$  at  $x$ , which must comply to:  $T_0 < T_w(x) < T_{avg}(x)$  is reconstructed iteratively by an algorithm which minimises the difference between the local  $q''_{meas}(x)$  (experiment-data based heat-flux) and the calculated local heat flux  $q''_{calc}(x)$  determined from:  $q''_{calc} = h_c(T_{avg} - T_w) + F_{12}\sigma(\epsilon_g T_{avg}^4 - \alpha_g T_w^4)$ .

The results for the  $q''(x)$ ,  $T_{avg}(x)$ , and the iteratively-computed  $T_w(x)$ , along with a relative-error in  $T_w(x)$ -determination, expressed as a relative difference between  $(q''_{meas} - q''_{calc})/q''_{meas}$  [%], are plotted together in Fig.4.b.

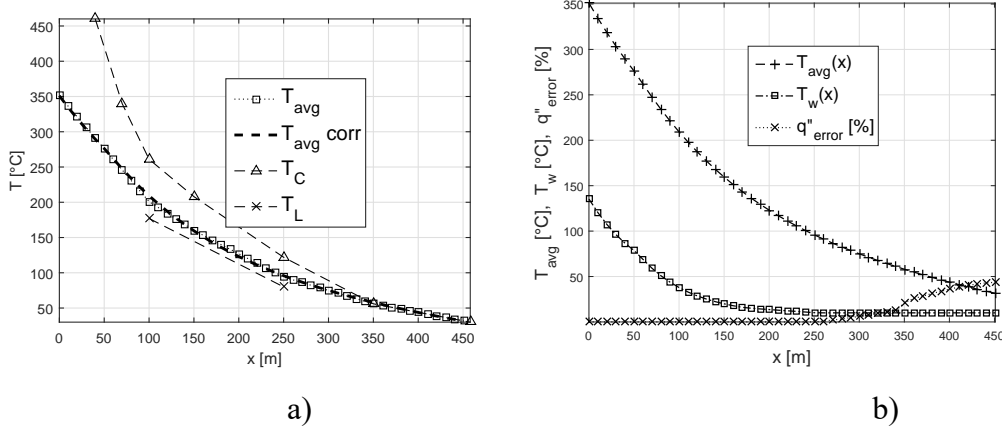


Fig.4. 70 MW fire-test processed data: a) Interpolated  $T_{avg}(x)$ , using  $\eta_r=2/3$ , and the measurements  $T_L$ ,  $T_C$ , step ( $^{\circ}4$ ); b) The distributions of  $T_{avg}(x)$ ,  $T_w(x)$ , and the relative error of the  $T_w$  calculation procedure in [%], step ( $^{\circ}5$ ).

The error appears only at the end of the analysed section, when all the relevant variables and the temperature difference are already very low, and can be attributed to the inaccuracies of the interpolation in that area. The calculation of  $T_w(x)$  shown was carried assuming  $\epsilon_g \approx \alpha_g = \epsilon_{12}=0.8$ , see [3], [7]. If a very sooty smoke-mixture is assumed and the value increased to  $\epsilon_{12} \approx 1.0$ , the results do not change much.

The results obtained for the distribution of heat transfer coefficients:  $h_c$ ,  $h_r$ ,  $h_{cr}$ ,  $h_{crc}$ , with respect to  $x$  are given in Fig.5. Obviously, local  $h_{cr}$  is equal to local sum  $h_c+h_r$ . As it can be seen from the previous two figures, at approx  $\sim 300$  m the  $h_{cr}$  and  $h_{crc}$  collapse into an equal value, since from that location, the average wall-temperature  $T_w(x)$  returns back to the undisturbed wall (rock-masive) temperature  $T_0$ , and both coefficients operate with the same temperature difference. The mean values over the analysed relevant length are given in Table 4. Analogous analysis was carried for the 120MW test-data, the results are given in Fig.5.b and in Table 4.

For the 70MW case, the convective, and the radiative heat transfer rate (not including the local flame-to-wall loss  $(1-\eta_r)HRR$  at fire-site), over the analysed length are:  $\dot{Q}_r=1.496 \cdot 10^7$  W,  $\dot{Q}_c=2.792 \cdot 10^7$  W. Thus, the share of the radiative part is approx. 35%, and can not be neglected. For the 120MW case, the same results are:  $\dot{Q}_r=2.83 \cdot 10^7$  W,  $\dot{Q}_c=4.02 \cdot 10^7$  W, and the radiative part share is 41.3%.

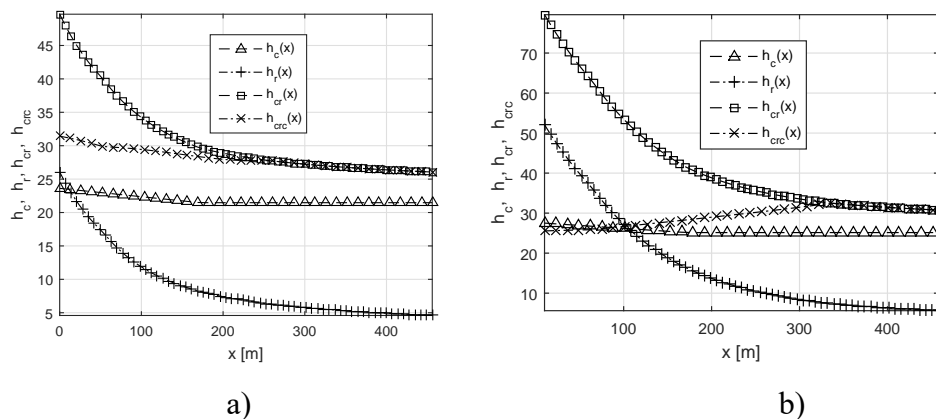


Fig.5. Computed heat transfer coefficients: a) 70MW test-data; b) 120MW test-data

Table 4: Mean values of the heat transfer coefficients for the 70MW and 120MW tunnel-fire test-data.

HRR	$h_{c,m}$	$h_{r,m}$	$h_{cr,m}$	$h_{crc,m}$
70 MW	22.14	11.81	34	28.95
120 MW	25.54	17.88	43.6	28.24

Depending on the calculation approach to estimate the  $T_{avg}(x)$  as a best-fit approximate solution [1],[2],[5], the designer may be interested in either  $h_{cr,m}$  and  $T_w$ , [1], or in  $h_{crc,m}$  only, [2], when in order to determine  $T_{avg}(x)$  and  $\Delta p_{ch}$  eqs.(3,4,5) are used.

When compared to the generic-tunnel numerical example ( $HRR_{max}=50MW$  fire) the values obtained from the data processing of the 70MW test-fire data are higher, which can be attributed to: (i) higher  $HRR$ 's (70MW vs 50MW) effect on Re and  $h_c$ , (ii) a higher (above the limit) roughness effect on higher  $h_c$ , (iii) higher radiative share, (iv)  $HRR$ 's time-evolvement in test [5] vs simulated case. Having in mind  $h_{c,m}$ 's  $HRR$ -trend (i) and friction-trend of Fig.2 (ii), the  $h_{r,m}$ 's  $HRR$ -trend (iii), one could extrapolate back for an estimate value at the generic-tunnel example inputs (50MW,  $f_D=0.0275$ ):  $h_{c,m}\sim 16$ ,  $h_{r,m}\sim 9.3$ ,  $h_{cr,m}\sim 25.3$ ,  $h_{crc,m}\sim 22.5 W/m^2K$ .

### 3. SUMMARY AND CONCLUSION

For most commonly encountered tunnels with cast-concrete walls ( $D_h\approx 8m$ ,  $u_{cr}\approx 3m/s$ ,  $f_D\approx 0.0275$ ), longitudinally ventilated, at a time 15-20 min from the fire-onset, with standardized 50MW fire, the following numerically-computed  $h_{cr,m}$  and  $h_{crc,m}$  values can be expected: 21.3, 16.1 W/m<sup>2</sup>K, respectively. They can be used to asses  $T_{avg}(x)$  and the  $\Delta p_{ch}$  in ventilation design.

For larger fires, and/or tunnels with a higher wall-roughness, higher values of  $h_{c,m}$ ,  $h_{cr,m}$  or  $h_{crc,m}$  than the given numerical example will occur. Care must be exercised in evaluating them in each design case, given the complex influence of wall-roughness, radiation, flow-velocity, fire size, and a numerical approach is recommended.

Test-based values given in Table 4. can be considered as good upper-value test-based estimates given the limiting-effect of surface-roughness value in these tests, on maximizing the convective part of the overall heat transfer, at a given  $HRR$  value.

### 4. REFERENCES

- [1] PIARC, 2007. Committee on Road Tunnels Operation. Systems and Equipment for Fire and Smoke Control in Road Tunnels.
- [2] CETU, 2003. Centre d'Etudes des Tunnels. Le dossier pilote des tunnels equipements, section 4.1 – Ventilation. France, ISBN 2-11-084740-9.
- [3] Incropera FP, DeWitt DP, Bergman TL, et al. Fundamentals of Heat and Mass Transfer”, Wiley and Sons 1996. ISBN-13: 978-0471457282.
- [4] RVS 09.02.31, 2014. Tunnel, tunnel equipment, ventilation, basic principles. Austrian Research Association for Roads, Rail and Transport.
- [5] Loennermark A, and Ingason H. Fire spread and flame length in large-scale tunnel fires. *Fire technology* 2006; 42: 283-302.
- [6] Sturm P, Bacher M, Beyer M, et al. Fire loads and their influence on ventilation design - A simple model for use in regulations. *14th ISAVT*, Dundee, May 2011.
- [7] CAMATT 2.20, 2011. Centre d'Etudes des Tunnels, France.

- [8] Jang HM and Chen F. On the determination of the aerodynamic coefficients of highway tunnels. *Journal of Wind Engineering and Industrial Aerodynamics* 2002; 90: 869–896.
- [9] Levoni P, Angeli D, Stalio E, et al. Fluid dynamics characterization of the Mont Blanc tunnel by multi-point airflow measurements. *Tunneling and underground space technology* 2015; 48: 110-122.
- [10] Kays WM, and Crawford ME. Convective heat and mass transfer. McGraw – Hill, Inc. 1980. McGraw Hill series in mechanical engineering. ISBN 0-07-033457-9.
- [11] Zhao S, Liu F, Wang F, Weng M. Experimental studies on fire-induced temperature distribution below ceiling in a longitudinal ventilated metro tunnel. *Tunnelling and Underground Space Technology* 72 (2018) 281–293



# METHODOLOGY FOR INVESTIGATIONS ON THE TUNNEL CLIMATE IN LONG RAILWAY TUNNELS - OPTIMIZATION OF THE DESIGN PROCESS FOR CROSS-PASSAGE COOLING SYSTEMS

<sup>1</sup>Daniel Fruhwirt, <sup>1</sup>Peter Sturm, <sup>2</sup>Helmut Steiner,

<sup>1</sup>Graz University of Technology, AT

<sup>2</sup>ÖBB Infrastruktur AG, AT

## ABSTRACT

The operation of long railway tunnels requires numerous technical installations. Parts of these installations react sensitively on thermal loads and dust loads and require protection from the tunnel atmosphere. In the case of modern twin-tube single track tunnels such components are often placed in utility rooms which are situated in cross-passages. In order to meet the temperature requirements of the utility rooms, cross-passage cooling systems have to be installed. Designing these cooling systems requires extensive investigations on the tunnel climate. This represents a big challenge, as information about the tunnel climate in long railway tunnels is rare. For this reason, a method to support the design process of cross-passage cooling systems had to be developed. The application of this method on a certain tunnel provided the required information for a data based system design of the cooling systems in the Koralmtunnel (AT). This includes both, details about the technical feasibility of ventilation and air conditioning systems as well as economic considerations.

*Keywords: tunnel climate, cooling systems, CFD simulations, life cycle cost*

## 1. INTRODUCTION

Tunnel systems are an important part of the world’s transport infrastructure. Wherever mountains have to be crossed or transit traffic needs to be diverted underground, tunnels are indispensable. Rail transport is considered one of the key factors for sustainable transport of goods and people. For this reason, the European Union forces the expansion of the trans-European railway network [3].

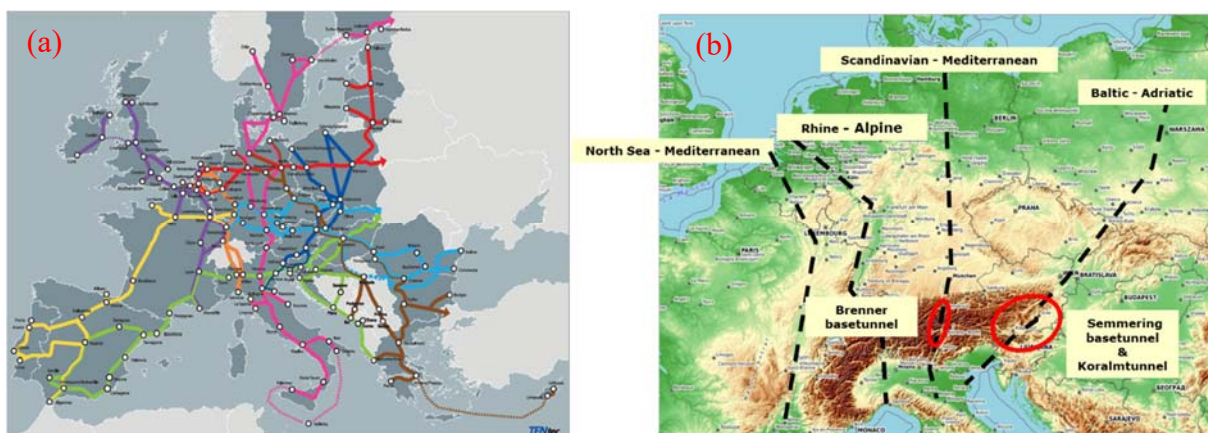


Figure 1: European railway network, (a) – Trans-European Network Transport (TEN-T) [2], (b) - selected trans-Alpine railway routes

This expansion includes the Alpine region that will be crossed by four main railway routes in north-south orientation. Figure 1 shows a scheme of the future railway network as it is aspired

today. Two of the depicted routes (Figure 1) (b), the Scandinavian-Mediterranean route in the west and the Baltic-Adriatic axis in the east, are passing Austria. The core sections of these routes are three newly built very long railway tunnels. On the Scandinavian Mediterranean route the Brenner basetunnel is situated. It will be the world's longest sub-surface railway track when it will be set in operation at the beginning of the next decade. In addition to that, there are two more very long railway tunnels on the Baltic-Adriatic axis, the Semmering basetunnel (28 km) and the Koralmtunnel (33 km).

Such long railway tunnels require a lot of technical installations for operation, such as power supply, telecommunication, remote control etc. Some components have to be installed inside the tunnel tubes, but sensitive ones have to be protected from the tunnel atmosphere. This tunnel atmosphere usually is characterized by high thermal loads or temperature variations and high dust loads, due to massive particulate matter emissions from railway operations. Both stresses result in an enormous maintenance effort for the tunnel equipment [17] [20]. While thermal stress accelerates the aging process of electronic components [10] [7], electrically conductive particles can cause malfunctions and damage to sensitive components [22].

In modern twin-tube single-track tunnels, such components usually are housed in so-called cross-passages. The basic structure of such cross-passages is shown in Figure 2. In general, they can be divided into two halves. While one half serves as an escape route in the event of a tunnel incident, the second half offers the possibility of setting up dedicated utility rooms. To create favourable conditions for sensitive systems in the utility rooms, there are certain requirements for room temperatures, relative humidity and air quality. The strictest requirement usually refers to the room air temperature [8].

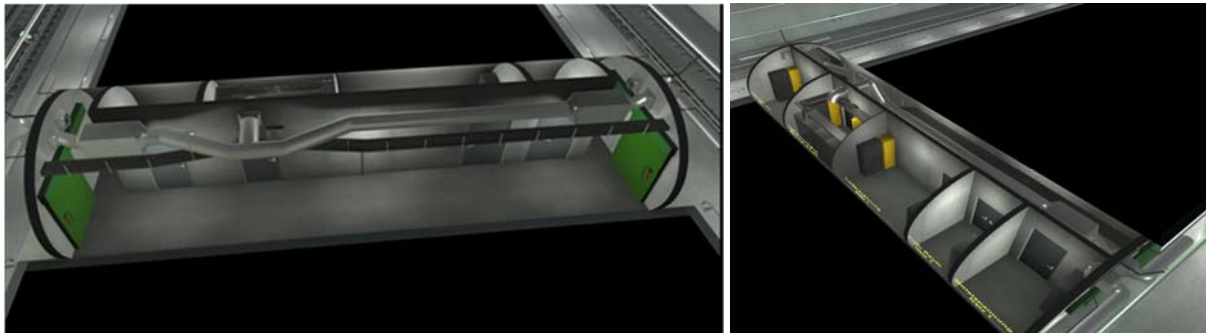


Figure 2: Principle layout of cross-passages in a modern twin-tube single track tunnel [14]

The design process of cross-passage cooling systems requires valid data about the tunnel climate or the expected tunnel air conditions respectively. Today only little information is available about the climate in very long railway tunnels. This is because the total number of railway tunnels longer than 25 km is low (four in Europe and seven in Asia). In addition, tunnel climate is strongly dependent on local parameters such as the rock temperatures. Hence, the tunnel climate needs to be investigated individually for every tunnel. Because information is rare and investigations of the tunnel climate are highly specific, a proper method that supports the design process of cooling systems and provides the required input data had to be developed.

## 2. METHODOLOGICAL APPROACH

Tunnel climate depends on many parameters, which vary from tunnel to tunnel, due to local environmental conditions and tunnel geometry. This fact makes the prediction of tunnel climate and the design of cooling systems in long railroad tunnels extremely complex. For this reason,

a proper method had to be developed in order to be able to carry out systematic investigations of the tunnel climate and to support the design of cooling systems.

The developed investigation method comprises four main investigation steps including numerical simulations and economic considerations. Hence, both the technical as well as the economic perspective are taken into account. A flow chart summarizing the basic procedure of the method is shown in Figure 3

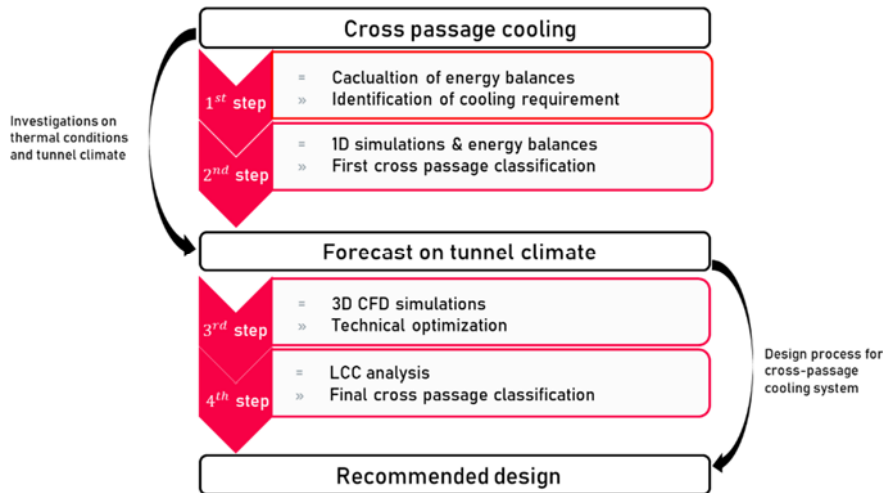


Figure 3: Flowchart of the developed method for the investigations on the tunnel climate of long railway tunnel (Fruhwirt Daniel, 2021)

The method developed is described in more detail below and applied to a specific case study.

## 2.1. Identification of cooling requirements

In order to identify the need for a cooling system, a model needs to be developed which is based at an energy balance between heat sources and heat sinks. Care must be taken to ensure that all relevant thermal processes (heat flows) are considered in the model and within certain system boundaries (i.e. individual rooms or so-called thermal zones). The temperature in a thermal zone is the result of all incoming and outgoing heat flows. Incoming heat flows are, for example, the waste heat from switch cabinets in the rooms or heat flows through walls from adjacent rooms or the surrounding rock.

In the end the energy balance of each individual zone can be expressed as shown in equation (1). There heat sources  $\dot{Q}_S$ , heat transfer through walls  $\dot{Q}_{wall}$ , the heat transfer between room air and rock layers  $\dot{Q}_{rock}$  as well as the impact of cooling systems  $\dot{Q}_{cool}$  as a sink are taken into account. Except the cooling term  $\dot{Q}_{cool}$ , all terms are a function of the room air temperature. Hence, the room air temperature can be explicitly expressed and calculated by the energy balance of the heat fluxes. In addition to that the undisturbed rock temperature has to be known in order to approximate  $\dot{Q}_{rock}$  accurately.

In order to determine an equilibrium temperature that will be achieved through thermal self-regulation the term representing the cooling requirement is set zero in equation (1). This results in effective, averaged room temperatures which than can be compared with room target temperatures. If a cooling demand has been identified the calculation must be repeated with constant room temperatures corresponding to the target temperatures. This requires the consideration of the cooling term in the energy balances of the rooms characterized by a certain

cooling demand. The final output of this second calculation run is the cooling demand of each individual thermal zone.

$$\dot{Q}_S + \sum_i \dot{Q}_{wall_i} + \dot{Q}_{rock} + \dot{Q}_{cool} = 0 \quad (1)$$

## 2.2. Cooling concepts

If required to meet the room target temperature, a cooling system must be implemented. In the case of long railroad tunnels, two systems seem suitable. One is a ventilation system that uses tunnel air for cooling purposes and the other is an air conditioning system. An air conditioning system needs another medium for heat exchange, which could either be tunnel air or a continuous water supply. For the design of either of these systems the conditions of the climate inside the tunnel needs to be known.

## 2.3. Forecast on tunnel climate

As mentioned above, the knowledge of the tunnel climate is necessary for further design steps. In order to forecast tunnel climate, some specifications need to be made before. One of them is the projection time. Based on experience, the service life of cooling systems can be assumed by ten years for air conditioning and twenty years for ventilation systems. However, when performing a feasibility study any projection periods should cover several replacement cycles for system components. This leads to time spans of several decades. Extended projection periods as well as large computational domains result in general in long computational times. Hence, simple numerical models like 1D CFD or Bernoulli equation based models are recommended for this purpose.

Special attention has to be paid on the definition of the initial conditions and the boundary conditions. The former are strongly dependent on the rock temperatures as well as on the applied ventilation strategies during the tunnels construction and equipping phase. Because the utility room cooling systems are being designed at a time when tunnel construction is on-going for several months or even years, the initial conditions cannot be determined by measurements in the actual tunnel. This means that the initial conditions must be determined in a pre-simulation covering the entire period of time in which the tunnel climate changes from the last known state.

In a next step boundary conditions need to be defined. Basically, there are boundary conditions that depend on local parameters, while others are related to activities like the operation schedule. The former category includes outside air conditions (temperature and humidity) and the rock temperature, while the latter one concerns the train frequencies (train schedule) and the train speed as the most important rail-operation related parameters.

Due to the long period of time to be considered, long-term effects such as climate change must also be taken into account. Especially in the Alpine region, this can lead to a significant change in outside air conditions over the decades. In the end the application of a 1D CFD model or a Bernoulli based model respectively provides data about the tunnel air temperature and relative humidity as a function of the tunnel position and time. Based on this information, the design of cross-passage cooling systems can be carried out. This design process requires the

determination of the utility room air temperatures that can be achieved by ventilation or air conditioning.

#### 2.4. Forecast of utility room temperatures – cooling by ventilation

In order to determine the expected utility room air temperatures, once more the calculation of energy balances is required. If a ventilation system is considered, equation (1) has to be modified including the mass flow over the system boundaries (equation (2)). In this equation,  $\dot{Q}_S$  denotes the heat sources represented by the waste heat of technical systems,  $\dot{Q}_{fan}$  denotes the heat output of the supply air fan motor, and  $\dot{m} * (h_{in} - h_{out})$  is the increase in supply air enthalpy  $h$  along the flow path. Assuming ideal gas behaviour and constant property values, this enthalpy increase can be determined as shown in equation (3).

$$\dot{Q}_S + \dot{Q}_{fan} + \dot{m} * (h_{in} - h_{out}) = 0 \quad (2)$$

$$h_{in} - h_{out} = c_p * (t_{in} - t_{out}) \quad (3)$$

Based on this simple approach, the expected room air temperatures ( $t_{out}$ ) that can be achieved by an active ventilation system are determined. It has to be noted that these values represent ideal ones that can be interpreted as an average room air temperature.

#### 2.5. Forecast of 3D temperature distribution in the utility rooms

Because the actual temperature distribution can not be displayed by the simple calculation regime (energy balances) as described above, in a third investigation step detailed 3D CFD simulations have to be carried out to get more information about the impact of the inlet air flow and the temperature distribution within the utility rooms. This temperature stratification or temperature distribution respectively, depends on the general temperature level within the utility room, the heat sources, the arrangement of the cabinets, as well as of the momentum of the incoming cooling air.

To serve this purpose, standard 3D CFD models are employed. The geometric 3D model of the cross-passage has to cover all relevant components that have noticeable influence on the room air temperatures. If the rock temperature and the room air temperatures of adjacent utility rooms are lower than the room air temperature of the assessed utility room, the thermal interaction with rock layers and the adjacent rooms can be neglected if a conservative approach should be applied. If the temperature gradient from rock to air is negative, the impact of thermal interaction becomes relevant and should be taken into account.

The 3D model provides information about the temperature distribution in the room and thus also about the thermal load on the devices. If ventilation is not sufficient an air conditioning system must be installed. In addition to that, 3D CFD simulations can be used to analyze different operation modes of the ventilation system (e.g. variable speeds or on/off modus).

#### 2.6. Economic consideration

In addition to technical feasibility, economic considerations are always important when planning an infrastructure project. For this reason, the fourth step in the methodological approach is a life cycle cost analysis (LCCA) that covers the relevant technical systems. In the case of cross-passage cooling systems, the analysis includes the cooling systems as well as all technical installations that are effected by the room air temperatures. Such a LCCA aims to determine an optimal target temperature for the utility rooms and provide additional data for the final system selection of the cross-passage cooling system.

There are several approaches to create an economic model. If a long period of time has to be assessed, it is recommended to use a dynamic approach, where each cash flow is valued at a specific date. This valuation is necessary to ensure comparability of investments. The net present value method [1] represents such a dynamic approach, as it takes into account the period in which an investment is made or an inflow of funds occurs [13]. In order to get a clear result, all cost relevant aspects like investment, maintenance, debugging services, operation and the replacement of systems need to be considered.

The net cash received (NCR) is defined as the difference between all cash inflows and cash outflows in a certain period of time  $\tau$  (see equation (4)). Equation (5) shows the definition of the net present value (NPV) which is defined as the sum of all NCRs divided by  $(1 + i)^\tau$  where  $i$  denotes the interest rate under consideration.

$$NCR = i_\tau - o_\tau \quad (4)$$

$$NPV = \sum_{\tau=0}^n \frac{i_\tau - o_\tau}{(1 + i)^\tau} = \sum_{\tau=0}^n \frac{NCR}{(1 + i)^\tau} \quad (5)$$

In the end, the total life cycle cost of the assessed systems can be determined. Based on this the final system selection of cross-passage cooling systems can be made.

### 3. CASE STUDY

The methodological approach as defined in section 2 is generally valid. However, any application needs input data which are of course site dependent. Such an application of the model has been performed in a case study for the 33 km long Koralm rail tunnel in Austria [14].

#### 3.1. Project description

The Koralm Tunnel (KAT), where the technical equipment phase has recently started, is a twin-tube single-track tunnel with a total length of 32.9 km. It consists of the two tunnel tubes and 70 cross-passages spaced 500 m apart. In addition, there is an emergency stop station directly in the centre of the tunnel and two ventilation stations with vertical air supply shafts that are operated both in case of fire and during maintenance phases. The maximum overburden of the tunnel in the centre is about 1'200 m, which is the main reason for locating the ventilation shafts near the portals. Figure 4 shows a longitudinal section and schematic diagram of the KAT.

Most of the cross-passages host five utility rooms, one for the telecommunications systems and four rooms housing the equipment for the power supply (low and medium voltage components). Temperature requirements were defined by the client individually for each of the utility rooms dependent on the systems installed within the utility rooms (see Table 1).

Table 1: Target temperature ranges for the utility rooms in the Koralm tunnel [8]

Utility room	T min [°C]	T target [°C]	T extreme [°C]
Low voltage room 1	-5	0-30	40
Telecommunication room	10	15-22	30
Low voltage room 2	-5	0-30	40
Transformer room	-25	0-35	70
Medium voltage room	-5	0-30	40

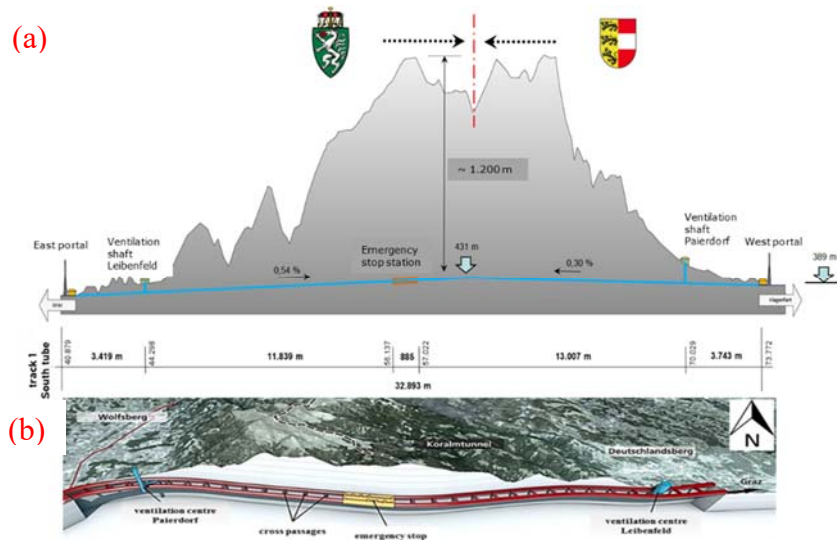


Figure 4: KAT tunnel system - (a) longitudinal section, (b) general scheme [16].

While the minimum and extreme values represent absolute boundary values, the third column (T\_target) shows the target temperature ranges for normal operation. Accordingly, the target temperature range for the telecommunication rooms is defined as 15°C to 22°C. Keeping the room air temperature within this temperature range is quite a challenge because the telecommunication equipment produces significant waste heat. For standard telecommunication equipment, the heat dissipation is about 6 kW and for telecom base stations, this increases to as much as 26 kW. This high off-heat together with the rock temperatures in the tunnel (see section 3.3) requires room air cooling.

### 3.2. Identification of the actual cooling requirement

The first investigation step requires the definition of an accurate thermodynamic system. In the case of the KAT this thermodynamic system covers an entire cross-passage including five utility rooms, one for telecommunication systems (TC) and four rooms to house components for the power supply. Each of the utility rooms as well as the escape way were modelled as an individual thermal zone. Figure 5 shows a scheme of a cross-passage covering eight thermal zones (thermodynamic systems).

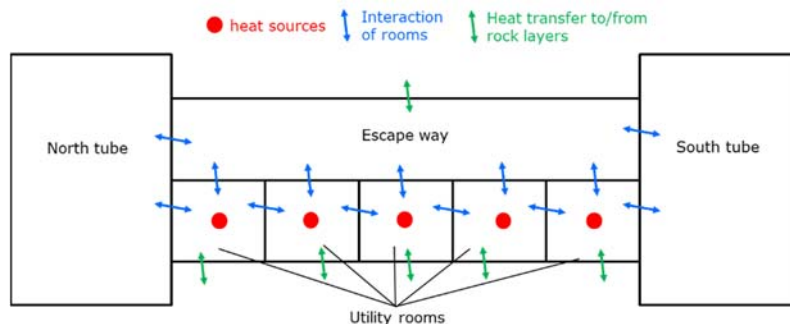


Figure 5: System configuration for the determination of the expected utility room air temperatures.

As illustrated in Figure 5 every utility room, the escape way and the adjacent tunnel sections are defined as separate but interconnected systems for which an energy balances are calculated.

The final outcome of this investigation step are the room temperatures reached in a steady state. It has to be noted that these values represent an averaged room air temperature, as an idealized, non-dimensional system (constant temperature in the entire utility room) is assumed. The energy balances applied to the thermal zones can be expressed as described in section 2.1.

Figure 6 shows the determined room air temperatures for every utility room in the Koralm tunnel in case of self-regulation (no active cooling system). It can be seen that the telecommunication room (TK), with a max. target temperature of 22°C and the adjacent low voltage room (target temperature 30°C) require an active cooling system.

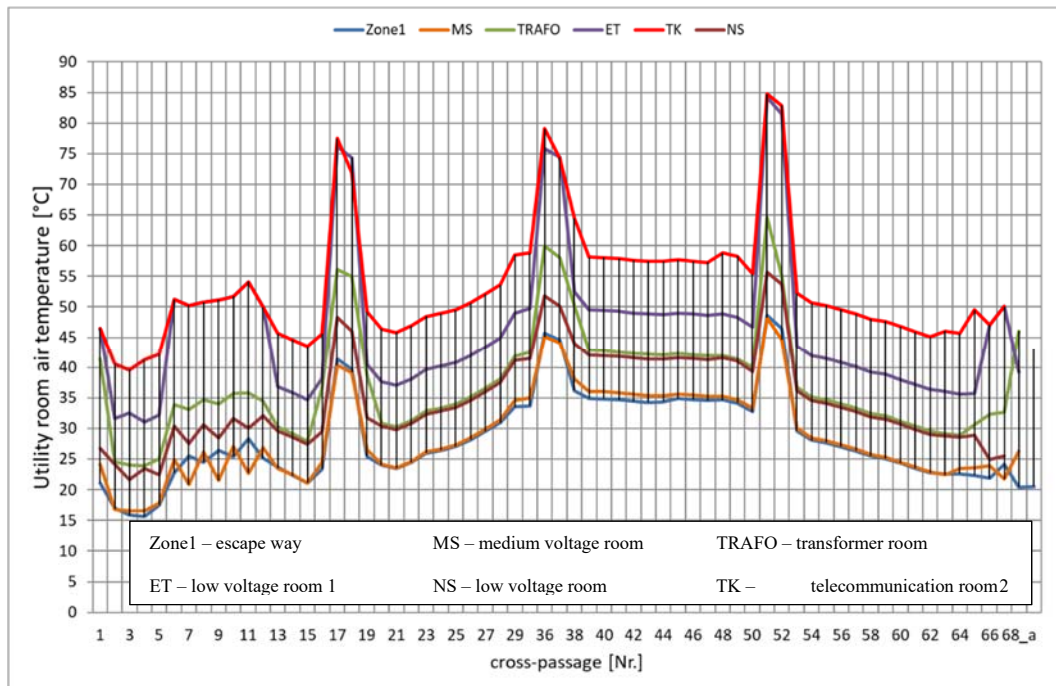


Figure 6: Expected utility room air temperatures without active cooling systems [19]

### 3.3. Forecast of the tunnel climate

At the beginning of the second investigation step some specifications have to be defined. This includes the definition of the period of time to be assessed in the tunnel climate investigations (see section 2.3). In the case of the KAT a period of 50 years had to be assessed, as several replacement cycles of cross-passage cooling systems should be included.

In the KAT tunnel climate investigations, IDA tunnel [11] was used. It is a commercial solver for the conservation of mass and a balance of total pressure.

#### Initial conditions:

The initial conditions for the simulation of the tunnel operation phase refer to the conditions at the end of the equipping phase and can vary significantly from the thermal conditions recorded in the construction phase or the early equipping phase of the tunnel. In order to determine these initial conditions for the operation phase, the last two years of the construction/equipping period were considered in the model. Input data for this model were the original rock temperatures, the heat sources and sinks during this period (off-heat from vehicles, evaporation heat during concreting of the trackways and the ventilation system applied during that period. The activity data for calculation these thermal loads was provided by the client on basis of technical reports [15]. The impact of the activities during these two considered years is demonstrated in Figure 7 in which the wall surface temperature curves along the south tube of the KAT for selected time steps are depicted.

Two important aspects have to be highlighted in this context. On the one hand the general temperature level is expected to decrease during the equipping phase and portal regions are strongly affected by the outside air conditions and thereby a certain bandwidth of temperatures can be observed in these areas. Furthermore, the discontinuity right in the tunnel centre has to



be explained in more detail. This special fact is a result of the applied construction ventilation system in the KAT. The construction and equipment of the tunnel is done in two totally separated lots, west and east. Most of the time a U-shape ventilation system that uses the south tube for supply air and the north tube as the return air tube will be operated independently in each of these two sections. While the black line in Figure 7 represents the initial rock temperature – as starting condition in the simulation – the other lines show a dedicated temperature offset at the boundary of the both lots, due to the aerodynamic separation by a brattice. Rock temperatures were known from permanent measurements during construction phase.

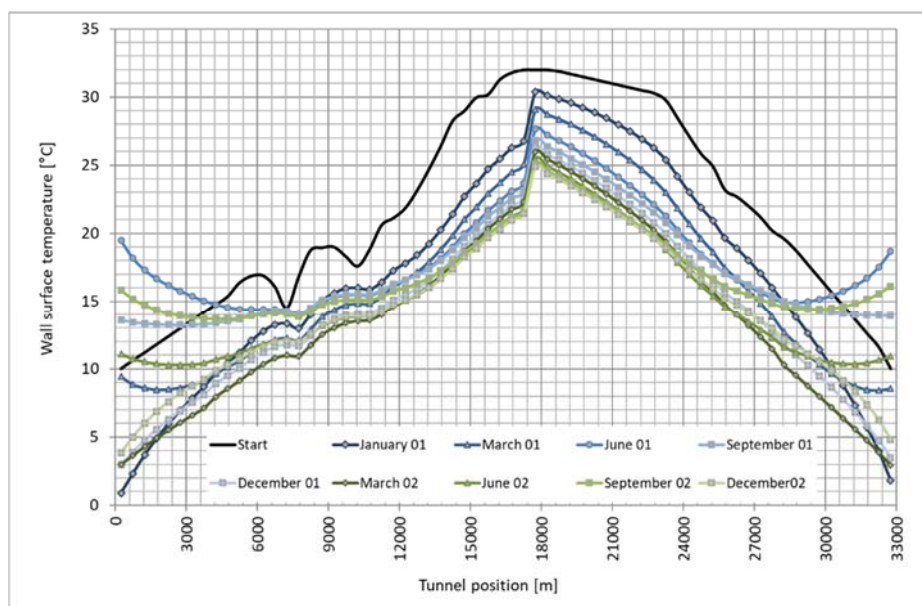


Figure 7: Wall surface temperature curves along the south tube of the KAT at selected points of time in the equipping phase. [9]

### Boundary conditions:

#### *Rock temperature:*

The most important parameters are the local rock temperatures, the outside air conditions and the train schedule. However, it should be noted that there are many more parameters (e.g. train speed) that have an influence on the tunnel climate. Consideration of all parameters results in a complex system that must be studied if a tunnel climate forecast is to be made.

Nevertheless, one of the most crucial physical effects for the tunnel climate is the heat transfer between the tunnel air and the tunnel wall due to heat transfer by convection. However, long-term effects on the tunnel climate also require the consideration of heat conduction. Therefore, the solid layers of the tunnel lining (concrete), shotcrete layers as well as the rock material have to be discretized in the numerical model. An important aspect in this context is that the rock material may change along the tunnel. Such changes can be caused by different water content in the solid layers or by different geological formations. In the KAT, the solid layers in most tunnel sections were modelled as rock layers with constant property values. In portal sections, the rock layers were replaced by neogene layers with different property values. The rock temperatures up to a penetration depth of 285 m at the end of the pre-simulation were used as initial conditions for the tunnel climate simulations.

#### *Outside air conditions:*

The second crucial parameter that has a strong influence on the tunnel climate is the outside air temperature. In order to have accurate data for this boundary condition, long-term

measurements from the project area are needed. In the case of the KAT, such data were available [6], since the Federal state of Styria operates a meteorological station near the KAT's east portal. This data set contains hourly mean values of outside air temperature and relative humidity. It has to be noted that daily or monthly average values are not applicable as the daily variations of the temperature have an influence on the thermal conditions in portal regions. The hourly average values of the past 20 years were analysed in detail. It turned out that the summer of the year 2012 was characterized by a high average temperature level and during summer of 2013 high peak temperatures up to 39 °C were recorded. For this reason, the data of both years were used to define the thermal boundary conditions. Because the forecast on the tunnel climate had to cover a period of 50 years, even long-term effects had to be taken into account. In order to do this, the impact of climate change was considered on basis of an expert statement from the local meteorological office [21]. Table 2 shows the monthly average values from a 30-year period in the past, as well as the expected values, 90<sup>th</sup> percentile values, and expected temperature increase for the period through 2070.

Table 2: Monthly average temperatures of the past and expected values for the period until 2070 for the area of Deutschlandsberg (KAT East portal) (Fruhwirt Daniel, 2021)

No.	Type	January	February	March	April	May	June	July	August	September	October	November	December
1	1971-2000	-3.1	-0.5	4.2	8.5	13.8	16.9	18.6	18.1	13.7	8.4	2.3	-1.8
2	Expected value	-0.6	1.9	6.5	10.7	15.9	19.0	20.6	20.2	15.9	10.6	4.6	0.6
3	90-percentile	0.0	2.5	7.1	11.3	16.7	19.9	21.6	21.1	16.7	11.4	5.3	1.3
4	$\Delta nr2 - nr.1$	2.5	2.4	2.3	2.2	2.1	2.1	2.0	2.1	2.2	2.2	2.3	2.4

The expected increase in monthly average temperatures by 2070 (No.4 in Table 2) is about 2.2°C, with a slightly higher temperature increase in winter than in summer. The development of the outdoor air temperature within this period is approximated by a linear function.

#### *Train frequency:*

The train frequency is another important parameter that strongly influences the tunnel climate. This is because train movements bring outside air into the tunnel and influence the heat transfer towards the walls. Hence, a plausible train schedule has to be implemented into the 1D simulations. As the train schedule was not defined at the design stage of the cross-passage cooling systems, a high traffic scenario and a low traffic scenario were considered. The low traffic scenario was defined by one single train per hour and direction and the high traffic scenario considered six trains per hour and direction.

#### Results from 1D simulations:

Finally, the result of the 1D tunnel climate simulations are the hourly average values of tunnel air temperature and relative humidity. Figure 8 shows as an example the curves of the maximum, minimum and average temperature along the south tube of the KAT for July in the first year of operation based on a high traffic scenario. Two important aspects should be emphasized in this context. On the one hand, a homogeneous temperature curve at a high temperature level can be observed in regions around the tunnel centre, and on the other hand, there is a strong influence of the outside air conditions in portal areas. This effect leads to a large temperature range, since the daily fluctuations of outside air temperatures have an impact to the tunnel sections near the portals. This fact underlines the importance of the hourly average temperatures used as thermal boundary conditions in the tunnel climate simulations.

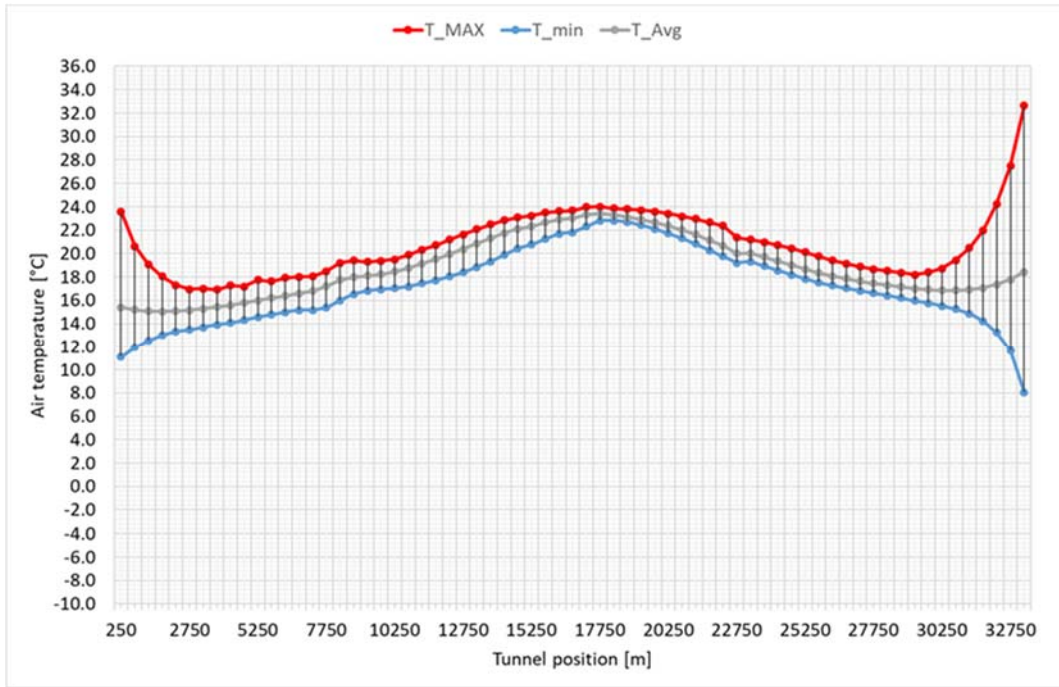


Figure 8: Tunnel air temperature curve in KAT south tube – July (1st year of operation) [8]

### 3.4. Determination of utility room air temperatures with active ventilation system

The results of the 1D simulations for tunnel climate provide boundary conditions for the design of the cross-passage cooling system. However, at this stage still no statement can yet be made concerning the type of cooling system required to keep the utility room air within the target temperature range. Therefore, an additional calculation of energy balances for the utility rooms with a certain cooling demand is necessary. The methodological approach used in this step is described in section 2.4. Figure 9 depicts the scheme of the thermodynamic system to determine the expected utility room air temperatures, in this case for the telecommunications room.

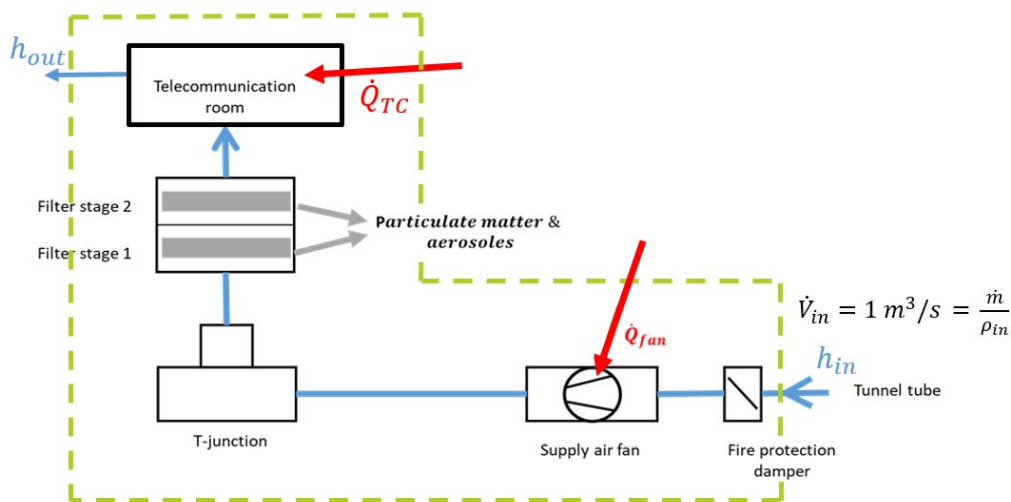


Figure 9: Thermodynamic system for the determination of the utility room air temperature

The final result of this calculation procedure is the average room air temperature in the TC room. This temperature is then compared to the target temperature of the TC room (22°C). Figure 10 shows how often the expected TC room air temperatures of selected cross-passages along the KAT will exceed the target temperature. The numbers are changing over operation time due to the projected change of tunnel climate over the years. At the beginning of the

operation phase, only a few exceedances of the target temperature (22°C) are expected in portal areas. In contrast, the target temperature will be permanently exceeded in the TC rooms located near to the centre of the tunnel. In the first twenty years of operation, two opposing trends can be observed. While temperature exceedances in the portal areas will increase significantly, temperatures in the centre of the tunnel are expected to decrease. These trends will continue until the effects of climate change become more pronounced and the temperature rise affects the entire tunnel system.

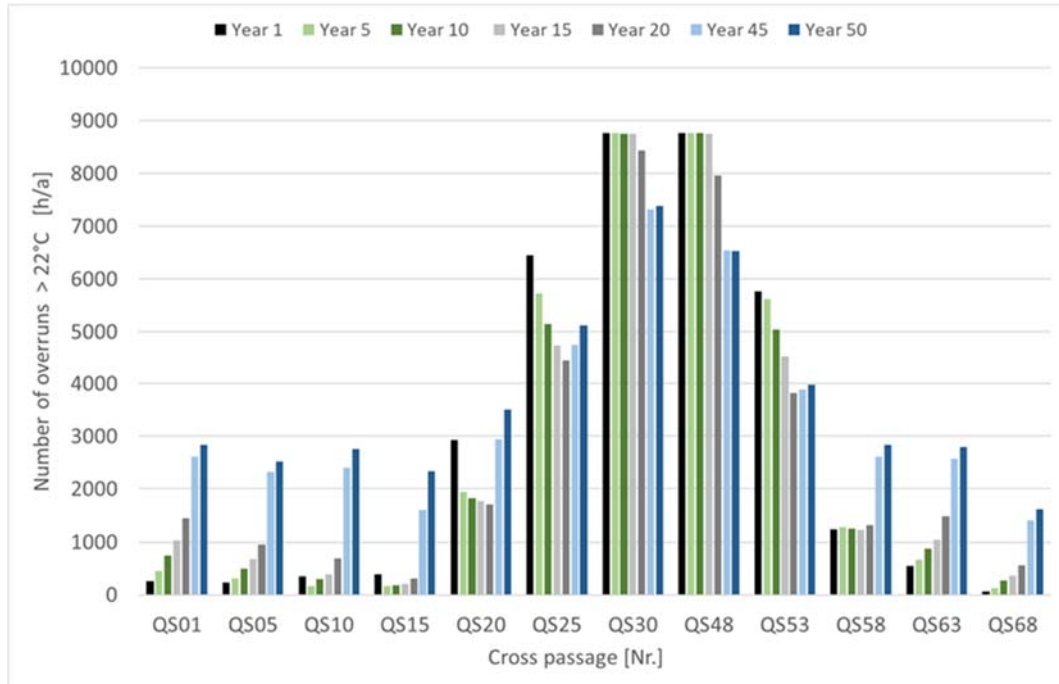


Figure 10: Number of exceedances of the target room air temperatures in the telecommunication room as a function of operation time in selected cross-passages along the KAT [8]

In a strict interpretation of these results, there is no cross-passage in which the TC room temperature can be kept permanently in the target temperature range. Consequently, every cross-passage would have to be equipped with an air conditioning system. However, the approaches used so far are subject to some uncertainty because the derived temperatures represent average room air temperatures and do not account for 3D effects such as temperature stratification. To obtain more information about these 3D effects, additional 3D CFD simulations were performed in the third investigation step.

### 3.5. Detailed 3D CFD Simulations

In the course of the 3D investigations of the utility room temperature (mainly the TC room), Ansys Fluent was the chosen 3D CFD solver. The geometrical 3D model covered a cross-passage equipped with a mechanical ventilation system. Utility rooms that do not require cooling are not included in the air path of the ventilation system and thus were neglected in the 3D CFD simulations.

The most relevant boundary conditions in the 3D simulations are the supply air temperature and the heat sources inside the TC room. For the simulation runs described below the supply air temperature was 20°C and a heat dissipation of 6 kW at the top of two implemented control cabinets were set. Heat transfer through walls was neglected, representing a thermal setup expected in tunnel sections with similar TC room air and rock temperatures.

Based on this setup, two simulation runs were performed. The first run included a permanent full load operation of the supply air fan with a constant supply air flow rate of 1 m<sup>3</sup>/s at the

inlet. In comparison, the second simulation run was performed in a transient mode with on/off operation of the supply air fan. While the first simulation run aimed at determining the temperature distribution in the TC room or the suitability of a ventilation system to meet the cooling requirement, the second simulation run aimed at some optimization of the control regime of the ventilation system. The results of the 3D CFD simulations are shown in Figure 11. The temperature contours are depicted on a vertical plane through the TC room. The exact location of the vertical plane is indicated in the image on the right side of Figure 11.

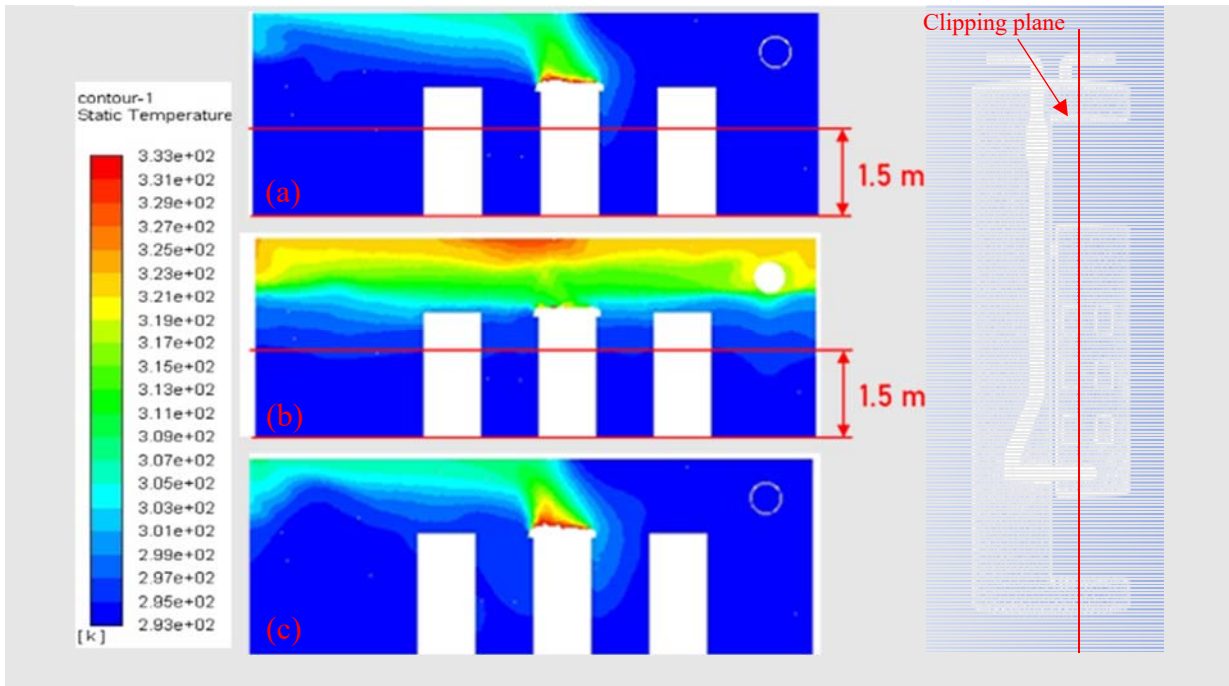


Figure 11: Results from 3D CFD simulations (a) steady state, (b) transient case, 75 sec after fan deactivation, (c) transient case, 65 sec after fan-reactivation [8]

Three important aspects are evidenced by the results of the 3D CFD simulations.

The first is the well-established temperature stratification within the TC room. While the space above the control cabinets acts as a thermal buffer with temperatures up to 45°C, the control cabinets themselves are not exposed to unacceptable temperatures. The 1D simulation as described in section **Fehler! Verweisquelle konnte nicht gefunden werden..** would have resulted in an average room air temperature of 24.8°C, i.e. above the target air temperature of 22°C.

The second aspect is the asymmetric temperature distribution, which is caused by the massive influence of the supply air. Cabinets located near the supply air inlet are permanently exposed to the cooler supply air temperature. As a consequence of the findings of the first simulation run (steady state – see (a) in Figure 11), the temperature criterion for the TC room was modified, in so far that the target temperature must be maintained at a height of 1.5 m. This should be sufficient, since room air extracted close to the floor is used for the internal cooling of the control cabinets.

The last important information was derived from the results of the transient simulation. The deactivation of the supply air fan leads to a temperature distribution as depicted in image (b) in Figure 11. Only 75 seconds after deactivation, the target temperature (22°C) is exceeded at a height of 1.5 m, resulting in reactivation of the supply air fan. After another 65 seconds, the warm TC room air is removed and the initial temperature distribution is reached again (see image (c) in Figure 11). Based on these results, an on/off control regime does not appear to be

appropriate and a control regime on two or more discrete fan speed levels is recommended to provide some flexibility.

Since the results of the 1D and 3D approaches are different, a validation of the 3D results was performed in the escape tunnel of an Austrian railway tunnel. Within this escape tunnel, a dedicated test room with similar characteristics compared to the KAT utility rooms was set-up and several test scenarios with variations of supply air temperature and heat release were performed [12]. The general outcome of the in-situ tests confirms the results of the 3D CFD simulations, as a well defined temperature stratification could be observed and the integrated control cabinets were never exposed to temperatures above the target temperature.

Based on the findings from the 3D CFD simulations, it can thus be concluded that 3D effects in the temperature distribution offer some potential for optimization of the target temperature. It should be noted that the results of the 3D CFD simulations depend on the arrangement of the cabinets. However, the basic conclusions concerning temperature stratification are found to be valid.

### 3.6. Cooling concepts

Since there is a need for active cooling in most of the KAT cross-passages, a principle cooling concept must be defined. Due to the fact that there is no continuous water supply in the KAT, tunnel air is the only available cooling medium. This limits the choice of cooling systems to two types. One is a mechanical ventilation system that uses tunnel air to cool the utility rooms, and the other is an air conditioning system that uses tunnel air for re-cooling. Figure 12 shows the principle layout of both cooling systems. Note that due to redundancy purposes both systems are duplicated in the same cross passage.

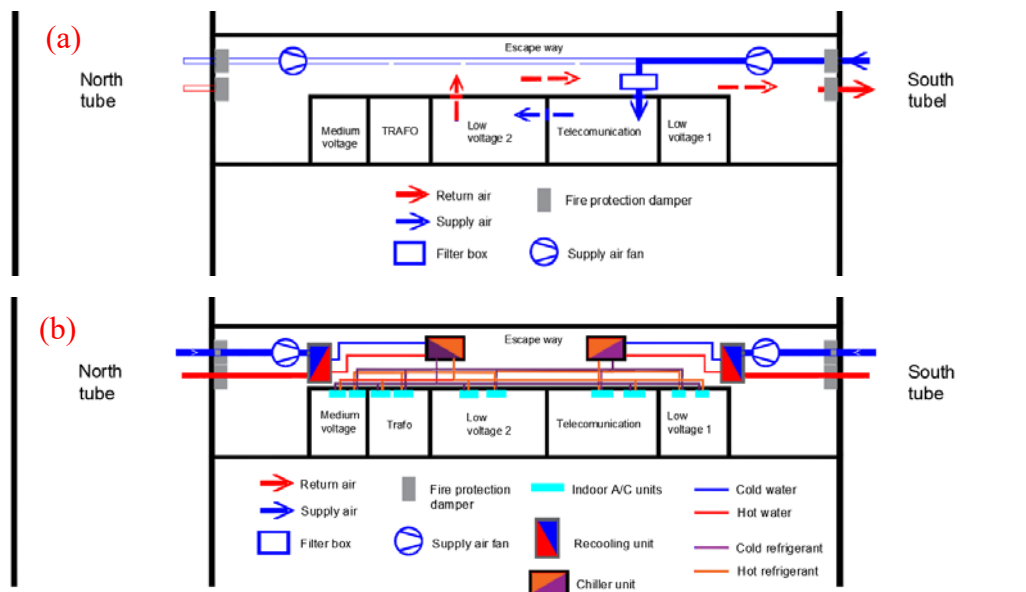


Figure 12: Principle layout of the cross-passage cooling systems in the Koralm Tunnel, (a) ventilation, (b) air conditioning [8]

Both systems have advantages and disadvantages. The ventilation system has its main benefits in its simplicity, as it contains only few electro-mechanical components (fans and dampers). This causes a moderate maintenance effort and keeps the power consumption and operation costs on an acceptable level. One disadvantage is the limited cooling effect due to the strong dependency on the tunnel air temperature respectively the tunnel climate. The second disadvantage is the required supply air treatment, since the tunnel air must be filtered due to high PM concentrations in the tunnel. This can be a knock-out criterion if the filter service life

does not reach an acceptable level. However, tests demonstrated that the expected filter life when using the KAT ventilation system is approximately between 4.5 and 21 months, depending on the filter specification [20]

In contrast to the ventilation system, the air conditioning system requires an increased electromechanical effort. The system design according to Figure 12 covers a refrigerant cycle, a water cycle and an air cycle. The necessity of a water cycle is mainly a result of regulations related to the maximum amount of refrigerant mass acceptable in an escape way [5]. In the end this results in higher cost for construction and operation compared to a ventilation system.

However, as a result of the investigations about tunnel climate it was concluded, that for many cross passages, a ventilation-based cooling system is not sufficient, hence air conditioning is required.

In the end the decisive criteria pro or against a system are the achievable track availability and the financial aspects. The ventilation system proved superior; however, the limitations imposed by the temperature requirements force the use of air conditioning systems at cross passages with enhanced cooling demand. The target temperature not to be exceeded in the telecommunication room is the decisive parameter for system selection. However, as this target temperature is given due to lifetime considerations of the equipment, a LCCA might be used to decide whether a reduced lifetime (higher target temperature) and lower system costs are beneficial compared to extended lifetime but higher system costs.

### 3.7. Economic considerations

In the last investigation step a LCCA was made for the cross-passage cooling systems and the TC systems. In general, the cost development for both system is driven by investment, operation and maintenance costs. The latter are dominant in the evaluation of the total life cycle cost of the cross-passage cooling systems and the TC systems. For this reason, accurate approaches to estimate all relevant cost elements are required.

The service life of both cooling systems (ventilation and air conditioning) was assumed to be 20 years for ventilation and 10 years for air conditioning systems. These values represent empirical values derived from previous tunnel projects. In contrast, the service life of TC systems was assumed to be a function of the room air temperature. To account for this, an Arrhenius approach was applied to the Eyring equation [4], which is commonly used to approximate ageing processes on chips and sensors due to thermal stresses. This results in a formulation as shown in equation (6).

$$\tau_E = \tau_Q * e^{\frac{E_a}{R} * \left( \frac{1}{T_E} - \frac{1}{T_Q} \right)} \quad (6)$$

Using this equation, the service life of the TC systems was determined for selected TC room air temperatures in the range from 22 °C up to 60 °C (Table 3). Consequently, a temperature range of 22 °C up to 35 °C appears to be suitable, since a further increase in room air temperature reduces the expected service life of TC systems to less than 6 years, which reduces the track availability significantly due to tunnel closures that would be needed for the replacement of broken down systems.

Table 3: Approximation of the Telecommunication system service life as a function of the utility room air temperature [8]

Operation temperature	22°C	25°C	30°C	35°C	40°C	45°C	50°C	55°C	60°C
Service life [years]	16	12	9	6	4	3	2.1	1.5	1.2

For the estimation of maintenance service costs, a similar approach was found as for the estimation of the service life. The annual cost for maintenance services of the cooling systems were approximated as a constant on basis of investment costs (1 % ventilation and 6 % air conditioning). In contrast, the annual maintenance cost for the electrical installations (TC systems)  $I_m$  were approximated by equation (7). There  $I_0$  denotes the initial investment cost for the TC systems and  $\frac{\tau_{22^\circ\text{C}}}{\tau_T}$  is the quotient of expected service life at a target temperature of 22 °C and a target temperature  $T$  according to the selected scenario. This quotient expresses the dependence of the maintenance cost on the room air temperature and takes into account increasing cost with increasing room air temperature.

$$I_m = I_0 * 0.0638 * \frac{\tau_{22^\circ\text{C}}}{\tau_T} \quad (7)$$

Within the temperature range of 22 °C to 35 °C, four temperature scenarios were defined and evaluated in the LCCA. For each temperature scenario, a cross-passage classification was made as to whether they can be equipped with a mechanical ventilation system (low cooling demand) or an air conditioning system (enhanced cooling requirement). Figure 13 shows the cross-passage classification for each of the temperature scenarios. While for the 22°C scenario almost no cross-passages could be equipped with ventilation systems, in the 35°C scenario, cooling by ventilation would serve for almost all cross passages.

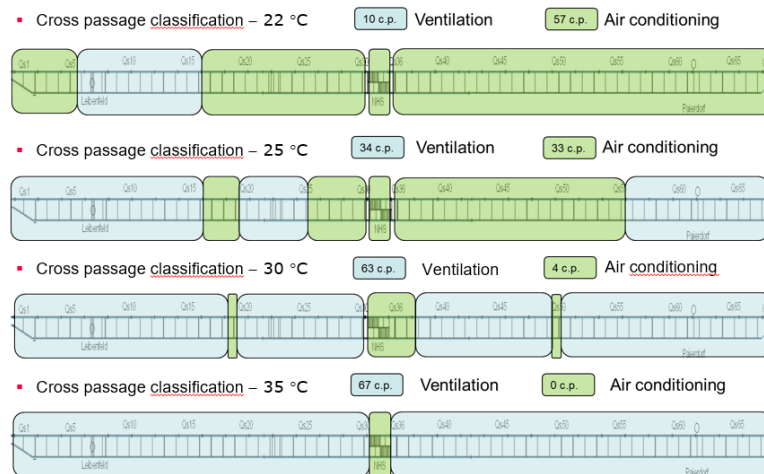


Figure 13: Cross-passage classification related to the implemented cooling system for four selected target temperature scenarios [8]

Based on a target temperature of 22°C, a comparison was made in the first simulation run between a cross-passage classification according to Figure 13 and a variant in which only air-conditioning systems are used. Figure 14 shows the results derived from this simulation run. The offset already at the beginning is due to the variation in initial investment cost. During the considered 50 year of operation the total life cycle cost (LCC) differ at the end by roughly 30% in which a cross-passage classification according to Figure 13 (roughly 15% ventilation and 85% air conditioning) accounts for the lower cost compared to a full installation of air conditioning systems. Hence, in cross-passages with lower cooling requirement the installation of a ventilation system should be aspired.



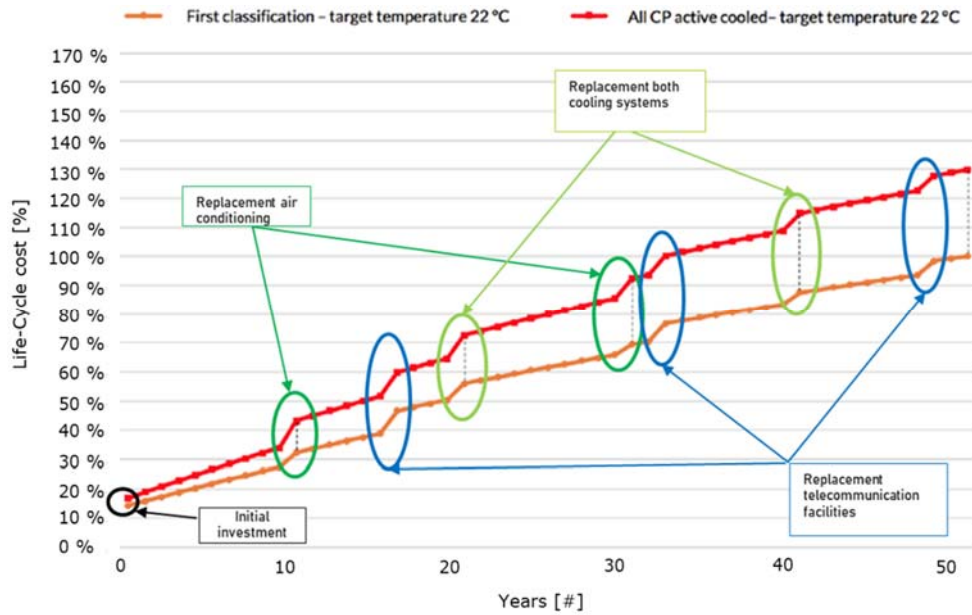


Figure 14: Comparison of life cycle cost for a combination of ventilation and air conditioning and for full equipment with air conditioning units [8]

Therefore, in further simulation runs, the remaining temperature scenarios were evaluated. The higher the room target temperature the smaller the number of cross-passages being equipped with air conditioning systems. Figure 15 shows the cost development and total LCCs of the studied target temperature scenarios. The total LCCs in the 22°C scenario were defined as reference costs (100%). The results show a decreasing trend in total LCCs as the target temperature increases. This trend continues until a target temperature of 30°C is reached. At the end of the 50-year period, the difference between the reference costs and the lowest LCC in the 30°C scenario is about 21 %. A further increase of the target temperature to 35°C leads directly to the highest LCC (107 %) due to increased costs for reinvestments and maintenance.

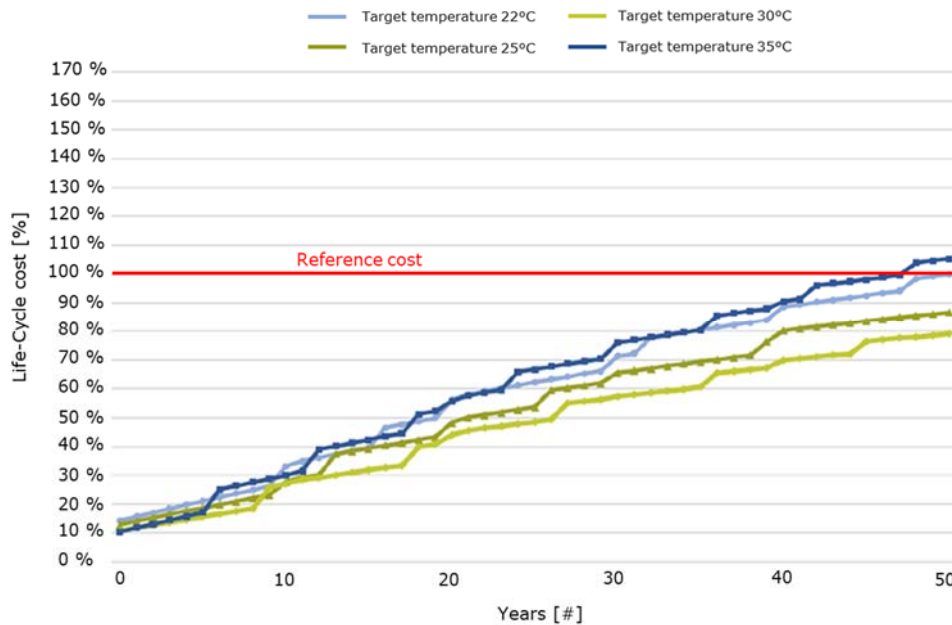


Figure 15: Life-Cycle cost in four selected target temperature scenarios [18]

The accuracy of these results was tested by a dominance analysis and a sensitivity analysis for each temperature scenario. The dominance analysis provided information about the cost elements and their impact on the total life cycle cost. The operation cost (86% of total life cycle

costs) dominate over initial investment cost (14%). When examining the total cost for the individual systems, it was found that the cost for TC systems (79.6 %) are dominant and the cost for ventilation systems (15.8 %) and air conditioning systems (4.6 %) are of minor importance.

From an economic point of view, 30°C seems to be the optimal target temperature for the TC rooms. Nevertheless, at the end the 25°C target temperature scenario was recommended with a cross-passage classification similar to Figure 13. The longer lifetime of the equipment (3 years) increases the track availability, and this outweighs the small loss in LCCs (8%) between the 25 and the 30°C scenario. (Remark: the track availability was not considered in the objective LCCA).

#### 4. CONCLUSIONS

This paper contains a model chain applicable for investigating the tunnel climate of very long railroad tunnels as well as the design processes for cooling systems in such tunnels. The derived method consists of four main examination steps that have to be run through one after the other.

As the tunnel climate is specific for each geographical location it must be investigated individually for each tunnel. The first question to be answered is always whether there is a cooling demand (mainly for the technical equipment) in the tunnel under investigation. Conservation equations for energy are the core of the calculation procedure. Since there is a temperature criterion for all electrical systems, the first step it is to be investigated whether external cooling is required in order not to exceed the target temperatures.

In many cases, tunnel air is the only available cooling medium, so there is a dependency on the tunnel climate or thermal conditions regardless of the type of cooling system. Therefore, in the next investigation step a forecast of the tunnel climate is required. For this investigation step important parameters like rock temperature, the outside air conditions (temperature and relative humidity) and the train frequency are needed. It should also be mentioned that the tunnel climate in the first years of operation is strongly influenced by the thermal conditions prevailing during the construction phase. Therefore, these situations have to be taken into account when defining the initial and boundary conditions for the simulation. The derivation of applicable data for outdoor air conditions should be based on long-term measurements in the project area. Depending on the time period to be assessed, long-term effects such as climate change should also be taken into account. Methods based on a 1D simulation of the aerodynamics and thermodynamics of the tunnel have proven to provide the required information about the tunnel climate. The results of this second investigation step can be used for a first statement on which type of cooling system is sufficient to meet the temperature requirements.

However, this statement has only an indicative character, since no 3D effects in the temperature distribution within the individual locations of the electrical equipment are considered. In order to close this information gap, additional 3D CFD simulations should be performed in the third investigation step. The results of these simulations are characterized by a higher accuracy and offer a certain optimization potential with regard to the equipment arrangement and cooling systems to be applied.

At this point, the basic design of cross-passage cooling systems has been completed and technical feasibility has been demonstrated. However, feasibility is only one aspect, the final design must also be cost effective. For this reason, a life cycle cost analysis should be performed for the most relevant systems. Ultimately, the developed method provides the necessary information for a data-based decision on the design of the equipment/cross-passage cooling system in a long railway tunnel.

## 5. REFERENCES

1. Allendorf, G.J. (Ed.), 2008. Immobilienökonomie. 1: Betriebswirtschaftliche Grundlagen / unter Mitarb. von Georg J. Allendorf, 4. überarb. Aufl. ed. Oldenbourg, München.
2. European Commission - Directorate-General for Mobility and Transport, 2016. Transport infrastructure: The work plans of the 11 European Coordinators for the TEN-T have been finalised, establishing the basis for action until 2030.
3. European Commission, 2022. Trans-European Transport Network (TEN-T).
4. Eyring, H., 1935. The Activated Complex in Chemical Reactions. The Journal of Chemical Physics 3, 107–115. <https://doi.org/10.1063/1.1749604>
5. Federal Ministry of Social Administration; Federal Ministry of Trade, Commerce and Industry; Refrigeration Plant Ordinance; Federal Republic of Austria, 2020. Grenzwerteverordnung 2021.
6. Federal State of Styria, 2022. Environmental monitoring system - Onlinedata. (available: <https://www.umwelt.steiermark.at/cms/ziel/2060750/DE/>, last access: April 14<sup>th</sup> 2022)
7. Frivaldsky, M., Pridala, M., Drgona, P., 2017. Implementation of mathematical model of thermal behavior of electronic components for lifetime estimation based on multi-level simulation. Archives of Electrical Engineering 66, 339–350. <https://doi.org/10.1515/ae-2017-0025>
8. Fruhwirt Daniel, 2021. Investigations of thermal- and climate conditions in the Koralm railway tunnel. PhD thesis, Graz University of Technology, Graz.
9. Fruhwirt Daniel, Sturm Peter, Bacher Michael, Steiner Helmut, 2018. CHANGE IN THERMAL CONDITIONS DURING CONSTRUCTION AND OPERATION OF A LONG RAILWAY TUNNEL – TAKING THE KORALMTUNNEL AS AN EXAMPLE, in: 9th International Conference TUNNEL SAFETY AND VENTILATION - New Developments in Tunnel Safety -. Presented at the 9th International Conference ‘Tunnel Safety and Ventilation,’ Verlag der Technischen Universität Graz, Graz, pp. 30–45.
10. Hertl, M., Weidmann, D., Lecomte, J.-C., 2009. An advanced quality and reliability assessment approach applied to thermal stress issues in electronic components and assemblies. Microelectronics Reliability 49, 1148–1152. <https://doi.org/10.1016/j.microrel.2009.07.045>
11. IDA tunnel, 2020. . EQUA Sweden. (available: <https://www.equa.se/de/events/join/276-introduktion-till-modellering-pa-avancerad-niva>, last access: April 14<sup>th</sup> 2022)
12. Institute of internal combustion engines and thermodynamics, 2020. In Situ Tunnelklimaversuche Unterwaldertunnel – Final report, No. I-11/20/DFr V & U I-17/06/642, Graz University of Technology, Graz.
13. Nwogugu, M.C.I., 2016. Anomalies in Net Present Value, Returns and Polynomials, and Regret Theory in Decision-Making. Palgrave Macmillan UK, London. <https://doi.org/10.1057/978-1-137-44698-5>
14. ÖBB Infrastruktur AG, 2022. Austrian Federal Railways - general information (Website).
15. ÖBB Infrastruktur AG, 2019. KORALMBAHN GRAZ - KLAGENFURT Bahntechnische Ausstattung KAT Baulos 30.6.1 / B15850 / ProVia ID 36150 GU1-BA Bau-Ausrüstung AUSSCHREIBUNGSPROJEKT TEIL 2.2 ANHANG 03 BESCHREIBUNG BAUABLAUF; tendering document
16. Richter, H., Theberath, J., Studiengesellschaft für Tunnel und Verkehrsanlagen (Eds.), 2017. STUVA-Tagung 2017 - Internationales Forum für Tunnel und Infrastruktur: STUVA-Tagung 2017, Stuttgart; ISBN: 978-3-433-03247-3
17. S. Ehrbar, 2017. Staub löst im Gotthard-Tunnel Fehlalarme aus. (available: <https://www.20min.ch/story/staub-loest-im-gotthard-tunnel-fehlalarme-aus-567769398149>, last access: April 14<sup>th</sup> 2022)

18. Scherz, M., Fruhwirt, D., Bacher, M., Steiner, H., Passer, A., Kreiner, H., 2019. Influence of cross passages temperatures on the life-cycle cost of technical equipment in a railway tunnel. IOP Conf. Ser.: Earth Environ. Sci. 323, 012090. <https://doi.org/10.1088/1755-1315/323/1/012090>
19. Steiner Helmut, Sturm Peter, Bacher Michael, Fruhwirt Daniel, 2017. Kühlung von Technischen Räumen in Eisenbahntunneln zur Erhöhung der Standzeiten und Minimierung der Wartung: Möglichkeiten der Optimierung am Beispiel Koralmtunnel. Presented at the STUVA Conference 2017, Stuttgart.
20. Sturm, P., Fruhwirt, D., Steiner, H., 2022. Impact of dust loads in long railway tunnels: In-situ measurements and consequences for tunnel facilities and operation. Tunnelling and Underground Space Technology 122, 104328. <https://doi.org/10.1016/j.tust.2021.104328>
21. Zentralanstalt für Meteorologie und Geodynamik, 2022. ZAMG - meteorological services.
22. Zhang, J.G., 2007. Effect of Dust Contamination on Electrical Contact Failure, in: Electrical Contacts - 2007 Proceedings of the 53rd IEEE Holm Conference on Electrical Contacts. Presented at the Electrical Contacts - 2007 Proceedings of the 53rd IEEE Holm Conference on Electrical Contacts, IEEE, pp. xxi–xxx. <https://doi.org/10.1109/HOLM.2007.4318186>

# EMPIRICAL VALIDATION OF SEASONAL 1D TEMPERATURE PREDICTIONS IN A 9 KM NORDIC TRAIN TUNNEL

<sup>1</sup>Erik Östblom, <sup>2</sup>Per Sahlin

<sup>1</sup>EQUA Solutions AB, Sweden, <sup>2</sup>EQUA Simulation AB, Sweden

## ABSTRACT

Reliable long-term predictions of tunnel temperatures are critical in several ways, such as for passenger comfort, buoyancy driven air flows, risk of ice formation, thermal loads on tunnel lining etc. In this work, IDA Tunnel temperature predictions are compared with long term measurements in a 9 km twin-bore train tunnel in Sweden. Comparisons were made with measured as well as computed tunnel air velocities. Predictions were in both cases in good agreement with measured data. Barometric pressure differences between the portals were shown to have a significant impact on results, as did the background deep ground temperature level.

*Keywords: tunnel simulation, tunnel environment, long term-prediction*

## 1. INTRODUCTION

### 1.1. Background

In this paper, measured temperatures in the Hallandsås tunnel in Sweden are compared with results from an IDA Tunnel simulation model. The Swedish Transport Administration (STA) decided to perform such measurements in the Hallandsås tunnel and to use the measurement data to validate a simulation model of the tunnel. The tunnel consists of two 8.7 km long tunnel tubes with single-track, one-way traffic.

Air velocities are continuously measured in the tunnel by STA. Measurements of air and wall temperatures in the tunnel have been carried out by the Swedish Road and Transport Research Institute. The measurement data have been compared with results from a simulation model created in IDA Tunnel version 1.2.1. IDA Tunnel is used to analyse climate and 1D airflow in railway and road tunnels. The simulations consider, among other things, actual weather conditions at the site during the measurement period, heat storage in tunnel walls and ground, moisture conditions and the impact of train traffic.

In a separate work, cold and ice in tunnels of a proposed high-speed railway through Sweden have been studied using IDA Tunnel [1]. Two small validation studies using measurements in the Glödsberg and Åsa tunnels are presented in the same report.

### 1.2. Methods for seasonal temperature predictions in underground tunnels

In the 1970's, the 1D Subway Environment Simulation (SES) program was developed by US public authorities. SES allows for dynamic simulation of train piston action and outputs airflows, temperatures, and humidity. SES focuses on the simulation of a single metro rush hour under constant operating conditions but also has a simplified method for predicting annual and diurnal temperatures based on assumed sinusoidal temperature variations. The basic structure of SES, with constant tunnel operating conditions, does not permit the study of tunnel ventilation system control. The last major release of SES, version 4.1, was in 2001.

More recently, the Subway Thermal Environment Simulation Software (STESS) has been developed by researchers at Tsinghua University [2] with the explicit purpose of studying control strategies for metro systems. It is based on an incompressible aerodynamic model that

is similar to SES (and thereby to IDA Tunnel). Also similar to IDA Tunnel, it has a finite-difference ground model and can thereby, in principle, compute arbitrary time variations in tunnel operation including the effect of buoyancy driven flows.

STESS relies on a cartesian 2D model of the ground around a tunnel segment, and, thereby, permits the definition of inhomogeneous ground properties. The software applies a combination of monthly and hourly timesteps to capture long-term as well as short-term ground heat-up. The details of this process is not clearly described in [2].

The IDA Tunnel ground model is based on superposition of multiple 1D temperature fields, to capture the true 2D field of (at most) two identical tunnel bores, including the influence from the ground surface. Multiple tunnel wall material layers can be described, but contrary to STESS the surrounding ground is assumed to have constant thermal properties.

Another method for seasonal temperature predictions in train tunnels is using the simulation tools Thermo and ThermoTun coupled, as reported by HBI in [3]. Thermo is developed by HBI and is used for simulation of thermal conditions in train tunnels. ThermoTun is developed by Dundee Tunnel Research and is used for simulation of aerodynamic and thermodynamic phenomena in rail and metro tunnels.

## 2. MEASUREMENT CAMPAIGN

Measurements of air temperature, relative humidity, wall surface temperature and wall inside temperature were carried out during a 27-month period starting in February 2019 [4]. The tunnel has been equipped with sensors that samples values once an hour.

The positions of the measuring stations are shown in Figure 1.

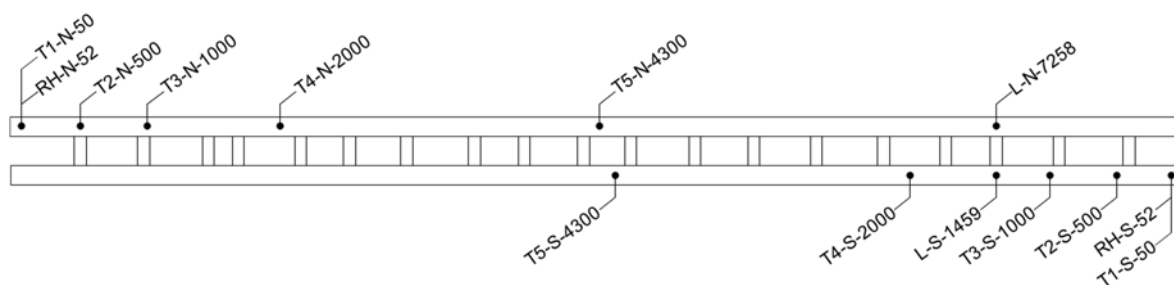


Figure 1: Position of measuring stations. T1-T5=Temperature measuring stations, RH=Relative humidity measuring stations, L=Air velocity measuring stations, N=Measuring station is located in the tunnel with northbound traffic, S=Measuring station is located in the tunnel with southbound traffic. The numbers at the end indicate the distance from the entrance in metres.

Air temperature and surface temperature are measured at measuring stations 50, 500, 1000, 2000 and 4300 m from the entrance to each tunnel tube. Air temperature is measured 1.5 m above the walkway. Surface temperature at measuring stations 50 m from the entrances is measured 0.3 and 3 m above the walkway. Surface temperature at other measuring stations is measured 0.3 and 2 m above the walkway. Wall inside temperature is measured 5 cm into the wall, 50 m from the entrance and 1.3 m above the walkway. Relative humidity is measured 52 m from the entrance and 1.5 m above the walkway.

Air velocities are collected from one anemometer in each tunnel tube from January 20, 2020, and onwards with a sampling period of 10 s. Both anemometers are located 1460 m from the northern portal and around 4.2-4.5 m above top of rail level. The measurements are sensitive to turbulence caused by train passages.

Due to various problems with the data collection, the period between March 2, 2020 and May 31, 2021 was selected for the comparison.

### 3. SIMULATION MODEL INPUT DATA

#### 3.1. Model variants

Two different variants of simulation models with respect to air velocities have been used in the comparison:

- Simulated with measured air velocity: In this variant, measured air velocity is used as a boundary condition. Simulated air velocity is then equal to measured air velocity.
- Simulated with computed air velocity. In this variant, the air velocity is a simulation result that varies with the influence of buoyancy, portal barometric pressure variations and aerodynamic impact from train passages.

The tunnel became operational by the end of 2015 and the comparison period starts almost five years later. To estimate the initial temperature state of the ground around the tunnel at the beginning of the comparison period, the time until the beginning of the comparison period is simulated separately. Due to the lack of air velocity measurement data during this period it was simulated with computed air velocity only. The resulting ground temperature at the end of the simulation period is used in describing the initial state for both model variants used in the comparison.

#### 3.2. Geometry and height profile

Figure 2 shows the tunnel height profile, cross section area and which part that has concrete lining. The southern portal is located 13 m above the north portal. There is a high point 6440 m from the northern portal. The gradient is 3 ‰ between the high point and the portals.

Around 84 % of the lined tunnel length consists of precast concrete segmental linings and the rest of cast in-situ concrete lining. About 30% of the rock tunnel sections are covered by insulated drains. All changes to the cross-sectional area consist of smooth geometric transitions that are assumed to result in negligible pressure losses.

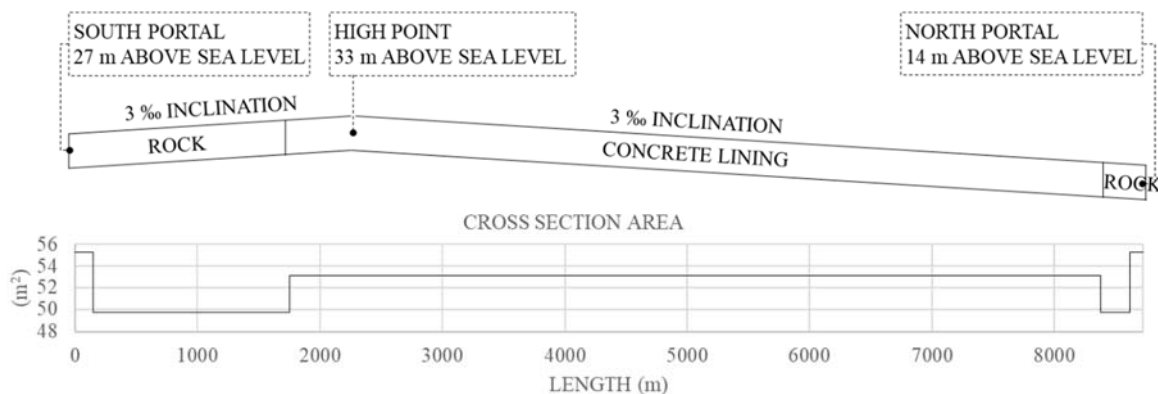


Figure 2: Tunnel height profile, cross section area and parts with concrete lining vs bare rock.

A Darcy-Weisbach friction factor of 0.02 is assumed as an average value for the whole tunnel.

There are 19 cross passages for emergency evacuation between the tubes. The cross passages have fire doors in each end which are closed during normal operation. Air leakage through the fire doors is considered to be insignificant and the cross passages have therefore not been modelled.

### 3.3. Ground

Table 1 shows values for thermal parameters of the ground around the tunnel and tunnel construction materials used. All values in the table are assumed. Polyethylene mat and air gap are used in insulated drains. The thickness of all construction material layers varies and is not reported here.

Table 1: Thermal parameters of ground and tunnel construction material.  $\lambda$  is thermal conductivity W/mK;  $\rho$  is density, kg/m<sup>3</sup>;  $c_p$  is specific heat capacity, kJ/kgK;.

Material	$\lambda$	$\rho$	$c_p$
Ground (rock)	3.5	2 700	880
Concrete	1.7	2 300	880
Shotcrete	1.7	2 300	880
Polyethylene mat	0.04	20	940
Air gap	0.5	1.2	1 006

The deep, undisturbed ground temperature is an important boundary condition and initial value. An accurate measurement of this key input is difficult to achieve, especially in an urban environment. Normally, the historic average air temperature is applied with some compensation for the heat island effect. Here, the value of this input parameter has been adjusted through a parametric study to increase agreement between measured and simulated wall surface temperature during the comparison period. This has resulted in the value +9.6°C being used for the deep, undisturbed ground temperature. Incidentally, this corresponds to the average air temperature that was measured by a nearby weather station during the period from when the tunnel became operational until the start of the comparison period.

Heat flux through the ground and wall between the parallel tunnel tubes are simplified by superposition of temperature fields where one tunnel tube is considered to have an exact copy 20 m next to it, i.e. the temperature of the actual adjacent tunnel tube (which has the opposite direction of traffic) is not considered. This simplification is considered to have limited impact on the results.

Groundwater seepage into the tunnels varies during the comparison period varies between 2.0 and 4.5 l/s in the north and 5.3 and 5.6 l/s in the south, respectively [5]. The advected heat will influence the temperature profile into the tunnel wall. It is assumed that no groundwater is exposed to tunnel air.

### 3.4. Ambient

Recorded ambient air temperature, relative humidity and pressure is used as boundary conditions at the portals.

For air temperature and relative humidity, the monitoring station closest to the north portal is located about 4.5 km northeast of the northern portal [6] and the monitoring station closest to the south portal is located about 9.25 km northwest of the southern portal [6]. The monitoring stations sample data with half hour intervals.

For barometric pressure, the monitoring stations closest to the tunnel are located about 60 km north-northeast of the north portal [7] and 8 km south-southeast of the south portal [8]. Due to the large distance between the monitoring stations, a barometric gradient has been calculated between them which has been used to estimate the barometric pressure at the portals. The monitoring stations sample data with hourly intervals.



Impact from wind pressure is assumed to have a negligible influence on results and is not considered.

### 3.5. Trains

Table 2 shows train types and a number of relevant parameters used to model them.

Table 2: Train types used in the simulation and some of the parameters describing them.

Parameter	Unit	X31	X55	X61	Freight train
Train length	m	79	107	74	466
Front area	m <sup>2</sup>	9.3	11.5	11.4	13.2
Perimeter of front area	m	11.4	12.6	12.6	12.8
Nose drag coefficient	-	0.50	0.45	0.45	0.62
Skin friction coefficient	-	0.012	0.014	0.012	0.031
Total weight incl. pass./cargo	ton	180	310	179	1125
Tractive power	kW	2 300	3 180	2 000	3 600
On-board services heat	kW	40	85	40	0
Average number of passengers	-	115	123	117	-
Davis formula coefficient A	m/s <sup>2</sup>	0.0103	0.0071	0.0092	0.013
Davis formula coefficient B	1/s	0.0003	0.00019	0.0004	0.00027
Speed	km/h	180	200	160	86

The number of train passages per day and tunnel tube is shown in Table 3.

Table 3: Number of train passages per day in each tunnel tube.

	X31	X55	X61	Freight trains
Weekdays	19	2	7	0.8 – 8.8
Saturdays	16	5	0	0.8 – 8.8
Sundays	16	5	0	0.8 – 8.8

### 3.6. Heat loads

The only heat loads in the model are the ones generated by the trains.

## 4. RESULTS

To improve readability, the graphs show measurement data and simulation results as daily averages. However, no averaging has been applied to any of the input data.

Since several measuring stations in the tube with southbound traffic were not able to record data during long periods of time, results are shown only for the tube with northbound traffic. The level of agreement between measured values and simulation results in the tube with southbound traffic, during periods when recording of measured values worked, is similar to that observed for the tube with northbound traffic.

Figure 3, 4 and 5 shows air and wall temperatures 50, 1000 and 4300 m, respectively, into the tube with northbound traffic (from the entrance). Figure 6 shows air speed and wall inside temperature at 7258 and 50 m, respectively, into the tube with northbound traffic (from the entrance).

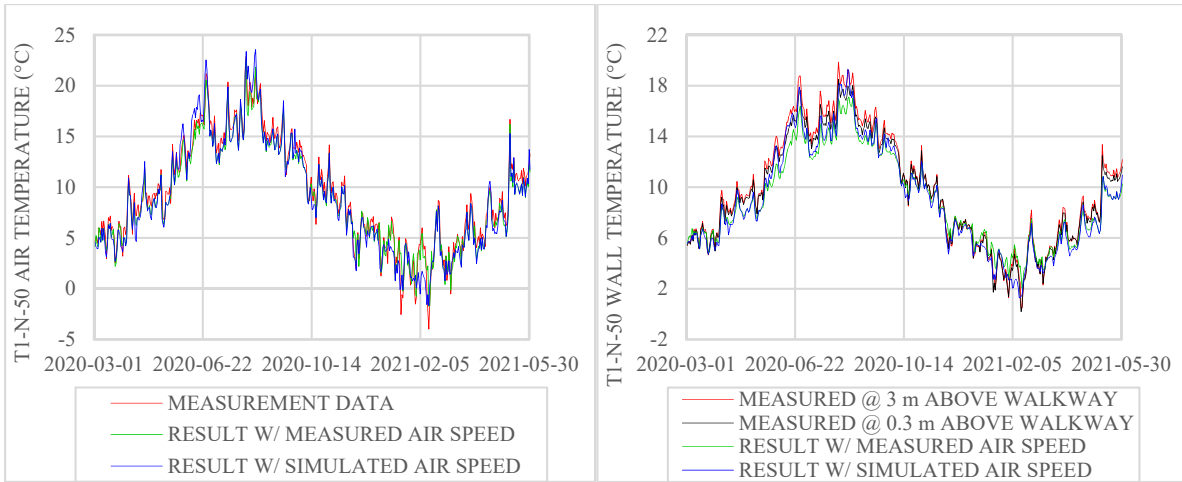


Figure 3: Daily average air and wall surface temperature 50 m into the tube with northbound traffic (from the entrance).

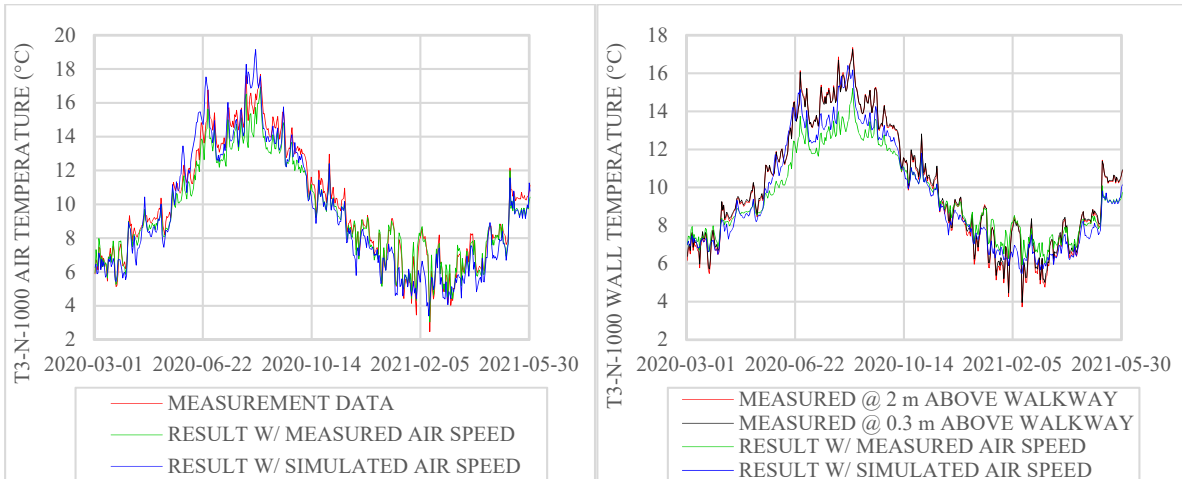


Figure 4: Daily average air and wall surface temperature 1000 m into the tube with northbound traffic (from the entrance).

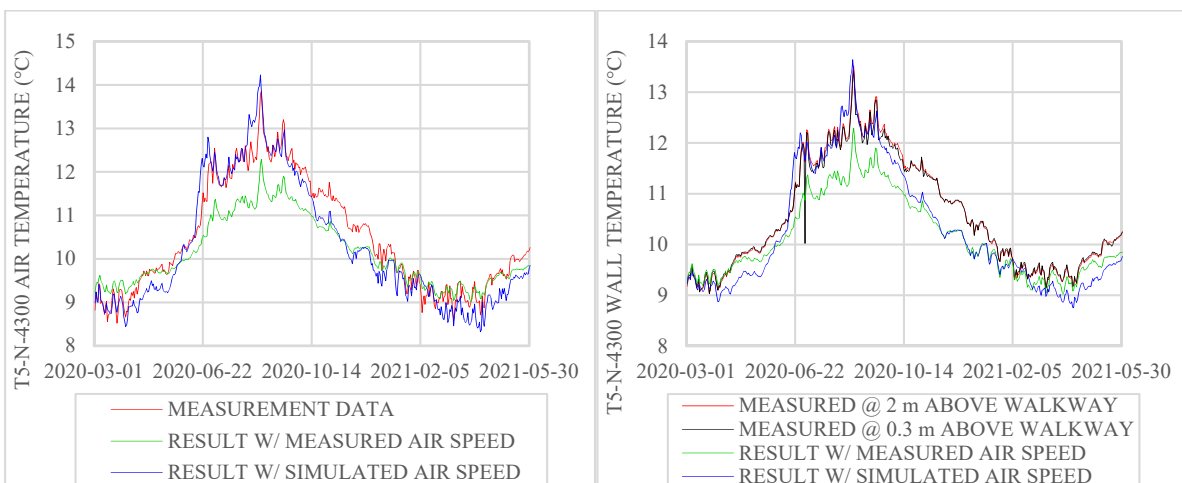


Figure 5: Daily average air and wall surface temperature 4300 m into the tube with northbound traffic (from the entrance).

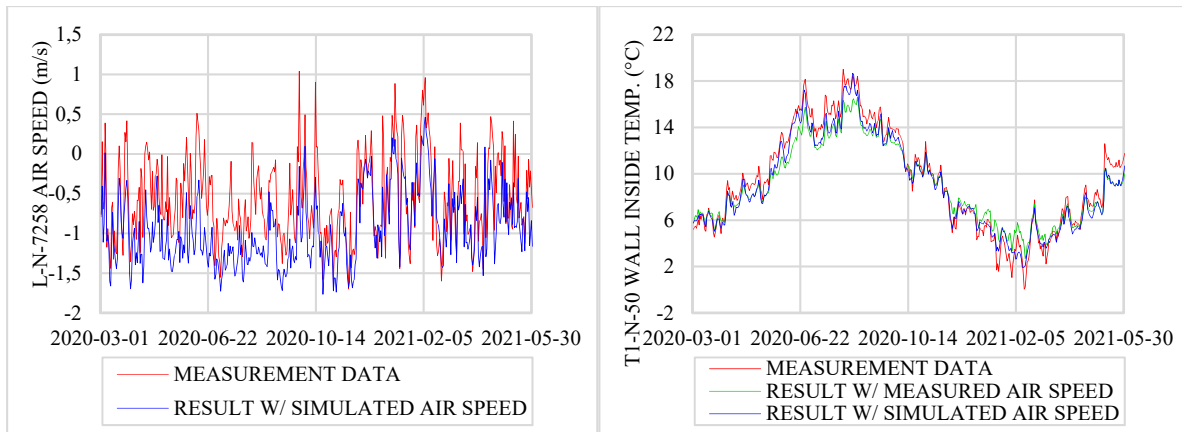


Figure 6: Left: Daily average air velocity (negative value means in the direction of traffic) 7258 into the tube with northbound traffic (from the entrance). Right: Temperature 5 cm into the wall, 50 m into the tube with northbound traffic (from the entrance).

## 5. DISCUSSION

The comparisons show that the simulation results are generally in good agreement with the measured values. The simulation models deal with a large set of parameters that are important in temperature studies of tunnels, such as thermal properties of tunnel construction materials and surrounding ground, geometry, elevation profile, actual weather conditions and train traffic.

Two important sources of error are uncertainties in the input data indicating the barometric pressure at the tunnel portals and the deep, undisturbed ground temperature. These parameters have a significant impact on results and are typically difficult to find input data for. The weather stations from which air pressure measurements were taken are located at great distances from the portals. This introduces uncertainty in the barometric gradient calculated from the weather station data that is used to estimate the barometric pressure difference between the portals.

The value used for the deep, undisturbed ground temperature was  $+9.6^{\circ}\text{C}$ , as this value provided the best agreement between simulation results and measurement data. This value was found to correspond to the mean temperature of the weather station nearest to the southern portal for the four previous full years before the start of the comparison period. The corresponding mean temperature for the weather station closest to the northern portal was  $+8.6^{\circ}\text{C}$ . In sparsely populated areas the deep, undisturbed ground temperature usually corresponds to the annual mean temperature for the site, so a better agreement would have been expected if the deep, undisturbed ground temperature had been set equal to the mean of the temperatures of both the northern and southern portals for a large number of years before the comparison period. Here, effects from groundwater flow may be part of the explanation.

Another obvious source of error is the estimate of traffic in the tunnel. Although good records of timetables and types of trains were found, the mixture of passenger and freight trains is not ideal for this type of study. No tuning of the traffic parameters was done and as Figure 6 (left) indicates, the computed air velocities were slightly higher than those measured. It may be somewhat counterintuitive that the simulations with computed air velocities sometimes show better agreement between simulated and measurement temperatures, than simulations based on measured air velocities.

Air velocities are measured with only one anemometer in each tunnel and the measurements are sensitive to turbulence caused by train passages. As air velocity affects the temperature in the tunnel, this is a source of error in the simulation where measured air velocities are used as

a boundary condition. In addition, it makes it difficult to assess how well simulated air velocities correspond to the actual ones.

## 6. CONCLUSION

The present study gives an indication of the type of accuracy that can be achieved with a reasonable amount of data collection and effort in using IDA Tunnel. As for any field study, the agreement is not perfect, but trying to achieve improved accuracy by a more elaborated physical model, e.g., in 2D or 3D, is difficult to motivate. The accuracy of the predicted results is well in line with inherent inaccuracies in measurements and obtainable input parameters.

## 7. REFERENCES

- [1] Wikström, N. Sahlin, P. (2019) Simulering av typtunnlar på höghastighetsbanan med avseende på kyla och isbildning, VTI rapport 1019. ISSN 0347-6030.
- [2] Wang, Y. Li, X. (2018) STESS: Subway thermal environment simulation software. *Sustainable Cities and Society* 38, 98–108.
- [3] Reinke, P., Wehner, M. (2018) Statistical distribution of air flow in rail tunnels and resulting risk of flow reversal during fire incidents. 9<sup>th</sup> International Conference ‘Tunnel Safety and Ventilation’, Graz, 93-100.
- [4] Wilhemsson, H. (2021) Tunneltemperaturer Hallandsåsen - Installationer och mätningar 2019-2021. VTI.
- [5] Björkman, F. Årsrapport 2020 - Prövotidsmätningar: Vatten. WSP, 2021-03-25.
- [6] The Swedish transport administration's weater information system VViS (2021) Data from measuring stations MS 1104 and MS 1124. <https://bransch.trafikverket.se/tjanster/trafiktjanster/VViS/>
- [7] Swedish Meteorological and Hydrological Institute (2021) Data from measuring station 63590. <https://www.smhi.se/data/meteorologi/ladda-ner-meteorologiska-observationer#param=airPressure,stations=all,stationid=63590>
- [8] Swedish Meteorological and Hydrological Institute (2021) Data from measuring station 62180. <https://www.smhi.se/data/meteorologi/ladda-ner-meteorologiska-observationer#param=airPressure,stations=all,stationid=62180>

## **THE PISTON EFFECT TEST BENCH FOR THE GRAND PARIS EXPRESS**

<sup>1</sup>Elisa BERAUD, <sup>1</sup>Fabien JOUVE, <sup>1</sup>Benoît HOUSEAUX

<sup>1</sup>Eiffage Énergie Systèmes, Ventilation of tunnel & underground spaces

### **ABSTRACT**

The "Grand Paris Express" railway network is currently under construction. It has been very quickly predicted that piston effect created by train will be greater than the traditional Parisian metropolitan network and all other networks in the world. This piston effect will be reflected in the stations and in all the shafts positioned roughly every 800 m in the tunnels for the intervention of emergency services.

These shafts are also used for ventilation for passenger comfort and safety. As a consequence, the equipment in the shafts will face with piston effect and will be subjected to strong variations in pressure. At reduced fan speed, it is expected the fans will be passed through with a negative airflow and also operated in negative pressure. Therefore, they will be operated in areas that are not defined by the usual.

In order to characterize a "Grand Paris Express" type fan, Eiffage carried out a platform to test the behavior of a model fan to the train piston effect. This test bench has been designed to reproduce the train passage on a cycle representative of the estimated pressure variation. The fan is therefore operated with successive negative and positive forced pressure on hundreds of thousands of cycles to ensure the durability of the equipment on several years of operation.

*Keywords: metro tunnel, train piston effect, test bench, model fan*

### **INTRODUCTION**

The new Grand Paris Express (GPE) railway network differs from the traditional Parisian metropolitan network for several combined reasons. On the one hand, the infrastructure is constituted of a succession of 1,000-2,000 m single bore bidirectional tunnels and stations with optimized sections of 50 m<sup>2</sup> and, on the other hand, it is operated with trains that travel at 110 km/h with a frequency passage of 90 s in rush hours.

It is expected the piston effect created by the overpressure due to the mass of air pushed in front the train and by the depression created behind the train would be exceptional in the tunnels: about  $\pm 1,000$  Pa in a few seconds.

The piston effect would be specific to each part of the lines depending of interdistance between stations, the slope and the curve of the track giving accelerating and braking behavior of the trains.

Piston effect would be also a function of train rate depending of peak hours (8:00 to 10:00 am then 5:00 to 8:00 pm) and off-peak hours (the rest of the day) or during weekend with a frequency passage of several minutes.

The following figure gives an illustration of the total pressure in the tunnel during the passing of two carousels of 10 trains spaced 90 s apart:

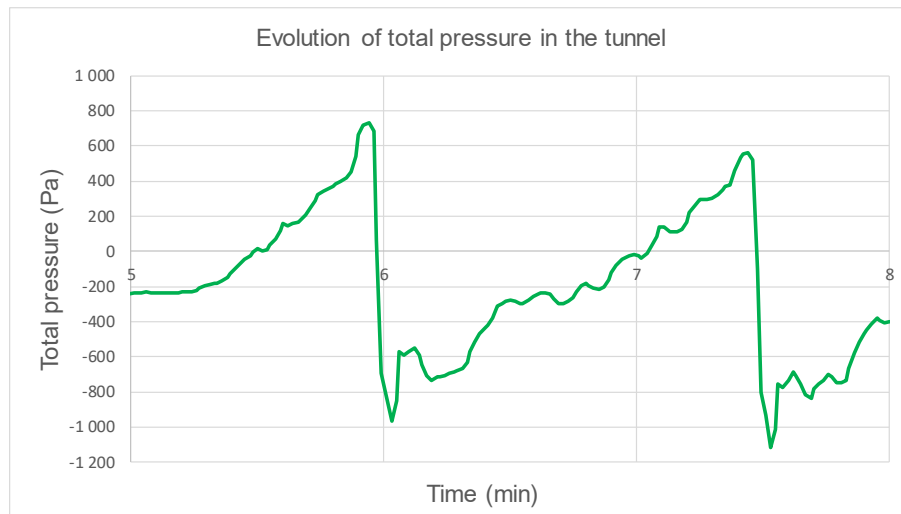


Figure 1: the evolution of total pressure in the tunnel (calculated by 1D code)

For the studies, the piston effect of Grand Paris Express has been characterized as follow:

- A criterion of total pressure of + 900 Pa and – 1400 Pa (conservative);
- A criterion of pressure gradient that is:
  - A decrease in pressure of 2,100 Pa at a rate of decrease of up to -500 Pa/s,
  - An increase in pressure of 1,600 Pa at a rate of up to 450 Pa/s.

These pressure fluctuations are reflected in the ventilation shafts located between the stations where the ventilation equipment is installed. And this at each train passage.

As a consequence, they are subjected to strong variations in pressure, which will modify the operating points. Therefore, they could be operated in areas of negative pressure and / or negative flow rates that are not defined for fans. With each passage of trains, the fans could be taken to unexplored operating zones.

We were aware that the consequences could be dramatic for operation: the fans could explode quickly after commissioning and would cause restrictions (or closure) of lines while operating.

Therefore, these new operating zones had to be explored. Several tests have been carried out with manufacturer to characterize the behaviour of the fan in the three quadrants of the curve (including negative flow and negative pressure) according to international standards (AMCA 802 and NF EN ISO 5801).

Then the endurance and resistance of the fans to these stresses had to be assessed. That is why a test bench has been designed, developed and build on Eiffage site to study the piston effect on a test fan which is similar but in smaller scale to the fans installed in Grand Paris Express shafts. Continuous operation of the bench makes it possible to simulate the operation of the real fan over several years and to test its durability.

The paper is more specific about the test bench (the description and characterisation of the model fan can be found in [4]). After a brief presentation of piston effect on GPE network, the paper will present the design of the test bench. Then it will present the principle of the test to reproduce the piston effect on the model fan.

## THE GRAND PARIS EXPRESS METRO

### The network

Grand Paris Express (GPE) will be a 100% automatic metro system of the Capital Region in France [1]. With its 68 brand new interconnected stations and 200 kilometers of new railway lines, this transit network will consist of a ring route around Paris (line 15) and lines connecting developing neighborhoods (lines 16, 17 and 18). Additionally, Grand Paris Express will also involve the extension of existing metro lines (line 14 to South). They will provide connections with Paris' airports, business districts and research clusters. It will service 165,000 companies and daily transport 2 million commuters.

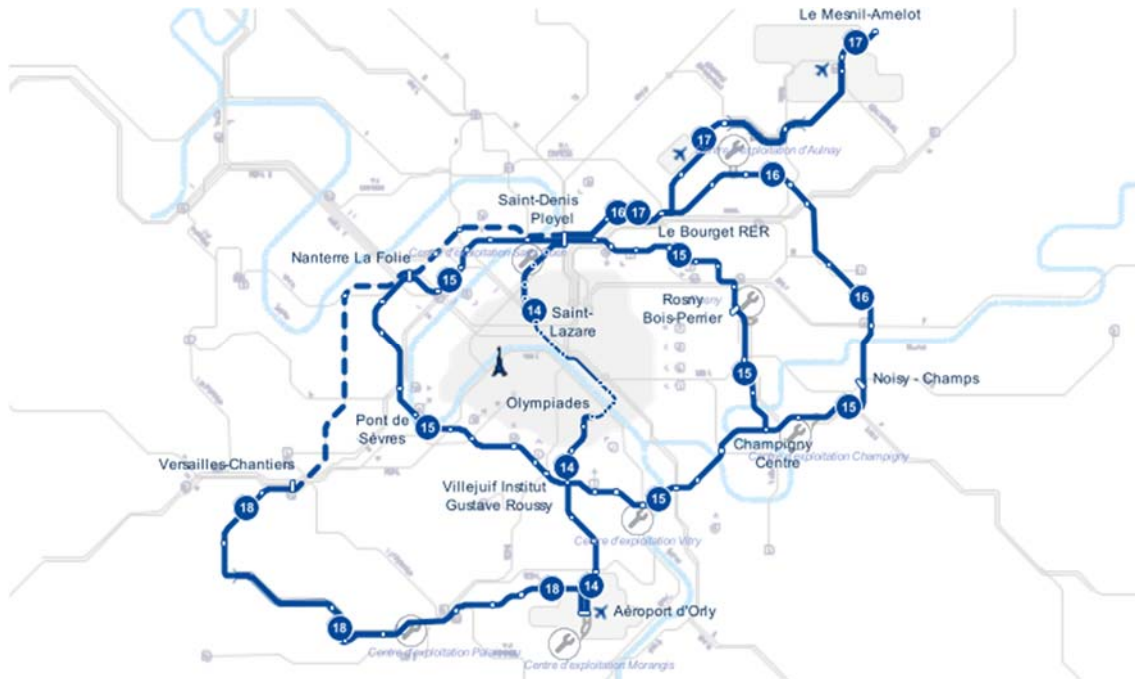


Figure 2: Grand Paris Express network

With 90 % of lines built underground, the good functioning of the new metro is ensured by the essential “service structure” positioned between stations.

Three times more numerous than stations, the 160 service structures will combine several functions, in particular related to passenger comfort and safety. Especially 120 of them will be equipped by ventilation equipment first to control smokes and protect the stations in case of fire in the tunnel, then to ensure air quality in the tunnel.

### The ventilation system

The design of the Grand Paris Express ventilation system must comply with the regulation of 22 November 2005 related to safety in tunnels of metros. [2]

As often, the ventilation system is sized by smoke extraction.

In the tunnel of GPE, the spread of smoke to facilitate evacuation of users and intervention of emergency services is controlled by a push-pull system. [3] It consists of using adjacent ventilation shafts in supply and/or extraction to ensure a distribution of the flows satisfying requested velocities.

To generate a velocity greater than 1.5 m/s upstream of the fire and a containment velocity of 0.5 m/s, the extraction smoke airflow in the tunnel is evaluated at 150 m<sup>3</sup>/s.

In operation, the comfort of passenger and air quality of tunnels is ensured by natural ventilation and reinforced during rush hours by mechanical ventilation working at reduced speed. The airflow is sized at 75 m<sup>3</sup>/s.

For this running point, fan are extremely sensitive to piston effect.

### THE PISTON EFFECT ON FAN

This last point can be illustrated on the operating curve of the fan (see Fig. 3).

The fans that will be installed by Eiffage in the ventilation service structures of lines 15 South, 16 and 17 of GPE are from Howden. The model ANR-2371/1122 will allow an operation for both fire extraction mode (operating point 1) and normal mode ventilation (operating point 2).

In case of fire, the fan will generate a flowrate of 150 m<sup>3</sup>/s and counter a network resistance of 1,200 Pa. The operating point is represented in red. In normal mode, the fan will work half speed and will generate a flowrate of 75 m<sup>3</sup>/s for a total pressure of 300 Pa. The operating point is represented in blue.

Resistance is the green line. The effect of train arriving (overpressure of + 900 Pa in the tunnel experienced as decrease of 900 Pa for the fan) and train leaving (depression of – 1,400 Pa in the tunnel) is represented with the two green dotted lines.

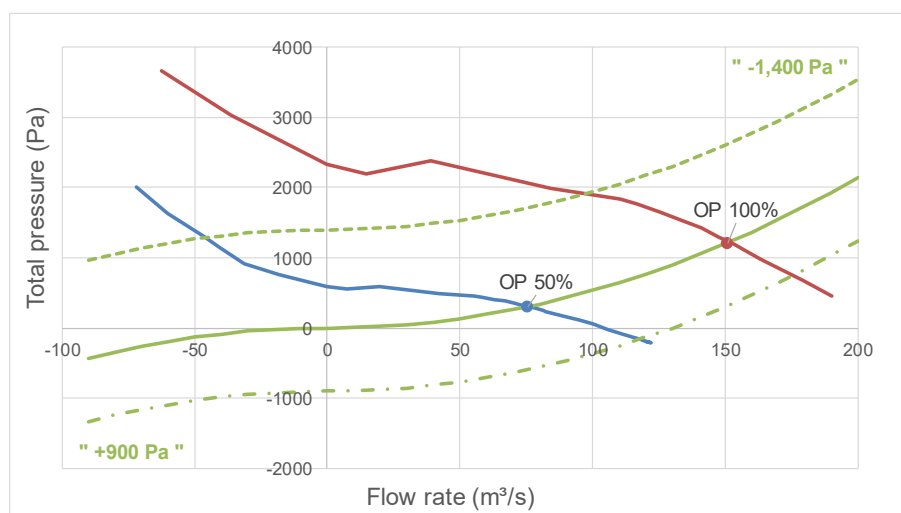


Figure 3: the piston effect on fan operation

The blue curve at reduced speed shows the displacement on the operating curve implying the need for anti-stall treatment. At the maximum pressure point (+ 1,400 Pa), the fan will be passed through with a negative airflow even though the fan is still running the same direction.

Extrapolation of the blue curve with the network curve for a tunnel pressure of + 900 Pa suggests that the two curves would intersect in negative pressure. This implies *a priori* the operation of the motor as a generator (negative mechanical power).

It appeared the fans would be taken in operating zones never encountered. As a consequence, they have to be characterized in these zones and then operated to test their resistance and durability with strong pressure variations.

It would not worth to test the piston effect on a real fan. It would take place and use a lot of power to be fully representative of the phenomenon. With a similitude of Reynolds and with same constraints on blades (with about the same tip velocity), the consequences of piston effect (both in the thresholds and in the pressure gradients) can be characterized on a model fan.



Common sense and scale consideration led Eiffage to carry out the tests on a fan with a diameter of 1,000 mm. This model fan has been installed on a test bench we designed and build - and then used - to reproduce the phenomenon of piston effect.

### THE TEST BENCH

The test bench is made up of a circuit in which are inserted the model fan and a generator fan which makes it possible to impose a pressure (or train passage) in this circuit.

The model fan can be forced with flow in one direction or the other by means of a dampers system, thus making it possible to simulate the effect of alternative overpressure and depression that are identical to the one encountered in real size.

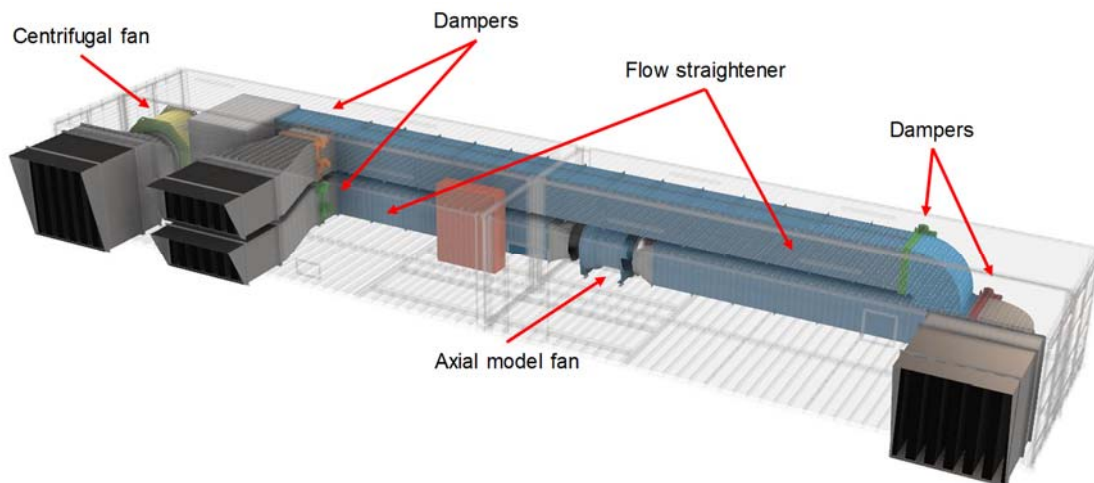


Figure 3: The test bench (front view)

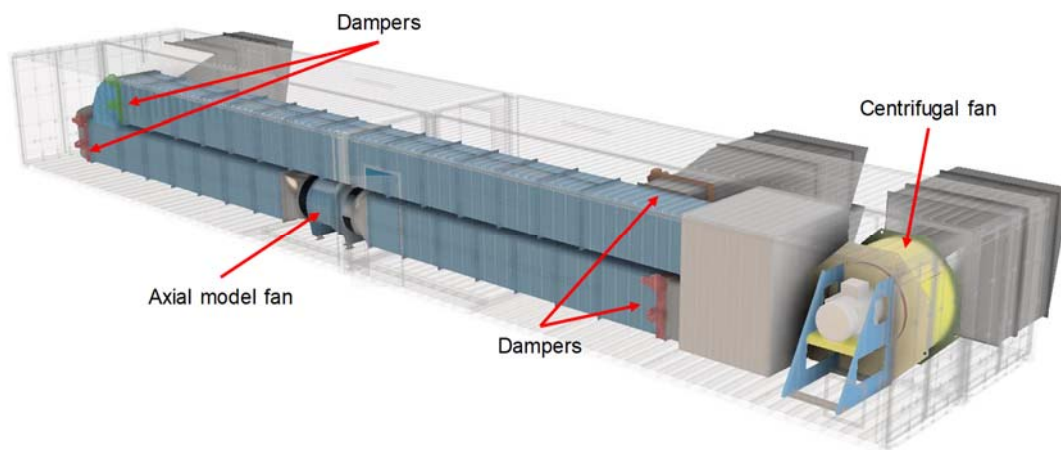


Figure 4: The test bench (behind view)

More precisely, the test bench has the size of 4 x 40 ft. containers (see Fig. 3 and 4).

The circuits are 1m x 1m metal ducts. Grids (or “flow straightener disposal”) have been added in upper part and lower part of circuits to reduce swirl and homogenize the flow in the ducts (according to standards NF EN ISO 5801).

The model fan is a 37 kW ANR-1000/473 axial fan, where both geometric and dynamic similarity have been respected with the full size fan installed in the GPE shafts. [4]

The following table gives the scaling and operating points of the model fan.

Table 1: real size and model fan characteristics

	Real size	Model
Impeller diameter	2,371 mm	1,000 mm
Hub diameter	1,122 mm	473 mm
Operating point 1		
Airflow	150 m <sup>3</sup> /s	26.7 m <sup>3</sup> /s
Total pressure	1,200 Pa	1,200 Pa
Rotation speed	980 rpm	2,324 rpm
Operating point 2		
Airflow	75 m <sup>3</sup> /s	13.3 m <sup>3</sup> /s
Total pressure	300 Pa	300 Pa
Rotation speed	490 rpm	1,162 rpm

The model fan will always rotate at the same speed and in the same direction (with a shaft power of about 5.5 kW) and would generate a flow from left to right on the test bench (Fig. 3).

The generator fan is a 75 kW centrifugal fan with an impeller diameter of 1,250 mm that produces 25 m<sup>3</sup>/s for a pressure difference of 1,800 Pa. It will be operated at constant speed and constant power (about 70 kW).

Air flow is sucked from outside by the 2m x 2m portal on the left; it is rejected in a plenum of 2m high, 1m large and 2m long. Then airflow is oriented in one or other ducts.

When the dumper in the top ducts are closed, the flow circulates in the bottom 1m x 1m ducts and evacuates outside by the 2m x 2m portal on the right (Fig. 3). The model fan is passed through with a flow in the same direction. This is operation in positive direction (see Fig. 5). The pressure is imposed by means of the flow rate. On the operation curve, the point is displaced in the negative pressure zone as if the train was arriving. The fan receives works as a generator.

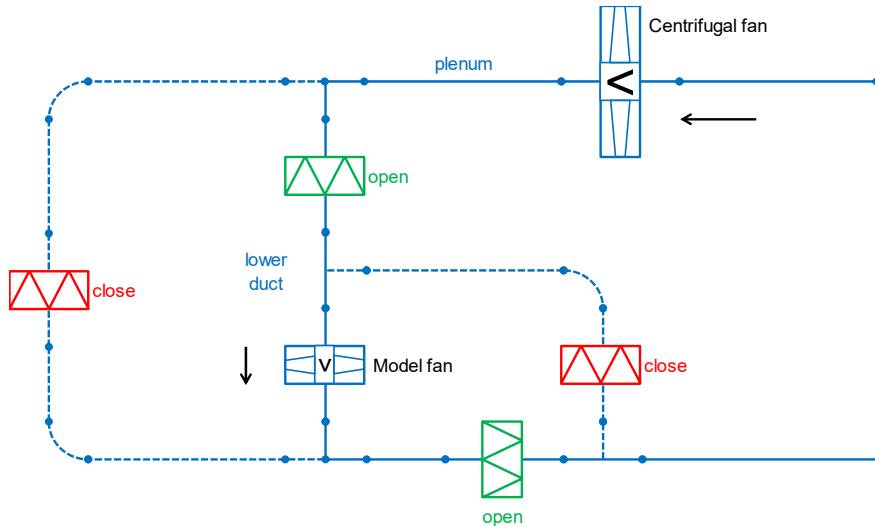


Figure 5: Operation in positive direction

When the dumper in the bottom ducts are closed, the flow circulates in the top 1m x 1m ducts, comes back in the bottom ducts, and evacuates outside by the 2m x 1m bottom portal on the middle (Fig. 3). The model fan is passed through with a flow in the opposite direction. This is operation in negative direction (see Fig. 6). On the operation curve, the point is displaced in the negative airflow zone as if the train was leaving. The fan generates a flow in one direction and receives a flow in opposite direction. The fan is under high pressure.

As the need to bring fan in negative airflow is less important, there is a discharge regulated by a damper in the plenum through the 2m x 1m top portal on the middle (Fig. 3 and 4).

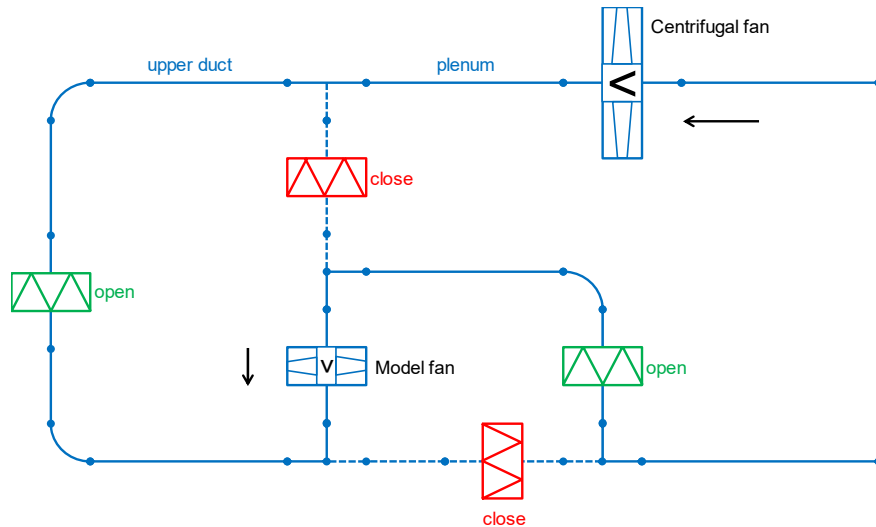


Figure 6: Operation in negative direction

The test bench can be operated alternatively in negative pressure and negative airflow to simulate passage of trains with a programmed sequence of dampers. Opening and closing have been adjusted to simulate the pressure gradient of arriving and departing train but have been accelerated to concatenate frequency of passage.

They can be opened or closed in 2 seconds; the kinetics can be determined and intermediate position can be ordered (see Fig. 7). Dampers are operated with 4-20 mA. An example of opening and closing curves of dampers can be illustrated on Fig. 7.

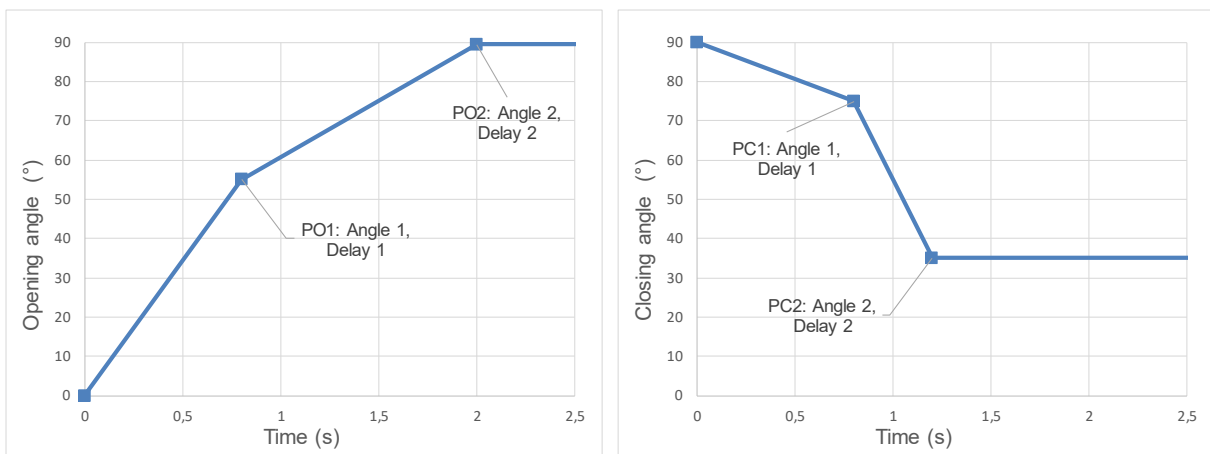


Figure 7: Opening and closing of dampers

### Instrumentation

The test bench is equipped with many captors. On each upper and lower ducts of the circuit, there at least two means of airflow determination, which could be:

- Vane anemometers;
- Static pressure probes;
- Measurement wings.

There are three anemometers: one is placed in the upper duct to measure airflow upstream the fan when operated in negative direction and the two others are in the lower duct to measure airflow upstream and downstream the fan when operated in positive direction.

Flow is also measured with pressure probes in the area of the model fan impeller and the flow straighteners. Moreover, we have placed a measurement damper (a classic damper whose blades are fitted with pressure taps) that allow to determine the flow through the duct. [5]

The bench has been calibrating with Pitot probe measurement on 36 vertical and horizontal points on a section with log-Tchebycheff distribution (according to NF EN ISO 5802). All the sections close to anemometers have been tested. In parallel, the “dzeta” or pressure drop coefficient of the disposal has been determined.

The fan is of course equipped with vibration captors. Temperature bearings and windings are also measured. All data are send to SCADA cabinet and registered to be analyzed.

The test bench can be automatically operated (train passage cycle) for endurance tests. All equipment can also be separately and manually operated. Under these conditions, the fan can be operated stationary in all configurations.

## CONCLUSION

The train piston effect that fan installed in the ventilation shafts of the Grand Paris Express network will endure is currently studied on a homothetic model fan.

The model fan has been first characterized by manufacturer for the specified operating points in smoke extraction mode and normal mode. It has also to be tested at negative pressure and negative flow, both in forward and reverse direction. [4]

Then the model fan has been installed and operated on the test bench designed by Eiffage to simulate the train piston effect. The model fan has been yet operated over 300,000 cycles of train passages, which can be equivalent to an operation over more than 10 years.

The test bench has allowed to test the resistance and the durability of the fan submitted to pressure variations with very strong pressure gradients both positive and negative over a very short time interval. At the end of the test, the blades will be tested to study and verify mechanical fatigue the fan has endured.

The bench has allowed to test the behavior of the fan with significant airflow disturbances in operation. It has been experienced especially in extreme configuration of train passage: with the train adding a flow to the flow of the fan (fan as a wind turbine) or with the train imposing a flow in the opposite direction the fan is operating.

## REFERENCES

- [1] <https://www.societedugrandparis.fr>
- [2] Arrêté du 22 Novembre 2005 relatif à la sécurité dans les tunnels des systèmes de transport public guidés urbains de personnes
- [3] Ventilation et désenfumage des réseaux de métro, P. Carlotti, J.-F. Burkhart, A. Mos, A. Dusserre and J.-M. Passelaigue, Techniques de l'Ingénieur, March 2022
- [4] A model fan to test the train piston effect at Grand Paris Express metro, E. Béraud, B. Houseaux, F. Duet, FAN 2022, Senlis (France), 27 – 29 June 2022
- [5] The measurement damper tested and validated in the B5 ramp, E. Béraud, V. Jury, B. Houseaux, J.P. Margrita, ISAVFT 2022, Brighton (UK), 28 – 30 Sept 2022

## **RAPID FIRE DETECTION AND NOTIFICATION USING A DUAL THERMAL+OPTICAL CAMERA**

<sup>1</sup>Takuya Matsumoto, <sup>1</sup> Tatsuya Oshiro, <sup>1</sup> Kazuki Furuhashi, <sup>2</sup> Hideyuki Uemura, <sup>3</sup> Alan Vardy

<sup>1</sup> Sohatsu Systems Laboratory Inc., Kobe, Japan

<sup>2</sup> Teledyne FLIR, Osaka, Japan, <sup>3</sup> University of Dundee, Dundee, Scotland, UK

### **ABSTRACT**

The latest fire detection standard of the Japanese Ministry of Land, Infrastructure, Transport and Tourism (“MLIT”) requires that a 0.5m<sup>2</sup>, 2 litre gasoline fire at a distance of 25 m must be detected and reported within 30 seconds of ignition. The paper shows that this requirement can be met reliably by using 'dual' video cameras, each with both thermal and optical functionality. It then describes how this capability can be incorporated into tunnel monitoring systems. The effectiveness of the method is demonstrated by the results of nine tests in a full-scale tunnel, namely three tests for each of three rates of airflow, nominally 0, 2.5 & 5.0 m/s. Every fire was detected in less than 10 seconds, thereby far exceeding the MLIT standard. Also, the passage of hot body vehicles through the test tunnel did not trigger false alarms. In addition to describing the system and the tests, the paper discusses related issues of practical importance to tunnel operators.

*Keywords: rapid fire detection, rapid fire notification, thermal camera, fire test*

### **1. INTRODUCTION**

In 2019, the Japanese Ministry of Land, Infrastructure, Transport and Tourism (“MLIT”) issued a revised tunnel-fire standard. The new standard requires that a 0.5 m<sup>2</sup>, 2 litre gasoline fire at a distance of 25 m must be detected and reported within 30 seconds of ignition. It also requires that the detection must be linked to automated emergency notification equipment and it called for a new technology for such equipment.

The required speed of detection is very challenging for existing systems. For example, a relatively recent system based on a linear temperature sensor cable has not been proven to meet it. That system has been shown to be capable of detecting fire from a 12 litre N-Heptane on 1.0m<sup>2</sup> fire pan within 30 seconds [1], but it has not been validated with smaller fires. It cannot be assumed to be able to meet the new standard because smaller fires will generate less heat and hence will increase the time before detection. Linear temperature sensor cables continue to have a valuable purpose (see Section 5), but a different technology is needed to be certain of meeting the new MLIT standard.

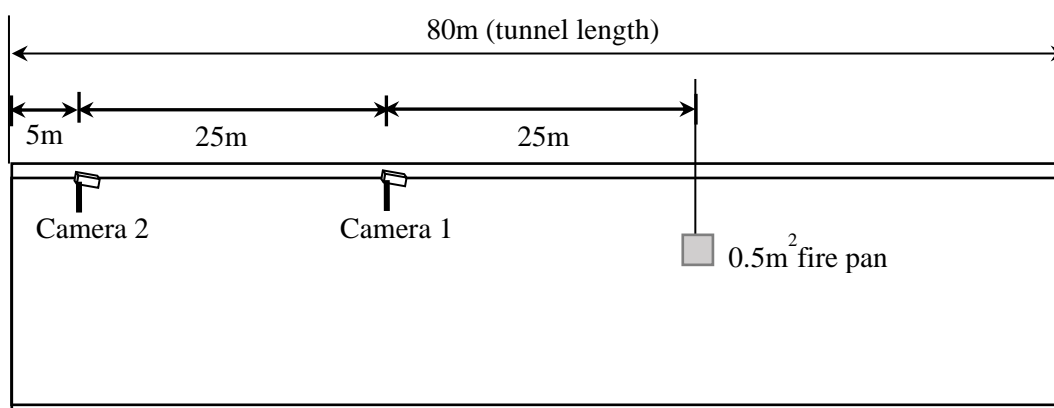
### **2. DUAL-SENSOR VIDEO CAMERAS**

The detection system introduced herein is based on the use of dual-sensor video cameras that have one optical sensor and one thermal sensor [2]. The thermal sensor fulfils the primary function of rapid detection. It is targeted to do this much sooner than the 30 s limit prescribed in the MLIT standard. Thermal cameras enable visibility in bad weather and in dark environments. They detect infrared wavelengths that correspond to the temperature of the object. Accordingly, they are highly suited to detecting temperature increases caused by fires. Furthermore, they can detect the presence of people and animals even in situations where an optical camera's view is obstructed by smoke or lack of light.

The optical sensor enables rapid verification of incidents reported by the thermal sensor. This is an important intended use, but it is far from being the only one because it will also be available for continuous monitoring during routine operation. The particular camera chosen for testing provides optical images of a similar quality to those of conventional high definition (“HD”) optical cameras. If linked to suitable image-processing technology, it could be used for rapid detection of non-fire incidents.

### 3. FIRE DETECTION TESTS IN A FULL-SIZE TUNNEL

In February 2021, a series of fire tests was undertaken in a full-size, experimental tunnel owned by Japan Construction Method and Machinery Research Institute (near Mount Fuji). The tunnel is 80m long and 7.8m high and its cross-sectional area is 78m<sup>2</sup>. The purpose of the tests was to determine whether the cameras could detect fires reliably within the required maximum time of 30 s. Two cameras were installed, one at a distance of 25 m from the fire pan and the other at a distance of 50 m. Each was mounted at a height of 3.5 m, which is the same as the height of CCTV cameras in Japan. There was no communication between the cameras. The reason for having two of them was to enable their performance at different distances from the fire to be assessed. **Figure 1** shows the arrangement of the two cameras and the fire pan in the tunnel.



**Figure 1 Arrangement of fire pan and cameras in the test tunnel**

Tests were conducted at three airflow speeds along the tunnel, namely 0, 2.5 and 5.0 m/s. Three tests were undertaken at each speed so that repeatability could be monitored. The reason for testing at different wind speeds is that this influences the behaviour of fires. For instance, the greater the speed, the smaller the size of the image seen at the camera – because the flame bends over. In addition, higher wind speeds cause greater turbulence and this causes flames to fluctuate. One consequence of this is that true repeatability is not possible in tests such as this, thereby increasing the importance of undertaking repeat tests.

One limitation of the tests was the length of the tunnel. It is intended that further tests will be carried out at another location in future to test the performance of the cameras at greater distances – 100 m or even more. The results of such tests will influence the number of cameras needed for safe operation. This is important for maintenance and supervision as well as for initial capital costs.

#### 3.1 Test results - fire

The middle and right-hand columns in Figure 2, 3 and 4 show thermal images at the instants when the fires were detected. The images in the middle column are from Camera-1, which was 25m from the fire, and those in the right-hand images are from Camera-2. The left-hand columns give the Test Number together with the measured speed of air flow. The time from

ignition of the fire until detection is listed beneath each image. In colour versions of the figure, the fire is seen as a red blob. In all cases, Camera-1 detected the fire before Camera-2, but the additional delay was only about 2 s on average even though doubling the distance reduced the size of the fire image by a factor of two (width) and a factor of four (area). Importantly, all nine fires were detected by both cameras in less than 10 s, which is far inside the 30 s window required by the new MLIT standard.







No. Air velocity [m/s]	Thermal image at the moment of detection Detection time	
	Camera 1 (25m)	Camera 2 (50m)
No. 1 0.22 [m/s]	 3.0 [s]	 5.0 [s]
No. 2 0.15 [m/s]	 2.9 [s]	 5.7 [s]
No. 3 0.01 [m/s]	 3.8 [s]	 7.0 [s]

Figure 2 Thermal image at the instant of detection (air velocity = 0 m/s)







No. Air velocity [m/s]	Thermal image at the moment of detection Detection time	
	Camera 1 (25m)	Camera 2 (50m)
No. 4 2.96 [m/s]	 6.3 [s]	 8.7 [s]
No. 5 2.60 [m/s]	 7.1 [s]	 7.7 [s]
No. 6 2.57 [m/s]	 4.0 [s]	 5.8 [s]

Figure 3 Thermal image at the instant of detection (air velocity = 2.5 m/s)



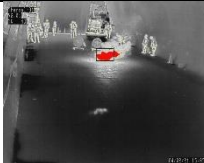

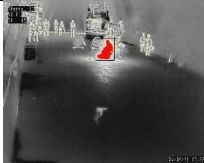

No. Air velocity [m/s]	Thermal image at the moment of detection Detection time	
	Camera 1 (25m)	Camera 2 (50m)
No. 7 5.53 [m/s]	 4.0 [s]	 5.0 [s]
No. 8 5.62 [m/s]	 6.1 [s]	 8.1 [s]
No. 9 5.95 [m/s]	 4.8 [s]	 6.0 [s]

Figure 4 Thermal image at the instant of detection (air velocity = 5.0 m/s)

Further quantitative data about the test configuration are given in Table 1. The outer columns give the same numerical values as those shown in Figures 2, 3 & 4 and the inner columns list environmental data. The correlation between the detection times and the air velocity was somewhat unexpected. For camera-1, the average detection times at air speeds of 0, 2.5 and 5.0 m/s were approximately 3.2, 5.8 and 5.0 s respectively and those for Camera-2 were approximately 5.9, 7.4 and 6.4 s. Of these six averages, only the value of 3.2 s stands out from the rest. This gives some cause to suspect that the influence of air speed on behaviour of a flame (as described in Section 3) is significant only at small velocities. However, the evidence of the 2.5 and 5.0 m/s data certainly does not support any expectation that the effect would increase with increasing speed. This suggests that the thermal sensors are more sensitive to the overall heat amplitude than to the size of the image presented by the heat source.

The illumination in the location of the cameras themselves was measured because, in principle, it can influence the performance of various types of camera. However, the evidence in Table 1 suggests that this did not have a significant influence on the performance of the thermal sensors. Camera-2 performed well even though it was at twice the distance of Camera-1 and also was close to the tunnel portal and thereby in an especially brightly-lit location.

**Table 1 Results of fire tests**

Case No.	environment						detection time [s]	
	air velocity on fire pan [m/s]	illuminance [lx]			temperature [deg. C]	humidity [%]	camera 1 (25m)	camera 2 (50m)
		fire pan	camera 1 (25m)	camera 2 (50m)				
1	0.22	120	140	1300	13.3	32.4	3.0	5.0
2	0.15	100	140	1300	14.0	30.7	2.9	5.7
3	0.01	100	140	1300	15.1	28.2	3.8	7.0
4	2.96	100	140	1300	15.1	20.9	6.3	8.7
5	2.60	100	160	1600	16.5	17.2	7.1	7.7
6	2.57	100	140	1700	15.1	19.0	4.0	5.8
7	5.53	80	140	2100	16.8	18.2	4.0	5.0
8	5.62	80	160	2500	15.4	18.0	6.1	8.1
9	5.95	80	140	2500	14.2	21.1	4.8	6.0

The other environmental parameters recorded on site were the temperature and humidity of the inflowing air. Of course, such data cannot be controlled, but, instead, are climate and weather-dependent. In practice, the temperatures did not vary significantly during the tests and, although the specific humidity varied by almost a factor of two, all values were quite low. In practice, therefore, little can be inferred about any possible influence of either of these parameters.

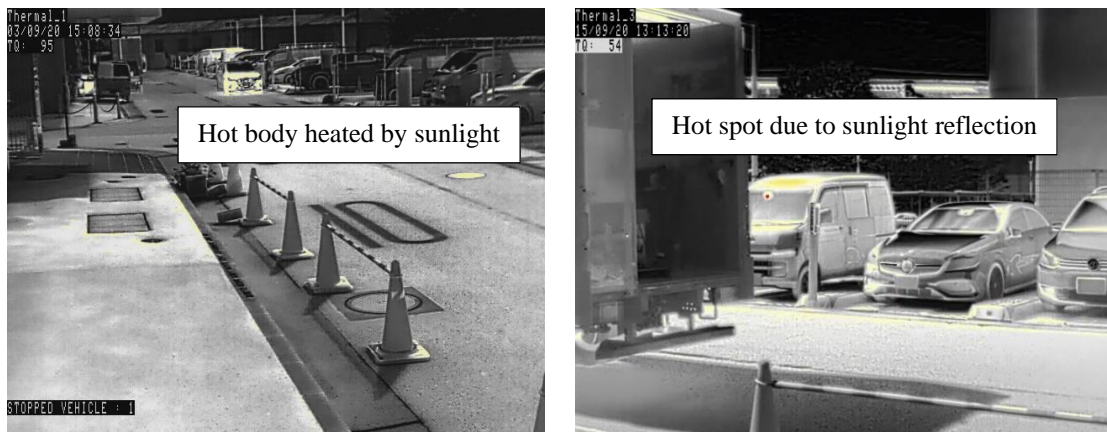
### 3.2 Test results – non-fire heat sources

The 100% detection performance of the cameras in the fire tests is highly encouraging. However, it is also important that this is not achieved at the expense of allowing non-fire heat



sources to trigger unacceptable numbers of false alarms. Accordingly, additional tests were conducted in which vehicles with hot spots (exhausts gases, etc) and hot body shells (from engines and long exposure to direct sunlight) passed through the factory road (Fig.5). These did not trigger alarms even though some (highly) local temperatures will have been close to those expected in the early stages of a fire. In addition, tests were conducted outside the tunnel on vehicles that had been exposed to hot sunshine for lengthy periods. Again, these did not trigger alarms.

Experience of continuous, day-to-day operation in an existing tunnel will be necessary before the true likelihood of false alarms can be determined unequivocally. However, the 0% record in tests designed to replicate real behaviour as closely as practicable is a strongly encouraging sign.



**Figure 5: Hot body testing failed to cause false alarms**

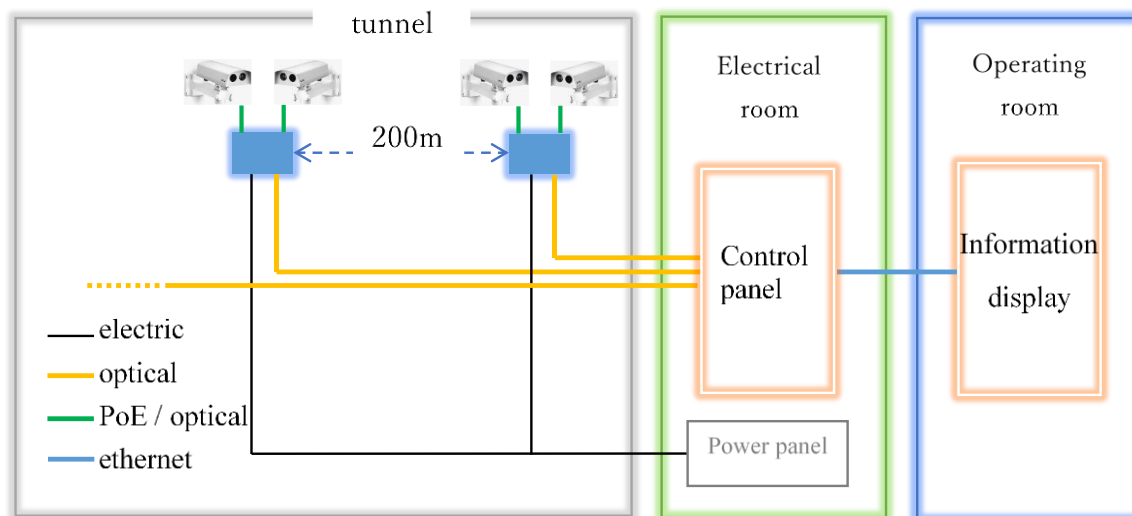
#### **4. FIRE DETECTION AND TUNNEL MONITORING SYSTEMS**

In a practical implementation in a road tunnel, there would be multiple cameras. The most suitable distance between successive cameras cannot be finalized until further tests have been undertaken at greater distances that were possible in the test tunnel. Provisionally, however, it is assumed that reliable detection will be possible in much less than 30 s at distances in excess of 100 m. Accordingly, it is expected that cameras will be installed in pairs at intervals of 200 m, with one facing in each direction. This arrangement has the following practical benefits:

- It enables fires to be seen from both directions. This has obvious advantages for the optical sensors, but it is also useful for the thermal sensors because it reduces the possibility of non-detection caused by vehicles blocking lines of sight to a fire.
- If it is found to be necessary to install a local panel or box adjacent to the camera, the required number of such boxes will be halved.

The integration of the cameras into the tunnel monitoring system is illustrated in Figure 6. The left-hand box shows successive pairs of cameras, one from each pair being needed to cover both sides of an incident in the intervening 200 m. The signals from the cameras are passed to the control panel that is responsible for triggering automatic responses as well as for communicating with operators when the system is being monitored by humans. The details of the control panel and its algorithms are not given here, partly because some will be site-specific even though others will be universally applicable. However, the proposed

methodology closely resembles that described by Sakaguchi et al [3] for detection using linear-temperature sensor cables.



**Figure 6 Integration of cameras in the tunnel monitoring system**

## 5. OPERATIONAL CONSIDERATIONS

The system can provide fire detection comparable to conventional systems using combinations of infrared sensors and CCTV cameras. However, the use of dual cameras that combine the two types of sensor in single unit has obvious advantages for installation and maintenance purposes as well as for system integration and capital cost. Furthermore, the tests reported above give preliminary evidence that the proposed system is likely to be both quicker and more reliable than existing systems, although there is not yet enough evidence to justify such a conclusion rigorously. Also, any new approach requires careful attention be paid to possible disadvantages, inadequacies and maintenance issues and this process has revealed some scope for future development as well as issues that can be addressed during further development and/or through appropriate maintenance specifications. One example of each of these possible types of counter-measure is now given.

Any surveillance system that relies upon having a direct line of sight between a sensor and an incident can be rendered ineffective by obstructions to the line of sight. In road tunnels, such obstructions can be caused by intervening vehicles. This is especially likely when one or more such vehicles are large and stationary – although that is less likely during the early stages of a fire when detection is most effective at reducing potential consequences. Examples of such detection delays with existing systems using flame-based sensors have been reported where a fire was not detected for many minutes due to the vehicles blocking the line of sight to the fire flame. In principle, this issue could be addressed by installing the cameras at shorter intervals than currently envisaged, but that is not the only option. Another possibility is to make use of linear-temperature sensor cables that are easily installed and, as indicated above, have been shown to effective, albeit not sufficiently responsive to meet the new MLIT requirements.

As an example of potential maintenance issues, attention is drawn to the need for one of the dual cameras at any particular location to face in the direction opposite to the main traffic flow. This will increase the rate at which the lenses become dirty and thereby cause the quality of the images to deteriorate. Specially-designed hoods are being developed to reduce this problem. In the case of bi-directional tunnels, the problem could also be reduced by installing each

camera on the side of the tunnel in which the direction of traffic flow is the same as the camera direction.

## 6. SUMMARY AND CONCLUSIONS

A new fire detection system for road tunnels is at an advanced stage of development and its core function has been tested in a full-scale tunnel. The system is based on the use of dual video cameras that have two sensors, one for thermal imaging and one for optical imaging. The motivation of the development is the existence of a new fire standard in Japan, requiring fire to be detected and automatic responses initiated within 30 seconds of ignition. This has to be achieved for a 2 litre gasoline fire size of 0.5 m<sup>2</sup> at a distance of 25 m.

An outline of the new system has been presented. One pair of dual cameras is installed at intervals of 200 m along the whole of the tunnel. One camera in each pair faces forwards and the other faces backwards, giving cover of any incident from both directions.

The full-scale tests were conducted in a tunnel that is used only for R & D and is only 80 m long so the new system has yet to be proven at distances implied by the proposed design. However, in the tests, a camera at a distance of 50 m from the pan fire achieved a 100% detection rate in less than 10 s. Furthermore, the passage of vehicles with hot-spots did not trigger false alarms.

Attention has been drawn to examples of issues that need to be addressed by any detection system and possible counter-measures have been identified. These include tunnel-specific modifications to hardware that will reduce implications for maintenance schedules.

There is a strong expectation that the required detection standards will be met with existing technology and that future developments in camera technology will enable even greater distances between successive camera locations to be acceptable.

## 7. REFERENCES

- [1] Nakahori, I., Oshiro, T., Fukuda, K., Matsumoto, T., & Abe, S. (2018). *Fast fire detection by linear temperature sensor cable and its application*, 9th International conference 'tunnel safety and ventilation', Graz, pp. 165-174.
- [2] Teledyne FLIR, ITS Series DualAID 316L Datasheet, 21-0337-INS-USL, Revised March 2021.
- [3] Sakaguchi, T., Matsumoto, T., Yamamoto K. & Takegaki M., I., (2020). *Road tunnel temperature monitoring system using a simulation mode*, 10th International conference 'tunnel safety and ventilation', Graz.

## EXPERIMENTAL STUDY ON GENDER DIFFERENCE IN MENTAL STRESS AND WALKING SPEED DURING TUNNEL FIRES

<sup>1</sup>Wenhao Li, <sup>1</sup>Miho Seike, <sup>1</sup>Akimasa Fujiwara, <sup>1</sup>Makoto Chikaraishi

<sup>1</sup>Hiroshima University, JP

### ABSTRACT

To investigate the relationship between mental stress and walking speed in a smoke-filled tunnel, an evacuation experiment was conducted in a smoke-experience tent, where 16 students (8 males and 8 females) participated. The heart rate change rate before and during the experiment (Group 0: <1, Group 1: 1–1.2, Group 2: >1.2) was used as an index of mental stress. The mean walking speed in smoke of each group were calculated based on gender. At  $C_s = 0.5\text{--}1.0\text{ m}^{-1}$ , the mean walking speed values of the females of Groups 0, 1, and 2 were 0.72, 0.94, and 1.23 m/s, respectively. the mean walking speed gradually increased as the heart rate change rate increased. However, the mean walking speed values of the males of Groups 0, 1, and 2 were 1.05, 0.83, and 0.75 m/s, respectively. the mean walking speed gradually decreased as the heart rate change rate increased. This indicates that males and females possess different spatial cognitive styles, implying that the influence of mental burden on walking differs based on gender.

*Keywords: tunnel fire, smoke, walking speed, mental stress, gender, experimental.*

### 1. INTRODUCTION

When a fire occurs in a tunnel, people evacuate through smoke, and there is a substantial risk of human casualties. To minimize this risk, evacuation behavior in smoke-filled tunnels should be investigated. There are several evacuation behavior studies in smoke-filled tunnel like spaces [1–9].

However, there are few studies on mental stress-related evacuation behavior other than Jin [10] and Seike et al. [11]. Leach [12] reported that during ship and airplane disasters, 10%–20% of evacuees can act and decide calmly, whereas 70%–75% freeze and 10%–15% cry or scream. In addition, because of heart rate increasing and breathing difficulties due to acute stress reaction in the evacuation [13], the smooth evacuation is difficult. Therefore, it is necessary to consider mental stress in the evacuation. Jin [10] evaluated mental stress based on heart and breathing rates and reported that when people experienced mental stress caused by smoke, their walking speed slowed down. However, Jin's experiment was conducted over 40 years ago, and mental stress and walking speed had not been measured at the same time. Additionally, the gender differences had not been investigated.

Seike et al. [11] evaluated mental stress based on the heart rate and blood pressure, and reported that when the participants felt mental stress owing to the loss of visibility caused by wearing an eye mask, their walking speed slowed by 0.1 m/s. However, Seike et al. [11] did not consider smoke and the gender differences. Therefore, to investigate the relationship between mental stress and walking speed in smoke-filled tunnels, and differences in this relationship based on gender, we conducted a smoke evacuation experiment.

This paper focused on the gender behavior difference in the case of individual evacuation for the fundamental data to expand group dynamics based on this data in the future topic.

## 2. METHODOLOGY

### 2.1. Smoke experience tent

The experiment was conducted in a smoke-experience tent (tent, Figure 1). The length, width, and height of the tent were 10, 2, and 2 m, respectively. Four checkpoints (CPs) were set up inside the tent (Figure 2). The longitudinal and vertical directions were indicated by  $x$  and  $y$ , respectively, and the origin was set at CP1. For smoke density, three smoke density measurements were used to calculate the intensity of the incident light and the intensity of light passing through the smoke. Then, the following Lambert–Beer law was used to convert these values into smoke density:

$$Cs = \frac{1}{l} \ln \frac{I_0}{I}$$

Where  $Cs$  is the smoke density,  $I_0$  is the intensity of the incident light,  $I$  is the intensity of light passing through the smoke, and  $l$  is the light path length ( $l = 0.8$  m).



Figure 1: Inside (left) and outside (right) the smoke tent

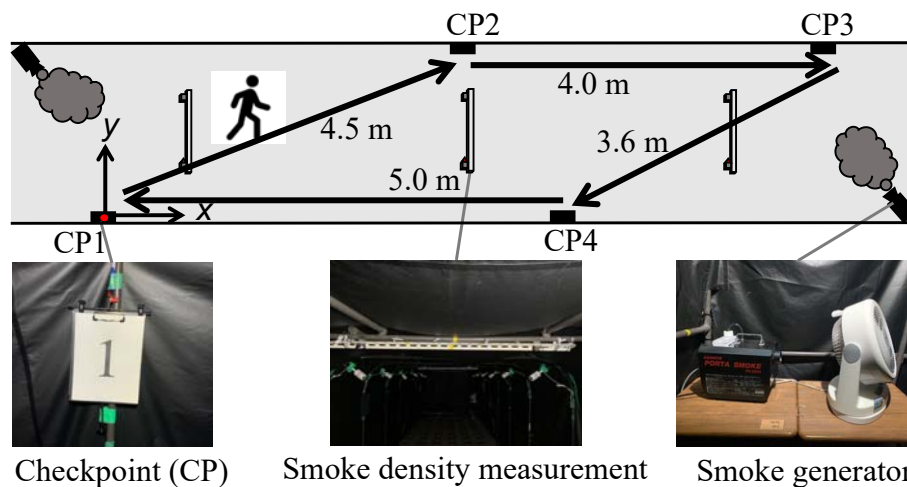


Figure 2: Evacuation route

### 2.2. Scenario

Participants were asked to evacuate by passing through CP1, CP2, CP3, CP4, and CP1. The evacuation route includes two paths along the wall (CP2–CP3, and CP4–CP1) and two diagonal paths (CP1–CP2, and CP3–CP4). To confirm the fundamental data of mental stress and walking speed under the smoke condition, this study focused on the paths along the wall. Each participant was asked to participate in five experiments with different smoke densities ( $Cs = 0–2.35 \text{ m}^{-1}$ ). Before the experiment, the participants were given an instruction, as stated below:

“A fire occurred in the tunnel, and the space became completely dark filled with smoke, therefore, please evacuate on an urgent basis.”

### 2.3. Heart rate measurement

Ettema et al. [14] reported that heart rate is influenced by sympathetic and parasympathetic nerves and increases during mental stress load. Therefore, this study evaluated mental stress using heart rate variability as an index. Heart rate was measured in the experiment using Wahoo Tickr WF124 (arm-wound activity meter).

### 2.4. Participants

Sixteen students participated in the experiment (eight males and eight females). The age of the males ranged from 21 to 25 (mean age of 23 years), and the age of the females ranged from 20 to 23 (mean age of 21.4 years). The participants were instructed to wear a safety vest, a helmet, a mask, and knee and elbow pads and carry a stopwatch during the experiment. In addition, they were instructed to carry flashlights, referring to news [15, 16] that evacuees used the light of their cell phones during tunnel fire accidents.

## 3. RESULTS

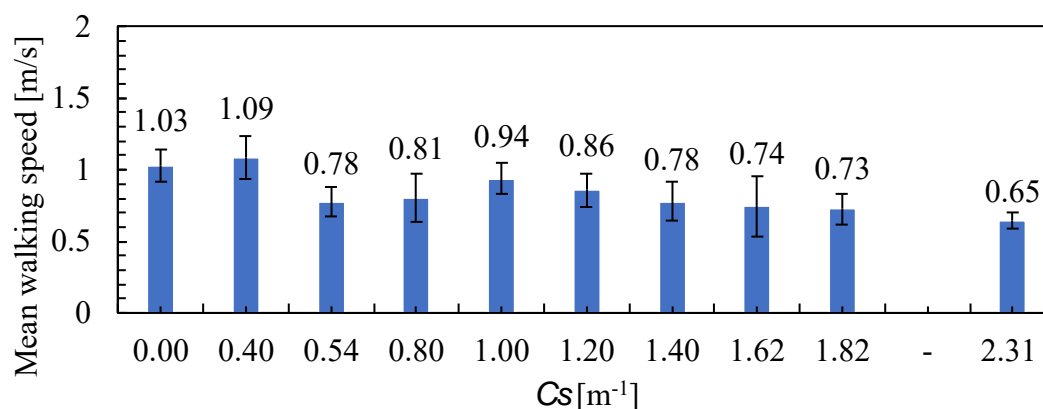
### 3.1. Walking speed

To investigate the walking speed under the smoke condition and its differences based on gender, the mean walking speed was calculated considering a smoke density increment of  $0.2 \text{ m}^{-1}$  starting from 0 (i.e., 0, 0.3–0.5, and 0.5–0.7  $\text{m}^{-1}$ ) (Figure 3). The horizontal and vertical axes corresponded to  $C_s$  and mean walking speed, respectively. The error bars corresponded to 95% confidence intervals. And the smoke density levelling was determined in this section.

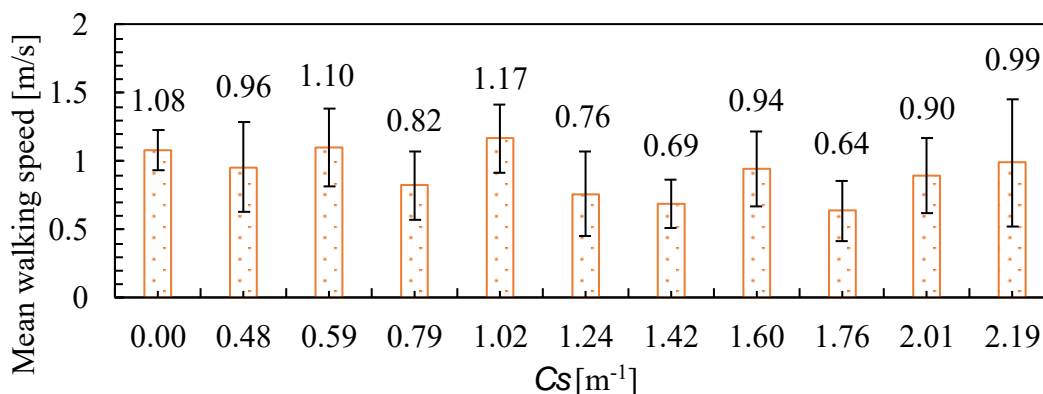
For males (Figure 3(i)), the mean walking speeds were 1.03 and 1.09 m/s at 0 and 0.40  $\text{m}^{-1}$ , respectively. The mean walking speed at 0.4  $\text{m}^{-1}$  was faster than that at 0  $\text{m}^{-1}$ . From 0.50 to 1.00  $\text{m}^{-1}$ , the mean walking speeds decreased to <1 m/s but tended to gradually increase. After 1.00  $\text{m}^{-1}$ , the mean walking speed gradually decreased, and after 1.40  $\text{m}^{-1}$ , the mean walking speed decreased to <0.8 m/s. There were no participants at 1.9–2.1  $\text{m}^{-1}$ . For females (Figure 3(ii)), the mean walking speeds were 1.08 m/s at 0  $\text{m}^{-1}$ , and 0.96 m/s at 0.48  $\text{m}^{-1}$ , which was slower than that at 0  $\text{m}^{-1}$  and decreased to <1 m/s. After 0.50  $\text{m}^{-1}$ , the mean walking speed was 0.82 m/s at 0.79  $\text{m}^{-1}$ , which was less than 0.9 m/s. After 1.00  $\text{m}^{-1}$ , the mean walking speed was 0.76 m/s at 1.24  $\text{m}^{-1}$ , which was less than 0.8 m/s. However, the mean walking speeds at 0.59 and 1.02  $\text{m}^{-1}$  were faster than that at 0  $\text{m}^{-1}$  as the error bars were larger, ranging from 0.82 to 1.38 m/s and 0.91 to 1.42 m/s, and the sample sizes were small (9 and 10, respectively), suggesting that the mean walking speeds were influenced by the faster participants. Moreover, after 1.40  $\text{m}^{-1}$ , the mean walking speeds were 0.69 m/s at 1.42  $\text{m}^{-1}$  and 0.64 m/s at 1.74  $\text{m}^{-1}$ , which were less than 0.7 m/s. However, the mean walking speeds were faster than 0.9 m/s at 1.60, 2.01, and 2.19  $\text{m}^{-1}$  owing to the smaller number of samples (9, 4, and 4, respectively) and larger error bar ranges (0.67–1.22, 0.69–1.17, and 0.52–1.46 m/s, respectively).

In summary, for the males, except for 0.40  $\text{m}^{-1}$ , the mean walking speeds at all the smoke densities were slower than that at 0  $\text{m}^{-1}$ . From 0.50–1.00  $\text{m}^{-1}$ , the mean walking speeds tended to increase. From 1.00–1.40  $\text{m}^{-1}$ , the mean walking speeds gradually decreased. After 1.40  $\text{m}^{-1}$ , the mean walking speeds decreased to <0.8 m/s. For females, except for 0.59 and 1.02  $\text{m}^{-1}$ , the mean walking speeds at all the smoke densities were slower than that at 0  $\text{m}^{-1}$ . From 0–0.50  $\text{m}^{-1}$ , the mean walking speed decreased to <1 m/s. From 0.50–1.00  $\text{m}^{-1}$ , the mean walking speed decreased to <0.9 m/s. From 1.00–1.40  $\text{m}^{-1}$ , the mean walking speed decreased to <0.8 m/s. From 1.40–1.76  $\text{m}^{-1}$ , the mean walking speeds decreased to <0.7 m/s. And after 1.76  $\text{m}^{-1}$ , the mean walking speeds increased. It was found that the walking speeds of males and females under the smoke condition were different. However, the mean walking speeds of the males and

females changed at 0.50, 1.00, and 1.40  $\text{m}^{-1}$ . Therefore, we classified the smoke density into five  $C_s$  levels, L0 (Level 0) ( $0 \text{ m}^{-1}$ , no smoke), L1 ( $0\text{--}0.50 \text{ m}^{-1}$ ), L2 ( $0.50\text{--}1.00 \text{ m}^{-1}$ ), L3 ( $1.00\text{--}1.50 \text{ m}^{-1}$ ) and L4 (over  $1.50 \text{ m}^{-1}$ ).



(i) Male



(ii) Female

Figure 3: Mean walking speed at  $0.2 \text{ m}^{-1}$

### 3.2. Heart rate

To investigate the mental stress under the smoke condition and its differences based on gender, the heart rate change rate (the ratio of the heart rate before the experiment to the mean heart rate under the smoke condition during the experiment) was calculated as an index of mental stress. We calculated the mean heart rate change rate of the participants whose heart rate increased during the experiment based on the gender and  $C_s$  level (Figure 4). The horizontal and vertical axes correspond to the  $C_s$  level and mean heart rate change rate, respectively. The error bars correspond to 95% confidence intervals. As the participants were nervous and anxious about the experiment before the start of the first experiment, the heart rate before the experiment was used as the mean heart rate for 3 minutes before the start of the second experiment.

The mean heart rate change rates of the males were 1.23 at L0, 1.22 at L1, 1.24 at L2, 1.15 at L3, and 1.11 at L4. The mean heart rate change rates of the females were 1.22 at L0, 1.26 at L1, 1.19 at L2, 1.10 at L3, and 1.15 at L4. At L0, the difference between the mean heart rate change rates of the males and females was almost equal at 0.01. However, at L2 and L3, the mean heart

rate change rates of the males were larger than those of the females. The reason for this is that, as reported by Sandstrom et al. [17], when recognizing space, males are characterized using the entire spatial image, whereas females are characterized using familiar objects in space as landmarks. Therefore, the males had difficulty grasping the whole spatial image because of less visibility under the smoke condition, whereas the females used checkpoints or something else as landmarks and were able to recognize space more easily than males, which may have resulted in less mental stress. In contrast, at L1 and L4, the heart rate change rates of females were larger. The reason for this is that the smoke became denser at L4, making it difficult for participants to recognize the space, even for females. As the males may have become slightly accustomed to the smoke-filled tent, the females may feel more mental stress than the males. Meanwhile, the heart rate change rate of females at L1 was larger because the error bar ranges of the 95% confidence intervals were larger for the males (1.08–1.36) and females (1.16–1.37), and the samples were smaller (5 and 5, respectively).

The mean values of heart rate change rate of males and females were almost equal at L0, whereas the mean values of males were larger than the females at L2 and L3. But the mean value of females was larger than the males at L4.

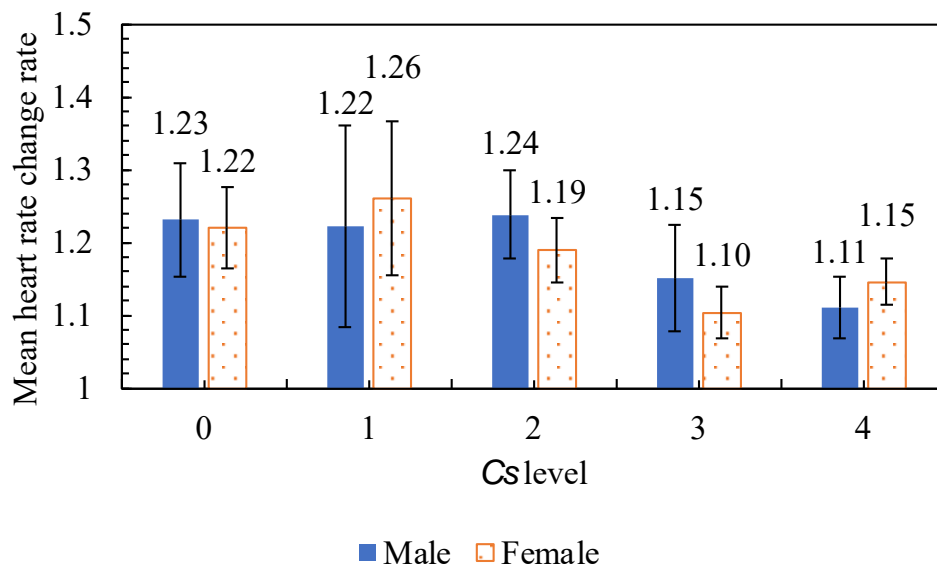


Figure 4: Mean heart rate change rate before and during the experiment

### 3.3. Heart rate and walking speed

To investigate the relationship between mental stress (heart rate change rate) and walking speed under the smoke condition and the differences in this relationship based on gender, we classified heart rate change rate into three groups (Group 0: <1, Group 1: 1–1.2, Group 2: >1.2). To divide Groups 1 and 2 using a heart rate change rate of 1.2, Whitley et al [10] conducted a walking experiment on 12 female students and found that the heart rate after walking for 50 s at 3.31 km/h (0.92 m/s) increased by ~1.19 times, compared with that before walking. Therefore, this study referred to the results of Whitley et al. [18] and classified mental stress into groups. We investigated the distribution and mean values of the walking speed of each group based on the gender and Cs level (Figure 5). The horizontal and vertical axes correspond to the Cs and mean walking speed, respectively. Groups 0, 1, and 2 are denoted by circles, rhombuses, and triangles, respectively. The filled plots correspond to the mean values.

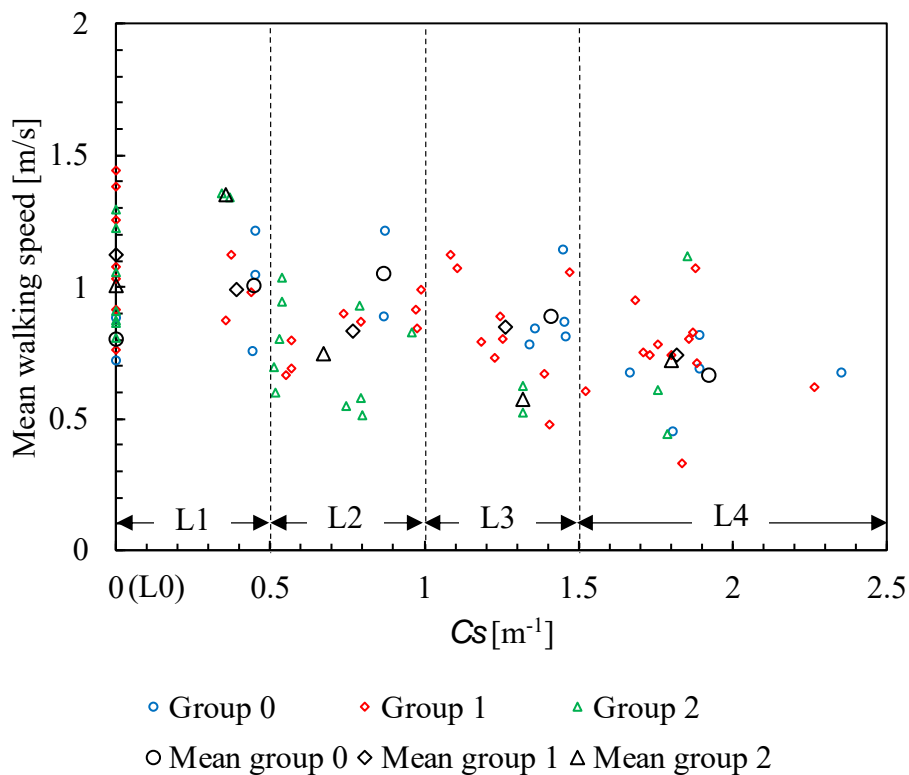
For the males (Figure 5(i)), the walking speed changed by 0.33–1.44 m/s at 0–2.35 m<sup>-1</sup>. For the females (Figure 5(ii)), the walking speed changed by 0.19–1.89 m/s at 0–2.24 m<sup>-1</sup>. The females



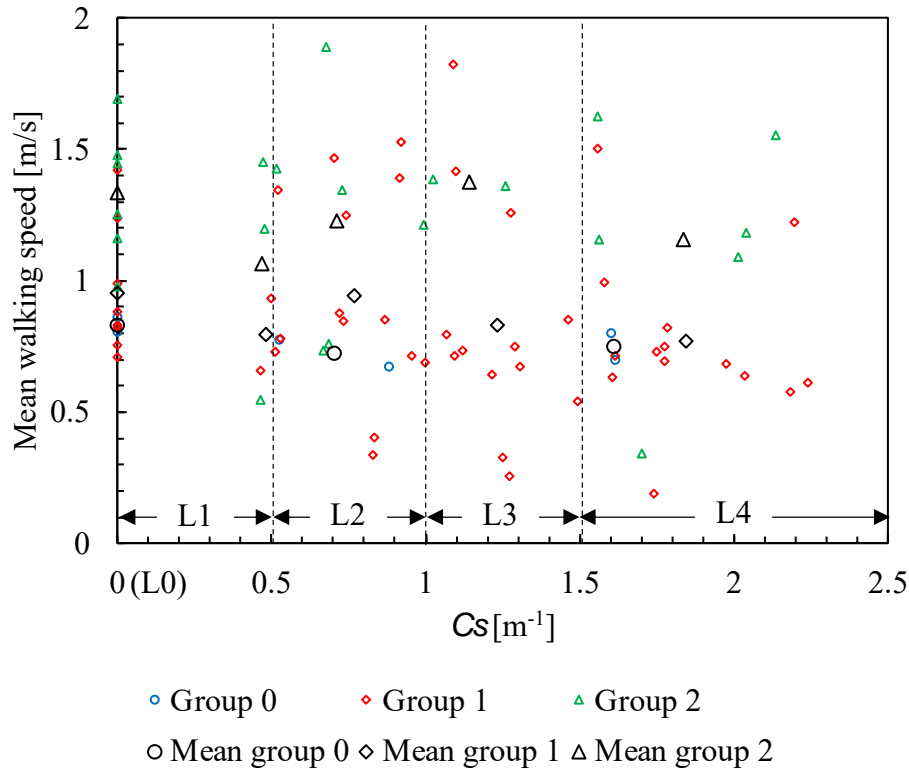
exhibited a larger difference between the maximum and minimum walking speeds than the males. Moreover, as all the participants whose walking speed exceeded 1.5 m/s were females, it was found that most females walked faster than the males owing to the difference in the spatial cognitive characteristics between males and females reported by Sandstrom et al. [17].

For the females, at L0, the mean walking speeds of Groups 0, 1, and 2 were 0.83, 0.96, and 1.33 m/s, respectively. The mean walking speed increased as the heart rate change rate increased, and a similar tendency was observed under the smoke condition. There were no Group 0 participants at L1 and L3. For the males, at L0, the mean walking speeds of Groups 0, 1, and 2 were 0.80, 1.12, and 1.00 m/s, respectively. However, at L1, the mean walking speeds of Groups 0, 1, and 2 were 1.01, 0.99, and 1.35 m/s, respectively. This tendency was similar to that observed for the females. At L2, the mean walking speeds of Groups 0, 1, and 2 were 1.05, 0.83, and 0.75 m/s, respectively. At L3, the mean walking speeds of Groups 0, 1, and 2 were 0.89, 0.85, and 0.57 m/s, respectively, which is in contrast with the females. The mean walking speed decreased as the heart rate change rate increased. At L4, the tendency was similar to that observed at L0.

For the females, the mean walking speed increased as the heart rate change rate increased, regardless of the smoke and  $C_s$  levels. For the males, the mean walking speed decreased as the heart rate change rate increased at L2 and L3. It was speculated that the walking speeds of the males and females varied when they experienced mental stress caused by smoke. As reported by Su et al. [19], under mental stress, males tend to take risks, whereas females tend to avoid risks. Therefore, it is considered that the walking speeds of the females were different from those of the males because the females had a stronger desire to escape faster from smoke than the males under the mental stress load.



(i) Male



(ii) Female

Figure 5: Walking speed at each group based on the  $C_s$  level

#### 4. CONCLUSIONS

To investigate the relationship between mental stress (heart rate change rate) and walking speed in a smoke-filled tunnel ( $C_s = 0\text{--}2.35\text{ m}^{-1}$ ), an evacuation experiment was conducted in a smoke-experience tent, where 16 students aged 20–25 (8 males and 8 females) participated. The results of the present study are summarized as follows:

- Regarding the heart rate change rate, compared with the females, the mean values with regard to the males were almost equal at  $0\text{ m}^{-1}$  but larger at  $0.50\text{--}1.50\text{ m}^{-1}$ . However, at  $>1.50\text{ m}^{-1}$ , the mean values of females were larger.
- With regard to the relationship between the heart rate change rate and walking speed, for the females, the mean walking speed increased as the heart rate change rate increased under the no-smoke and smoke conditions. For the males, the tendency was similar to that of the females at  $0\text{--}0.50\text{ m}^{-1}$ , whereas the tendency was opposite for the females at  $0.50\text{--}1.50\text{ m}^{-1}$ , where the mean walking speed decreased as the heart rate change rate increased.

#### 5. ACKNOWLEDGMENTS

This study was supported by the Obayashi Foundation (A2020-10-28-001) and JSPS KAKENHI under Grant No. JP20K15006. We express our sincere gratitude to all the participants of the experiments.

#### 6. REFERENCES

- [1] Jin, T., and Yamada, T., (1985), Irritating effects of fire smoke on visibility, Fire Science 11<sup>th</sup> International Conference ‘Tunnel Safety and Ventilation’ 2022, Graz

- and Technology, 5(1), pp. 79-90.
- [2] Frantzich, H., and Nilsson, D., (2001), Evacuation experiments in a smoke filled tunnel, 3rd international symposium on human behaviour in fire, Inerscience Communications Ltd, pp. 229-238.
- [3] Nilsson, D., Johansson, M., and Frantzich, H., (2009), Evacuation experiment in a road tunnel: A study of human behaviour and technical installations, Fire Safety Journal, Vol. 44, pp. 458-468.
- [4] Fridolf, K., Ronchi, E., Nilsson, D., and Frantzich, H., (2013), Movement speed and exit choice in smoke-filled rail tunnels, Fire Safety Journal, Vol. 59, pp. 8-21.
- [5] Fridolf, K., Andress, K., Nilsson, D., and Frantzich, H., (2014), The impact of smoke on walking speed, Fire and Materials, Vol. 38, No. 7, pp. 744-759.
- [6] Seike, M., Kawabata, N., and Hasegawa, M., (2016), Experiments of evacuation speed in smoke-filled tunnel, Tunnelling and Underground Space Technology, Vol. 53, pp. 61-67.
- [7] Seike, M., Kawabata, N., and Hasegawa, M., (2017), Evacuation speed in full-scale darkened tunnel filled with smoke, Fire Safety Journal, Vol. 91, pp. 901-907.
- [8] Ronchi, E., Fridolf, K., Frantzich, H., Nilsson, D., Walter, A. L., and Modig, H., (2018), A tunnel evacuation experiment on movement speed and exit choice in smoke, Fire Safety Journal, Vol. 97, pp. 126-136.
- [9] Seike, M., Lu, Y. C., Kawabata, N., and Hasegawa, M., (2021), Emergency evacuation speed distributions in smoke-filled tunnel, Tunnelling and Underground Space Technology, 122, 103934.
- [10] Jin, T., (1980), Studies on emotional instability in fire smoke, Bulletin of Japanese Association of Fire Science and Engineering, 30, pp. 1-6 (in Japanese).
- [11] Seike, M., Kawabata, N., Hasegawa, M., Tsuji, C., Higashida, H., and Yuhi, T., (2021), Experimental attempt on walking behavior and stress assessment in a completely darkened tunnel, Infrastructures, 6(75), pp. 2-14.
- [12] Leach, J., (2004), Why people 'freeze' in an emergency: temporal and cognitive constraints on survival responses, Aviation, Space, and Environmental Medicine, 75, pp. 539-542.
- [13] American Psychiatric Association., (2000), Diagnostic and statistical manual of mental disorders, Fourth Edition, Text Revision.
- [14] Ettema, J. H., and Zielhuis, R. L., (1971), Physiological parameters of mental load, Ergonomics, 14(1), pp. 137-144.
- [15] Tokachi Mainichi Newspaper, Inc., May 29th 2011 (in Japanese). <http://www.tokachi.co.jp/news/201105/201105290009334.php> (See May 25th in 2015).
- [16] Next Digital Limited, May 8th 2012 (in Chinese). <https://tw.news.appledaily.com/local/realtime/20120508/121709/> (See November 25th in 2018).
- [17] Sandstrom, N. J., Kaufman, J., and Huettel, S. A., (1998), Males and females use different distal cues in a virtual environment navigation task, Cognitive Brain Research, 6, pp. 351-360.
- [18] Whitley, J. D., and Schoene, L. L., (1987), Comparison of heart rate responses: water walking versus treadmill walking, Physical Therapy, 67(10), pp. 1501-1504.
- [19] Su, R., Rounds, J., and Armstrong, P. I., (2009), Men and things, women and people: A meta-analysis of sex differences in interests. Psychological Bulletin, 135, pp. 859-884.

# ON THE ACCURACY OF FDS SMOKE PROPAGATION MODELS IN THE CONTEXT OF TUNNEL RISK ANALYSIS

<sup>1</sup>Oliver Heger, <sup>2</sup>Peter Sturm

<sup>1</sup>ILF Consulting engineers Austria GmbH, Austria

<sup>2</sup> Institute of Thermodynamics and Sustainable Propulsion Systems, Graz University of Technology, Austria

## ABSTRACT

In the recent past the Fire Dynamics Simulator (FDS) has become one of the primary tools for fire- and smoke propagation simulation in the context of tunnel fire safety. FDS has been extensively validated for compartment fires but validation for tunnels is scarce. After a quantitative validation against a full scale fire test is presented, the paper demonstrates how specific numerical options, in particular the size of the CFD mesh, influence the accuracy of the smoke propagation results. By doing so the investigated FDS modelling concepts are related to achievable prediction accuracies as well as the expected computation times. This enables informed decisions about the choice of model characteristics based on the necessary accuracy and available computational resources for future tunnel fire consequence analysis, typically used in tunnel risk models.

*Keywords: FDS, CFD validation, CFD accuracy, risk model, tunnel fire simulation.*

## 1. INTRODUCTION & OUTLINE

For more than two decades, tunnel risk models have been an important tool to increase road tunnel safety. With the implementation of EC Directive 2004/EC [1] tunnel risk assessment became a mandatory part of the safety design process for road tunnels on the European network. While the general methodology of tunnel risk assessment is well defined on an international level, for instance in [2], specifications for the detailed implementation are given at a national level through standards and guidelines. Therefore, detailed implementations can vary considerably from country to country [3],[ 4]. However, fire risk is one of the main aspects in each tunnel risk assessment methodology. Therefore, the capability to predict the consequences of a tunnel fire is of high importance for every quantitative tunnel risk model, being part of a tunnel risk assessment methodology.

A core feature of every fire consequence model is the smoke propagation model. Such models in general are used to predict the movement of smoke and convective heat and allow to calculate toxic gas concentrations, temperature and visibility at any location for any time inside the tunnel. This further allows to estimate the effects of a tunnel fire on evacuating persons by combination with evacuation and/or survivability models. This procedure is generally called fire consequence modelling.

In tunnel fire studies, the 3D CFD software Fire Dynamics Simulator (FDS) [5] has become one of the primary tools to model tunnel fire dynamics numerically. FDS is based on a low Mach number approximation of the Navier-Stokes equations, applying a LES formulation and particular suited for buoyant flows [6]. This formulation, in combination with the use of so called wall functions to treat boundary-layer effects without the need to resolve the boundary layer with great detail, allow for significantly larger cell volumes of the numerical mesh. This results in much shorter computation times compared to other 3D-CFD codes and in particular allow to use full 3D-CFD fire simulations in probabilistic, system-based tunnel risk models [7].

However, even though much larger cell dimensions are possible compared to other 3D-CFD codes, the accuracy of course decreases with increasing volume of the numerical grid cells. In addition to mesh resolution, also other numerical modelling options - like the treatment of convective heat transfer, accounting for thermal radiation, the utilized pressure solver, etc. – influence the accuracy of the smoke propagation prediction. The remainder of this paper documents the methods used to investigate these dependencies and presents results in terms of a relation between modelling options, prediction accuracy and necessary computation time.

In section 2 the general FDS model used in this study is described and validated by comparison against the well-known Memorial Tunnel fire test 501 [8]. In section 3 the influence of different mesh resolutions on convective propagation and temperature stratification – the key parameters with respect to smoke propagation – are analyzed qualitatively and quantitatively by application of a vector analysis metric. The influence on convective transport and temperature stratification are important to understand, but it is even more important to understand the influence on the accuracy of the risk model estimates. Therefore, the smoke propagation results obtained in the CFD parameter studies were further processed with a tunnel evacuation model based on the FED/FIC dosage-endpoint approach [9]. The results of this process are presented in section 4. A conclusion in the form of a reference table, relating modelling option, prediction accuracy and necessary computational effort is then given in section 5.

## 2. FDS TUNNEL FIRE MODEL

The present study is based on the parameters of a 20 MW full-scale fire test under natural ventilation, documented during the Memorial Tunnel Fire Ventilation Test Program [8]. The basic geometric properties of the Memorial Tunnel for the selected fire test (Test number 501) are given in Table 1. The most important numerical parameters for the FDS model are stated in Table 2. A detailed explanation of the numerical parameters can be found in [5] and [6]. The variation of these parameters as a part of the study is presented in the later sections. The values stated in Table 2 represent the standard model options.

To model the tunnel fire, time-dependent surface boundary conditions for convective heat flux and mass flux for CO, CO<sub>2</sub>, HCN and soot have been applied to a 3m x 3m area 1.0 m above the tunnel floor. As an educated guess, 75% have been assumed for the share of convective heat on the overall heat release rate (HRR) of the gasoline fire. The radiative share of the HRR has been neglected. To resemble the natural ventilation during the fire test, velocity boundary conditions, based on the measured bulk airflow velocity at the measurement point closest to the southern portal has been used at the (initial) domain inlet (853 m). Open boundary conditions have been used at the (initial) domain outlet (0m). The heat release rate (HRR) time curve and the inlet bulk airflow used as velocity boundary condition are depicted in Figure 1. As can be seen in the figure, the longitudinal flow is reversed approximately 140s after the fire start, which is taken into account in the velocity boundary conditions.

Table 1: Tunnel parameters

Parameter	Value
<b>Tunnel Length</b>	853 m
<b>Cross-Section Type</b>	Horseshoe
<b>Cross-Section Area</b>	60.3 m <sup>2</sup>
<b>Tunnel Height / Tunnel Width</b>	7.5 m / 9.0 m
<b>Cross-passages</b>	None (in simulation)

Table 2: Numerical parameters of the standard model

Parameter	Value
Fire Model	Time-dependent surface boundary condition for convective heat flux and smoke mass flux (CO, CO <sub>2</sub> , HCN, soot) at fire location
Ventilation Model	Velocity boundary condition at domain inlet, open boundary condition at domain outlet
Cell Dimensions	0.5 m x 0.5 m x 0.5 m
Convective Heat Transfer	Default
Radiative Heat Transfer	Default
Subgrid Closure	DEARDORFF
Simulation Method	VLES
Pressure Solver	FFT

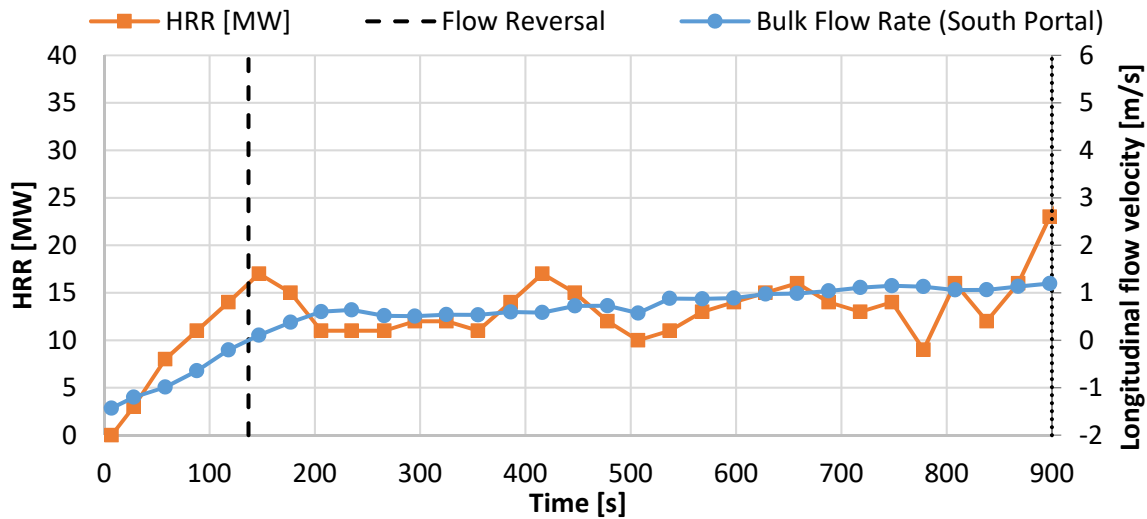


Figure 1: Velocity- & HRR time series used as boundary conditions in the CFD model

Figure 2 shows the temperature profile 170 seconds after fire start for the simulation and 120 seconds after fire start for the measurement data. The 50 seconds delay between experimental and numerical data has been added because of an observed irregularity on the measurement time-stamp. The temperatures at the majority of measurement locations start to rise unreasonably early after the nominal fire ignition. For instance, at a measurement position 31 m downstream of the fire, a strong increase of cross-sectional average temperature, indicating the arrival of the hot smoke layer, is documented three seconds after nominal fire start, which is, for a bulk airflow velocity of approximately 1.3 m/s physically not realistic. The temperature developments, however, at all measuring points, seem to be plausible in general. They in particular match well with the numerical results, despite the mentioned overall time gap. To estimate this time gap, the point in time, when the hot tunnel air from the fire source should theoretically arrive at the respective locations, was calculated based on the measured bulk flow velocity, assuming that propagation in the first phase is mainly driven by longitudinal airflow, not by buoyancy forces between hot and cold layer. By doing so, a time-stamp deviation between 40 seconds and 55 seconds was estimated for the experimental time stamp. This estimated time-delay was taken into account in the further validation process, by comparing results of the numerical computation with experimental results with a 50 s later time-stamp.

This on the one hand leads to a plausible downstream propagation speed of the hot smoke layer and to a good agreement between experimental measurement and numerical results.

Figure 2 shows the comparison of temperature contours for 37.8 °C (100°F) and 93.3 °C (200°F) in the longitudinal-vertical plane, 120s (170s time stamp for experimental data) after fire start. The contours show some deviation, in particular for the higher temperature contour. But with deviations between 0% ( $\Delta x_1$ ) and 34 % ( $\Delta x_3$ ), the results are interpreted to be in reasonable agreement, if the underlying uncertainties are taken into account. These uncertainties are on the one hand related to the measurements themselves, in particular with respect to the uncertainty of the heat release rate and the low time resolution of the measurements (30s measurement intervals), and on the other hand to missing model input data, e.g. rock temperature, portal pressure difference and wind pressure.

In addition to temperature contours also the time development of the cross-sectional average temperature has been compared along the tunnel. As an example, the comparisons at two longitudinal positions are shown in Figure 3. The general time-development is very well resembled by the simulations. The quasi steady temperature after the fire was fully developed deviate by approximately 10 - 20 °C (20% - 40%). The average temperatures suggest that back-layering is over pronounced in numerical simulations, as temperatures upstream the fire are above the measured values and temperatures downstream of the fire are below the measured temperatures. However, if the general uncertainties are again taken into account, the results can be understood as in good agreement.

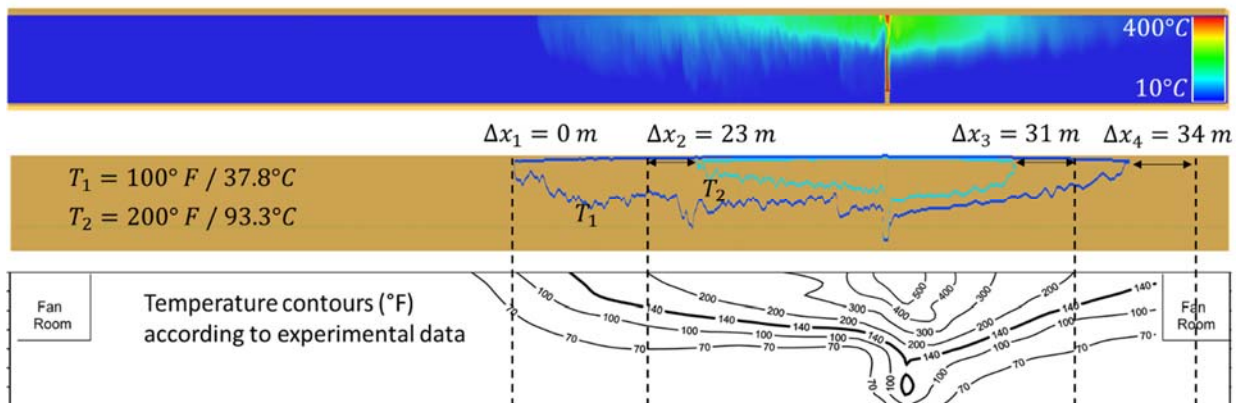


Figure 2: Comparison of temperature contours – experimental measurement (bottom) vs. FDS simulation (middle) and full FDS temperature profile (top), 170 s after fire start (120s according to experimental data).

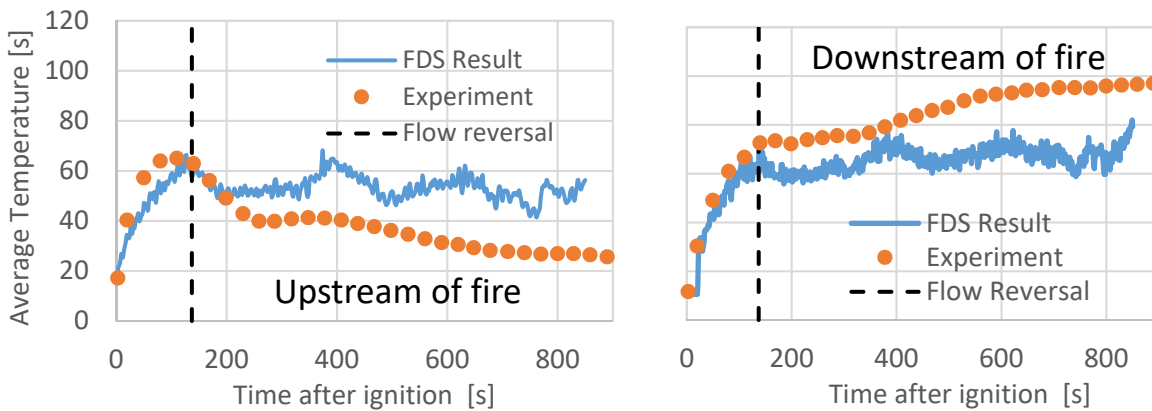


Figure 3: Comparison of cross-sectional average temperature development 62 m left (left) and 66 m right (right) of fire.

### 3. DEPENDENCE OF SMOKE PROPAGATION ON CFD MESH RESOLUTION

The propagation and distribution of hot smoke is closely related to temperature stratification and the distribution of hot gases. It is therefore convenient to analyse temperatures instead of smoke concentrations. In particular because smoke-/gas concentrations also depend on fire gas emissions, which are harder to measure than heat release rates. Therefore, the time-series of three parameters, describing convective propagation and layer formation are compared for different mesh resolutions in the following.

Figure 4 shows the time series of calculated cross-sectional average gas temperature, layer height and layer temperature difference, at one exemplary longitudinal position for different numerical mesh options, compared to the standard model according to Table 2. The curves clearly separate into two groups, differing in the chosen mesh resolution in z direction. Only small differences for meshes with 0.25 m resolution in z direction are observable. The variants with coarser resolution, including the standard model, deviate with respect to average temperature and layer height from the fine mesh results. Also a refined mesh around the fire site – 0.25 m x 0.25 m x 0.25 m +/- 15 m around fire location, 0.5 m x 0.5 m x 0.5 m elsewhere – does not further increase the model accuracy in relation to the standard model, which is already in good agreement with the experimental result, see section 2.

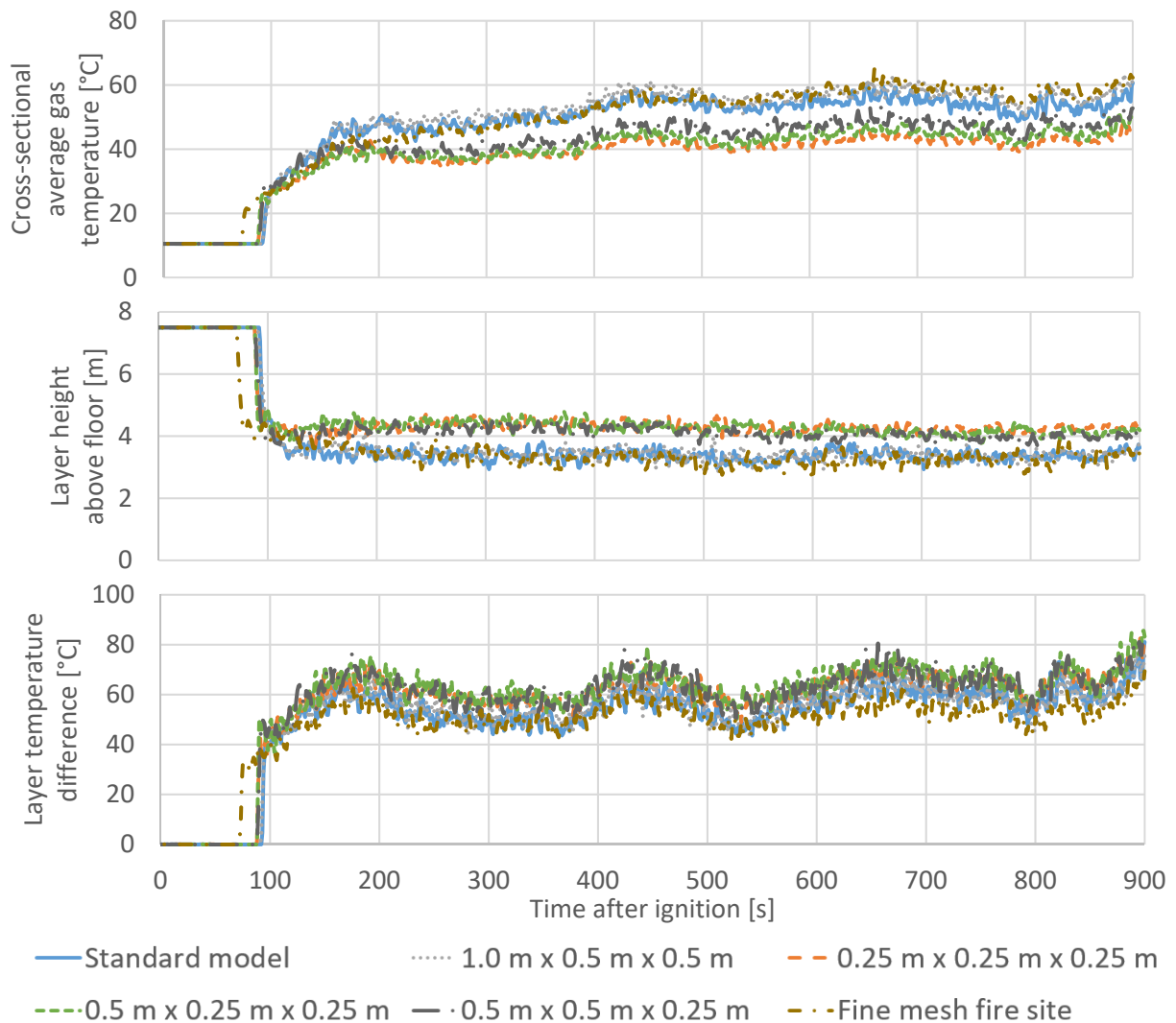


Figure 4: Comparison of average gas temperature, layer height and layer temperature difference 100 m before the fire



For the quantitative comparison, a vector algebra metric, suitable to measure the deviation of two time-series [10] is utilized. This metric assumes the two compared time series as two vectors in an Euclidean space. The relative difference used to quantify the deviation between the two time series – a and b – is then defined as the length of the difference vector – a-b – relative to the length of the base vector:

$$r_{pos} \equiv \frac{\|a - b\|}{\|a\|} = \sqrt{\frac{\sum_{i=1}^n (a_i - b_i)^2}{\sum_{i=1}^n a_i^2}}, \bar{r} = \frac{\sum_{pos} r_{pos}}{\sum_{pos}}$$

Equation 1: Relative difference between two measured time seires according to [Reference Peacock et al.] and averaged relative difference

A similar approach is also used in [11]. The standard model according to Table 2 has been shown to be in good agreement with the experimental measurement. Therefore, it is used as a reference in the quantitative comparison. Table 3 summarizes the averaged relative difference ( $\bar{r}$ ) of average temperature, layer height and layer temperature difference, according to Equation 1, for the different meshing options, in relation to the standard model.. The difference is evaluated based on the time series at seven longitudinal positions along the tunnel – 214 m, 414 m, 514 m 594 m, 638 m, 718 m and 818 m. The values given in Table 3 represent the respective relative difference, averaged over all seven longitudinal positions.

Table 3: Relative difference for the investigated modelling options with respect to the standard model, averaged over seven longitudinal positions along the tunnel

<b>Modelling Variant</b>	<b>Average Temperature</b>	<b>Layer Height</b>	<b>Layer Temperature Difference</b>
<b>Standard model</b>	-	-	-
<b>1.0 m x 0.5 m x 0.5 m</b>	6 %	7 %	12 %
<b>Fine mesh fire site</b>	14 %	16 %	24 %
<b>0.5 m x 0.5 m x 0.25 m</b>	8 %	10 %	13 %
<b>0.5 m x 0.25 m x 0.25 m</b>	11 %	12 %	14 %
<b>0.25 m x 0.25 m x 0.25 m</b>	14 %	13 %	17 %

The quantitative comparison shows deviations of roughly 6 % to 24 %. Surprisingly, the mesh with increased resolution around the fire site shows the largest differences in relation to the standard model. Intuitively, one would expect it to be closer to the standard model than the 0.25 m x 0.25 m x 0.25 m, but instead it shows the largest difference. One reason could be that the solvers applied in FDS prefer homogenous meshes over meshes with changing resolutions. Despite the refined mesh around the fire location, the resulting deviations of the remaining (homogenous) meshes are between 6 % and 17 %. These deviations can in principle be significant, in particular because the mesh independence for the finest resolution has not been further investigated, which means that the deviations from the standard model could still increase in case of even finer meshes. However, the comparison with experimental measurements in section 2 showed a good agreement for the standard model. Therefore, deviations are expected to be overall limited, also for even finer mesh resolutions. Also, deviations in terms of temperature/smoke propagation and layer formation are important to know, but in order to understand how these deviations influence tunnel risk analysis results, consequences based on the respective fire simulation results need to be assessed. This is presented in the following section.

#### 4. DEPENDENCE OF FIRE CONSEQUENCE MODELS ON MESH RESOLUTION

In general, a variety of different metrics to quantify the consequence of a tunnel fire exist, trying to model the impact of fire hazards on persons inside a tunnel.

One rather simple method is to use a visibility threshold. As long as the visibility is above a certain value (e.g. 5 m), evacuation is possible and persons continue to egress. When the visibility drops below the threshold value, evacuation is assumed to have failed. More sophisticated methods for consequence analysis aim to model the physiological impact of fire hazards on the human body, taking the effect of reduced visibility, toxin- and temperature dosage intake as well as respiratory and visual irritancy into account. An example for such a consequence model, based on the approach of [9], is utilized in the Austrian Tunnel Risk Model [12].

A common process to visualize the severity of a fire scenario with respect to such fatality thresholds is to evaluate the time until the respective threshold value is met at any position inside a tunnel. This is presented in Figure 5, where the time until the respective fatality criteria are met at any longitudinal location along the tunnel are compared for the different mesh options. For this purpose, gas concentrations, visibility and temperature at 1.6 m height have been extracted from the CFD results discussed in section 3.

Apparently, the time until incapacitation happens strongly depends on the chosen fatality criterion, much more than on the investigated mesh resolutions. While evacuation is possible for more than 600 seconds according to the FED/FIC criterion (except at locations very close to the fire source), safe egress times of only 200 to 400 seconds result from the visibility-threshold approach. However, the sensitivity to mesh resolution seems to be similar for both threshold values: Similar to the findings before, the results depend on the mesh resolution in z direction. Incapacitation times for a given fatality criterion are almost identical for all CFD meshes with a resolution of 0.25 m in z direction but strongly deviate from the results with coarser resolutions in z direction, in particular for longitudinal positions between 400 m and 600 m (0 m – 200 m left of the fire).

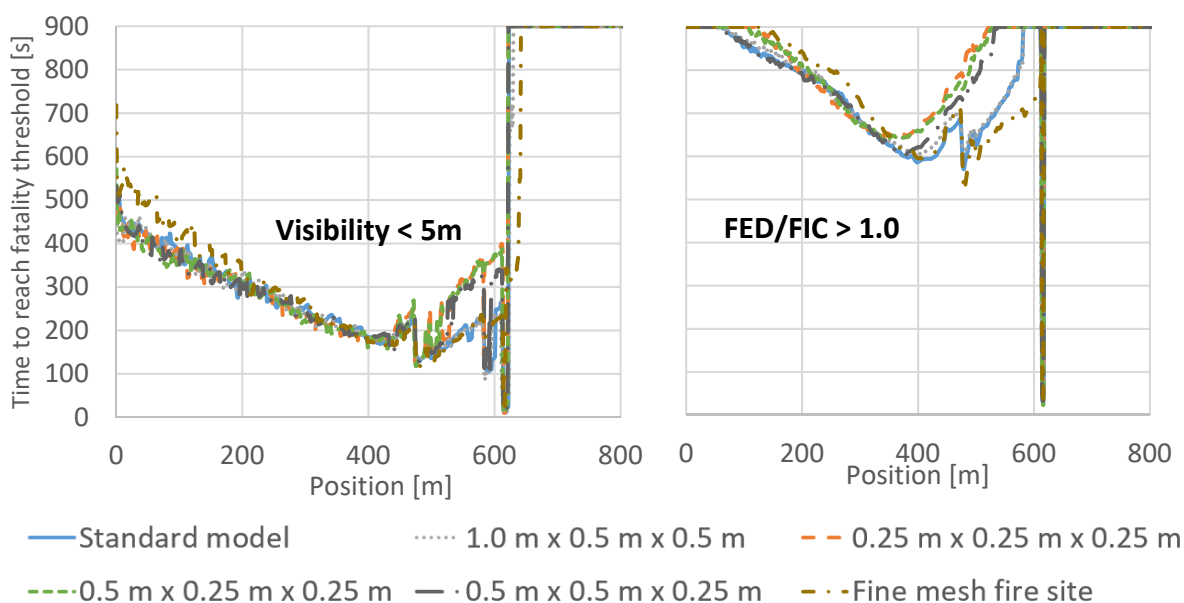


Figure 5: Time to reach fatality threshold values as a function of longitudinal position along the tunnel for visibility criterion (left) and FED/FIC criterion (right).

#### 4.1. Resulting Consequence Numbers

In order to quantify the sensitivity of risk analysis results on the CFD model options, the number of expected fatalities in case of a tunnel fire (consequence number) has been calculated based on a simple agent-based egress model, relying on the FED/FIC fatality threshold. The egress model is used to resemble the evacuation of tunnel users for a hypothetical congested traffic scenario. Therefore, agents start to egress at every tunnel meter 150 s after fire ignition. A walking speed of 1 m/s has been chosen for the agents which is modified based on local visibility and level of agent intoxication [12]. In addition it was assumed that a share of 3% of all tunnel users remain at their initial location for the whole simulation time of 15 minutes (representing people with reduced mobility, injured, wrong behaviour, etc.).

In addition to the mesh resolution also the influence of other CFD (FDS) parameter selections has been investigated:

**Convective Heat Transfer Option:** Typically, large gradients with respect to normal velocity and temperature (in case of hot flows) arise at the boundary layer of a viscous flow. This can be treated either by a fine resolution of the boundary layer or by so called wall models. A logarithmic wall model for near wall temperature has been used in addition to the standard near-wall model for normal velocity. This is supposed to increase the accuracy of the convective heat flux from hot tunnel air to colder tunnel surface without the need of small near-wall cell size. (HEAT\_TRANSFER\_MODEL = 'LOGLAW')

Also an additional time step constraint, limiting the size of the time step between two solver iterations, has been used which acknowledges the convective heat flux from tunnel air to the tunnel surface. (CHECK\_HT=.TRUE.)

**Radiative Heat Transfer:** As described in section 2, only the convective share of the fire HRR has been taken into account in the investigations. This is true for all investigated variants. However, also without a direct radiative heat source, the convective heating of the tunnel air leads to a temperature increase and therefore induces radiative heat flux from the tunnel air to the tunnel surface. In this variant, this radiative heat flux (or any radiative heat flux from a hot surface) is neglected (RADIATION = .FALSE.).

**Subgrid Closure:** In LES only a certain part of the turbulent dynamics is directly modelled on the numerical grid. The remaining share of the turbulent dynamic, in particular the final cascade to thermal energy, is treated by a so called subgrid model. As an alternative to the standard "Deardorff" subgrid model for the subgrid kinetic energy and the WALE near-wall subgrid model, the "Constant Smagorinsky" subgrid model and the "Van Driest" near-wall subgrid model have been used. (CONSTANT SMAGORINSKY + VAN DRIEST)

**Pressure Solver:** In the low Mach number approximation, applied in FDS, a fast non-iterative algorithm that utilizes Fast Fourier Transforms (FFT) is used to solve the pressure equation. In default mode the FFT is applied to each individual numerical mesh separately and the pressure solutions of the individual meshes are then matched together. As an alternative, the global Poisson equation can also be solved over the entire domain. (SOLVER='GLMAT')

Figure 6 shows the resulting consequence numbers for different numerical mesh options (left) and CFD parameter selections (right). The deviations in relation to the standard model are given as percentage values. The differences in terms of fire consequences are between - 8 % and + 6 %. These deviations are significantly smaller than the deviations in terms of temperature/smoke propagation and layer formation, discussed in section 3. However, whether such deviations are significant for a given risk model application, depends on the actual use case. Very often, only rough estimates are known for the necessary input parameters and the overall accuracy of the

model results is generally limited. In such a situation the deviations shown in Figure 6 might be very small in comparison, and therefore be negligible overall. In other applications high accuracy CFD results can be of utmost importance, in particular when design options related to the flow profile (e.g. jet fan installation positions, etc.) are investigated. Generally speaking, a deviation in fire consequence numbers of roughly 5 % can be assessed as minor, in particular in combination with the computational effort associated with the higher accuracy variants.

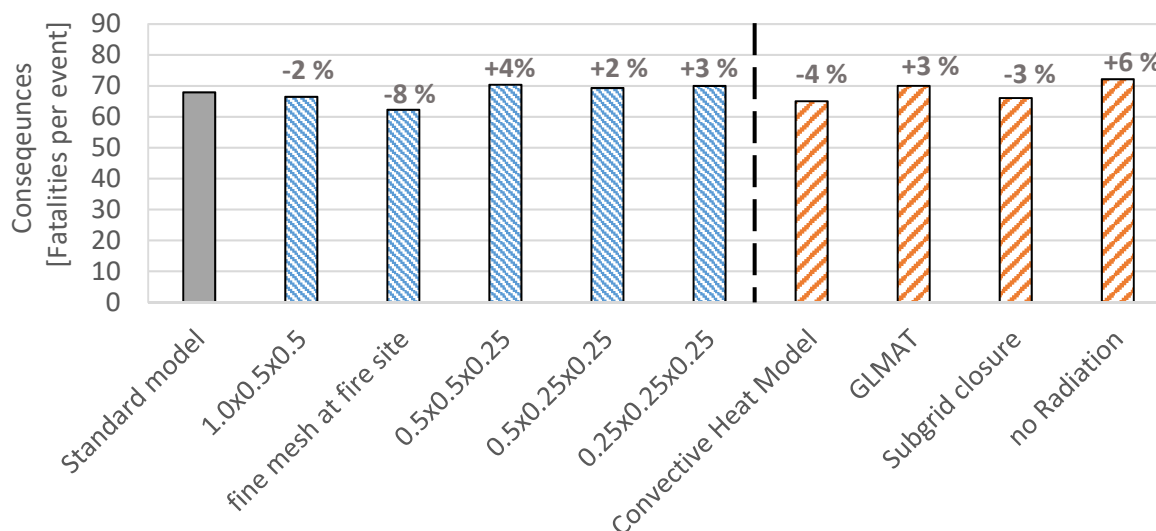


Figure 6: Comparison of fatality numbers resulting from the quantitative consequence analysis of a congested traffic scenario based on the CFD results with respect to different numerical mesh options and CFD parameter selections

## 5. SUMMARY AND CONCLUSION

Comparison of FDS results and experimental measurement showed a good agreement for the FDS standard model with parameters according to Table 2. Based on this qualitative validation, a parameter study was carried out to investigate the effect of different CFD mesh resolutions and parameter selections on temperature/smoke propagation and layer formation, as well as fire consequence numbers (fatalities). The main result of the paper is presented in Table 4. The deviation of the investigated mesh resolutions from the standard model variant, in terms of temperature propagation and layer formation, is between 6% and 24%. This deviation significantly reduces to a deviation between -8% and 6% in terms of fire consequences to tunnel users (fatalities). The same observation can also be made for the other CFD model parameter variations where deviations between 4% and 35%, in terms of temperature and stratification, reduce to deviations of -3% to +6% in terms of fire consequences. The reasons for this reduced dependency of consequence numbers on mesh resolution and CFD model options are assumed to be manifold and the effect may also vary for different fire scenarios and tunnel setups. However, one important property of the FED/FIC fatality threshold approach is the accumulative nature. In contrast to the pure threshold-value (concentration, visibility) based approaches, which only depend on momentary values, localized variations over limited periods of time are naturally smoothed out by the FED/FIC approach. This should not be misunderstood as a model peculiarity but as the way the human body is believed to react on fire hazards based on fundamental research [9].

While the influence of the investigated mesh resolutions and CFD parameter settings on consequence numbers seem to be minor, the effect on the necessary computation time is tremendous. As an example, if we compare the finest mesh resolution – 0.25 m x 0.25 m x 0.25 m – with the standard model, an accuracy increase in fire consequence numbers of 3 % requires an increase of computational cost from 112 CPU hours to 1697 CPU hours. A reference system with 64 physical cores and a base frequency of 2.2 GHz has been used. The computation time represents the sum of the CPU times of all involved cores (60 - 30 nodes, depending on the variant).

It can therefore be concluded that the numerical costs for mesh resolutions finer than 0.5 m in any direction outweigh the benefit in terms of consequence number prediction accuracy. This is in particular important for probabilistic system-based risk assessment approaches, where a large number of fire scenarios has to be treated and an increase in numerical cost scales up with the number of scenarios. However, if numerical resources are available, an increase in mesh resolution in the vertical direction is recommended.

Table 4: Comparison of model accuracy and necessary computation times for investigated FDS model options

<b>Variant</b>	<b>Temperature &amp; Stratification</b>	<b>Consequences</b>	<b>Computation Time</b>
<b>Standard model</b>	base value	67.9 fatalities	112 CPU hours
<b>1.0 m x 0.5 m x 0.5 m</b>	6 % - 12 %	4 %	- 85 %
<b>Fine mesh fire site</b>	14 % - 24 %	8 %	+ 179 %
<b>0.5 m x 0.5 m x 0.25 m</b>	8 % - 13 %	4 %	+ 87 %
<b>0.5 m x 0.25 m x 0.25 m</b>	11 % - 14 %	2 %	+ 655 %
<b>0.25 m x 0.25 m x 0.25 m</b>	14 % - 17 %	3 %	+ 631 %
<b>Convective Heat Model</b>			
	14 % - 28 %	4 %	+ 1596 %
<b>GLMAT</b>			
	4 % - 8 %	3 %	+ 203 %
<b>Subgrid closure</b>			
	8 % - 15 %	3 %	+ 16 %
<b>No Radiation</b>			
	10 % - 35 %	6 %	- 34 %

## 6. REFERENCES

- [1] European Union, “Directive 2004/54/EC of the European Parliament and of the Council on minimum safety requirements for tunnels in the trans-European road network,” 2004.
- [2] World road Association (PIARC), Technical Committee 3.3 Road Tunnel Operations, “Risk analysis for road tunnels,” 2008.
- [3] Ntzeremes P., Kirtopoulos K., “Evaluating the role of risk assessment for road tunnel fire safety: A comparative review within the EU,” Journal of Traffic and Transport Engineering, Volume 6, Issue 3, pp. 282-296, 2019 .
- [4] Wahl, H., Vollmann, G., Thewes, M., „Multi-Parameter Study of Interactions and Uncertainties within CFD-Based Consequence Analysis Using Elementary Effects Analysis,” Virtual Conference ‘Tunnel Safety and Ventilation’, December 2020, Graz.
- [5] McGrattan, K., Hostikka, S., Floyd, J., McDermott, R., Vanella, M., “Fire Dynamics Simulator User’s Guide,” November 19, 2021, Revision FDS6.7.7 -0-gfe0d4ef38.

- [6] McGrattan, K., Hostikka, S., Floyd, J., McDermott, R., Vanella, M., “Fire Dynamics Simulator Technical Reference Guide Volume 1: Mathematical Model,” November 19, 2021, Revision FDS6.7.7 -0-gfe0d4ef38.
- [7] FSV (Austria Society for Research on Road, Rail and Transport), “Guideline RVS 09.03.11 Methodology of Tunnel Risk Analysis”, Vienna, 2015.
- [8] Bechtel/Parsons Brinckerhoff, “Memorial Tunnel fire Ventilation Test Program,” Massachusetts Highway Department and Federal Highway Administration, November 1995.
- [9] Purser D.A., McAllister J.L., „Assessment of Hazards to Occupants from Smoke, Toxic Gases, and Heat,” in *SFPE Handbook of Fire Protection Engineering*, National Fire Protection Association, pp. 2308-2428, 2016.
- [10] Peacock, R.D., Reneke, P.A., William, D.D., Jones, W.W., “Quantifying fire model evaluation using functional analysis,” *Fire Safety Journal*, Volue 33, pp. 167-184, 1999.
- [11] McGrattan, K., Hostikka, S., Floyd, J., McDermott, R., Vanella, M., “Fire Dynamics Simulator Technical Reference Guide Volume 3: Validation,” November 19, 2021, Revision FDS6.7.7 -0-gfe0d4ef38.TuRisMo
- [12] Forster C., Lentz A., “Erweiterung und Vertiefung des österreichischen Tunnelmodells – TuRisMo 2: Arbeitsbericht zum Arbeitsausschuss Tunnel-Sicherheit,“ Bundesministerium für Verkehr, Innovation und Technologie, Austria, 2015. [Online]. Available:  
[https://www.bmvit.gv.at/dam/bmvitgvat/content/themen/strasse/infrastruktur/tunnel/sicherheit/bericht\\_tunnelsicherheit.pdf](https://www.bmvit.gv.at/dam/bmvitgvat/content/themen/strasse/infrastruktur/tunnel/sicherheit/bericht_tunnelsicherheit.pdf). [April 11<sup>th</sup> 2022]

# UPGRADE OF THE GERMAN METHODOLOGY FOR TUNNEL RISK ASSESSMENT

<sup>1</sup>Dr.-Ing. Georg Mayer, <sup>2</sup>Harald Kammerer, <sup>3</sup>Christoph Zulauf, <sup>4</sup>Christof Sistenich

<sup>1</sup>BUNG Ingenieure AG, DE

<sup>2</sup>ILF Consulting Engineers Austria GmbH, AT, <sup>3</sup>EBP Schweiz AG, CH, <sup>4</sup>Bundesanstalt für Straßenwesen (BASt), DE

## ABSTRACT

The currently used methodology of safety assessment of road tunnels in accordance with BASt booklet B66 “Sicherheitsbewertung von Straßentunneln” [1] dates from 2009, extensive knowledge has been gained when implementing and applying the developed method in risk analysis studies. Numerous research projects have provided new findings on parameters previously not considered. As some methodological elements and basic assumptions no longer correspond to the state of the art, it became necessary to re-analyze the methodology and to develop appropriate adjustments. The updated holistic approach is based on the current evaluation of incidents in German road tunnels as well as the state of the art regarding the assessment of road users’ risks in tunnels. The upgrade suggested as output of the BASt research project FE15.0663/2019/ERB<sup>1</sup> funded by the German Federal Ministry of Digital and Transport deals with risk evaluation, frequency analysis as well as the consequences of collisions and fires in tunnels. The implementation of the proposed adjustments allows analyzing tunnel risks more realistically and improves the evaluation of a large number of safety measures. The present paper summarizes the main adaptations developed and their influence on the risk assessment of road tunnels.

*Keywords: Tunnel risks, risk analysis methodology, frequency analysis, risk assessment, evaluation of safety measures, Computational Fluid Dynamics (CFD), evacuation simulation*

## 1. INTRODUCTION

With the introduction of the RABT 2006 [2] and the publication of the EABT-80/100 [3] in 2019, the requirements of the EC-Directive 2004/54/EC [4] on the use of risk analyses for the assessment of safety of road tunnels were transferred to German regulations. So, risk analyses are required if a road tunnel either has special characteristics or deviates from the specifications laid down in the regulations as regards its geometric design or safety-related equipment. Risk analyses also become necessary to verify if longitudinal ventilation for bi-directional tunnels and tunnels with daily congestion is admissible.

The required depth of risk analyses (qualitative/quantitative) as well as the verification of whether there is a special characteristic and/or a significant deviation from guideline specifications is determined according to the procedure described in Leitfaden für Sicherheitsbewertungen von Straßentunneln [5] gemäß RABT 2006 [2]. The methodology how to carry through quantitative risk analyses is described in the BASt booklet B66 Sicherheitsbewertung von Straßentunneln [1].

Since its publication in 2009, extensive knowledge has now been gained in the implementation of the procedure and its practical application in risk analysis studies. In addition, numerous research projects on special issues were carried out and significant new findings were made on parameters that were previously not taken into account. Among other things, the underlying accident statistics (event database) has been updated in the meantime and provides additional information on the frequencies of collisions and fires in road tunnels.

Therefore, both the methodological approach and the basic parameters and assumptions of the method no longer reflect the current state of the art. For the reasons mentioned above, it is necessary to re-

---

<sup>1</sup> FE15.0663/2019/ERB „Überprüfung der Annahmen und Parameter für Risikoanalysen für Straßentunnel (review of the assumptions and parameters for risk analyses for road tunnels) im Auftrag des Bundesministeriums für Digitales und Verkehr (BMDV) vertreten durch die Bundesanstalt für Straßenwesen (BASt), 2020-2022.

analyze the currently applicable methodology for the safety assessment of road tunnels and to suggest appropriate adjustments.

For this purpose, in a first step, new statistical bases were collected, accident rates were updated and influencing factors were determined. In addition, previously used input parameters and assumptions of the methodology, which affect the tunnel safety level as a whole as well as individual equipment features, were further completed, their influence on the risk checked and adjusted.

In addition, the methodology was expanded to include parameters that were previously not taken into account. This comprises, for example, the influence of speed on the accident rate and severity, fire development rates differentiated according to faster or delayed progression, a more detailed consideration of reaction times and human behavior during evacuation processes, the positive effects of third-party rescue, etc. From the investigation of the parameters mentioned with regard to their influence on risk, statements were derived regarding the need to take these parameters into account in risk-oriented studies in the future.

Another aim of the project was to standardize the procedures in order to be able to compare better the results of specific risk-oriented investigations on the features of safety-relevant equipment in road tunnels.

When working on the project, it was essential to obtain a broad, as comprehensive as possible view of the experience in the implementation and application of the procedure. To ensure this, a wide range of participants from practice and science were addressed in a workshop at the beginning of the project.

## **2. PRACTICAL EXPERIENCE**

The analysis of the existing methodology shows that basically the methodology is still suitable for assessing the safety of road tunnels and, thanks to its modular structure, it is open to expansion. The fact that it does not focus on the use of special models guarantees a high degree of future viability.

In the last ten years, numerous different sets of rules have been developed or adapted in order to implement the requirements of the European directive. For the present research project, primarily the regulatory requirements of those countries were analyzed in-depth, in which the topic of tunnel safety is particularly important. The findings can be summarized as follows:

**Degree of standardization:** The current regulatory requirements or the established procedures for risk assessment in accordance with the requirements of EC Directive 2004/54/EC are (as expected) very different. Nonetheless, there are a number of methods comparable in terms of their basic principles. In comparison to the methods of other countries which have been evaluated in depth, it turned out that the method according to BASt booklet B66 [1] allows a greater degree of freedom in implementation. Other procedures have more detailed specifications for individual elements or their model consideration. Here, the evaluations show a general area of tension as to which extent which specifications should be made for risk-based evaluations or which extent of freedom is allowed in the implementation. In the first case, the comparability between different practical applications and the traceability are enhanced, in the second case there are more possibilities to map specific tunnel properties that can be mapped less or not at all in highly formalized procedures.

**Risk analysis / model parameters:** In comparison to the method according to BASt booklet B66 [1], some of the other established methods, e.g. the models in Switzerland [6] and in the Netherlands [7], take into account more / additional tunnel properties (design characteristics and measures) than the direct influencing variables and parameter values. This includes, for example, an increased number of lanes or curve radii. There are also, in some cases, more pronounced specifications and notes on the parameter values to be used. Furthermore, more specific instructions and specifications for modeling event sequences and models are taken into account (e.g. behavior of tunnel users).

There are several investigations and studies on many influencing factors that can be used for implementation in the further development of the process in accordance with BASt booklet B66 [1].



Risk evaluation: There is also considerable heterogeneity with regard to the criteria for risk assessment. While some procedures are based on comparative procedures with a reference tunnel (as often is the case in Germany today), others use absolute limit criteria relating to the level of safety or considerations of proportionality for any additional measures. There are also procedures that use not only collective risks but also individual risks for tunnel users as an evaluation measure.

Complexity and effort: The majority of the procedures established today tend to be complex. For practical application, in-depth specialist knowledge in the field of road tunnels and risk-based procedures is required. Today, there are software programs associated with several established processes that support implementation and thus reduce effort. However, even in these cases, the users have to be well familiar with the methodological basics and have to bring in system knowledge of tunnels in order to model the respective tunnel properties and possible event sequences realistically.

### **3. SUGGESTED UPGRADE FOR THE RISK ASSESSMENT METHODOLOGY**

The suggested adaptations for the assessment methodology are divided into the following issues:

1. Risk evaluation
2. Frequency analysis
3. Analysis of the consequences of tunnel collisions
4. Analysis of the consequences of tunnel fires

When determining the adjustments, special attention was paid at the procedural level to the following general properties in the application of the methodology:

- Flexibility in use
- Minimum required level of complexity and effort
- Transparency, traceability and comparability of the (interim) results
- Process-related comparability of risk-reducing measures

In addition, the effects of the proposed adaptations were examined intensively. The previous safety level of a tunnel according to the specifications in booklet B66 [1] was compared with the calculations for a model tunnel, taking into account the new model parameters and evaluation approaches. The focus was on the comparative approach to assess differences in risk. The extensive results are presented in detail in the final report.

#### **3.1. Risk evaluation**

According to the procedure described in booklet B66 [1], it is proposed that the (collective) risks determined in the course of the risk assessment are shown in the form of cumulative curves in a FN-diagram, using an absolute evaluation criterion to assess the acceptability. At the time of the development of the B66 procedure, however, it was foreseeable that it would not yet be possible to establish an absolute acceptability criterion. For this reason, it was recommended that the risk assessment be carried out based on a relative comparison between the planned case and the corresponding value for the theoretical case of a guideline-compliant design. As experience has shown, this comparative assessment of the risks largely has become established in practice. However, practice has also revealed that there is a need to sharpen the definitions with regard to the reference tunnel.

Basically, the reference tunnel is a theoretical tunnel similar to the real tunnel to be examined, but fully meets all requirements and conditions of the guidelines and regulations to be applied in the specific case. A relative assessment approach is made, in which compliance with the required safety level is determined by a relative comparison with this reference tunnel. Using a relative assessment approach, the influence of uncertainties on the assessment result can be minimized.

In the present research project, specifications for the reference tunnel were defined for all safety parameters relevant according to RABT [2]/ EABT [3] and compared with the tunnel to be examined. The focus was on setting parameters for the majority of tunnels in Germany. For tunnels that represent special cases, it is recommended that the reference tunnel be determined individually in consultation with the relevant decision-makers, depending on the objective of the investigation.

### 3.2. Frequency analysis

The suggested adaptation as regards the frequency analysis contains the findings from the evaluations of the nationwide event database, the definition of influencing factors for the accident rate as well as a proposal for updating the structure of the event tree.

The frequency of vehicle accidents and fires can be derived from long-term event statistics. In contrast to analytical methods, here statistical methods are clearly in the focus. Analysis is based on the nationwide event database consisting of the basic data for each tunnel and the event report for each reportable event. The database includes 168 tunnels and approx. 49,000 events (years 2006 to 2020).

After extensive data processing, numerous parameters could be derived directly from the database. The primary focus was on checking the current event rates and, if necessary, their updating based on new statistical data.

The analysis in the research project has revealed that the values from the BAST booklet B66 [1] for the (base) accident rate, the distribution of different accident types and the fire rate have to be updated. In addition to the new, updated values, the report includes a comparison with the values from BAST booklet B66 [1] and a comparison with event rates from other countries.

However, accidents in road tunnels are influenced by numerous geometric and traffic-related factors. Therefore, it is necessary to include these influencing factors when determining the frequency of accidents. For this purpose, corresponding correction factors for unidirectional and bidirectional road tunnels were determined, by which the respective base accident rate is multiplied.

Accident rates derived from the event database as well as expert estimates and comparison with approaches from other risk models form the basis for this factor model. Correction factors could be determined for the following influences:

- Existence of entrances / exits ( $f_{ZA}$ )
- Tunnel length ( $f_L$ )
- Number of traffic lanes ( $f_{FS}$ )
- Traffic lane width ( $f_{FSB}$ )
- Existence of break down lane ( $f_{SS}$ )
- Traffic volume per lane ( $f_{DTV/FS}$ )
- Permissible speed ( $f_V$ )
- Differential speed ( $f_{\Delta V}$ )

To determine the frequency, all possible intermediate states between the initial events up to the final system states are determined and quantified with regard to their expected frequency. The intermediate states are examined for system responses in the same way as those of the triggering event. In this way, until a final state is reached, different branches of the event sequence are created, which are provided with different branch probabilities.

The following branches are considered within the event sequence for mapping fire incidents:

- Event location (e.g. entrance area / inner tunnel section / center of the tunnel ...)
- Traffic volume (day / night / ...)

- Traffic status (free-flow traffic / congested traffic)
- Fire load (5/30/100 MW)
- Fire development (fast / delayed)
- Detection successful (yes / no)
- Tunnel user alert successful (yes / no)
- Tunnel closure systems activated (yes / no)
- Ventilation system activated (yes / no)
- Other security systems available and activated (yes / no)
- Increased extent of damage (yes / no)
- Start of third-party rescue measures

The report specifies standard values for the relative frequencies of the individual branches and explains specific differences to BASt booklet B66 [1].

### **3.3. Analysis of the consequences of tunnel collisions**

In addition to the accident rate, the speeds driven in the tunnel also have an impact on the resulting extent of damage in the event of collision. Since no meaningful relationships could be derived from the event database, the influence was justified with the help of the Nilsson Power Model [8]. It is based on the direct relationship between the change in mean speed and the resulting change in the severity of the accident.

The different influence of the speed on these two sub-areas and equally on the frequency of accidents with different degrees of severity is represented by the numerical value of the exponent. Therefore, it is recommended to model the extent of damage for collisions with the exponent 1, also due to the good agreement with the statistically proven dependencies.

### **3.4. Analysis of the consequences of tunnel fires**

In the event of a fire inside a road tunnel, smoke particles, heat and toxic gases can endanger road users. High concentrations of smoke particles lead to restricted visibility and to irritation of the respiratory tract and eyes, and thus hinder users in their orientation and movement. In order to be able to take these effects into account when determining the extent of the damage, a simulation model is required that enables the time and space-discrete calculation of the heat, smoke and toxic substances depending on the development of the fire and fluid-mechanical boundary conditions.

For the computer programs (CFD models) suitable for this purpose, essential parameters and boundary conditions were specified in the suggested adaptations in order to determine the impact models for estimating the consequences of fire. Approaches for simulating the effects of smoke, the effects of toxic gases and the effects of heat were defined.

An essential part of the revision of the damage scale model concerns the discussion and, if necessary, the definition of a detailed timeline on which the model is based. The focus was primarily on the definition of fire curves and the associated energy and pollutant release rates. A major innovation is the implementation of a fast and a delayed fire curve. They allow evaluating additional measures that have a significant influence on the individual time steps. These measures include, for example, the different behavior of detection devices, the reaction of operators, the activation of safety devices, and the degree of compliance with activated tunnel closure systems and the reaction of tunnel users.

One of the major innovations in the revised and upgraded methodology is the implementation of an accumulation-based escape mode. It aims at mapping the effects of a tunnel fire on people trying to escape as realistically as possible. The current risk model provides for the evaluation of successful or unsuccessful escape solely based on visibility. By implementing intoxication models (based on a

"fractional effective dose" (FED) or a "fractional effective concentration" (FIC)) it is possible to model variable escape speeds as a result of restricted visibility or highly irritant gas concentrations. Another focus when revising the consequence model was the definition of model approaches and the requirements for models to analyze self-rescue processes. Possibilities were created to evaluate different escape velocities, the perception of security facilities or hazards in the tunnel, inadequate behavior during the self-rescue and the influence of people with restricted mobility. Approaches for evaluating third-party rescue activities, both concerning firefighting and rescue of people, were implemented, too.

#### **4. SUMMARY AND CONCLUSION**

Within the framework of the research project FE 15.0663/2019/ERB (Review of the assumptions and parameters for risk analyses for road tunnels), various recommendations for the further development have been made. They are based on the experience gained from practical application of the methodology described in BAST booklet B66 [1] and on the results of general developments in the field of risk analyses for road tunnels. The analysis of the presently used assessment method has shown that basically it is still suitable for safety assessment of road tunnels and that due to its modular structure it is open to expansions. Since the method does not focus on the use of special models, it features great sustainability. The method was expanded to include a factor model that allows further consideration of traffic-related and structural influences on accident rates. Furthermore, in order to represent more realistic fire processes, fire developments with both rapid and delayed progression were integrated into the procedure. In addition, an accumulation-based escape model was implemented to determine the impacts of fire on tunnel users. As a result, the extent of damage is now determined based on a "fractional effective dose" (FED) or a "fractional effective concentration" (FIC). Moreover, fire-fighting measures are now part of the procedure. By the implementation of the suggested adjustments, it is now possible to analyze the risks in tunnels more realistically and to better evaluate a large number of safety measures.

#### **5. REFERENCES**

- [1] Zulauf et. al.: FE 03.378/2004/FRB „Bewertung der Sicherheit von Straßentunneln“, Berichte der Bundesanstalt für Straßenwesen (BAST), Heft B 66, ISBN 978-3-86509-909-9, 2009.
- [2] Forschungsgesellschaft für Straßen- und Verkehrswesen – Arbeitsgruppe Verkehrsführung und Verkehrssicherheit (Hrsg.): „Richtlinien für die Ausstattung und den Betrieb von Straßentunneln (RABT)“, 2006.
- [3] Forschungsgesellschaft für Straßen- und Verkehrswesen – Arbeitsgruppe Verkehrsmanagement (Hrsg.): „Empfehlungen für die Ausstattung und den Betrieb von Straßentunneln mit einer Planungsgeschwindigkeit von 80 km/h oder 100 km/h (EABT-80/100)“, 2019.
- [4] European Union (ed.): "Directive 2004/54/EC of the European Parliament and of the Council on minimum safety requirements for tunnels in the trans-European road network," 29 April 2004.
- [5] Bundesministerium für Verkehr, Bau und Stadtentwicklung (BMVBS)/Bundesanstalt für Straßenwesen (BAST) (Hrsg.): Leitfaden für Sicherheitsbewertungen von Straßentunneln gemäß RABT 2006 (Abschnitt 0.5), 2008.
- [6] Bundesamt für Strassen (Hrsg.), Richtlinie „Risikoanalyse für die Tunnel der Nationalstrassen“, Richtlinie 19004, Ausgabe 2014
- [7] QRA-tunnels 2.0, Achtergrondsdocument, Rijkswaterstaat (Hrsg.) , Ministerie van Infrastructuur en Milieu, 2012
- [8] G. Nilsson: Traffic Safety Dimensions and the Effect of Speed on Safety, Bulletin 221, Lund Institute of Technology, Department of Technology and Society, Traffic Engineering, 2004.

# INFLUENCE OF ALTERNATIVE ENERGY CARRIERS ON TUNNEL SAFETY – A QUANTITATIVE CONSEQUENCE ANALYSIS

<sup>1</sup>Regina Schmidt, <sup>2</sup>Anne Lehan, <sup>3</sup>Patrik Föbtleitner, <sup>1</sup>Harald Kammerer

<sup>1</sup>ILF Consulting Engineers GmbH, Austria

<sup>2</sup>BAST Federal Highway Research Institute, Germany,

<sup>3</sup>Institute of Thermodynamics and Sustainable Propulsion Systems, Austria

## ABSTRACT

The composition of road traffic is nowadays clearly dominated by petrol and diesel powered vehicles. However, one of the major goals against further climate change is the decarbonisation of road traffic by the use of vehicles with alternative energy carrier technologies. The currently most promising ones are the Li-Ion battery-powered vehicles, fuel-cell-powered vehicles and vehicles powered with internal combustion engines using hydrogen or liquefied natural gas. Although the latter do currently represent only a small share of the total traffic, it can be assumed that alternative powered vehicles will soon take on greater significance. Therefore, a deeper understanding of possible additional risks, especially in considering incidents in tunnel structures, is of greatest interest and is currently investigated in various research projects, such as [1], [2], [3]. In these projects, the focus lies only on one of the alternative energy carriers mentioned above. However, in order to obtain a thorough overview of relevant possible additional dangers as well as related consequences on the safety of tunnel users, the aim of the BAST-project FE 15.0675/2020/ERB [4] as well as of the present paper is to consider all relevant alternative powered vehicle types in order to identify possible need for adaption of the risk-analytical assessment method for road tunnels. To this aim, dangerous zones according to, for example battery fires, jet fires or vapor cloud explosions have been assessed by using numerical as well as analytical models. In the course of a detailed evacuation model, considering a large variety of agents with different velocities and respiratory volumes, the corresponding consequences of alternative energy carriers on tunnel users can be assessed. This paper will demonstrate and discuss in detail the foundation of the research project with focus on the evacuation simulation, as well as the resulting consequences analysis on tunnel users.

*Keywords: Alternative energy carrier technologies, tunnel risk assessment, evacuation and consequence model, road tunnel, research project.*

## 1. INTRODUCTION

Road traffic is currently clearly dominated by petrol and diesel-powered vehicles. The annually growing number of vehicles and increasing mileage result in a steadily increasing energy requirement. Therefore, the transport sector makes a significant contribution to greenhouse gas emissions. The decarbonization of road traffic through the establishment of climate-friendly alternatives as a substitute for petroleum-based fuels is therefore a basic requirement for achieving climate protection goals. The use of vehicles with new alternative energy carrier technologies, above all electric batteries, but also hydrogen and LNG (liquefied natural gas) are supposed to increase rapidly in the future. Moreover, as a result of the increasing urbanization the traffic is shifted to the underground.

Existing recommendations and regulations for tunnel safety, as well as methods for risk assessment however, have so far been limited exclusively to events in connection with vehicles operated by conventional energy carrier systems. In order to be able to maintain the existing

level of safety in the future, the effects of events in road tunnels involving vehicles with alternative energy carriers must constantly be determined and evaluated. To this aim, the traffic composition now and in twenty years is discussed in section 2. Section 3 deals with leaks, collisions and vehicle fires in combination with alternative energy carrier technologies and the corresponding consequences on the safety of tunnel users is discussed in section 4. Results presented in section 5 can eventually be used to adapt the risk-analytical assessment method for road tunnels and to derive any necessary adjustments to the requirements for road tunnels.

## 2. TRAFFIC COMPOSITION – NOW AND IN 20 YEARS

In course of a thorough analysis of the existing vehicle fleet for the year 2020, a starting point for the development on the new car market could be found. The average value for the years 2016-2020 was used to quantify the found data, since due to the Covid 19 pandemic, the year 2020 alone can be assumed to not be representative in terms of new registrations. This analysis was carried out for the vehicle categories passenger cars, light trucks, heavy trucks and buses and data from the EU and worldwide studies were also applied.

All of the forecast studies that were analyzed in this regard showed that conventional energy carriers will become less important for all vehicle categories, but will nonetheless make up a large part of the vehicle fleet. The greatest change can be expected for passenger cars and buses, since a quarter of all newly registered vehicles already use energy carriers based on alternative energy sources.

Table 1 shows the relevance of the energy carrier types for each of the four vehicle types for the years 2020, 2030 as well as for the year 2040 and thus summarizes the forecasts identified in a clear form. Basically, it is difficult to reliably predict the vehicle mix to be expected. Many influencing factors, in particular leaps in technological development and political decisions, influence the assertiveness of the individual technologies and the forecasts presented show a currently valid trend rather than a reliable forecast.

Table 1: Relevance of energy carrier types to vehicle types for 2020, 2030 and 2040<sup>1</sup>

	Cars			Light HGV			Heavy HGV			Bus		
	2020	2030	2040	2020	2030	2040	2020	2030	2040	2020	2030	2040
Conventional	high	high	medium	high	high	high	high	high	high	high	high	high
Hybrid <sup>2</sup>	high	medium	medium	low	medium	medium	low	medium	low	high	medium	high
BEV	medium	high	high	low	medium	medium	low	low	low	medium	high	high
CNG	low	low	low	low	low	low	low	low	low	low	low	medium
LNG	low	low	low	low	low	low	low	low	medium	low	low	medium
LPG	low	low	low	low	low	low	low	low	low	low	low	low
FCEV	low	low	medium	low	low	medium	low	low	medium	low	low	medium
H <sub>2</sub>	low	low	low	low	low	low	low	low	medium	low	low	medium

<sup>1</sup> Conventional: Gasoline, Diesel, BEV: battery electric vehicle, CNG: compressed natural gas, LNG: liquified natural gas, LPG: liquified petroleum gas, FCEV: fuel cell electric vehicle,

<sup>2</sup> Note, that the carrier "Hybrid" includes all different types of hybrid vehicles

### 3. IDENTIFICATION OF ADDITIONAL RISKS DUE TO ALTERNATIVE ENERGY CARRIERS

Based on traffic mix forecast for the year 2040 presented in Table 1, possible tunnel events involving battery-powered electric vehicles, fuel cell-powered vehicles and vehicles with internal combustion engines (CGH2, LNG), were investigated risk-analytical. This was done in constructing as a first step simplified exemplary hazard trees according to accidents involving vehicles with the mentioned alternative energy carriers. Each of the energy carriers exhibit special physical properties that are directly related to the type of storage and may result in differentiated types of risk when involved in an accident.

As an example, Figure 1 shows the schematic representation of a hazard tree according to the battery electric engine and it will now be used to discuss the different hazard-tree branching-points in a bit more detail. For each of the alternative energy carrier types mentioned above, four different vehicle types (car, light truck, heavy truck, bus) have been considered according to their respective relevance shown in Table 1. The splitting in four vehicle types is of main importance since not every new energy carrier system is suitable for every vehicle type. For example, due to the high weight of the battery a battery-powered heavy transporter is not an alternative to a heavy truck that runs on a conventional energy source. Furthermore, the energy storage devices of different vehicle types may be of different sizes and most often are placed in different positions and thus may lead to differentiated danger zones or hazards. The next branching points in the hazard tree relate to the type of event. Is the event under consideration a fire incident – a hot incident – or a purely mechanical one – a cold incident. Is the built-in safety device functional or damaged respectively not functional. The branching point concerning the object of hazard does in addition to the risk of tunnel users also consider the risk of third-party rescue teams as well as the risk for the tunnel infrastructure. However, the focus lies on the last branching point, the potential hazard types - such as heat, toxic gases, acid, electricity, overpressure, the effects of a rapidly expanding flame front (fireball) and cryogenic burns.

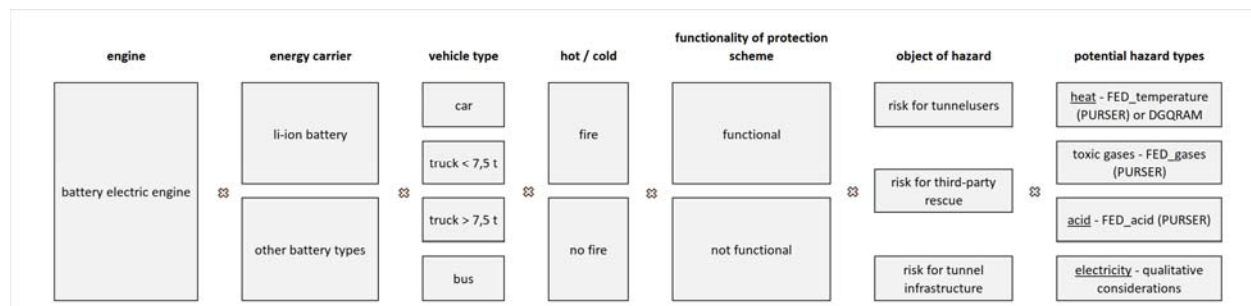


Figure 1: Battery electric engine hazard tree – schematic representation

### 4. RISK ANALYSIS

Based on the very general hazard trees presented in chapter 3 in combination with available experience reports and expert assessments event trees were developed. The latter contain a manageable number of relevant hazard scenarios. Depending on the type of scenario, numerical methods such as numerical flow models, analytical models or already existing models have been used. Necessary adaptations have been made to identify the influence of vehicles with alternative energy carriers on the hazard extent in the tunnel structure in order to estimate the potential extent of damage with regard to people in the tunnel.

#### **4.1. Determination of frequencies**

Initially, it should be noted that the proportion of alternatively powered vehicles is too small to derive frequencies based on statistical methods, so that estimates of the probability of occurrence for each hazard scenario can currently only be made on the basis of qualitative assessments. However, this may change in the future and therefore the possibility for considering adapted data has been provided.

Wherever possible, frequencies from the general road tunnel risk analysis in accordance with the adapted BAST-booklet B66 [5] have been used in quantifying the event tree branches described above – for example in the collision and fire frequencies, or in the distribution of fire sizes for truck fires. Where there have been no corresponding frequencies available, estimates have been made by the experts involved in the project by taking into account the findings and assumptions from similar research projects.

#### **4.2. Damage extent modeling of alternative energy carriers**

##### **Li-Ion battery fire**

In the case of Li-ion battery fires, analogous to fires in conventional vehicles, three main hazards with regard to personal safety were considered. These refer to the danger of heat, restricted visibility (smoke gases) and the danger of inhaling toxic substances. As a result, the model fire curves defined in the research project BRAFA [1] and the associated pollutants released were used as the basis for the three-dimensional CFD simulations.

##### **Hydrogen VCE**

In case of an accident involving a hydrogen-powered vehicle, the hydrogen tank can rupture due to the mechanical impact or due to thermal stress (in case the safety device on the tank is not working) and a vapor cloud explosion (VCE) may occur. When modeling the VCE, two different hazards were considered: the hazard of a fast expanding fireball and the overpressure hazard. The hazard area corresponding to the fireball was estimated with an experimentally founded relationship between the diameter of the fireball and the mass involved [6]. To estimate the overpressure hazard area, the generally valid relationship between overpressure and distance from the origin of the detonation corresponding to hydrogen tank explosions was used [7].

##### **Hydrogen jet fire**

If a hydrogen-powered vehicle catches fire and the temperature at the safety valve reaches the threshold value, hydrogen is released. Due to the already existing fire, the released hydrogen is immediately ignited and consequently leads to a jet fire. The corresponding risk area was estimated for all considered vehicle types by using model results that were experimentally verified in [8]. In particular, the different number of tanks, the different tank volumes, the possible different storage pressures and possible different blow-out directions were explicitly taken into account.

##### **LNG BLEVE**

The overpressure of an exploding LNG tank in the tunnel was modeled with the well-established TNT equivalence model (similar to the OECD/PIARC DG-QRAM model [9]). The existing mass of LNG in the tank is converted into an equivalent mass of TNT. From numerous experiments relating to the damage caused by TNT explosions, the damage respectively the hazard area of the LNG BLEVE (Boiling Liquid Expanding Vapor Explosion) was estimated.



### 4.3. Evacuation model

The applied, elaborate and in general terms defined evacuation model is now discussed in a nutshell. Instead of repeating the evacuation simulation for statistical reasons with a changed arrangement of so called agents along the tunnel, at each position in the tunnel, the number of persons is decomposed into 18 different agent types. This number results from assuming three age categories for both genders, i.e. six agents. Further on, for each of the six agents, three evacuation speeds are assumed – leading to 18 different agent types. Moreover, at each position in the tunnel, for each of the 18 agent types, five starting times are considered. It can be assumed, that agents going by car or by truck as well as the first part of bus passengers are able to start their respective evacuation process without any delay. The evacuation start time according to the second part of bus passengers is assumed to be shifted via 10 seconds, the third part via 20 seconds and the fourth via 30 seconds. In addition, 3% of the persons (sum of passenger car occupants, HGV occupants and Bus occupants) are assumed to stay in their vehicle and are not evacuating due to limitations in mobility or because they behave incorrect.

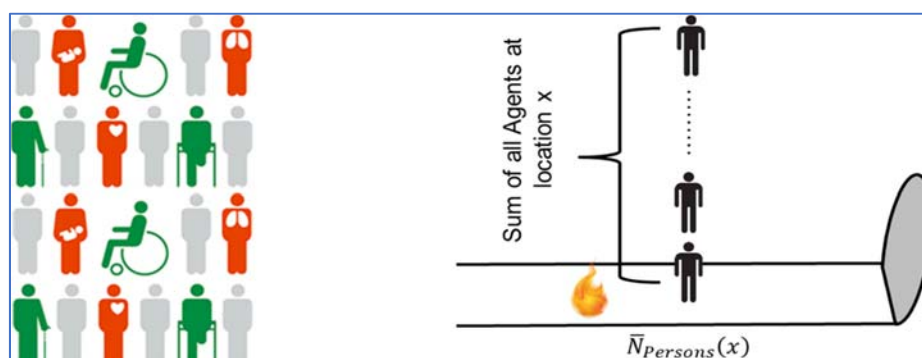


Figure 2: Evacuation model: Agent configuration

### 4.4. Survivability model

Each agent starts its individual evacuation process from its respective starting location into the direction of the next emergency exit. However, it is assumed that the agents do never evacuate across the fire. In this case they are assumed to decide to take the longer, but safer, way to the emergency exit in opposite direction.

For every evacuation point  $x$  in the tunnel, success or failure is calculated for each of the different agent types. This is done for all the distinct mentioned dangers according to the different energy carriers – conventional fire, Li-Ion battery fire, hydrogen VCE, hydrogen jet fire and LNG BLEVE. In case of conventional fires as well as for battery fires, the FED / FIC<sup>3</sup> approach according to Purser and McAllister [10] is used, i.e. inhaled toxic fire products are summed up for each agent along its individual evacuation path and if one of the values exceeds the respective fatality threshold before the emergency exit or the tunnel portal is reached, the agent is considered as incapacitated. As to identify the fatality zones of the jet fire scenarios or the explosion scenarios, various different danger zones, depending on the size as well as the position of the tanks, were calculated. If in course of the evacuation process, an agent happens to be within one of the danger zones, the agent is considered as incapacitated.

## 5. EVALUATION AND INTERPRETATION OF RISKS

In order to be able to evaluate and identify possible additional risks due to alternatively powered vehicles in the tunnel, a suitable hypothetical comparison tunnel (one-way traffic tunnel without

<sup>3</sup> FED: Fractional Effective Dose; FIC: Fractional Irritant Concentration

traffic congestion) based on the results of the BAST-research project FE 15.0663/2019/ERB [11] was chosen. On the basis of this tunnel, a relative assessment approach was pursued, in which different safety levels were compared through a relative comparison of different vehicle fleet constellations. By using a relative evaluation approach, the influence of imprecision on the evaluation result can be minimized and accordingly even the smallest safety-related changes can be made visible.

In order to objectively compare the potential risk of the individual energy carriers, the determined risk values for each vehicle type and each energy carrier technology have been compared, whereby it has been assumed in each case that the vehicle type is operated to 100% with the respective energy carrier technology. Representative for all vehicle types, the results according to all three, most promising alternative engines according to cars are shown in Figure 3 and the results show that in comparison to the conventional engine, there can no relevant increase in the overall risk be identified. Fire and explosion risks are not relevant for the selected comparison tunnel in absolute terms since the major part of the risk is due to mechanical incidents – collisions without fire development or explosion. This is due to the tunnel being a unidirectional tunnel with longitudinal ventilation at critical velocity as well as due to the fact that mechanical incidents do statistically occur ten times more often than fire incidents. However, in considering the pure fire and explosion risks there is a significant increase in risk from gas-powered vehicles visible. This increase in fire risk is mainly due to the additional jet-fire scenarios taken into account in considering the fuel-cell engine.

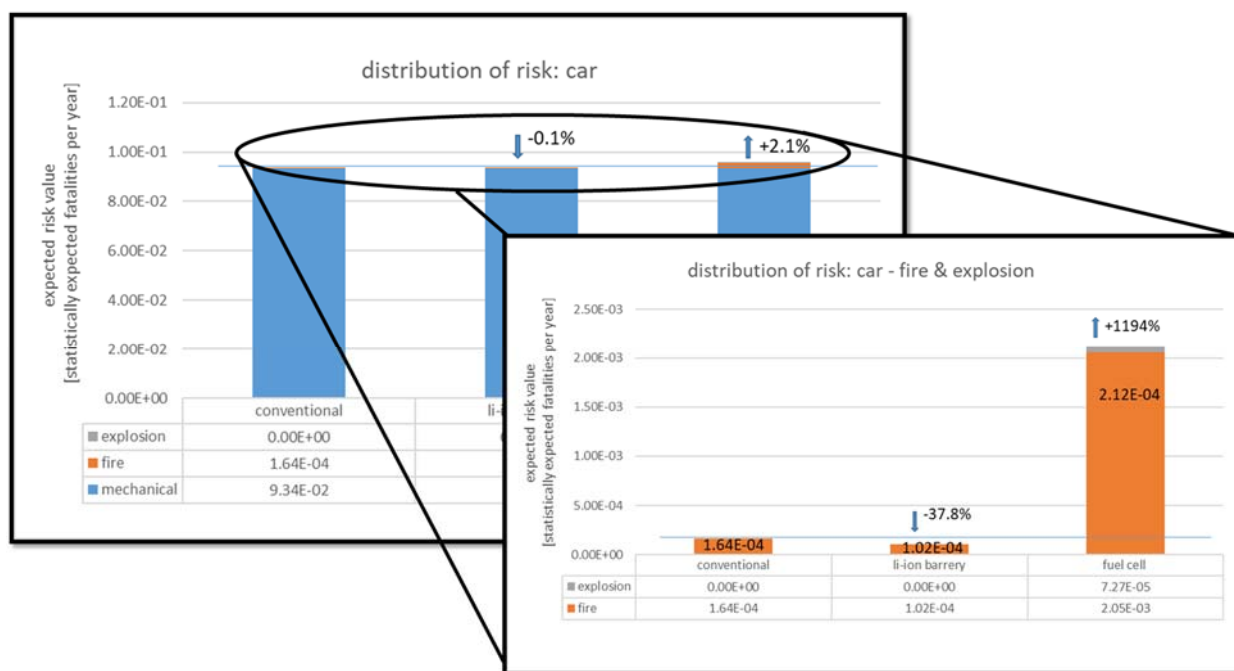


Figure 3: Comparison of total risk respectively fire and explosion risk according to the three alternative energy carriers that will most probably be used for cars in future. 100% share for each propulsion technology for each vehicle type, here the car, is assumed

In calculating the risks according to the predicted share of the respective energy carriers in the total traffic, the results presented in Figure 4 show that no increase in the overall risk for the traffic forecast compared to 100% conventional engines can be derived. As has already been mentioned before, fire and explosion risks are not relevant for the considered tunnel in absolute terms, but can increase significantly for changed shares of vehicles powered by alternative energy carriers in the tunnel. The extent to which the increase in the risk according to fire and explosion is relevant under other conditions or to what extent the overall risk increases with

changed conditions - especially for tunnels with a relevant proportion of traffic jams - is still to be clarified.

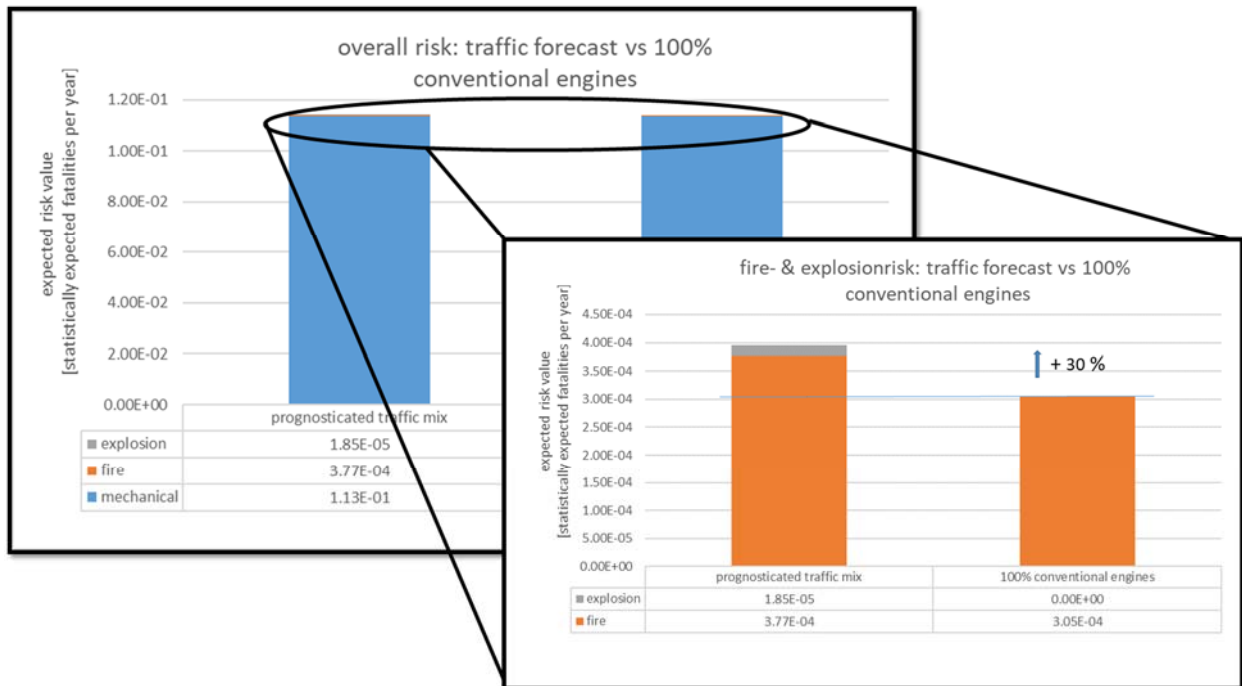


Figure 4: Comparison of the total risk as well as the fire and explosion risks according to the traffic forecast 2040 and for 100% conventional engines

## 6. SUMMARY AND CONCLUSION

The current paper outlines a thorough risk assessment procedure how to identify possible additional risks due to alternatively powered vehicles in tunnel structures. Based on the research efforts, it can be concluded that, according to the current state of knowledge, battery-powered vehicles do not cause a significantly higher fire risk than conventional vehicles. According to gas-powered vehicles, the risk assessment showed that the overall risk remained almost the same as for conventional powered vehicles; however, a significant increase in the risk regarding to fire and explosion scenarios could be identified. Even if the jet-fire, the VCE or the BLEVE incident are extremely unlikely from today's perspective, the same statement applies to them as to large fire events, namely that they may not be relevant in the overall risk context, however, they will rouse socially a lot of attention and have therefore to explicitly taken into account. Therefore, the development of the vehicle share of these energy sources should be regularly reviewed in order to be able to take precautions here accordingly at an early stage.

## 7. REFERENCES

- [1] FFG. (2021). Brandauswirkungen von Fahrzeugen mit alternativen Antriebssystemen (BRAFA). <https://doi.org/10.3217/8vj91-gc832>.
- [2] HyTunnel. (2022). <https://hytunnel.net/>
- [3] Sandia. (2020). <https://energy.sandia.gov/tag/hyram/>.

- [4] B. Kohl; H. Kammerer; O. Heger; R. Schmidt; P. Sturm; P. Fößleitner. (2022). *Einfluss von Fahrzeugen mit neuen Antriebstechnologien auf die Tunnelsicherheit, FE 15.0675/2020/ERB. Unveröffentlichter Projektbericht der ILF Consulting Engineers und der TU Graz im Auftrag der Bundesanstalt für Straßenwesen, Deutschland*
- [5] BMVBS and BAST, "Heft B 66: „Bewertung der Sicherheit von Straßentunneln“ Bericht zum Forschungsprojekt FE 03.378/2004/FRB," 2009.
- [6] R. Zalosh and N. Weyandt, "Hydrogen Fuel Tank Fire Exposure Burst Test," SAE Paper Number 2005-01-1886, 2005.
- [7] V. Molkov and W. Dery, "The blast wave decay correlation for hydrogen tank rupture in a tunnel fire," *International Journal of Hydrogen Energy* 45, 2020
- [8] H. Hussein, S. Brennan and V. Molkov, "Hydrogen Jet Fire from a Thermally Activated Pressure Relief Device (TPRD) form Onboard Storage in a Naturally Ventilated Covered Car Park," MDPI, 2021
- [9] OECD/PIARC/EU, "Transport of dangerous Goods through tunnels: Quantitative Risk Assessment Model (v4.04) - Reference Manual," 2019
- [10] D. A. Purser; J. L. McAllister, "Assessment of Hazards to Occupants from Smoke, Toxic Gases and Heat," *SFPE Handbook of Fire Protection Engineering*, 5th ed., Springer-Verlag, USA, 2016.
- [11] B. Kohl, H. Kammerer, O. Heger, G. Mayer, S. Brennberger, C. Zulauf and P. Locher, "Überprüfung der Annahmen und Parameter für Risikoanalysen für Staßentunnel: FE 15.0663/20197," 2019.

# THE APPLICATION OF ZONE MODELLING IN THE RISK ANALYSIS OF TUNNELS WITH ARTU SOFTWARE

<sup>1</sup>Michele Fronterre, <sup>2</sup>Rugiada Scozzari

<sup>1</sup>Cantene s.r.l., IT

## ABSTRACT

Cantene has developed a software tool called ARTU, acronym for “Risk Analysis in Tunnels”, that calculates the societal risk related to fire in tunnels. The tool combines probabilistic and deterministic approaches, including different sub-models: 1D fluid dynamics, queue formation, egress, interaction between fluid-dynamic conditions and people. Recently, a new version has been released, that includes zone modelling in the representation of fluid dynamics. Zone modelling makes it possible to represent phenomena like back-layering and smoke stratification that cannot be represented by 1D fluid-dynamic tools. These phenomena are particularly significant in the first phase of the fire, when mechanical ventilation has not reached the nominal airflow and the egress takes place. The stratification of smoke has particular importance in tunnels without mechanical ventilation due to the fact that the fire products move undisturbed. A zone modelling tool developed by Lund University was chosen and many adjustments were made along with the developers in order to make the software suitable to the tunnel fire application. The areas of applicability of the tool were also investigated. As a results, the zone modelling software has been integrated into ARTU, in order to automatically manage a multiscale analysis depending on the characteristics of the analysed tunnel.

*Keywords: Risk analysis, 2004/54/EC, 1D fluid dynamics, probabilistic approach, validation, zone modelling, tunnel.*

## 1. INTRODUCTION

Tunnels often represent crucial nodes of a road network, as they may represent points of connection between two otherwise disconnected areas or even allow for transnational connection between countries. For this reason, tunnel fires can have catastrophic consequences in terms of traffic disruption, property damage, and, more importantly loss of lives [1]. Since the publication of the Directive 2004/54/EC of the European Parliament (related to tunnels within the Trans-European Road Network which are longer than 500 meters [2]), risk assessment has become an integral part of tunnel design [3]. Furthermore, an appropriate risk assessment of existing and new facilities can be a useful tool to assess tunnel safety levels and inform decision makers and designers upon solutions to be adopted [4].

Based on these premises, the Italian fire engineering and thermal science company Cantene srl developed a tunnel risk analysis tool called ARTU (acronym in Italian for Risk Analysis in Tunnels). This tool adopts a probabilistic approach to estimate the expected number of fatalities per year in existing and new tunnels. ARTU uses an approach based on pseudo-random sampling from distributions to define hundreds of different fire and egress scenarios. Random variables include pre-movement time and egress velocity, fire position, and the type of vehicle on fire (design fire). A deterministic approach is used to describe the interaction between fire products and people involved in each scenario [5].

ARTU estimation of risk is based on the analysis of a large number of different scenarios. Hence, in order to keep the computational cost acceptable, fluid dynamics representation is based on 1D model. Despite its low computational requirement, this modelling approach prevents the representation of phenomena like smoke stratification and back-layering that can occur in presence of low longitudinal velocity. These phenomena are common in naturally

ventilated tunnels with small slope, when the fire is growing and not fully developed. Furthermore in mechanical ventilated tunnel, smoke stratification can be a desired effect during the egress of occupants, in order to ensure that a layer free of smoke in the lower part of tunnel section can be used as a mean of egress. ARTU's aim is to evaluate societal risk, namely expected number of fatalities per year, so its focus is on the first phase of the fire, i.e., during egress. A more detailed description of smoke stratification in the vicinity of the fire and during the first phase of the fire has the potential to better represent the interaction between occupants and fire, leading to a more accurate evaluation of societal risk [5].

## 2. TUNNEL FIRE MODELLING APPROACHES

The main modelling methods for the study of fire and smoke in tunnels are here presented considering increasing complexity and computational cost.

One-dimensional (1D) network models represent a system as a one-dimensional network of nodes, containing a single set of variables such as temperature, density, mass treated as homogeneous, and node connections that represent 1D transfer conduits between nodes [5]. The 1D model returns time-varying air temperature, air velocity, and volume airflow along the tunnel. The intrinsic limitations of 1D models are that the flow quantities are assumed to be homogeneous in each cross-section. As a consequence, 1D models are not suitable to simulate the fluid behaviour in regions characterised by high temperature or velocity gradients. These regions are the ones close to the flames or in the regions where well-defined smoke stratification is found [1].

Zone models represent a compartment as multiple uniform zones (typically two zones: a hot upper layer and a cooler lower layer). Zone models solve conservation equations between the uniform zones and typically include empirical relationships for phenomena such as fires and plume flow. Zone models are limited by the geometry they can represent (simple, cuboidal compartments) but are solved relatively quickly [5]. When applying control volume equations to tunnel fires, consideration should be given to the unique nature of some fire phenomena in tunnels. For example (i) an assumption that hot-layer properties are homogeneous along the length of the tunnel will only be tenable for very short tunnels; (ii) ambient and forced ventilation flows in tunnels may affect air entrainment in plumes; (iii) the relative velocities of hot and cold layers may mean that shear mixing effects at the interface may not be negligible [1]. Nevertheless, the use of tunnel fire zone models in probabilistic tunnel risk modelling is not a novel approach [6].

Field models, also called computational fluid dynamics (CFD) models, divide a domain into finite elements or volumes for which conservation equations are solved. Each finite element holds a set of conserved variables. Field models can be used to examine complex geometry but require large storage space, high computation requirements and have a high computational cost [7]. The physical behaviour of the fluid is represented by means of mathematical models, and it is possible to extend the description of the fluid to include effects such as turbulence, buoyancy, combustion and heat transfer by radiation and convection, all in a single simultaneous calculation. When solutions are obtained, they should be reviewed taking into account the influence of grid size and time step, what influence do boundary conditions have on the solution, adequate convergence of solution [1].

As systems in the built environment are getting larger and more complex, hybrid approaches (also called multiscale approaches) started arising. Computational limitations mean that the calculation domain must be curtailed, ignoring the two-way coupling between the total system and a fire. Coupled hybrid modelling (adoption of coupled fire dynamics sub-models with a range of computational costs) expands the domain and analyses of this two-way coupling within a reasonable timeframe [7].

### 3. DESCRIPTION OF THE SOFTWARE ARTU

ARTU estimates the expected number of fatalities per year in existing and new tunnels. A queue-formation model is used to determine the initial position of people along the tunnel, taking into account data about traffic conditions. The path of each person inside the tunnel towards the exit is calculated assuming that the people in a straight or curved tunnel can only move in one direction (along the tunnel wall), which can be approximated with a 1D modelling approach. ARTU takes into account the presence of other people in the surroundings and the reduction of visibility due to smoke. The estimation of damage is based on the effects of smoke on people, estimated by means of the FED (Fractional Effective Dose) parameter. For the majority of toxic products in a fire atmosphere, incapacitation or death occurs when the victim has inhaled a particular product dose of toxicant [8]. As with toxic gases, an exposed occupant can be considered to accumulate a dose of convected heat over a period of time [9]. ARTU calculates the FED for each person in the domain, based on oxygen, carbon monoxide, carbon dioxide concentration and gas temperature, obtained from the results of the fluid-dynamics routine.

For the fluid dynamics representation, the first release of ARTU used a third party software based on 1D fluid dynamics which includes geometrical data and characteristics of the ventilation system. The software returns time-varying air temperature, air velocity, and volume airflow along the tunnel. Since it is a 1D tool, it returns only one value for each variable at a set distance from the fire. This value represent an average over the cross-section of the tunnel.

To improve the resolution of the fire modelling representation available in ARTU, Cantene initiated a research project together with the Division of Fire Safety Engineering at Lund University. The aim of the project was to include zone modelling in ARTU with a multiscale approach.

### 4. THE MULTI-ZONE MODEL

The multi-zone model integrated within ARTU is based on an existing tool, the MZ Fire model [10], used to calculate the effects of a fire in an enclosure. The overall concept of a multi-zone model has been presented in previous publications [11].

The enclosure is divided into several regions (horizontal) and layers (vertical) this means that the entire enclosure is made up of several smaller computational volumes or zones that extends in the x-, y- and z-direction. The conservation of mass and energy are applied for each zone and the calculated properties (like temperature) are uniform in each zone. The fire is specified as a heat release rate and the heat and hot gases rises upwards from the fire in a plume that enters the highest located layer in the fire region, until it hits the ceiling. Plume mass flow is calculated with Heskestad's plume model [12]. The plume equation is developed from data of pool fires up to a diameter of 2.5 m [13] that is assumed to be axisymmetric and not influenced by wind. Air and hot gases are entrained in the plume from the layers that it passes through. Mass is transported horizontally to layers in adjacent regions due to hydrostatic pressure differences. The driving mechanism behind the transport of smoke in the MZ Fire model is temperature differences between the different zones. This makes the implementation difficult when momentum forces become important. To account for momentum resulting from when a fire plume hits the ceiling and a horizontal flow created, an empirical ceiling jet model is used. The vertical flow of mass between layers is calculated based on the conservation of mass.

Heat is transferred to solid obstructions through convection and radiation, and through 1-D conduction in obstructions. Heat is transferred between zones through the flow of hot gases and radiation [5].

## 5. APPLYING MULTI-ZONE MODEL TO TUNNELS

The MZ Fire model, which originally was developed for large enclosures, has been updated and adapted for tunnel environments. In fact, the use of zone models requires carefully consideration of: (i) the ratio between length and height of the simulated domain; (ii) the representation of ventilation devices used in tunnels, such as jet-fans, that may require dedicated model input calibration efforts. The integration of MZ Fire model into ARTU involved a set of developments needed specifically for tunnel fire scenarios (e.g. tunnel gradient and tunnel section representations). In addition, an analysis has been done to determine the MZ model domain of application. Analysis was done by means of a benchmarking with full scale test data and field model simulations. Figure 1 compares the ceiling gas temperatures at different distance from fire obtained by empirical test, FDS field model simulation and MZ model simulation. The data refers to the Runehamar tunnel test T1, where an HRR with peak equal to 205 MW after 20 minutes from ignition was estimated.

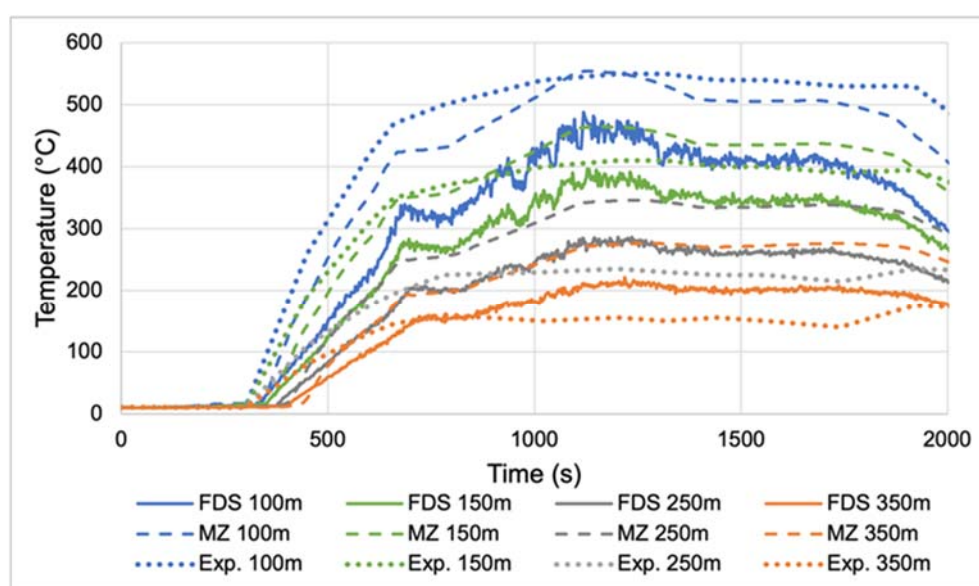


Figure 1: ceiling gas temperatures at different distances from the fire for the Runehamar tunnel test T1 [5]

Figure 1 shows that the ceiling jet temperatures closer to the fire source (100-150 m) are predicted well by the MZ Fire model, while the temperatures further away (250+ m) are over predicted. In general, MZ predicts a higher temperature closer to the ceiling, and lower temperature at the lower levels. The average temperature over the height is corrected. Nevertheless, since the focus is on predict the interaction between people and smoke, the under estimation of temperature in the lower height is not acceptable. For this reason, applicability of MZ model is set to HRR lower than 20MW, based on the extensive benchmark reported in [5]. In addition, benchmark results showed that MZ model can be suitably applied to short portion of tunnels (<200m from fire). These applicability limits make the zone model particularly appropriate to determine the tenability conditions in the vicinity of fire, during the first phase of emergency, when egress takes place.

## 6. CASE STUDY

The selected case study is a bidirectional tunnel with natural ventilation.



Table 1: the case study

Length	910m
Cross sectional area	60m <sup>2</sup>
Slope	0.5%
Number of emergency exit	None
Traffic direction	Bidirectional
Average annual daily traffic	8.460 veh/day
% of heavy goods vehicle	9%
Ventilation system	Natural
Fixed-fire extinguishing system	None

An analysis was done for a fire 50m from left portal involving a light vehicle. The corresponding HRR is taken from [13]. Peak value is reached in 300s from the ignition and corresponds to 8MW.

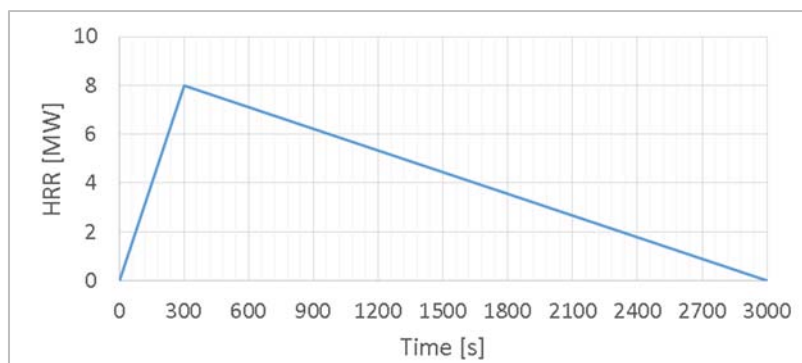


Figure 2: HRR curve

Figure 3 and Figure 4 show a comparison between the results obtained by the 1D and the zone modelling tool. In each figure, the upper graph shows the results from 1D model. The second graph shows the results from zone model that are related to a shorter domain (100m) in the vicinity of fire. The lower graph shows the combination of the two models, thus the multiscale approach result. Results from 1D model are averaged on the cross section of tunnel, while results from zone model are taken at 2 m from the floor, along the tunnel axis.

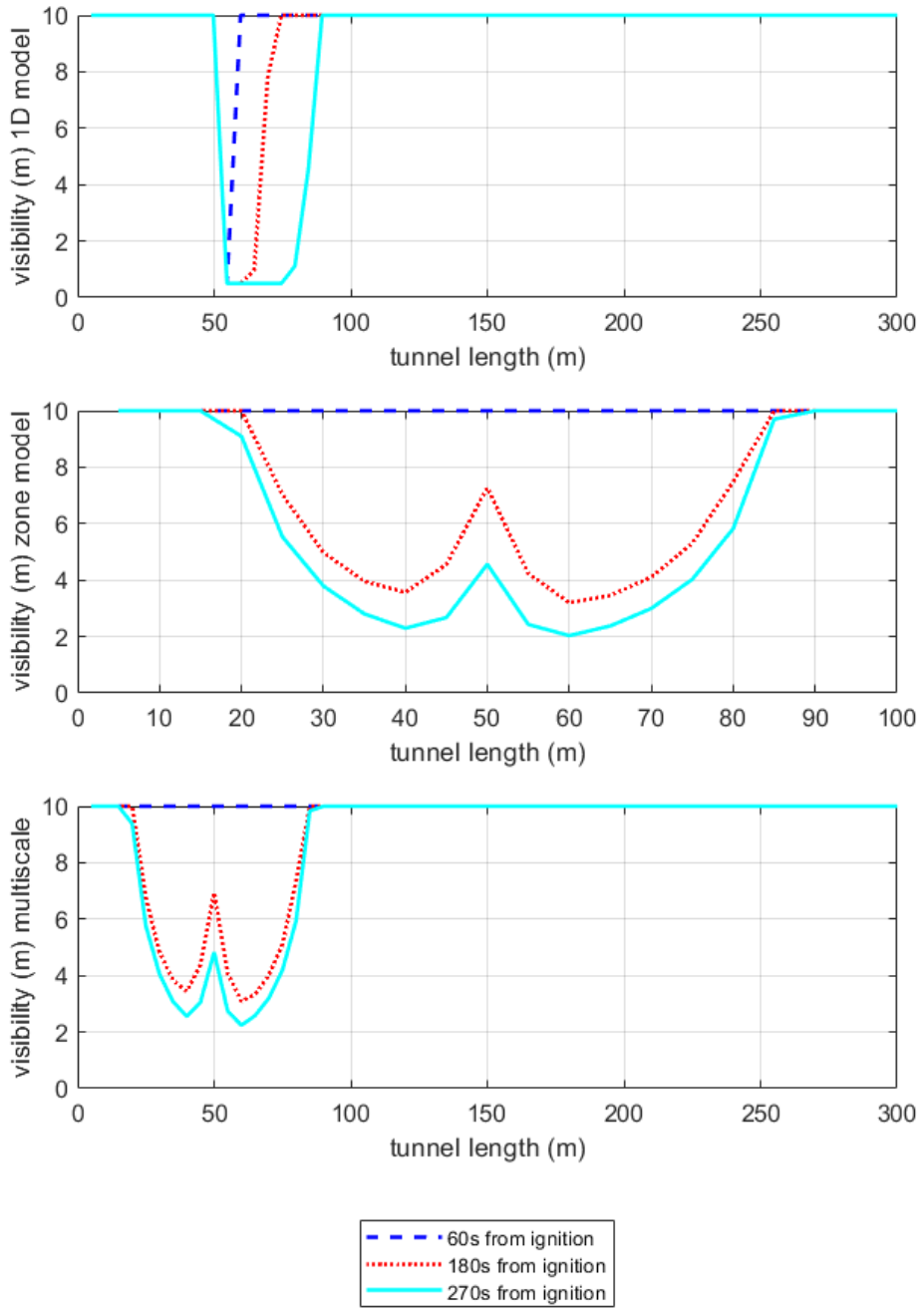


Figure 3: visibility along the tunnel at 3 different times

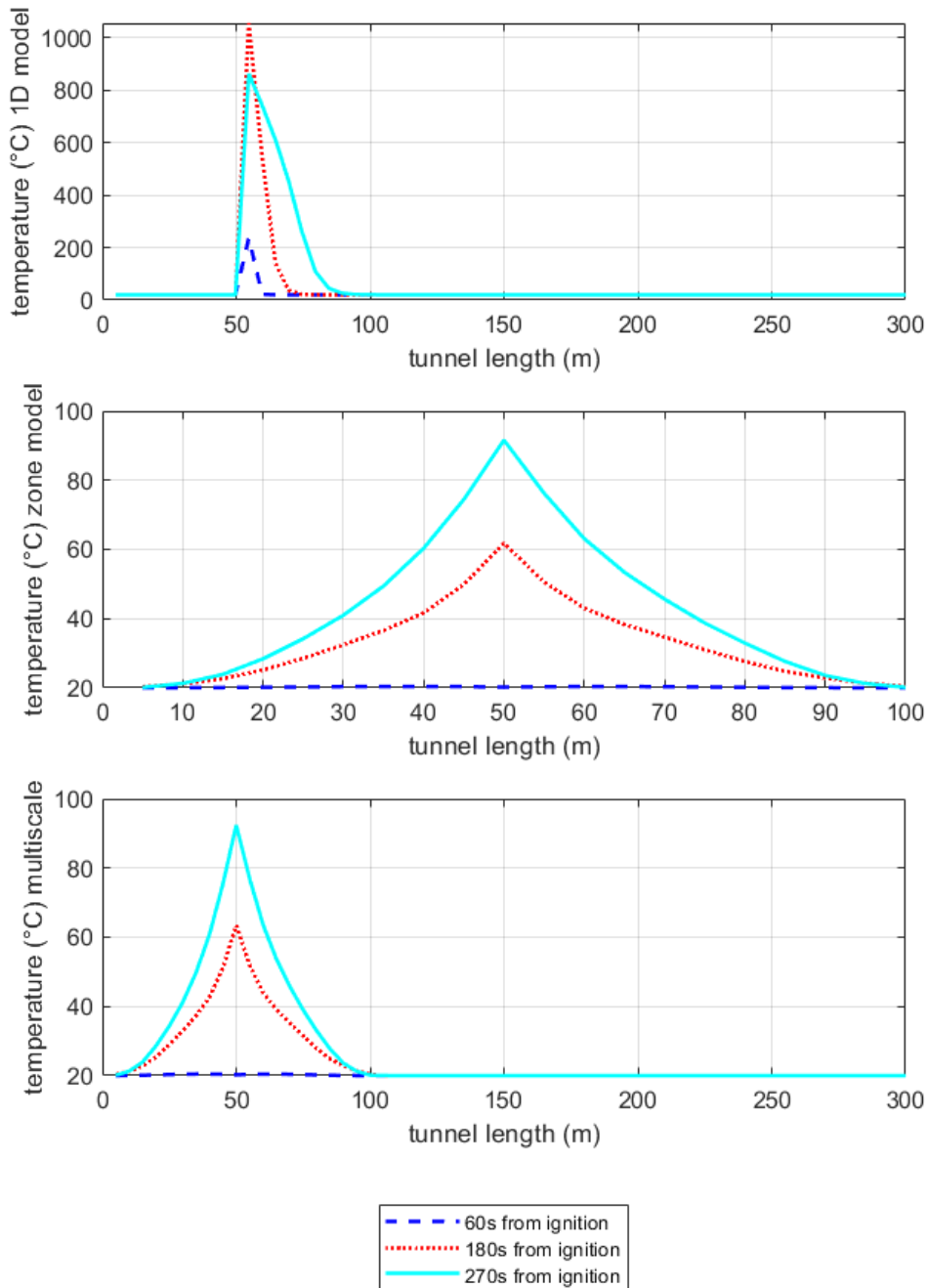


Figure 4: temperature along the tunnel at 3 different times

Applying zone modelling instead of 1D modelling makes the risk estimation more accurate, as explained in the following.

(i) 1D models gives a too conservative estimation for both temperature and visibility, in particular in the first 60 seconds from the ignition. In fact, when using 1D models, an implicit hypothesis is done that if there is smoke in a section of tunnel, people interact with it, because smoke is assumed as homogeneously spread in the tunnel cross section. Zone models instead, make it possible to estimate the smoke layer height, thus leading to a more precise estimation of users-smoke interaction (Figure 5).

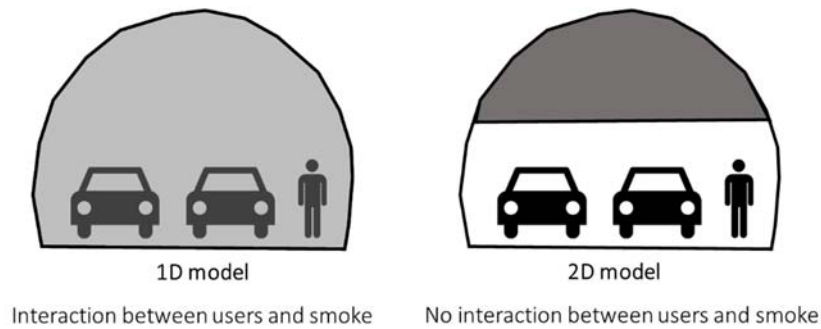


Figure 5: different estimation of users-smoke interaction

(ii) Zone modelling makes it possible to investigate the dynamic of smoke in the vicinity of fire. As described by [15], at a short distance from the point where the fire plume impinges on the tunnel ceiling, the smoke flow transits to a longitudinal flow on both sides in a tunnel with essentially no longitudinal ventilation and nearly no slope. Eventually such a layer will become thicker and descend towards the tunnel floor. This can be seen in the particular shape of the visibility output from zone model.

(iii) The zone model estimates the effect of slope in a more precise way than the 1D model. In 1D results, the smoke is pushed through the right portal by the effect of buoyancy. No back layering is represented because of the intrinsic limitation of this kind of model. 1D modelling cannot describe back-layering in case of a longitudinal velocity lower than critical value (Figure 6). The zone model instead shows the presence of back-layering through the left portal.

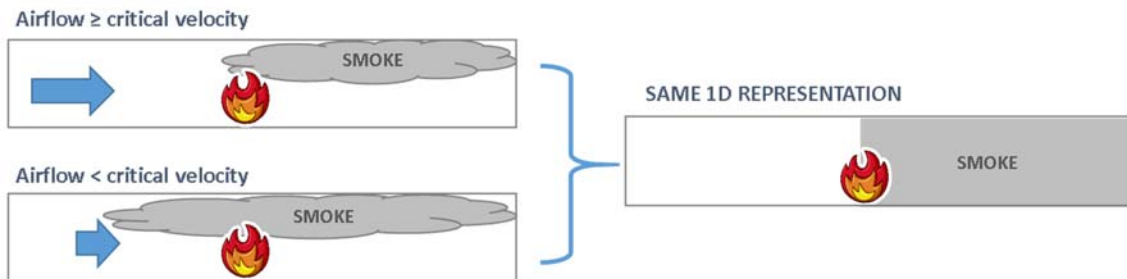


Figure 6: 1D representation of cases with different longitudinal ventilation

## 7. SUMMARY AND CONCLUSIONS

Zone modelling provides an alternative modelling concept to simple one-dimensional models and more advanced CFD models. The strength of the zone modelling compared to the 1D models is that it is possible to get the vertical and horizontal distribution of e.g., temperature and visibility in the simulated domain. Regarding more advanced models, the benefit of the MZ Fire model is that the simulation time is much smaller. Even if the results are promising caution should be taken when using the model, since it includes several simplifying assumptions. For this reason, it should be kept in mind that the zone modelling is a complement to other models and tools. For some situations a one-dimensional model might be more adequate. All in all, the possibility to switch between a more or less refined representations of tunnel fire dynamics (still having computational times that do not impede the use of this approach) offers more flexibility to the tunnel fire safety designer and expands the possible range of applicability of ARTU [5].

## 8. REFERENCES

- [1] Beard, A., & Carvel, R. (2012). Handbook of Tunnel Fire Safety, 2nd edition. London, UK: ICE Publishing.
- [2] The European Parliament. (2004). DIRECTIVE 2004/54/EC. Official Journal of the European Union.
- [3] Kohl, B., Botschek, K., & Hörhan, R. (2007). Austrian Risk Analysis for Road Tunnels. Development of a new Method for the Risk Assessment of Road Tunnels. First International Tunnel Safety Forum for Road and Rail. Lisbon, Portugal.
- [4] Beard, A. (2010). Tunnel safety, risk assessment and decision-making. *Tunnelling and Underground Space Technology* 25, 91-94.
- [5] Johansson, N., Ronchi, E., Scozzari, R., & Fronterre, M. (2021). The use of multi-zone modelling for tunnel fire risk analysis. Lund, Sweden: Lund University.
- [6] Riess, I., Bettelini, M., Brandt, R., "Sprint - a Design Tool for Fire Ventilation," 10th International Symposium on Aerodynamics and Ventilation of Vehicle Tunnels, Boston, 2000.
- [7] Ralph, B., & Carvel, R. (2018). Coupled hybrid modelling in fire safety engineering; a literature review. *Fire Safety Journal*, 157-170.
- [8] Purser, D., & McAllister, J. (2016). Assessment of Hazards to Occupants from Smoke, Toxic Gases, and Heat. In M. Hurley, *SFPE Handbook of Fire Protection Engineering*, 5th edition (pp. 2308-2428). Springer Science+Business Media.
- [9] NFPA. (2011). NFPA 502 Standard for Road Tunnels, Bridges, and Other Limited Access Highways. Quincy, USA: National Fire Protection Association.
- [10] Johansson, N. (2021). Evaluation of a zone model for fire safety engineering in large spaces. *Fire Safety Journal* 120.
- [11] Suzuki, K., Tanaka, T., Harada, K., Yoshida, H., 2004. An application of A Multi-layer Zone Model to A Tunnel fire. *Fire Saf. Sci.* 6, 7b-2.
- [12] Heskestad, G., 1983. Virtual origins of fire plumes. *Fire Saf. J.* 5, 109-114.
- [13] Kung, H.-C., Stavrianidis, P., 1982. Buoyant plumes of large-scale pool fires. *Symp. Int. Combust.* 19, 905-912. [https://doi.org/10.1016/S0082-0784\(82\)80266-X](https://doi.org/10.1016/S0082-0784(82)80266-X)
- [14] CETU. (2003). Guide to Road Tunnel Safety Documentation booklet 4. France: CETU Centre d'études des tunnels.
- [15] Ingason, H., Li, Y. Z., & Lönnemark, A. (2015). *Tunnel Fire Dynamics*. New York: Springer Science+Business Media.

## **FIERCE: A COST BENEFIT ANALYSIS FOR TUNNEL FIRE SAFETY**

<sup>1</sup>Schepers Melchior, <sup>1</sup>Deckers Xavier, <sup>2</sup>Jovanović Balša, <sup>2</sup>Chaudhary Ranjit Kumar,  
<sup>2</sup>Van Coile Ruben

<sup>1</sup>Jensen Hughes, Ghent, Belgium

<sup>2</sup>Department of Structural Engineering and Building Materials, Ghent University, Ghent,  
Belgium

### **ABSTRACT**

The Belgian fire engineering consultancy FESG – A Jensen Hughes Company - has been developing a risk assessment framework for tunnels called FIERCE (Fire Integrated Environment for Risk Comprehension and Evaluation) in cooperation with Ghent University. The goal of the framework is to develop a probabilistic approach towards fire safety measures in tunnels taking into account specific fire safety measures (sprinklers, water mist systems, ventilation) but also structural and financial considerations. The framework couples, CFD, 1D and evacuation simulations in order to assess the impact of a tunnel fire in terms of potential casualties. In order to evaluate the structural damage and subsequent downtime a finite element model of a representative tunnel was built in ‘SAFIR’. This model was subjected to several fire curves, with a heating phase conforming to the RWS curve and an exponential decay phase. The evaluation of the damage and associated cost was done by mapping the depth of the 300 °C isotherm and residual deformations at the end of the decay phase to a damage state leading to an assessment matrix correlating the fire curve and the damage state. The damage state was subsequently linked to a repair cost as well as a cost associated with the unavailability of the tunnel.

*Keywords: QRA, Tunnel Fire Safety, SAFIR, downtime, cost-benefit*

### **1. INTRODUCTION**

Notable accidents such as the Mont Blanc tunnel fire, the Tauern tunnel fire and the Channel tunnel fire have raised awareness for the need of effective fire safety measures in tunnels. This awareness was also reflected in the European Directive 2004/54/EC [1,2,3] which aimed at bringing the safety level of the tunnels throughout the Trans European Road Network to a higher level. In this directive a strong emphasis is placed on the importance of a thorough risk analysis as forming the basis for the measures that need to be put into place to achieve an acceptable safety level. This triggered the development of several risk assessment methods for road tunnels [4, 5]. As a result different countries developed different risk assessment methods independently, based on local accident databases and fire events [6]. Currently there is no proprietary risk analysis tool for tunnels in Belgium. The FIERCE project therefore set out to investigate and develop a holistic framework that would allow an all-encompassing probabilistic, risk-based approach towards the design and assessment of fire safety systems in tunnels. By taking a probabilistic approach an integrated solution can be provided, considering structural, life safety and economic aspects optimized to the lifecycle of the tunnel.

### **2. QRA FRAMEWORKS IN EUROPE**

The current risk assessment methods in use throughout Europe all have different levels of complexity and accuracy. The methods are either quantitative or qualitative, system based or scenario based and may or may not consider dangerous goods [7]. Depending on the risk assessment method that is applied to a certain tunnel, the outcome in terms of measures that need to be taken, might be vastly different. There is however always a trade-off that needs to be made between the cost and benefits of certain proposed measures. The current risk assessment methods do not allow to take such trade-offs into account, neither do they allow an easy integration of the probabilistic nature of the parameters and boundary conditions involved with the occurrence of a fire. When not taking into account the probabilistic nature of these variables the different methods can lead to widely different results for the same tunnel. This should be avoided and a more uniform approach should be used in order to provide

consistent results [8]. A lot of the risk assessment tools in use today, such as the OECD/PIARC QRA model and the RWS method are spreadsheet-based tools working with a pre-set number of scenarios. Since the number of scenarios is limited these tools do not always deliver an optimal solution. Furthermore only the scenarios imposed by the issuing member states are considered in the respective QRA methods, while the type of road infrastructure might deviate substantially between different member states [7]. These methods focus mainly on possible control measures, while for example the reliability of the measures (e.g. reliability of sprinklers vs smoke and heat control systems) is not taken into account. Some notable shortcomings of the most used current methods are the inability to take into account one or more of the following aspects: sprinklers, new energy carriers, transversal ventilation, structural stability, the propagation of smoke or the impact of smoke on the evacuation of people from the tunnel. By providing a framework which can be extended with additional modules the proposed framework aimed to overcome the inherent deficiencies of the existing methods.

Besides the inability of most of the existing methods to address structural and monetary considerations, in Europe, differently than in other countries such as Japan or Australia, active suppression systems are not employed in tunnels [9] and thus not taken into account in the existing risk assessment tools. Water suppression systems can however strongly limit the growth and the size of the fire and as a result also the negative effects related to a large fire. On the other hand the suppression system will also affect the smoke stratification which in turn will affect evacuation conditions. Research has however showed that the use of water suppression in tunnels generally has a positive impact and consequently it should be possible to include such safety measures in the risk analysis [10, 11].

### **3. THE FIERCE FRAMEWORK**

Fire safety in tunnels is a complex process with multiple interacting elements such as the fire, the traffic flow, the tunnel's structure and the fire safety measures influencing one another in multiple ways [12, 13, 14, 15]. The development of a new approach for assessing fire safety in tunnels, including the probabilistic nature of the processes involved, thus requires the integration of different fields of expertise combined in a single holistic approach. The FIERCE tunnel safety framework, encompasses different sub-models within a Performance Based Design (PBD) framework. As an alternative to the prescriptive approach a performance based design allows the fire safety engineer to propose alternative solutions which allow to satisfy the performance criteria in an optimized way. A deterministic approach takes into account only a prescribed set of expected worst case scenarios. These are then used to design the different safety systems: ventilation, suppression and or passive protection and detection. However, in choosing the fire scenario a lot of assumptions are made. Ambient conditions, traffic, failure rates of components,... all these variables rely on the constraints of the project on the one hand and on the experience of the designer on the other hand. They thus often rely on engineering judgement. As a result a too conservative choice of the input parameters leads to an overly expensive design while a non-conservative choice leads to a high risk in case of fire. Therefore, in order to propose design solutions which are optimized both in terms of life safety, structural safety and business continuity the risk assessment has to take into account all possible scenarios that can occur throughout the lifecycle of the tunnel. In order to do so a probabilistic approach is proposed.

In a probabilistic design it is possible to include a continuous set of fire scenarios which are then sampled and used to represent the probability of a certain scenario occurring throughout the lifecycle of the tunnel. The consequences of the design fire scenarios are then evaluated with a performance based approach and the final result of the assessment is represented in an FN curve. Such an FN curve is used to evaluate the risk for life safety by correlating the number of fatalities with the frequency of a certain accident. This concept of risk evaluation is further extended by the framework to also include the financial consequences of the fire and the effect of the fire on the structural stability of the tunnel. The framework aims to provide an integrated design approach where the different submodels, as shown in figure 1, influence one another and their mutual dependence is taken into account.

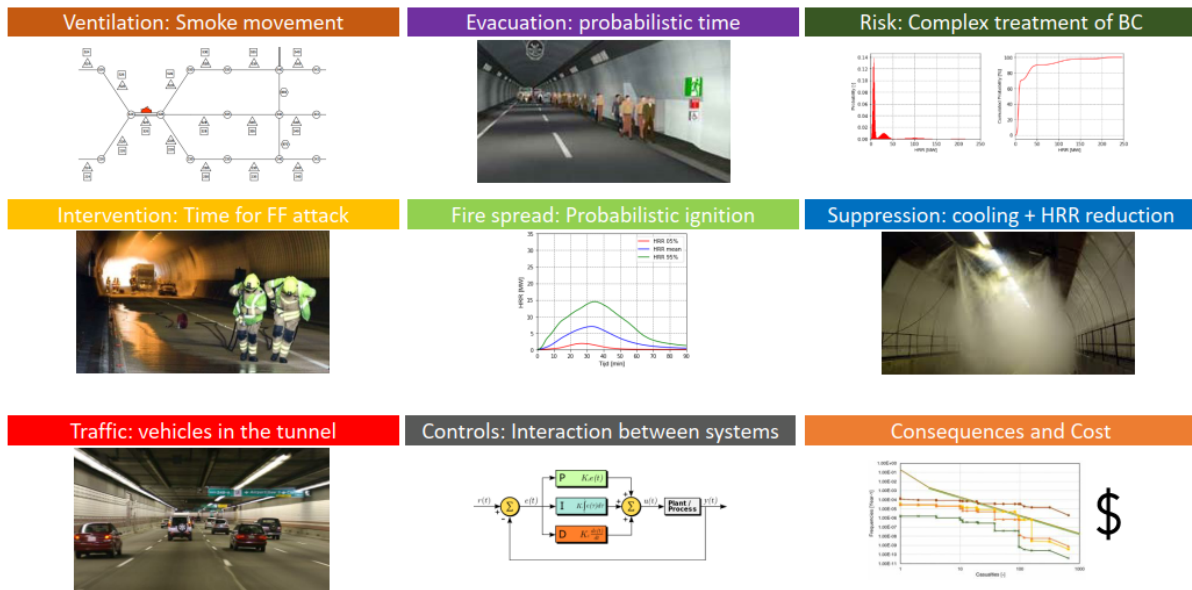


Figure 1: submodules making up the integrated design approach

### 3.1. Submodule interaction

The first layer in the consequence modelling of the FIERCE framework deals with ventilation and evacuation modelling. The ventilation modelling is based on a 1D approach in order to be able to run a great number of simulations in a reasonable time frame, which is not possible with current CFD packages. The evacuation model in turn is capable of running a large amount of simulations and directly takes into account the effect of the fire and smoke spread on occupant movement, slowing down occupants when they have to evacuate through smoke conditions. The coupling of the smoke spread and evacuation models allows for the calculation of the FED or FID and as such an assessment of the amount of possible casualties.

In the second layer the events that directly affect the HRR of the fire are considered such as suppression systems that may be present and possible suppression efforts by the fire brigade. In order to evaluate the effects of the suppression system a simplified model was developed that allows for a quick determination of the cooling effect of a watermist system. The firefighter intervention model is based on an event based approach where fire brigade operations are broken up into several activities including: gathering information, dispatch of resources, equipment set up, control and extinguishment of the fire, and search and rescue [16]. Amongst several parameters the success of the firefighter intervention largely depends on the intervention time, more specifically the so called ‘time to water on fire’, the moment at which the suppression activities are started [17,18]. The intervention time can be split into several stages as shown in the figure 2.



Figure 2: event flow for the fire brigade intervention

The model provides an estimation of the time required for the firefighters to reach and possibly suppress the fire, thus influencing the HRR of the fire [19].

In the final layer, the novelty of the proposed approach lies in the structural model that was developed and which allows for both a structural and financial assessment of the consequences of the fire. This model is expanded upon in the following section.



## 4. STRUCTURAL MODEL

To allow for a comprehensive risk evaluation, also the structural performance during and after fire is assessed. First of all, structural integrity during fire allows for evacuation and search and rescue operations. Secondly, service interruption following a fire can constitute very large indirect consequences, i.e., through increased travel times for users. In situations where structural repairs or reconstruction are required post-fire, this service interruption can extend over many months.

### 4.1. Fire exposure

Tunnel structures are commonly designed or assessed considering a heating phase exposure only. The structure's minimum capacity is however obtained during the decay phase, and permanent deformations and load redistribution imply that heating phase stability is no proxy for post-fire usability. Considering Li and Ingason [20], the temperatures achieved in severe tunnel fires (i.e., structurally significant fires) are capped by the characteristics of the tunnel, and not by the potential heat release rate (HRR) of the burning heavy goods vehicles. Therefore, as soon as the HRR is sufficiently high (order of 90 MW), the heating phase can be modelled considering the RWS fire curve. Here, the decay phase is modelled considering the equation below, with the decay phase coefficient  $b$  ranging between  $0,0015\text{min}^{-1}$  and  $0,0611\text{min}^{-1}$ , based on experiments listed in [21]. The average value of  $0,025\text{min}^{-1}$  is adopted. Resulting exposures are visualized in figure 3

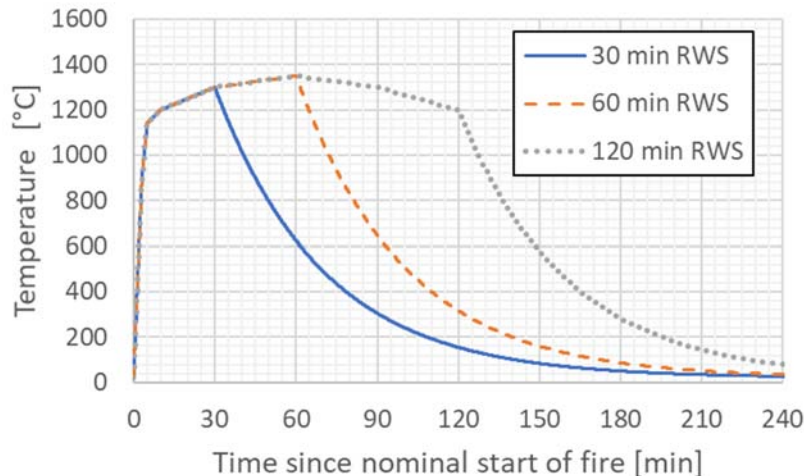


Figure 3: Exposure considered for structurally significant fires.

### 4.2. Concrete spalling

Spalling is modelled considering nominal spalling rates, as recommended in [22] and applied by Hua et al. [23]. Specifically, a set time for the onset of spalling is considered, followed by a constant spalling rate of, for example, 3 mm per minute. Spalling is stopped as soon as either (i) the reinforcement layer is reached, or (ii) when the fire enters the decay phase. Hua et al. [23] report spalling rates for tunnels of up to 5mm/min. In the current study nominal spalling rates of 1/2/3/3.75/5 mm/min are considered, as well as a no-spalling case. For each spalling rate a corresponding probability is specified considering the experimental dataset listed by Hua et al.

### 4.3. Structural model and performance during fire

A twin tunnel section with a smaller internal connecting tube is considered. This section is evaluated in order to allow for a fast and approximate assessment of similar designs. Cross-sectional dimensions for the tunnel are indicated in figure 4. The springs representing the soil restraint to outwards movement are represented by the blue lines. The tunnel section is symmetrical. Fire exposure is modelled for the left tube only, heating the walls and ceiling (not the floor). The calculations are done using the dedicated structural fire engineering software SAFIR [24]. Further details on the structural model are provided in [25]. Structural failure during fire was observed for high load combinations. When considering the

expected load values (as is required for a risk-based design optimization), all considered tunnel structures maintained stability for the full fire duration.

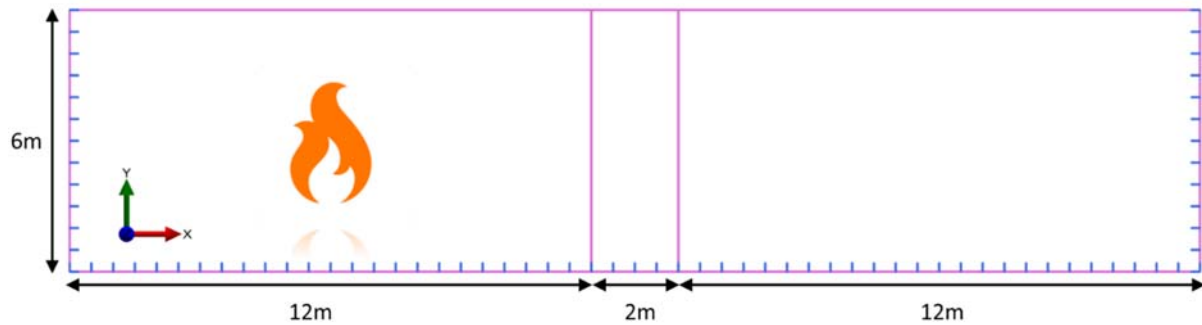


Figure 4: Tunnel section and dimensions (axis position).

#### 4.4. Post-fire damage and downtime assessment

Post-fire damage is considered to relate to (i) permanent damage to heated concrete, and (ii) permanent deformations in the tunnel cross-section. Damage limit states based on [26] are adopted. Specifically, concrete heated above 300°C is considered to require replacement, while deflection limits apply for the walls and ceiling (e.g., a ceiling deformation exceeding span/120 requires full reconstruction).

The resulting damage states are defined for different nominal spalling rates and cases where the concrete is protected with fire protection boards, considering different RWS heating phase durations. For the ceiling the thermal damage state generally dominates the mechanical (deformation) damage state, meaning that the repair strategy for the ceiling is defined by the thermal ingress. The obtained damage state due to the thermal and mechanical damage is listed in figure 5. As the damage state relates to a repair strategy, the damage states are then directly linked with a cost for repair and repair duration (i.e., downtime). The repair costs of the tunnel structure can then be estimated, based on the damage parameters D300 and the residual deformations, and its associated damage state classification. The repair cost for a repairable structure is the sum of cost of labor and materials required to carry out the repair, while in case of an irreparable structure, the cost is a sum of demolition and reconstruction cost. The same applies to the evaluation of downtime, which can also be represented as a cost. Depending on the level of damage, and the considered costs, it may be ‘cheaper’ to rebuild than to repair. Considering [27], downtime costs can be very high for critical infrastructure (order of 1M EUR per day) and these downtime costs can dominate the overall cost-benefit assessment. In other words, decisions on the effectiveness of fire protection measures (notably passive fire protection) are generally governed by downtime considerations.

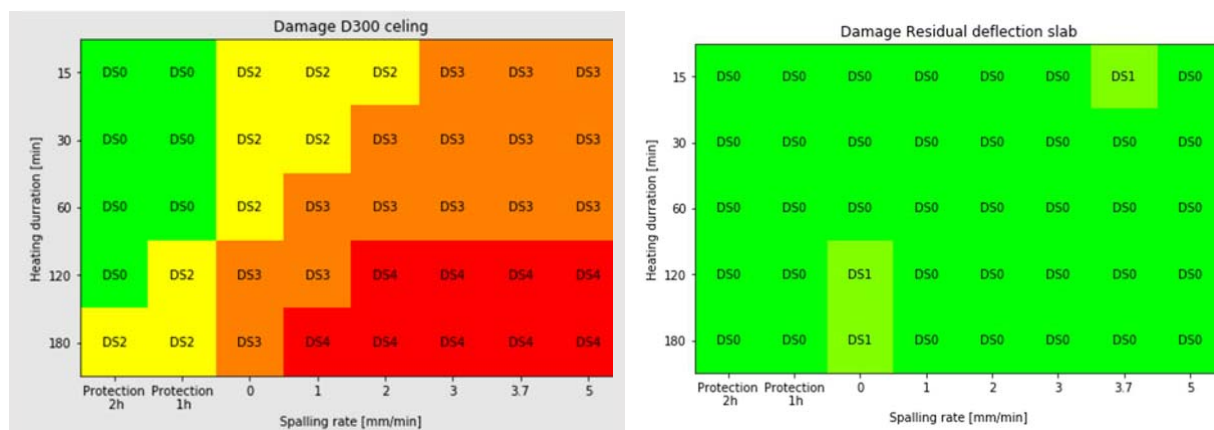


Figure 5: thermal damage state classification (left) and mechanical damage state for the ceiling (protected and unprotected) under RWS fire exposure in function of heating phase duration and nominal rate of concrete spalling.

## 5. SUMMARY AND CONCLUSION

The FIERCE framework provides a holistic approach to the risk assessment of tunnels under fire conditions. The different submodules making up the framework interact with another to ensure the dependencies between them are taken into account as accurately as possible. The ventilation, evacuation and additional submodules that may influence the HRR of the fire allow the assessment of the fire safety measures in terms of life safety. The structural module on the other hand allows insight into the structural fire performance, the possibility of structural failure, and the extent of the damages post-fire. This in turn allows for an assessment of the damage caused by the fire and the associated cost due to repairs and downtime of the tunnel. The results of an analysis via the framework allow for a trade-off to be made between the fire safety measures and their cost, thus allowing an optimal solution to be obtained in terms of costs versus benefits.

### Acknowledgement

This research project has been made possible via the support of Flanders Innovation & Entrepreneurship under grant number HBC.2019.2839.

## 6. REFERENCES

- [1] EC. 2004 “Minimum Safety Requirements for Tunnels in the Trans-European Road Network. Directive 2004/54/EC”. European Commission and the Council, Brussels.
- [2] Thamm, B. "The new Directive 2004/54/EC on road tunnel safety." Routes/Roads 324 (2004)
- [3] Brandt, R. “Upgrading the Karavanken Tunnel according to the EU-Directive 2004/54/EC.” (2010).
- [4] EC. 2015 “Study on the implementation and effects of Directive 2004/54/EC on minimum safety requirements for road tunnels in the trans-European road network”, European Commission and the Council, Brussels.
- [5] PIARC, 2008. “Risk Analysis for Road Tunnels. World Road Association”, Paris.
- [6] Ntzeremes, P., and K. Kirytopoulos. 2019 “Evaluating the role of risk assessment for road tunnel fire safety: A comparative review within the EU.” Journal of Traffic and Transportation Engineering (English Edition) (2019).
- [7] Ntzeremes, P., Kirytopoulos, K., 2018a. “A stochastic-based evacuation model for risk assessment in road tunnel fire accidents and the importance of educating users”. In: The 28th International European Safety and Reliability Conference (ESREL 2018), Trondheim
- [8] Ntzeremes, P., Kirytopoulos, K., 2018b. Applying a stochastic-based approach for developing a quantitative risk assessment method on the fire safety of underground road tunnels. Tunnelling and Underground Space Technology 81, 619e631
- [9] Mawhinney, J. R. 2013 "Fixed fire protection systems in tunnels: issues and directions." Fire technology 49.2: 477-508.
- [10] Mosen: <https://mosen.global/wp-content/uploads/2011/01/New-Tyne-Crossing-Fire-Suppression.pdf>
- [11] Lemaire, T., and Y. Kenyon. 2006 "Large scale fire tests in the second Benelux tunnel." Fire Technology 42.4: 329-350.

- [12] Beard, A., and R. Carvel, 2012 “Handbook of tunnel fire safety”. ICE publishing,.
- [13] Ingason, H., Y. Z. Li, and A. Lönnemark. Tunnel fire dynamics. Springer, 2014.
- [14] Caliendo, C., et al. 2012 “Numerical simulation of different HGV fire scenarios in curved bi-directional road tunnels and safety evaluation.” *Tunnelling and Underground Space Technology* 31: 33-50
- [15] Fridolf, K., D. Nilsson, and H. Frantzich. 2013 "Fire evacuation in underground transportation systems: a review of accidents and empirical research." *Fire technology* 49.2 : 451-475
- [16] Buckley, G., Bradborn, W., Edwards, J., Terry, P. and Wise, S.. 2000 The Fire Brigade Intervention Model. *Fire Safety Science* 6: 183-194
- [17] Kim, H. K., A. Lönnemark, and H. Ingason 2010. “Effective firefighting operations in road tunnels”
- [18] De Sanctis, G; Kohler, J.; Fontana, M., 2013 On the use of fire brigade statistics for structural fire safety engineering, Conference ‘Application of Structural Fire Design’
- [19] Bergqvist, A. 2004 “What can the fire brigade do about catastrophic tunnel fires?.” SP RAPPORT-STATENS PROVNINGSANSTALT: 161-176
- [20] Li, Y.Z. en H. Ingason, “Maximum ceiling temperature in a tunnel fire” SP Rep, 51(2.1), 2010.
- [21] Ingason, H., Gustavsson, S., & Dahlberg, M. (1994). Heat release rate measurements in tunnel fires. Brandforsk project 723-924 (SP Report 1994:08). Swedish National Testing and Research Institute, Boras, Sweden.
- [22] *fib.* (2021). *Performance-based design of concrete structures (committee draft 2021-06-24)*. The International Federation for Structural Concrete. Lausanne, Switzerland.
- [23] Hua, N., Tessari, A., & Khorasani, N. E. (2021). Characterizing damage to a concrete liner during a tunnel fire. *Tunnelling and Underground Space Technology*, 109, 103761.
- [24] Franssen, J. M., & Gernay, T. (2019). User’s manual for SAFIR 2019. A computer program for analysis of structures subjected to fire. Liege University and Johns Hopkins University.
- [25] Chaudhary, R.K., Jovanovic, B., Schepers, M., Deckers, X., Van Coile, R. (2022). Reinforced-concrete tunnel lining under RWS heating curve, followed by a cooling branch. *Proceedings of the fib Congress 2022*. 12-16/06, Oslo, Norway.
- [26] Ni, S., & Gernay, T. (2021). A framework for probabilistic fire loss estimation in concrete building structures. *Structural Safety*, 88, 102029.
- [27] RWS. (2010). Grote vrachtwagenbrand in tunnel A2 Leidsche Rijn. Document 4818-2010-0037. RWS Steunpunt Tunnelveiligheid, the Netherlands. Available at: [https://puc.overheid.nl/PUC/Handlers/DownloadDocument.ashx?identifier=PUC\\_146958\\_31&versionnummer=1](https://puc.overheid.nl/PUC/Handlers/DownloadDocument.ashx?identifier=PUC_146958_31&versionnummer=1)

## **INFLUENCE OF THE REDUNDANCY OF TUNNEL VENTILATION SYSTEMS ON THE AVAILABILITY OF ROAD TUNNELS**

<sup>1</sup>Leonhard Pölzer, <sup>2</sup>Maximilian Weithaler, <sup>3</sup>Reinhard Gertl, <sup>4</sup>Markus Gröblacher

<sup>1</sup>ILF Consulting Engineers Austria GmbH, AUT

<sup>2</sup>ILF Consulting Engineers Austria GmbH, AUT, <sup>3</sup>ILF Consulting Engineers Austria GmbH, AUT, <sup>4</sup>ASFINAG Bau Management GmbH, AUT

### **ABSTRACT**

Tunnel ventilation plays a significant role in road tunnel availability. Especially in single-tube, but also in twin-tube road tunnels with transverse ventilation, the failure of an exhaust fan often leads to complete tunnel closure – at least in Austria.

Comparison of international guidelines shows that different countries have different specifications regarding exhaust fan redundancy for transverse ventilation systems in tunnels. Almost all stipulate the need for redundancy in the design and operation of transverse ventilation systems. The Austrian guidelines and regulations are the only ones of those investigated not containing information on the requirement for a redundant ventilation system.

Increasing the availability of road tunnels through a redundant ventilation concept is always associated with increased investment costs. However, these are justified when considering the loss of revenue as a result of tunnel closure. Redundancy can be achieved through various approaches. On the one hand, redundancy can be achieved by setting up additional fans in parallel; on the other hand, a redundant ventilation system can be achieved by using structural solutions.

In future there will be an increasing need to ensure the availability of major road networks. It is therefore necessary to update the Austrian guidelines and regulations to make them state of the art.

*Keywords: Tunnel, Ventilation, Redundancy, Availability*

## 1. INTRODUCTION

Tunnel ventilation plays a significant role in road tunnel availability. Especially in single-tube, but also in twin-tube road tunnels with transverse ventilation, the failure of an exhaust fan often leads to complete tunnel closure. The Austrian Guidelines and Regulations for the Planning, Construction and Maintenance of Roads (RVS 09.02.31) do not stipulate that redundancy is a requisite for exhaust fans in transverse-ventilated tunnels.

Since complete tunnel closure is associated with massive financial losses and also has economic consequences, the position that other countries take with regard to the issue of failure safety has been examined. In addition, the different specifications for the dimensioning of transverse-ventilated tunnels in different countries are shown, as well as the requirements for exhaust fans.

As there are no specifications related to redundancy in RVS 09.02.31, the possibilities for counteracting failure of one of the exhaust fans are discussed, as exhaust fans are essential for tunnel operation. Due to the fact that setting up redundant systems involves additional costs that should not be underestimated, the costs incurred and the effect on the availability of the individual systems are also evaluated and compared.

## 2. REDUNDANCY: GUIDELINES, REGULATIONS AND POSSIBILITIES

### 2.1. Comparison of guidelines and regulations with regard to the requirement for a smoke extraction system

The specifications of the country-specific guidelines and regulations for road tunnel smoke extraction systems in Austria, Germany, Switzerland and the USA are outlined in the following. An overview of all of the specifications is given in Table 1: Overview of Design Criteria for Exhaust Fans.

#### ***RVS 09.02.31 (Guidelines and Regulations for the Planning, Construction and Maintenance of Roads – Austria)***

RVS 09.02.31 stipulates a heat release rate (HRR) of 5 MW for car traffic only and 30 MW for mixed car and heavy goods vehicle (HGV) traffic. When the share of HGVs is more than 15%, the HRR is to be increased depending on the result of the respective tunnel risk analysis. [1]

The exhaust fans must be designed in such a way that their functionality at a smoke gas temperature of 400°C is guaranteed for a period of minimum 120 min. [1] This corresponds to fire class F400 in accordance with the European standard (EN 12101-3). [2] RVS 09.02.31 does not stipulate that redundancy is a requisite for exhaust fans. [1]

#### ***EABT-80/100 (Recommendations for Equipping and Operating Road Tunnels with a Design Speed of 80 km/h or 100 km/h – Germany)***

The HRR stipulated in EABT-80/100 depends on the HGV kilometres travelled per day and tube. A HRR of 30 MW applies when up to 4,000 HGV-km are travelled per day and tube. If the number of HGV-km travelled per day and tube is between 4,000 and 6,000, the HRR must be increased to 50 MW. If the number of HGV-km travelled per day and tube exceeds 6,000, a HRR of 50 to 100 MW must be assumed for the design of the ventilation systems, depending on the result of the respective tunnel risk analysis. [3]

In the case of smoke extraction via an exhaust duct with a length greater than 50 m, the functionality of the exhaust fans, at a temperature of up to 250°C, must be guaranteed for 90 min. In the case of point extraction, or smoke extraction via a shorter exhaust duct, with a length less than 50 m, the functionality of the exhaust fans, at a temperature of up to 400°C, must also be guaranteed for 90 min. [3] As this information is not classified in EN 12101-3, fire class F400 must be used. [2]

The redundancy requirement for the exhaust fans in EABT-80/100 stipulates that it should be possible to extract at least 70% of the total design flow rate in the event that an exhaust fan fails. [3]

***ASTRA 13001 (Swiss Federal Roads Office – Switzerland)***

The HRR stipulated by the Swiss ASTRA is 30 MW, independent of the traffic load. [4]

In the case of smoke extraction via an exhaust duct with a length greater than 50 m, the functionality of the exhaust fans, at a temperature of up to 250°C, must be guaranteed for 120 min. In the case that the distance between the first exhaust damper and the exhaust fan is less than 50 m, the functionality of the exhaust fans, at a temperature of up to 400°C, must be guaranteed for 120 min. [4] To ensure this, fire class F400 must be used for the exhaust fans in accordance with EN 12101-3. [2]

Swiss ASTRA's redundancy requirement for the exhaust fans stipulates that it should be possible to extract at least 65% of the extraction flow rate from the tunnel traffic area in the event that an exhaust fan fails. This requirement applies to each tube individually, even if other structural measures, such as ventilation cross passages, are in place to increase the extraction flow rate. [4]

***NFPA 502 (National Fire Protection Association - USA)***

NFPA 502 stipulates a HRR of 15 to 300 MW. The HRR used for the design depends on the type of vehicles that are to be expected. In addition, in tunnels with life-saving safety systems, such as fixed fire-fighting systems, NFPA 502 allows for mitigation of the design fire scenario. [5]

The exhaust fans must be designed in such a way that operation, at a smoke gas temperature of up to 250°C, must be guaranteed for 60 min. [5] When considering EN 12101-3, this specification does not correspond to any fire class. For reasons of comparison, fire class F300 is used. [2]

The redundancy requirement in NFPA 502 stipulates 100% redundancy in the event that an exhaust fan fails. This means that the ventilation system must be designed in such a way that it is still possible to extract 100% of the flow rate in the event that an exhaust fan fails. [5]

Table 1: Overview of Design Criteria for Exhaust Fans

Guideline	Exhaust fan redundancy	Heat Release Rate (HRR)	Exhaust fan fire class
<i>RVS 09.02.31 [1] (Austria)</i>	not required	5 MW for car traffic only 30 MW for mixed car and HGV traffic >30 MW for >15% share of HGVs; risk analysis required	120 min at 400°C → Fire class F400
<i>EABT-80/100 [3] (Germany)</i>	70% of design flow rate if one exhaust fan fails	30 MW for up to 4,000 HGV-km/day and tube 50 MW for up to 4,000 HGV-km/day and tube 50–100 MW for > 6,000 HGV-km/day and tube; risk analysis required	90 min at 250°C 90 min at 400°C → Fire class F400
<i>ASTRA 13001 [4] (Switzerland)</i>	65% of design flow rate per tube if one exhaust fan fails	30 MW	120 min at 250°C 120 min at 400°C → Fire class F400
<i>NFPA 502 [5] (USA)</i>	100% of design flow rate if one exhaust fan fails	15–300 MW, depending on type of vehicles expected and installed fire protection measures	60 min at 250°C → Fire class F300

## 2.2. Possibilities for increasing availability and achieving redundancy

In a tunnel with transverse ventilation or point extraction, the exhaust fans in the ventilation buildings are the most important components. Due to their size and the requirements, these fans are in most cases individually manufactured. As a result, long waiting times must be expected, in most cases, for replacements in the event of damage.

There are several possible ways to achieve redundancy in tunnel ventilation systems. However, the goal remains the same: to increase the availability of road tunnels and subsequently maintain operation of important main traffic routes.

### Increasing availability by keeping replacement parts in stock:

The motor is the component of an exhaust fan which is most likely to be damaged. Therefore, procurement of a replacement motor is a possibility for reacting quickly in an emergency and for counteracting long tunnel closure. However, the necessary storage space must be available for this measure. If this is not the case, it is possible to store the replacement motor with the manufacturer for a storage fee. The respective manufacturer then also takes care of the necessary maintenance works, such as regularly moving the rotor. This solution is well suited to increasing availability in existing tunnels where the required storage space is not available, without the need for structural measures. Another possibility to increase availability is to keep a complete replacement fan in stock (n+1).

### Increasing availability by means of redundant systems:

#### *Fully redundant systems*

For every individual exhaust fan, there is an additional parallel fan that can completely (100%) replace the failed exhaust fan (= fully redundant system: 1+1) in case of an incident. If the fans are all in operation during normal operation (part-load operation), this is referred to as hot redundancy. If the parallel exhaust fans are not in operation during normal operation, this is called cold redundancy. Fully redundant systems are very cost-intensive, but also offer the highest standard in terms of failure safety.

Transverse-ventilated tunnels with ventilation systems designed according to NFPA 502 always have a fully redundant system.



### ***Partially redundant systems***

As some guidelines and regulations do not require 100% redundancy, the system can be designed in such a way that all components have to be operated in part-load operation during normal operation, in order to achieve the design flow rate and reduce costs. In the event that an exhaust fan fails, the remaining exhaust fans are operated in full load mode. In total, depending on the design, only 70% of the design flow rate is achieved. As all exhaust fans are needed to achieve the design flow rate, partially redundant systems always comprise a hot redundancy. In a partially redundant system, the costs can be slightly reduced in comparison to a fully redundant system, as the individual exhaust fans will be smaller, depending on the redundancy requirement. The availability is not affected, provided the applicable guidelines and regulations permit a partially redundant system. It is to be noted that, in some cases, parallel operation of fans may lead to significant fluctuations in electricity demand. This problem particularly occurs at fans with asymmetrical inflow.

Tunnels for which the EABT-80/100 or the ASTRA specifications were used for the dimensioning of the ventilation system have at least one partially redundant system.

### ***Structural redundancy:***

In twin-tube tunnel systems, the exhaust air ducts of both tubes can be connected via ventilation cross passages. In the event that an exhaust fan fails, both of the exhaust fans in the second tube can replace the exhaust fan that has failed. However, this type of redundancy is not permitted by all guidelines and regulations.

Example: Karawanken tunnel, see Chapter 2.3

## **2.3. The Karawanken tunnel as a project-specific example of structural redundancy**

The approx. 8 km long Karawanken road tunnel connects the A11 Karawanken motorway and the A2 motorway (which forms part of the Slovenian road network). Since March 2015, the first tube of the Karawanken tunnel has been operated as a bidirectional road tunnel with a ventilation system rehabilitated in accordance with the requirements of RVS 09.02.31. After completion of the second tube, the twin-tube tunnel will be operated as a unidirectional tunnel system with 2 lanes for each direction of traffic. The ventilation system is planned as a semi-transverse ventilation system that has jet fans in the lay-bys, as illustrated in Figure 1.

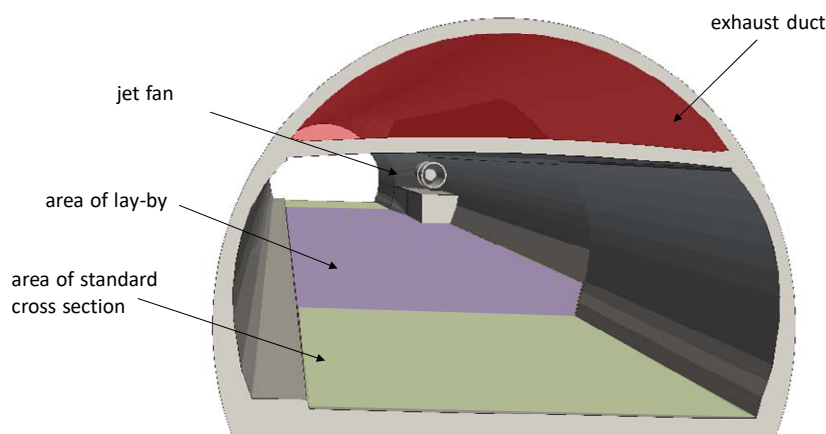


Figure 1: Lay-by niche [6]

A concept for a redundant tunnel ventilation system has been developed by ILF Consulting Engineers Austria GmbH in collaboration with ASFINAG for the construction of the second tube of the Karawanken tunnel. Although it is not stipulated in RVS 09.02.31 that redundancy is a requisite for exhaust fans, the interconnection of the ventilation systems in both tunnel tubes, via four ventilation

cross passages, as shown in Figure 2, increases the tunnel’s availability. The great advantage of this combined ventilation system is that if an exhaust fan fails, it can be replaced by one or both fans in the neighbouring tube. For this, only the dampers at the end of the cross passages have to be opened, see Figure 3.

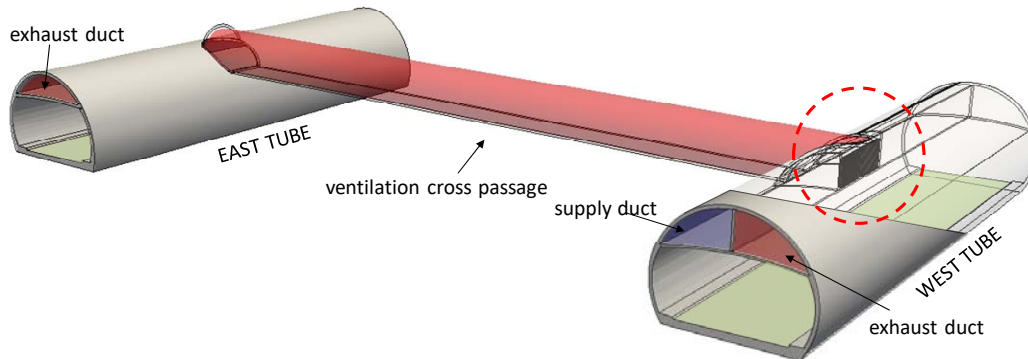


Figure 2: Ventilation cross passage [6]

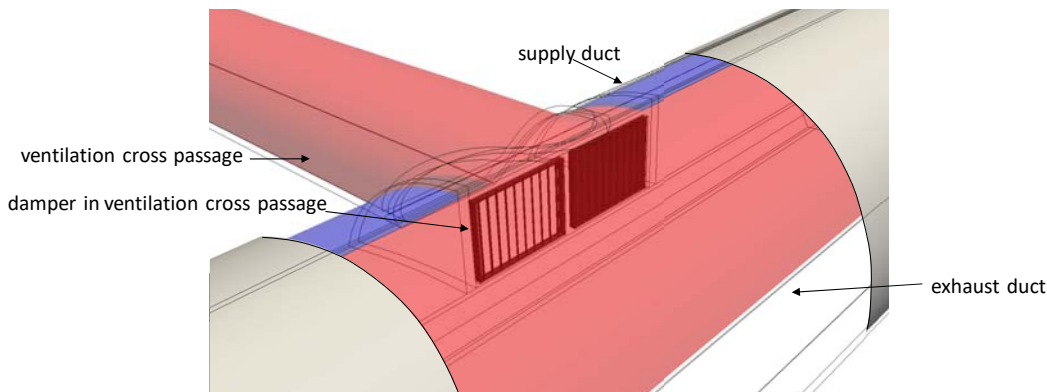


Figure 3: Detail: Connection of the ventilation cross passage [6]

This ventilation system ensures the availability and thus the continued operation of the tunnel in case of an incident or planned maintenance works. This makes it possible to achieve redundancy through a structural solution – in this case ventilation cross passages – without needing to change the number or size of exhaust fans. Consequently, there are no extra costs for additional ventilation equipment. As the ventilation cross passages are constructed as part of the construction of the second tube, the investment costs are kept within reasonable limits.

***Estimated loss of revenue as a result of tunnel closure***

To illustrate the costs arising in the event of tunnel closure, the loss of toll revenue has been calculated and is shown in Table 2. The cost estimate is based on the annual average daily traffic (ADT) volume (the ADT volume used for the dimensioning of the tunnel system) as well as the current toll costs of EUR 7.60.

Table 2: Loss of toll revenue as a result of tunnel closure

<b>Toll costs</b>	<b>Loss of toll revenue</b>
per hour	~ EUR 4,000
per day	~ EUR 100,000
per week	~ EUR 700,000
per month	~ EUR 3,000,000
per year	~ EUR 36,000,000 €

The economic consequences for other companies – due to delivery delays resulting from detours and traffic jams, additional costs as a consequence of longer delivery routes, etc. – have not yet been taken into account.

## 2.4. Comparison of different systems for achieving redundancy

For a better understanding of the different types of systems available for achieving redundancy, an evaluation matrix showing different alternatives is included below. A comparison of the additional costs and the increase in availability is made. The reference case is the case without redundancy, as it is described in the current version of RVS 09.02.31, where:

0 ... the same, + ... better, ++ ... much better, - ... worse, -- ... much worse.

Table 3: Comparison of different solutions

Redundancy system	Availability	Costs
No redundancy	0	0
Fully redundant systems	++	--
Partially redundant systems	++	-
Keeping replacement parts in stock	+	-
Structural redundancy	++	--

## 3. SUMMARY AND CONCLUSION

The comparison of guidelines and regulations showed that the respective design specifications for the HRR in each of the respective countries differ greatly from each other. In almost all of the countries considered, the HRR used for the design depends on the expected transport mix. The exception is Switzerland, where a recommended value is specified. When allocating the fire classes given in EN 12101-3 to the requirements prescribed for the exhaust fans, it can be seen that there is consensus on this topic among European countries. Internationally, the requirements are somewhat less stringent. In all of the guidelines and regulations examined, with the exception of the Austrian RVS 09.02.31, redundancy for exhaust fans is required to varying degrees. It is mostly specified as a percentage availability and refers to exhaust fan failure. If permitted by the applicable guidelines and regulations, redundancy can be achieved through a structural solution without the need for keeping additional equipment in stock. In twin-tube tunnels, for example, redundancy can be achieved by connecting the ventilation systems of the two tubes by means of ventilation cross passages.

Increasing the availability through a redundant ventilation concept is always associated with increased investment costs. For redundant or partially redundant systems, the investment costs for the ventilation equipment increase noticeably. If the resulting additional costs are compared with those which are incurred in the event of complete tunnel closure, the investment already pays off within a few weeks. This is why the option of implementing a redundant system should be considered for greenfield tunnel projects in Austria, especially for important main traffic routes.

In order to effectively counteract the high loss of revenue and the economic consequences associated with tunnel closure due to defective ventilation equipment, the safety-relevant systems required for tunnel operation have to be constructed as redundant systems. Thus, the growing need for major road networks to have a higher availability can be met.

Evaluation of the country-specific guidelines and regulations showed that the Austrian RVS 09.02.31 constitute an exception, when compared internationally, as regards the non-existent requirement of redundancy. In order to keep pace with the state of the art, at least in Europe, it is necessary to revise and update the content of RVS 09.02.31.

#### 4. REFERENCES

- [1] Richtlinien und Vorschriften für das Straßenwesen: Tunnel, Tunnelausrüstung, Belüftung (RVS 09-02-31), Arbeitsgruppe „Tunnelbau“ und Arbeitsausschuss „Betriebs- und Sicherheitseinrichtungen“, 2014
- [2] Grundlagen der maschinellen Entrauchungsanlagen nach EN 12101 und DIN 18232, Fachjournal: Fachzeitschrift für Erneuerbare Energien & Technische Gebäudeausrüstung, Dipl.-Ing. Herbert Schmitt, 2010
- [3] Empfehlungen für die Ausstattung und den Betrieb von Straßentunneln mit einer Planungsgeschwindigkeit von 80 km/h oder 100 km/h (EABT-80/100), Forschungsgesellschaft für Straßen- und Verkehrswesen (FGSV): Arbeitsgruppe Verkehrsmanagement, Ausgabe 2019
- [4] Lüftung der Strassentunnel: Systemwahl, Dimensionierung und Ausstattung (ASTRA 13001), Bundesamt für Strassen ASTRA, Ausgabe 2021 V3.00
- [5] Standard for Road Tunnels, Bridges and Other Limited Access Highways (NFPA 502), Edition 2020
- [6] ASFiNAG Planungsunterlagen

# VALIDATION OF A MODEL ROAD TUNNEL USING FIRE EXPERIMENTS DATA

<sup>1</sup>Klein, Andreas, <sup>2</sup>Jessen, Wilhelm, <sup>3</sup>Sistenich, Christof

<sup>1</sup> ISAC GmbH, Aachen, Germany

<sup>2</sup> Institute of Aerodynamics, RWTH Aachen University, Germany

<sup>3</sup> Federal Highway Research Institute (BASt), Bergisch Gladbach, Germany

## ABSTRACT

This paper describes the validation of a model tunnel designed for investigations on the design and operation of ventilation systems in road tunnels. The model tunnel in a scale of 1:18 allows flow visualisation and velocity measurements via particle image velocimetry technique (PIV). For isothermal investigations on fire scenarios, a buoyant helium-air-mixture is injected into the tunnel. Analogue scaling based on the preservation of the Froude number is used to correlate the results to real scale.

Two experiments with mechanical longitudinal ventilation from the “Memorial Tunnel” test program were considered suitable for validation. The investigations were carried out in parallel experimentally with the model tunnel and numerically with the Fire Dynamics Simulator (FDS). The validation comprised a qualitative comparison of the smoke propagation and a quantitative comparison of vertical flow profiles in the tunnel axis to the original data.

Overall, a good agreement with the original data was found in the evaluation of the results, so that a successful validation was assumed. The results show that it is possible to obtain similar flow characteristics applying analogue scaling in fire scenarios including the operation of model jet fans.

*Keywords: model tunnel, mechanical ventilation, validation, analogue scaling.*

## 1. INTRODUCTION

The design and operation of ventilation systems for road tunnels has been the object of experimental studies since the 1960s when the number and length of tunnels started to increase considerably in industrialised countries. Usually, these kind of studies are conducted in a model scale and exploit the possibility to establish a geometric similarity of the tunnel and a kinematic similarity of the flow between model and real scale. Since real scale experiments especially on the ventilation in emergencies are costly and limited in scope, experiments in model scale have proven to be useful, even though there are limitations due to the partial nature of the physical similarity that can be achieved. For example, current guidelines on the estimation of the critical velocity are mainly based upon experiments in model scale whose results were combined with theoretical considerations afterwards [1; 2; 3].

In addition to the concept of similarity, the results from model scale should be subject to a validation with data from real scale in order to demonstrate that the model can give meaningful insight if it is applied in a reasonable way.

## 2. MODEL TUNNEL

The model tunnel in question was designed in a preceding research project in a scale of 1:18 [4; 5]. Numerous modular segments were constructed that allow to model two-lane tunnels with typical rectangular or arched profiles and variable slopes. In order to model mechanical

ventilation systems, working jet fans in different sizes and with adjustable jet velocities were constructed. The effect of moving vehicles on the tunnel flow can be included based on a modified slot-car system. Since gravitational effects dominate the tunnel flow in emergency situations, fire plumes are modeled isothermally based on the preservation of the Froude number (section 4.2).

Multiple series of experiments addressed e. g. the blockage effect of vehicles, the positioning of jet fans and the influence of the tunnel slope during normal and emergency situations with longitudinal mechanical ventilation. In the end, the tunnel and the preliminary results were seen as a “proof of concept” for subsequent investigations.

A distinguishing feature of the model tunnel is the ability to measure instantaneous and mean flow fields by particle-image velocimetry (PIV). PIV is a laser-optical, non-intrusive measurement technique whose principle is based on the illumination and tracking of seeding particles that are added to the flow. This enables to obtain velocity distributions in the measurement plane. The model tunnel is built of transparent plastic to guarantee the optical accessibility to conduct 2C (two component)-PIV measurements. The principle of this technique is sketched in (Figure 1).

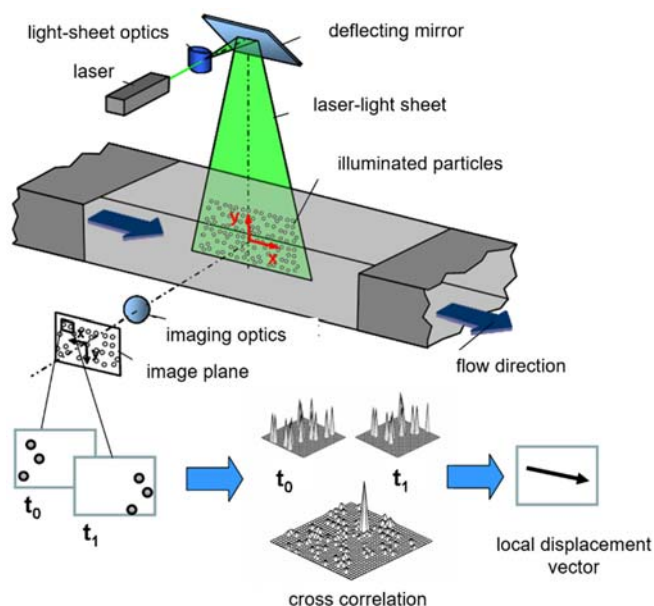


Figure 1: Principle of a 2C-PIV measurement and the subsequent data processing

### 3. FIRE EXPERIMENTS DATA (MEMORIAL TUNNEL)

In order to gain or derive suitable data for validation, literature on real-scale fire tests and commissioning tests in tunnels was reviewed. As expected, the number of real-scale tests that document the effect of ventilation was quite limited. Most of the tests in research projects were performed in structures that are noticeably different from typical road tunnels. In addition, they are lacking thorough data on the operation of the ventilation system and its effect on the flow field; the latter is true for commissioning tests as well.

As a result, the well-known tests on fire ventilation in the “Memorial Tunnel” [6] were chosen as the single source for validation data. These tests, conducted 1993-1995 in a disused two-lane road tunnel of 853 m length, can be considered the most extensive source on the problem at hand to this day. Out of the 98 tests in total, 15 tests were performed with longitudinal mechanical ventilation that differed mainly in fire size and jet fan activation pattern. Out of

these, tests no. 606A and 608 were chosen and modelled both experimentally and numerically. This paper addresses the results for test 608.

The available data for modelling and subsequent comparison comprised the heat release rate, jet fan activation patterns, observed smoke propagation and verbal descriptions in test protocols as well as flow profiles in the tunnel axis and estimations on the volume flow at several positions distributed over the length of the tunnel.

## **4. EXPERIMENTAL RESULTS**

### **4.1. Adaptations in order to model the Memorial Tunnel**

The testing facility offered a free length of approximately 45 m. Considering some clearance that was necessary beyond the portals, this allowed for the assembly of the model tunnel with a length of 40 m, equivalent to 720 m with respect to the model scale. This restriction required the reduction of the real scale tunnel length that could be represented by 133 m (-15 %). Therefore, the section downstream of the jet fans between the fire site and the south portal was shortened. The slope of 3.2 % was considered by adjusting the supporting frames beneath the model tunnel. Its shell was built out of transparent polycarbonate geometrically similar to the original horseshoe profile.

The Memorial Tunnel originally featured a full transverse ventilation system with fan rooms at both portals that situated the axial fans above the traffic space. The geometry of these fan rooms reduced the tunnel cross-section from a horseshoe profile to a rectangular profile and was reproduced in the model tunnel.

The available data also shows the tunnel flow in uphill direction prior to the test due to meteorological effects (wind) and possibly natural convection; in order to include these effects a set of computer case fans was assembled and placed in front of the higher north portal that was able to generate the corresponding pressure difference.

Over the course of test 608, 7 out of the 15 installed jet fans were operated. The power supply of the model tunnel was limited to provide for jet fans or fan groups at three different longitudinal positions. Therefore, only the first half of this test could be simulated (2 minutes of natural convection after fuel pan engulfment followed by 12 minutes of forced convection; Figure 2). The three jet fans that were operated in different groups during this period were placed in the tunnel axis similar to the original test.

### **4.2. Analogue Scaling (Froude Scaling)**

For isothermal investigations on fire scenarios, a buoyant helium-air-mixture was injected into the model tunnel (Figure 3). Analogue scaling based on the preservation of the Froude number was used to correlate the results to real scale [5; 7].

Test 608 was prepared with fuel pans that were expected to produce a nominal heat release rate of approximately 20 MW. According to the test data, the actual heat release rate reached 3.5 MW during natural convection and ranged from 7 to 19 MW during forced convection ( $t_{\text{end}} = 14 \text{ min} = 840 \text{ s}$ ).

Adequate flow rates and compositions of the helium-air-mixture with an equivalent buoyancy were derived according to the following steps:

1. Simplification of the heat release rate by identifying key values that represent the development over the course of the test (Figure 2).

- Derivation of suitable smoke flow rates and temperatures for these key values by applying the model by Mégret/Vauquelin [8]. Assuming ideal gas conditions, flow densities could be deduced from the general gas equation.
- Application of analogue scaling for the smoke flow rates. With respect to the model scale, the underlying relations equate to:

$$Fr = \frac{v_R}{\sqrt{g \cdot L_R}} = \frac{v_M}{\sqrt{g \cdot L_M}} \Rightarrow v_R = v_M \cdot \left[ \frac{L_R}{L_M} \right]^{\frac{1}{2}} \quad \wedge \quad \dot{V}_R = \dot{V}_M \cdot \left[ \frac{L_R}{L_M} \right]^{\frac{5}{2}}$$

The analogue scaling was applied to the jet fans as well, i. e. the original jet velocity of 34.2 m/s was scaled to 8.1 m/s.

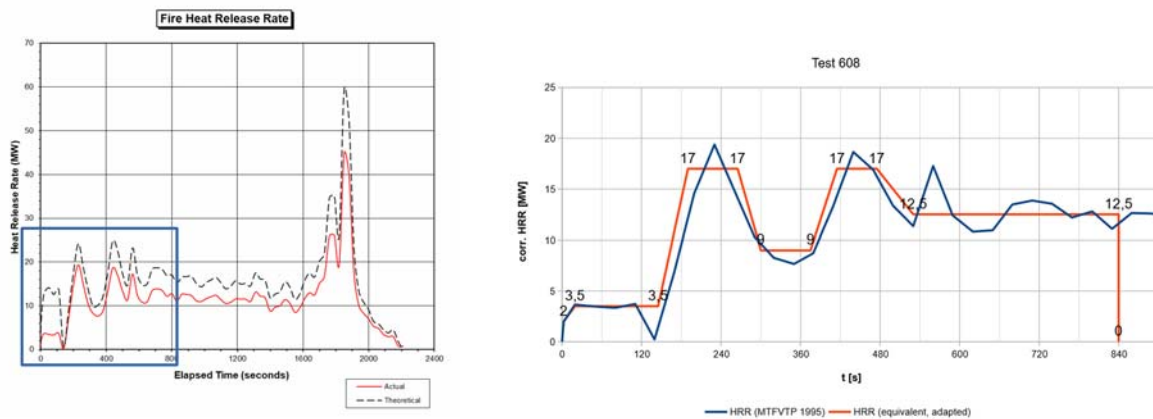


Figure 2: Measured heat release rate (left; [2]) and simplified heat release rate used to model the composition and flow rate of the helium-air-mixture (right)

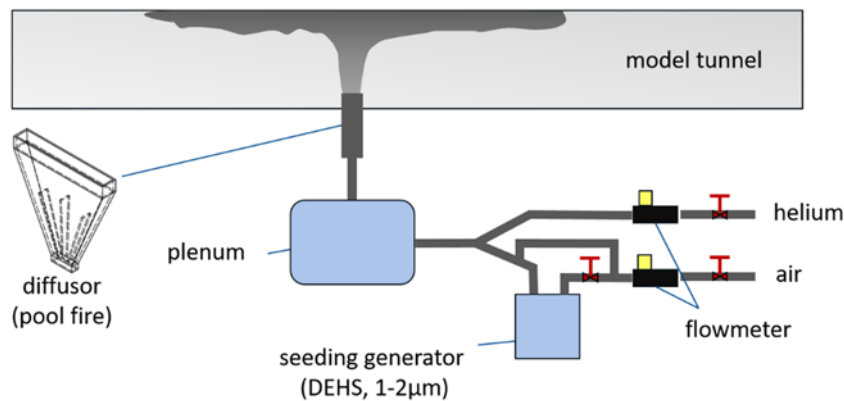


Figure 3: Seeding and injection of the helium-air-mixture into the tunnel

#### 4.3. Comparison of flow profiles

The 2C-PIV measurements were performed in the tunnel axis at three different positions that correspond to the original tests (named Loop 207-209 in [6]). These positions were located 1,90-2,61 m downstream of the operated jet fans (equivalent to 34-47 m in real scale). Over the course of the test, the motion of the tracer particles was recorded with a sample frequency of 2 Hz. The processed profiles extracted from the velocity distributions show the development of the flow (Figure 4). The diagrams therein include the standard deviation so that fluctuations due to the inherent turbulent nature and more prominently due to the flow reversal after jet fan activation become apparent.



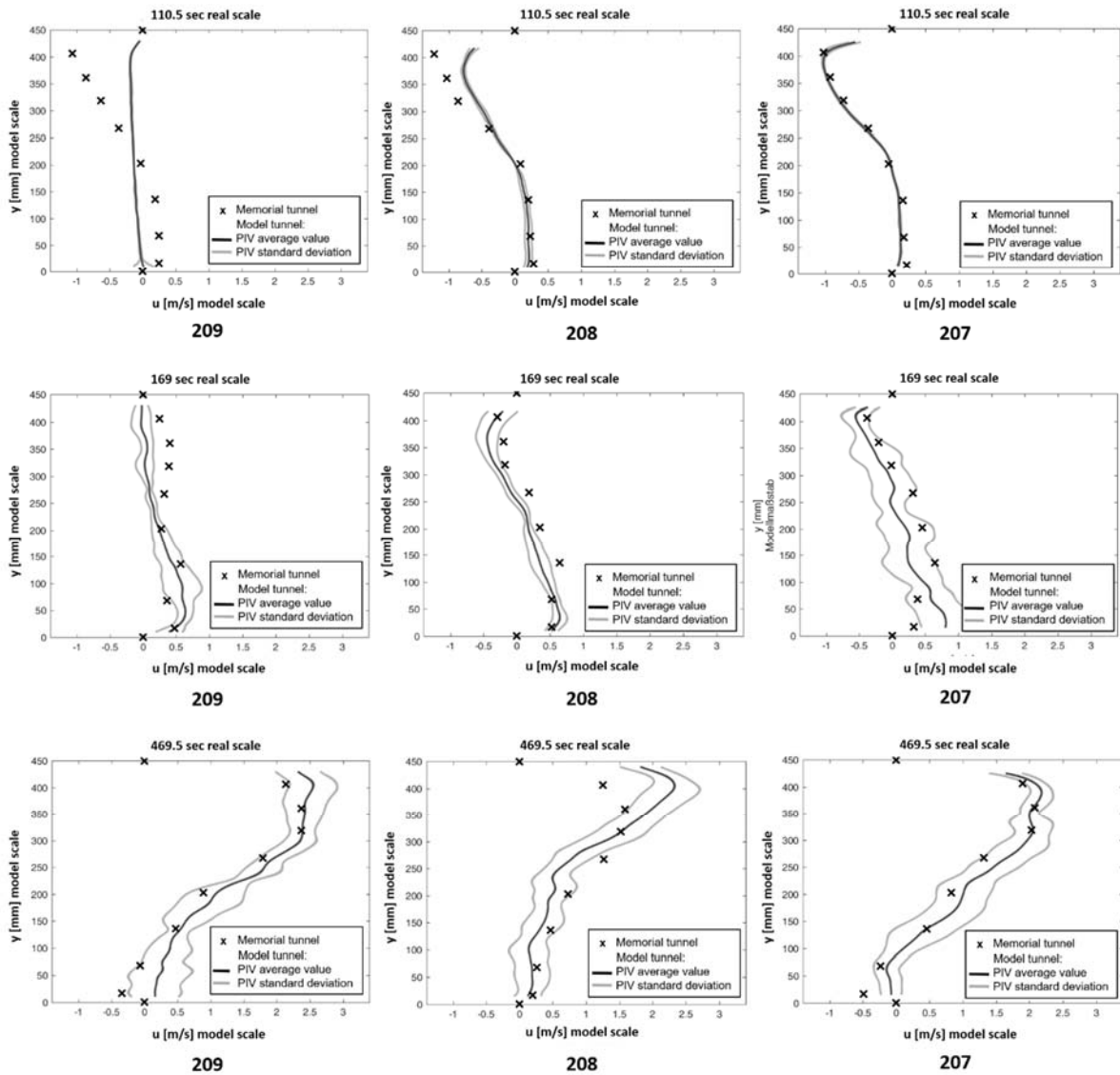


Figure 4: Flow profiles in the tunnel axis at 110.5 s, 169 s and 469.5 s compared to the original data at loops 209, 208 and 207 (original flow velocities scaled to model scale). Model tunnel values were averaged over 3.5 s, equivalent to 15 s in real scale. Reading direction of diagrams correspond to flow direction during forced convection (downhill towards south portal).

At 111 s during natural convection, there is very good agreement at loop 207 closest to the fire site, but progressively weaker agreements at the loops uphill. According to the test report, the smoke front moved over a distance of almost 300 m within 60 s (from  $t = 60$  s to  $t = 120$  s), equivalent to a very fast propagation velocity of approximately 4.5 m/s. However, this is possibly an overestimation since there is an offset of 53 s between the fuel pan engulfment as referential point in time in the original data and the preceding ignition of the fuel pan when smoke started being produced. The implications of this offset are difficult to account for whether it be in experiments or simulations.

At 169 s, 49 s after the activation of three jet fans, flow reversal is imminent. With respect to the transient nature of this process, there is convincing agreement between original and experimental data at all loops.

At 469 s, there is a good agreement as well with the exception of loop 208 where the original velocities are lower in the upper half. There are two possible reasons for this discrepancy: first, assumptions had to be made regarding the longitudinal jet fan positions because they are not clearly stated in the report. Second, the report mentions the positioning of test equipment

upstream of the fire site that partially obstructed the flow. Because they are not disclosed in detail, they could not be modelled [cf. 9].

## 5. NUMERICAL RESULTS

In order to bridge between the original and the experimental results, the tests were modelled numerically with the Fire Dynamics Simulator (FDS V6.5.2) both in real scale and model scale. Boundary and initial conditions were modelled as closely as possible to the original test and the experiments, respectively (e. g., wall roughness, fan thrust, initial flow prior to the test). The only exception from that was the length of the real scale model which was reduced to 720 m corresponding to the restricted length of the model tunnel (section 4.1). In real scale, a gas burner was specified with the heat release rate depicted in Figure 2. In model scale, the injection of the helium-air-mixture was identical to the experiments.

An evaluation of the flow velocities showed that the numerical velocities are rising faster than in the original tests (Figure 5). However, the actual discrepancy is hard to determine since the temporal resolution in the original data is quite low (1/60 Hz) with an undisclosed averaging interval. Another contributing factor to this effect might be that the original jet fans require longer start-up times. In addition, the numerical velocities are approximately 10 % higher in quasi-stationary conditions both in real scale and model scale. This difference is probably mostly due to additional flow losses in the original test related to the test equipment upstream of the fire site that could not be modelled.

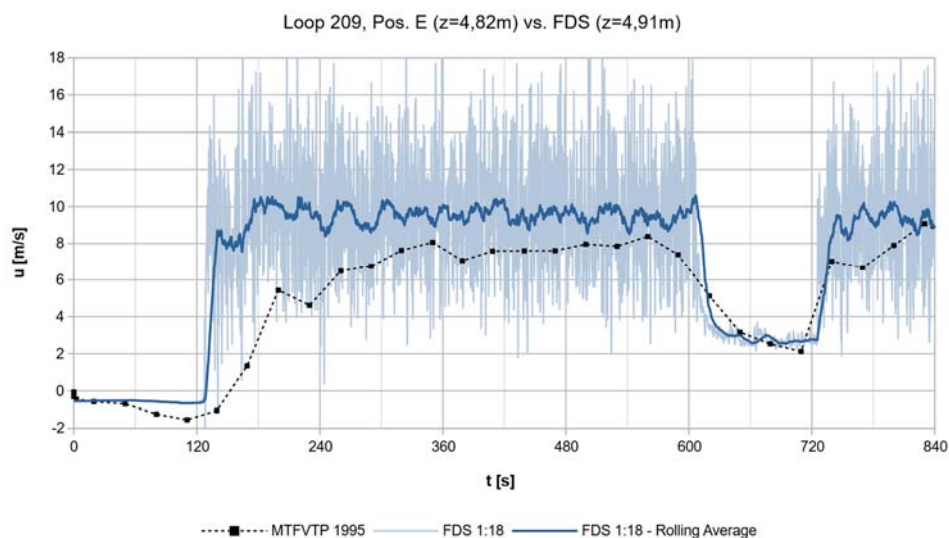


Figure 5: Comparison of the velocity development at loop 209, Pos. E ( $z = 4,82 \text{ m}$ ) - original data vs. scaled numerical data

The flow profiles generally show the same trends as in the experiments (Figure 6). An additional characteristic is that the numerical peak flow velocities tend to be 20-25 % higher. This can be attributed to the grid resolution which was derived with the goal to resolve the buoyant plume appropriately (cartesian grid with  $\delta x = 280 \text{ mm}$  in real scale and  $15.6 \text{ mm}$  in model scale;  $D^*/\delta x \approx 9.4$  for  $\dot{Q} = 12.5 \text{ MW}$ ). While all loops are located at the beginning of the self-similar zone of the jet, the momentum is mostly transferred within the mixing zone that is closer to the jet fan. In order to realistically resolve the entrainment in this zone that causes the jet to decay quickly, a smaller grid size would have been necessary [9]. As a result, the momentum transfer is stretched over a longer distance.

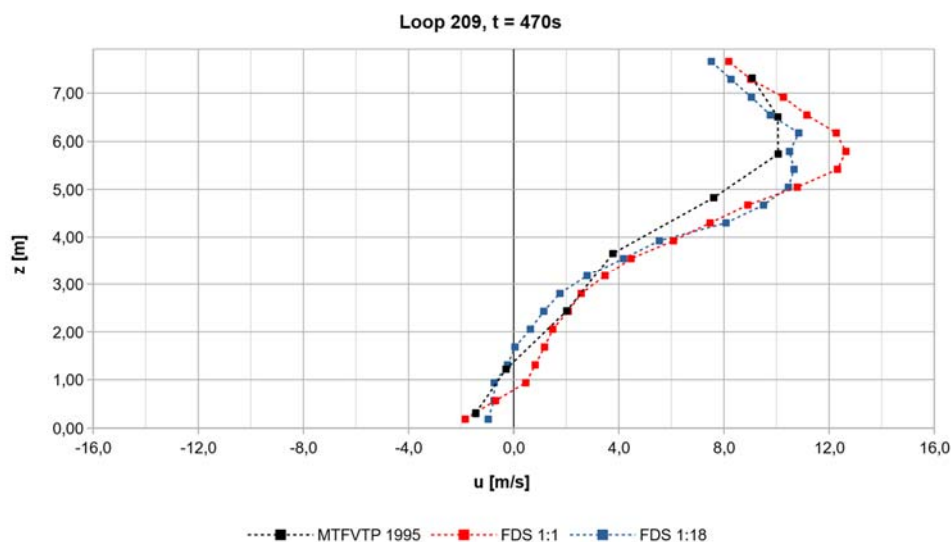


Figure 6: Comparison of the flow profile at loop 209 at 470 s - original data vs. numerical data in both real scale and model scale

## 6. CONCLUSION

Overall, a good agreement with the original data was found in the evaluation of the results, so that a successful validation was assumed. This is true for the other points in time that are not shown in this paper as well. The results show that it is possible to obtain similar flow characteristics applying analogue scaling in fire scenarios including the operation of model jet fans.

Residual discrepancies to the original data were mostly small or moderate and could be attributed partially to the limitations of scaled model tests in general as well as to additional adaptations that were necessary for these particular tests (section 4.1). Equally important, the incomplete documentation of the original experiments and the available scope of data limited both the experimental and the numerical model. The spatial and temporal resolution of the original data is too low in order to be able to compare transient processes in detail. In addition, some ambiguities and discrepancies were found in the original data. These results also correspond to the preliminary findings of Ingason/Li who were able to consider details not disclosed in the original report; they concluded that there is a level of uncertainty in the data that still needs to be fully analysed [10].

## 7. REFERENCES

- [1] Bakke/Leach: Turbulent Diffusion of a Buoyant Layer at a Wall. Applied Scientific Research, Section A, Vol. 15 (1), pp. 97-136, 1966
- [2] Lee/Chaiken/Singer: Interaction Between Duct Fires and Ventilation Flow: An Experimental Study. Combustion Science and Technology, Vol. 20, pp. 59-72, 1979
- [3] Danziger/Kennedy: Longitudinal ventilation analysis for the Glenwood Canyon Tunnels. Proceedings on the 4th International Symposium on the Aerodynamics and Ventilation of Vehicle Tunnels, York/UK, 1982
- [4] Oeser/Steinauer/Klein/Jessen/Schröder: Untersuchungen zur Optimierung von Längslüftungssystemen für Straßentunnel auf der Basis der Entwicklung eines

Modelltunnels. FE 15.0539/2011/ERB im Auftrag des Bundesministeriums für Verkehr und digitale Infrastruktur, vertreten durch die Bundesanstalt für Straßenwesen (BASt), Bergisch Gladbach, 2016

- [5] Klein/Jessen/Oeser/Schröder/Sistenich: Investigations on smoke propagation with longitudinal ventilation by means of a model tunnel. 8th International Conference ‘Tunnel Safety and Ventilation’, Graz 2016
- [6] Bechtel/Parsons Brinkerhoff: Memorial Tunnel Fire Ventilation Test Program - Comprehensive Test Report. Massachusetts Highway Department, Boston/USA, 1995
- [7] Vauquelin: Experimental simulations of fire-induced smoke control in tunnels using an “air-helium reduced scale model”: Principle, limitations, results and future. Tunnelling and Underground Space Technology, Vol. 23 (2), pp. 171-178, 2008
- [8] Mégret/Vauquelin: A model to evaluate tunnel fire characteristics. Fire Safety Journal, Vol. 34 (4), pp. 393-401, 2000
- [9] Klein/Jessen: Untersuchungen zur Lüftung von Straßentunneln anhand eines generischen Modells. FE 15.0643/2017/ERB im Auftrag des Bundesministeriums für Verkehr und digitale Infrastruktur, vertreten durch die Bundesanstalt für Straßenwesen (BASt), Bergisch Gladbach, 2022
- [10] Ingason/Li: Understanding of critical velocity in Memorial Tunnel Fire Tests using longitudinal ventilation. Virtual Conference ‘Tunnel Safety and Ventilation’ 2020

# EGRESS-DOORS IN ÖBB RAILWAY TUNNELS – BASICS, DECISIONS, RECOMMENDATIONS

<sup>1</sup>Helmut Steiner, <sup>2</sup>Michael Bacher

<sup>1</sup>ÖBB Infrastructure plc, A; <sup>2</sup>Graz University of Technology, A

## ABSTRACT

Increasing demands on a modern public transport infrastructure result in ever more extensive and complex projects including long tunnels. This usually also entails increased expenditure on rail technology equipment (including control and instrumentation systems and sensors). The aim of the overall rail tunnel system must be to ensure that railway operations must be safe, punctual and, as far as possible, uninterrupted. Aspects of maintenance, servicing and renewal must never be forgotten in this context.

Emergency exit doors represent an important element in a rail tunnel, especially in the event of an incident for people fleeing and seeking for safe areas. It is of great importance and in many aspects a great challenge to define reasonable requirements for egress doors with regard to statics, serviceability, fire protection, operability, among others. Such requirements are finally often associated with compromises.

*Keywords: Egress-door, tunnel-door, emergency exit door, swinging door, double-action swinging door, sliding door, railway tunnel, tunnel safety*

## 1. INTRODUCTION

Modern transport infrastructure is playing an increasingly important role in the area of conflict between constantly increasing mobility needs, the associated traffic volume and the fight against the global climate crisis. This requires efficient, fast and convenient connections between urban areas, coupled with high frequency. Only rail-based systems can provide these options to the required extent (e.g. transport capacity) and in accordance with today's general conditions and targets (e.g. reduction of CO<sub>2</sub> emissions).

The existing topography in Central Europe (e.g. the Alpine arc), settlement structures, environmental considerations, require underground and tunnel systems to an ever increasing extent. In this context, safe operation and, in case of incidents, safe escape of the passengers are of eminent importance. Escape routes must be adapted to the tunnel system (e.g. single- or double-tube or double-track line) and the external boundary conditions (e.g. topography and geology) and can therefore vary considerably. In tunnels, emergency exit doors are an essential component to ensure a safe fire protection separation of the different areas such as tunnel, cross passage, emergency exit, etc. The long tunnel projects currently under construction in the ÖBB network, such as the Semmering Base Tunnel (SBT) and the Koralmtunnel (KAT), as well as the transnational Brenner Base Tunnel (BBT), require a large number of such doors.

In Austria, in a double-tube tunnel system, cross passages are built in general at intervals of around 500 m, connecting the two tubes. These not only provide the escape route, but also serve technical rooms with various technical equipment like electrical power supply, telecommunications, etc. In order to protect these areas from high pressure fluctuations and dust loads due to the train service, the aspect of leakage must also be taken into account.

## 2. BOUNDARY CONDITIONS / REQUIREMENTS

Doors let people in, but they also lock them out. They create safety, security, protection against weather, wild animals, uninvited guests and much more. Doors have been around since people began building shelters of all kinds, for different reasons and with different materials. Especially in railroad tunnels of high-performance tracks, the requirements for emergency exit doors are multi-layered and diverse in nature. These doors can therefore in no way be described as "off-the-shelf product", but are "special units" of great complexity and high quality.

Requirements for emergency exit doors arise on the one hand from static and dynamic aspects, mainly resulting from the pressure effects of fast-moving trains. On the other hand, since they also serve as partitions for fire compartments, corresponding fire resistance classes must be specified. In order to meet these two requirements, very stable, solid and therefore heavy constructions are required. In the interest of easy escape, however, low opening forces are defined by standards and regulations. The high door weight in combination with easy usability almost automatically results in a motor-assisted or motor-driven door, which on the other hand must be equipped with additional safety elements to avoid escaping passengers being crushed or pinched.

In total, this results in a very complex, high-tech component that should be available with a high degree of reliability and availability in conjunction with the lowest possible expenses for maintenance [1, 2].

## 3. ASPECTS - DECISIONS

Table 1 provides an overview of possible aspects that influence the project-related decision when selecting an emergency exit door. The order in which the topics and keywords are listed does not represent a ranking or evaluation, nor does it claim to be complete.

Table 1: Aspects of emergency exit doors

<b>General</b>	<ul style="list-style-type: none"> <li>• RAMS – Reliability, Availability, Maintainability, Safety</li> <li>• Life Cycle Costs (LCC)</li> <li>• Live Cycle Management (LCM)</li> <li>• Quality - e.g. steel grade, coating thicknesses</li> <li>• Pressure-, smoke-, dust-proof</li> </ul>
<b>Type</b>	<ul style="list-style-type: none"> <li>• Swinging door</li> <li>• Double-action swinging door</li> <li>• Sliding door - articulated sliding door, sectional sliding door</li> <li>• Special door – e.g. pressure-neutral door, telescopic sliding door</li> </ul>
<b>Structural analysis</b>	<ul style="list-style-type: none"> <li>• Boundary conditions - e.g. tunnel cross-section, train speed, railway system, train split</li> <li>• Design – structural- and fatigue safety</li> <li>• Durability</li> </ul>
<b>Fire</b>	<ul style="list-style-type: none"> <li>• Functional integrity</li> <li>• Fire resistance class</li> <li>• Heating curve - e.g. unit temperature-time curve</li> </ul>
<b>Geometry</b>	<ul style="list-style-type: none"> <li>• Shell geometry, shell clearance</li> <li>• Clearance and height</li> <li>• Assembly conditions</li> <li>• Space requirements for open door</li> </ul>
<b>Operation</b>	<ul style="list-style-type: none"> <li>• Operating and opening elements</li> </ul>

	<ul style="list-style-type: none"> <li>• Operating and opening forces</li> <li>• Labelling, symbols, lighting, colour</li> <li>• Safety devices</li> </ul>
<b>SCADA / sensors</b>	<ul style="list-style-type: none"> <li>• Remote control</li> <li>• Status indication</li> </ul>
<b>Tender process</b>	<ul style="list-style-type: none"> <li>• Type of tender process</li> <li>• Prequalification (suitability, selection criteria)</li> <li>• Best bidder and quality criteria</li> <li>• Validation of required criteria</li> </ul>

### 3.1. Type of doors

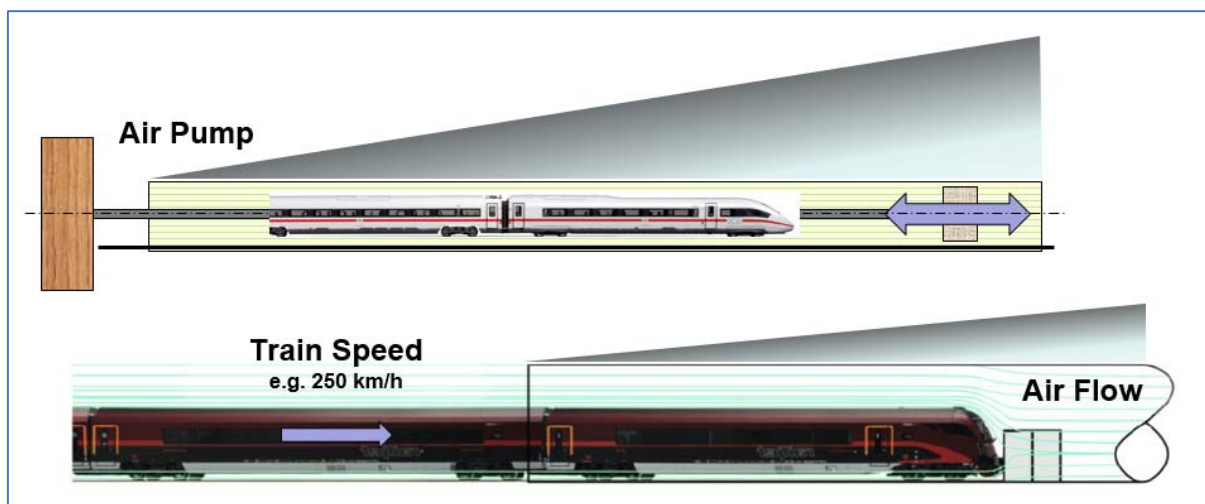
Currently, different types of doors are used by railroad operators in Europe. For example, double-action doors are used in Germany and sliding doors in Switzerland. Each type has advantages as well as disadvantages, which depend on the specific application and the boundary conditions. The basic principle is: keep it as simple as possible. Doors should have as few sources of error as possible, but at the same time offer high availability and lower maintenance and service costs [6].

The ventilation system plays a decisive role in the selection of the door type, because in event of an incident, the escape routes must be kept smoke-free. By generating a positive pressure gradient between the escape route and the location of the incident, fresh air flows from the safety tube into the event tube, avoiding any penetration of smoke into the escape route. However, this pressure difference has a big influence on the door opening forces. Especially in the case of swing and double-action doors additional components such as overpressure relief flaps or mechanical door opening aids are indispensable.

Last but not least, the geometry of the escape route as well as the installation situation also influence the decision as to which door type is finally selected.

### 3.2. Aspects of structural analysis

High speed trains in a railway tunnel cause multiple phenomena and thus also affect the various installations in the tunnel. One of them is the piston effect which generates an air flow in the tunnel. The other one is the sonic boom at the exit portal, generated by train induced pressure waves (Figure 1).



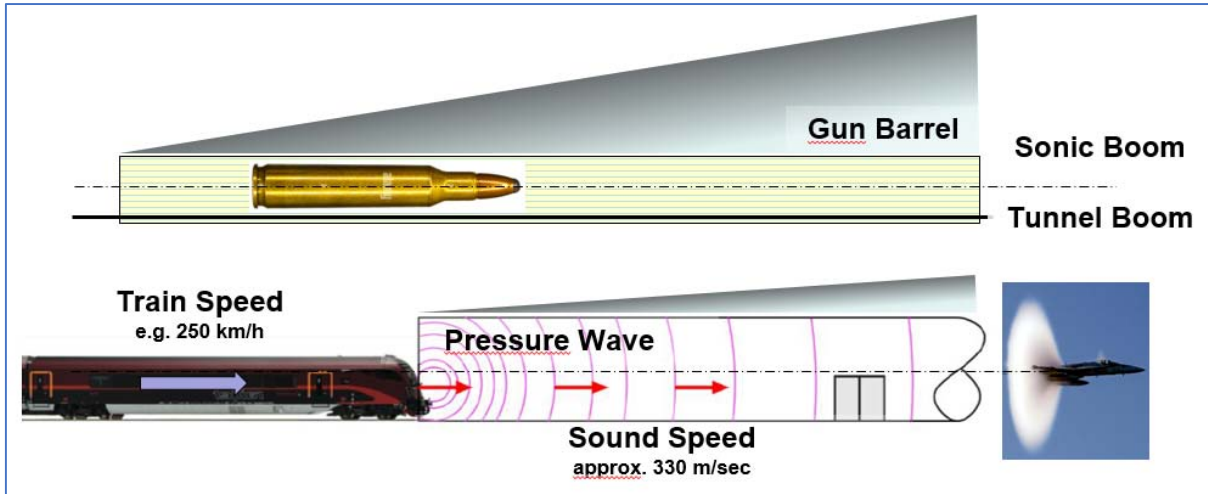


Figure 1: Air flow and pressure wave phenomena in a railway tunnel

It is important to distinguish in which way pressure can be balanced in a tunnel. In the case of an emergency exit door, were no pressure balance between inside and outside take place, very high-pressure differences occur within milliseconds when a high-speed train enters, passes through and exits the tunnel. These pressure differences lead to dynamic loads on the emergency exit doors. Figure 2 shows a typical pressure load profile in a tunnel resulting from a ÖBB RailJet train.

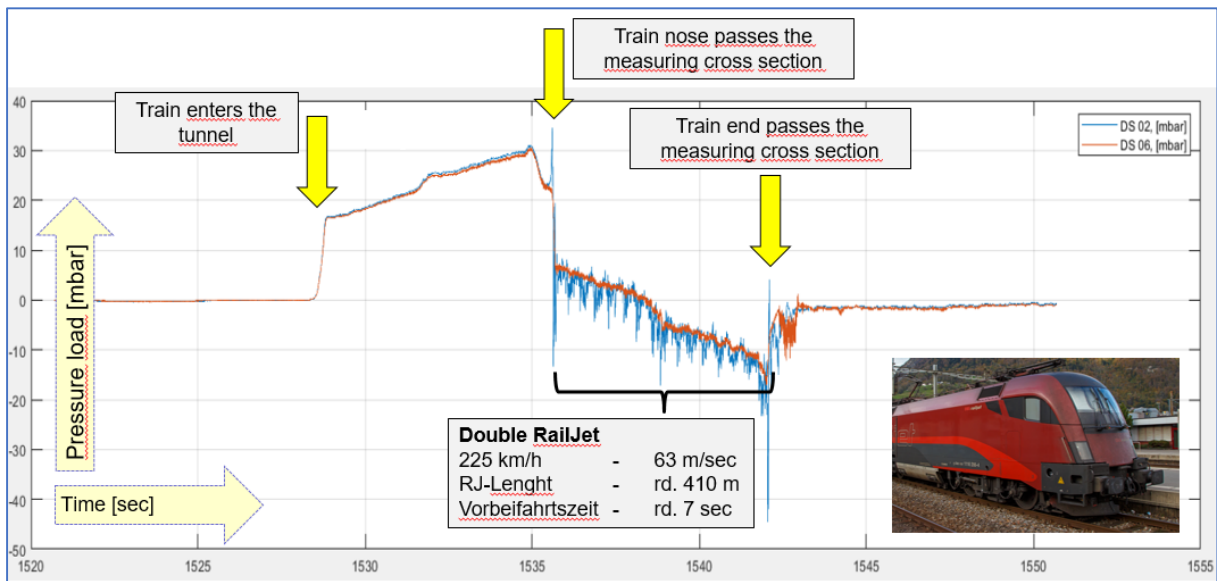


Figure 2: InSitu measured pressure curve of a double RailJet

With the help of in-situ measurements in railway tunnels (e.g. Unterinntal, west route) on various components (e.g. sole drainage lid, emergency exit doors, telecom cable brackets), the loads that actually occur could be determined. The results of these measurements serve as the basis for the design of the components and their mounting [8, 9].

Using numerical simulations on an idealized model tunnel, the influence of the tunnel length (including the reflection of the pressure waves at the portals), the clear cross-section and the train speed were examined and subjected to an overall assessment [4].



### 3.3. Fire resistance

Every building structure as well as every underground system must be divided into fire compartments in order to provide safe areas for escaping persons in the event of an incident. In the case of the Koralm Tunnel the two tunnels are connected with cross passages at intervals of about 500 m. In case of an incident, passengers can escape from the emergency tube via the cross-passages into the opposite safe tube. According to the safety plan fire resistance must be provided over a time span of 180 min. This is done by the two wall slabs – including the escape doors, which separate the cross passage from both tunnel tubes (Figure 3).

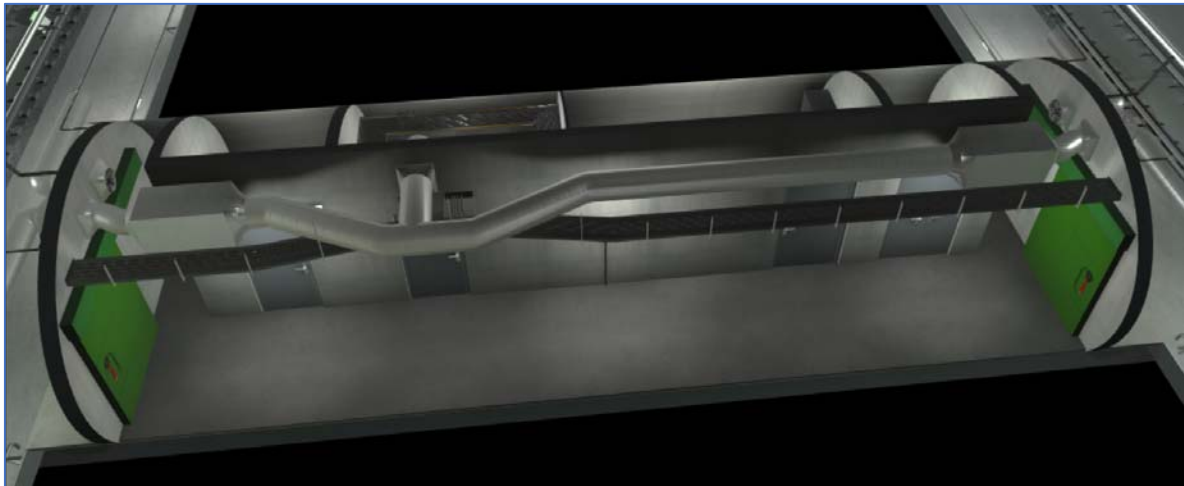


Figure 3: 3D view of a koralm tunnel crosscut / shown in green the emergency exit doors / the closing on both sides to the running tunnels

The fire classification is based on test criteria which include a temperature-time curve. Since various temperature-time curves for such classifications exist, it is essential to select the appropriate curve for the specific application. Figure 4 shows various curves widely used for different applications in tunnels. The so called RWS curve is sometimes used in road tunnel applications while the ISO standard temperature versus time curve (ISO 834 or EN 1991-1-2) is often used for ‘standard’ fire testing applications.

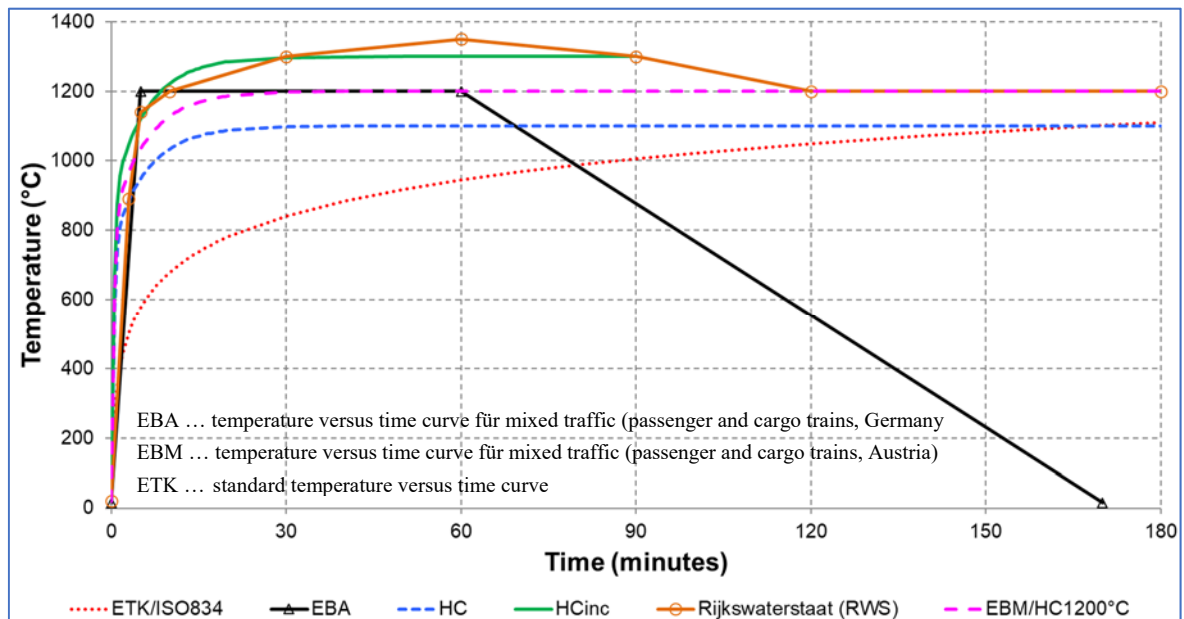


Figure 4: Comparison of different temperature-time curves

In order to be able to select the most appropriate temperature-time curve for the specific project, detailed analyses (e.g. CFD simulation with different fire loads, geometries, boundary conditions) were carried out e.g. for the Koralm railway line [5]. Figure 5 shows the results from a 100 MW (75 MW convective heat) fire event concerning a train stopping very close to cross passage door.

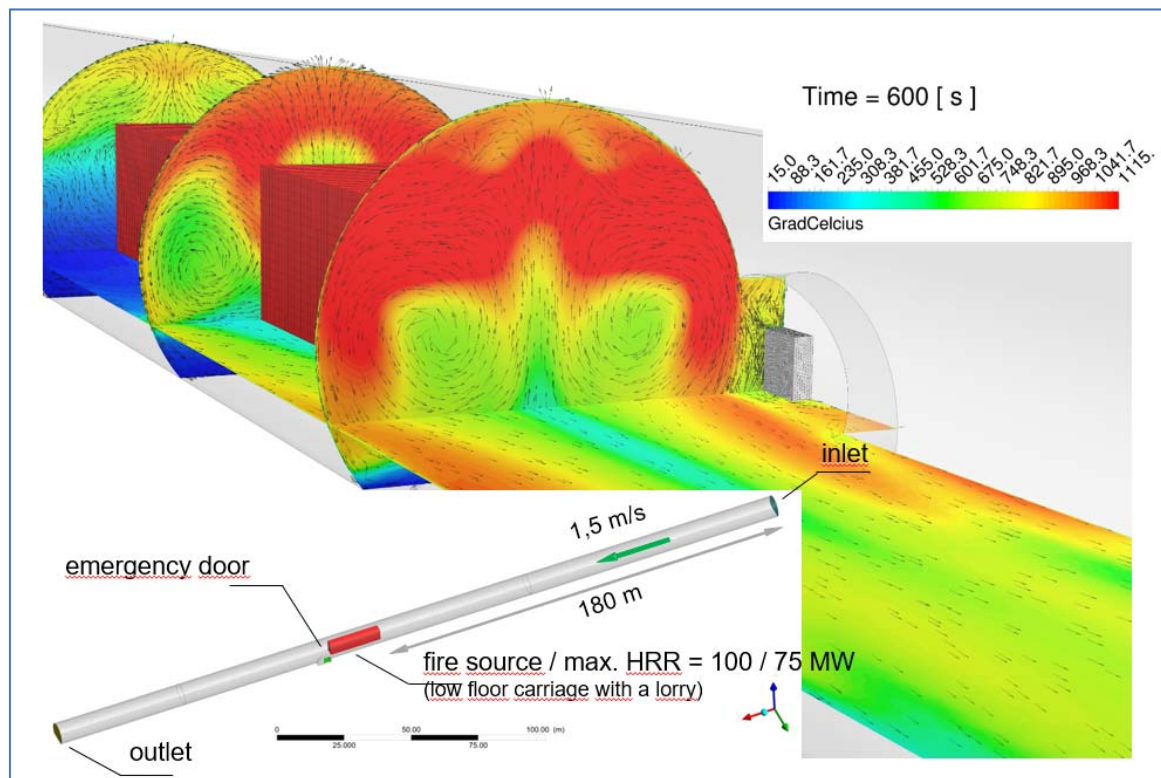


Figure 5: CFD simulation - 75 MW HRR after 600 sec.

From the results in connection with existing technical literature, it was concluded that the application of the unit temperature versus time curve is sufficient and correct in this case.

### 3.4. Clearance of the passageway

It is very important to provide sufficiently dimensioned passageways. The dimensions of the cross section of the passageways was determined with the help of egress simulations. The critical input parameters are the type of trains and the associated maximum number of escaping passengers (Double RailJet - approx. 1,000 persons), the width of the escape route in the tunnel (pavement width for the KAT is between 1.8 and 2.1 m), the stop position of the train in the tunnel (directly in front of a cross- passage or between two cross-passages) and the escape route length (distance between two cross-passages). For the KAT, the following minimum clearance of the passageways through the door were obtained (see table 2).

Table 2: Emergency exit doors - clearance of the passageway

location	type of door	clear width	clear height
outside the emergency stop escape routes every 500 m	sliding door	1.6 m	2.2 m
within the emergency stop escape routes every 50 m	sectional sliding door	1.4 m	

### **3.5. Opening force**

To ensure that the emergency exit door can also be opened easily by physically impaired persons, children, etc. in the event of an incident, the corresponding maximum opening forces (100 Newton) must be observed. The doors are intended to be used for a period of at least 30 to 50 years (depending on train frequency and train mix). During this period, soiling and abrasion occur, which leads to an increase in the opening forces over the service life. Therefore, it makes sense to define a lower limit value (e.g. 80 N) for the new egress door. By mechanizing the door, which can be achieved by e.g. completely motorized opening and closing process, the maximum opening forces can be guaranteed over the life cycle of the door. However, in the case of mechanized doors, it is necessary to take measures against crushing, shearing, impact and retraction.

## **4. TENDER PROCESS**

In order to ensure that the desired product can be produced, delivered and installed on time in the required quality, sufficient time for tests must be calculated already for the tendering and contract awarding process.

Since large projects such as the Koralm tunnel require a large number of emergency exit doors (approx. 200 pieces), order and production delays can take on proportions that jeopardize the entire project process.

An EU-wide published multi-stage award procedure with the stages - Prequalification, Bidding, Negotiation and Clarification, Last and Final/Best Offer - offers the best chances of obtaining the defined product in terms of quality as well as price.

However, it must not be forgotten that a large number of accompanying services, supplies and construction work are still required and that these costs must not be forgotten in the project budget.

In this connection it must be mentioned that suppliers of suitable emergency exit doors can be found only in very limited numbers in Europe.

## **5. REALISTIC STEADY-LOAD TEST**

Commissioning the planned, designed and finally built emergency exit door is an essential point. Above all, the checks should be carried out under boundary conditions that are as close to reality as possible.

A very special issue is the steady-load test, which is necessary to simulate the dynamic pressure effects caused by fast-moving trains in the railway tunnel. In Switzerland and Germany, a test procedure was established at testing institutes in which the pressure load is applied to the door by means of air.

However, since the real load changes occur in fractions of a second and not in seconds, this method was discarded for the Koralm tunnel project. It has been replaced by a more realistic process utilizing a servo-hydraulic load-controlled loading device simulating the pressure waves. Figure 6 depicts the pressure load in the Wienerwald Tunnel as a result of a train passing through.

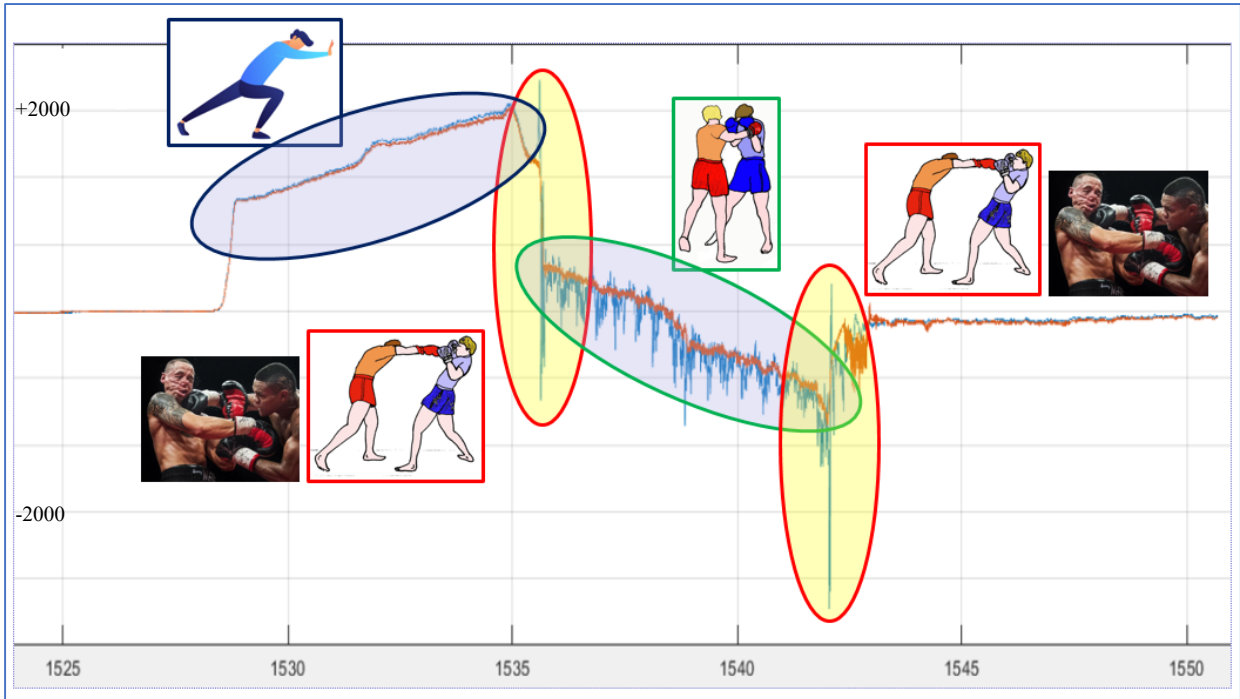


Figure 6: Pressure curve impact analogies (x-axis = time [sec]; y-axis = pressure load [Pa])

In order to uniform the load on the door leaf, an appropriately designed load transmission construction is essential.

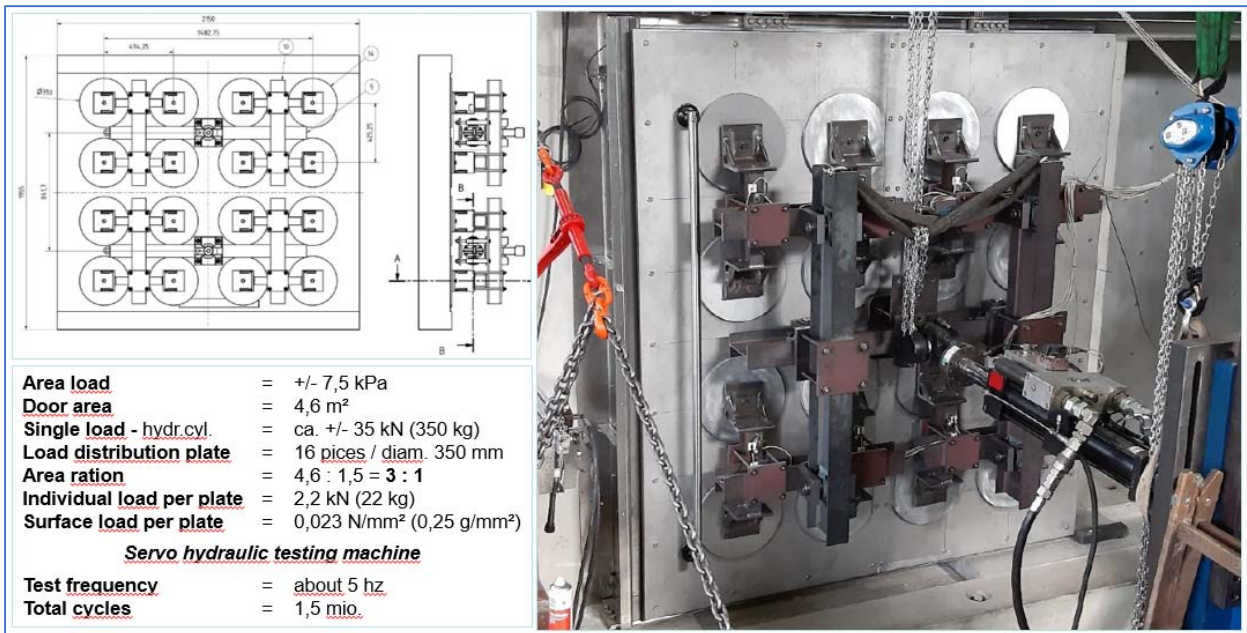


Figure 7: Test set up: concrete frame, sliding door, load transmission construction (servo-hydraulic testing device)

For the testing of the different types of emergency exit doors for the Koralmtunnel, a special test arrangement was developed, evaluated and extensively tested for its practical suitability. The test results were in line with the objectives [3, 7]. Figure 7 shows the load transmission equipment for the tests.

## 6. SUMMARY AND CONCLUSION

This paper is intended to provide an overview of the different aspects that can influence decisions regarding emergency exit doors in a railway tunnel. Every decision is in the most cases a compromise and depends on the particular boundary conditions of the project and can vary from project to project.

It is important to rank and weight the different aspects and thus to make the decision-making process comprehensible and transparent for third parties and outsiders. A good basis for a profound decision-making process can be an overall project assessment that begins at a very early stage of the project. In this context, a building information modelling (BIM) process can make an important contribution.

## 7. REFERENCES

- [1] Fabbri Davide, Strass Christian, Peggs Simon; Safety doors in world's longest tunnel under the Gotthard: Outstanding requirements and performance. Feedback from the bidding phase and results from the testing phase on selected prototypes; Proc. of the 33rd ITA AITES World Tunnel Congress; Prague; 5.-10. May 2007
- [2] Peggs Simon, Pochop Frank; Anforderungen und ganzheitliche Projektabwicklung am Beispiel Gotthard-Basistunnel; Rosenheimer Tür- und Tortage 2008
- [3] Steiner Helmut, Kari Hannes, Reiterer Michael; Erste Schritte zur Entwicklung von "neuen" ÖBB-Tunneltüren; STCE - Dynamik Tage Wien 2016; Tagungsband
- [4] Steiner Helmut, Kari Hannes, Reiterer Michael; Baudynamische Analysen bei der Entwicklung von Tunneltüren für die ÖBB: Simulationsberechnungen der Druck- und Sogbelastungen, Stoßspektrern, Eigenfrequenzen, Ermüdungsbemessung; STUVA Conference 2017; Forschung + Praxis 49
- [5] Steiner Helmut, Beyer Michael, Sturm Peter-Johann; Requirements for escape doors in the tunnels of the Koralm railway line – special focus on the thermal loads during fire; 9th Int. Conv. „Tunnel Safety and Ventilation“ 2018, Graz, proceedings ISBN 978-3-85125-606-2
- [6] Baltzer Wolfgang, Brungsberg Torsten, Riepe Werner; Anforderungen an die Ausbildung von Notausgangstüren in Straßentunneln: Barrierefreiheit, Druck-/Sogbelastungen, Geometrie, Ausführungsbeispiele; STUVA Conference 2019; Forschung + Praxis 53
- [7] Steiner Helmut, Reiterer Michael; Experimentelle Untersuchung der Dauerhaftigkeit von Tunneltüren für schnellbefahrene Bahntunnel der ÖBB; STCE - Dynamik Tage Wien 2021; Tagungsband
- [8] Schellander Janez, Reiterer Michael, Steiner Helmut; Messtechnische Untersuchungen von druckwellen- und strömungsinduzierten aerodynamischen Belastungen in Hochgeschwindigkeitstunneln; 17. D-A-CH-Tagung 2021 Luzern
- [9] Reiterer Michael, Schellander Janez, Steiner Helmut; Bahntechnische Einbauten in schnellbefahrenen Eisenbahntunneln der ÖBB – Realitätsnahe Belastungsansätze in Theorie und Praxis, Laborversuche und In-situ-Messungen, STUVA Conference 2021; Forschung + Praxis 56

# RECOMMENDATIONS TOWARDS THE STANDARDIZATION OF THE VENTILATION EQUIPMENT IN ROAD TUNNELS

<sup>1</sup>Justo Suárez

<sup>1</sup>INGENIERIC, ES

## ABSTRACT

The road tunnel safety regulations specify the requirements of the ventilation system to achieve an acceptable level of risk in the tunnel, but they do not provide specific guidelines about the standardization of the equipment to be installed. This is an important point that must be taken into account to reduce the life cycle cost of the ventilation equipment throughout its lifetime, improving its maintainability, compatibility and integration with other systems. The present paper summarizes the outcome document, recently released by the Spanish National Committee of PIARC, assessing minimum requirements and recommendations towards the standardization of the ventilation equipment in road tunnels and the advantages linked to this standardization.

*Keywords: Standardization, Ventilation Equipment, Maintenance, Integration, Life Cycle Cost.*

## 1. INTRODUCTION

The safety requirements in road tunnels have been significantly increased in the latest years. The directives, laws and regulations that rule safety in tunnels have been focused in specifying the safety levels that must be guaranteed, as well as the systems that are needed to be installed to achieve these levels. However, they do not embrace other important matters related to the standardization of the equipment, its maintainability, compatibility and integration with other systems. These issues must also be considered to ensure a reliable performance of the equipment along its operational life, paying especial attention to the aggressive environment existing in most of the road tunnels.

Taking into account the above considerations, the Spanish Tunnel Committee of PIARC decided to set up several “standardization” Working Groups, each one focused on a different tunnel system. The objective of these WGs is to develop documents with baseline recommendations about the functional characteristics and the requested values that should be specified for each electro-mechanical equipment to be installed in the tunnel.

Among all different electro-mechanical systems in road tunnels, the ventilation is probably the most critical one to guarantee the safety and comfort of the users. In addition, the ventilation system takes up a substantial part of the total investment in tunnel installations, it has a significant energy consumption during normal tunnel operations and it also takes most of the budget and resources assigned for equipment maintenance.

## 2. DOCUMENT ON STANDARDIZATION OF VENTILATION EQUIPMENT

### 2.1. Considerations for standardization assessment

Under the coverage of the ATC (Spanish Tunnel Committee of PIARC), a Working Group for standardization of ventilation equipment in road tunnels was established in October 2018. The WG included 26 professionals from 17 different companies and organizations involved in the tunnel industry. The objective of the Working Group was to develop a useful and practical guideline document with recommendations towards the standardization of the ventilation equipment [1].

To facilitate the standardization assessment, the ventilation machinery was classified in four main categories according to its functionality, with different types of equipment in each category, as shown in figure 1.

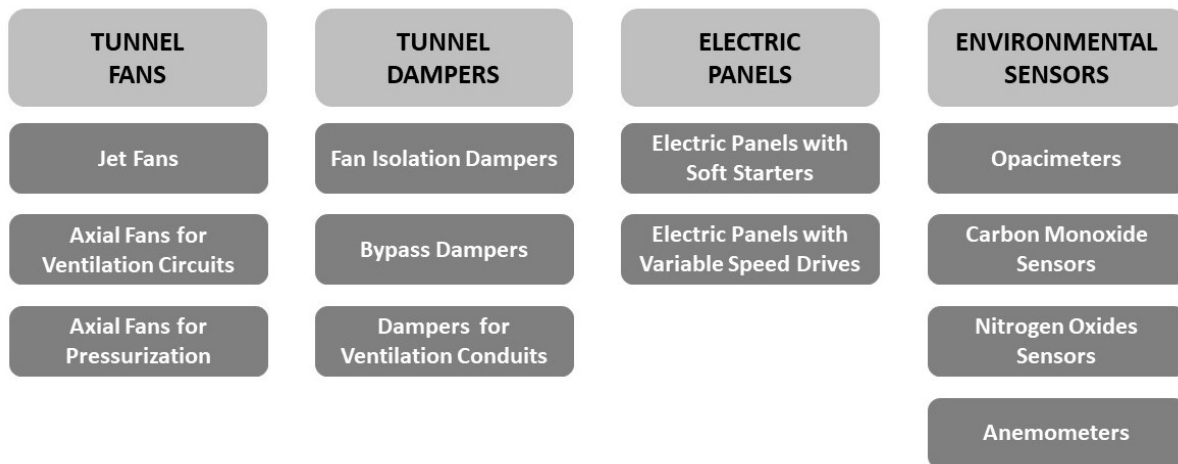


Figure 1: Ventilation equipment classification

Following this classification, the most important technical characteristics of each type of equipment were analysed and recommended values were defined to guarantee its functionality and its durability in the tunnel environment. Some technical characteristics were equally relevant to all the types of equipment on the same category, while others were applicable only to one type of equipment. As an example, the corrosion resistance has been assessed for all the equipment to class C5 according to ISO 12944 [2], as this is the most predictable environment inside the tunnels.

Tunnel fans were the machinery with more possibilities for being standardized. Over sixty technical characteristics were identified and assessed for their standardization, providing suitable values and recommendations. These characteristics were gathered in the following areas (between brackets the number of characteristics subjected to standardization in each area):

1. Electric motor parameters (12)
2. Devices for control and monitoring (6)
3. Junction boxes for power supply and signals (7)
4. Power supply cables (3)
5. Aerodynamic performance (5)
6. Impeller balancing (3)
7. Sound level (2)
8. High temperature resistance (2)
9. Corrosion protection (1)
10. Quality of materials (3)
11. Fan types (12)
12. Installation in tunnel (9)

Regarding tunnel dampers were identified the following areas where several characteristics were assessed for standardization:

1. Installation in tunnel (3)
2. Typology, size, and modules (6)
3. Aerodynamic performance (4)
4. Actuators and operating system (17)

5. High temperature resistance (4)
6. Corrosion protection and quality of materials (9)

With respect to electrical panels the use of variable speed drives (VSD) was recommended to start-up and control the tunnel fans. VSDs provide a smooth start-up of the motor and reduce the power consumption by adjusting the rotational speed of the fan to the requested ventilation performance at each moment, as a result, significant savings in electric power consumption are achieved. VSDs can also control the electrical parameters and the signals from the fan. Soft starters were proposed as a lower cost alternative to VSDs. The use of direct on line starting for the fans was rejected.

Regarding environmental sensors, different technologies were assessed and minimum technical requirements were defined.

## **2.2. Engagement of the stakeholders**

The standardization of the ventilation equipment is a joint task that should involve all stakeholders of the tunnel project. These are some recommendations to be followed for achieving a certain level of standardization on the equipment.

- Consultants and designers: During the design stage of the ventilation system, standardization criteria should be used to specify the equipment, for example minimizing the number of different models for the same type of equipment, especially in the case of fans.
- Contractors: During project execution the standardization criteria used at the design stage must be maintained, avoiding changes based exclusively in economic considerations. Standardization principles shall also be followed for any project requirement that has not been clearly defined in the design, such as possible additional accessories on the main equipment.
- Equipment manufacturers: All units of equipment of the same type must be manufactured with consistency in their uniformity. Manufacturers must facilitate the interchangeability of spare parts for similar types of equipment. In addition, the availability of spare parts must be ensured throughout the lifetime of the equipment. It is advisable that equipment manufacturers take an active role with proposals that could improve the standardization.
- Maintenance Teams: The maintenance of the equipment must be carried out by qualified personnel, using recommended original spare parts. The level of standardization of the installed equipment must be kept along all its lifetime, avoiding replacement of parts or components that can generate exceptions or singularities.
- Tunnel owners: They are the ones who should promote and demand standardized ventilation equipment, taking advantage of all the related benefits, optimizing the tunnel management and reducing costs.

## **3. ADVANTAGES OF THE VENTILATION EQUIPMENT STANDARDIZATION**

### **3.1. Maintenance optimization**

Maintenance of the tunnel installations ensures the durability and good performance of the equipment over the years. There are two types of maintenance to be considered:

- Preventive (planned) maintenance. It is related to routine activities carried out on the equipment to guarantee the reliability during all its lifetime.



- Corrective maintenance. It includes all those activities that are carried out to set back in operation any equipment that has been damaged. This type of maintenance is carried out as a matter of urgency because the detection of any anomaly or dysfunction in the equipment or installation may affect to the tunnel safety.

The standardization of the ventilation equipment optimizes both types of maintenance activities. The standardization must be oriented to increase the quality of the equipment to be standardized. Following this principle, the installation of standardized equipment with higher quality will result in less maintenance requirements and the implementation of more effective maintenance procedures. Furthermore, a standardized ventilation equipment reduces the quantity and variety of spare parts that must be kept in stock to face any replacement during maintenance. Corrective maintenance activities are also reduced as the installation of higher quality equipment leads to lower rate of failures.

On the other hand, equipment standardization also leads to a “Maintenance Standardization”. A reliable maintenance programme can be scheduled based on standardized equipment parameters that have been previously assessed. The periodicity of preventive maintenance can be adjusted to the real equipment conditions, avoiding unnecessary stoppages on the tunnel.

Ventilation equipment with highly standardized characteristics will simplify the maintenance training. Equipment from different manufacturers will be subjected to uniform maintenance training courses as their characteristics will be the same.

### **3.2. Streamlined technical specifications**

Each tunnel project requires a bespoke design of its ventilation system, and the ventilation equipment specifications are based on that design. Most of the times, the ventilation equipment is selected according to one of these practices:

- Brief and general specifications. They are outlined by the designer of the tunnel ventilation system, leaving technical details of the equipment to relevant regulations (PIARC guidelines, handbooks, ...) and ultimately to the Contractor. Any lack of definition is usually solved based on economic criteria. In the absence of a design obligation, the cheapest option is usually chosen.
- Very detailed specifications. They are included as part of the ventilation design. This generates an additional workload in the design phase. The result is often a very rigid specifications that complicates their practical implementation in the tunnel. Once the design has been approved, it is very difficult to implement any modification, if it would be needed. The equipment specifications must satisfy the design criteria and be suitable for the tunnel conditions but taking especial care that the technical requirements of the equipment are not oversized.

A reference document providing recommended standardized values for the main equipment characteristics could be a useful tool to assist the ventilation designers in the task of issuing consistent equipment specifications. It would also avoid equipment selection based on lowest price criteria and barely compliance options, due to unspecified ventilation equipment characteristics.

### **3.3. Constructability and durability**

Standardized ventilation equipment allows simple installation procedures and methods of statement, saving time for installation and on-site testing and reducing their related costs.

The equipment standardization shall facilitate the onsite constructability of the ventilation system under severe space restrictions. It should also be considered to keep enough space around the equipment for installation and maintenance activities, as well as possible replacements of the equipment or some parts during its operational life.

The parameters related to durability of the ventilation equipment has been standardized to withstand the harsh tunnel conditions.

### **3.4. Compatibility and integration with other systems**

The ventilation is one of the most critical systems in the tunnels, therefore it must be compatible and perfectly integrated with other systems.

The interface between the ventilation equipment and the ventilation control system must be fail-safe to guarantee the reliability of the whole system and the tunnel safety.

The signals to be provided by the ventilation equipment to the control system must be standardized, as well as the protocols of communication between the local control panels and the control system. Clear mapping of the signals to be managed must be defined on the ventilation design.

The ventilation control system must collect and record updated data coming from the ventilation equipment (tunnel fans, dampers, electric panels and sensors) being some of these data the input signals for the ventilation algorithms. Data collection should be made according to pre-defined sampling times. It is recommended a statistic analysis of these data, as they can provide valuable information about equipment performance, optimising its maintenance and extending its operative lifetime.

### **3.5. Improvements in Life Cycle Cost Analysis**

The directives of the European Union and the Administrations of many countries have been paying attention, since years ago, to the economic cost of infrastructures construction, maintenance and operation throughout their lifetime. In this sense, the European Union Directive 2014/24/EU on public procurement [3] and other national regulations stimulate or directly dictate to consider the Life Cycle Cost as a key factor for awarding public contracts.

Life Cycle Cost (LCC) is defined as the total cost of ownership related to acquisition, operation and maintenance over the life of the infrastructure system and is the actual cost that the buying organization will have to bear during the years that the system will be in operation. For most electro-mechanical systems maintenance costs increase over time, while the residual value of installed equipment decreases. Infrastructure owners must ensure that their total cost of ownership is as low as possible.

The figure 2 shows a typical example of how is divided the total life cycle cost of a ventilation system considering a lifetime of 25 years. The operational cost, mainly the electricity consumption, is the highest one, followed by the acquisition and maintenance costs, being marginal the resell value.

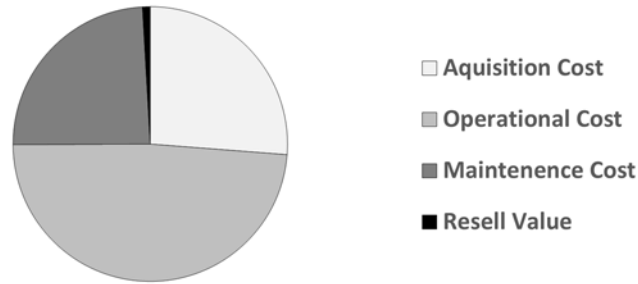


Figure 2: Typical LCC share for a Tunnel Ventilation Project

The acquisition costs are easy to calculate as they are directly related to the purchasing price of the ventilation equipment. In most of the cases the standardization upgrades the technical characteristics of the ventilation equipment increasing its acquisition cost, in any case, this negative consequence is compensated by the reduction of the other costs. One example could be the recommendation for using variable speed drives to operate the fans: the purchase of these devices increases the acquisition cost but the savings in power consumption reduces significantly the operational cost and therefore, the life cycle cost of the ventilation system is significantly lower.

The operational cost involves all the expenses needed for the operation of the ventilation system. Among all these expenses the electricity consumption is by far the highest one. The standardization must be oriented towards the use of higher efficiency equipment, setting a minimum rate of output performance per kilowatt.

The maintenance costs are the ones more directly related to the equipment standardization. An important drawback to get a reliable LCC analysis is how to estimate realistic costs of preventive and corrective maintenance. These costs are the most uncertain ones, as the preventive maintenance depends on manufacturer's recommendations and the corrective maintenance on the MTBF (Mean Time Between Failures) of the equipment, also to be provided by the manufacturer.

Although the equipment has to comply with mandatory technical specifications, there are many parameters that are subjected to the manufacturer criteria, therefore the maintenance requirements cannot be fairly assessed and subsequently the level of uncertainty on its associated costs is very high. Similar situation occurs on the MTBF, which also rely on manufacturer's information. On the contrary, when the main parameters of the ventilation equipment have been standardized, the maintenance requirements can be established according to uniform criteria for all the manufacturers.

To illustrate the positive impact of the equipment standardization and the use of VSDs on the LCC a case study of a motorway tunnel with longitudinal ventilation system has been assessed. The LCC analysis was made for 32 jet fans during 25 years of operational life and considering two different scenarios:

- with standardization and using VSD.
- without standardization and direct on line starting.

The inputs for the calculations were based on rough estimates and cost assumptions. The results are shown in figure 3.

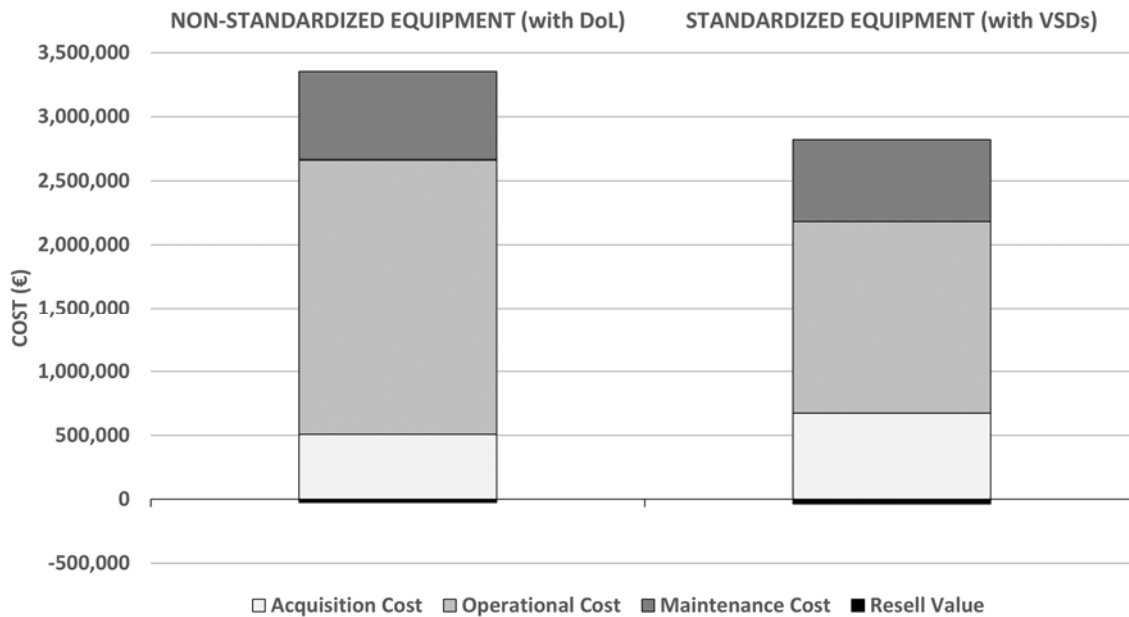


Figure 3: Example LCC of Tunnel Ventilation Equipment (25 years)

#### 4. SUMMARY AND CONCLUSIONS

It has been noted the necessity of improving the standardization of the electro-mechanical equipment installed in road tunnels, being the ventilation one of the systems with more possibilities to be standardized. In this regard, a guideline document with recommendations towards the standardization of the ventilation equipment has been prepared by a Working Group under the Spanish Tunnel Committee of PIARC. The equipment standardization is a joint task that must involve all the stakeholders in a road tunnel project. The common goal must be to achieve a maximum level of standardization not only in a single tunnel, but also among all the tunnels in a road network.

The standardization of the ventilation equipment improves the constructability, durability of the whole ventilation system and its integration with other systems. It improves and facilitates the development of technical specifications for ventilation systems at the design stage of a road tunnel project. Furthermore, if the main technical characteristics of the ventilation equipment are standardized, the task and periodicity of the maintenance activities can be adjusted to the real needs of the equipment. This leads to a cost-cutting on the budget assigned to maintenance and a significant reduction on the life cycle cost of the equipment.

#### 5. REFERENCES

- [1] ATC Comité de túneles "Túneles de carretera: Recomendaciones para la normalización de equipos de ventilación", May 2022.
- [2] ISO 12944-2:2017. "Paints and varnishes. Corrosion protection of steel structures by protective paint systems. Classification of environments".
- [3] Directive 2014/24/EU of the European Parliament and of the Council of February 26, 2014.

# ON THE RISK OF A PRESSURE VESSEL EXPLOSION INSIDE ROAD TUNNELS

Jonatan Gehandler, Chen Huang, Ying Zhen Li & Anders Lönnermark

RISE Research Institutes of Sweden, SE

## ABSTRACT

Biogas and hydrogen are two renewable fuels that are needed in a transition from fossil fuels. Biogas and hydrogen tanks are equipped with a melt fuse that should release in the event of fire. However, on a few occasions, both nationally and internationally, the tank failed and the high pressure compressed gas was released instantaneously causing a pressure vessel explosion. If the explosion occurs inside a tunnel, the problems related to the pressure wave will be even more challenging, so the question whether the rescue service should be allowed to enter the tunnel has been raised, in particular with regards to the risk of hearing impairment. The Swedish civil contingency agency (MSB) takes such a stance. However, there are many uncertainties and assumptions that lead to such a decision that may need to be further discussed. It is argued that the limit value of 200 Pa is too low for such short and rare source of noise that a pressure vessel explosion is, and that such a decision also must consider the low likelihood of occurrence. A distinction should be made between pressure limits that has an immediate damaging effect and those which causes hearing damages from long-term exposure.

*Keywords: CNG, biogas, hydrogen, pressure vessel explosion, tunnel, safety distance, firefighting, rescue service.*

## 1. INTRODUCTION

Biogas and hydrogen are two fuels that are needed in a decreased use of fossil fuels, transition towards cleaner fuels, and lowered green-house gas emissions. These vehicle fuel tanks are equipped with a melt-fuse, a thermally activated pressure relief device (TPRD), that should release the gas in the event of fire before a pressure vessel explosion occurs. However, a pressure vessel explosion in the event of fire has occurred twice in Sweden, and several times internationally. The reason that often have been put forward is a local fire that does not heat the TPRD, or that extinguishing media cool the TPRD. RISE have been investigating CNG tanks exposed to local fire exposure [1] and extinguishing [2] in field experiments.

The Swedish civil contingency agency, MSB, are considering to recommend very strict measures for rescue service interventions of gas vehicles in road tunnels in a future guideline. This is mainly due to the risk of hearing impairment in the event of pressure vessel explosion, by which the entire tunnel tube is considered a "prohibited area", regardless of tunnel length if there is a risk of a pressure vessel explosion. In the event of a tunnel incident, this decision would be taken by the local rescue leader as soon as a gas vehicle is confirmed on fire. This is of great importance to the Swedish Transport Administration, as a rescue intervention is part of the tunnel safety concept. MSB bases its conclusions on work carried out at Lund University [3]. The purpose of this paper is to explore the reasonableness of MSB's future recommendations regarding requirements for rescue operations in tunnels with gas vehicles. In particular, the following factors will be analyzed.

- How likely a CNG or hydrogen pressure vessel explosion is.
- How a pressure wave propagates in a tunnel, considering vehicle and tunnel characteristics.
- Pressure magnitude limits used in literature.

- An occupational health perspective for firefighters' hearing.
- A decision and risk theory perspective.

## 2. REVIEW

### 2.1. The risk for a pressure vessel explosion in the event of fire

As was stated in the introduction, RISE have investigated whether a local fire exposure and extinguishing can cause a pressure vessel explosion. In total 15 field experiments were conducted, either with a local fire source [1] (see left hand of Figure 1) or extinguishing with water [2] (see right hand side of Figure 1).



Figure 1. Left: small fire pan (i.e. local fire exposure) below CNG steel tank. Right: application of water onto CNG composite tank with widespread fire pan below the tank. (Photo: RISE)

Only one of the 15 tests led to a pressure vessel explosion; a CNG composite tank filled to 150 bar that was exposed to the local fire exploded after 20 min, see Figure 2. While application of water was efficient at cooling the TPRD and thus put it out of operation, the water also cools the tank and for the different types of tanks that were tested, this did not lead to a tank rupture. Water was applied for 20 min. The tests show that it is difficult to create the necessary conditions to reach a pressure vessel explosion. In many real situations, fires will only result in a local exposure for a limited period of time, and application of water will often result in that the fire is extinguished. Despite, as was stated in the introduction, a pressure vessel explosion in the event of fire has occurred, e.g., twice in Sweden during the last 20 years during which Sweden has had about 50000 CNG vehicles [2].



Figure 2. A pressure vessel explosion.

### 2.2. Pressure wave propagation

The pressure wave propagation is commonly studied using empirical methods and numerical simulations. Baker et al. [4] has developed a methodology for evaluating physical bursting of a

sphere in the free space using data fitting from numerical calculation, comparing with measurement, and solving one-dimensional shock wave equation together with blast scaling law. By specifying the initial tank volume and pressure, tables can be looked up, and the tank rupture explosion overpressure versus distance can be obtained. For example, Molkov and Kashkarov [5] applied the empirical method developed by Baker et al. for estimating pressure wave correlations for a stand-alone hydrogen tank rupture. It is possible to apply Baker et al.'s empirical method to tunnel condition by introducing a factor for considering the congestion of the tunnel geometry. It is then important to be aware of the uncertainty of this factor of congestion.

More efforts have been focused on applying detailed 1-dimensional (1-D) and 3-dimensional (3D) numerical tools for estimating consequences of a pressure vessel explosion. Li [6] developed an in-house 1-D code for simulating gas tank ruptures in tunnels. Runefors [3] used a commercial 3-D Computational Fluid Dynamics (CFD) code to do similar tasks, and found that the differences in explosion overpressure at different distances were within 10% between the results and Li's work [6]. A correlation for blast wave decay after hydrogen tank rupture in a tunnel fire was obtained by performing CFD simulations involving turbulence and combustion [7]. CFD simulations using a simplified method [8] by ignoring turbulence and combustion with substantial lower computational cost, was also performed using an open-source code OpenFOAM for the same tunnel geometry and scenario as in [7]. The simplified method showed quantitative agreement with RISE CNG tank rupture experiment [1]. An explicit dynamic code Autodyn was also used to simulate tank rupture at ro-ro space, which is similar to tunnel conditions [9]. Assumption of an analogy between gas tank rupture and TNT explosion was taken although this needs further verification.

As an example of the pressure wave propagation from a pressure vessel explosion, a single-lane tunnel with a width and height of 5.5 m and 4.5 m, respectively, and a length of 150 m is used. Figure 3 shows a comparison between the calculated explosion overpressures versus distance by Ulster [7] and RISE [8] for an 86 L tank filled with 700 bars hydrogen. The tank is exposed to fire so that the temperature increase to 395 K and 945 bar pressure at the time of tank rupture (the plastic is burnt away so that the composite lose its strength). It is worth noting that in the work of Ulster, 11% of chemical energy from burning of hydrogen is included in the simulation, whereas only the physical tank burst is simulated in the RISE model. Such difference in the model results in a lower overpressure at far-field, i.e., 30 m from the tank centre but reasonable agreement with Ulster's simulation results in the near-field. The far field difference is likely attributed to the combustion of the hydrogen. The discontinuity of the fourth sampling point in the figure is due to that the RISE 3D CFD model considers the detailed tunnel geometry, and that the pressure waves are interacted and magnified close to the ceiling of the tunnel at about 4 m distance and tunnel height.

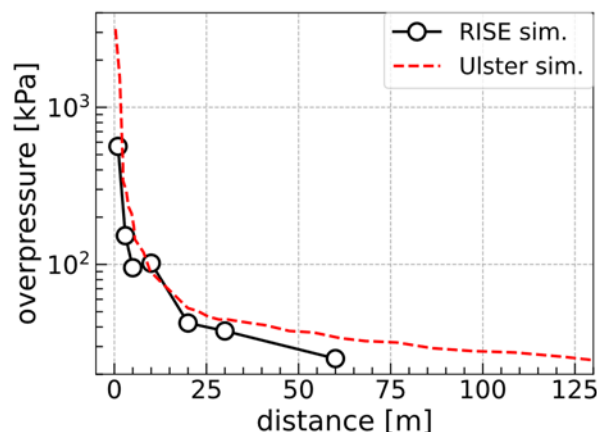


Figure 3. The pressure wave propagation along a tunnel following a pressure vessel explosion.

It is known that the pressure wave from a pressure vessel explosion decreases along the tunnel. The pressure wave may also decrease with number of objects in the tunnel. Therefore, simulated pressures without objects tends to be conservative compared to reality.

### 2.3. Pressure wave impact on firefighters

Different injury criteria are used by different organizations depending on the damage level on humans and on buildings. Pressure-impulse diagrams are commonly used for specifying the damage criteria for buildings based on experience gained during the second world war [4]. Here, we focus exclusively on the damage level of humans. The Swedish Civil Contingencies Agency (MSB) accepts a maximum pressure wave of 200 Pa to avoid hearing impairment [3]. This corresponds to a sound pressure level (SPL) of 140 dB, which is comparable to the 135 dB, which is level that is allowed by the Swedish Work Environment Authority as the peak value.<sup>1</sup> Overpressures of 13.8 kPa, 34.5 – 48.3 kPa, and 137.9 – 172.4 kPa were proposed by Jeffries et al. [10] as thresholds for temporary loss of hearing, 50% probability of eardrum rupture and 50% fatality from lung hemorrhage, respectively. Similar values were found in Ref. [11] with thresholds for 50% probability of eardrum rupture and 50% fatality from lung hemorrhage being 43.5 kPa and 140 kPa, respectively.

It is clear that a very conservative limit (200 Pa corresponding to 140 dB) is used by MSB, compared to other limit values found in literature. It is argued that for rare explosions that last for less than one second, higher values (e.g., 13.8 kPa) recommended in other papers may be more appropriate. This would for instance yield a safety distance in the order of 50 – 100 m in Runefors' [2] simulations, instead of that the whole tunnel is prohibited area.

### 2.4. An occupation health perspective

An initial literature search about hearing protection for firefighters shows that firemen have an apparent risk of hearing disorder. This is mainly attributed to high noise-levels in their daily work environment such as the siren in the fire truck and noise from equipment, e.g., water pumps. The literature search could not find other, more rare events such as pressure vessel explosions to be a reason for hearing disorder among firemen [e.g., 12]. At the same time, it is clear that more could be done to improve firefighter's hearing health, e.g., through the use of hearing protection devices (HPD) that are integrated with the radio and helmet, and through programmes that monitor and limit exposure to noise.

It appears that hearing impairment indeed is an occupational health issue for firefighters, however, the main contributors, according to literature, are from ordinary noise sources rather than extreme events such as explosions.

### 2.5. A decision and risk theory perspective

If we, as most philosophers, would believe the Scottish philosopher David Hume (1711–1776), we cannot derive an ought from an is. The level of safety, e.g., for firefighters during intervention inside a tunnel, is a normative question. Such issues are studied within normative ethics and there are primarily two ethical thought patterns that are used to justify decisions, namely, deontology and utilitarianism [13].

Within deontological ethics the core idea is that there are certain rules or duties which must not be violated, regardless of the consequences of adhering to these rules or duties. At least these consequences play a subordinate role. For instance, an authority could claim that firemen should

---

<sup>1</sup> <https://www.av.se/halsa-och-sakerhet/buller/krav-vid-olika-bullernivaer/>



not be exposed to noise levels above 200 Pa. A strict adherence to a deontological principle, may ultimately lead to the banning of all risky activities, and may infringe on the same values set out to be protected, which may cause more risks than it could possibly prevent [13].

Utilitarianism is about specifying the advantages and disadvantages of each alternative and choosing the alternative with the greatest net advantage. Another way to phrase this is to maximize the utility. Thus, one can argue that enough safety is achieved if the overall utility is maximized [13]. Most decision theories are based on the idea that the choice depends on the probabilities of various consequences and their utility, or value, to the decision-maker. Risk is most often understood as a combination of consequences and probability. A utilitarian approach highlights, not only the consequences side of risk, but also the probabilistic side of risk.

Based on these two thought patterns, the soundness of decisions can be debated. If one would, for example, require that firefighters under no circumstances should be exposed to noise levels above 200 Pa, this would, for instance, require that they could not go near burning trucks (truck tires can explode in the event of fire resulting pressures in the order of 5 kPa [8]), and most likely no fires at all since most vehicles and facilities contain pressure vessels of various kinds, that may explode. It appears that a strict adherence to the deontological limit 200 Pa for the firefighting profession seem unrealistic. Thus, a utilitarian basis for such decisions seems more plausible, this would give weight to the very low likelihood of occurrence of a tank rupture (in Sweden, once per year and 500 000 CNG vehicles and much less probable inside tunnels). Besides, an intervention whereby the fire is extinguished (with or without fixed firefighting systems) lowers the risk further. This decision, whether an intervention is worth the risk, is made at each incident scene by the rescue leader, and in rescue service guidelines by the MSB.

### **3. SUMMARY AND CONCLUSION**

This paper presents preliminary investigations of the risk to firefighters from a pressure vessel explosion inside a tunnel. This is analyzed from five perspectives:

- How likely a CNG or hydrogen pressure vessel explosion is.
- How a pressure wave propagates in a tunnel, considering vehicle and tunnel characteristics.
- Pressure magnitude limits used in literature.
- An occupational health perspective for firefighters' hearing.
- A decision and risk theory perspective.

It is argued that the low likelihood of occurrence is an important risk-reducing factor, in particular in the event of sprinkler activation or manual fire extinguishing, which further lowers the risk of a pressure vessel explosion. There are many assumptions and uncertainties in pressure wave propagation simulations inside tunnels and real experimental data are lacking. It is argued that a pressure limit for this type of event should be in the order of 10-20 kPa, and that this event has little to do with an occupational health perspective which concerns ordinary noise sources such as siren and equipment. If firefighters would not be allowed to be exposed to higher pressure waves than 200 Pa, it would be difficult to perform the profession of firefighting. A distinction is necessary between pressure levels that has an immediate damaging effect and those which causes hearing damage with long-term exposure. At the same time, more could be done to improve firefighters' hearing, e.g., the use of HPD and programmes to monitor and limit noise exposure.

#### 4. REFERENCES

- [1] Gehandler, J. and Lönnermark, A. (2019). CNG vehicle containers exposed to local fires, in RISE Report 2019:120\_rev1.
- [2] Gehandler, J., Olofsson, A., Hynynen, J., Temple, A., Lönnermark, A., Andersson, J., Burgén, J. and Huang, C. (2022). BREND 2.0 - Fighting fires in new energy carriers on deck, in RISE Report 2022:47.
- [3] Runefors, M. (2020). Zonindelning vid räddningsinsatser mot fordon med alternativa bränslen – Beräkningsunderlag, Avdelningen för Brandteknik, Lunds Tekniska Högskola.
- [4] Baker, W.E., Cox, P.A., Kulesz, J.J., Strehlow, R.A. and Westine, P.S. (2012). Explosion hazards and evaluation. New York: Elsevier Scientific Publishing Company. Vol. 5.
- [5] Kashkarov, S., Li, Z., and Molkov, V. (2020). Blast wave from a hydrogen tank rupture in a fire in the open: Hazard distance nomograms. *International Journal of Hydrogen Energy*, 45(3): p. 2429-2446.
- [6] Li, Y. Z. (201). Study of fire and explosion hazards of alternative fuel vehicles in tunnels. *Fire Safety Journal*, 110, 102871.
- [7] Molkov, V. and Dery, W. (2020). The blast wave decay correlation for hydrogen tank rupture in a tunnel fire. *International Journal of Hydrogen Energy*, 45(55): p. 31289-31302.
- [8] Burgén, J., Gehandler, J., Olofsson, A., Huang, C., and Temple, A. (2022). Safe and Suitable Firefighting, in RISE report 2022:32.
- [9] Vylund, L., Gehandler, J., Karlsson, P., Peric, K., Huang, C. and Evegren, F. (2019). Fire-fighting of alternative fuel vehicles in ro-ro spaces, in RISE report 2019:91
- [10] Jeffries, R. M., Gould, L., Anastasiou, D. and Franks, A. P. (1996). Derivation of fatality probability functions for occupants of buildings subject to blast loads, in *Probabilistic Safety Assessment and Management'96* (pp. 669-675). Springer, London.
- [11] Lees, F. (2012). *Lees' Loss prevention in the process industries: Hazard identification, assessment and control*, Butterworth-Heinemann.
- [12] Ewigman, B.G., Coleen, H. K., Michael, C. H. and Darla, H. (1990). Efficacy of an Intervention to Promote Use of Hearing Protection Devices by Firefighters, in *Public Health Reports* 105(1): p. 53-59.
- [13] Basta, C. (2014). Siting risky facilities: Probabilism, determinism and beyond, in *Planning Theory*, 13(1): p. 44-64.

# DETERMINATION OF AERODYNAMIC LOADS IN RAIL TUNNELS USING MEASUREMENTS

Rodler J.<sup>1</sup>, Huber A.<sup>2</sup>

<sup>1</sup>FVT mbH, Austria

<sup>2</sup>GRUNER GmbH Ingenieure und Planer, Austria

## ABSTRACT

When a train passes through a tunnel, pressure variations are generated which propagate along the tunnel at sonic speed and are reflected back at portals into the tunnel. These pressure variations may cause aural discomfort or, in the worst case, aural damage to train passengers and train staff and will produce transient loads on the structure of trains and the infrastructure components. [4]

To define a clear interface between the subsystems of rolling stock and infrastructure, the train-induced aerodynamic pressure variations inside tunnels need to be known and limited. In order to specify and to limit the train-induced aerodynamic pressure variations inside tunnels, reference cases for rolling stock assessment are defined. [4]

The increase of the speed limit up to more than 200 km/h for trains of VR Group (Finland) on coastal line (between Helsinki and Turku) in the unrestricted mixed rail-traffic operation required analyses and measurements regarding possible pressure loads. In this process, the relevant aerodynamic properties of the rolling stock are determined based on full-scale tests and compared with the directives of TSI and national directives.

This paper describes the test procedure with sophisticated in-house developed pressure measurement device. The difficulties of pressure measurement using differential pressure sensors especially for this application is pointed out and a new solution is shown.

*Keywords: TSI, aerodynamic loads, rail tunnel, train-tunnel pressure signature, pressure measurements*

## 1. INTRODUCTION

When a train passes through a tunnel, pressure waves at sonic speed are propagated in the tunnel. The compression wave (frontal wave) generated currently the train enters the tunnel is reflected at the opposite portal as an expansion wave. Just when the train tail enters the tunnel, an expansion wave (rear wave) is generated and reflected at the portal as compression wave. Due to unfavourable superposition of waves the pressure amplitude increases, which effects high loads on tunnel equipment and built in components.

However, a small part of the compression wave exit the tunnel and radiates outside, in the form of an impulse-like micro-pressure wave. This can create a booming noise and causes noise pollution in a wide area around the tunnel exit.

Furthermore, pressure variations affects aural pressure comfort for passengers and staff in trains and in worst case, they can cause permanent health damages.

Pressure variations are described by means of the gauge pressure,  $p(t)$ , measured in time and referenced to atmospheric pressure. The external pressure,  $p_e$ , usually denotes the pressure outside a train, or equally inside a tunnel. The internal pressure,  $p_i$ , usually denotes the pressure inside the train or generally in any enclosed air volume that is present in the tunnel system. The internal pressure responds to the external pressure and is dependent on the pressure sealing of the train or generally any structure that separates its internal volume from the external environ-

ment. In order to assess the effects at the surface between the external and internal environments, the pressure difference  $p_a$  is determined. This pressure difference is one source of structure loading. [4]

With regard to aerodynamics, a train have to fulfil the required characteristic pressure changes for a given combination (reference case) of train speed and tunnel cross-section. The assumption is that a single train passes through a standard, straight tubular tunnel (without shafts etc.). Since full-scale measuring of every combination is not possible, calculation results with validated simulation models are accepted. The model building and validation bases on measured pressure curves. The possible procedure of measuring the pressure curve is described below.

## 2. IMPORTANT GUIDELINES

### 2.1. Technical specifications for the interoperability (TSI)

The European Commission has passed technical specifications for the interoperability (TSI) in the trans-European high-speed railway system and in the conventional trans-European railway system and has published them in the respective gazettes of the European communities.

The technical specification for interoperability (TSI) relating to the ‘rolling stock — locomotives and passengers rolling stock’ subsystem of the rail system in the entire European Union, can be found in Commission Regulation (EU) No 1302/2014 of 18 November 2014. [2]

### 2.2. EN 14067-5

The EN 14067-5 document establishes aerodynamic requirements, test procedures, assessment methods and acceptance criteria for operating rolling stock in tunnels. Aerodynamic pressure variations, loads, micro pressure wave generation and further aerodynamic aspects to be expected in tunnel operation are addressed in this document. Requirements for the aerodynamic design of rolling stock and tunnels of the heavy rail system are provided. [4]

## 3. AERODYNAMIC CRITERION / TRAIN-TUNNEL PRESSURE SIGNATURE

The train-tunnel pressure signature can determine the aerodynamic properties of a running train in a rail tunnel. Figure 1 schematically shows the pressure variations generated when a train enters a tunnel.

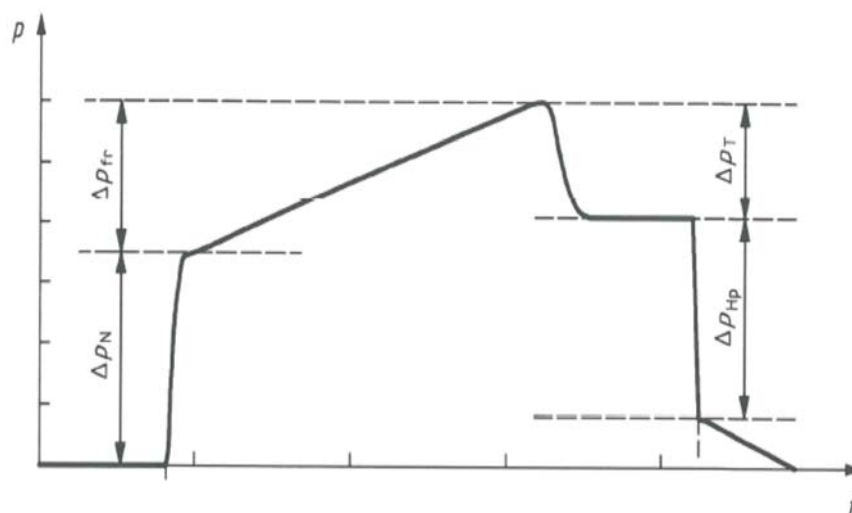


Figure 1: Train-tunnel pressure signature at a fixed place in the tunnel [4]

$\Delta p_N$	Pressure rise generated by the frontal wave of the train nose entering the tunnel
$\Delta p_{fr}$	Pressure rise generated during the tunnel passage due to the friction
$\Delta p_T$	Pressure drop due to rear wave generated by train tail entering the tunnel
$\Delta p_{Hp}$	Pressure drop during the passage of the train nose

The applicable characteristic limits for  $\Delta p_N$ ,  $\Delta p_{fr}$  and  $\Delta p_T$  are compiled in Table 1.

Table 1: Maximum tunnel characteristic pressure changes for the reference case [4]

Maximum design speed km/h	Reference case		Criteria for the reference case, Pa		
	Reference speed, $v_{tr,ref}$ km/h	$A_{tu}$ [m <sup>2</sup> ]	$\Delta p_N$ [Pa]	$\Delta p_N + \Delta p_{Fr}$ [Pa]	$\Delta p_N + \Delta p_{Fr} + \Delta p_T$ [Pa]
$v_{tr,max} < 200$	No requirements				
$200 \leq v_{tr,max} \leq 230$	200	53,6	$\leq 1750$	$\leq 3000$	$\leq 3700$
$230 < v_{tr,max}$	250 or $v_{tr,max}^a$	63,0	$\leq 1600$	$\leq 3000$	$\leq 4100$

<sup>a</sup>The lower value of  $v_{tr,max}$  and 250 km/h shall be applied

Evidence must be provided based on full-scale tests, carried out with the reference speed or a higher speed in a tunnel with a cross-section as close as possible to the reference case. The transfer to the reference requirement can be done with verified simulation software calibrated with the performed measurements.

#### 4. QUANTIFICATION OF PRESSURE VARIATIONS

The quantification of pressure variations can be done with full-scale measurements at a given position in the tunnel or alternative with pressure measurements on a moving train and subsequent calculation of the values  $\Delta p_N$ ,  $\Delta p_{fr}$  and  $\Delta p_T$ .

##### 4.1. Measurements in the tunnel

Ideally, the values  $\Delta p_N$ ,  $\Delta p_{fr}$  and  $\Delta p_T$  are measured at a fixed position in the tunnel. In EN 14067-5 [4] the equation for the distance  $x_p$  between the entrance portal and the measurement position is given:

$$x_p = \frac{c * L_{tr}}{c - v_{tr}} + \Delta x_1 \quad \text{Formula 1}$$

The extra length  $\Delta x_1$  (approx. 100 m) ensures a clear time-related separation of the pressure variations over time. The installation of the measurement devices near to the portal is meant to avoid a deadening of the pressure wave.

Figure 3 shows the pressure signals recorded in a tunnel for a specific train. The train speed was measured within the range of 198.9 to 201.6 km/h. Therefore, all curves are quite similar. Two curves (measurement 4 and measurement 6) are remarkable different. At the time of both measurements, flow speed of about 4 m/s was measured in the tunnel before the train passed. The direction of the flow was in opposite to the driving direction of the train in the tunnel. This resulted in higher pressures. All the other measurements were performed with air speeds less than 1.2 m/s, which resulted in a very good match of the pressure curves.

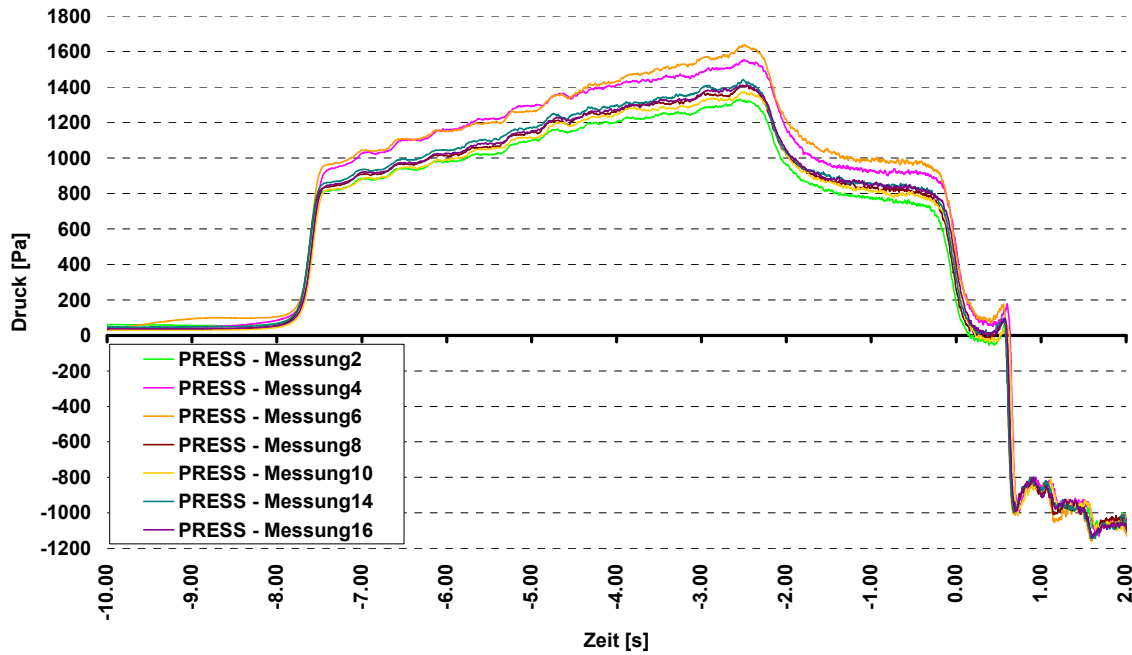


Figure 2: TSI pressure signal from a train measured on a fixed position in tunnel

#### 4.2. Measurements on the train

Measurements on the exterior of the train are possible as well.  $\Delta p_N$ ,  $\Delta p_{fr}$  and  $\Delta p_T$  can be approximated by measurements of  $\Delta p_{N,o}$ ,  $\Delta p_{fr,o}$  and  $\Delta p_{T,o}$  (comp. Figure 3). If needed,  $\Delta p_{HP}$  can be derived either from predictive formulae or assumed to be equal to  $\Delta p_{N,o}$ .

The tunnel shall have a constant cross-sectional area, no side passages or airshafts and no residual pressures waves. Ideally, there should be no initial airflow in the tunnel. However, if there is, its influence on the measurements shall be checked.

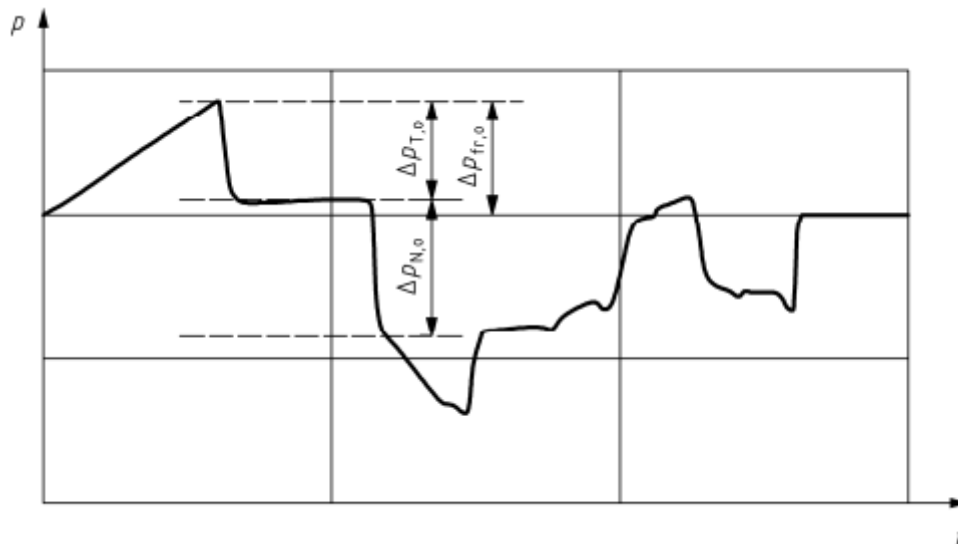


Figure 3: Train-tunnel-pressure signature on the nose of the train [4]

Pressures are measured using transducers on the exterior of the train. To get the complete frictional pressure rise,  $\Delta p_{fr}$ , it is necessary to measure the pressures on the outside of the train at a position just behind the nose at the position where the full cross-sectional area is reached. [4]

## 5. EXAMPLE FOR MEASUREMENTS ON A TRAIN

VR Group is a government-owned railway company in Finland. VR's most important function is the operation of Finland's passenger rail services. In 2019, the Finnish Transport Infrastructure Agency (FTIA) decided to increase train speeds on the coastal line. The coastal line located between Kirkkonummi and Turku is an approximately 162 km long railway track in the south of Finland. Along the track there are 15 single-bore, single-track tunnels with lengths from 43 m up to 1240 m.

The train speeds for each train (ICS, SM3) are limited by the track geometry. The actual speed for SM3 (Pendolino) on this route is 180 km/h to 200 km/h and is going to be increased to max. 220 km/h. The actual speed for ICS on this route is 140 km/h to 160 km/h and is going to be increased to max. 200 km/h.



Figure 4: SM3 (Pendolino) (left) (© Otto Karikoski) and ICS2 (right) (© Antti Leppänen)

### 5.1. Measurement Setup

Both test trains were equipped with several sensors outside and inside the train. The ideal sensor positions are right behind the nose, right before the rear and in the middle of the train. At the nose and at the rear the pressure maxima respectively minima along the train can be expected in long tunnels. The center position provides additional information about the pressure evolution along the train during tunnel passages, which might be useful especially in short tunnel.

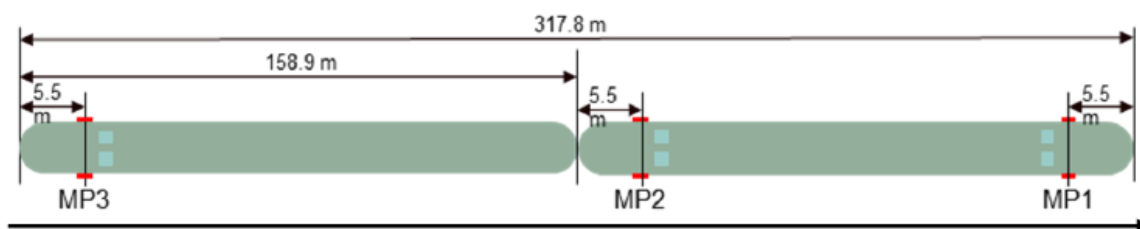


Figure 5: SM3, sensor position along the train [5]

Every measurement position (MP1 - MP3) per train consisted of four external sensors (two on both sides of the train in different heights) and two sensors inside the train. The use of four external sensors provides redundancy and information about possible perturbation of the signal due to train geometry and local non-static pressure effects that can be caused by tunnel geometry. The sensor heights were chosen with respect to train geometry to avoid unnecessary noise on the signals.

Two sensors in the interior are used for redundancy reasons, furthermore they validate each other. If they are placed in the same coach as the outside sensors, their detailed position has negligible influence on the sensor readings because pressure travels at the speed of sound inside the train.

## 5.2. Measurement Devices

The requirements to measurement technique with regard to measurement frequency and accuracy is given in [4].

The pressure transducers shall be calibrated within the expected pressure range, typically  $\pm 4$  kPa. The combination of pressure sensors and probes used shall be capable of measuring the pressure with a minimum of 150 Hz resolution. The measurement error of the measurement chain comprising the pressure transducer and the data acquisition system shall be less or equal than 2% of the expected value for  $\Delta p_N + \Delta p_{fr}$ .

The measurement of static pressure shall be made in a way to ensure that airflow in the tunnel does not affect the measurement. A suitable realization of such an installation is to use a flat mounting board with pressure taps set in it. The mounting board shall be as thin as possible. An example is shown in Figure 6. [4]

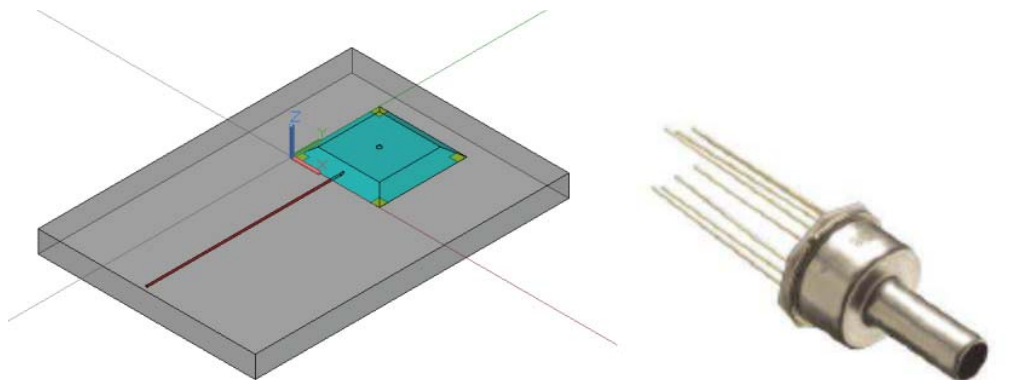


Figure 6: Mounting board with pressure tap (left) and the sensor used in the present case

In order to prevent a loss in (dynamic) information, the tubes and pipes between the pressure tap and the pressure transducer shall not exceed an overall length of 50 cm. The static pressure may be measured as a differential pressure relative to a common reference pressure (e.g. as stored in an insulated pressure reservoir). The structural flexibility and the volume of air in the tubes compared to the pressure reservoir shall be dimensioned to reduce this effect. A small leakage in the pressure reservoir may be necessary to adjust the reference pressure to slow ambient pressure changes. It shall be demonstrated that the leakage is not affecting the test during testing. [4]

Usual differential pressure sensors are used with reference volumes on their negative pressure input. However, experience has demonstrated that differential pressure measurement is not ideal because:

- Pressure changes in the tunnel act on the tubes connected to the pressure reservoir and may affect the reference pressure
- Reference volumes tend to extreme drifts caused by temperature change and poor tightness.
- Mechanical movement can lead to perturbation of the measured signals, which leads to major, not quantifiable inaccuracies of the measurement readings.
- Furthermore, the mounting of tubes along the train is not practicable within a suitable time span.

A new solution was developed and used for the present case using absolute pressure sensors. Naturally absolute pressure sensors are more inaccurate than differential pressure sensors due to their high measurement range therefore a precise ultra-stable high performance, temperature



compensated piezo resistive silicon pressure sensor were used in each mounting board. Table 2 shows the characteristic parameters of the pressure transducer.

Table 2: Pressure sensor and barometer specification

Pressure sensor		Barometer	
Parameters	Value	Parameters	Value
Measurement range	0 to 15 psi	Measurement range	600 - 1100 hPa
Compensated temperature range	-20°C to +85°C	Temperature range	-25°C - +60°C
Working temperature	-40°C to +125°C	Accuracy	± 0.05 hPa
Non linearity	± 0.05% Span	Stability	< 100 ppm/year
Sample rate	500 Hz		
Response time	1 ms		

The pressure sensors are integrated in a mounting board (150 mm x 150 mm) to protect it against mechanical loads and weather effects. The pressure signal reaches the sensor via a perforation (1 mm diameter). The transfer properties of this system were taken into account in the installation of the measurement equipment.

The data recording was performed with a portable data logger (DEWE 43). This logger has eight analogue channels and multiple digital inputs and is able to capture measurement signals at scan rates up to 100 kSamples/s for each canal. The filtering and the averaging are done automatically inside the logger. The pressure signal were captured at a scan rate of 500 Hz.

Sensors shall be calibrated prior to use over the expected pressure range. This was done using a pressure vessel, which can be evacuated and pressurised. As reference, a calibrated very precise barometer was used (see specifications in Table 2).

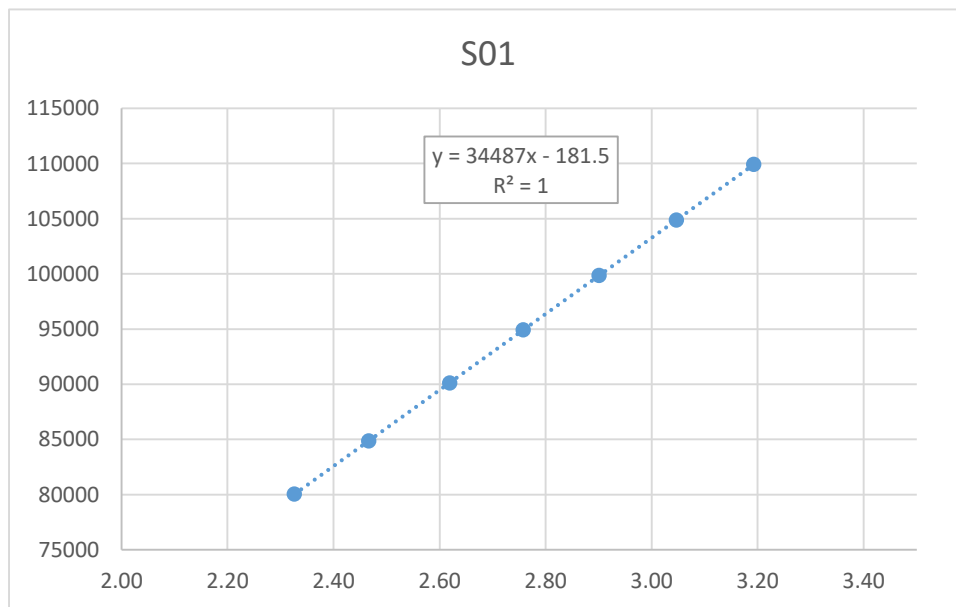


Figure 7: Calibration function for sensor S01 (sensor, amplifier, data acquisition)

## 6. RESULTS

Each tunnel passage was exported separately (150 passages x 3 measurement positions correspond to overall 450 passages).

All obtained signals were filtered with a 75 Hz zero phase shift low pass to reduce noise. Right before a tunnel passage, outside and inside pressure can be considered equal if the inside pressure had enough time to compensate (no tunnel exits right before the tunnel entry).

Based on this assumption, offsets were removed by subtracting the first value of each sensor from each of its samples. Figure 8 shows an example of the corrected data. The green line corresponds to the inside pressure. The four remaining lines correspond to the four outside pressures per measurement position. As expected, there are no major differences between the four measurement positions outside the train. During the full-scale test, pressure was measured during overall 150 tunnel passages on board of the SM3 and the ICS train.

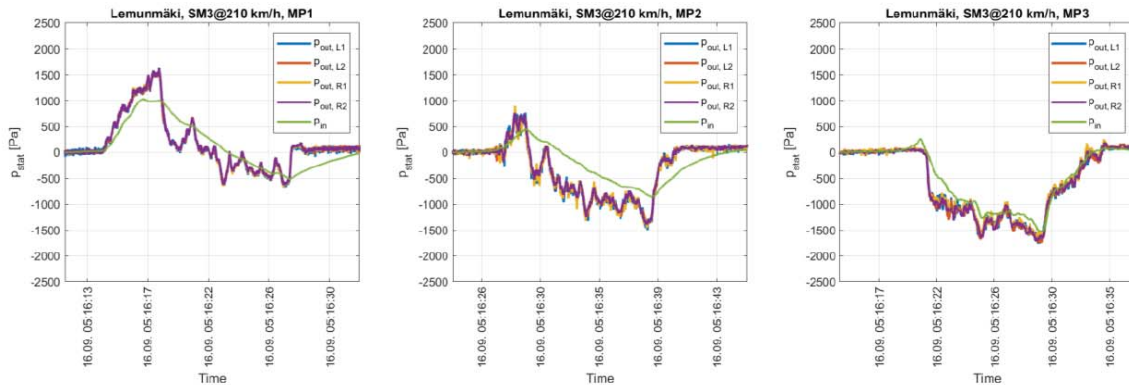


Figure 8: Outside and inside pressures at three measurement positions [5]

Each tunnel passage was visualized to identify invalid data like failure of the power supply, temporary failure of single sensors or data acquisition system, pressure-sealing malfunction, mistakes during export etc. Non-valid data were excluded from the results. Every data set was analyzed and documented concerning:

- maximum pressure outside the train,
- minimum pressure outside the train,
- TSI Health criterion,
- maximum positive pressure on the train wall (maximum of pin-pout),
- maximum negative pressure on the train wall (minimum of pin-pout),
- maximum pressure changes per second outside the train,
- maximum pressure change per second inside the train,
- comfort criterion within 1 second and
- comfort criterion within 4 seconds.

## 6.1. Simulation Program

The software ThermoTun was used for numerical simulation. ThermoTun is a computer programme accepted worldwide for the simulation of trains in tunnels and of tunnel systems. The correctness is confirmed by extended measurement campaigns (cf. [6]). With the programme, e.g. the following, aerodynamically relevant, unsteady values can be determined:

- Pressure variations of trains passing tunnels and on rolling stocks,
- Traction power requirements for trains in railway tunnels,
- Averaged air speed in the railway tunnel tube,
- Distribution and concentration of pollutants and smoke in railway tunnels.

The measurement results were recalculated with this software. Some parameters of the analysed train are varied as often as necessary until a good matching with the measurement was reached.

Subsequently, the pressure signatures could be calculated with the programme for the in TSI specified tunnel cross-section ( $A_{\text{Tunnel}} = 53.6 \text{ m}^2$ ).

## 7. CONCLUSION

A train must have aerodynamic properties that no damages occur for the train and for the tunnel installations when the train passes through a tunnel or passes by an oncoming train. Besides this, the comfort of the passengers must also be taken into consideration.

The increase of speed limit for trains on a specific railway section especially with tunnels requires full-scale measurements of pressure variations, because evidence must be produced about the aerodynamic properties of the train.

This paper describes the authorisation procedure to increase the train speeds on a specific route. It consists in full-scale measurements, which were done in Finland on the coastal line located between Kirkkonummi and Turku, which leads to a data set of several train / tunnel pressure curves. Finally Gruner Ltd Vienna performed various aerodynamic simulations focussing on aerodynamic loads and pressure comfort considering the higher train speeds in several single bore tunnels on this line.

## 8. ACKNOWLEDGEMENT

We would like to thank SWECO Infra & Rail Oy, Helsinki and VR Group for their kind permission to publish this work.

## 9. REFERENCES

- [1] Union International Des Chemins Des Fer (UIC)-Code 779-11., "Détermination de laire de la section transversale des tunnels ferroviaires à partir dune approche aérodynamique", Paris, 2005
- [2] TSI LOC&PAS, VERORDNUNG (EU) Nr. 1302/2014 DER KOMMISSION über eine technische Spezifikation für die Interoperabilität des Teilsystems „Fahrzeuge — Lokomotiven und Personenwagen“ des Eisenbahnsystems in der Europäischen Union, 18. November 2014
- [3] TSI Infrastructure, VERORDNUNG (EU) Nr. 1299/2014 DER KOMMISSION über die technische Spezifikation für die Interoperabilität des Teilsystems „Infrastruktur“ des Eisenbahnsystems in der Europäischen Union, 18. November 2014
- [4] EN 14067-5:2006+A1:2010, Railway applications - Aerodynamics, Part 5: Requirements and test pro-cedures for aerodynamics in tunnels; January 2011
- [5] Huber A., Langner V., Tunnel Aerodynamics on Costal Line – Full Scale Test, Aerodynamic Analysis – Full Scale Test, Report GRUNER R215'034'000 for SWECO Infra & Rail, Helsinki, 12.01.2022
- [6] Vardy, A., Reinke, P., Estimation of train resistance coefficients in tunnels from measurements during routine operation, Proc. Instn. Mech. Eng. VI 213 Part F, 1999

# INCREASING SAFETY AND SECURITY BY USING MODERN INTERDISCIPLINARY APPROACHES FOR UNDERGROUND FACILITIES

<sup>1</sup>Nina Gegenhuber, <sup>1</sup>Robert Galler

<sup>1</sup>Montanuniversitaet Leoben/Chair of Subsurface Engineering, AT

## ABSTRACT

In the last couple of years, the need for extended safety and security methods in underground facilities for users, operators and emergency services became more and more important. Especially when it comes to terroristic attacks or accidents in underground structures where toxic gases and hardly any visibility can be part of, emergency services need to be as good as possible supported and protected. Therefore, various projects starting with a robot for mapping, augmented/virtual and mixed reality applications or navigation systems are carried out at ZaB - Zentrum am Berg in Eisenerz, a tunnel research, development, training and education facility, belonging to the Montanuniversität Leoben. This enables safety-related research without prejudice to the necessary operating times and high availability of conventional traffic tunnels. For the generation of a situational picture, the 3D representation of the underground branches of the facility, the recording of the number, the whereabouts of the tunnel users and the effective range of the sensors integrated in the operational and safety systems (BuS) are necessary. The goals also include positioning systems that allow real-time position determination despite darkness, smoke and very high temperatures. The presentation deals with research projects in the above-mentioned fields and some first findings.

*Keywords: emergency services, underground positioning, real-time, safety and security, ZaB*

## 1. INTRODUCTION

Underground structures, such as tunnels, subways or underground stations, represent a major challenge for emergency services due to the extraordinary conditions, especially when it comes to complex scenarios. Poor visibility, smoke development, temperature, emissions, the use of explosives, released hazardous substances (CBRN substances) and structural hazards among the influencing factors, not only place special demands on the emergency services, but also push the equipment and devices to their limit.

Autonomously operating systems for reconnaissance and logistics tasks are currently not available due to the lack of sensors. It is therefore still necessary for the emergency personnel to go directly to the danger areas. Positioning must take place without external infrastructure, since its availability in the event of a disaster cannot be guaranteed. The same applies to any navigable a priori map information. It is therefore necessary to find a positioning system which, without external sensors or infrastructure and without available map data, determines the position of the robot or persons in the tunnel in darkness, smoke and great heat, precisely and reliably in real time, in order to automatically guide them on this basis.

The real-time availability of situation information is an essential prerequisite for optimized command support in underground crisis scenarios. Solutions offer mobile, flexible multi-sensor platforms, rapid data processing, data management and the integration of external information sources. Multi-sensor solutions, on the other hand, also use in-situ installed tunnel equipment such as video cameras. They can provide valuable additional information for the point in time before a dangerous situation occurs and improve the real-time capability of situation picture generation in order to be able to supply the emergency services with current data when they arrive. This data is intended to provide the number and location of infrastructure users prior to

the critical event. In addition, knowledge and models of human behaviour in underground crisis situations are essential prerequisites for the development of technical concepts and innovative assistance solutions. The organization and management of the emergency services must be coordinated in detail with the scenario requirements and structural/spatial framework conditions.

Therefore, research projects focusing on the support in safety and security in tunnels in emergency cases is essential. The Zentrum am Berg gives us the possibility to try and train within these projects in a 1:1 scale. In various projects positioning of people and a robot underground, bringing together virtual and augmented reality for training and emergency cases and testing sensors for smoke and heat are brought together to increase safety and security in tunnels.

## **2. ZENTRUM AM BERG**

With the Zentrum am Berg on the Styrian Erzberg, the Montanuniversität Leoben operates an independent research infrastructure for the construction and operation of underground facilities which is unique in Europe. The facility consists of an extensive tunnel system and enables research and development on a 1:1 scale as well as education and training under real conditions.

The underground research facility consists of two parallel railway tunnels, two parallel road tunnels and a test tunnel (Fig. 1). The tunnels can be reached via three entry portals and are connected underground by a cavern. A total of five different tunnel tubes are therefore available for research and test purposes. The facility enables national and international research projects to be carried out on a wide range of issues along the entire life cycle of underground facilities:

- Geotechnical monitoring
- Numerical simulation in geotechnics
- Safety research, safety technology/ventilation, tests of fire detection and fire protection devices, risk management
- Rescue Conditions
- Thermo and aerodynamic issues
- Long-term stability and durability of materials
- Rehabilitation of underground structures
- Impact of climate change: mudslides, rock fall, landslides and forecasting technologies
- Innovative and low-vibration driving methods
- Equipment technology such as control systems, gate systems (tightness requirements vs. dirt) or electrical equipment in the railway tunnel

The fully equipped road, railway and test tunnels allow a wide variety of training options and test executions for emergency services, as well as for operating and maintenance personnel. This should make a decisive contribution to increasing the safety of users of underground transport systems.

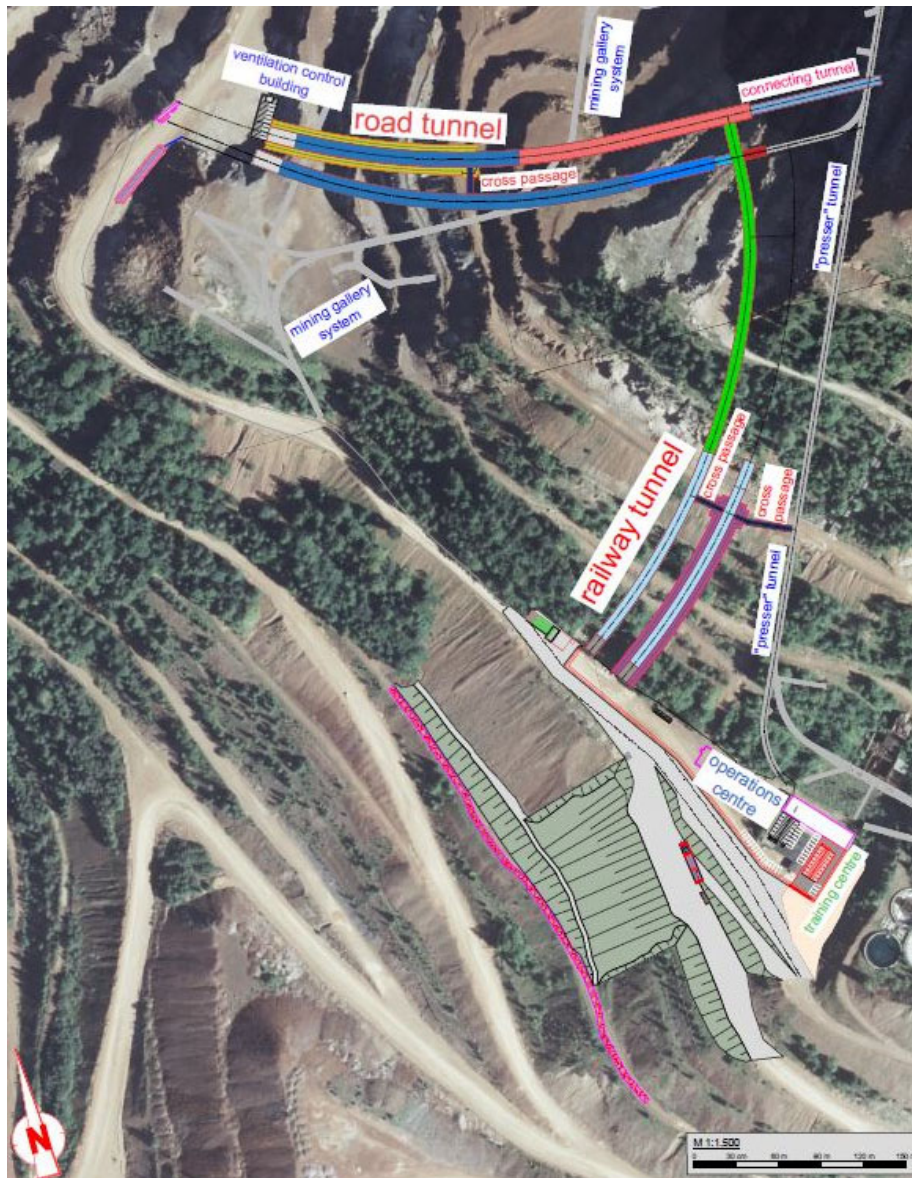


Figure 1: Overview Zentrum am Berg in Eisenerz (Styria)

The instruction of service and maintenance personnel should also take place on the basis of training courses and the practical training for relevant professions should be settled.

- Testing of evacuation scenarios using different protection and control devices, signaling technology and others
- Experiments with automated firefighting systems
- Training for very high fire loads (e.g. truck fire)
- Impact of different operating scenarios for plant and operating technicians and optimized handling of maintenance processes
- Training of relevant professions

The Zentrum am Berg serves researchers, students, emergency organizations, industry, as well as operators and users of the road and rail infrastructure as an event infrastructure and international hub. This is intended to initiate excellent, international and interdisciplinary cooperation in the field of underground research.

### 3. PROJECTS OVERVIEW

The first important approach for safety is the position of people or a robot within the underground infrastructure. Navigation of the robot and the blue on blue problem from the military are just two issues, which need to be solved. Due to the multidimensional branching of underground structures and the limited view and the resulting difficulties in orientation, the precise positioning of one's own forces is essential for survival. Therefore, NIKE Bluetrack deals with a blue force tracking system (Fig. 2) that provides the location information of the own forces on a map to commanders. In underground structures (e.g. tunnels or subways), the localisation is challenging due to the lack of GNSS signals.



Figure 2: Test subject with sensors mounted on helmet and shoes. [1]

First outputs including detailed analyses of the tests, algorithms and analysis with IMU and UWB are summarized in [1]. Those first results are promising and the final tests are planned at ZaB in summer.

The multidisciplinary use of semi-autonomous robots equipped with sensors for supporting analysis tasks, on the one hand, enables situation-adapted deployment techniques and quick decision-making. On the other hand, intelligent, mobile and portable multi-sensor solutions directly on site and on the person, as well as the real-time generation of an overall situation picture, can provide support for the safety of the emergency services.

In the two KIRAS projects ROBO-MOLE and NIKE-SubMoveCon, this is considered from two different perspectives, one with an autonomous robot and the other with equipment for the emergency services and with installed tunnel equipment that meets current standards. [2]



Figure 3: Laser scan data by RIEGL at ZaB

Within ROBO-MOLE first measurements carried out, have been laser scan data by RIEGL Laser Measurement Systems GmbH at ZaB. The tunnel structure was scanned down to the centimetre in order to obtain an up-to-date inventory of the tunnel structure with all its installations (Fig. 3). Further experiments included fire tests to see, where the limitations of the various sensors for the robot (Fig. 4) are. The selected sensors are IMU, thermal cameras, laser scan, RGB camera, odometry and CBRN sensors for positioning of the robot and deliver further information for the emergency services. Especially the smoke from a fire is challenge for the various sensors. Final tests of the full robot system will be conducted in October.



Figure 4: Fire tests for the sensor evaluation (railway tunnel, ZaB)

Further experiments with video cameras and thermal sensors from Joanneum Research were carried out. In order to be able to support the generation of a picture of the situation, a localization of the direction of movement and the position of individual people is a prerequisite for clarifying the situation, where and how many people were in the underground facility. The video cameras have different orientations and installation locations within the ZaB tunnel system, which must be determined metrologically.



Figure 5 shows those control points that are helpful in determining the orientation of a video camera and must be provided as a 3D position. Such thermal camera recordings serve as the basis for further tasks in generating situation images for any crisis scenarios. The technical implementation of converting the video cameras of the tunnel equipment into a measuring system is being carried out in cooperation with Joanneum Research Forschungsges.mbH. The areas of responsibility of the partners in NIKE-SubMoveCon break down into the provision of image material, control points and first approximate values for the camera parameters by the ZaB and the calculation of the camera parameters and image processing by Joanneum Research.

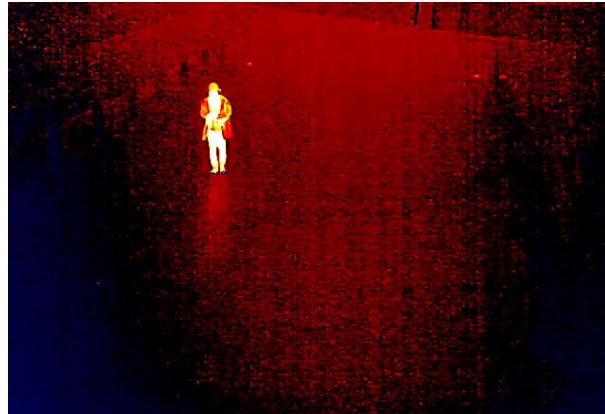


Figure 5: Thermalvideo -camera with a person visible (NIKE Submovecon)

Two new projects started last autumn: NIKE DHQ-Radiv and NIKE Med. Both include first results from the other already existing projects and intertwine. NIKE DHQ-Radiv is an essential sub-project of the overall NIKE program and will develop the process of rapid data integration and visualization of this information in a truly comprehensive Common Operational Picture [3]. It is important to ensure the lateral continuity of different visualization systems in the entire reality - virtuality continuum (2D & 3D & Mixed Reality). Only individual applications are actually available, there is currently no collaborative collaboration option.



Figure 6: Usage of Virtual Reality (VR) for mission preparation. (Pictures: ÖBH/laabmayr)

NIKE Med evaluates the required and available emergency capacities, develops an application to optimize care for responders, and identifies development needs for building strategic reserve capacities. NIKE Med makes an essential contribution within the framework of the NIKE research and development program to achieving full operational readiness of a specialized task force with the capability to operate underground, thus adding essential value to state crisis and disaster management. At this stage of the project the needs of the various emergency services is evaluated as input for the planned app.

#### 4. CONCLUSIO

The projects NIKE Bluetrack, ROBO-MOLE and NIKE-SubMoveCon complement each other perfectly and are a first example of interdisciplinary approaches in disaster management. The safety of the emergency services and optimal support for them in the event of a complex emergency is the top priority. The results of these projects will contribute to supporting emergency services and protecting lives in dangerous situations. Positioning within an underground structure is essential and can be realized with those projects for the future. All projects have various emergency service partners, to make the research output practical in operation. The new projects NIKE DHQ Radiv and NIKE Med, extend the already running projects and add new developments on the one hand with the various mixed, augmented and virtual reality applications, which already used for different training and on the other hand include the medical input which results in complex scenarios. The overall target is to make underground structures safer for users and emergency services, who risk their lives to safe others.

#### 5. REFERENCES

- [1] Mascher, K., Watzko, M., Koppert, A., Eder, J., Hofer, P. and Wieser M., 2022, NIKE BLUETRACK: Blue force tracking in GNSS-denied environments based on the fusion of UWB, IMUs and 3D models, Sensors, submitted
- [2] Wenighofer, R., Gegenhuber, N. and Perko, R., 2021, Interdisziplinäre Unterstützung für Einsatzkräfte bei Untertage-Katastrophenszenarien, DRD 2021, Universität Innsbruck
- [3] Hofer, P., Eder, J., Hager, L., Strauß, C and Jacobs, S., 2021, RApid Data Integration and Visualization (RADIV) in Complex Subterranean/Subsurface Operations, ATC<sup>2</sup>, Leoben

#### 6. ACKNOWLEDGEMENT

Significant parts of the developments presented are funded by the FFG in the following projects:

FFG-Nr. 879691, NIKE Bluetrack (Nachhaltige Interdisziplinarität bei Komplexen Einsätzen unter Tage / BLUE Force TRACKing), Partner: OHB Digital Solutions GmbH, IL-Ingenieurbüro Laabmayr & Partner, BMLV, TU Graz

FFG-Nr. 879720, NIKE-SubMoveCon (Nachhaltige Inter-disziplinarität bei Komplexen Einsätzen unter Tage - Subsurface Movement Control), Partner: Joanneum Research Forschungsgesellschaft mbH, Montanuniversität Leoben, Ingenieurbüro Laabmayr & Partner, IFR - Ing. Richard Feischl, Experience Research & Consulting, BMLV, ASB Stmk.

FFG-Nr. 879693, ROBO-MOLE (ROBOtik für 3D-Mapping, Orientierung und Lokalisierung bei untertägigen Einsatz-szenarien) Partner: Montanuniversität Leoben, AIT Austrian Institute of Technology GmbH, Berufsfeuerwehr Graz, Berufsfeuerwehr Innsbruck, Bundesfeuerwehr Linz, BMLV, CBRN Protection GmbH, DCNA, e-netic, IQSOFT Gesellschaft für Informationstechnologie m.b.H., JOANNEUM RESEARCH Forschungsgesellschaft mbH, RIEGL Research Forschungsgesellschaft mbH, Technische Universität Graz (Institut für Software-technologie und Institut für Geodäsie/Arbeitsgruppe Navigation)

FFG-Nr. 886340, NIKE Med (Nachhaltige Interdisziplinarität in Komplexen Einsätzen - MEDical treatment), Partner: SimCampus, Mindconsole GmbH, DCNA, IL Laabmayr & Partner, Universität Innsbruck, BMLV

FFG-Nr. 886302, NIKE DHQ Radiv (Digital Head Quarter-Entwicklung RApid Data Integration and Visualization als Kernprozess der Stabsarbeit), Partner: Syncpoint GmbH, Realsim, IL Laabmayr & Partner, Meixner Vermessung, BMLV, OHB Digital Solutions GmbH, JOANNEUM RESEARCH Forschungsgesellschaft mbH

# FEASIBILITY STUDY INTO THE IMPLEMENTATION OF ZERO FLOW TUNNEL VENTILATION IN THE SCHIPHOL KAAGBAAN TUNNEL

Hans Beljaars

Royal HaskoningDHV Netherlands

## ABSTRACT

The Schiphol Kaagbaan tunnel had to be refurbished to meet the European Standards. Due to secondary requirements from stake holders, an investigation was started to determine whether removing the evacuation corridor and using a Zero Flow Ventilation strategy was a viable option. Three steps were taken to reach a final design choice. In the final step, the Feasibility Study, the two most decisive requirements of the authorities were 1) to prove the concept through a CFD-simulation and 2) to prove the equivalence of the Zero Flow Ventilation compared to a traditional evacuation approach. Due to remaining risks it was eventually decided to adapt stake holder requirements and implement an adapted evacuation corridor for egress.

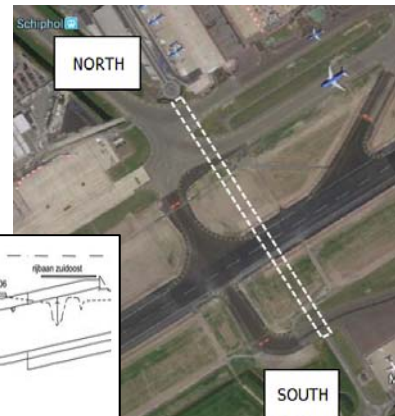
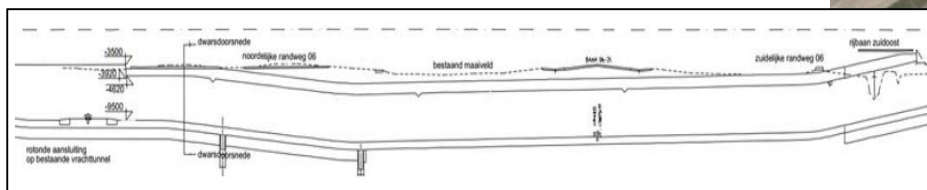
*Keywords: Zero Flow Tunnel Ventilation, conceptual ventilation design, CFD simulation.*

## 1. INTRODUCTION

At Schiphol Amsterdam Airport in the Netherlands renovation of the existing Kaagbaan tunnel (airside) was required. This was needed because following the new Building Permit requirements the European directive 2004/54/EC had to be implemented. The Kaagbaan tunnel is located under the Kaagbaan runway and is designed for bi-directional traffic. The tunnel was built in 1997. Before refurbishment, the tunnel had no escape doors and no ventilation system, but it had several CCTV cameras and a horizontal dry riser system with fire hydrants placed every 50 meters. It is partly built as an immersed tunnel and partly as a cut and cover tunnel. It is predominantly used for the transport of personnel, luggage and fuel.

**Fehler! Verweisquelle konnte nicht gefunden werden.)**

Location (right) and a longitudinal cross section

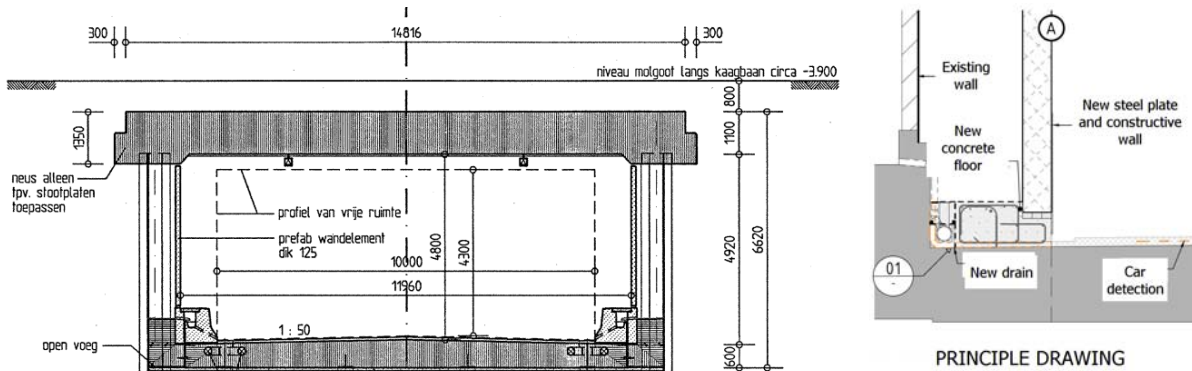


of the Kaagbaan tunnel

## 2. ORIGINAL SCOPE OF WORK / DESIGN CHANGE

To achieve the required safety level, one of the main requirements was an evacuation route that was separated from the traffic tube by a wall. The minimum width required for an evacuation route corridor in an existing tunnel in the Netherlands is 0,70 meter. During the construction phase a requirement regarding the maximum collision impact of the dividing wall was updated. A new civil design of the evacuation route wall was necessary and resulted in the implementation of a thicker wall. The minimum evacuation route corridor width and the

minimum required road width of 10 meter did not fit in the existing civil tunnel construction anymore. To complicate things further, an additional request from Stakeholder 'Asset Management' was to keep the tunnel operational during renovation works. By leaving out the evacuation route corridor and implementing 'Zero Flow Ventilation' (ZFV), a solution to these problems could be found. (See paragraph 3.1 for an explanation of ZFV.)



**Fehler! Verweisquelle konnte nicht gefunden werden.)** Original tunnel cross section and (part of) the evacuation route corridor.

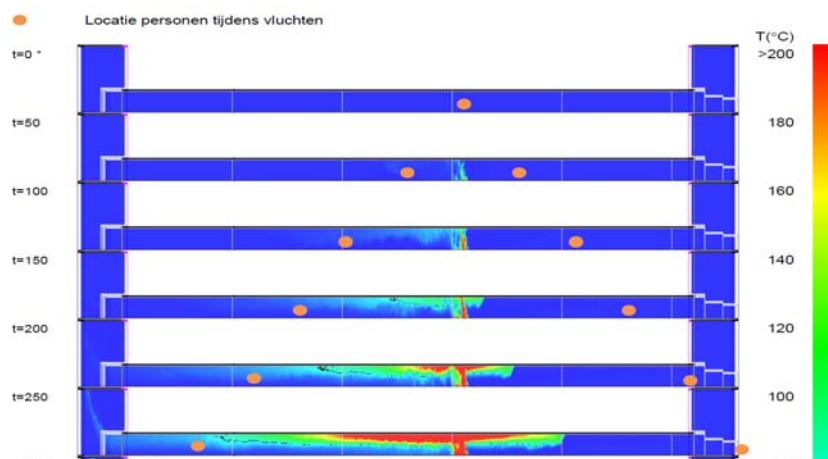
### 3. IMPLEMENTING A NEW VENTILATION CONCEPT.

The issue came to light just before the start of actual construction works in 2018. An updated tunnel ventilation design and the design changes would have a large impact on the tunnel safety concept. To implement the new tunnel safety concept during this phase of the project several steps had to be taken in a very short period. According to the license, the tunnel had to be renovated before May 2019. Initially, a high-level management report was necessary to describe the existing design, update the requirements and describe the ensuing construction steps in the project. The background and underlying reasons for the possible design changes had to be described in relation to current and future safety concepts, including the effect on the tunnel's technical systems. The management report was accepted and a plan for the implementation of the design changes had to be set up. The first step was to gather more detailed information in order to understand all related consequences. The second step was a Feasibility Study which contained a description of all the relevant consequences. This study had to include the project interfaces, risk assessments, cost assessments, a trade off matrix, etc. The third step, combined with the second step, was an inventory of the consequences related to the stakeholders such as 'Asset Management' and 'Operations', the Schiphol Tunnel Safety employee, the Fire Department and other authorities. All the consequences of implementing a new safety concept had to be elaborated. Based on this report the Schiphol Board made its final decision. The implications of the new safety concept for the project costs and schedule were large. For the implementation of Zero Flow Ventilation a new detailed design would be necessary. In December 2017 the initial management report was completed, the preliminary study was finished in January 2018 and the Feasibility Study was developed from February up to April 2018.

#### 3.1. Zero Flow Ventilation

With Zero Flow Ventilation the air velocity in the tunnel is kept at a low speed so pedestrians can evacuate the tunnel before the heat or smoke reaches dangerous levels at their egress position. It uses variable speed jet-fans to control the impulse, and thus the air velocity, induced by the jet-fans. The direction of the jet-fan air flow is controlled and will be the opposite direction of the existing air velocity in the tunnel. The system can manipulate the maximum air velocity in the tunnel within a short period of time within boundaries of -0,5 to +0,5 m/s.

This air velocity is low enough to allow healthy people to evacuate the tunnel safely at both sides. A swift startup of the Zero Flow Ventilation system is required to reduce the air velocity in the tunnel quickly and allow enough time for accident awareness, including the escape reaction, of the tunnel users to start egress. Several systems are used for this awareness. A swift automatic response or a manual response by the tunnel operator can be achieved by implementing the correct protocols, continuous measurement of wind speed and wind direction and technical facilities like Traffic Low Speed Detection, Linear Heat detection and CCTV-cameras.



**Figure 3)** Escaping pedestrians (orange dots) able to stay ahead of smoke and toxic gasses.

### 3.2. Preliminary Study

In this study the system uses two clusters of four jet-fans each. The jet-fans are placed 100 meters from the tunnel entrances. This configuration was determined by the 1D-simulation performed by the supplier of ZFV control cabinets, the company Sohatsu (Kobe, Japan). The jet-fans are not located directly at the tunnel entrance to avoid a short circuiting of air (the exact positioning, the number of fan clusters, the number of jet-fans and other parameters are to be validated later with Computational Fluid Dynamics modelling (CFD)). The decrease of air velocity is examined in this phase with the help of 1D-simulations. This was done for different scenario's and with various locations of the fire. If a fire starts in the proximity of a jet-fan cluster the thrust of that jet-fan cluster will be reduced. The thrust can be negligible, depending on the exact exposure of fans to high temperatures and the air temperature.

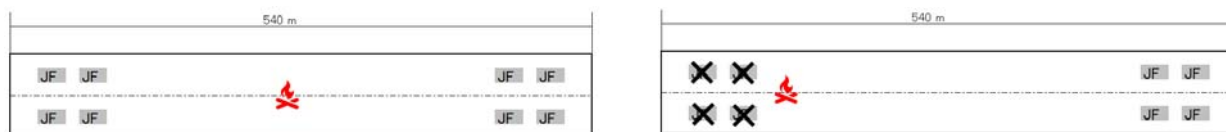
#### 3.2.1. Starting point fire scenarios for the Preliminary Study.

Taking into account the various scenarios and using past experiences resulted in a design with four jet-fans at each portal. This preliminary study had to prove whether ZFV would be able to reduce the air velocity in a short period of time and in a short and wide tunnel such as the Kaagbaan tunnel.

#### Main starting points

Measurements and calculations have shown a maximum air velocity in the tunnel of 4 m/s due to wind and traffic. It was assumed that healthy tunnel users can walk at 2,2 m/s. To allow the person to evacuate the tunnel safely a longitudinal air velocity reduction of 2 m/s within 60 seconds needs to be achieved. After this period of 60 seconds a further reduction to 0 m/s is intended. In the scenario where a fire is not in the vicinity of the jet-fans, all eight jet-fans can operate to control airflow velocity. In case of a fire close to a cluster of jet-fans, only the other cluster of jet-fans can reduce the air velocity conform the limitations. The impulse created by the cluster close to the fire is unknown because of their exposure to high temperatures. In this study two simulations for the behavior of air in the tunnel have been conducted: one simulation

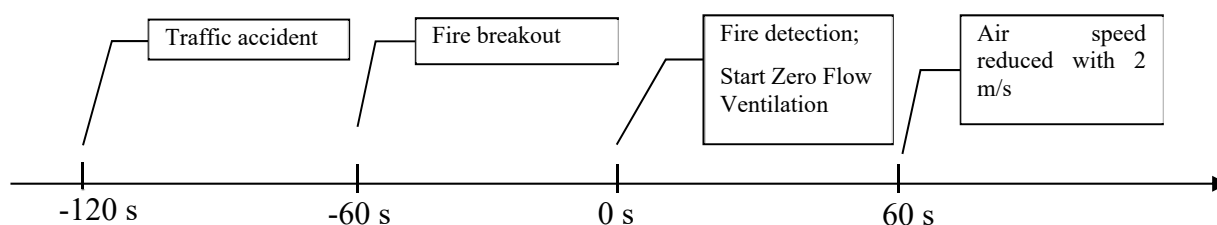
with one active cluster of jet-fans operating and one simulation with both clusters of jet-fans operating. The two scenarios are compared in order to examine the effectiveness of the clusters and to determine if more jet-fan clusters are required.



Fehler! Verweisquelle konnte nicht gefunden werden.) Fire locations with four or eight jet-fans in operation.

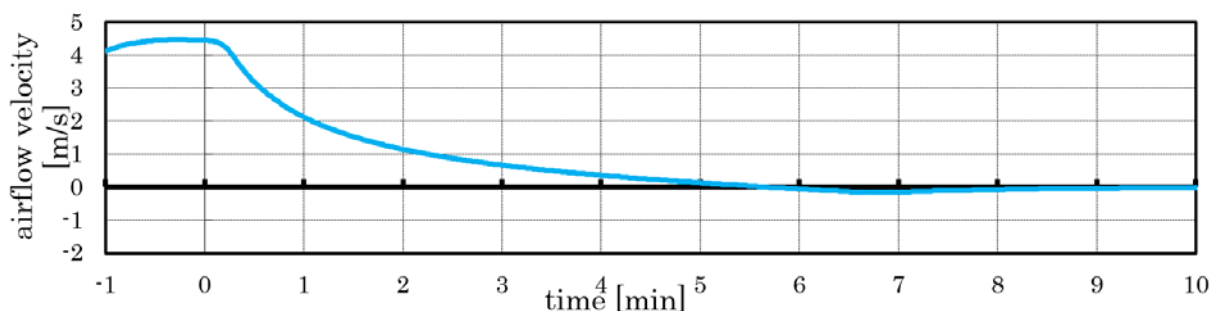
### Fire Breakout Scenario

The fire breakout scenario is defined by three events: traffic accident at time  $t = -120$  s, fire breakout at time  $t = -60$  s, and fire detection at time  $t = 0$  s. As the Zero Flow Ventilation control is initiated by fire detection, the system starts operating at  $t = 0$  s. For the Kaagbaan study it was vital to establish the period that the system requires to control the airflow in the tunnel. The target was set at 2 m/s air velocity reduction within the first 60 seconds.



Fehler! Verweisquelle konnte nicht gefunden werden.) Time sequences

### 3.2.2. Results



Fehler! Verweisquelle konnte nicht gefunden werden.) 1D simulation result; scenario with 4 jet-fans operating.

Fig. 6 shows the reduction of airflow velocity where only one active cluster of jet-fans is operating. The airflow velocity is reduced to 2 m/s within 60 seconds. Calculations with two active clusters of jet-fans illustrate that zero-flow ventilation can reduce the airflow velocity to less than 2 m/s within 30 seconds, and a further reduction to 0 m/s within 120 seconds after activation at  $t = 0$  s.

**Conclusion in December 2017:** a Zero Flow Ventilation system is effective in a short and wide tunnel such as the Kaagbaan tunnel. The required thrust and the number and type of jet-fans will be determined at a later stage during the Feasibility Study. Then there will be more clarity about the system requirements, the type of fires that and the various scenarios.

*In January 2018 several stakeholders (including the local Authorities, the tunnel owner, the tunnel safety authority, the Fire Department) came together for a scenario analysis session*

with regards to fire and other calamities in the Kaagbaan tunnel. Consensus was achieved on how all systems and authorities should operate following fire detection and the response to calamities. The scenario analysis gave insight into the procedures in case of fire when a Zero Flow Ventilation System is in operation. It became clear that this safety concept would only be accepted after a proven and agreed safety case. A detailed CFD-model showing the safe evacuation of tunnel users would be accepted as proof. An independent third party was to conduct the CFD-modeling. As required by local regulations, when an alternative system is to be used, the performance of that system should be equal or better than the previously used system. This needs to be proven for the aspects Safety, Environment, Use, Energy and Health. Safety appeared to be the most important subject for implementation of ZFV at this stage. It was also decided that the walking speed of evacuating healthy pedestrians was reduced from 2.2 m/s to 1.6 m/s in the models to meet requirements in other standards. The air velocity in the models as result of the outside wind influences was increased to the conservative value of 5 m/s.

### 3.3. FEASIBILITY STUDY

The feasibility study was important to prove that the implementation of this new ventilation concept was possible. Three subjects in the feasibility study, shown in bold and underlined below, were the most important aspects that could cause the discontinuation of the implementation of a ZFV-system.

Table of contents of the feasibility study with most relevant subjects highlighted:

1. System architecture
2. Performance of the system
  - a. **CFD analysis**
  - b. Energy availability
  - c. Electromagnetic Compatibility (EMC)
  - d. Civil impact
  - e. RAMS
  - f. Maintenance
3. Total Cost of Ownership
4. **Building Permit / Safety Analysis**
5. Risk Analysis
6. Time Schedule
7. Contractual impact

#### **Item 2a: CFD analysis**

An independent consultant *Efectis NL* created the CFD-simulations in conjunction with *Royal HaskoningDHV*. Stakeholder requirements, the civil, mechanical, electrical parameters, the fire and smoke scenarios and the response scenarios had to be agreed upon with the various stakeholders. The critical parameters to be used in the models had to be agreed upon before the simulations could be started. Critical parameters such as the air temperature, air quality and radiation are shown in figure 7.

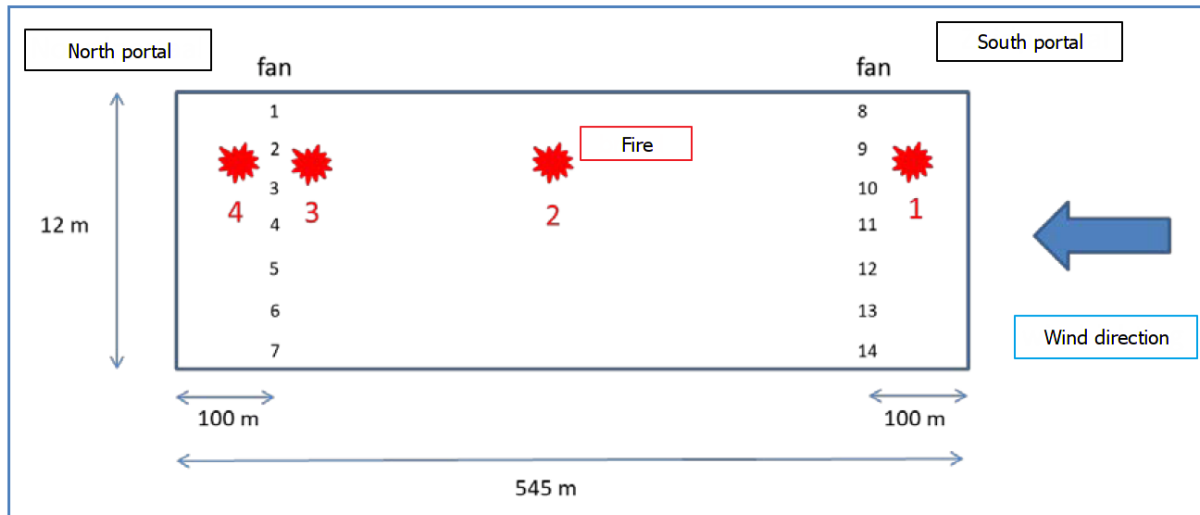
	<b>Critical Parameter</b>	<b>Acceptance Value</b>
1	<b>Sight distance</b> on light emitting subjects in horizontal direction at 2.5 m height:	$\geq 30$ meter
2A	<b>Temperature</b> over the total height of the smoke layer:	$\leq 200$ °C.



2B	If the temperature of the top of the smoke layer is > 200 °C. and at the bottom is < 200 °C. then: <b>heat radiation</b> at 2.1 meter:	$\leq 2.5 \text{ kW/m}^2$
----	--	---------------------------

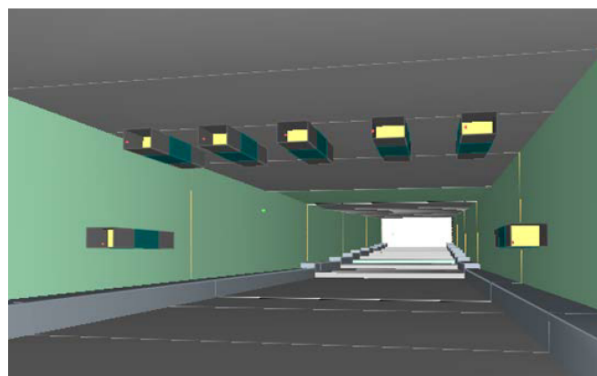
Figure 7) Critical values

The 1D simulation was completed to determine the necessary impulse and thus the required number of jet-fans. A scenario analysis led to 4 critical scenarios and several additional starting points such as the maximum wind influences, available electrical power, etc. Four locations of a fire are important (Figure 8).



Fehler! Verweisquelle konnte nicht gefunden werden.8) The four decisive fire locations

The simulation program Fire Dynamic Simulator (FDS v6.6.0) and the visualization program 'SmokeView' were used. The Dutch Ministry of Infrastructure has validated this simulation program since 2003. The following parameters were placed in the model: the geometry of the civil construction, jet-fans with accompanying airflow patterns, the jet-fan maximum operational temperature of 300°C, location based grid sizes including the accompanying time steps were important to receive correct simulation results around the decisive locations. The model contained more than 1.1 billion cells. The largest cells were 0.4x0.5x0.33 and the smallest cells were 0.4x0.25x0.16 (in meters). Later on a 'cold' CFD simulation was carried out for the verification of the 1D calculation and other traffic parameters like the positions of vehicles, fans etc.



Fehler! Verweisquelle konnte nicht gefunden werden.) Cross section of the tunnel with one of the two clusters of seven jet-fans

From the models it was determined that 2 jet-fan clusters of 7 jet-fans (thrust 540 N each) were required. During the scenario analysis it became clear that the third scenario (fire at location 3, see figure 8) was the decisive scenario. In this scenario the visibility conditions were poor as soon as the fire started. Additional CFD's were run to show what would happen in the location around the fire in the first two minutes after a fire started. See fig. 10 and 11.

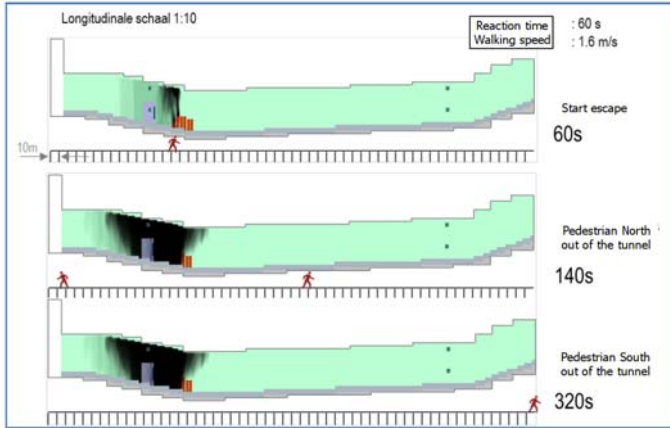


Figure 10:  
Smoke dilution and  
evacuation positions in  
scenario 3.

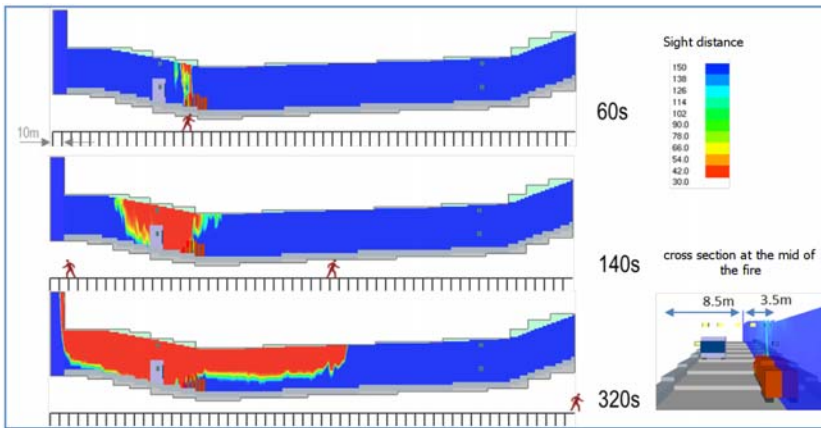
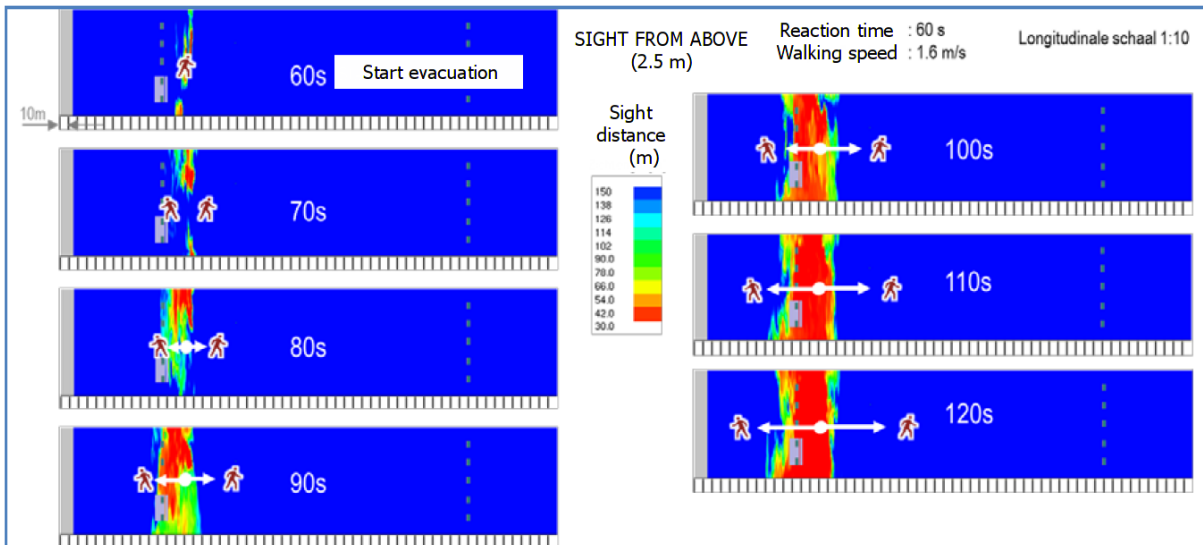


Figure 11:  
Sight distances to light  
emitting objects and  
evacuation positions in  
scenario 3.

Picture left: side view.  
Picture below: top  
view.



From the illustrations above it can be concluded that the sight distance to illuminating objects in evacuation positions will always be 30 meters or more. From  $t = 90$  s evacuees will escape in both directions in front of the moving smoke blanket. Heat radiation also stays within

acceptable limits, the illustration showing this is not included in this paper. Conclusion: with a reaction time of maximum 60 seconds from the start of the fire and with a walking speed of 1.6 m/s, safe egress is possible in all the scenarios.

(CFD motion pictures will be shown during the presentation at the conference in May 2022.)

#### **Item 4: Building Permit / Safety Analysis**

The reason for the whole project was to obtain an updated Building Permit. Approval of the original tunnel design would have been received from the local authorities without any issues. By deviating from the original tunnel design and introducing a different tunnel safety and ventilation concept, such as ZFV, risks were introduced in the Permit Application process. The table below is a comparison between the original and the proposed new variant on important aspects:

<b><u>Building Permit 2012</u></b>	<b><i>Variant 'Evacuation route'.</i></b>	<b><i>Variant 'Zero Flow Ventilation'.</i></b>
<b><i>Decisive aspects</i></b>		
1) Evacuation route		
- Self-rescue	+	0
- Rescue assistance	0	+
2) Ventilation		
- Health	0	+
- Self-rescue	0	0
- Rescue assistance	0	0 / +
3) Reliability		
- System reliability	0	0 <sup>1)</sup>
- Installation reliability	0	0 / - <sup>2)</sup>

- 1) The system reliability had to be proven in a CFD report (as described in chapter 3).
- 2) The reliability of the technical installations had to be proven by a RAMS report. To meet requirements several additional redundant systems were required.

#### **4. PROJECT PROGRESS AFTER THE FEASIBILITY STUDY AND CONCLUSION**

During the process from January to April 2018 an additional Impact Analysis as well as a Risk Analysis were carried out. The conclusion from these analyses was that the risks and impact of a non-approval of the Building Permit application as well as some of the technical risks were too large. Schiphol decided that the disadvantages from the 'Evacuation route' variant (narrower road and 6 – 8 months of traffic obstructions due to building activities) were not large enough to revise the project design to a Zero Flow Ventilation design concept and changed these initial requirements.

The renovation project 'Kaagbaantunnel' was finished with an accepted time delay by the Authorities in December 2019 using the original concept of an evacuation route corridor.

With the results of this Feasibility Study, it is concluded that Zero Flow Tunnel ventilation can be part of a safe(r) evacuation strategy in bi-directional tunnels with or without an escape gallery. For implementation in projects additional time and cooperation of authorities is needed when legislation aspects are debated. Certainly for countries where Zero Flow Tunnel Ventilation systems are not common practice.

## 5. REFERENCES

Lemaire A., E. Ferad (2018) *CFD berekeningen Zero Flow Ventilatiesysteem Kaagbaantunnel Schiphol*. Schiphol Group. (SNBV)

Nakahori I., Sakaguchi T., Kohl B., Forster C., Vardy A. (2016) *Risk assessment of zero-flow ventilation strategy for fires in bidirectional tunnels with longitudinal ventilation*. BHR Group.

# VENTILATION STRATEGY AND DESIGN OF INTERTWINING TUNNELRAMPS, OOSTERWEEL LINK ANTWERP

<sup>1</sup>T. Bouwhuis, <sup>1</sup>T.J.A. Dolle, <sup>2</sup>A.J.M. Snel  
<sup>1</sup>RoTS / Witteveen+Bos, Amsterdam, The Netherlands  
<sup>2</sup> Lantis / RoTS, Antwerpen, Belgium

## ABSTRACT

The Antwerp Oosterweel Link will consist of 5 intertwined TERN-tunnels (Trans-European Road Network tunnels), which will be, together with underpasses and depressed highways, all operated, controlled and secured by an integral safety concept.

The most interesting tunnel complex of the Oosterweel Link, in terms of tunnel safety and tunnel ventilation, are the 2x2 stacked Kanaalzone tunnels. Near the Oosterweel junction intertwining ramps of the Kanaalzone tunnels create a specific geometry regarding tunnel safety and smoke control.

The paper presents analyses of the preliminary design of the ventilation system of the Kanaalzone tunnels, comprising 74 jet-fans, and the accompanying ventilation strategy.

The following steps in analyzing the smoke control can be determined:

- basic ventilation design, based on probabilistic analysis;
- quasi one-dimensional pressure balance relations;
- cold (smoke-free) CFD-simulations to analyze the system behavior in detail;
- hot-run CFD-simulations to analyze the smoke behavior and to optimize the ventilation strategy.

Relevant preliminary results are:

- Full jet-power on all fans is not always the best solution for smoke control in intertwined tunnel tubes.
- Air balances between the tubes are important for effective smoke control in interconnected ramps and are affected by many parameters.
- Interconnected tunnel tubes require a ventilation strategy on cluster level instead of tube level.

*Keywords: Tunnel ventilation design, intertwined tunnels, Oosterweel Link.*

## 1. INTRODUCTION

In order to improve the traffic flow around the city of Antwerp, the existing ring road R1 will be closed by the Oosterweel Link. The Oosterweel Link consists of 5 complexly intertwined TERN tunnels, a number of underpasses and several kilometres of depressed highways.

### 1.1. Oosterweel Link Antwerp

The existing ring road of Antwerp is not a full circle: it lacks a direct connection between the west and the north side of the city, including a second crossing of the Schelde river (figure 1-1). With increasing expected traffic densities this leads to more and more problems regarding traffic management, incident handling, noise and pollution.

By closing the ring road with the Oosterweel Link the traffic flow will improve, the possibilities for integral traffic management will grow and the port of Antwerp will become better accessible.

The Oosterweel Link consists of 5 tunnels: the Schelde tunnel (crossing the Schelde river), the Kanaalzone tunnels (crossing the port), the OKA tunnel (crossing the Albert channel), the Luchtbal tunnel and the Schijnpoort tunnel (both under passing urban areas). Further the link consists of the Oosterweel junction, a depressed infrastructural node that connects the Schelde tunnel, the Kanaalzone tunnels and the local road network north of Antwerp. The link is completed by several depressed highways and underpasses, connecting the tunnels and facilitating the inflow and outflow of local traffic to the link.



Figure 1-1 A) Oosterweel Link as closing element of the existing ring road; B) Components of the Oosterweel Link.

## 1.2. Tunnel safety and road safety

The safety concept of the Oosterweel Link is based on two pillars: tunnel safety and road safety. Tunnel safety starts by complying to the EU directive 2004/54/EC on minimum safety requirements for tunnels in the Trans-European Road Network (TERN) and its translation in the Belgian legislation. Next to this a quantitative risk analysis (QRA) has to be performed for every tunnel tube, in which a variety of parameters regarding the geometry, the traffic and the safety measures have to be taken into account. The calculated group risk has to be checked against the legal standard, that limits the chance of casualties at  $0.1/N^2$  per kilometre of tunnel tube per year (with N the number of casualties per incident). In the final design iteration all tunnels of the Oosterweel Link comply to the legislation and the legal standard for the group risk, by applying an elaborate set of safety measures.

The second pillar of the safety concept of the Oosterweel Link is road safety. Road safety starts with a safe road design that complies to the so called “10-seconds rule” in the EU directive 2004/54/EC. This rule puts restrictions on the location of convergence and divergence points in relation to the location of the tunnel portals. Therefore the road design was subjected to a human factor analysis, that checked whether the total road system including all marks and signs is clear to the drivers and can be used safely. Finally an analysis of the dynamic traffic management in relation to tunnel safety was performed in order to guarantee that traffic flows can be guided through the tunnels safely.

## 1.3. Kanaalzone tunnels and Oosterweel junction

The most interesting tunnel complex of the Oosterweel Link, in terms of tunnel safety and especially tunnel ventilation, are the Kanaalzone tunnels. These are 2x2 stacked tunnels with connections to the Oosterweel junction, the Luchtbal tunnel and the OKA tunnel. Near the Oosterweel junction, multiple intertwining ramps of the Kanaalzone tunnels create a complex geometry regarding tunnel safety in general and smoke control in particular (figure 1-2 and figure 3-3).

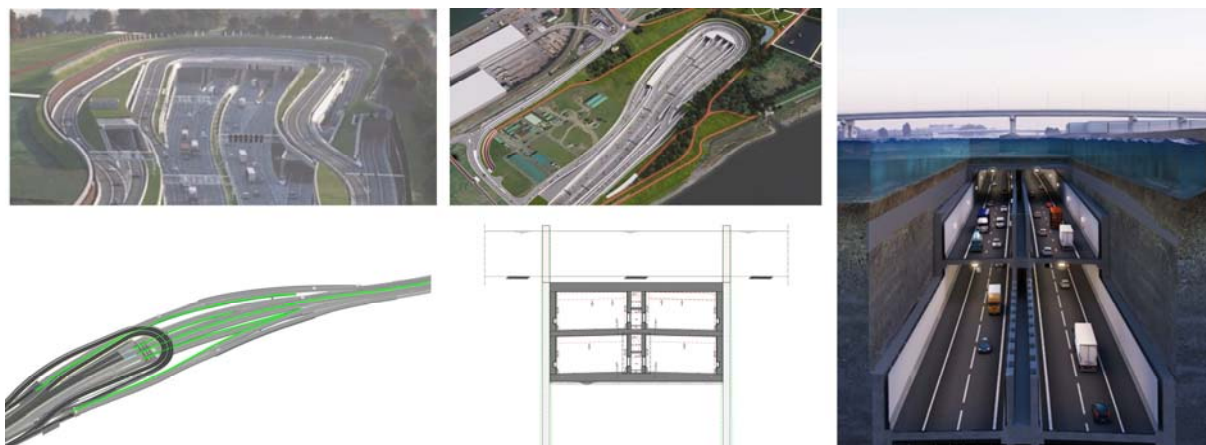


Figure 1-2 Top left: Tunnel portals of the Kanaalzone tunnels (tubes and ramps) at the Oosterweel junction; Top center: Top view of the Oosterweel junction; Bottom left: Schematic overview of Kanaalzone tubes, ramps and escape galleries; Bottom center: Cross section of stacked Kanaalzone tunnels; Right: Impression of stacked Kanaalzone tunnels.

The lower tubes of the Kanaalzone tunnels have a length of approximately 3.5 kilometers and connect the Oosterweel junction in the west to the existing ring road R1 and the new Luchtbal tunnel in the north. In the same way the upper tubes have a length of approx. 3.2 km and connect the Oosterweel junction to the R1 and the new OKA tunnel in the east. The upper and lower tubes are stacked when crossing the docklands and diverge near the Albert channel.

The east side of the Oosterweel junction is not only the entrance and exit of the upper and lower tubes of the Kanaalzone tunnels, but also the connection of the local traffic to the highway system. Therefore two additional tunnels portals are situated at the junction, which are the entrance and exit of the ramps. Although those ramps only have one tunnel portal, they split or merge just behind the portal in order to connect the traffic to both the upper and the lower main tubes. This results in a system of interconnected tubes and ramps that should be studied in detail related to smoke control conditions.

All tunnels of the Oosterweel Link will be equipped with a longitudinal ventilation system, since such a system can handle big fire sizes and can be fitted into the complex geometry of stacked tunnels.

Since Antwerp has one of the biggest ports of Europe, the amount of heavy goods vehicles at the ring road is large, just as the transport of highly flammable materials and fuels. Accidents with these trucks can result in scenarios with fire sizes up to 200MW. A transverse ventilation systems would not be able to control the smoke and heat produced by such fires. Besides, such a ventilation system would be difficult to fit into the complex geometry of the Oosterweel Link. Therefore longitudinal ventilation systems are applied.

## 2. METHOD

When designing the ventilation concept and corresponding ventilation strategy, a number of consecutive analyses with increasing levels of detail are necessary. In this chapter, a brief overview of the different steps is given, while the next chapter elaborates on every individual step and its results.

The probabilistic analysis can only be applied in isolated tunnel tubes however does not account for junctions, hence for design purposes the Kanaalzone tunnels are considered in two parts: the main tube, where probabilistic calculations are applicable, and the intertwining ramps near the Oosterweel junction where separate analyses are required.

The first step in designing the ventilation in the ramps is an analytical calculation, based on the pressure balance in the connected tubes. Hereafter, a detailed analyse is done by means of CFD calculations, first without and then with smoke and fire.

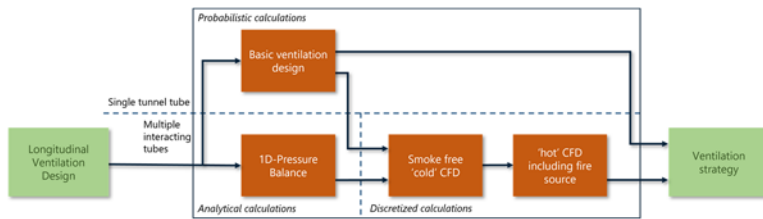


Figure 2-1 Calculation, simulation and design proces for the longitudinal ventilation of the Kanaalzone tunnels.

### 3. ELABORATION AND RESULTS

#### 3.1. Probabilistic analysis

The basic design of the tunnel ventilation system is based on failure rate analyses. Probabilistic calculations determine the failure rate where the critical ventilation velocity is not achieved [1]. This is the minimum air velocity (fire size dependent) that must be achieved by the tunnel ventilation system in order to prevent backlayering of smoke.

The probabilistic calculations account for:

- External conditions: Wind conditions and terrain roughness.
- Tunnel design: Tunnel orientation related to wind, entrance and exit configuration, vertical tunnel alignment (chimney effect), tunnel roughness.
- Traffic: Traffic composition (e.g. number of trucks) and congestion.
- Fire conditions: Fire size and location. The location affects the length of the congested traffic and the chimney effect.
- Ventilation design: Ventilation power, number and locations of fans, fan efficiencies and heat resistance of fans.

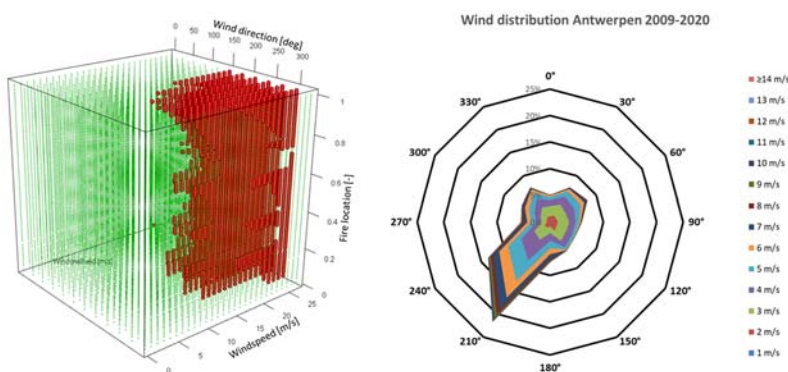


Figure 3-1 A) pointcloud of probabilistic calculations. Green indicates a pass, i.e. the ventilation speed is larger than the critical velocity, a red point indicates a failure; B) The winddistribution of Antwerp: an 11 year average of hourly measurements.

The probabilistic variables in the calculations are the non-dimensional fire location [-], the wind direction [deg] and the windspeed [m/s]. All unique combinations of the variables result in over 30.000 calculations, where a resultant ventilation speed can be compared with the critical ventilation speed.

In the figure above the results are shown for a 200MW fire in the TKZO main tunnel tube. Every green point indicates a situation where the critical velocity is reached, every red data point indicates a failure, i.e. the critical ventilation speed is not achieved. This success- and



failure data is combined with the chances of occurring of a certain wind condition, resulting in the required acceptable level of failure rate, per fire size [2].

### 3.2. Quasi one-dimensional pressure balance relations

The airflow from the main tunnel tube will split, according to a certain distribution, at the location of the exit ramp. At the exit of both branches of the tunnel the outside pressure is assumed to be equal to atmospheric pressure, hence the pressure drop over the tunnel sections 1 and 2 (figure 2-2) must be the same.

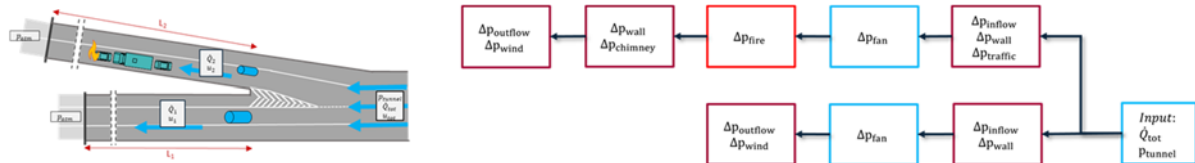


Figure 3-2 A) Simplified situational sketch of an incident at an exit ramp; B) Schematic overview of all contributions to the pressure drop in the incident tube (top row) and non-incident tube (bottom row).

Since some of the resistances faced by the air flow are velocity dependent, there is a volume flow distribution where the following relations hold:

$$\begin{aligned} \dot{Q}_{tot} &= \dot{Q}_1 + \dot{Q}_2 \\ \Delta p_1 &= \Delta p_2 = p_{tunnel} - p_{atm} \end{aligned}$$

In this the pressure drops in branches 1 and 2 are considered to be a summation of all the individual contributions according to the scheme above.

In this scheme, the fans provide a ‘negative pressure drop’ ( $\Delta p_{fan}$ ) and can be determined such that the requested air flow distribution at the junction is reached. This method can be extended to accompany multiple junctions and has resulted in a first ventilation design for the ramps. Merging the designs of the main tubes and the ramps results in the ventilation set-up as presented below.

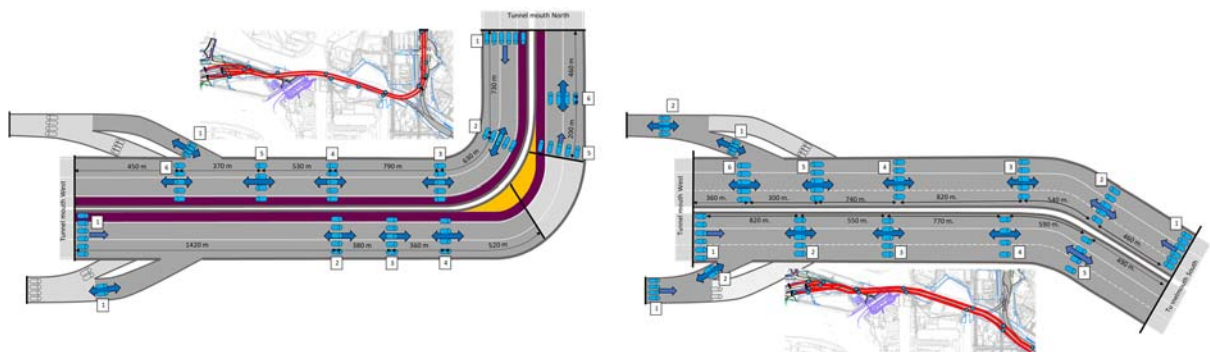


Figure 3-3 Schematic overview of the ventilation design for the Kanaalzonetunnel; A) Lower Kanaalzone tunnel. B) Upper Kanaalzone tunnel.

### 3.3. CFD model

In order to simulate the performance of the tunnel ventilation design in detail a CFD model of the entire Oosterweel junction has been created. The figure below shows an exploded view of the model. The full length of the exit ramps is modelled and over 600 meters of both main tubes. The total length of the geometry is roughly 800 meters. The mesh contains 5.5M cells of 0,5m x 0,5m x 0,5m, in line with [2]. The boundary conditions represent a wind pressure on all tunnel exits and a fixed inflow from the main tubes in line with earlier results (section 3.1).

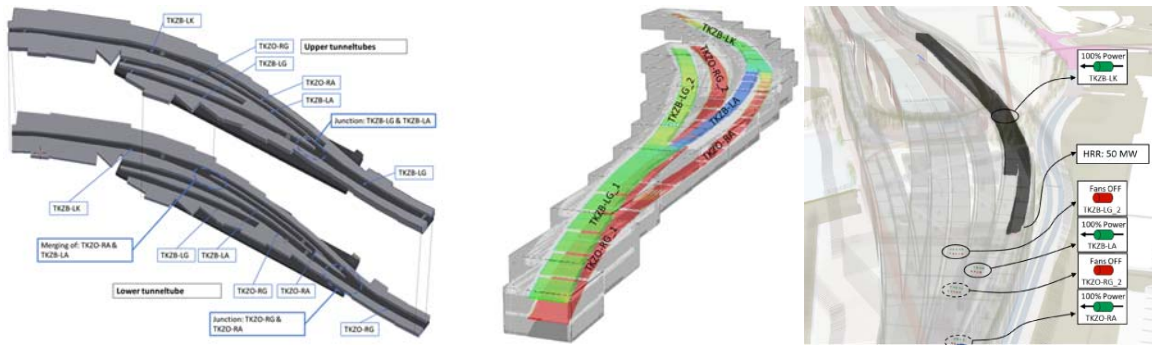


Figure 3-4 A) Exploded view of the geometry of the CFD-model; B) Impression of the airflows; C) Impression of smoke.

### 3.4. Smoke-free CFD-calculations

The air flows in the entire system of connected traffic tubes have been mapped systematically. The focus is on the influence of the different fan clusters (system input) on the resulting air flows in the system of tunnel tubes (system output). This determines the (degree of) controllability of the system.

For presentation purposes the resulting airflows in the tunnels are translated to schematic diagrams, see figure 3-5.

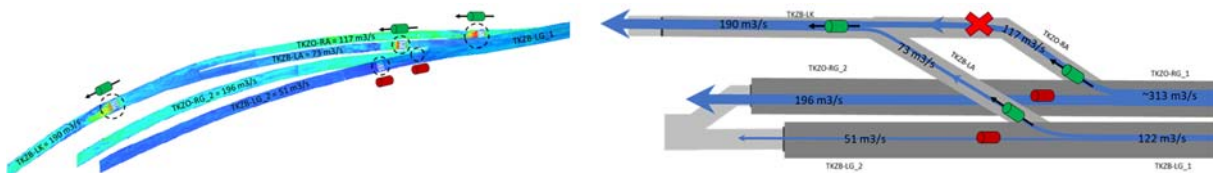


Figure 3-5 A) resulting airflows in CFD simulation; B) Schematic representation of the CFD results.

Over 10 different scenario's, with mixed conditions regarding inflow from the main tubes, ventilation settings in the junctions and traffic conditions yield the following main findings based on 'cold' smoke-free simulations:

- The volume flows in the two main tubes have a dominant influence on the system behaviour of air flows in the Oosterweel junction and are therefore also dominant in whether or not the required air flows and speeds in the various ramps are met. A correct balance is a strict requirement for the airflow in the incident ramp.
- Switching tunnel clusters on or off in a non-incident ramp can have a major (positive or negative) influence on the airflow speed in the incident ramp.
- In the event of an incident in one of the ramps, an excessive volume flow in the non-incident ramp can block the airflow in the incident ramp.
- The results of the 'cold runs' confirm the results of the previously made pressure balance analyses, where this concerns the distribution of an airflow at a split.
- Based on the airflow and system analysis (the 'cold runs'), only the basic information is acquired. This analysis only determines the system behaviour and the mutual influence of the tunnel tubes. To determine whether there is sufficient smoke control, additional CFD analyses are required, in which a fire source is also modelled ('Hot Runs').

### 3.5. CFD-calculations including fire and smoke simulation

The actual possibilities to control smoke are calculated using a 'hot run' CFD analysis. The 'cold run' analyses showed that the volume flows in the two main tubes (TKZO-RG & TKZB-LG) have a dominant influence on the system behaviour of air flows in the Oosterweel junction and were therefore also considered dominant in whether or not the required airflows will be met in

the various ramps. The translation of the system behaviour of the air flows in the various ducts into a usable ventilation strategy is done in this step of the process. Several ventilation strategies are calculated for one fire incident scenario. The situation in which the exit TKZO-RA is the incident tube has been analysed. This situation is considered to be the characteristic case, as the 'cold run' analyses showed that realizing sufficiently large air flows in the exits could be critical. A 50 MW fire is simulated. Different ventilation strategies have been simulated. The inflow conditions from the main tunnel tubes are varied, since the cold simulation showed that these have a dominant influence on the system behaviour.

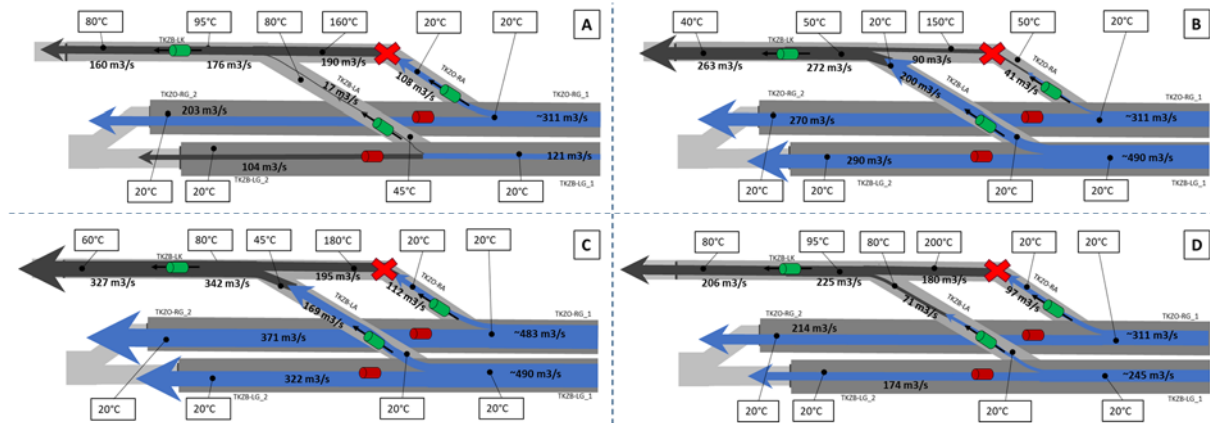


Figure 3-6 Ventilation strategies: A) Standard; B) Balanced, with congested traffic in main tube (TKZO-RG); C) Balanced, without traffic in main tube (TKZO-RG); D) Balanced and economic, without using full power.

The main findings of hot-run CFD calculation of a 50 MW fire scenario in the exit lane TKZO-RA are:

- With standard ventilation strategy (Fig. 3-6 A):
  - Complete smoke control in incident ramp;
  - Smoke backlayering in adjacent ramp TKZB-LA;
  - Escalation of incident to main tube TKZB-LG\_2.
- With an adapted 'balanced' ventilation strategy (Fig. 3-6 B & C):
  - No smoke in KZ main tubes;
  - No backlayering in adjacent ramp (TKZB-LA);
  - Backlayering in incident ramp for lower flow rate in TKZO-RG (Fig. 3-6 B);
  - No backlayering in the incident ramp and full smoke control with a balanced inflow in the main tubes TKZO-RG and TKZB-LG (Fig. 3-6 C).
- With a balanced energy-efficient ventilation strategy (Fig. 3-6 D):
  - No smoke in KZ main tubes;
  - Limited backlayering in adjacent ramp (TKZB-LA);
  - No backlayering in the incident ramp and full smoke control with a balanced inflow in the main tubes TKZO-RG and TKZB-LG.

## 4. PRACTICAL IMPLEMENTATION OF VENTILATION STRATEGY

### 4.1. Ventilation strategy

The calculations discussed in section 3.5 all relate to the same incident location. In order to come to a practical ventilation strategy for the Kanaalzone tunnels, the method was applied on fire locations in the other tubes and ramps. This results in the so-called “Tunnel reflex matrix”: an elaborate matrix in which the fire locations are listed in the columns and the ventilation clusters in the rows (figure 4-1). The cells then indicate how the fans of each specific cluster

have to be activated in the specific fire scenario. Based on this matrix the total power available in the electrical system has been analysed.

Incident tube	Kanaalzone upper tubes														Kanaalzone lower tubes								Kanaalzone split/merged ramps		Power required
	TKZB-GL 1		TKZB-GL 2		TKZB-GL 3		TKZB-GL 4		TKZB-GL 5		TKZB-GL 6		TKZB-GL 7		TKZB-GL 8		TKZB-GL 9		TKZB-GL 10						
	1	2	1	2	1	2	1	2	1	2	1	2	1	2	1	2	1	2	1	2					
	6 x 30 kW (uni-direct)	5 x 20 kW (Bi-direct)	4 x 20 kW (Bi-direct)	4 x 20 kW (Bi-direct)	6 x 30 kW (uni-direct)	14 x 20 kW (Bi-direct)	2 x 20 kW (Bi-direct)	6 x 30 kW (uni-direct)	19 x 20 kW (Bi-direct)	5 x 20 kW (Bi-direct)	4 x 20 kW (Bi-direct)	6 x 30 kW (uni-direct)	14 x 20 kW (Bi-direct)	2 x 20 kW (Bi-direct)	4 x 20 kW (Bi-direct)	4 x 20 kW (Bi-direct)	4 x 20 kW (Bi-direct)								
Kanaalzone upper tubes	TKZB-GL	scenario 1	Incident tube	Active ventilation (100%)	Active ventilation (100%)	Active ventilation (100%)	Active ventilation (100%)	Active ventilation (100%)	Active ventilation (100%)	Active ventilation (100%)	Active ventilation (100%)	Active ventilation (100%)	Active ventilation (100%)	Active ventilation (100%)	Active ventilation (100%)	Active ventilation (100%)	Active ventilation (100%)	Active ventilation (100%)	Active ventilation (100%)	Active ventilation (100%)	Active ventilation (100%)	1095.00 kW			
		scenario 2	Active ventilation (100%)	Active ventilation (100%)	Active ventilation (100%)	Active ventilation (100%)	Active ventilation (100%)	Active ventilation (100%)	Active ventilation (100%)	Active ventilation (100%)	Active ventilation (100%)	Active ventilation (100%)	Active ventilation (100%)	Active ventilation (100%)	Active ventilation (100%)	Active ventilation (100%)	Active ventilation (100%)	Active ventilation (100%)	Active ventilation (100%)	Active ventilation (100%)	Active ventilation (100%)	Active ventilation (100%)	Active ventilation (100%)	985.00 kW	
		scenario 3	Active ventilation (100%)	Active ventilation (100%)	Active ventilation (100%)	Active ventilation (100%)	Active ventilation (100%)	Active ventilation (100%)	Active ventilation (100%)	Active ventilation (100%)	Active ventilation (100%)	Active ventilation (100%)	Active ventilation (100%)	Active ventilation (100%)	Active ventilation (100%)	Active ventilation (100%)	Active ventilation (100%)	Active ventilation (100%)	Active ventilation (100%)	Active ventilation (100%)	Active ventilation (100%)	Active ventilation (100%)	Active ventilation (100%)	Active ventilation (100%)	960.00 kW
	TKZB-GL	scenario 4	Active ventilation (100%)	Active ventilation (100%)	Active ventilation (100%)	Active ventilation (100%)	Active ventilation (100%)	Active ventilation (100%)	Active ventilation (100%)	Active ventilation (100%)	Active ventilation (100%)	Active ventilation (100%)	Active ventilation (100%)	Active ventilation (100%)	Active ventilation (100%)	Active ventilation (100%)	Active ventilation (100%)	Active ventilation (100%)	Active ventilation (100%)	Active ventilation (100%)	Active ventilation (100%)	Active ventilation (100%)	Active ventilation (100%)	440.00 kW	
		scenario 5	Active ventilation (100%)	Active ventilation (100%)	Active ventilation (100%)	Active ventilation (100%)	Active ventilation (100%)	Active ventilation (100%)	Active ventilation (100%)	Active ventilation (100%)	Active ventilation (100%)	Active ventilation (100%)	Active ventilation (100%)	Active ventilation (100%)	Active ventilation (100%)	Active ventilation (100%)	Active ventilation (100%)	Active ventilation (100%)	Active ventilation (100%)	Active ventilation (100%)	Active ventilation (100%)	Active ventilation (100%)	Active ventilation (100%)	440.00 kW	
		scenario 6	Active ventilation (100%)	Active ventilation (100%)	Active ventilation (100%)	Active ventilation (100%)	Active ventilation (100%)	Active ventilation (100%)	Active ventilation (100%)	Active ventilation (100%)	Active ventilation (100%)	Active ventilation (100%)	Active ventilation (100%)	Active ventilation (100%)	Active ventilation (100%)	Active ventilation (100%)	Active ventilation (100%)	Active ventilation (100%)	Active ventilation (100%)	Active ventilation (100%)	Active ventilation (100%)	Active ventilation (100%)	Active ventilation (100%)	Active ventilation (100%)	560.00 kW
Kanaalzone lower tubes	TKZD-GL	scenario 7	Active ventilation (100%)	Active ventilation (100%)	Active ventilation (100%)	Active ventilation (100%)	Active ventilation (100%)	Active ventilation (100%)	Active ventilation (100%)	Active ventilation (100%)	Active ventilation (100%)	Active ventilation (100%)	Active ventilation (100%)	Active ventilation (100%)	Active ventilation (100%)	Active ventilation (100%)	Active ventilation (100%)	Active ventilation (100%)	Active ventilation (100%)	Active ventilation (100%)	Active ventilation (100%)	Active ventilation (100%)	Active ventilation (100%)	1010.00 kW	
		scenario 8	Active ventilation (100%)	Active ventilation (100%)	Active ventilation (100%)	Active ventilation (100%)	Active ventilation (100%)	Active ventilation (100%)	Active ventilation (100%)	Active ventilation (100%)	Active ventilation (100%)	Active ventilation (100%)	Active ventilation (100%)	Active ventilation (100%)	Active ventilation (100%)	Active ventilation (100%)	Active ventilation (100%)	Active ventilation (100%)	Active ventilation (100%)	Active ventilation (100%)	Active ventilation (100%)	Active ventilation (100%)	Active ventilation (100%)	830.00 kW	
		scenario 9	Active ventilation (100%)	Active ventilation (100%)	Active ventilation (100%)	Active ventilation (100%)	Active ventilation (100%)	Active ventilation (100%)	Active ventilation (100%)	Active ventilation (100%)	Active ventilation (100%)	Active ventilation (100%)	Active ventilation (100%)	Active ventilation (100%)	Active ventilation (100%)	Active ventilation (100%)	Active ventilation (100%)	Active ventilation (100%)	Active ventilation (100%)	Active ventilation (100%)	Active ventilation (100%)	Active ventilation (100%)	Active ventilation (100%)	Active ventilation (100%)	945.00 kW
	TKZD-GL	scenario 10	Active ventilation (100%)	Active ventilation (100%)	Active ventilation (100%)	Active ventilation (100%)	Active ventilation (100%)	Active ventilation (100%)	Active ventilation (100%)	Active ventilation (100%)	Active ventilation (100%)	Active ventilation (100%)	Active ventilation (100%)	Active ventilation (100%)	Active ventilation (100%)	Active ventilation (100%)	Active ventilation (100%)	Active ventilation (100%)	Active ventilation (100%)	Active ventilation (100%)	Active ventilation (100%)	Active ventilation (100%)	Active ventilation (100%)	Active ventilation (100%)	640.00 kW
		scenario 11	Active ventilation (100%)	Active ventilation (100%)	Active ventilation (100%)	Active ventilation (100%)	Active ventilation (100%)	Active ventilation (100%)	Active ventilation (100%)	Active ventilation (100%)	Active ventilation (100%)	Active ventilation (100%)	Active ventilation (100%)	Active ventilation (100%)	Active ventilation (100%)	Active ventilation (100%)	Active ventilation (100%)	Active ventilation (100%)	Active ventilation (100%)	Active ventilation (100%)	Active ventilation (100%)	Active ventilation (100%)	Active ventilation (100%)	Active ventilation (100%)	640.00 kW
		scenario 12	Active ventilation (100%)	Active ventilation (100%)	Active ventilation (100%)	Active ventilation (100%)	Active ventilation (100%)	Active ventilation (100%)	Active ventilation (100%)	Active ventilation (100%)	Active ventilation (100%)	Active ventilation (100%)	Active ventilation (100%)	Active ventilation (100%)	Active ventilation (100%)	Active ventilation (100%)	Active ventilation (100%)	Active ventilation (100%)	Active ventilation (100%)	Active ventilation (100%)	Active ventilation (100%)	Active ventilation (100%)	Active ventilation (100%)	Active ventilation (100%)	730.00 kW
Kanaalzone split/merged ramps	TKZS	scenario 13	Active ventilation (100%)	Active ventilation (100%)	Active ventilation (100%)	Active ventilation (100%)	Active ventilation (100%)	Active ventilation (100%)	Active ventilation (100%)	Active ventilation (100%)	Active ventilation (100%)	Active ventilation (100%)	Active ventilation (100%)	Active ventilation (100%)	Active ventilation (100%)	Active ventilation (100%)	Active ventilation (100%)	Active ventilation (100%)	Active ventilation (100%)	Active ventilation (100%)	Active ventilation (100%)	Active ventilation (100%)	Active ventilation (100%)	945.00 kW	
		scenario 14	Active ventilation (100%)	Active ventilation (100%)	Active ventilation (100%)	Active ventilation (100%)	Active ventilation (100%)	Active ventilation (100%)	Active ventilation (100%)	Active ventilation (100%)	Active ventilation (100%)	Active ventilation (100%)	Active ventilation (100%)	Active ventilation (100%)	Active ventilation (100%)	Active ventilation (100%)	Active ventilation (100%)	Active ventilation (100%)	Active ventilation (100%)	Active ventilation (100%)	Active ventilation (100%)	Active ventilation (100%)	Active ventilation (100%)	Active ventilation (100%)	450.00 kW

Figure 4-1 Tunnel reflex matrix for the Kanaalzone tunnels.

## 4.2. Coherence with related management- and technical systems

In the safety concept of the Kanaalzone tunnels, the tunnel ventilation system plays an important role. The concept is based on self evacuation via escape galleries next to the traffic tubes and ramps. It assumes that upstream of a fire location the traffic gets congested and people have to evacuate, while downstream the traffic is able to leave the tunnel. This concept works together with the traffic management system that takes care of the traffic handling downstream of the fire location and the tunnel ventilation that guarantees a smoke-free escape route upstream towards the escape gallery (in which over pressure is applied to prevent smoke inflow). Integrating the tunnel ventilation system with the other safety systems results in a robust safety concept for the complex Kanaalzone tunnels.

## 5. CONCLUSIONS

The main findings of the tunnel ventilation design process for the complex Kanaalzone tunnels can be summarized as follows:

- Full jet-power on all fans is not always the best solution for smoke control in intertwined tunnel tubes.
- Air balances between the tubes are a dominant factor for effective smoke control in interconnected ramps and are affected by a wide range of sensitive parameters.
- Interconnected tunnel tubes require a fan control strategy on cluster level instead of on tube level.

## 6. REFERENCES / CONTACT

Oosterweelverbinding.be / info@lantis.be / Lantis contact conference: peter.verbois@lantis.be

[1] Ministry of Transport, Infrastructure and Environment, 2011, ProTuVem Probabilistisch rekenmodel Tunnelventilatiesystemen, handleiding ProTuVem v2.0

[2] Rijkswaterstaat, 2005, Aanbeveling ventilatie van verkeerstunnels, Steunpunt tunnelveiligheid, Ministerie van verkeer en waterstaat

## RISK-BASED VENTILATION DESIGN STUDY FOR THE LA LINEA TUNNEL

<sup>1</sup>Jorge Luis Rios Portilla, <sup>2</sup>Juan-Carlos Rueda, <sup>2</sup>Harald Kammerer, <sup>2</sup>Reinhard Gertl,  
<sup>3</sup>Bernhard Kohl

<sup>1</sup> DISICO S.A Ingeniería Eléctrica, Civil y Telecomunicaciones, Colombia

<sup>2</sup> ILF Consulting Engineers Austria GmbH, Austria

<sup>3</sup> ILF Group Holding GmbH, Austria

### ABSTRACT

With a length of 8,650, the La Linea tunnel is the longest road tunnel crossing the central Andes mountain range in Colombia, with one tube for unidirectional traffic, connected via several cross passages with the parallel rescue tube. In 2016, at the beginning of the study, the civil works were concluded and the tunnel equipment had to be defined. According to relevant regulations and guidelines, the tunnel would require a transversal ventilation system. However, in the tunnel were no provisions for the implementation of such a ventilation system, respectively an intermediate ceiling for an air duct. In the ventilation study, different ventilation concepts were investigated. The aim was to identify the most appropriate ventilation system for normal operation and in case of fire. The equivalency of each alternative ventilation system including additional required risk-mitigation measures was investigated by a detailed quantitative risk assessment study. Thereby, the Austrian Tunnel Risk Model (TuRisMo) according to RVS 09.03.11 was used as a decision-making tool for the ventilation design and other safety-related aspects. The results obtained from the quantitative risk assessment study as well as the ventilations study show that the longitudinal ventilation system is the best and most suitable ventilation concept for the La Linea tunnel.

*Keywords: Tunnel risk assessment, transversal and longitudinal ventilation system, road tunnel, decision-making tool.*

### 1. INTRODUCTION

The La Linea tunnel is the longest tunnel of the 24 tunnels which are part of the project “Crossing the central mountain range”. The 8,650 m long tunnel system has one traffic tube for unidirectional traffic which is connected via 16 cross passages (connecting galleries) with the parallel rescue tube. The traffic is operated in uphill direction at a slope of 1%. The tunnel is at an average altitude of about 2,450 m above sea level and is part of a main transport route of the country. The predicted traffic for 2036 is approximately 5,747 vehicles per day.

The La Linea tunnel has a long design history since the 1990 decade: Several different options for a ventilation system have been studied and proposed. Finally it was intended to implement a semi-transversal ventilation system. At the beginning of this study in 2016, the tunnel was in the final phase of construction, with finalized civil works, without equipment and installations at this stage. Normally, the decision on the ventilation system is taken in an early planning phase, because it provides an important basis for defining the requirements for the design of the civil structures of a tunnel (like tunnel cross section). In particular, the implementation of any smoke extraction system requires the provision of a properly dimensioned air duct (for smoke extraction) in the upper part of the tunnel cross section. However, as the project was already in an advanced stage of realization, the cross section could not be modified any more. These

boundary conditions provided considerable constraints for the decision on the ventilation system.

## 2. INITIAL SITUATION

As the project was already in an advanced stage of realisation, the cross section could not be modified anymore. Referring to the key design parameters for fire for a semi-transversal ventilation a cold exhaust flow rate of  $211 \text{ m}^3/\text{s}$  would be required (see Figure 1 – concept 1). In principle the existing tunnel cross section would provide sufficient space above the traffic clearance gauge to achieve this design objective, but then no space would be available for the implementation of the planned overhead signalling system (according to international state of the art and regulations – see for instance RVS 09.02.22 [1] – the lane dependant traffic signs must be positioned on top of its corresponding lane). Vice versa, providing the space required for the installation of the overhead signalling system would reduce the capacity of the smoke extraction system to  $84 \text{ m}^3/\text{s}$ , which would impede its efficiency considerably (see Figure 1 – concept 2).

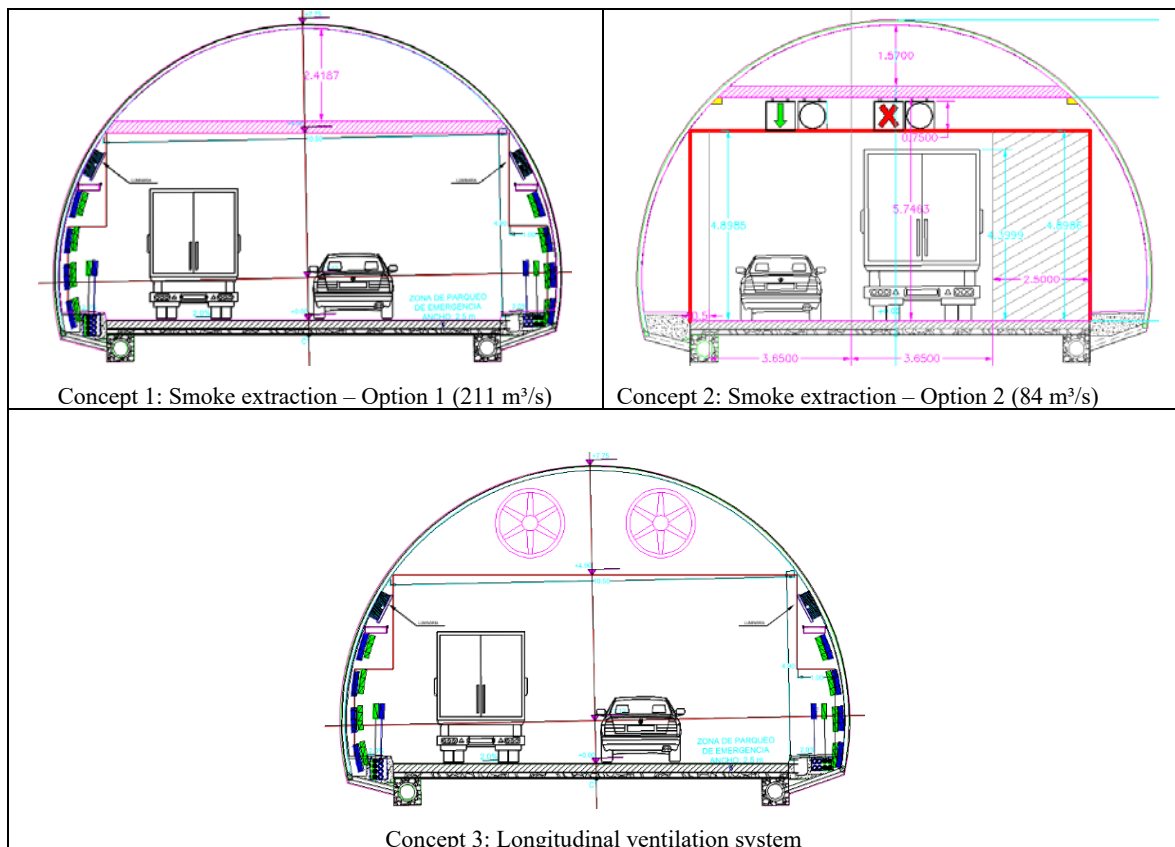


Figure 1: Alternative ventilation concepts feasible in existing tunnel profile

Therefore, a detailed quantitative risk assessment model was used as a decision-making tool to investigate different possible ventilation systems and define the most appropriate ventilation design and other safety-related aspects.

## 3. TWO DIFFERENT APPROACHES TO TUNNEL SAFETY

According to international best practice (see for instance PIARC reports “Risk analysis for road tunnels” [2], “Current practice for risk evaluation for road tunnels” [3]) two different approaches are applied to guarantee a satisfying level of tunnel safety, which are as well relevant for the selection of important safety systems like tunnel ventilation: (a) The

(traditional) prescriptive approach, based on technical design guidelines, providing technical specifications of the safety features of a tunnel; the underlying safety principle of this approach postulates, that a tunnel is sufficiently safe, if these technical specifications are met. However, even if all requirements are fulfilled there is a residual risk, which is not specifically addressed in this approach; and (b) the (innovative) risk-based approach, based on a structured, harmonised and holistic safety analysis of the whole tunnel system, considering all safety-relevant specific characteristics of an individual tunnel. A tunnel is considered as sufficiently safe, if predefined risk criteria are met.

These two approaches shall be used as complementary elements of tunnel design (see PIARC report “Current practice for risk evaluation for road tunnels” [3]). These two different approaches are as well established in up to date international tunnel regulations, like the EC-Directive 2004/54/EC [4]. The EC-Directive 2004/54/EC on Minimum Safety Requirements for Road Tunnels is a regulatory framework which is mandatory for all EU member states; it has been implemented in the national legislation of all countries. The EC-Directive 2004/54/EC defines in Annex I a list of mandatory safety measures, also addressing ventilation aspects; defines in Article 13 the requirement for a risk analysis; and establishes the principle of compensation: if a prescriptive requirement cannot be met for relevant reasons, this can be compensated by alternative measures, if it can be demonstrated by a risk analysis, that at least the same level of safety can be achieved. National guidelines may be stricter and more detailed, but must be within this frame work.

#### **4. RELEVANCE OF TUNNEL LENGTH WITH RESPECT TO DECISION ON VENTILATION SYSTEM**

##### **4.1. EC-Directive**

In the European Directive 2004/54/EC [4] there are no general length limitations for unidirectional tunnels with longitudinal ventilation systems. The only length limitations for longitudinal ventilation (>1000m) refers to traffic parameters – bidirectional traffic or unidirectional traffic with regular congestion (due to traffic overload). The traffic study for the La Linea tunnel [5] confirms, that even in the long-term perspective the expected peak hour traffic will be clearly below the capacity of the tunnel. In all future peak hour scenarios investigated the level of saturation will be clearly below 50%. Additionally, in the risk assessment study requirements are defined (regarding the position of the toll station) to avoid building up of a queue of vehicles in the tunnel exit zone, which may reach back to the tunnel exit portal. Hence, the basic conditions for the implementation of a longitudinal ventilation system in La Linea tunnel are met.

##### **4.2. National guidelines**

In some European countries there are national tunnel design guidelines – in addition to the EC-Directive; in many cases, these national guidelines are older than the EC-Directive. Some of these guidelines have length limitations for the application of longitudinal ventilation systems in unidirectional tunnels. The main reason for these limitations was that in the past the fresh air supply during normal operation due to the high emission level of old vehicles could be a limiting factor, because the maximum permissible air velocity in the tunnel could be exceeded.

In Austria – like in some other European countries - there is a set of national technical guidelines (RVS) relevant for elements of civil tunnel structure and tunnel equipment (including ventilation). These guidelines are continuously updated, implementing new findings and developments. In older versions of RVS 09.03.11 [6] the application of longitudinal ventilation systems for unidirectional tunnels was limited to tunnels shorter than 3,000 m. In an update

(2014) of national guidelines (RVS 09.02.31 [7]) these limitations have been adapted as follows: In general, RVS 09.02.31 suggests for unidirectional tunnels longer than 5,000 m a semi-transverse ventilation system. However, an alternative ventilation system is permissible, if the equivalency is confirmed by means of a risk analysis. These regulatory definitions define the requirements for risk assessment as well as the conditions for the acceptability of a longitudinal ventilation system from a risk-based perspective: In the risk assessment it has to be demonstrated that the risk of the tunnel with longitudinal ventilation (including additional risk-mitigation measures required) is equal to or less than the risk of the tunnel with semi-transversal ventilation; thus defining the semi-transversal ventilation as reference case relevant for risk evaluation.

#### **4.3. Technical aspects**

In addition to the regulatory aspects, also technical aspects have to be considered when designing a ventilation system for a (long) unidirectional road tunnel.

##### **Fresh air demand**

The fresh air demand depends on the emissions of the vehicles in the tunnel. The number of vehicles in the tunnel is a function of the hourly traffic volume and the tunnel length. The longer the tunnel, the more vehicles are inside the tunnel at the same time. Hence, a long tunnel requires more fresh air than a short tunnel.

The amount of fresh air itself is no restriction for any ventilation system. However, guidelines like the PIARC, NFPA, the German RABT or the Austrian RVS limit the maximum longitudinal air velocity in the tunnel. Since a high fresh air demand causes a high longitudinal air velocity in the tunnel, the maximum amount of fresh air is indirectly also limited by the velocity limitation. Therefore, the application of ventilation systems with a fresh air supply via the tunnel portals like a longitudinal ventilation system or a semi-transverse ventilation system has limits. Thus, for long tunnels with a high fresh air demand a transverse ventilation system may be required for normal operation. In case of the La Linea Tunnel it could be demonstrated that the required amount of fresh air allows to apply a longitudinal ventilation system (see chapter 6)

##### **Pressure loss caused by wall friction**

The friction between the flowing air and the static concrete walls causes a pressure loss, which has to be overcome by the ventilation system. The pressure loss rises if the length of a tunnel/exhaust duct gets longer and if the cross section gets smaller. In case of a longitudinal ventilation system a long tunnel causes a higher pressure loss than a short tunnel. That is why a long tunnel requires more jet fans for reaching a required air velocity than a short tunnel. However, the application of a longitudinal ventilation system is not restricted by the required amount of jet fans. For a semi-transverse ventilation system there is a pressure loss in the main tunnel and in the exhaust duct. The longer and the smaller the exhaust duct, the higher is the pressure loss along the duct while extracting air and the higher is the pressure difference between the exhaust duct and the main tunnel. The maximum permissible pressure difference between the exhaust duct and the main tunnel is limited by guidelines for technical reasons (e.g. by the Austrian RVS 09.02.31 to 3,000 Pa). This limitation restricts the application of a semi-transverse ventilation system

#### **4.4. Safety Aspects**

From the safety perspective only fire incidents are relevant for the decision on the ventilation system. The EC-Directive as well as national guidelines limit in general the application of



longitudinal ventilation systems to unidirectional tunnels which do not have congested traffic (with some exceptions under specific conditions – see chapter 4.1 and 4.2). This regulation refers to the fact, that in case of a fire incident, vehicles in front of the fire should be able to leave the tunnel without problems, if the traffic is not congested. In this respect two different scenarios for congested traffic need to be distinguished:

- **Congestion due to traffic overload:** Stop-and-go traffic caused by insufficient capacity of the tunnel itself or road sections downstream of the incident location. This type of congestion excludes the application of longitudinal ventilation for longer tunnels.
- **Evolving congestion after a previous initial event:** Congestion caused by an initial event, like vehicle breakdown or collision. This type of congestion may happen in every tunnel and cannot be excluded. Therefore, this type of congestion is not meant by the regulatory requirements mentioned above.

However, both congestion types lead to different fire scenarios with different probability of occurrence, exposition (number of vehicles potentially affected) and preconditions for smoke propagation. Especially in the latter, there is an influence of tunnel length. Hence, the consequences of this scenario need to be specifically addressed in a quantitative risk assessment study.

## 5. RESULTS OF RISK ASSESSMENT STUDY

Taking the conditions and requirements defined in chapter 3 as basis, a quantitative risk assessment study was performed for the La Linea tunnel. For that, the Austrian Tunnel Risk Model TuRisMo (defined in RVS 09.03.11 [6]) was applied, following the principles defined by PIARC for the risk assessment process.

The risk assessment study was performed for the 3 ventilation systems shown in Figure 1. The risk evaluation was carried out using a relative approach: The tunnel options which shall be investigated were compared to the risk value of an idealised reference tunnel defining the “reference risk profile” (see Figure 2). Following the definitions in the ventilation design guideline RVS.09.02.31 [7] for the decision on the ventilation system of La Linea tunnel, the reference tunnel is a tunnel with a semi-transverse ventilation system with a exhaust flow rate of 211 m<sup>3</sup>/s (see chapter 2) – an ideal case, without taking into account possible consequences of space requirements in cross section.

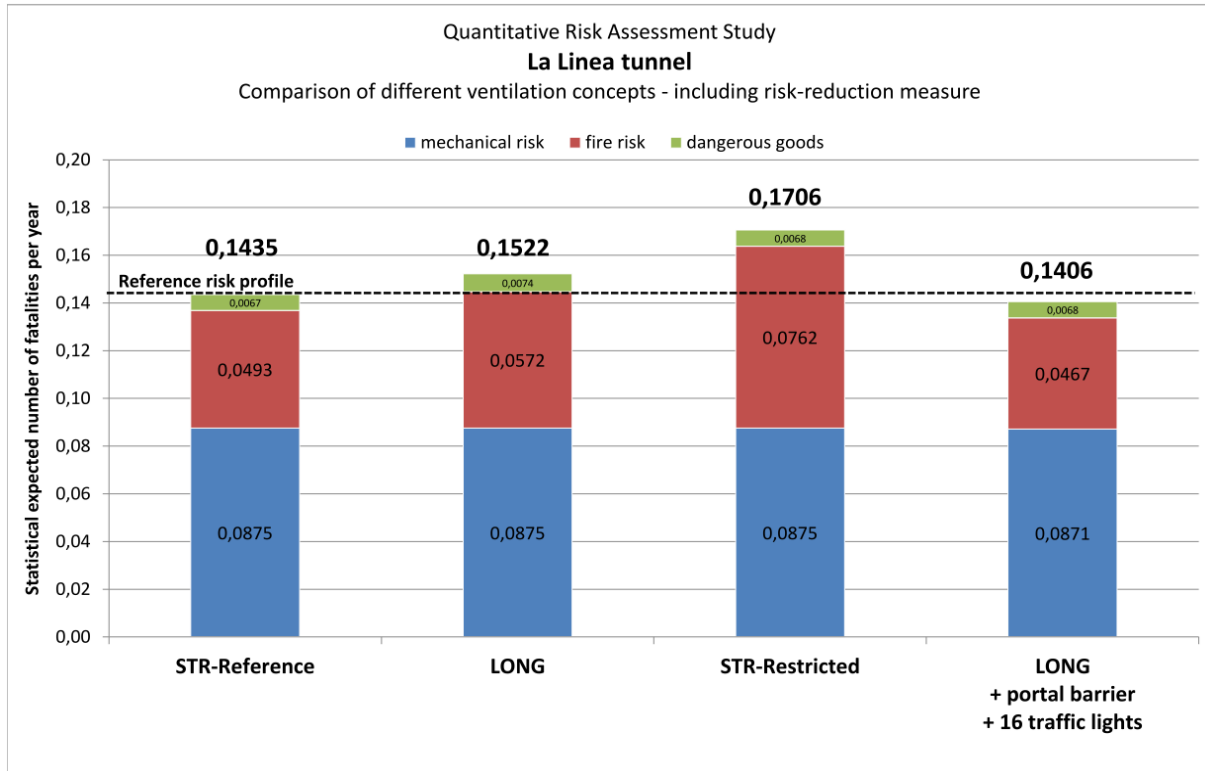


Figure 2: Quantitative risk assessment study – final results

These results can be interpreted as follows: The optimum semi-transverse smoke extraction system (Concept 1: “STR-Reference”) defines the reference risk profile. A realistic but restricted semi-transverse smoke extraction system (Concept 2: “STR-Restricted”), taking into account the space requirements, considerably exceeds the reference risk profile (due to high fire risk as a consequence of a restricted smoke extraction capacity). The longitudinal ventilation system (Concept 3: “LONG”) slightly exceeds the reference risk profile due to a slightly higher fire risk.

Therefore, additional risk mitigation measures are required to allow the use of a longitudinal ventilation system from a risk perspective. A more detailed analysis of the fire risk of Concept 3 revealed, that a relevant share of risk is due to secondary fire scenarios (influence of tunnel length – high number of vehicles still moving in the tunnel – increased likelihood of secondary collisions and fires). Hence, the additional measures are proposed to reduce this specific part of the risk: stop vehicles in tunnel as soon as possible by implementing additional traffic barriers at the tunnel portal and 16 traffic signals throughout the tunnel – thus, reducing exposition of vehicles to a potential fire. During the adaption of the Austrian tunnel model TuRisMo respectively RVS 09.03.11 both, the time for vehicles to stop in front of a red light as well as a in front of a traffic barrier were discussed. Based on the experience of Austrian tunnel operators it takes approximately 30 seconds to stop in front of a red light. When using a traffic barrier it was assumed, that this time is reduced to zero. Of course, the time to detect the incident and react has to be added (e.g. 60 seconds). Due to the faster stopping time less vehicles enter the tunnel and less people are exposed in case of a fire. In addition, traffic signals inside the tunnel stop vehicles in regular distances and increase the distance of people to the fire location. Since the traffic signals (and additional vehicle queues) are located next to the emergency exits, the evacuation time in the tunnel is increased. The results show that this specific measure was able to reduce the risk of the tunnel with longitudinal ventilation below the reference case.

## 6. RESULTS OF FRESH AIR DEMAND CALCULATIONS

The amount of required fresh air depends on the traffic volume through the tunnel. Hence, the fresh air demand is the same for all ventilation concepts. As with a longitudinal ventilation system the fresh air supply underlies some limitations (due to tunnel length), this requirement is crucial for the assessment of the feasibility of a longitudinal ventilation system. Hence, an investigation of the fresh air requirements to meet the air quality limits in the tunnel, which is necessary for carbon monoxide (CO) and visibility in the conceptual ventilation design, and result in a minimum flow rate has been performed. Particle emission rates are used for the calculation of fresh air to meet the visibility limits. The NO<sub>2</sub>/NO<sub>x</sub> concentration is not considered for the fresh air demand, what is state of the art for European and North-American road tunnels. The reason for the neglect of the NO<sub>x</sub> concentration is it's irrelevance for short term exposure. The fresh air calculation defines the minimum flow rate and is set up for different speeds for CO and turbidity. Due to the increasing number of vehicles equipped with catalytic converters. CO emissions have decreased. Therefore, in most cases the visibility due to particulates (exhaust and non-exhaust) is relevant for the ventilation design.

Under the assumption of a traffic control system that can limit the minimum collective vehicle speed to 10 km/h, the design flow rate for normal operation was calculated to 211 m<sup>3</sup>/s. This flow rate is equal to a longitudinal air velocity of 2.8 m/s. The design flow rate for maintenance operation is calculated by applying a limiting value of 0,003 m<sup>-1</sup> according to PIARC and is 375 m<sup>3</sup>/s. Due to the high fresh air demand for maintenance operation, maintenance works shall be performed during low traffic hours to avoid too high air flow rates. The minimum required air velocity in the tunnel according to the PIARC for normal operation is 1.5 m/s. According to the guideline NFPA 502 [8] maximum air velocities in the traffic tunnel during normal operation should be less than or equal to 11 m/s. Hence, the fresh air demand can be provided without exceeding maximum velocity limits. According to the calculation results all vehicle speeds down to 10 km/h can be handled by the ventilation system. The calculation results are summarized in Table 1

Table 1: Required jet fans for normal operation

collective vehicle speed [km/h]	number of required activated jet fans	
	traffic scenario with max HGV- percentage	traffic scenario with maximum traffic
≥50 km/h	self-ventilated	self-ventilated
40 km/h	self-ventilated	4
30 km/h	2	6
20 km/h	6	10
10 km/h	11	14

## 7. SUMMARY AND CONCLUSIONS

A risk assessment study was performed in order to investigate and quantify the influence of different ventilation systems on the risk, and used as a decision-making tool on the ventilation design. The study compared an reference smoke extraction system (=fulfilling all guidelines) with a realistic smoke extraction system and a longitudinal ventilation system. The results show, that from a safety point-of-view the realistic smoke extraction system (taking into account the space requirements in the La Linea tunnel) considerably exceeds the reference risk profile and cannot be taken into consideration. Furthermore it was demonstrated, that the fresh air supply of La Linea tunnel can be guaranteed by an adequately designed longitudinal ventilation system.

Besides the safety aspects the longitudinal ventilation system is superior to the semi-transverse ventilation system regarding the following: the reliability of the system; the simple ventilation control; the power consumption during emergency operation and therefore a less costly energy supply system; the combination with a simple and effective pressurization system for the rescue tunnel; the testing and commissioning effort; the required space for overhead traffic signs; the investment costs.

The results obtained from the quantitative risk assessment study as well as the ventilations study showed, that the proposed longitudinal ventilation system is the best and most suitable ventilation concept for the La Linea tunnel. Therefore, that was the system that finally was implemented and operates with no issues since September 2020.

## 8. REFERENCES

- [1] Österreichische Forschungsgesellschaft Straße-Schiene-Verkehr, „RVS 09.02.22 Tunnelausrüstung“, 28.05.2014
- [2] World Road Association (PIARC), Technical Committee 3.3 Road Tunnel Operations, “Risk analysis for road tunnels,” 2008.
- [3] World Road Association (PIARC), Technical Committee 3.3 Road Tunnel Operations, “Current practice for risk evaluation for road tunnels,” 2013
- [4] Directive 2004/54 / EC of the European Parliament and of the Council „on minimum safety requirements for tunnels in the trans-European road network“; Brussels, 29.04.2004
- [5] Estudio de Tránsito para El Túnel, UT DGG, Bogota, Septiembre 2016
- [6] Österreichische Forschungsgesellschaft Straße-Schiene-Verkehr, “RVS 09.03.11 Tunnel Risk Analysis Model”, 2015
- [7] Österreichische Forschungsgesellschaft Straße-Schiene-Verkehr, “RVS 09.02.31 Tunnel Ventilation”, 01.06.2014
- [8] National Fire Protection Association NFPA 502, Standards for Road Tunnels, Bridges, and Other Limited Access Highways

## TESTING THE THRUST OF JET FANS IN A WIND TUNNEL

Tomasz Burdzy<sup>1</sup>, Wojciech Węgrzyński<sup>1</sup>, Marek Borowski<sup>2</sup>,

<sup>1</sup>Fire Research Department, Building Research Institute (ITB), Poland.

<sup>2</sup>AGH University of Science and Technology, Krakow, Poland.

### ABSTRACT

In this research item we present a comparison on the calculated theoretical thrust of jet-fans and the values measured on a test station located within a high-velocity wind tunnel. The aim of this research was to perform a direct measurement of the thrust of the jet fan, along with the electrical parameters of the fan motor and direct velocity measurements in the jet fan stream, in an environment with a pre-defined air velocity (wind tunnel). The research was performed on two types of jet-fans ((1) 355mm diameter, approx. 37 N nominal thrust and (2) 50 mm diameter, approx. 2,8 N nominal thrust). The jet fans were placed in a boundary layer wind tunnel, in a test section of approx. 4 x 3 x 10 m (W x H x L). As the wind tunnel has a rectangular cross section, different locations of the jet-fans were tested (bottom, middle), to unravel the effect of the configuration factor on the jet fan performance. The inlet air velocity varied from 0 m/s to 20 m/s. The goal of this research was to identify the performance characteristic of jet-fans, related to the ambient air velocity. This subject is important in the estimation of the jet-fan performance in analytical methods (such as PIARC manual) or in 1D modelling systems. Furthermore, the estimation of such performance is highly relevant to the use of jet-fans in ventilation ducts, as a mean to reduce the required operational pressure of exhaust fans in a long tunnels with transversal ventilation systems. The presented work will give an overview of the standardized methods for measuring and calculating the thrust of jet-fans, the results of the measurements performed in the road tunnel and a numerical analysis of a long exhaust duct with jet-fans installed (with and without modifications introduced after the wind tunnel tests).

*Keywords: thrust, ventilation design, road tunnels systems, longitudinal ventilation,*

### 1. INTRODUCTION

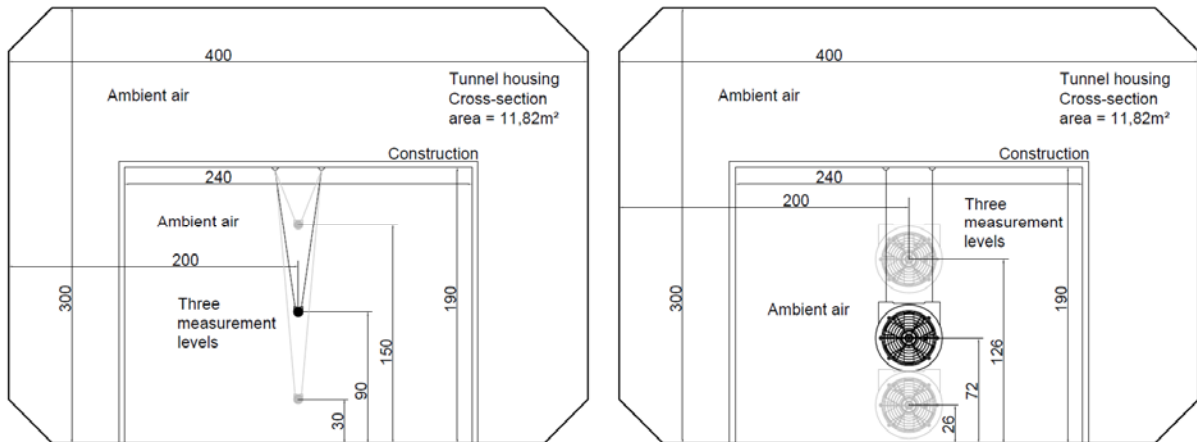
Tunnels built in Poland in most cases have longitudinal ventilation. The selection of appropriate jet fans is still very difficult due to the variability of their parameters in relation to the prevailing conditions inside the tunnel. Their effectiveness depends on the temperature, the flow velocity of the surrounding air as well as their location in relation to the tunnel geometry.

In longitudinal ventilation systems, the most important task is to maintain the appropriate flow velocity, necessary to maintain appropriate conditions in the comfort or fire ventilation mode. So the most important thing in the selection and design of jet fans is the appropriate determination of their ability to force flow in the tunnel. When fans are installed in a tunnel, their effective thrust will be limited compared to the value measured in ISO 13350. This is due to unfavorable fan placement (versus near walls and ceiling), non-centric placement within cross-section the tunnel and the ambient air velocity in the tunnel. These factors were investigated in this study.

### 2. MEASUREMENT INSIDE THE WIND TUNNEL

The measurements were based on continuous and simultaneous measurement of thrust, air velocity in the tunnel with temperature and fan power consumption. The thrust was measured in the fan axis, above the fan, while it was hanging freely on the lines (see figure 2 and 3). The power consumption of the fan with a diameter of 355 mm was measured separately for each phase. The fan was tested in the configuration of star "Y" (1st gear) and double star "YY" (2nd

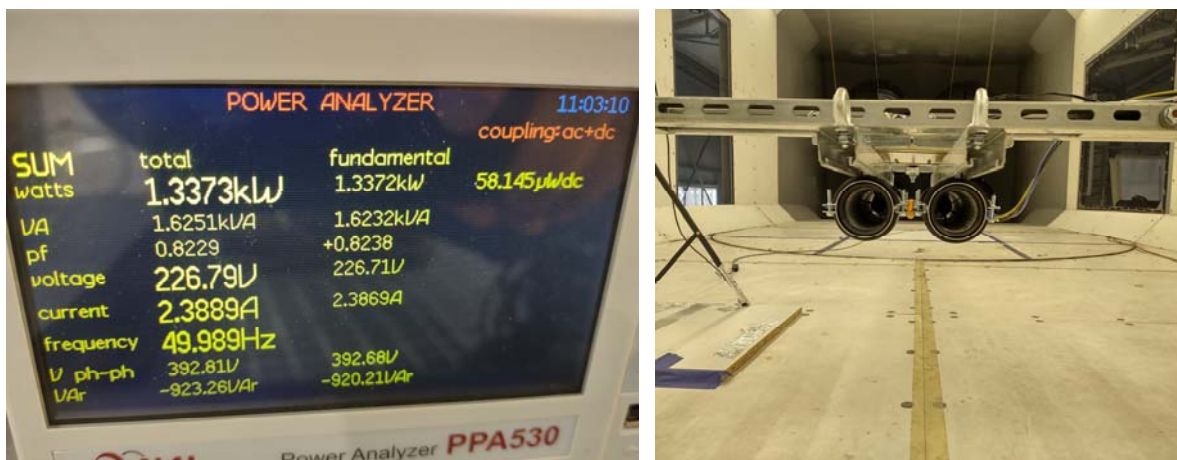
gear) at 50Hz power frequency. The Y configuration gives approximately half of the volume flow of the YY configuration. Additional variable was the location of the fan within the tunnel, as shown on Fig. 1. The smaller jet fan (50 mm, 2,7 N) was installed in various configurations near the floor of the tunnel, and also in a configuration of the pair of devices see Fig. 3, right.



**Figure 1:** Measuring station, three measurement levels for jet fan 355mm, and three levels for jet fan 50 mm.



**Figure 2:** Thrust measurement (left) Jet Fan 355mm on the station (right)



**Figure 3:** Power consumption measurement (left) A pair of jet fans 50mm (right)

All the measured thrust forces were brought to comparative values, ie. multiplied by  $(1,2/\rho)$  in accordance with [1]. Moreover, the thrust force determined theoretically, i.e. according to the formula, has been introduced:

$$T = \dot{m} \cdot (v_{jet} - v_{ambient})$$

Table 1. Theoretical thrust data

$T$	N	thrust
$\dot{m}$	kg/s	mass stream
$v_{jet}$	m/s	velocity in jet fan
$v_{ambient}$	m/s	ambient velocity

Table 2. Jet fan data to determine theoretical thrust

	$v_{jet}$	$T$
355, YY 2nd gear	18.08	37.34
355, Y 2nd gear	9.04	9.41
50, 1920x125	34.3	2.75
50, 1860x125	30.3	2.16

Theoretical thrust was always determined based on the thrust given by the manufacturer or measured outside the wind tunnel. The same as it is in design practice see table 2.

### 3. RESULTS

During the measurements in the “Y” configuration, the thrust in the range of about 5÷6 m/s corresponded to the theoretical thrust force. When measuring in the “YY” configuration, the thrust was always 0 N before the ambient velocity reached 14 m/s. The electric power consumption always decreased insignificantly with the increase of the ambient velocity.

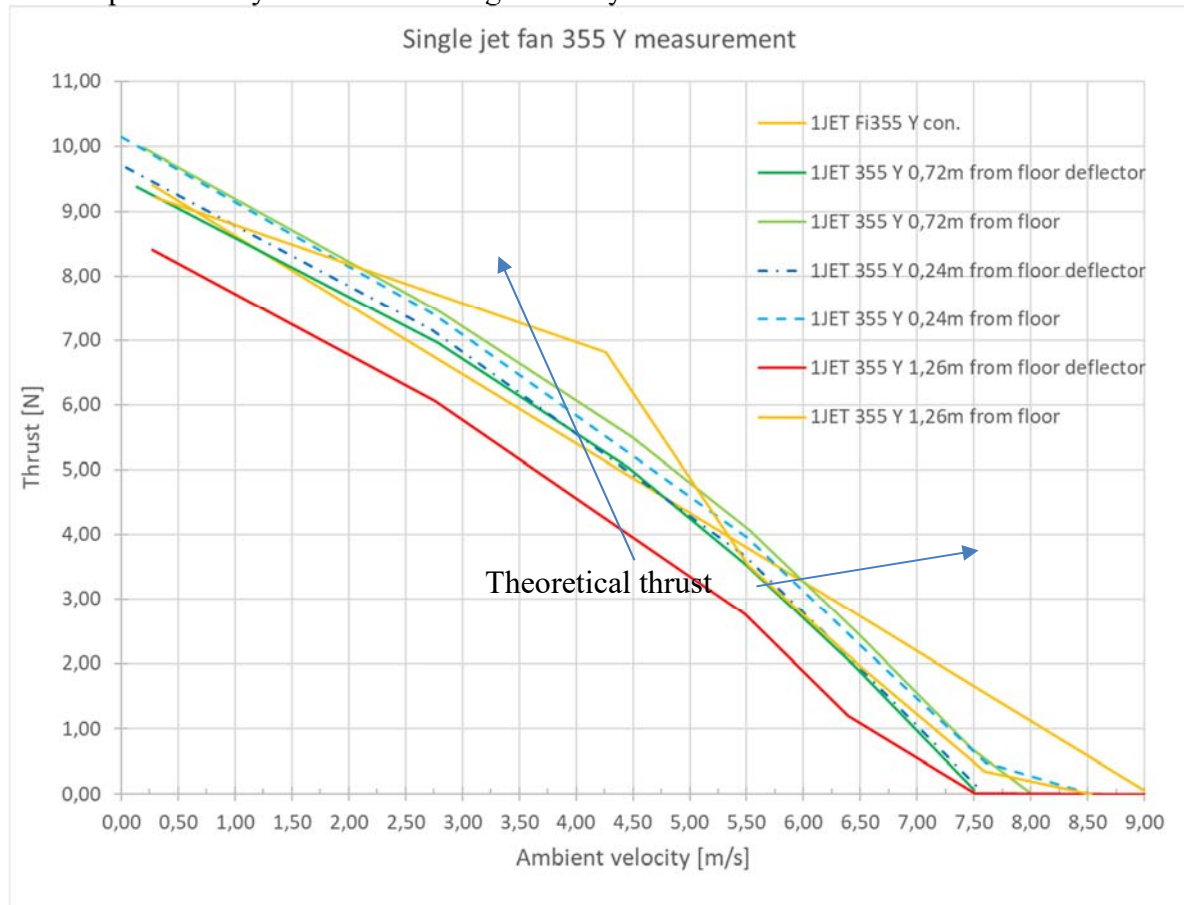


Figure 4: Measurement results for a 355mm jet fan in “Y” configuration.

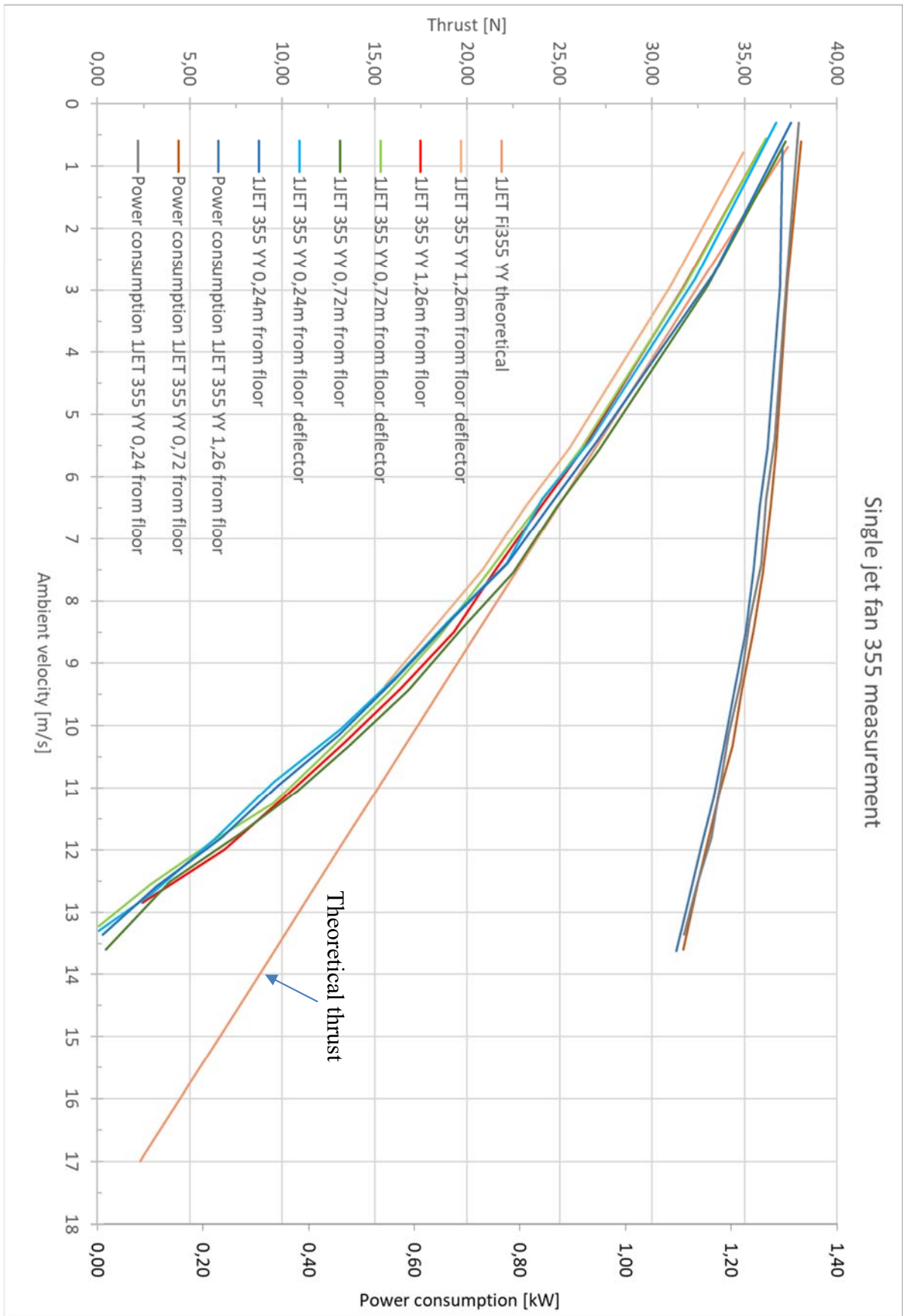
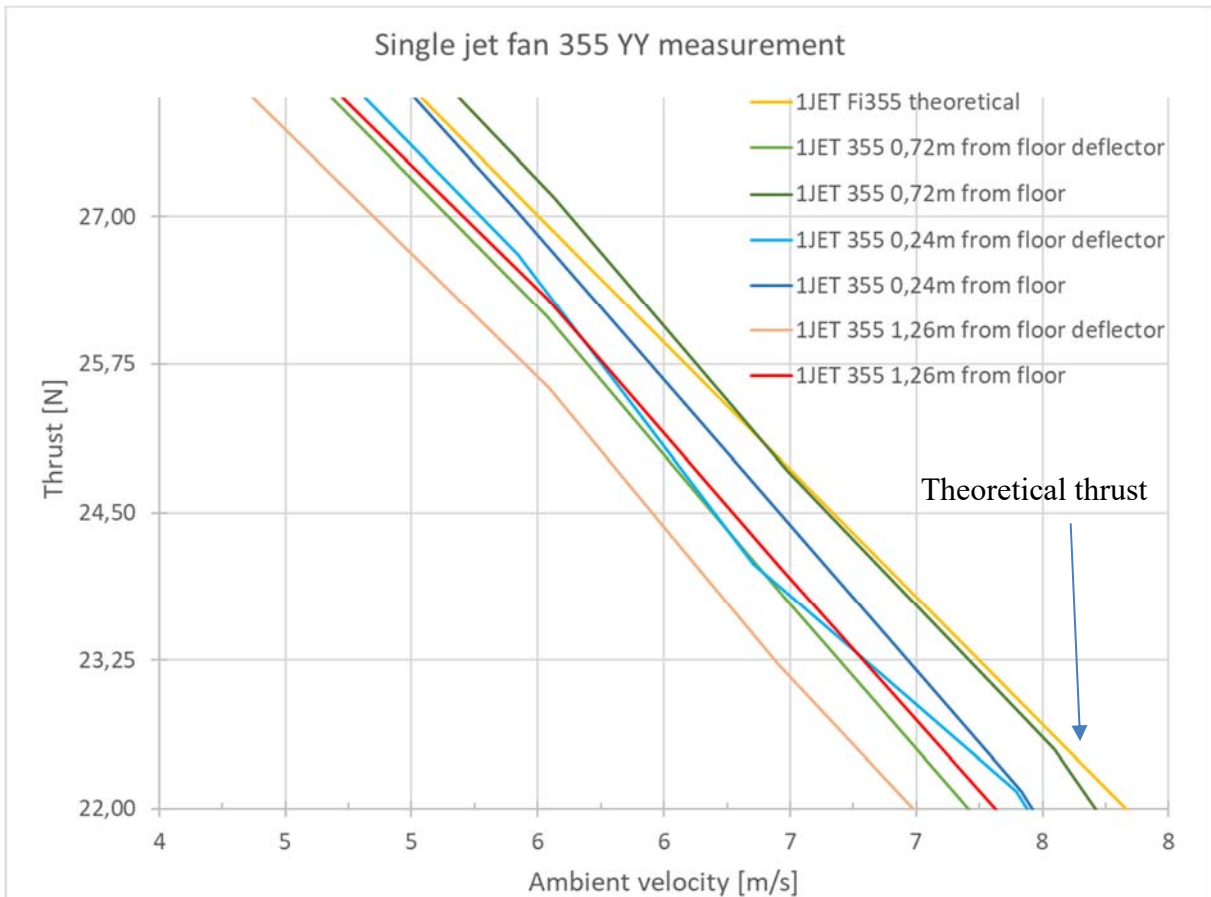


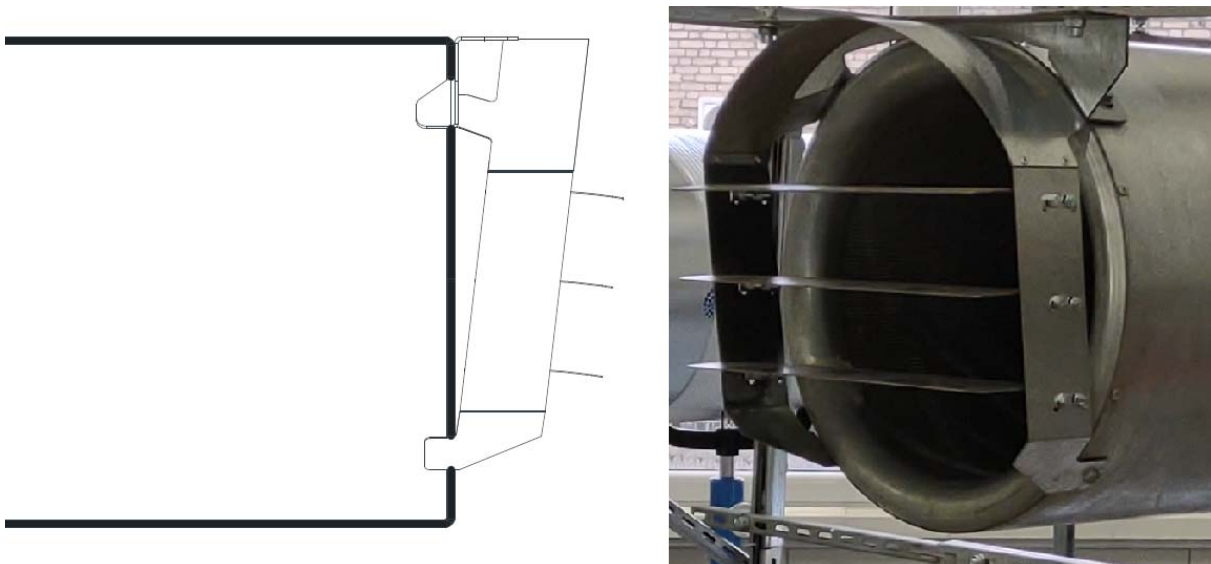
Figure 5: Measurement results for a 355mm jet fan in “YY” configuration.



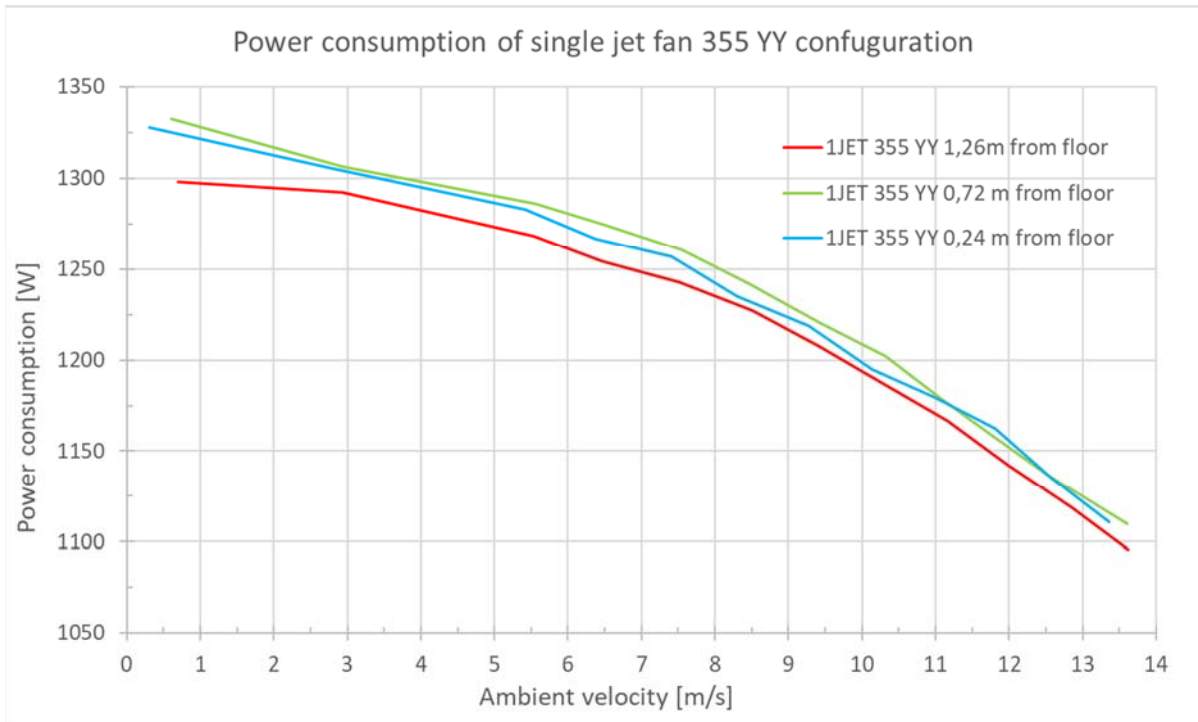


**Figure 6:** Clipping measurement results for a 355mm jet fan in “YY” configuration.

On the figure of the results from the YY configuration, it can be seen that the thrust force in each case for that particular jet fan had a greater value without the deflector than with the deflector.

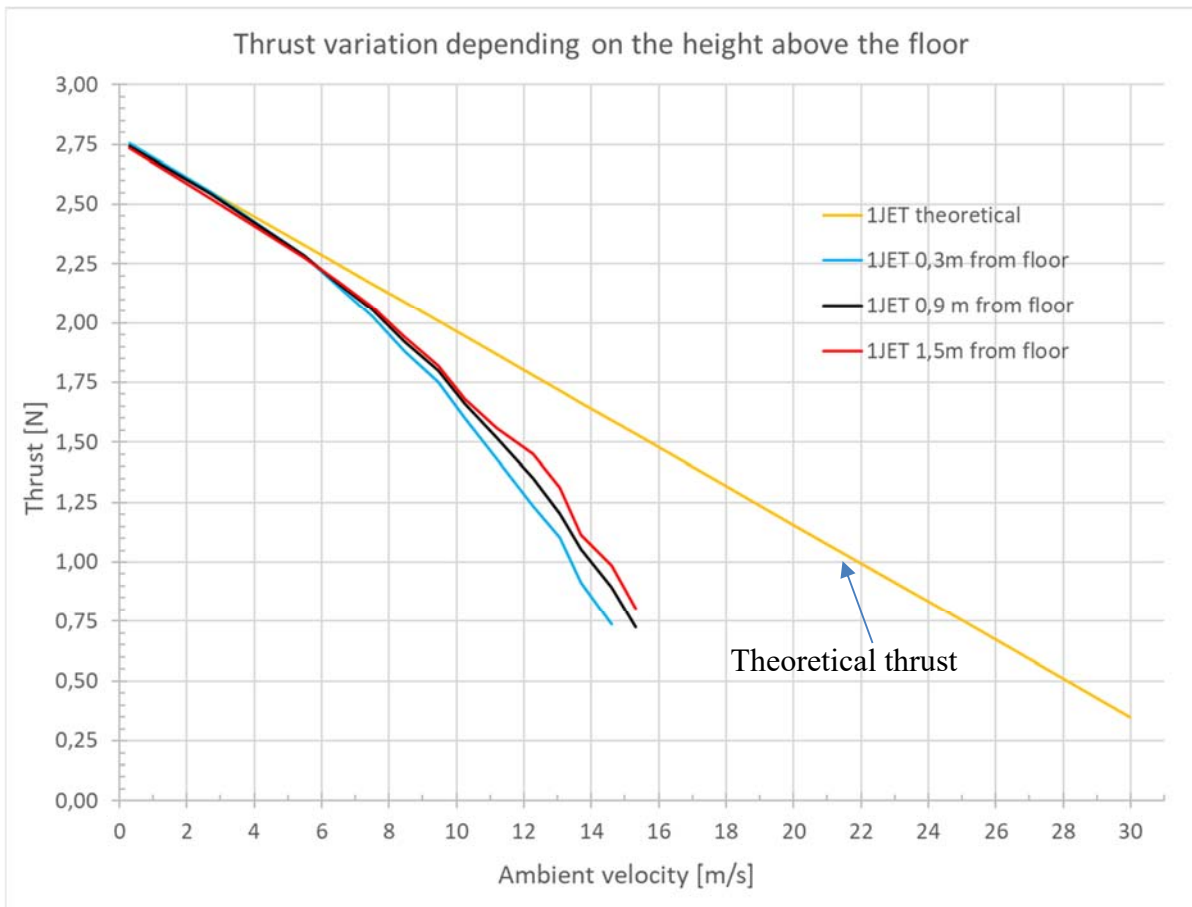


**Figure 7:** Detail of the deflector. Lamellas 0.1 m wide and  $0^\circ$  angle with respect to the flow axis

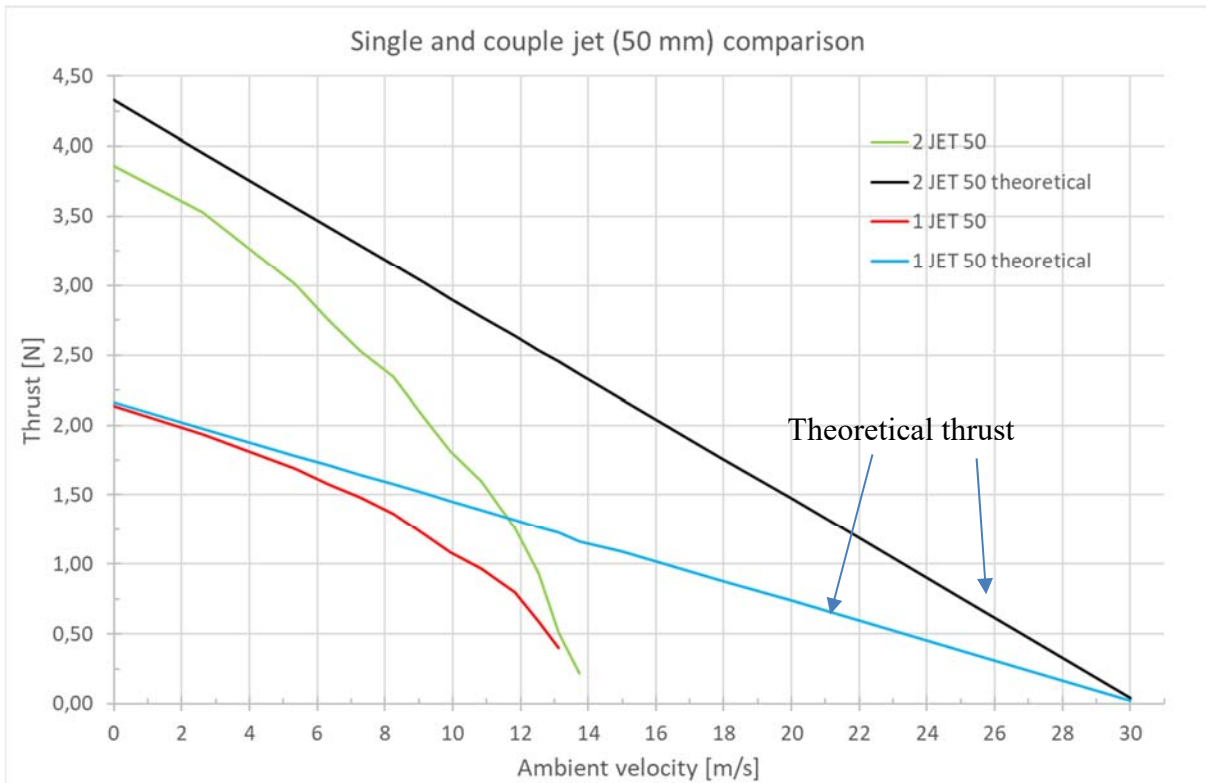


**Figure 8:** Power consumption measurement for a 355mm jet fan in “YY” configuration.

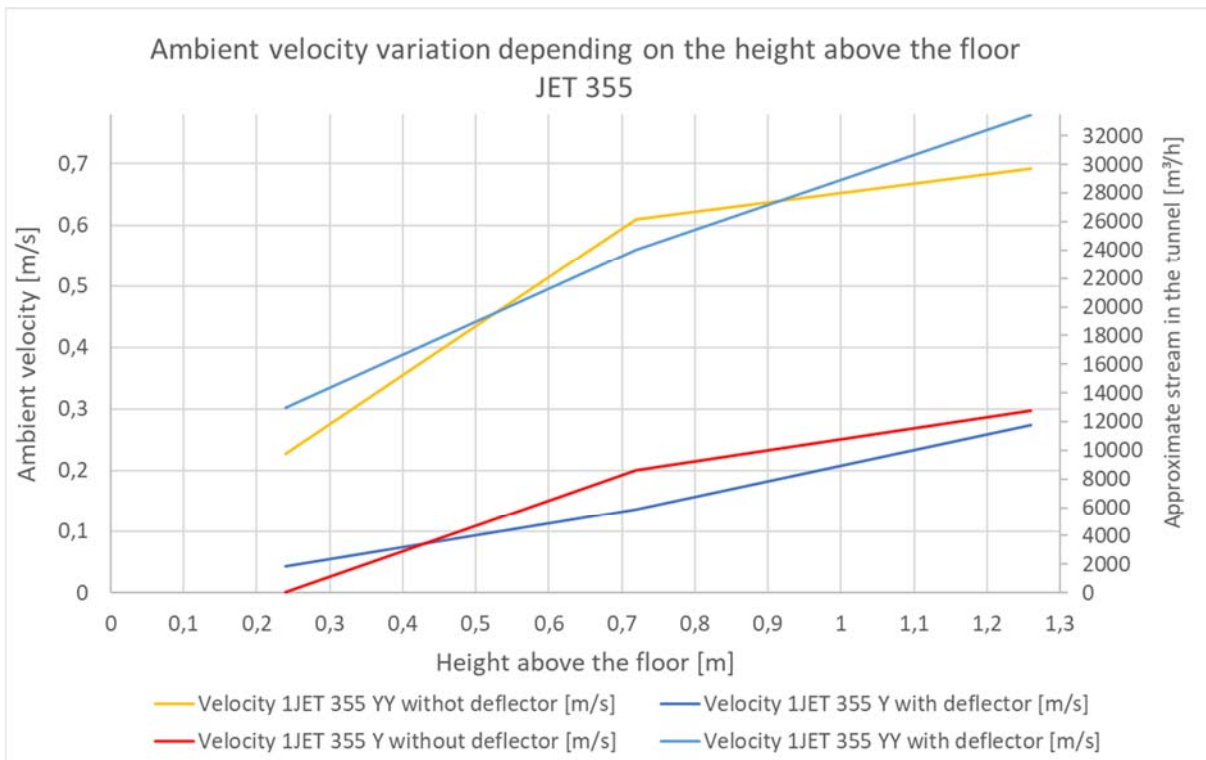
Figure 7. The jet fan gets its power from the mains also when its thrust is 0 N as it still generates the flow.



**Figure 9:** Measurement results for a 50mm jet fan in 1920x125 configuration (brushless motor).



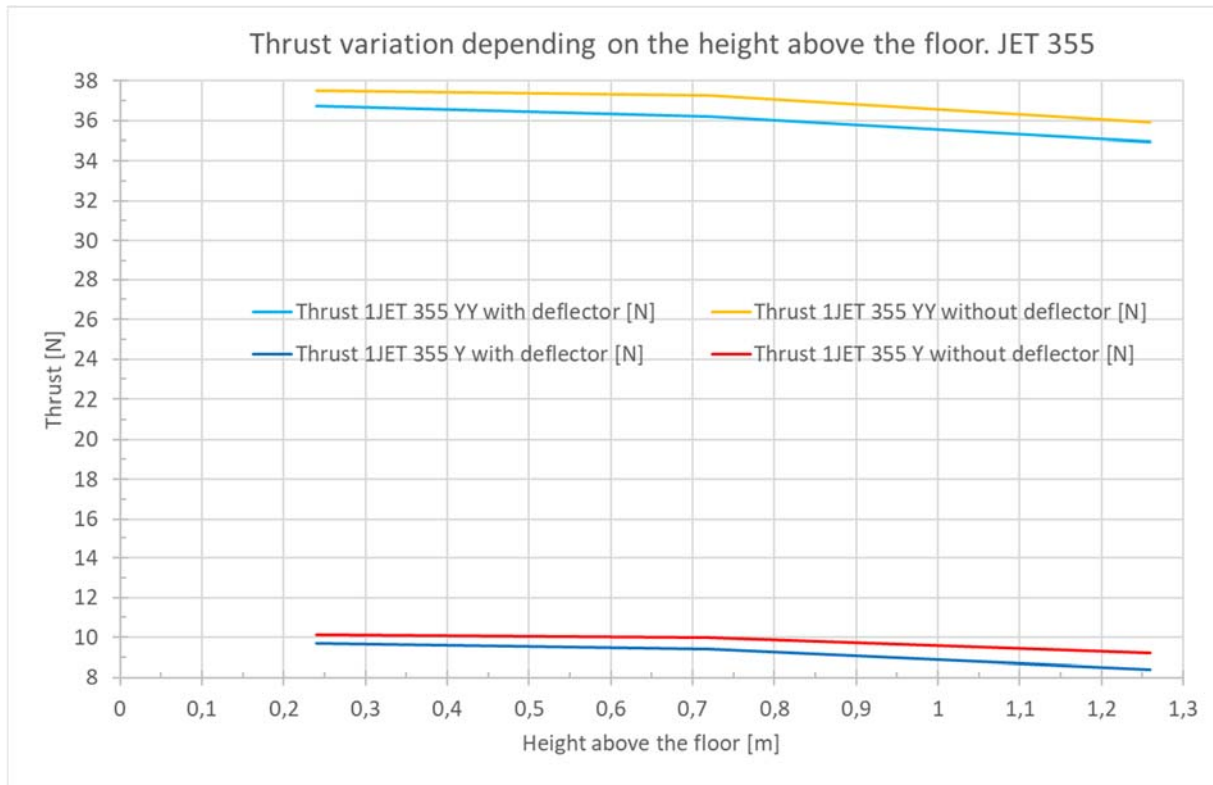
**Figure 10:** Measurement results for a pair of 50mm jet fans in 1860x125 configuration (brushless motor).



**Figure 11:** Measurement of ambient velocity during a 355mm jet fan working. Forcing the flow in the wind tunnel only by jet fan.

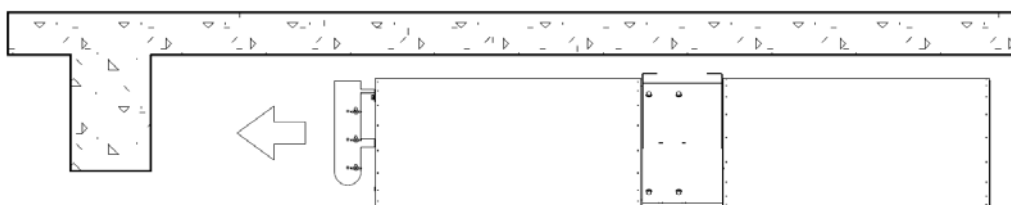
Induced air speed is highest if a deflector is used, but for the position 0,72m above the floor the induced air speed is highest without a deflector (same tendency for the Y and YY - configuration). The reason is that the induced air speed is a result of both the theoretical thrust

of the jet fan and the mounting factor as a measure for the efficiency of thrust conversion to generating the flow.



**Figure 12:** Measurement of thrust a 355mm jet fan. Forcing the flow in the wind tunnel only by jet fan.

Figures 11 and 12 relate to the same measurements who were taken when the fans of the wind tunnel were off. So the ambient velocity was induced by the jet fan 355 installed inside the wind tunnel. The magnitude of the generated speed and the approximate air flow in the wind tunnel are shown in Fig. 11. The flow generated in this way influenced the inlet of the jet fan, thereby reducing its thrust slightly see fig.11. It works like a feedback loop.



**Figure 13:** Obstruction in front of jet fan outlet

The thrust remains constant regardless of obstructions in front of the jet fan outlet fig. 13 as long as the fan is able to maintain its own flow. Parallel rough surface of the tunnel wall in relation to the flow does not affect the thrust.

#### 4. CONCLUSIONS

Theoretically determined thrust from a practical design perspective may deviate significantly from actual flows in the higher velocity range f.e. above 6÷7m/s. In practice, however, design speeds are below 5 m/s.

In Figure 11 it can be seen that the same fan suspended at different heights generates different amounts of flows in the tunnel by induction. Flows differ from one another many times, although the thrust force varies slightly depending on the location above the floor in Fig. 12.

The thrust force does not determine the ability to induce air by the jet fan, nor the value of the generated flow.

There are many analytical factors in the literature that define the efficiency of jet fans depending on their location. On the basis of these measurements, it can be concluded that they relate to a large extent to the efficiency of generating the flow expressed by the basic value of the thrust force, and not to the thrust itself in practical terms.

In the practical design the thrust of the fan may not reach the expected value, due to installation factors and the loss of thrust with the airflow within the tunnel. The experiments performed here will be expanded to measure the flow generated by the jet fans, in order to determine the most efficient way to induce flow in tunnels.

## Literature

- [1] ISO 13350:2015 Fans — Performance testing of jet fans
- [2] Michael Beyer, DI (FH) Eindimensionale Berechnungsmethoden zur Auslegung von Lüftungsanlagen in Tunneln unter besonderer Berücksichtigung dreidimensionaler Strömungseffekte. Institut für Verbrennungskraftmaschinen und Thermodynamik, TU Graz
- [3] Road and Transportation Research Association (2006) Regulations for the equipment and operation of road tunnels. RABT.
- [4] PIARC Technical Committee 3.3 Road Tunnel Operation (2008) Road tunnels: a guide to optimising the air quality impact upon the environment.
- [5] Control of smoke flow using a jet-fan in an underground car park / Marek BOROWSKI, Marek JASZCZUR, Michał KARCH, Tomasz BURDZY // E3S Web of Conferences [Dokument elektroniczny]. - Czasopismo elektroniczne ; ISSN 2267-1242. — 2019 vol. 128 art. no. 10007, s. 1–5. — Wymagania systemowe: Adobe Reader. — Bibliogr. s. 4–5, Abstr.. — Publikacja dostępna online od: 2019-11-08. — ICCHMT 2019 : XII International Conference on Computational Heat, Mass and Momentum Transfer : Rome, Italy, September 3–6, 2019. — tekst: [https://www.e3s-conferences.org/articles/e3sconf/pdf/2019/54/e3sconf\\_icchmt2019\\_10007.pdf](https://www.e3s-conferences.org/articles/e3sconf/pdf/2019/54/e3sconf_icchmt2019_10007.pdf)
- [6] Parametry aerodynamiczne i charakterystyka wentylatorów strumieniowych — [Aerodynamic parameters and characteristics of jet fans] / Tomasz BURDZY // Chłodnictwo i Klimatyzacja ; ISSN 1425-9796. — 2020 nr 2, s. 50–51. — Bibliogr. s. 51.
- [7] PIARC (2008), “Road Tunnels: Operational Strategies for Emergency Ventilation”, Technical Committee C3.3 Tunnel Operations, Working Group No. 6 Ventilation and Fire Control, World Road Association.
- [8] S. Nawrat , S. Napieraj, Wentylacja I Bezpieczeństwo w tunelach komunikacyjnych, KU 0171pozycja wydawnictw naukowych Akademii Górniczo Hutniczej im. S. Staszica w Krakowie, ISBN 83-7464-026-X.
- [9] Cao J, Tamura Y, Yoshida A (2013) Wind tunnel investigation of wind loads on rooftop model modules for green roofing systems. J Wind Eng Ind Aerodyn 118:20–34. <https://doi.org/10.1016/j.jweia.2013.04.006>.
- [10] Ono Y, Tamura T, Kataoka H (2008) LES analysis of unsteady characteristics of conical vortex on a flat roof. J Wind Eng Ind Aerodyn 96:2007–2018. <https://doi.org/10.1016/j.jweia.2008.02.021>
- [11] Wojciech Węgrzyński, Grzegorz Krajewski, and Grzegorz Kimbar. A concept of external aerodynamic elements in improving the performance of natural smoke ventilation in wind conditions. <https://doi.org/10.1063/1.5019109>
- [12] Kempf, J. (1965), “Einfluss der Wandeffekte auf die Treibstrahlwirkung eines Strahlgeblases”, Schweizerische Bauzeitung, 83. Jahrgang, Heft 4.

- [13] F. Tarada R. Brandt Impulse Ventilation for Tunnels – A State of the Art Review. 13th International Symposium on Aerodynamics and Ventilation of Vehicle Tunnels, New Brunswick, New Jersey, USA, May 2009.
- [14] Analiza poprawności odwzorowania wpływu strugi swobodnej izotermicznej z wentylatora strumieniowego — Analysis of the correctness projection of jet fan free isothermal airstream / Tomasz BURDZY, Marek BOROWSKI // Rynek Instalacyjny ; ISSN 1230-9540. — 2019 R. 27 nr 1-2, s. 19–22. — Bibliogr. s. 22.

# MEASUREMENTS AND CFD CALCULATIONS WITH A MOJET AND A CONVENTIONAL JET FAN

<sup>1</sup>Fathi Tarada, <sup>2</sup>Lars Lehmann, <sup>1</sup>Pier Bertacche

<sup>1</sup>Mosen Ltd, Forest Row, UK

<sup>2</sup> TLT-Turbo GmbH, Zweibrücken, DE

## ABSTRACT

A series of measurements were undertaken with a 1.25m internal diameter, fully reversible jet fan in a factory and in the Rendel Street branch of the Mersey Queensway tunnel in Birkenhead, England. The jet fan was fitted with conventional and shaped (MoJet) silencers on both sides of the fan. The MoJet silencers were designed to deflect the airflow away from the tunnel soffit, in order to reduce the friction between the discharged jet and the soffit. The measurements showed an increase in the in-tunnel MoJet thrust of nearly 30%, compared to the conventional jet fan. The power consumption figures of the MoJet and the conventional jet fan were approximately the same, both in factory tests and in the tunnel, within the defined uncertainty limits. The measured tunnel velocities were very close to the results of detailed 3D CFD calculations using ANSYS Fluent, which incorporated the full geometry of the jet fan (including the rotating blades) and the tunnel. Our measurements imply that the MoJet can be employed to reduce the number of jet fans and to decrease the power consumption required for longitudinal tunnel ventilation.

*Keywords: Jet fan, MoJet, aerodynamics, thrust, power, CFD, Coanda, installation factor*

## 1. INTRODUCTION

Jet fans are the most commonly used means of generating mechanical ventilation in tunnels. This is because of the relatively low capital costs associated with jet fans compared to alternative technologies (such as transverse or semi-transverse ventilation systems), since the alternatives generally require the construction of ventilation stations, shafts and ducts, and thereby entail higher construction costs. Despite the attraction of the jet fan solution from a capital cost perspective, the operating and maintenance costs of jet fans can be disproportionately high. This is partly due to inherent inefficiencies with conventional jet fans, with typical installations wasting over half the supplied electrical power, Ref. [1]. This inefficiency is due to two main reasons: aerodynamic friction between the jet discharged by jet fans and neighbouring tunnel surfaces, exacerbated by the Coanda effect, and the unloading of jet fans due to ingestion of high-speed jets from upstream jet fans, Ref. [2].

The MoJet is the latest innovation that has been implemented to improve the in-tunnel thrust delivered by jet fans and thereby to significantly improve their overall efficiency. MoJets incorporate shaped silencers, which direct the discharged flow away from adjacent tunnel surfaces, whilst avoiding flow separation at the intake silencer, Ref. [3]. Measurements with unidirectional MoJets installed within corners of a rectangular tunnel were shown to deliver 100% more in-tunnel thrust than conventional jet fans, Ref [4]. The study in this paper relates to aerodynamic measurements with a fully reversible MoJet and a conventional jet fan installed in a horseshoe-shaped tunnel.

The factory and tunnel measurements reported here were carried out by TLT-Turbo GmbH. The design of the MoJet and the 3D CFD calculations were undertaken by Mosen Ltd. Assistance with the aerodynamic measurements was provided by the Technical University at

Aachen. The tunnel measurements were undertaken with the kind permission of the public-sector transport provider for the Liverpool region, Merseytravel.

## 2. MOJET DESIGN

Our study was based upon a 1.25m internal diameter fan, with 10 blades mounted on the rotor. Two different sets of silencers were attached to this fan: conventional 1D (1.25m long) silencers and MoJet silencers with the same lower edge length as for the conventional jet fan. The outside diameter of the MoJet (1.65m) was the same as that of the conventional jet fan.

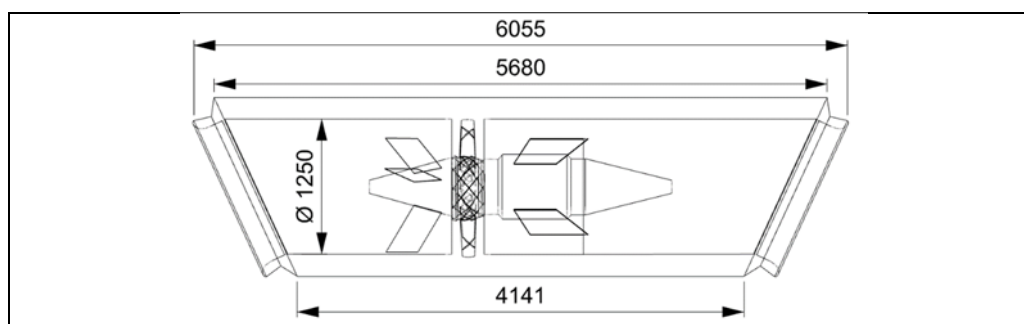


Figure 1: MoJet used in this study (dimensions in mm)

## 3. TUNNEL TEST ARRANGEMENTS

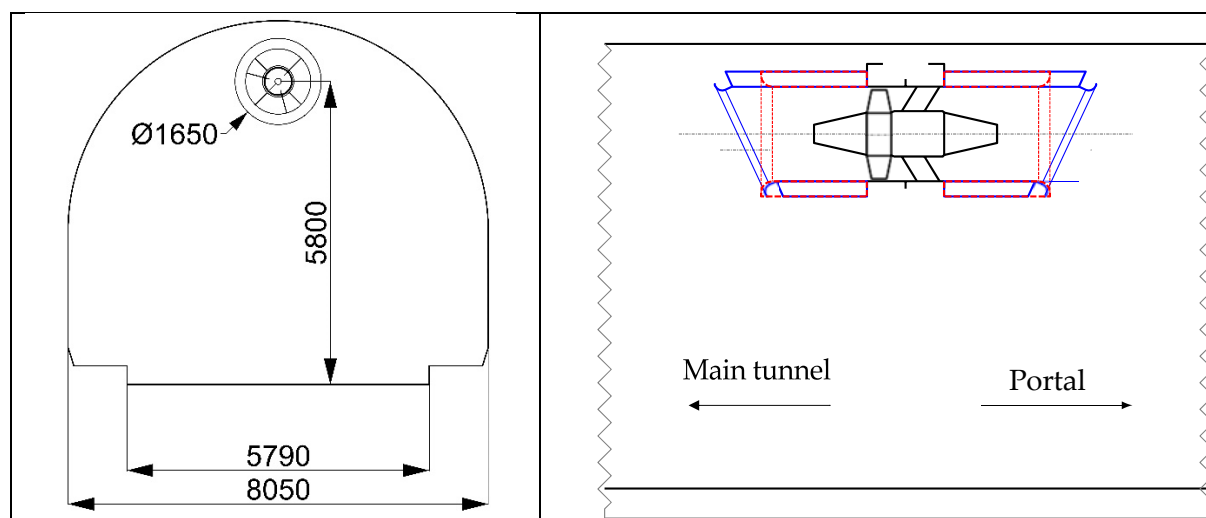


Figure 2: Locations of installed jet fan in tunnel (red=conventional jet fan, blue=MoJet), with dimensions in mm

The tests were undertaken in the disused branch Rendel Street branch of the Queensway Tunnel which connects the Birkenhead to Liverpool. The tunnel has two lanes, and has a horseshoe profile (figure 2). The total length of the branch tunnel is approximately 500 m. From the junction with the main tunnel, the branch tunnel runs straight for about 270 m. After that, there are two slight curves with intermediate lengths of about 100 m. After the second curve up to the portal, the tunnel is straight again. Furthermore, the tunnel has a slight incline along its entire length.

The jet fan was installed below the tunnel soffit, as shown in figure 2 and figure 3. The longitudinal axis of the fan was aligned parallel to the tunnel axis. The distance between the junction of the branch tunnel with the main tunnel to the location of the jet fan discharge was about 25 m. The clearance between the upper edge of the silencer and the tunnel ceiling was approximately 0.35 m.





Figure 3: MoJet installation in the Rendel Street branch tunnel

Velocity measurements were carried out at a distance of about 140 m downstream of the outlet from the jet fan over the entire tunnel cross-section. For that purpose, the velocities were measured at a total of 36 measuring points located at the tunnel cross section in accordance with the log-Tchebycheff distribution in BS EN ISO 5802:2008+A1:2015 (Ref. [5]). The locations of the velocity measuring points are shown in figure 4.

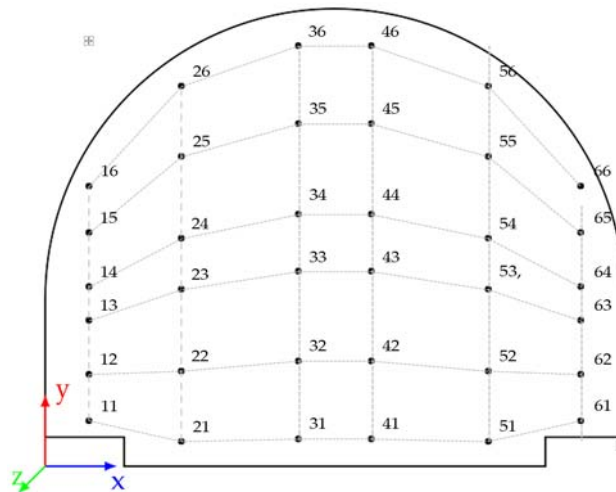


Figure 4: Distribution of the velocity measuring points over the tunnel cross section

Calibrated hot wire anemometers (Trotec BA30WP) were used, with Bluetooth connections to a tablet for data capture. Readings were taken every second for one minute at every measurement location, and then time-averaged.

Background airflow measurements were taken before and after each of the two tests (with the conventional jet fan and with the MoJet). Corrections were then applied to the air velocities in the following manner:

$$V_{effective}^2 = V_{av}^2 \pm V_{background}^2 \quad (\text{Equation 1})$$

In practice, the corrections due to background velocities were found to be very small.

#### 4. MEASUREMENT UNCERTAINTIES

The tunnel aerodynamic measurements were subject to systematic uncertainties (e.g. due to anemometer calibrations, direction of probes, finite number of measuring points) and to random measurement errors. We estimate that the random errors were within 3.5%, to 95% confidence in accordance with Ref. [5]. Most systematic uncertainties “cancelled out” due to comparative nature of exercise, since the same layout and measurement equipment was used for both the conventional jet fan and MoJet tests.

#### 5. FACTORY TESTS

Prior to the tunnel tests, factory tests of the thrust and power consumption were undertaken for the conventional jet fan and the MoJet, in accordance with BS EN ISO 13350:2015 (Ref. [6]). Only the horizontal component of thrust was measured in these tests. The factory measurements are summarised in table 1 below. All measurements were referred to an air density of 1.2 kg/m<sup>3</sup>.

Table 1: Factory measurements

	<b>Horizontal component of thrust in forward direction (N)</b>	<b>Electrical power consumption (kW)</b>
<b>Conventional jet fan</b>	2221	87.6
<b>MoJet</b>	2123	87.7

The thrust and electrical power consumption values for the conventional jet fan and the MoJet are within the measurement uncertainties specified in Ref. [6] ( $\pm 5\%$  for thrust and  $\pm 2\%$  for power consumption).

#### 6. TUNNEL TEST RESULTS

The evaluation of the measured data results in the velocity profiles shown in figure 5. In both cases, the flow profile 140m downstream of the jet fan discharge is well developed and is reasonably evenly distributed over the tunnel cross-section. Certain areas with significantly higher velocities due to the discharged jet are not visible in either case, due to the long distance from the fan discharge. In the left part of the tunnel cross-section viewed in the direction of flow (right in figure 5), the MoJet reaches higher velocities overall. This is due to the swirl exhibited by the jet flow. Viewed in the direction of flow, the fan rotor turned in a counterclockwise direction. Since the discharged flow from the MoJet is deflected away from the soffit and towards the tunnel centre, this results in lower frictional losses. This allows the swirl to be maintained longer and to convey a larger volumetric flowrate in the left half of the tunnel cross-section.

With the MoJet silencers, an average air velocity in the tunnel of 3.78 m/s was achieved compared to an average air velocity of 3.33 m/s with conventional silencers, i.e. a 13.5% velocity increase with the MoJet. Since the thrust ratio is proportional to the square of the velocity ratio, it follows that the MoJet delivered 28.9% more in-tunnel thrust than the conventional jet fan. Since velocity measurements are subject to random errors estimated at  $\pm 3.5\%$ , to 95% confidence (please refer to section 5 above), the measurements of the in-tunnel thrust will be subject to random errors estimated at  $\pm 7\%$ .

The electrically absorbed power for the MoJet during the test was measured at 87.5 kW, which is 1.7 % higher than with conventional silencers (86.0 kW). These two power consumption measurements are however within the uncertainty limits in Ref. 6 ( $\pm 2\%$ ).

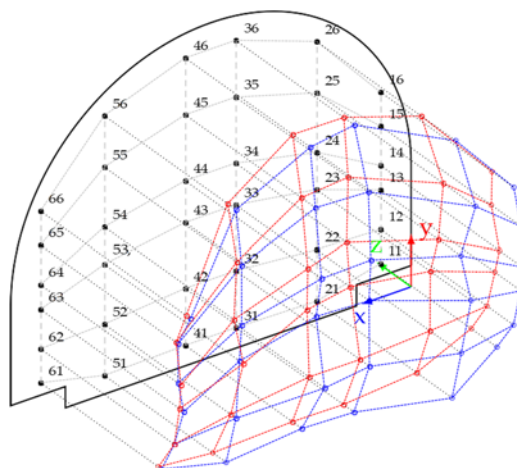


Figure 5: Measured velocity distribution for the conventional jet fan (in red) and the MoJet (in blue)

## 7. 3D CFD CALCULATIONS

The factory tests and tunnel measurements were modelled through 3D CFD, in order to better understand the flow physics and to gain confidence in future CFD modelling of similar cases.

Steady-state CFD models were built using ANSYS Fluent version 2022R1 and the effects of turbulence were resolved using the two-equation  $k-\omega$  shear stress transport model. A single blade set at a pitch angle of  $39.5^\circ$  and rotating at 1485 rpm was modelled, with periodic boundary conditions used to simulate the remaining blades. Mixing planes were applied upstream and downstream of the rotor. The turbulence in the blade's boundary layer region were accurately captured by refining the computational grid with prism layers giving a maximum  $y^+$  value of 25. In addition, prism layers were generated for all other wall boundaries. The maximum  $y^+$  recorded for the bellmouth, the silencer and the internal components of the conventional jet fan and the MoJet was approximately 60. The jet regions were refined using conical refinement zones. The computational grid comprised approximately 6 million polyhedral cells for the bench thrust models and 9 million polyhedral cells for the tunnel models.

In order to compute the tunnel cases efficiently, only the first 225 m length of the branch tunnel was modelled, and the main tunnel was not included in the simulations. Instead, a loss coefficient was applied at the junction between the main tunnel and the Rendel Street branch tunnel, to simulate the aerodynamic losses through the main tunnel portals, along the main tunnel and at the entry to the branch tunnel. This entry loss coefficient ( $\frac{1}{2}K\rho V^2$ ) was calibrated at  $K=2.895$  in order to meet the measured tunnel velocity for the MoJet case. The same loss coefficient was used for the conventional jet fan calculations. In order to reflect the relatively rough tunnel surfaces, a sandgrain roughness was set to 70 mm for the roadway, and 80 mm for the soffit and walls.

Table 2: Bench thrust test CFD vs measurements

Fan Type	Fan Mass Flow (CFD)	Fan Air Density (CFD)	Fan Discharge Velocity (CFD)	Thrust (CFD)	Measured Thrust	% Difference (CFD to measurements)
	kg/s	kg/m <sup>3</sup>	m/s	N	N	
<b>MoJet</b>	56.66	1.20	38.48	2179	2123	2.6%
<b>Conventional</b>	57.71	1.20	39.19	2260	2221	1.8%

Table 3: Tunnel test CFD vs measurements

Fan Type	Fan Mass Flow (CFD)	Fan Air Density (CFD)	Fan Discharge Velocity (CFD)	Average tunnel air velocity (CFD)	Average tunnel air velocity (measurements)	% Difference (CFD to measurements)
	kg/s	kg/m <sup>3</sup>	m/s	m/s	m/s	
<b>MoJet</b>	63.63	1.20	43.27	3.78	3.78	(calibrated via tunnel entry loss coefficient)
<b>Conventional</b>	59.42	1.20	40.39	3.37	3.33	1.2%

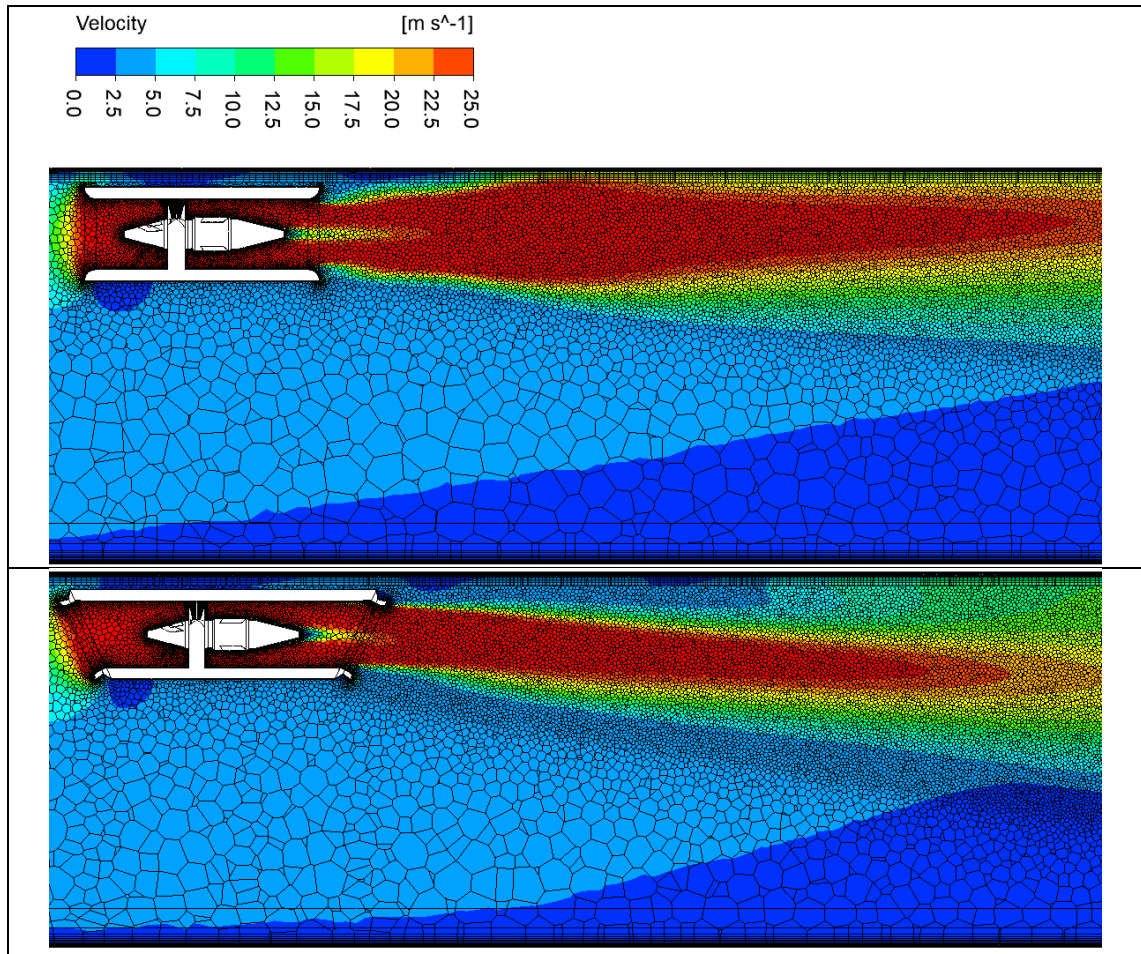


Figure 6: CFD-calculated velocity contours for a conventional jet fan (above) and for a MoJet (below)

The CFD-calculated velocity contours for the conventional jet fan (figure 6) show that the discharged jet attaches to the tunnel soffit, causing significant aerodynamic shear and loss of thrust. In contrast, the velocity contours for the MoJet show that the jet is deflected downwards by approximately 5°, such that the aerodynamic shear stress on the tunnel soffit is significantly reduced, and the in-tunnel thrust is increased. Another reason for the additional thrust of the MoJet in the tunnel is its 7% increased mass flow, compared to the conventional jet fan (table 3). This is due to the higher tunnel airflow in the MoJet case.

The installation factors implied by the CFD calculations were estimated using the following formula:

$$\eta_i = (A_T \Delta P_s + \Delta M_x + S_x) / \{T_B (1 - \frac{V_T}{V_j})\} \quad \text{Equation (2)}$$

where

$A_T \Delta P_s$  = Longitudinal pressure drop along the tunnel [N]

$\Delta M_x$  = Increase in the longitudinal component of momentum across the tunnel domain [N]

$S_x$  = Shear stress acting on the tunnel surfaces in the longitudinal direction, for the case of an equivalent tunnel without jet fans, but with the same longitudinal air velocity [N]

$T_B$  = Jet fan bench thrust for the fan present in the tunnel domain [N]

$V_T$  = Area-averaged longitudinal velocity in tunnel [m/s]

$V_j$  = Jet longitudinal discharge velocity for bench thrust conditions, referred to the fan cross-sectional area [m/s]

The installation factors for the MoJet and the conventional jet fan were calculated on the basis of equation (2) and are presented in figure 7 below. The installation factor estimated using the Kempf correlation (Ref. [7]) is also presented in the same figure. The Kempf correlation generally over-predicts the installation factor for the conventional jet fan, and under-predicts the MoJet installation factor.

The installation factors for both the conventional jet fan and (to a lesser extent) the MoJet are predicted to decrease with increasing tunnel velocity, due to the stretching of the “friction patch” between the jet and the soffit. This phenomenon has been reported by other researchers, e.g. Ref. [8].

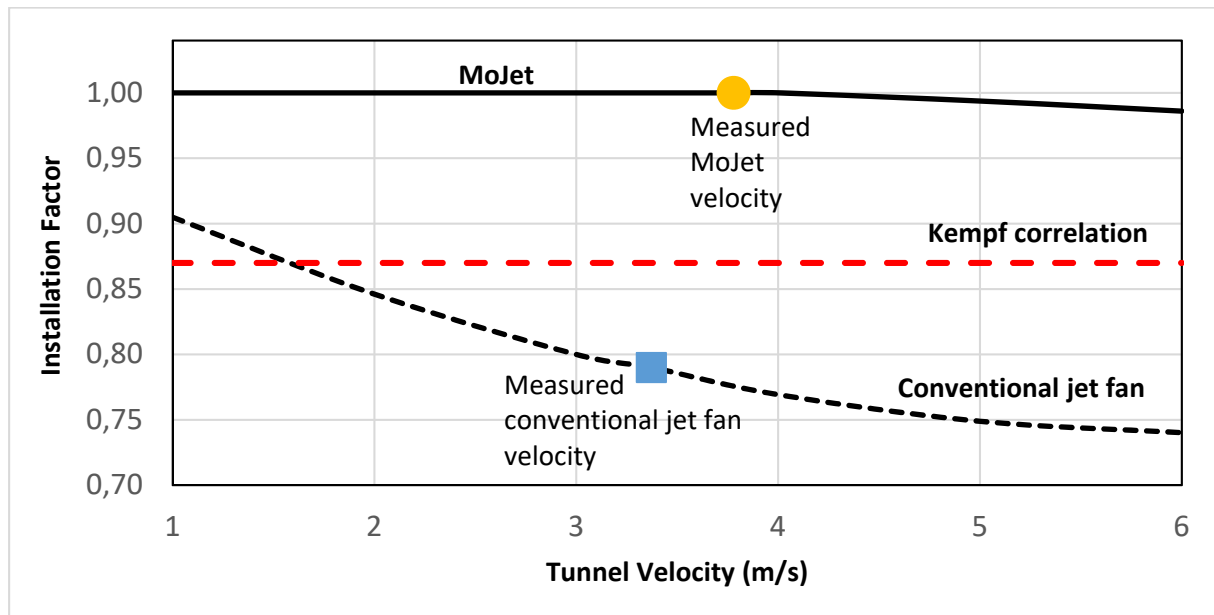


Figure 7: Jet fan installation factors estimated via 3D CFD

## 8. SUMMARY AND CONCLUSION

Our factory measurements of the bench thrust and power consumption of a conventional jet fan and a MoJet indicated approximately the same values, within the uncertainty limits defined in Ref. [6]. However, the two products behaved very differently within a tunnel, with the MoJet delivering almost 30% more in-tunnel thrust than a conventional jet fan. Our CFD calculations show that the main reason for this improvement is the significant reduction in the shear stress on the tunnel soffit with the MoJet, compared to a conventional jet fan. Another reason for the

improved in-tunnel thrust with the MoJet is a 7% calculated increase in the mass flow through the fan, compared to a conventional jet fan. This is due to the shape of the inlet bellmouth, which has a larger cross-sectional area than the fan cross-sectional area.

Our findings suggest that the MoJet can be used to significantly reduce the required number of jet fans, and to substantially reduce the overall power consumption required for longitudinal tunnel ventilation. The actual reduction that can be achieved will be dependent on the specific tunnel geometry (including the surface roughness, which was high in the present case), as well as the ventilation design scenario – e.g. the fire heat release rate that is assumed, the number of jet fans assessed to be destroyed in a fire and the number of jet fans deemed to be out of service due to maintenance.

The research presented here considered only one jet fan installed within a tunnel at any given time. However, the majority of longitudinally ventilated tunnels require multiple jet fans to deliver the required airflow. In cases where the jets from upstream jet fans are ingested into downstream jet fans, a reduction in the jet fan thrust can be expected, due to the unloading of the fan blades (Ref. [2]). Such unloading can be expected to occur if the jet sticks to the tunnel soffit (or corner), and persists for a distance longer than the longitudinal spacing between the jet fans. It is likely that the deflection of the discharged jet away from the tunnel surfaces achieved by the MoJet will prove beneficial in avoiding the penalty of blade unloading, as well as reducing the aerodynamic shear downstream of the jet fans.

## 9. REFERENCES

- [1] “Innovation in Jet Fan Design”, F. Tarada, 7<sup>th</sup> International Symposium on Tunnel Safety and Security, Montreal, 2016.
- [2] “Impulse Fans”, N. Costeris, in “Aerodynamics and Ventilation of Vehicle Tunnels”, pp. 827-846, 1991.
- [3] “Optimised Tunnel Ventilation Device”, F. Tarada, International PCT Patent Application Number PCT/GB2018/000029, 2018.
- [4] “MoJet Tunnel Ventilation – Full-Scale Testing and CFD Analysis”, F. Tarada, K. Else, A. Domoney, P. Hendrick, A. Tarhach, A. Mugisha and A. Kabuya, 18<sup>th</sup> International Symposium on Aerodynamics, Ventilation and Fire in Tunnels, Athens, Greece, 25<sup>th</sup> – 27<sup>th</sup> September 2019.
- [5] BS EN ISO 5802:2008+A1:2015, “Industrial fans – Performance testing in situ”.
- [6] BS EN ISO 13350:2015, “Fans - Performance testing of jet fans”.
- [7] “Impulse Ventilation for Tunnels – A State of the Art Review”, F. Tarada and R. Brandt, 13<sup>th</sup> International Symposium on Aerodynamics and Ventilation of Vehicle Tunnels, New Brunswick, New Jersey, USA, May 2009.
- [8] “Evaluation of Jet Fan Performance in Tunnels”, Beyer M., Sturm P.J., Saurwein M., Bacher M. (2016), 8<sup>th</sup> International Conference ‘Tunnel Safety and Ventilation’, Graz.

## **BEST PRACTICE FOR SELECTION OF FAN- AND DRIVE TECHNOLOGY IN TUNNEL VENTILATION APPLICATIONS**

<sup>1</sup>Simon Frey, <sup>1</sup>Matthias Lempp, <sup>1</sup>Christina Zimmermann, <sup>2</sup>Stefan Herger, <sup>3</sup>Jürg Pargätzi,  
<sup>4</sup>Diego Tschuppert

<sup>1</sup> HBI Haerter AG, CH

<sup>2</sup> Brüniger + Co. AG, CH, <sup>3</sup> Parmeltec GmbH, CH, <sup>4</sup> FEDRO, CH

### **ABSTRACT**

When designing and defining the ventilation systems of road tunnels and safety tunnels, the question of possible combinations of fan and drive technologies and their evaluation regarding technical realisation and economic efficiency very often arises. A well-founded decision-making process for the selection of suitable combinations is only partially available and therefore, selection is often based on personal experience and preferences.

The FEDRO research project AGT 2015/005 addresses this issue by presenting the relevant fundamentals such as an overview of typical fan and drive technologies, the aerodynamic requirements issued by the Swiss design codes as well as grid-compatibility requirements. The start-up currents as well as the harmonics related to the most common drive technologies are determined for typical ventilation applications by means of on-site tests.

Based on these fundamentals, aerodynamic and electric selection processes are developed, allowing to determine the suitable combinations of fan- and drive technology for a specific project. The aerodynamic selection process assesses e.g., the need for multiple operating points for an axial fan or the impact on longitudinal airspeed. The grid compatibility assessment analyses the voltage drop at start-up and harmonic interference, based on the effective, project specific grid topology. The following evaluation process allows to identify, within those suitable combinations, the technically and economically most interesting solution. Within this evaluation, technical aspects (aerodynamics and system-integration) as well as life-cycle cost for fans, drives and wiring are considered. These costs include initial investment, maintenance as well as intermediate replacements when components do not fulfil the needed lifetime.

The developed best practises are transparent and easy to use and therefore a useful tool when designing a road tunnel ventilation system.

*Keywords: Best Practice, Fan- / Drive Technology, Selection Process, VFD, DOL, Life-Cycle Cost*

### **1. INTRODUCTION**

When designing the ventilation systems of road tunnels and safety tunnels, the question of possible combinations of fan and drive technologies and their evaluation regarding technical realisation and economic efficiency arises on a regular basis. Hence, a well-founded and concise knowledge base for the selection of suitable combinations is only partially available. Therefore, the selection is often based on personal preferences and the experiences of the persons involved.

The research project summarizes the relevant basics (aerodynamics and fan technologies, tunnel ventilation specific system requirements, drive technologies and grid compatibility) and confirms / extends these findings by on-site measurements. Based on these findings, a four-step selection and evaluation process is developed allowing confirming the technical compatibility

of a fan / drive combination and to evaluate the most suitable solution for a specific project / application. This so-called most suitable solution is determined using technical criteria such as the capability to precisely control the longitudinal airflow (in case of longitudinal ventilation) or the energy consumption and using life-cycle cost (25 years) including initial investment (fan, drive, cable system), annual maintenance as well intermediate refurbishment for components having a life expectancy less than the considered period.

## 2. BASICS

### 2.1. Fan-Technology

Fans are subdivided according to the curvature of the flow in axial, semi-axial and radial. In tunnel ventilation applications, mostly axial fans are used – other fan types (e.g. radial fans) are rather exotic and are therefore not covered by the present research.

Besides the basic fan type, a distinction can be made based on how the duty point is varied. Common techniques are throttling, variation of rotational speed, variation of pitch angle and variable inlet guide vanes. However, in tunnel ventilation applications, most often variation of pitch angle and variation of rotational speed are used. Hence, only those two techniques are considered in the research project. Figure 1 shows the fan characteristics of a fixed pitch fan with variation of rotational speed as well as the characteristics of a variable pitch, fixed rotational speed fan. The main differences are the size / position of the stall region and the characteristics of the aerodynamic efficiency.

When having to deal with initial counter-pressure (either caused by shaft pressures or by other fans), the extended operational region of a variable pitch fan is clearly advantageous and can determine the technical solution. Speed variation does not affect the stall limit and, depending on the effective fan curve, throttling of the other fans may be required to allow for a sequential start-up. According to [3], fans with variable pitch angle are also slightly advantageous regarding start-up time. No significant difference exists whether the pitch angle is controlled by hydraulics or by electric drives.

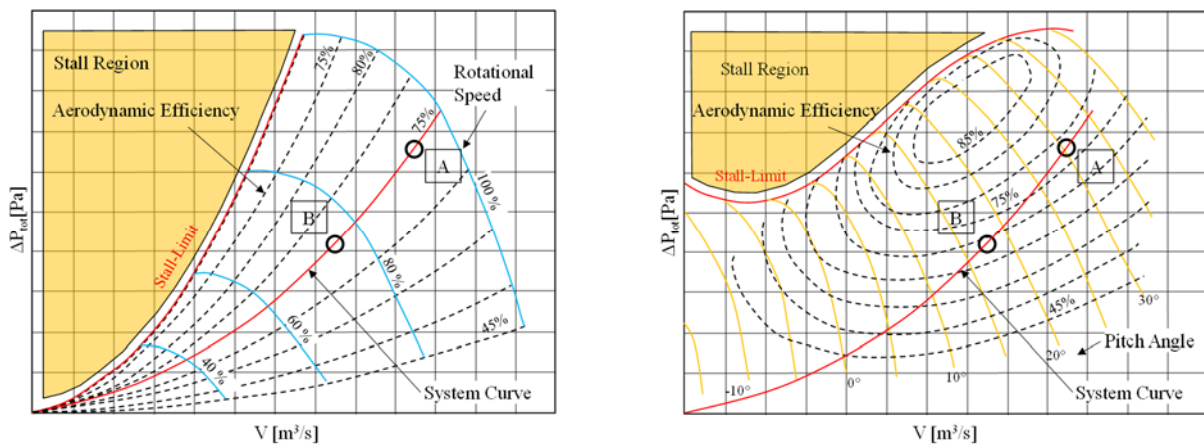


Figure 1: Comparison of fan characteristics affected by variation of rotational speed (left) and by variation of pitch angle (right). For a variable pitch fan, the stall region has much smaller extents and a stall-free zone is present at very low flow rates. For a fixed pitch angle fan, the aerodynamic efficiency remains constant along a specific system curve whereas in case of a variable pitch fan, the aerodynamic efficiency varies [2].

Regarding longitudinal ventilation for smoke management, the effect of a single jet fan on the airflow is an important characteristic. [4] presents a method to evaluate the airflow modulation by jet fans as well as considerations regarding proper acceptance criteria. This criterion will be used during the latter selection process.



## 2.2. Drive-Technology

Nowadays, most of the fans in tunnel ventilation applications are driven by three-phase squirrel-cage induction motors (asynchronous motors). Recent motor technologies such as synchronous reluctance motors appear to be very interesting regarding efficiency but, as up to now, no temperature rated motors are commonly available, asynchronous motors remain by far the most common technology. Significant electrical current peaks and corresponding grid perturbations occur when connecting the motor directly to the grid (direct online, DOL). Different drive systems allow limiting these current peaks at start-up: star-delta connection, pole-changing method (Dahlander Motor), soft starter, and variable frequency drive (VFD). Most often, the ratio of start-up current  $I_s$  to nominal current  $I_N$  is used to characterize these peaks.

In order to confirm literature as well as manufacturer data, on site measurements of the current and the voltage per phase are performed as well as measurements of the harmonics. When assessing grid compatibility, measurements must be performed using sufficient temporal resolution. According to [6], 10 ms RMS values have to be considered in order to sufficiently resolve the current / voltage evolution.

Table 1 summarizes the measured ratio  $I_s/I_N$  as function of the start-up method as well as the recommended value. One can see, that especially when using the pole-changing method, no significant reduction of start-up current peaks can be achieved. When using star-delta connection, the peak currents are reduced by a factor of two compared to DOL start-up. Even though soft starters theoretically allow for very low current peaks, in ventilation applications, the ratio of  $I_s/I_N$  cannot be reduced below 4 to 5 as otherwise, the available torque is not sufficient for driving the impeller. When using variable frequency drives, the current peaks can be ignored.

Table 1: Start-up currents for different drive technologies (measurement / recommendation)

Drive Technology	Tunnel	Measured $I_s/I_N$	Recommendation $I_s/I_N$
Direct online (DOL)	Tunnel Fluelen, exhaust fan	7,5	8 – 10
	Tunnel Fluelen, jet fan	7,9	
	Tunnel Islisberg, jet fan	11,3	
Star-delta connection (Y/D)	Tunnel Sachseln, exhaust fan	4,1	4 – 6
	Tunnel Islisberg, exhaust fan	4,6	
	Tunnel Gubrist, exhaust fan	4,1	
	Tunnel Uetliberg, exhaust fan	4,0	
Pole-changing method (Dahlander: 50% / 100%)	Tunnel Sachseln, safety gallery fan	5,7 (0% → 50%)	8 – 10
		9,5 (50% → 100%)	
Soft starter	Tunnel Kirchenwald, exhaust fan	4,0	3 – 5
	Tunnel Lopper, exhaust fan	4,3	
Variable frequency drive (VFD)	Tunnel Fluelen, exhaust fan	1,04	1,0 – 1,5
	Tunnel Saas, exhaust fan	1,27	
	Tunnel Crap Teig, exhaust fan	1,03	

Besides limitation of current peaks at start-up, pole-changing connection and variable frequency drives also allow for different rotational speeds and therefore for different duty points. Whereas pole changing motors only allow for a fixed, predetermined ratio of rotational speeds, VFDs allow to specifically adjust the rotational speed in order to match, as close as possible, the requirements. This allows for adequate controls (e.g. longitudinal smoke management) and important savings in energy consumption. However, for VFDs with rated power less than about 100 kW, the VFDs efficiency is strongly affected by the effective load (rotational speed /

torque). Figure 2 shows the VFDs efficiency as function of rated power and as function of the load (100% / 50% rotational speed) of a fan application. One can see that for mid-size VFDs, efficiency is reduced by 5% to 10% when operated at 50% nominal speed. Especially for very small VFDs, the efficiency drops by nearly a factor of two, strongly affecting overall efficiency. This is mainly governed by the power needed to drive the electronics of the VFD becoming important compared to the power of the driven machine.

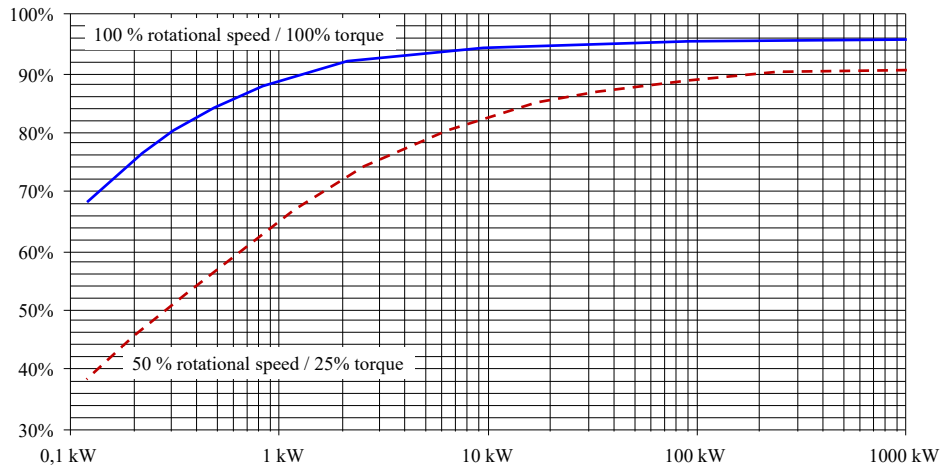


Figure 2: VFD efficiency as function of VFD rated power and rotational speed for applications with quadratic speed / torque relation [5]. For a 500kW VFD (typical exhaust fan), efficiency drops by about 6% when the rotational speed is reduced to 50%. In case of a 15 kW VFD (typical safety gallery / escape route fan), the reduction is roughly 10%.

### 2.3. Grid Perturbations

Grid perturbations can impact the selection of drive technology as well as its technical details. Hence, it's recommended to do first evaluations regarding grid compatibility already in the early design phase. Otherwise, cost relevant measures are required in case grid compatibility is not fulfilled during commissioning.

According to [6], grid perturbations are evaluated using the two following criteria: voltage drop (switching related voltage changes) as well as harmonic interference.

Voltage drops may cause sudden shutdown of equipment, loss of data in control systems as well as sudden relay-switching operations. Therefore, voltage drops need to be limited to tolerable values. Such values are given by technical rules [6] applicable in Germany, Austria, Switzerland, and Czech Republic. Hence, the voltage drop shall be limited to 3% at mid-voltage level (1 kV to 36 kV) and to 6% at low-voltage level (< 1 kV) being usually the secondary side of the transformers. The voltage drop is estimated, during the design phase, by the ratio of switched power and the short-circuit power at the corresponding voltage level. The data from Table 1 can be used to determine the switched power. The short-circuit power is either the power of the transformer divided by the short-circuit voltage (at mid-voltage level) or the grid specific short-circuit power.

Harmonics have a negative impact on the power quality and should therefore be avoided. Depending on their type<sup>1</sup>, frequency converters and soft starters generate harmonics with different harmonic currents. An assessment of the harmonics according to [6] should only be performed if loads causing harmonic interferences are operated within the considered grid. The harmonic spectra of individual installations were measured and compared during the field tests. Harmonics can be reduced either by adding line chokes / filters or by more advanced VFD-

<sup>1</sup> E.g. 6-pole drives, 12-pole drives, active front end drives

types. According to the on-site tests, line chokes are appropriate to reduce harmonic currents for 6-pulse VFDs. In case of AFE VFDs, harmonics are normally not critical. During the design phase, harmonics can be assessed by evaluating the ratios of short-circuit power  $S_{KV}$  to installed power  $S_A$  and harmonics relevant power  $S_{OS}$  to installed power  $S_A$ . Depending on the voltage level, measures may be required or not as shown in Figure 3.

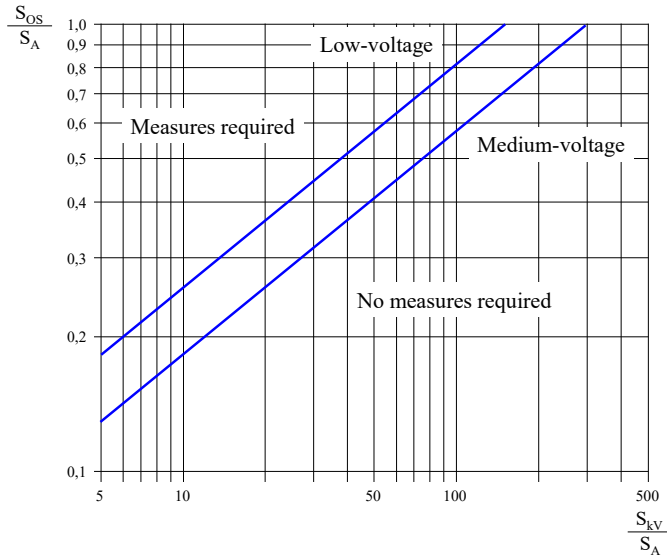


Figure 3: Evaluation of the need for measures to reduce harmonics for low- and medium-voltage installations, [6]

### 3. SELECTION AND ASSESSMENT PROCESSES

The research project [1] presents for each basic type of ventilation application (smoke extraction, longitudinal ventilation, and escape route ventilation) a four-step process to determine the project specific compatible solutions and, considering an estimation of life-cycle cost, the best option within those compatible solutions (see Figure 4).

In the following, this process is presented in more detail using the generic example "Tunnel Musterloch", being a bidirectional road tunnel of 1'300 m length. According to the system design, on overall thrust of 3'700 N is required for longitudinal ventilation. This thrust can be obtained by either 12 22 kW jet fans with nominal diameter of 630 mm, 8 30 kW jet fans with nominal diameter of 800 mm or 5 37 kW jet fans with nominal diameter of 1120 mm. According to the system type, the ventilation system must allow for proper airflow control. Hence, the effect of a single jet fan on longitudinal airflow shall not be bigger than the defined threshold (e.g. less than 0.4 m/s). If this is not the case, either the drive technology must be adapted or a jet fan with less standstill thrust has to be selected. Using the findings presented in [4] or any other calculation method for the impact on longitudinal ventilation, one can determine that, from a pure aerodynamic point of view, the 22 kW jet fan as well as the 30 kW allow for suitable airspeed control independent of the associated drive whereas the 37 kW jet fan needs to be equipped with VFD. Details of this evaluation process can be found in [1].

When assessing grid compatibility, the voltage drop as well as the harmonics need to be evaluated. The full report, [1] presents in detail the different steps to perform. However, it must be noted that no general rule exists as the grid compatibility depends on the effective topology of the installation (e.g. the installed power and the ventilation-related power per transformer). Depending on the overall power and depending on the chosen connection point, it may result that based on voltage drop, any drive technology and especially DOL is admissible for the 22 kW as well as for the 30 kW jet fan. As for the 37 kW jet fan, VFD is needed due to

aerodynamics, voltage drop is not an issue. However, in order to limit harmonics, rather low-tech VFDs (6-pulse) may only be allowed when using line chokes / complex filters. Technically more advanced VFDs (e.g. AFE drives) are less problematic regarding harmonic perturbations.

Having defined the admissible solutions, these can be assessed regarding their technical quality. In case of longitudinal ventilation, the corresponding criteria are: the required space (within the technical rooms), the degree of grid perturbations (voltage drop, harmonics), the energy efficiency, the performance to control the airspeed in case of an emergency (accuracy, time needed to obtain the required airspeed), the complexity of the integration (e.g. relays vs. a complex, specific communication protocol), the cabling system (e.g. number / diameter of the power cables), the eventual impact on HVAC systems in the technical rooms (e.g. in case of VFD). Each of these criteria has its own weighting factor which can be individually adjusted. This allows to consider, at best, the project specific boundary conditions. The grading of each individual solution is given by this weighting factor and a predetermined baseline evaluation. More details regarding the technical evaluation can be found in [1]. For the "Tunnel Musterloch", due to the more precise control of the longitudinal airspeed, the solution using VFD is technically advantageous compared to the others. Nevertheless, the 22 kW / 30 kW jet fans with DOL drive are valid options basically due to their technical simplicity. However, it must be noted that the use of the evaluation mechanism needs an appropriate expertise and awareness of the underlying mechanisms. Otherwise, by imprudently adjusting the weighting factors, any solution can be brought forward.

The financial assessment, the life-cycle cost evaluation, considers the initial investment for the fans including drive and wiring as well as the maintenance costs. The estimate is based on the project specific solution as costs are determined among other things by the effective number of jet fans, by their specific drive, their nominal power, and cable length. The maintenance costs integrate annual maintenance as well as eventual component replacement e.g. for soft starter / VFD as their typical life expectancy is less than the considered life-cycle of 20 years (in case of longitudinal ventilation). Regarding the life-cycle cost within the example case "Musterloch", the most economical solution is the 30 kW jet fan with DOL drive. However, the difference to the 37 kW jet fan equipped with AFE VFD is only about 10%. It has to be noted that the cost evaluation is relative and does not allow for any estimate of absolute investment / maintenance cost as underlying prices (e.g. the price for metals) may have changed in the meantime.

When combining the technical and the economical evaluation for the "Tunnel Musterloch", the technical advantages of the 37 kW solution with VFD do compensate the higher life-cycle cost and so the recommended solution is to equip the tunnel with 5 37 kW jet fans, driven by active front end VFDs. Also, this overall result must be checked appropriately as even small differences may bring forward either of the solutions. Nevertheless, the results allow to distinguish in a quantitative, comprehensive manner the advantages / disadvantages of the individual combinations of fan technology / fan type and the corresponding drive.

Besides the detailed process for longitudinal ventilation, the research report also presents the corresponding processes for exhaust systems as well as for ventilation systems for escape routes / safety galleries

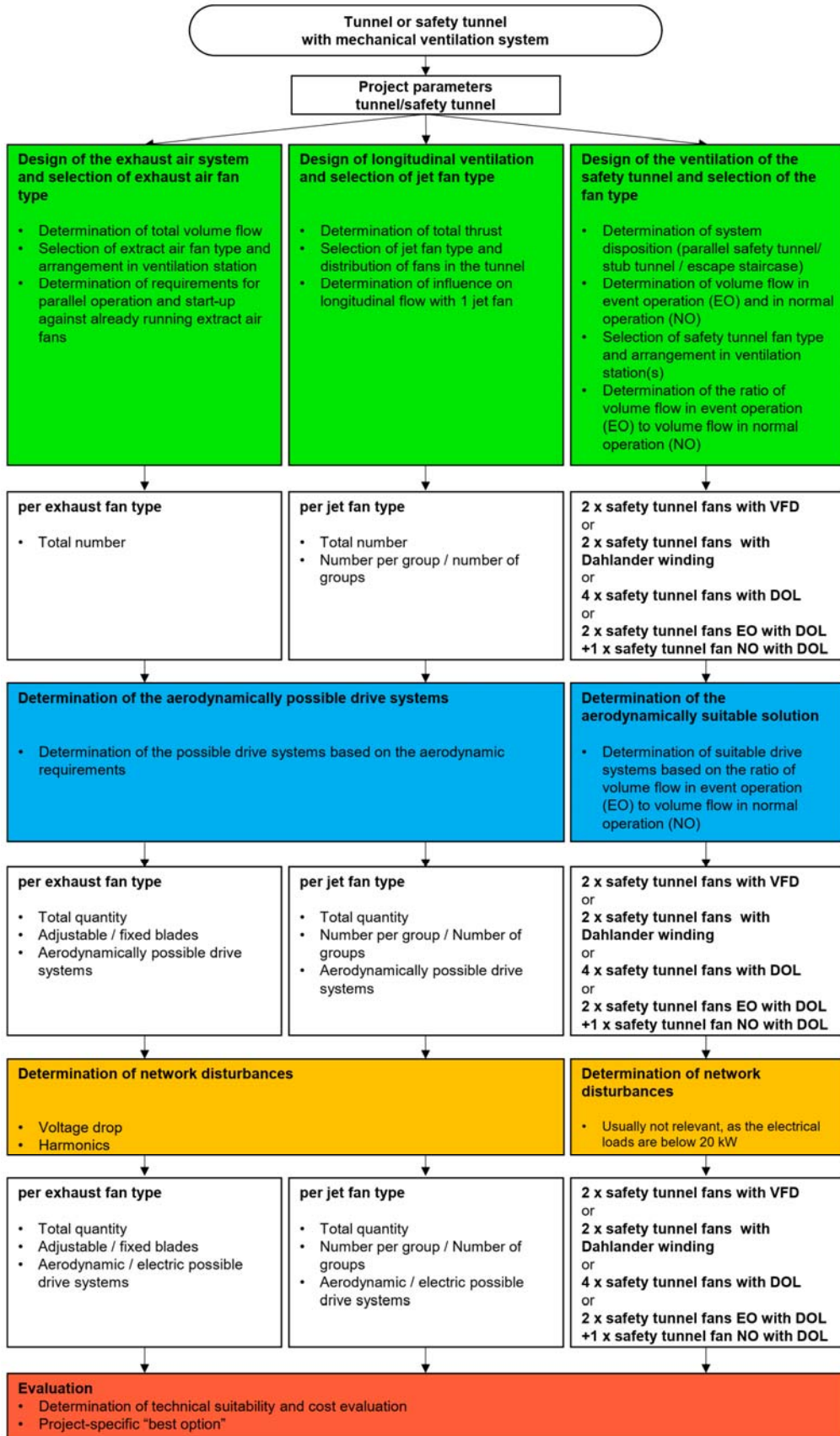


Figure 4: Overview of the selection and assessment process for the basic ventilation system types

#### 4. SUMMARY AND CONCLUSION

To overcome repeated discussions regarding the most suitable combination of fan and drive for a specific project, the ASTRA research project AGT 2015-005: Analysis of systems formed by fan- and drive technology used for tunnel and safety tunnel ventilation presents a best practice process to determine on one hand the technically suitable solutions (from an aerodynamics and grid compatibility point of view) and, on the other hand, to compare the technical benefits and the life-cycle cost of those solutions. As the method is available for smoke extraction fans, for longitudinal ventilation systems as well as for the ventilation systems of safety tunnels, most of the applications are covered. Hence, a transparent and profound tool is created and can readily be applied during the design phase to compare different technical solutions as well as to determine the most suitable one.

#### 5. REFERENCES

- [1] ASTRA Research Project AGT 2015/005, Analysis of systems formed by fan- and drive technology used for tunnel and safety tunnel ventilation, March 2022
- [2] ASTRA Fachhandbuch BSA, Merkblatt 23001-11340, Abluftsystem, 2011, V1.00
- [3] F. van Vemden, Starting-up-time and –methods of fans for emergency tunnel ventilation systems, 4. Int. Conference "Tunnel Safety and Ventilation" 2008 Graz
- [4] S. Frey et al., Aspects of longitudinal airflow control in road tunnels, 10. Int. Conference "Tunnel Safety and Ventilation" 2020 Graz
- [5] Topmotors, Merkblatt Nr. 25: Frequenzumrichter, Oktober 2014
- [6] VSE – Verband Schweizerischer Elektrizitätsunternehmen, D-A-CH-CZ Technische Regeln zur Beurteilung von Netzurückwirkungen, 2. Ausgabe, 2007

## **EVERY SECOND COUNTS - THE SAFETY OF PEOPLE AND GOODS IN TUNNELS.**

### **BEST PRACTICE: INNOVATIVE FIRE AND SECURITY SOLUTION USING THE EXAMPLE OF "ZENTRUM AM BERG".**

<sup>1</sup>Wolfgang Lahner

<sup>1</sup>Honeywell/Honeywell Life Safety Austria GmbH, Austria

#### **ABSTRACT**

Tunnels are among the most demanding environments for fire safety technology and require careful planning and rigorous testing before commissioning. From road tunnels to subway and railroad tunnels, these structures serve as an integral part of modern infrastructure and need to remain operational around the clock. The operational requirements, difficult-to-access installations and the safety of both the people and goods that pass through tunnels, pushes the expectations of fire safety equipment, software and knowhow to an even higher level.

To obtain approval for using the automated fire detection, the company must prove that the maximum fire detection time according to RVS (Guidelines and Regulations for Planning, Construction and Maintenance of Roads in Austria) is not exceeded.

For tunnel projects this test was essential to be able to deliver automated fire detection in Austrian tunnels.

#### **1. INTRODUCTION**

In 2010, a report by the Austrian Court of Audit showed the public that one-fifth of the investments in the road and rail tunnels examined in the report went toward safety. In the case of the road tunnels investigated, as much as a quarter of the costs are for safety. <sup>[1]</sup> This report gives a very deep insight on the safety of tunnels in Austria.

In the Brixlegg rail tunnel, the probability of a fatal accident is one in 10 billion and in the Sonnstein tunnel, one in 100 billion. A safety concept commissioned by ÖBB in 1995 is also mentioned:

"Marginal costs for the prevention of a "perceived fatality" weighted higher on the basis of the aversion factor in the amount of approx. 7.27 mill. EUR (100 mill. ATS), up to which cost-effectiveness ratio measures are sensibly to be realized. Because of the consideration of the aversion factor, ÖBB actually invests about 36 mill. EUR to prevent a (real) fatality;" <sup>[1]</sup>

In contrast to rail tunnels, an average of six fatalities occurred in Austrian freeway and expressway tunnels in the period 1999-2019 and the average economic accident costs amounted to 24.0 million euros per year. According to ASFINAG's incident database, there were 130 fire incidents in tunnels over 500m and its portal areas in the period 2006-2019. In these fire incidents, four people lost their lives, the last time in May 2016. <sup>[2]</sup>

All this and much more illustrates the investment needed to make safety a reality in tunnels.

#### **2. DATA**

Let's have look at the basics of fire detection for tunnels in Austria.

### 2.1. Fire detection in railroad tunnel

According to the regulation concerning the technical specifications for interoperability relating to "safety in railway tunnels" of the rail system of the European Union, minimum safety requirements must be met.

The EU stipulates that all railroad tunnels longer than 1km must be equipped with fire detection in the technical rooms and the alarms are transmitted to the infrastructure managers. Stations that are in tunnels shall be in conformity with the national rules on fire safety. When they are used as safe areas and/or fire fighting points, they shall comply only with the relevant specifications must be met. <sup>[3]</sup>

These EU directives have been implemented in the Railway Act.

### 2.2. Fire detection in road tunnel

Tunnels in the Trans-European Road Network must meet minimum safety requirements. The EU stipulates that a system for automatic detection of traffic incidents and/or fires shall be installed in all road tunnels more than 500m in length with a control center. For road tunnels more than 500m in length without a control center, automatic fire detection systems shall be installed. <sup>[4]</sup>

In Austria, the EU specifications for minimum safety requirements were implemented in the Road Tunnel Safety Act (STSG). Here, only road tunnels with a ventilation system must be equipped with an automatic fire alarm system in case of fire. <sup>[5]</sup> For road tunnels in Austria, individual guidelines and regulations are declared binding by service instruction or decree according to §7 Para. 2 of the Federal Roads Act. <sup>[1]</sup> This brings into play the RVS (Guidelines and Regulations for Road Construction), which reflects the current state in Austria and the bindingly declared RVS 09.02.22 for tunnel equipment, which specifies everything that fire detection for road tunnels must be able to do and fulfill. The automatic fire detection system for the driving area must also ensure that it can trigger within a short time.

Table 1: maximum fire detection time, according to RVS for the fire detector in the road tunnel <sup>[6]</sup>

LONGITUDINAL AIR VELOCITY [m/s]	FIRE DETECTION [s]		FIRE LOAD
	PRE-ALARM	ALARM	
< 3	60	90	2 x 1m <sup>2</sup> pool fire with 10l ethanol each
≥ 3	120	150	2 x 1m <sup>2</sup> Diesel pool fire with 10l diesel each - and 5 liter gasoline each

Furthermore, for the road tunnels of highways and expressways there are still the planning manuals which then require, for example, that a pre-alarm is to be detected and reported, but which is not evaluated, or does not control anything.

### 2.3. Test fire Saalbach Hinterglemm

For our fire detection system to be allowed to be used in Austrian road tunnels, it had to be tested and approved by an accredited inspection body. This was achieved in 2015 with the following test results:

Table 2: Test fire Saalbach Hinterglemm



Tunnel test fire - Tunnel Hinterglemm - 23.11.2015 detection times / Linear Heat					
tripping times results	Airlongitudinal velocity m/s	DTS west		DTS east	
		pre alarm	alarm	pre alarm	alarm
ethanol fire					
14:29:00	< 3	14:29:52	14:30:02	14:29:56	14:29:56
		00:00:52	00:01:02	00:00:56	00:00:56
14:51:00	< 3	14:51:52	14:51:52	14:51:46	14:51:56
		00:00:52	00:00:52	00:00:46	00:00:56
petroleum diesel fire					
15:10:57	≥ 3	15:11:52	15:11:52	15:11:46	15:11:56
		00:00:55	00:00:55	00:00:49	00:00:59
15:33:52	≥ 3	15:34:52	15:35:02	15:34:56	15:34:56
		00:01:00	00:01:10	00:01:04	00:01:04

### 3. SUMMARY AND CONCLUSION

All this and more illustrates the investments we make to prove our technology in order to provide institutions such as the Tunnel Research Center of the University of Leoben "Zentrum am Berg" with the best possible solution.

#### WHICH SOLUTION SUITS BEST IN A TUNNEL; WHICH TECHNOLOGIES ARE USED?

Honeywell offerings installed at ZaB include fire detection solutions, public address and voice alarm system (PA/VA), and an alarm and video management system in the road and rail tunnels.

The main technology in Fire Safety is the latest generation of Honeywell's DTS (Distributed Temperature Sensing) linear heat detectors. In the ZAB, there are two DTS detectors installed, each in redundant loop configuration to support reliable operations. They are connected in single-mode configuration by a fiberoptic essernet® network which is also processing signals from point detectors and new VES aspirating smoke detectors. By combining these fire detection systems, both fire and smoke can be detected in their very early stages, preventing false alarms even under challenging conditions.

The PA/VA system inside Zentrum am Berg's tunnels is realized with the Digital Output Module (DOM) from the VARIODYN D1 range which is EN54 certified and features multicasting and integrated power

amplifiers. For display and operation, the Ethernet Touchscreen Call Station (ETCS) offers a 7" touchscreen with a user-friendly interface.

The PC-based hazard management system WINMAG is a key element of the alarm and video management system. WINMAG's graphical user interface allows users to quickly localize hazards even in complex system environments with minimal training requirements, saving valuable time in incident response.

Thanks to its modular and scalable design, WINMAG allows full integration of Honeywell's server-based video management system MaxPro. By providing real-time alarms and detection of abnormal behavior without human supervision, MaxPro further contributes to the system's efficiency, both in terms of cost saving and safety requirements.

Every second is valuable in case of an incident in a tunnel. Modern Fire Safety and Security solutions and a fast evacuation is essential in a tunnel for saving lives and property. <sup>[7]</sup>

#### **4. REFERENCES**

- [1] <https://www.rechnungshof.gv.at/rh/home/home/tunnelsicherheit.pdf>
- [2] [https://www.bmk.gv.at/dam/jcr:b268b082-424d-429c-8026-7b60608e4ed7/tunnelbericht\\_1999-2019\\_20200904.pdf](https://www.bmk.gv.at/dam/jcr:b268b082-424d-429c-8026-7b60608e4ed7/tunnelbericht_1999-2019_20200904.pdf)
- [3] <https://eur-lex.europa.eu/legal-content/DE/TXT/PDF/?uri=CELEX:32014R1303&from=DE>
- [4] <https://eur-lex.europa.eu/legal-content/DE/TXT/PDF/?uri=CELEX:02004L0054-20090807&from=DE>
- [5] <https://www.ris.bka.gv.at/GeltendeFassung.wxe?Abfrage=Bundesnormen&Gesetzesnummer=20004722>
- [6] RVS 9.02.22 Tunnel Equipment
- [7] Case Study "Zentrum am Berg" by Honeywell Life Safety Austria GmbH

## **AN AFFORDABLE & SUSTAINABLE ALTERNATIVE: LED RETROFIT TUNNEL LIGHTING**

<sup>1</sup> Author: Thomas Nessel, <sup>2</sup>Markus Keller

<sup>1</sup> ASFiNAG Service GmbH, AT

<sup>2</sup> ASFiNAG BMG, AT

### **1. INTRODUCTION**

The operating technology department at ASFiNAG has found a sustainable way of converting existing lighting to LEDs cost-effectively and independently of manufacturers.

Lighting is one of the most important safety features in road tunnels.

There have been many improvements in lighting technology in recent years but the new systems were either very high maintenance or expensive. The metal halide lamps give white light but quickly lose luminosity, have high power consumption and need to be replaced every two years. The most recently installed LED fixed systems are very expensive, require their own wiring, and when they need to be replaced, you are dependent on the manufacturer's system.

Our research has shown that the existing stainless steel housings and wiring will last at least 25 years. Therefore, we looked for a manufacturer who was willing to develop with us a completely new modular system with LED inserts and lens technology. The specifications from the beginning were that the inserts must fit into any system, that more and even light must arrive on the road, that it must be a modular system where a spare part costs no more than 40 € and the installation must be possible under 5 minutes. After completing our tests, we knew that the implementation was technically possible and we released the specification for procurement.

Today, there are already five manufacturers supplying these highly compatible and sustainable inserts according to our specifications. The number is constantly increasing. Due to the competition, the price dropped and since 2020 even the powerful tunnel entrance lighting is equipped with LED inserts.

### **2. KNOWN PROBLEMS**

#### **Common problems with halogen metal vapour lamps:**

- become darker
- change colour
- high power consumption
- Reflector angle
- Ballasts
- Replace EVERY 2 years! Lock!

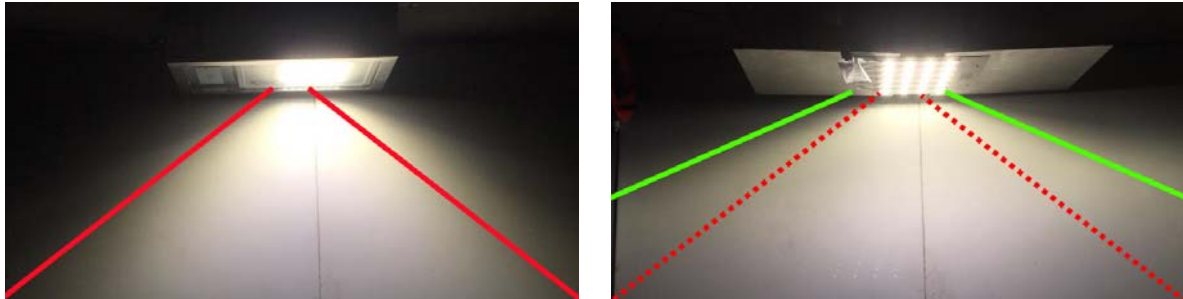
#### **Current problems with LED Fix System:**

- Expensive! >700€ per luminary
- Bespoke wiring
- Bespoke brackets
- Manufacturer-dependent

- Aluminium <Longevity

### 3. INNOVATION

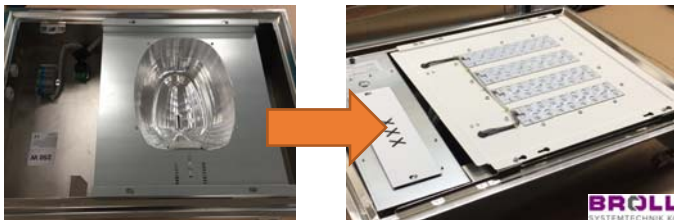
We started the **Lighting Insert Development**:



What we wanted:

- +Retrofit: old housing, old wiring
- +More light, more evenly dispersed
- +Modular system, < 70€ per spare part
- +Installation <5min
- +Use below 400€
- +Less power
- +Light quality (colour temp., colour reproduction)

With support of Detas DLeds and BROLL made a **simple modular retrofit design**



...simple and easy to install:



With great results:



#### 4. NEW LED INSERT SUCCESSES:

- Old housings + wiring last 30 years
  - + Item price starting from 200€
  - + Replaced in < 5 minutes
  - + 25% more light at 34% lower power consumption
- Since 2020 we install it also at the TUNNEL ENTRANCE

#### 5. NEXT STEPS IN THE ASFINAG BMG EM

- Study on Cri value correction in the RVS
- Introduction of changes to the RVS/FSV to reduce the energy demand & CosPhi
- Revise the design manual tunnel lighting considering stainless steel suitcase luminaires
- Determine the basis of replacement needs

#### 6. PLAPB CHANGES IN THE ASFINAG BMG EM

- Revise tender texts
- LEDs Cri & Energy & 80.000h
- Driver temperature & unifying the housing
- cd/m<sup>2</sup> measurements & what does the customer see?
- Ensure testing possibilities by local construction supervision (ÖBA)
  
- Ra CRI  $\geq 70$  checkable at data sheet !
- Control without series connection & 8-4 steps
- 3 parts = one luminaire in DACH & simple on-site exchange
  - stainless steel box & luminaire up to € 800 EFB
  - DFB driver & quick exchange (e.g. 2x150W € 300)
  - EFB unit & quick exchange (e.g. 1x400W € 400)

#### 7. QUALITY

##### QUALITY: Fail safety – temperature:

- The temperatures measured indicate whether the light meets the quality requirements.

- Temperature management
  - -> minimum volume required
  - -> high quality LED-drivers

QUALITY: Color consistency

What we never want to see again:



Color-over-angle (CoA) effect:

At normal incidence, a fraction of the blue pump light leaks out to produce a balanced white spectrum. At large angles, more blue light is absorbed, resulting in an off-color spectrum with less blue and more green+red=yellow than wanted.

Not on IR LED, but IR LEDs are half-efficient on Color consistency at  $Ra \geq 90$ .  
(Soraa/LEDinside)

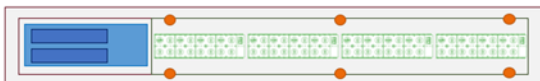
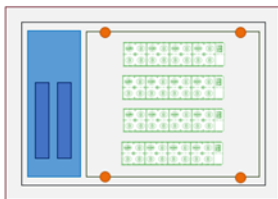
Solution:

We need a Lens LED combination without color-over-angle (CoA) effect

## 8. SUMMARY AND CONCLUSION

New ASFiNAG STANDARD

(2 modular, sustainable housing types)



- 2 Standard housings  
with flat glass – easy cleanable
- Standard equipment carrier  
for 2 drivers (failure safety,  
same quantity of LED Modules)
- Standard mounting points  
(only minimum volume defined)
- Add quality definition:

⇒ temperature &

11<sup>th</sup> International Conference 'Tunnel Safety and Ventilation' 2022, Graz

- ⇒ color consistency
- ⇒ makes  $Ra \geq 70$  possible

#### 10 Years & 30 years

- 📍 new optimized concept & sustainable use
- 📍 increase of life cycle
- 📍 reduction of energy consumption
- 📍 survey of the need for replacement
- 📍 adaptation RVS & PlaBP
- 📍 Stainless steel case lights (retrofit also for entrance area) & 17.5 up to 35 years lifetime

# VENTILATION IN SHORT TUNNELS AS A RISK MITIGATION MEASURE: "A SHORT TUNNEL CAN BE AS DANGEROUS AS A LONG ONE"

<sup>1</sup> D. Benitez Forero

<sup>1</sup> Electromechanics Department, Integral S.A., Colombia

## ABSTRACT

*When a tunnel capacity is foreseen by design and in operation results in a higher one, which produces almost permanent queues inside a tunnel, with a combination of light and heavy vehicle traffic, and an emergency management protocol mismatched to the reality of the operation, whether it is a short or long tunnel, with two-way or one-way flow, it is necessary to revisit the concept of tunnel classification based on its length and traffic volume, because a short tunnel can be as dangerous as a long tunnel".*

*Normally, tunnels between 50 m or less and up to 250 or less than 500 m are defined as short tunnels in the standards that regulate and legislate on road tunnels worldwide. It is also possible to intuit a priori, that short tunnels, being of really minimum lengths, if compared with tunnels defined as long (1000 m and above), do not present comparable risks as those that would be found in the latter. Therefore, the attention to any particularity that a short tunnel may have, during the design phase, is ruled out.*

*However, with a closer look, it is observed that in general terms from the regulations, short tunnels have been stripped of all series of protections, "possibly" because of the supposed lower level of risk compared to long tunnels. However, the fact that these short tunnels do not have a tangible safety compliance scheme, puts them in a potentially high-risk classification, just like long tunnels. Therefore, they are vulnerable to the shortcomings that can be ensured from a holistic view of safety, whose vision is almost never fulfilled in a project.*

## 1. CONTEXT OF THE PROBLEM

In several design standards and directives, there are stipulated a series of aspects that must be reviewed and taken into account when designing safe tunnels. Many standards [5], define the following factors that influence the tunnel to be more or less safe, among others, such as the following aspects:

- Tunnel length
- Amount of traffic and nature of the traffic (heavy, light, motorcycles, other)
- Dangerous goods
- Longitudinal slopes
- Natural ventilation, with forced ventilation
- One-way or two-way flow
- With or without emergency lane
- With or without drains for hazardous materials
- Emergency plans
- Fire extinguishing, fire detection and fire alarm systems

There are, in turn, numerous methods of risk analysis[6], both qualitative and quantitative risk measurement, there are of course prescribed as the above list, that each of these conditions must be taken into account in a design, however, these factors are usually associated in relation to the length of a tunnel and the amount of traffic, at most. Meanwhile, catastrophic accidents



continue to happen as the one reported in the tunnel called "Túnel de la Línea" in Colombia, Latin America, where in a set of 23 tunnels; one of them being only 190 m long, an accident occurred that left at least 7 dead and 30 injured. Then, in several engineering projects, it is found that tunnels between 50 m or less and up to 250 or 300 m, even less than 500 m, -as in the European Directive-, are defined as short tunnels and at the level of standards, more or less requirements are imposed based on the length of the tunnel.

On the other hand, although statistically an admissible margin of fatalities and injuries has been established in road tunnel projects, as used in the approach of risk analysis methodologies such as DG QRAM and others, it is unacceptable to allow the loss of human lives in a context as delimited as a short tunnel, and then there must be analyzed several concepts around the meaning of risk, and the dynamic nature of this for which are applicable in turn, dynamic systems for risk mitigation.

## **2. DYNAMIC NATURE OF RISK**

Any infrastructure made by man and for man, would be meaningless without a use. An infrastructure, be it a high-rise building, a hydroelectric power plant, a bridge, an airport, a road tunnel, etc., would be nothing more than "models" if they did not interact with man, since these are static systems in themselves, and only under interactions with man, dynamic processes are produced, as man uses these infrastructures. Therefore, the interactions between man and infrastructures produce processes that are dynamic, not static. There is no risk associated with the static nature of the infrastructures, but there is a risk associated when man interacts with them. Therefore, it can be said that "risk is dynamic in nature".

However, geometrically ill-conceived works impose conditions on the dynamics of a process from the outset, and to the extent that the statics of the infrastructures affect the dynamics of a process, the risk will vary in range, and therefore, it will oscillate between the dynamic and the static, the latter being a restriction imposed from the outset on the dynamics of the processes due to the invariable nature of their nature. In synthesis, the errors in the geometric design of tunnels, which have been identified in the norms, regulations or design guides, such as exaggerated lateral and longitudinal slopes, narrow radii of curvature, gauges, platforms, shoulders and lane widths, absence of emergency evacuation tunnels, inaccuracy of information and data of the traffic study, lack of characterization of dangerous goods, etc., impose per se, a restriction on the design of tunnels, impose per se, a restriction to the fulfillment of the goal of having a safe tunnel, thus transferring its potential risk to the dynamic systems of the processes that have to manage its variables to modulate the risk, control it or minimize it. According to the above, it is not correct to dimension and design the dynamic systems without first taking into account the non-compliances, at least regulatory, of the infrastructures, as if we were starting from an ideal structure, since then, we will have deficiently dimensioned systems for the attention of the risks in the operation of the tunnel.

## **3. DYNAMIC SYSTEMS**

Understanding that the processes happen by the interaction of man on the infrastructures (static), that is; man puts in use the structures to its service, example; when a road tunnel starts operating, then, the dynamic systems are all those that collaborate in a variable way in the time to modulate the risks that are generated by the interaction between the vehicles, the occupants, and the infrastructure itself. The dynamic systems will be: ventilation systems[8], detection systems, and fire extinguishing systems when they must be activated, ITS, signaling, communications, emergency brigades when they are activated, etc. These are all the resources

and systems that assist in a continuous and sustained manner over time the management of vehicular traffic through the tunnel or road corridor, and will vary in behavior and performance according to the variation of the events generated by the vehicles in transit.

In this way, the dynamic systems will only act according to some input variables, which initially would not satisfy previous requirements, such as a bad geometric design, and therefore, the sizing and specifications of the dynamic systems will never be adequate to satisfy safe operating conditions of the tunnel.

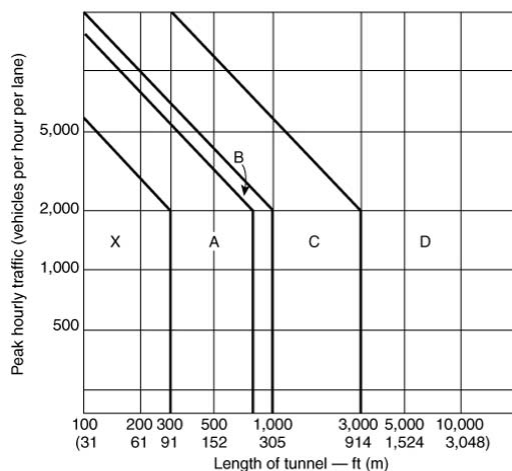
We have established then, that geometrically poorly dimensioned infrastructures impose restrictions to the fulfillment of the safety goals by the dynamic systems, so it can be deduced that no matter how many safety systems and emergency plans are available, the intrinsic risk of the previous non-compliances underlies and where the dynamic systems are not perfectly adjusted to the variables of the traffic regime, then, any kind of consequences as catastrophic as the ones happened in a tunnel of only 190 m in length could occur.

#### 4. RISK MITIGATION SYSTEMS

It should be defined that the need of ventilation for short tunnels is prescribed for sanitary needs, that is, only natural ventilation is required to guarantee the sufficient quantity of oxygen in the air and the cleaning of the air through the dissolution of contaminants in the normal operation of the tunnel. But under the definition of natural ventilation, the benefit of ventilation as a safety mechanism for a fire or smoke evacuation situation occurring in a short tunnel is practically ruled out. It should be shown then, the reasons why forced ventilation is required for certain short tunnels.

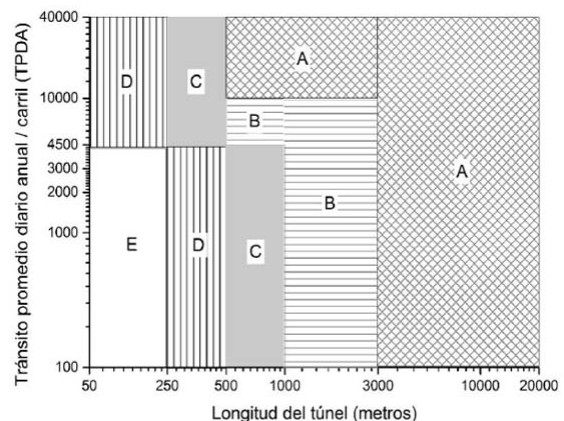
According to NFPA 502 [3], short tunnels are specifically defined as being between 31 [100 ft] and 91 m [300 ft] in length and are only intended to handle traffic of about 5,000 vehicle-hours/lane, as shown in Figure 1 below:

Figure 1: Tunnel Classification according to NFPA 502



Source: NFPA 502, 2020 edition

Figure 2: Tunnel Classification according to the Tunnel Manual, Colombia.



Source: Manual for the Design, Construction, Operation and Maintenance of Road Tunnels, 2021 edition.

Additionally, these tunnels are classified as "X", and have Mandatory Requirements (MR) and Conditionally Mandatory Requirement (CMR) protection and safety considerations, which can be summarized in table A.7.2 "Minimum Road Tunnel Fire Protection Reference Guide". But it is relevant that this standard recommends that absolutely, for "all" tunnel lengths, the respective engineering analysis must be developed, where at least each of the following aspects must be taken into account.

- (1) New installation or modification of an existing installation.
- (2) Modes of transport using the facility
- (3) Anticipated traffic volume and mix
- (4) Restricted vehicle access and egress
- (5) Fire emergencies ranging from minor incidents to major catastrophes (6) Potential fire emergencies ranging from minor incidents to major catastrophes (7) Fire emergencies ranging from minor incidents to major catastrophes
- (6) Potential fire emergencies including, but not limited to, the following.
  - (a) At one or more locations within or on the facility
  - (b) In the vicinity of the facility
  - (c) At facilities at a great distance from the emergency response facilities
- (7) Exposure of the emergency systems and structures to elevated temperatures
- (8) Traffic congestion and control requirements during emergencies (9) Emergency protection elements
- (9) Fire protection elements, including, but not limited to, the following
  - (a) Fire alarm and fire detection systems
  - (b) Standpipe systems
  - (d) Water fire extinguishing systems; (e) Ventilation systems
  - (e) Ventilation systems
  - (f) Emergency communication systems
  - (g) Protection of structural elements
- (10) Components of facilities, including emergency systems (11) Evacuation and rescue requirements
- (11) Evacuation and rescue requirements
- (12) Emergency response time (13) Access points for vehicles
- (13) Access points for emergency vehicles (14) Emergency communications to emergency responders (15) Access points for emergency vehicles
- (14) Emergency communications to appropriate agencies (15) Location of facilities, including emergency systems (16) Emergency communications to appropriate agencies

- (15) Location of facilities, such as urban or rural (level of risk and response capability)
- (16) Physical dimensions, number of traffic lanes and roadway geometry
- (17) Natural factors, including prevailing wind and pressure conditions
- (18) Expected loading
- (19) Impact on buildings or landmarks near the facility (20) Impact on the facility
- (20) Impact on the facility from external conditions and/or incidents (20) Impact on the facility from external conditions and/or incidents
- (21) Traffic operating mode (unidirectional, bidirectional, switchable or reversible).

From the above, and according to the "X" classification for short tunnels, the following means or safety resources are considered mandatory (MR):

- Structural elements of the tunnel protected to fire.
- Traffic control
- Emergency response plan

And as conditionally mandatory (CMR), the following safety means or resources:

- Emergency communications systems

However, of all the above, not a single system that is part of the fire protection for short tunnels, among others, for example, the ventilation system, is included. The following are the systems that are part of the fire protection in this standard, but could be others or similar in other standards:

- Fire vehicle.
- Piping network system for hose connections, hose cabinets or hydrants.
- Fire department water storage.
- Fire Department connections.
- Fire pumps
- Manual fire extinguishers
- Fixed water-based fire extinguishing system.
- Emergency ventilation system
- Drainage system
- Hydrocarbon detection
- Environmental hazards due to substances and fuels

#### COLOMBIAN STANDARD [4]

In the Colombian standard called the "Manual for the Design, Construction, Operation and Maintenance of Road Tunnels, 2021 edition, short tunnels are classified as "E", and are considered between lengths of 50 to 250 m, for traffic volumes of 100 to 4500 TPDA (Average Daily Annual Daily Traffic/Lane), see graph 2 above.

## **5. STATIC SYSTEMS AND DYNAMIC**

We have defined in the "dynamic nature of risk", that we have static and dynamic systems. The static systems are the infrastructures and the dynamic systems are all the resources that materialize according to the real time in the event of a contingency. If we review the mandatory requirements that a short tunnel must meet, such as "structural elements must be protected against fire", this is not a dynamic element against the contingency of an accident or a fire inside the short tunnel. And regarding the "traffic control" and the "emergency response plan", since these are very dependent on human decision making, they are subject to the risk of failure by not meeting the expectations that are necessary to cover, when an accident and/or fire occurs in a tunnel, in general, short or long length. The same happens with the "emergency communications systems", which result from the decision to implement them or not, according to the criteria of the engineering analysis proposed in standards such as NFPA 502.

Although an engineering analysis must be developed on a mandatory basis for any length of tunnel, it is not yet clear when, what, and why, some, all, or no systems, both static and dynamic, should be implemented to address safety.

Accordingly, at the very least, it should be clear that the systems, resources, and dynamic means to deal with a contingency for an automobile accident and/or fire in the tunnel will be those that can be made available in real time and materially, such as ventilation systems, water jet discharges from hoses or fixed water-based extinguishing systems, manual extinguisher discharges on a vehicle that is on fire or overheated and will soon cause a spreading fire. Therefore, it is of vital importance, before establishing for every tunnel the need to develop an engineering analysis, and beyond defining what is mandatory, and what is conditionally mandatory in safety equipment for a tunnel, is to recognize the nature of the static and dynamic systems that are part of the safety of a tunnel that is put into operation, where not even all risk analysis models are able to cope with these circumstances [11].

## **6. ANALYSIS OF THE SITUATION**

In view of the clear evidence shown by the statistics in the reports that are permanently published worldwide, there are still accidents due to vehicular collisions at the entrance of a tunnel, accidents with or without fire, many of them with catastrophic results due to the loss of human lives. It is necessary then, to understand that the structures or infrastructures already built, or to be built, that once poorly executed do not comply at least prescriptively with some or many geometric parameters such as those already mentioned above, and in addition, certain resources or systems are also static in nature to contribute to safety, then, it is also necessary to understand that they must be recognized as dynamic systems, that those systems that contribute materially and in real time to safety, such as emergency ventilation, water jet discharges, and manual extinguishing, should be recognized as dynamic systems, in order to consider a reclassification of tunnels[10] to include both forced ventilation and fire extinguishing.

### **6.1. CATASTROPHE IN A 190 M LONG TUNNEL**

In a 190 m long tunnel, there were no water-based extinguishing systems, no manual fire extinguishers, and even less forced ventilation. At the same time, an engineering analysis considered that other resources or fire protection systems were unnecessary. The communication systems were those that corresponded to communication via radios between surveillance personnel on the outskirts of each tunnel, and an emergency plan[7], possibly not adjusted to the changing reality of traffic depending on the time of day and the special vacation dates, where the number and intensity of travelers moving through a road corridor designed to

mobilize mostly freight vehicles increases. Therefore, light vehicles and cargo vehicles shared the same road corridor, which also consisted of 23 tunnels, all with different lengths.

An accident occurred inside the tunnel, which was only 190 m long and had a negative slope, when a tractor-trailer with no brakes collided with a line of vehicles inside the tunnel. Several of the light vehicles were carrying families, as well as intermunicipal buses full of passengers, but also cargo vehicles, so that the light vehicles were trapped in the middle of the cargo vehicles, producing a human "sandwich", which as a result of the accident left at least seven dead and 30 injured, according to official news reports and the rescue corps that attended the accident.

## **6.2. EFFECTS OF THE VEHICLE COLLISION**

After the vehicle collision, several light vehicles were ejected at the gauge level downstream of the tunnel, while others were trapped in the middle of the tractor-trailers, which remained with their engines running after the collision. The tractor-trailer that collided spilled the material it was carrying, such as engine lubricating oils and brake fluids. Minutes after the accident, visibility inside the tunnel was lost due to fumes from the burning engines, possibly also due to the combined combustion of the oil and brake fluid spills. The death of the people could have been caused by asphyxiation and intoxication[9], in addition to the mechanical impact.

## **6.3. VICTIM RESCUE**

For the rescue of the victims, the "external" emergency response personnel entered through the downstream portal of the tunnel, that is, at the lowest altitude of the tunnel. However, due to the obstruction of the vehicles trapped in the tunnel and close to the entrance portal, the rescue of the victims had to be done through the upstream portal of the tunnel, that is, at the highest altitude of the tunnel, as well as the extraction of the vehicles involved in the collision. This shows that, given the circumstances of the accident, where there is a short tunnel, also with a negative longitudinal slope, the rescue actions of the occupants were under the most adverse conditions of toxic and irritating fumes, because the rescue could not be downstream of the incident, due to the vehicular obstruction of the entire tunnel. However, there was no forced ventilation to mitigate the risk of death by asphyxiation and/or poisoning, nor was there an extinguishing system to cool the overheated and still burning engines after the multiple collisions.

## **7. VENTILATION AS A DYNAMIC SYSTEM FOR RISK MITIGATION**

It is documented in many specialist papers, statistics published by the different PIARC technical committees, and others, the serious events that can take place in short tunnels [1], a brief non-exhaustive list of accidents involving fires or just accidents, is presented below:

ACCIDENTS WITH/WITHOUT FIRES IN SHORT TUNNELS [2]

Year	Tunnel	Country	Tunnel Length m (ft)	Fire Duration	Damage		
					People	Vehicles	Structure
1967	Suzaka	Japan	244 (800)	11 h	2 injured	12 trucks	-
1968	Moorfleet	Germany	243 (800)	1 h	-	1 truck	Serious
1976	Crossing BP	France	430 (1,410)	1 h	12 injured	1 truck	Serious
1987	Gumefens	Switzerland	343 (1,125)	2 h	2 dead	2 trucks, 1 van	Slight
1989	Brenner	Austria	412 (1,350)		2 dead, 5 injured		
1993	Serra Ripoli	Italy	442 (1,450)	2h 30 min	4 dead 4 injured	5 trucks 11 cars	Limited
1996	Isolla delle Femmine	Italy	148 (485)	-	5 dead 20 injured	1 tanker, 1 bus, 18 cars	Serius
2001	Guldborgsund	Denmark	460 (1,509)	-	5 dead 6 injured		
2022	La Línea	Colombia	190 (623)	-	7 dead 30 injured	1 truck, 5 cars 3 buses	-

According to the context of the present document, the ventilation system is a dynamic system that must be considered for short tunnels due to the following circumstances that a priori may not be identifiable:

- 1- Longitudinal slope of the short tunnel greater than 3% finally constructed.
- 2- Dangerous goods content of the vehicle(s) involved.
- 3- Production of fumes due to combustion or spillage of hazardous materials from the vehicles involved.
- 4- Condition of the engines left running after the collision.
- 5- Unavailability of water for the cooling of the burning engines, to avoid the start of possible combustions of the crashed vehicles.
- 6- Difficulty for the emergency brigades to reach the exact spot due to the obstruction of the accident vehicles and the line of vehicles formed before and after the tunnel.
- 7- Rescue and extraction of the injured in the most unfavorable conditions upstream of the accident, under conditions of smoke either from fire or combustion of the spills, or smoke emission from the burning engines.

## 8. CONCLUSIONS

- Each design standard for the safety of road tunnels has defined a different length for the so-called short tunnels, ranging from 30 m to less than 500 m. This is a very wide range where the length of the tunnels can vary. This is a very wide range where there may be other conditions that are difficult to control through prescriptive design or through risk analysis.
- The infrastructure of a tunnel and the roads that connect to its entrance are static systems, because they have no variation or adjustment after operation.
- The interactions between man and infrastructure produce processes that are dynamic, not static.

- There is no risk associated with the static nature of the infrastructures, but there is a risk associated when man interacts with them.
- Dynamic systems are all those that collaborate in a time-varying manner to modulate the risks generated by the interaction between vehicles, occupants and the infrastructure itself.
- The dynamic systems will be: ventilation systems, detection systems, fire detection and extinguishing systems when they must be activated, ITS, signaling, communications, emergency brigades when they are activated, etc. They are all the resources and systems that assist in a continuous and sustained manner over time the management of vehicular traffic through the tunnel or road corridor, and will vary in behavior and performance according to the variation of the events generated by the vehicles in transit.
- The ventilation system is a dynamic system that should be considered for short tunnels, and therefore, a systematic review of the worldwide regulations should be initiated, with respect to the classification of tunnels that only prescriptively links the parameters of length and traffic volume.
- A conventional risk analysis methodology does not resolve design singularities by virtue of the interaction of static systems and dynamic systems.

## 9. REFERENCES

- [1] W.K. Chow, Ph.D., FSFPE, "Fire Hazards in Short Vehicular Tunnels
- [2] Igor Y Maevski, Transportation Research Board, "Design Fires in Roads Tunnels", List of Road Tunnels Fires, Table 3.
- [3] NFPA 502, "Standard for Road Tunnels, Bridges, and Other Limited Access Highways", 2020 edition
- [4] Manual for the Design, Construction, Operation and Maintenance of Road Tunnels, 2021 edition, "Classification of Road Tunnels by Length and TPD in Colombia, Figure 2-1
- [5] Directive 2004/54/EC of the European Parliament and of the Council of 29 April 2004, "Basis for Measuring Safety", pp 59
- [6] PIARC, Risk Analysis for Road Tunnels, Technical Committee C3.3, 2008R02ES
- [7] Centre D'Etudes Des Tunnels CETU, Booklet 5 "Emergency Response Plans", 2006
- [8] PIARC, Road Tunnels: Ventilation Control Strategies in Emergency Situations, Technical Committee C3.3, 2011R02
- [9] PIARC, Road Tunnels: Vehicle Emissions and Ventilation Air Demand, "Admissible In-Tunnel Concentrations Of Toxic Gases", Technical Committee C4, 2012R05EN
- [10] F.H. AMUNDSEN - O.L.SOVIK, "Classification Of Tunnels, Existing Guidelines And Experiences, Recommendations", PIARC Committee on Road Tunnels, 1995
- [11] Horhan R., Foster C., Kohl B., "RVS 09.03.11 - Upgrading Of The Austrian Tunnel Risk Model TuRisMo, BMVIT Federal Ministry for Transport, Innovation and Technology, Vienna, ILF Consulting REngineers, Linz